

Cardiac Repolarization

Basic Science and Clinical
Management

Nabil El-Sherif
Editor

Cardiac Repolarization

Nabil El-Sherif
Editor

Cardiac Repolarization

Basic Science and Clinical
Management

 Springer

Editor

Nabil El-Sherif
Department of Medicine and Physiology
State University of New York Downstate Medical Center
VA New York Harbor Healthcare Center
Brooklyn, NY
USA

ISBN 978-3-030-22671-8 ISBN 978-3-030-22672-5 (eBook)
<https://doi.org/10.1007/978-3-030-22672-5>

© Springer Nature Switzerland AG 2020

This work is subject to copyright. All rights are reserved by the Publisher, whether the whole or part of the material is concerned, specifically the rights of translation, reprinting, reuse of illustrations, recitation, broadcasting, reproduction on microfilms or in any other physical way, and transmission or information storage and retrieval, electronic adaptation, computer software, or by similar or dissimilar methodology now known or hereafter developed.

The use of general descriptive names, registered names, trademarks, service marks, etc. in this publication does not imply, even in the absence of a specific statement, that such names are exempt from the relevant protective laws and regulations and therefore free for general use.

The publisher, the authors, and the editors are safe to assume that the advice and information in this book are believed to be true and accurate at the date of publication. Neither the publisher nor the authors or the editors give a warranty, expressed or implied, with respect to the material contained herein or for any errors or omissions that may have been made. The publisher remains neutral with regard to jurisdictional claims in published maps and institutional affiliations.

This Springer imprint is published by the registered company Springer Nature Switzerland AG
The registered company address is: Gewerbestrasse 11, 6330 Cham, Switzerland

Foreword

Normal cardiac repolarization is vital to maintain optimal mechanical and electrical cardiac function. Repolarization that is too long or too short, or otherwise abnormal, puts the patient at risk for developing life-threatening cardiac arrhythmias. It is essential that scientists and clinical electrophysiologists understand cardiac repolarization. The textbook *Cardiac Repolarization: Basic Science and Clinical Management*, edited by Nabil El-Sherif, provides information critical to that understanding.

Chapter 1, “Physiology and Molecular Biology of Ion Channels Underlying Ventricular Repolarization of the Mammalian Heart,” reviews the key ion channels that underlie cardiac repolarization and focuses on critical potassium ion channels, while the Chap. 2, “Neuromodulation of Cardiac Repolarization and Arrhythmogenesis,” explores autonomic modulation of this activity at the cardiac channel, cellular, and organ levels.

Heart failure can predispose to the development of potentially fatal arrhythmias via multiple mechanisms including altered calcium handling, stretch, and changes in myocyte electrical and metabolic properties, as explored in Chap. 3, “Repolarization Remodeling in Structural Heart Disease.” A major advance in studying mechanisms impacting repolarization has been the use of pluripotent stem cell-derived cardiomyocytes to model cardiac disease states, a major advance presented in Chap. 4, “Cardiac Repolarization and Stem Cells: An Emerging Path Toward Precision Medicine.”

Voltage-gated sodium channels, responsible for the rapid upstroke of the action potential, are vital to maintain electrical excitability and coordinate excitation-contraction coupling, as explored in Chap. 5, “Role of Late Sodium Current during Repolarization and Its Pathophysiology.” How age, sex, and race impact cardiac repolarization and arrhythmogenesis is presented in Chap. 6, “Age, Sex, and Racial Differences in Cardiac Repolarization and Arrhythmogenesis,” emphasizing that testosterone appears to shorten the QTc interval in males, while in females, there is a more complex interaction between progesterone and estrogen.

With the initial chapters serving as a scientific foundation for clinical events involving repolarization, the text now turns to the clinical arena, beginning with a consideration of the standard electrocardiogram (ECG), still one of the most useful methods for risk stratification for sudden cardiac death, and an analysis of the QT interval, as explained in Chap. 7, “ECG-derived Evaluation of Cardiac Repolarization.” Microvolt T-wave analysis represents

another approach for investigating the QT interval to track T-wave alternans, a beat-to-beat fluctuation in ST-segment or T-wave morphology, and is discussed in Chap. 19, “Microvolt T-Wave Alternans: Pathophysiology and Clinical Aspects.”

The next several chapters feature clinical manifestations of the long QT interval. Chapter 8 delves into the phenotype-genotype relationship of clinical presentations, ECG patterns, risk stratification for cardiac events, and therapy in “Genotype-Phenotype Correlation in Congenital LQTS: Implications for Diagnosis and Risk Stratification,” concentrating on the three genes *KCNQ1*, *KCNH2*, and *SCN5A* underlying LQT1, LQT2, and LQT3, respectively, which account for about 95% of patients with an identified genetic cause. Chapter 9 discusses the clinical management of patients with the inherited long QT syndrome, “Clinical Management of LQTS Patients,” focusing on minimizing the adrenergic response, shortening the QTc, decreasing the dispersion of refractoriness, and improving the function of dysfunctional ion channel.

Chapter 10, “Drug-Induced Long QT Syndrome and Torsades de Pointes,” emphasizes drug-induced LQTS and its ventricular arrhythmia, noting that QT prolongation is a useful but imperfect predictor of patients at high risk of developing the serious and life-threatening arrhythmia, torsades de pointes. Chapter 11, “Acquired Long QT Syndrome and Electrophysiology of Torsade de Pointes,” stresses the electrophysiological mechanisms of acquired LQTS, its electrocardiographic (ECG) characteristics, clinical presentation, and management of the acquired long QT interval.

New mechanisms of QT prolongation are explored in Chap. 12, “Pathogenesis of Autoimmune-Associated Long QT Syndrome,” and Chap. 13, “The Role of Inflammation and Autoimmunity in Long-QT Syndrome.”

The QTc interval can be too short (<340 ms) as well as too long and provoke ventricular arrhythmias, as discussed in Chap. 18, “The Short QT Syndrome.”

A relatively newly described entity, the J-wave syndromes, appears to be a constellation of several clinical entities characterized by J-wave abnormalities, such as the early repolarization syndrome associated with variants in seven different genes, discussed in Chap. 14, “Genetics, Molecular Biology and Emerging Concepts of Early Repolarization Syndrome.” Chapter 15, “Electrocardiographic J-wave and Cardiovascular Risk in the General Population,” presents the prevalence and significance of the ECG pattern of early repolarization in the general population, while Chap. 16, “Benign Versus Malignant Early Repolarization Patterns,” differentiates benign from arrhythmogenic J waves, emphasizing the J-wave proper, the ST-segment, and the ensuing T-waves.

Brugada syndrome appears to be part of the J-wave group and is discussed in Chap. 17, “Genetic Architecture, Pathophysiology, and Clinical Management of Brugada Syndrome,” in which the authors stress the understanding of the pathophysiological mechanism(s), the ongoing efforts to reappraise the genetic architecture, and the advances in risk stratification and therapeutic approaches.

Chapter 20, the final chapter, “Action Potential Dynamics in Human Atrial Fibrillation,” explores the action potential variability in the most common sustained arrhythmia that affects more than 30 million people worldwide, atrial fibrillation.

This textbook, ably edited by Nabil El-Sherif and written by him along with a multitude of electrophysiology experts, is a must for basic and clinical electrophysiologists interested in cardiac repolarization.

Douglas P. Zipes, MD
Distinguished Professor
Indiana University School of Medicine
Krannert Institute of Cardiology
Indianapolis, IN, USA

Preface

Cardiac repolarization is a vital aspect for understanding normal cardiac rhythm, and its abnormal modulation is the basis of many potentially lethal cardiac arrhythmias. The last book that dealt exclusively with cardiac repolarization was published in 2003. It is overdue to readdress the many significant changes in the field.

This book was designed to provide a comprehensive up-to-date coverage of clinical and research aspects of cardiac repolarization, with several sections that are the domain of practicing physicians. The 20 chapters are sub-grouped into 4 parts. Part I deals with the basic, molecular biology and clinical aspects of cardiac repolarization at large, including the influence of the autonomic system, remodeling in organic heart disease, racial and gender difference in cardiac repolarization and arrhythmic risk, ECG-derived evaluation of cardiac repolarization, and future role of stem cells studies of cardiac repolarization.

Part II provides a comprehensive coverage of pathophysiology, molecular biology, and clinical aspects of long QT syndromes. While basic and clinical aspects of congenital long QT syndrome and torsade de pointes are usually the domain of academic cardiologists and cardiac electrophysiologists, acquired and drug-induced long QT syndrome should be of interest to a majority of medical professionals who prescribe drugs and take care of patients.

Part III provides updated basic and clinical coverage of the subject of early repolarization (ER), also called J-wave syndromes, and expound currently controversial aspects such as benign versus malignant ER in the 12-lead ECG and in the general population at large. Finally, Part IV covers the pathophysiology and clinical aspects of special cardiac repolarization syndromes that include short repolarization syndrome, repolarization alternans, the important role of microvolt T-wave alternans in arrhythmia risk stratification, and the recently recognized role of atrial repolarization and arrhythmogenesis.

The wide-ranging features of the book should be of interest not only to academic and clinical cardiologists and cardiac electrophysiologists but also to a much larger group of practicing internists and other medical professionals who would like to keep abreast of the important developments in this field.

Brooklyn, NY, USA

Nabil El-Sherif

Contents

Part I Pathophysiology, Molecular Biology, and Clinical Aspects of Cardiac Repolarization

- 1 Physiology and Molecular Biology of Ion Channels Underlying Ventricular Repolarization of the Mammalian Heart. 3**
Thomas W. Comollo, Chuangeng Zhang, Xinle Zou, and Robert S. Kass
- 2 Neuromodulation of Cardiac Repolarization and Arrhythmogenesis. 49**
Fabrice Extramiana and Pierre Maison-Blanche
- 3 Repolarization Remodeling in Structural Heart Disease 77**
Andreas S. Barth and Gordon F. Tomaselli
- 4 Cardiac Repolarization and Stem Cells: An Emerging Path Toward Precision Medicine. 87**
Massimiliano Gneccchi, Luca Sala, and Peter J. Schwartz
- 5 Role of Late Sodium Current During Repolarization and Its Pathophysiology 109**
Mohamed Chahine
- 6 Age, Sex and Racial Differences in Cardiac Repolarization and Arrhythmogenesis 119**
Arja Suzanne Vink, Sally-Ann B. Clur, Pieter G. Postema, Nico A. Blom, and Arthur A. M. Wilde
- 7 ECG-Derived Evaluation of Cardiac Repolarization 131**
Gioia Turitto and Nabil El-Sherif

Part II Pathophysiology, Molecular Biology, and Clinical Aspects of Long QT Syndromes

- 8 Genotype-Phenotype Correlation in Congenital LQTS: Implications for Diagnosis and Risk Stratification 141**
Ilan Goldenberg
- 9 Clinical Management of LQTS Patients. 165**
Wojciech Zareba

10 Drug-Induced Long QT Syndrome and Torsades de Pointes	185
Raymond L. Woosley and Peter J. Schwartz	
11 Acquired Long QT Syndrome and Electrophysiology of Torsade de Pointes	201
Nabil El-Sherif, Gioia Turitto, and Mohamed Boutjdir	
12 Pathogenesis of Autoimmune-Associated Long QT Syndrome	217
Mohamed Boutjdir, Pietro Enea Lazznerini, Pier Leopoldo Capecchi, Franco Laghi-Pasini, and Nabil El-Sherif	
13 The Role of Inflammation and Autoimmunity in Long QT Syndrome	227
Pietro Enea Lazznerini, Franco Laghi-Pasini, Nabil El-Sherif, Mohamed Boutjdir, and Pier Leopoldo Capecchi	
Part III Pathophysiology, Molecular Biology, and Clinical Aspects of Early Repolarization Syndromes	
14 Genetics, Molecular Biology, and Emerging Concepts of Early Repolarization Syndrome	255
Charles Antzelevitch and Gregory Dendramis	
15 Electrocardiographic J Wave and Cardiovascular Risk in the General Population	269
Heikki V. Huikuri	
16 Benign Versus Malignant Early Repolarization Patterns	277
Raphael Rosso and Sami Viskin	
17 Genetic Architecture, Pathophysiology, and Clinical Management of Brugada Syndrome	285
John R. Giudicessi and Michael J. Ackerman	
Part IV Pathophysiology and Clinical Aspects of Special Cardiac Repolarization Syndromes	
18 The Short QT Syndrome	303
Chiara Scrocco, Fiorenzo Gaita, and Carla Giustetto	
19 Microvolt T-Wave Alternans: Pathophysiology and Clinical Aspects	313
Richard L. Verrier	
20 Action Potential Dynamics in Human Atrial Fibrillation	333
Junaid Ahmed Bakhtiyar Zaman, Sanjiv M. Narayan, and Michael R. Franz	
Index	347

Contributors

Michael J. Ackerman, MD, PhD Departments of Cardiovascular Medicine, Pediatric and Adolescent Medicine, and Molecular Pharmacology and Experimental Therapeutics, Mayo Clinic Genetic Heart Rhythm Clinic and the Windland Smith Rice Sudden Death Genomics Laboratory, Rochester, MN, USA

Charles Antzelevitch, PhD, FACC, FHRS, FAHA Department of Cardiovascular Research, Lankenau Institute for Medical Research, Wynnewood, PA, USA

Lankenau Heart Institute, Wynnewood, PA, USA

Sidney Kimmel Medical School, Thomas Jefferson University, Philadelphia, PA, USA

Andreas S. Barth, MD, PhD, FAHA Department of Cardiac Electrophysiology, Johns Hopkins University, Baltimore, MD, USA

Nico A. Blom, MD, PhD Department of Pediatric Cardiology, Emma Children's Hospital, Amsterdam UMC, University of Amsterdam, Amsterdam, The Netherlands

Department of Paediatric Cardiology, Willem-Alexander Children's Hospital, Leiden University Medical Centre, Leiden, The Netherlands

Mohamed Boutjdir, PhD Department of Medicine and Physiology, SUNY Downstate Medical Center, Brooklyn, NY, USA

State University of New York Downstate Medical Center, New York, NY, USA

NYU School of Medicine, New York, NY, USA

Pier Leopoldo Capecchi, MD, PhD Department of Medical Sciences, Surgery and Neurosciences, University of Siena, Siena, Italy

Mohamed Chahine, PhD CERVO Research Center, Institut Universitaire en Santé Mentale de Québec, Quebec City, QC, Canada

Department of Medicine, Université Laval, Quebec City, QC, Canada

Sally-Ann B. Clur, MBBCh, MSc, FCP(SA)Paed, PhD Department of Pediatric Cardiology, Emma Children's Hospital, Amsterdam UMC, University of Amsterdam, Amsterdam, The Netherlands

Thomas W. Comollo, PhD Department of Pharmacology, Columbia University Irving Medical Center, Vagelos College of Physicians and Surgeons, New York, NY, USA

Gregory Dendramis, MD Cardiovascular Division, Pietro Cosma Hospital, Padova, Italy

Nabil El-Sherif, MD Department of Medicine and Physiology, State University of New York Downstate Medical Center, VA New York Harbor Healthcare Center, Brooklyn, NY, USA

Fabrice Extramiana, MD, PhD Arrhythmia unit, Department of Cardiology, Bichat Hospital, APHP, Paris University, Paris, France

Michael R. Franz, MD, PhD Division of Cardiology, Veterans Affairs Medical Center, Washington, DC, USA

Fiorenzo Gaita, MD Department of Medical Sciences, University of Turin, and Clinica Pinna Pintor, Turin, Italy

John R. Giudicessi, MD, PhD Department of Cardiovascular Medicine, Mayo Clinic, Rochester, MN, USA

Carla Giustetto, MD Division of Cardiology, Department of Medical Sciences, University of Turin, “Città della Salute e della Scienza” Hospital, Turin, Italy

Massimiliano Gnechi, MD, PhD Coronary Care Unit, and Laboratory of Experimental Cardiology for Cell and Molecular Therapy, IRCCS Policlinico San Matteo Foundation, Pavia, Italy

Department of Molecular Medicine – Unit of Cardiology, University of Pavia, Pavia, Italy

Department of Medicine, University of Cape Town, Cape Town, South Africa

Ilan Goldenberg, MD Cardiology Division, Clinical Cardiovascular Research Center, University of Rochester Medical Center, Rochester, NY, USA

Heikki V. Huikuri, MD Research Unit of Internal Medicine, University Hospital of Oulu, Oulu, Finland

Robert S. Kass, PhD Department of Pharmacology, Columbia University Irving Medical Center, Vagelos College of Physicians and Surgeons, New York, NY, USA

Franco Laghi-Pasini, MD, PhD Department of Medical Sciences, Surgery and Neurosciences, University of Siena, Siena, Italy

Pietro Enea Lazzerini, MD Department of Medical Sciences, Surgery and Neurosciences, University of Siena, Siena, Italy

Pierre Maison-Blanche, MD Arrhythmia unit, Department of Cardiology, Bichat Hospital, APHP, Paris University, Paris, France

Sanjiv M. Narayan, MD, PhD Department of Medicine, Stanford University, Stanford, CA, USA

Pieter G. Postema, MD, PhD Department of Clinical and Experimental Cardiology, Amsterdam UMC, University of Amsterdam, Heart Center, Amsterdam, The Netherlands

Raphael Rosso, MD Department of Cardiology, Tel-Aviv Medical-Center and Sackler School of Medicine, Tel Aviv University, Tel Aviv-Yafo, Israel

Luca Sala, PhD Center for Cardiac Arrhythmias of Genetic Origin – Laboratory of Cardiovascular Genetics, Istituto Auxologico Italiano IRCCS, Milan, Italy

Peter J. Schwartz, MD Center for Cardiac Arrhythmias of Genetic Origin – Laboratory of Cardiovascular Genetics, Istituto Auxologico Italiano IRCCS, Milan, Italy

Chiara Scrocco, MD Clinical Cardiology Academic Group, Molecular and Clinical Sciences Research Centre, St George’s University of London, London, UK

Gordon F. Tomaselli, MD The Albert Einstein College of Medicine, Department of Medicine, Bronx, NY, USA

Gioia Turitto, MD Cardiac Electrophysiology Services, Department of Medicine, New York-Presbyterian Brooklyn Methodist Hospital, Brooklyn, NY, USA

Richard L. Verrier, PhD Department of Medicine, Harvard Medical School, Beth Israel Deaconess Medical Center, Boston, MA, USA

Arja Suzanne Vink, MSc, MD Department of Clinical and Experimental Cardiology, Amsterdam UMC, University of Amsterdam, Heart Center, Amsterdam, The Netherlands

Department of Pediatric Cardiology, Emma Children’s Hospital, Amsterdam UMC, University of Amsterdam, Amsterdam, The Netherlands

Sami Viskin, MD Department of Cardiology, Tel-Aviv Medical-Center and Sackler School of Medicine, Tel Aviv University, Tel Aviv-Yafo, Israel

Arthur A. M. Wilde, MD, PhD Department of Clinical and Experimental Cardiology, Amsterdam UMC, University of Amsterdam, Heart Center, Amsterdam, The Netherlands

Raymond L. Woosley, MD, PhD Department of Medicine, Division of Clinical Data Analytics and Decision Support, University of Arizona, College of Medicine-Phoenix, Phoenix, AZ, USA

Junaid Ahmed Bakhtiyar Zaman, MA, BMBCH, MRCP Royal Brompton Heart and Vascular Institute, London, UK

Department of Medicine, Stanford University, Stanford, CA, USA

Wojciech Zareba, MD, PhD Cardiology Division, Clinical Cardiovascular Research Center, University of Rochester Medical Center, Rochester, NY, USA

Chuangeng Zhang, PhD Department of Pharmacology, Columbia University Irving Medical Center, Vagelos College of Physicians and Surgeons, New York, NY, USA

Xinle Zou, PhD Department of Pharmacology, Columbia University Irving Medical Center, Vagelos College of Physicians and Surgeons, New York, NY, USA

Part I

**Pathophysiology, Molecular Biology, and
Clinical Aspects of Cardiac Repolarization**



Physiology and Molecular Biology of Ion Channels Underlying Ventricular Repolarization of the Mammalian Heart

1

Thomas W. Comollo, Chuangeng Zhang, Xinle Zou, and Robert S. Kass

Introduction

The proper mechanical pumping of the mammalian heart depends upon a precise, cyclic cascade of electrical events, with each player from the anatomical region, down to the ion channels responsible for each ionic current playing its exact role in this symphonic-like mechanism. Cells in the sinoatrial node, the “pacemaker” region of the heart, are first activated and propagate the electrical activity through the remainder of the heart. This signal spreads due to the coupling of cardiac cells at gap junctions [1–5], inciting “action potentials” in each of the cells (cardiomyocytes), as the cell is electrically excited. The surface electrocardiogram (ECG) reflects the differences in voltage across different regions of the heart as this electrical cascade spreads through the organ.

The “action potentials” generated in each cell as the electrical signals spread throughout the heart are the result of activation and subsequent inactivation of both depolarizing, inward sodium (Na^+) and calcium (Ca^{2+}) currents that are then countered by repolarizing, outward K^+ currents [4, 6]. During this action potential cascade of events, the influx of Ca^{2+} triggers release of more Ca^{2+} from the myocyte version of the endoplasmic

reticulum, the sarcoplasmic reticulum (SR), through Ca^{2+} -sensitive ryanodine receptor channels [7]. This triggers the excitation-contraction (EC) coupling relationship that triggers calcium-dependent muscle contraction [7, 8]. Calcium ions bind a protein called troponin, exposing a myosin-binding site on the actin filaments, and myosin moves the actin by an adenosine triphosphate (ATP)-dependent mechanism [9]. Thus, the electrical signaling of the heart translates into mechanical pumping via rhythmic contraction of the myocardium.

Ventricular action potential waveforms reflect the coordinated activity of multiple ion channels that open, close, and inactivate on different time scales (Fig. 1.1). The rapid upstroke of the action potential (phase 0) is caused by a large inward current through voltage-gated Na^+ channels. It is followed by a transient repolarization (phase 1), reflecting Na^+ channel inactivation and the activation of voltage-gated outward potassium (K^+) currents (Fig. 1.1). This transient repolarization or “notch” influences the height and duration of the plateau phase (phase 2) of the action potential, which depends on the delicate balance of inward (Ca^{2+} and Na^+) currents and outward (K^+) currents. Although Ca^{2+} influx through high-threshold, L-type voltage-gated Ca^{2+} channels is the main contributor of inward current during the plateau phase, this current declines during phase 2 as the (L-type Ca^{2+}) channels undergo Ca^{2+} and voltage-dependent inactivation. The driving force for K^+ efflux through the voltage-gated

T. W. Comollo · C. Zhang · X. Zou · R. S. Kass (✉)
Department of Pharmacology, Columbia University
Irving Medical Center, Vagelos College of Physicians
and Surgeons, New York, NY, USA
e-mail: rsk20@cumc.columbia.edu

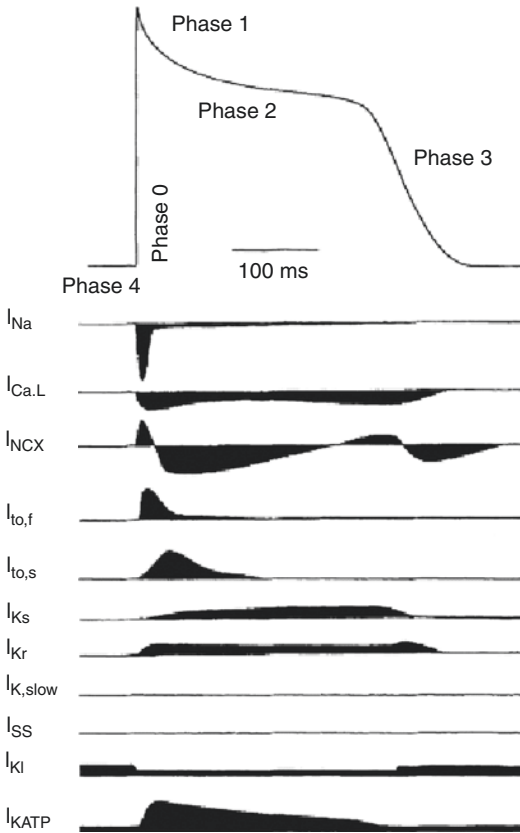


Fig. 1.1 Schematic of the action potential and underlying ionic currents in adult human ventricular myocytes. The contributions of some K^+ currents, such as $I_{K,slow}$ and I_{SS} which are expressed in other species, have not been defined in human ventricular cells

(and other) K^+ channels, however, is high during the plateau, and, as the Ca^{2+} channels inactivate, the outward K^+ currents predominate resulting in a second, rapid phase (phase 3) of repolarization back to the resting potential (Fig. 1.1). The height and the duration of the action potential plateau, as well as the time- and voltage-dependent properties of the underlying voltage-gated Na^+ , Ca^{2+} , and K^+ currents, therefore, also influence action potential durations. As a result, modifications in the properties or the densities of any of these channels could have dramatic effects on ventricular action potential waveforms, refractory periods, and cardiac rhythms.

Electrophysiological studies have detailed the properties of the major voltage-gated inward Na^+ and Ca^{2+} and outward K^+ currents (Table 1.1).

These currents determine the heights and the durations of ventricular action potentials. In contrast to the Na^+ and Ca^{2+} currents, there are multiple types of K^+ currents in ventricular myocytes. Of the various K^+ currents, the voltage-gated K^+ currents are the most numerous and diverse. At least two types of transient outward currents, $I_{to,f}$ and $I_{to,s}$, and several components of delayed rectification, including I_{Kr} ($IK_{(rapid)}$) and I_{Ks} ($IK_{(slow)}$), have been distinguished in ventricular myocytes in a variety of different species (Table 1.1). In addition, there are marked regional differences in the expression patterns of these (voltage-gated) K^+ currents. These differences contribute to the observed variability in ventricular action potential waveforms [10–12]. The time- and voltage-dependent properties of the various repolarizing currents in myocytes isolated from different species and/or from different regions of the ventricles in the same species are similar, suggesting that the molecular correlates of the underlying channels are also the same [13]. A rather large number of pore-forming (α) and accessory (β , δ , and γ) subunits that coassemble as Na^+ , Ca^{2+} , and K^+ channels have been identified in mammalian ventricles, and considerable progress has been made in defining the relationships between these subunits and functional ventricular Na^+ , Ca^{2+} , and K^+ channels. Importantly, these studies have revealed that distinct molecular entities underlie the various ion channels contributing to ventricular action potential repolarization.

Importantly, voltage-gated channels change between at least three different conformations. These are open, closed, and inactivated [14–16]. In the closed state, the channel pore is closed. Upon activation, due to rising intracellular voltage, the pore opens due to movement of the voltage sensor and the channel enters the “open” conformation. After time that varies from channel to channel, the voltage-gated ion channel will enter the “inactivated” conformation, a nonconducting state. Eventually, the channel will recover from the inactivated state and become capable of conducting ionic current again [14–16].

The densities and the properties of voltage-gated Na^+ , Ca^{2+} , and K^+ currents change during normal ventricular development, reshaping

Table 1.1 Ionic currents contributing to cardiac action potential repolarization

Current	Activation	Inactivation	Recovery	Blocker	Species
I_{Na}	Fast	Fast	Fast	TTX	Cat,dog, ferret, human, mouse, rat
$I_{Ca(L)}$	Fast	Ca ²⁺ -dep	Fast	DHP, Cd ²⁺	Cat, dog, ferret, human, mouse, rat
$I_{to,f}$	Fast	Fast	Fast	mM 4-AP, flecainide, HaTX, HpTX	Cat, dog, ferret, human, mouse, rat
$I_{to,s}$	Fast	Slow	Slow	mM 4-AP	Ferret, human, mouse, rat, rabbit
I_{Kr}	Moderate	Fast	Slow	E-4031, dofetilide, lanthanum	Cat, dog, guinea pig, human, mouse, rabbit, rat
I_{Kur}	Fast	Slow	Slow	μ M 4-AP	Human
I_{Ks}	Very slow	No		NE-10064, NE-10133	Dog, guinea pig, human, rabbit
I_{Kp}	Fast	No		Ba ²⁺	Guinea pig
I_K	Slow	Slow	Slow	mM TEA	Rat
$I_{K,slow1}$	Fast	Slow	Slow	mM 4-AP	Mouse
$I_{K,slow2}$	Fast	Very slow	Slow	mM TEA	Mouse
I_{ss}	Slow	No		mM TEA, A1899	Dog, human, mouse, rat
I_{KI}				Ba ²⁺	Cat, dog, ferret, human, mouse, rabbit, rat
$I_{K(ATP)}$	ATP depletion			SUR	Cat, dog, mouse, ferret, human, rabbit, rat
$I_{K(Ach)}$	Acetylcholine			Tertiapin-Q	Mouse, human,
I_{KCa}	Internal Ca ²⁺			Maurotoxin Apamin	Mouse, rat, guinea pig, rabbit dog, human

TTX tetrodotoxin, DHP dihydropyridine, 4-AP 4aminopyridine, HaTX hanatoxin, HpTX heteropoptoxin, SUR sulfonylurea, TEA tetraethylammonium

ventricular action potential waveforms [17] and modifying the sensitivity to antiarrhythmics. In addition, alterations in the densities and properties of voltage-gated Na⁺, Ca²⁺, and K⁺ currents occur in a number of myocardial disease states [18–26] changes that can lead to the generation of life-threatening ventricular arrhythmias. As a result, there is considerable interest in defining the molecular mechanisms controlling the regulation, modulation, and functional expression of the channels underlying action potential repolarization in the ventricles.

Inward Na⁺ and Ca²⁺ Currents in Mammalian Ventricles

Voltage-Gated Ventricular Na⁺ Currents

Voltage-gated Na⁺ channels open rapidly on membrane depolarization and underlie the rapid rising phases of the action potentials in mammalian ventricular myocytes (Fig. 1.1). The threshold for activation of these channels is quite

negative (~ -55 mV), and activation is steeply voltage dependent. The inward movement of Na⁺ through open voltage-gated Na⁺ channels underlies impulse conduction in ventricular muscle, as well as in the specialized conducting network of Purkinje fibers in the ventricle [27]. Voltage-gated Na⁺ channels also inactivate rapidly, and during the plateau phase of the ventricular action potential, most of the Na⁺ channels are in an inactivated and nonconducting state [27]. There is, however, a finite probability of channel reopening at voltages corresponding to the action potential plateau (Fig. 1.1), and present estimates are that approximately 99% of the channels are inactivated and 1% of the channels are open during the plateau phase [28–30].

The probability of Na⁺ channel reopening at depolarized voltages (i.e., during phase 2) is determined by the overlap of the curves describing the voltage dependences of channel activation (a measure of the probability of the channel transitioning from a closed, but available, to an open state) and steady-state inactivation (a measure of the availability of channels in the closed state). This overlap has been termed the “window”

current because it is conducted over a “window” of voltages where the two curves overlap [31]. Although the Na⁺ channel “window” current has been recognized as an important determinant of action potential duration in the heart for many years [31, 32], studies focused on exploring the mechanisms underlying inherited cardiac arrhythmias have shown that voltage-gated Na⁺ channels play an important role in ventricular action potential repolarization. In addition, there are regional differences in the expression of the persistent component of the voltage-gated Na⁺ current in the ventricles [33]. Together with the marked differences in voltage-gated outward K⁺ current densities and properties, differences in Na⁺ current densities may contribute to observed regional heterogeneities in ventricular action potential amplitudes and durations [12].

While some studies have suggested there are additional varieties of voltage-gated Na⁺ channels in the myocardium, the predominant cardiac sodium channel is Na_v1.5 [16, 34–36]. Na_v1.5 channel α subunits are encoded by the SCN5A gene [16, 27, 34, 37, 38]. Four different types of sodium channel β subunits modulate these Na_v1.5 channels [16, 34, 39]. There are four total sodium channel β subunit genes, SCN1B–SNC4B, each coding for a β subunit, all of which are expressed in cardiac tissue [16, 34, 39]. Subunit composition often modulates the exact properties of cardiac Na⁺ current [16, 34, 39]. Ionic sodium current is also shaped by exact structures of subunits as often dictated by genetically encoded mutation and factors affecting channel trafficking and regulation, both genetic and environmental [5, 34, 40–42]. Additionally, electrical and chemical factors of the environment also affect channel function and thus voltage-gated sodium channel conductance [5, 40–42].

Voltage-Gated Ventricular Ca²⁺ Currents

A number of different subtypes of voltage-gated calcium (Ca²⁺) currents/channels have been distinguished in neurons and in muscle cells based on differences in time- and voltage-dependent

properties and pharmacological profiles, and two (somewhat similar) classification schemes have evolved to describe the voltage-gated Ca²⁺ currents/channels in a variety of different cell types, including mammalian ventricular myocytes. In the first system, voltage-gated Ca²⁺ channels are referred to as low-voltage-activated (LVA) and high-voltage-activated (HVA) Ca²⁺ channels based primarily on differences in the (voltage) threshold of channel activation [43–48]. Similar to voltage-gated Na⁺ channels, for example, the LVA Ca²⁺ activate at relatively hyperpolarized membrane potentials, i.e., ~ -50 mV. In addition, LVA Ca²⁺ channels activate and inactivate rapidly. HVA Ca²⁺ channels, in contrast, open on depolarization to membrane potentials more positive than -20 mV and inactivate over a time course of several hundred milliseconds to seconds [47]. Only HVA Ca²⁺ currents are evident in adult mammalian ventricular myocytes [47, 49] (Fig. 1.1).

There is considerable variability in the detailed kinetic and pharmacological properties of the HVA Ca²⁺ channels expressed in different cell types, and it is now clear that HVA Ca²⁺ are considerably more heterogeneous than LVA Ca²⁺ channels. In the alternate Ca²⁺ channel nomenclature, the various HVA channels are referred to by a single letter designation, i.e., L, N, P, Q, or R. In this scheme, LVA channels are referred to as T (transient)-type Ca²⁺ channels. Although all HVA Ca²⁺ channels exhibit relatively large single-channel conductances (13–25 pS) and have similar permeation properties, the electrophysiological and pharmacological properties of L- (long-lasting), N- (neither L- nor T-), P- (Purkinje), and Q- and R- (remaining) type channels are distinct [43–48, 50].

In mammalian ventricular myocytes, the HVA current is through L-type voltage-gated Ca²⁺ channels, and the densities of the L-type Ca²⁺ channel currents do not vary appreciably in different species and/or in myocytes isolated from different region of the ventricles of the same species [47]. These channels require strong depolarization for activation, generate relative long-lasting calcium currents, (ICa(L)), when Ba²⁺ is the charge carrier, and are selectively

blocked by dihydropyridine Ca^{2+} channel antagonists, such as nifedipine and nitrendipine [47] (Table 1.1). The opening of L-type voltage-gated Ca^{2+} channels in response to membrane depolarization in ventricular myocytes is delayed relative to the voltage-gated Na^+ channels (Fig. 1.1). As a result, the L-type Ca^{2+} channels contribute little to the rapid rising phase (phase 0) of ventricular action potentials [10–12, 51] (Fig. 1.1). Ca^{2+} influx through the L-type Ca^{2+} channels triggers Ca^{2+} release from intracellular Ca^{2+} stores and contributes importantly, therefore, to excitation-contraction coupling. In addition, the inward Ca^{2+} current through these channels counters outward K^+ efflux and contributes importantly, therefore, to the prominent plateau phase of the action potential in ventricular myocytes (Fig. 1.1). Nevertheless, at positive potentials, L-type Ca^{2+} channels do inactivate, and the inactivation of these channels is voltage and Ca^{2+} dependent. Under normal physiological conditions with Ca^{2+} as the charge carrier, inactivation of ventricular L-type voltage-gated Ca^{2+} currents is rapid owing to Ca^{2+} -dependent channel inactivation. In addition to contributing to the termination of the action potential plateau and action potential repolarization, the spontaneous ceasing of conductance (inactivation) of ventricular L-type Ca^{2+} channels functions as a negative feedback system that is critical in governing intracellular Ca^{2+} concentration [10–12, 51].

Diversity of Voltage-Gated, Outward K^+ Currents in Mammalian Ventricles

Voltage-gated K^+ channel currents influence the amplitudes and durations of ventricular action potentials, and in most cells, two broad classes of voltage-gated K^+ currents have been distinguished: transient outward K^+ currents, I_{to} , and delayed, outwardly rectifying K^+ currents, I_{K} (Table 1.1). The transient currents (I_{to}) activate and inactivate rapidly and underlie the early phase (phase 1) of repolarization, whereas the delayed rectifiers (I_{K}) determine the latter phase (phase 3) of action potential repolarization in the ventricu-

lar myocardium (Fig. 1.1). These are broad classifications, however, and there are actually multiple types of I_{to} and of I_{K} (Table 1.1) expressed in ventricular cells. In addition, there are species and regional differences in the densities, as well as the detailed biophysical properties, of these currents, and these are evident in the waveforms of ventricular action potentials recorded in different cell types/species [10–12, 51].

Transient Outward K^+ Current Channels, I_{to}

Activating and inactivating quickly upon membrane depolarization, I_{to} does a part of the action potential shaping controlled by the differing densities and type of I_{to} present [4, 52]. Among these characteristics influenced by I_{to} are action potential height and duration [4]. Multiple types of I_{to} further diversify I_{to} influence on the various cardiac cell type action potentials [4, 52].

Although two transient outward current components, referred to as I_{to1} and I_{to2} , were originally distinguished in cardiac Purkinje fibers and assumed to reflect distinct K^+ conductance pathways [53–55], the Ca^{2+} -dependent I_{to2} appears to be a Cl^- (not a K^+) current [53–56]. The Ca^{2+} -independent, 4-aminopyridine (4-AP)-sensitive I_{to1} in cardiac Purkinje fibers, in contrast, is K^+ -selective [54, 55]. Numerous studies have described the properties of Ca^{2+} -independent, 4-AP-sensitive transient outward K^+ currents in ventricular cells (Table 1.1), although the currents have been variably referred to as I_{to} , I_{to1} , or I_{t} [13, 57, 58]. Electrophysiological and pharmacological studies, however, have now clearly demonstrated that there are two distinct transient outward K^+ currents, $I_{\text{to,fast}}$ ($I_{\text{to,f}}$) and $I_{\text{to,slow}}$ ($I_{\text{to,s}}$), in ventricular cells and that these currents are differentially distributed [11, 12, 59–62].

The rapidly activating and inactivating transient outward K^+ currents that are also characterized by rapid recovery from steady-state inactivation are referred to as $I_{\text{to,fast}}$ ($I_{\text{to,f}}$). The rapidly activating and inactivating transient outward K^+ currents that recover slowly from inactivation are referred to as $I_{\text{to,slow}}$ ($I_{\text{to,s}}$) (Table 1.1) following

the nomenclature suggested by Xu and colleagues [60]. Although prominent in ventricular myocytes from most species including cat [63], dog [64, 65], ferret [57], human [66–68], mouse [60, 69–71], and rat [66, 72] (Table 1.1), $I_{to,f}$ is recorded in guinea pig ventricular myocytes only when extracellular Ca^{2+} is removed [73]. The time- and voltage-dependent properties of ventricular $I_{to,f}$ in different species (Table 1.1) are similar in that activation, inactivation, and recovery from steady-state inactivation are all rapid [57, 60, 64–68, 72, 74]. In addition, $I_{to,f}$ is readily distinguished from other voltage-gated outward K^+ currents including $I_{to,s}$ using the spider K^+ channel toxins *Heteropoda* toxin-2 or toxin-3 [59–61, 75]. The fact that the properties of ventricular $I_{to,f}$ in different species are similar (Table 1.1) led to the hypothesis that the molecular correlates of functional ventricular $I_{to,f}$ channels in different species are the same [13], and considerable experimental evidence in support of this hypothesis has now been provided. Indeed, all available evidence suggests that members of the K_V4 subfamily of α subunits encode functional ventricular $I_{to,f}$ channels [10, 11]. Nevertheless, there are differences in the biophysical properties of ventricular $I_{to,f}$ channels, suggesting that there are subtle, albeit important, differences in the molecular correlates of these channels in different species.

The transient outward K^+ currents in rabbit ventricular myocytes (originally referred to as I_t) inactivate slowly and recover from steady-state inactivation very slowly, with complete recovery requiring seconds [76–78]. The properties of rabbit ventricular I_t are similar to the slow transient K^+ current, referred to as $I_{to,slow}$ or $I_{to,s}$, that was distinguished (from $I_{to,f}$) in mouse ventricular myocytes by the slow rates of inactivation and recovery from inactivation [60]. In adult mouse ventricle, $I_{to,f}$ and $I_{to,s}$ are differentially distributed [60–62]. In all cells isolated from the wall of the right (RV) and left (LV) ventricles, for example, $I_{to,f}$ is expressed and $I_{to,s}$ is undetectable [60–62]. There are, however, differences in $I_{to,f}$ densities in RV and LV cells [60–62]. In the ventricular septum, the currents are more heterogeneous: 80% of the cells express $I_{to,f}$ and $I_{to,s}$ and the remaining

(20%) express $I_{to,s}$ alone. In addition, when present, $I_{to,f}$ density is significantly ($p < .001$) lower in septum, than in RV or LV cells [60, 61].

The rates of inactivation and recovery from inactivation of the transient outward K^+ currents are significantly slower in ferret LV endocardial than epicardial cells [59]. Interestingly, the time- and voltage-dependent properties and the pharmacological sensitivities of the transient outward K^+ current in these cells are similar to mouse ventricular $I_{to,s}$ and $I_{to,f}$, respectively. The properties of I_{to} (I_t) in rabbit ventricular myocytes, in contrast, appear to be analogous to mouse ventricular $I_{to,s}$ (Table 1.1).

The greatly varying properties of $I_{to,s}$ and $I_{to,f}$ suggested that they are two different currents with different molecular determinants [13]. Evidence suggests that $I_{to,f}$ occurs as product of $K_V4.3/K_V4.2$ α subunits, with $K_V4.3$ being the prominent producer of $I_{to,f}$ in human ventricles and a mix of $K_V4.3/K_V4.2$ in rat, mouse, and ferret [52, 59, 79–85]. Alternately the cardiac $I_{to,s}$ is believed to be resultant of $K_V1.4$ α subunits [52]. This is because $K_V1.4$ in an expression systems yields currents that closely resemble $I_{to,s}$ [86–88].

Delayed Rectifier K^+ Currents/Channels, I_K

Delayed rectifier K^+ currents, I_K , have been characterized extensively in myocytes isolated from canine [65, 74, 89, 90], feline [91, 92], guinea pig [93–99], human [100, 101], mouse [60, 61, 71, 102, 103], rabbit [104, 105], and rat [72, 106, 107] hearts, and, in most cells, multiple components of I_K (Table 1.1) are co-expressed. In guinea pig ventricular myocytes, for example, two prominent components of I_K , $I_{K,r}$ ($I_{K,r,rapid}$) and $I_{K,s}$ ($I_{K,s,slow}$), were distinguished based on sensitivity to block by class III antiarrhythmic agents and differences in time- and voltage-dependent properties [72, 108, 109]. $I_{K,r}$ activates rapidly, inactivates very rapidly, displays marked inward rectification, and is selectively blocked by several class III antiarrhythmics, including dofetilide, E-4031, and sotalol [96]. No inward rectification

is evident for I_{Ks} , and this current is blocked by class III compounds, including NE-10064 and NE-10133, which do not affect I_{Kr} [110]. In human [100, 101, 111, 112], canine [74, 89], and rabbit [105, 113] ventricular cells, both I_{Kr} and I_{Ks} are expressed and are prominent repolarizing currents. In feline [91] and rat [107] ventricular myocytes, however, only I_{Kr} is detected. I_{Kr} and I_{Ks} are also readily distinguished at the microscopic level [93, 94, 104, 105], and molecular genetic studies suggest that the molecular correlates of these channels are distinct [10, 11].

The distinctively differing characteristics of I_{Kr} and I_{Ks} , both in voltage- and timing-related properties, elude to specialized roles for each in repolarization [4]. This is especially true of cells in Purkinje fibers and ventricles, though, perhaps even more indicative of specialized roles for I_{Kr} and I_{Ks} , in some cells only I_{Kr} or I_{Ks} is expressed [4]. Indeed, each is the result of a different α subunit. I_{Kr} normally makes the greatest contribution to repolarization and is a product of $K_V11.1$ known as the hERG channel [109, 114]. HERG stands for “human ether-a-go-go-related gene” [114]. I_{Ks} is resultant of the KCNQ1 α subunit in complex with the accessory subunit KCNE1 [4, 109]. KCNE1 confers the characteristic I_{Ks} traits to the KCNQ1 α subunit complex [4, 109].

A third type of delayed rectifier current exists, known as I_{Kur} , but is expressed primarily in the atrial myocardia and not in the ventricles [111, 115, 116]. I_{Kur} is a current conducted by the HK2 channel, also known as human $K_V1.5$ [116–118]. This channel is expressed on the protein and mRNA level in both the atria and ventricle, as well as several other organs [116, 119–121]; it is thought to only produce I_{Kur} current in the atria [116, 122].

In rodent ventricles, there are additional components of I_K with properties different from I_{Ks} and I_{Kr} (Table 1.1). In rat ventricular myocytes, for example, there are novel delayed rectifier K^+ currents, referred to as I_K and I_{ss} (Table 1.1) [72, 123]. In mouse ventricular myocytes, two voltage-gated K^+ currents, $I_{K,slow}$ and I_{ss} , have also been identified [60, 71, 102, 103, 124]. $I_{K,slow}$ is rapidly activating and slowly inactivating K^+ current with kinetic and pharmacological properties

distinct from $I_{to,f}$ and $I_{to,s}$ (and I_{ss}); in addition, $I_{K,slow}$ is blocked effectively and selectively by μM concentrations of 4-AP [102, 103, 124] which do not affect $I_{to,f}$ or $I_{to,s}$ in the same cells [60, 71]. The current, I_{ss} , remaining at the end of long (up to 10 s) depolarizing voltage steps, in contrast, is slowly activating and 4-AP insensitive [60, 71]. In contrast to the differential distribution of $I_{to,f}$ and $I_{to,s}$, however, $I_{K,slow}$ and I_{ss} appear to be expressed in all mouse ventricular myocytes [60, 61, 71].

Developmental Changes in Voltage-Gated K Channel Expression

During postnatal development, ventricular action potentials shorten, phase 1 repolarization (Fig. 1.1) becomes more pronounced, and functional $I_{to,f}$ density is increased [123, 125–134]. In neonatal canine ventricular myocytes, for example, the “notch” and the rapid (phase 1) repolarization that are typical in adult cells are not clearly evident [126]. Action potentials in neonatal cells are insensitive to 4-AP, and voltage-clamp recordings reveal that $I_{to,f}$ is undetectable [126]. In cells from 2-month-old animals, $I_{to,f}$ is present and phase 1 repolarization is clearly evident [126].

The density of $I_{to,f}$ is also low in neonatal mouse [127, 133] and rat [123, 125, 128, 130–132, 134] ventricular myocytes and then increases several fold [13, 17] during early postnatal development. In rat, the properties of the currents in 1–2-day ventricular myocytes [134] are also distinct from those of $I_{to,f}$ in postnatal day 5 to adult cells [123] in that inactivation and recovery from inactivation are slower in postnatal day 1–2 cells. Indeed, the properties of the transient outward currents in postnatal day 1–2 rat ventricular cells [134] more closely resemble $I_{to,s}$ than $I_{to,f}$. Neither $I_{to,s}$ nor $I_{to,f}$, however, is detectable in embryonic ventricular myocytes [135].

In rabbit ventricular myocytes, transient outward K^+ current density increases and the kinetic properties of the currents also change during postnatal development [129]. In contrast to rat, however, the rate of recovery of the currents (mean recovery time ~ 100 ms) is ten times faster

in neonatal than in adult (mean recovery time ~1300 ms) cells [129]. The slow recovery of the transient outward currents underlies the marked broadening of action potentials at high stimulation frequencies in adult (but not in neonatal) rabbit ventricular myocytes [129, 136]. In rabbit ventricular cells, therefore, it appears that the change in the transient outward K^+ currents is opposite to that seen in other species, i.e., $I_{to,f}$ is expressed in the neonate, whereas $I_{to,s}$ is prominent in the adult.

The expression patterns of delayed rectifier K^+ currents also change during postnatal development. Both I_{Kr} and I_{Ks} , for example, are readily detected in fetal/neonatal mouse ventricular myocytes [127, 137, 138], whereas these currents are difficult to detect in adult cells [60, 61, 71]. Although I_{Kr} appears to be the predominant repolarizing K^+ current in fetal mouse ventricular cells, I_{Kr} density decreases with age [60, 61, 137, 138]. The density of I_{Ks} increases during late embryonic development [137] and subsequently decreases during postnatal development [127, 133, 137]. Because I_{Kr} and I_{Ks} are prominent repolarizing K^+ currents in adult cardiac cells in several species, changes in the expression and/or the properties of these conductance pathways must be distinct from those observed in the mouse heart. In contrast to the marked changes in $I_{to,f}$, the density of I_K does not change significantly in rat ventricular cells after postnatal day 5 [123, 132].

Regional Differences in K^+ Current Expression

There are marked differences in $I_{to,f}$ densities in different regions of the ventricles in canine [64, 139], cat [92], ferret [59], human ([66]; but, *see* also [68]), mouse [60, 61], and rat [140]. In canine left ventricle, for example, $I_{to,f}$ density is 5–6-fold higher in epicardial and midmyocardial than in endocardial cells [139]. $I_{to,s}$ density is also variable in mouse and ferret left ventricles [59–61], being detected only in (ferret) endocardial [59] and (mouse) septum [60, 61] ventricular cells.

The densities of ventricular I_{Ks} and I_{Kr} are also variable. In dog, for example, I_{Ks} density is higher

in epicardial and endocardial cells than in M cells [89]. There are also regional differences I_{Kr} and I_{Ks} expression in guinea pig LV [141, 142]. In cells isolated from the LV free wall, for example, the density of I_{Kr} is higher in subepicardial, than in midmyocardial or subendocardial, myocytes [142]. At the base of the LV, in contrast, I_{Kr} and I_{Ks} densities are significantly lower in endocardial than in midmyocardial or epicardial cells. These differences in voltage-gated K^+ current densities contribute to the variations in action potential waveforms recorded in different regions (right vs left, apex vs base) and layers (epicardial, midmyocardial, and endocardial) of the ventricles [10–12, 57, 64, 89, 141, 142].

Other Ionic Currents Contributing to Repolarization in Mammalian Ventricles

In addition to the voltage-gated K^+ channels, there are other K^+ channels that play a role in action potential repolarization in mammalian ventricles. The inwardly rectifying K^+ channels (K_{ir}), which are readily distinguished biophysically from the voltage-gated, outwardly rectifying K^+ channels because these channels carry inward K^+ current better than outward K^+ current [143], contribute to myocardial action potential repolarization through I_{K1} [143–145]. This biophysical property of these channels, however, is of no functional importance because the membrane potential of cardiac myocytes never reaches values more negative than the reversal potential for K^+ (~ -90 mV). It is the outward K^+ currents through these channels that are important physiologically, and these currents also play a role in action potential repolarization. Three types of inwardly rectifying K^+ channel currents have been described in the mammalian ventricular myocytes: the cardiac inward rectifier current, I_{K1} , the ATP-dependent K^+ current, I_{KATP} , and $I_{K(ACh)}$ channels mediated by muscarinic acetylcholine receptor. Although the densities of these currents vary in different regions (atria, ventricles, and conducting tissue) of the heart, in the ventricles, these currents appear to be uniformly expressed.

I_{KCa1} is a small-conductance Ca^{2+} -activated K^+ current [146]. It is caused by SKCa channels, Ca^{2+} -activated K^+ channels that have a single-channel conductance of ~ 10 pS [147]. These channels are involved in repolarization, with SK channel blocker causing longer action potentials, most pronounced in the atria [148–150]. Some atrial fibrillation patients have been associated with a single nucleotide polymorphism in the SK channel coding KCNN3 gene [150–152].

$I_{K(ACh)}$ channels are gated through G protein-coupled mechanism, mediated by muscarinic acetylcholine receptor activation [153, 154]. $I_{K(ACh)}$ channels are activated by the binding of G protein $\beta\gamma$ -subunits in response to the acetylcholine released on vagal stimulation [155]. Although $I_{K(ACh)}$ channels are expressed in AVN, SAN, atrial, and Purkinje cells these channels are all activated by acetylcholine released on vagal stimulation. These channels are not thought to contribute appreciably to action potential repolarization under normal physiological conditions. Consistent with this hypothesis, targeted deletion of one of the Kir subunits (Table 1.6) encoding $I_{K(ACh)}$ channels Kir3.4 does not measurably affect resting heart rates [156]. However, atrial fibrillation is not evident in Kir3.4 null mice exposed to the acetylcholine receptor agonist carbachol, suggesting that activation of $I_{K(ACh)}$ channels is involved in the cholinergic induction of atrial fibrillation [157].

The weakly inwardly rectifying ATP-dependent K^+ channels, first identified in cardiac muscle, are inhibited by increased intracellular ATP and activated by nucleotide diphosphates [145]. These channels are thought, therefore, to provide a link between cellular metabolism and membrane potential [145, 158]. In ventricular myocardium, activation of I_{KATP} channels is thought to be important under conditions of metabolic stress, as occurs during ischemia or hypoxia and results in shortening action potential durations [158, 159]. The activation of I_{KATP} channels has also been suggested to contribute to the cardioprotection resulting from ischemic preconditioning [160, 161]. Unlike the voltage-gated K^+ channels expressed in the ventricular myocardium, I_{KATP} channels appear to

be distributed uniformly through the right and left ventricles and through the thickness of the ventricular wall. The I_{KATP} channels, however, are expressed at much higher density than other sarcolemmal K^+ channels [161]. Although these channels are inhibited under normal physiological conditions, the high density suggests that action potentials will be shortened markedly when only a small number of I_{KATP} channels are activated [162]. In mammalian ventricular myocytes, I_{K1} plays a role in establishing the resting membrane potential, the plateau potential, and contributes to phase 3 repolarization (Fig. 1.1). The fact that the conductance of these channels is high at negative membrane potentials underlies the contribution of I_{K1} to ventricular resting membrane potentials [163]. The voltage-dependent properties of I_{K1} channels, however, are such that the conductance is very low at potentials positive to approximately -40 mV [163]. Now I_{K1} channels have been found in human [164, 165], guinea pig [165, 166], and rabbit [76, 167, 168] atrial and ventricular myocytes and rabbit SAN cells [167]. The properties of I_{K1} channels are similar in that all are blocked by extracellular Ba^{2+} , intracellular Cs^+ and strongly inwardly rectifying [76, 93, 164, 165]. The strong inward rectification evident in cardiac I_{K1} channels is attributed to block by intracellular Mg^{2+} [169] and Ca^{2+} [170] and by polyamines [163, 171, 172]. Removal or depletion of intracellular polyamines, Mg^{2+} and/or Ca^{2+} , will eliminate the steep inward rectification of I_{K1} channels current and convert to a linear current-voltage relation [163, 169–172].

The fact that the strongly inwardly rectifying I_{K1} channels conduct at negative membrane potentials suggests that these channels will play a role in establishing the resting membrane potentials of Purkinje fibers, as well as of atrial and ventricular myocytes. Direct experimental support for this hypothesis was provided with the demonstration that ventricular membrane potentials are depolarized in the presence of Ba^{2+} [163], which blocks I_{K1} channels. In addition, action potentials are prolonged, and phase 3 repolarization is slowed in the presence of extracellular Ba^{2+} [143], suggesting that I_{K1} channels

also contribute to repolarization, particularly in the ventricular myocardium.

Similar to the K_v channels, I_{K1} densities and the detailed biophysical properties of the currents do vary in different myocardial cell types. In the human heart, for example, I_{K1} density is more than twofold higher in ventricular, than in atrial, cells [165]. In guinea pig, the properties of the atrial and ventricular I_{K1} currents are also distinct in that ventricular I_{K1} inactivates during maintained depolarizations, whereas atrial I_{K1} does not [93, 166]. In addition, changes in extracellular K^+ modulate the magnitude of ventricular I_{K1} but have little effect on atrial I_{K1} [93]. At the microscopic level, (guinea pig) atrial and ventricular I_{K1} channels are also distinct. Mean channel open times of ventricular I_{K1} channels, for example, are approximately five times longer than those of atrial I_{K1} channels, whereas the single atrial and ventricular I_{K1} channel conductance are indistinguishable [93].

Taken together, these observations suggested the interesting possibility that distinct molecular entities underlie ventricular and atrial I_{K1} channels, and experimental support for this hypothesis has now been provided [166].

Molecular Correlates of Voltage-Gated Na^+ and Ca^{2+} Currents in Mammalian Ventricle

Voltage-Gated Na^+ Channel (Na_v) Pore-Forming α Subunits

Voltage-gated Na^+ (Na_v) channel pore-forming (α) subunits (Fig. 1.2a) belong to the “S4” superfamily of genes encoding voltage-gated ion channels. Although a number of Na_v α subunits (Fig. 1.2a) have been identified to date (Table 1.2), only one of these, $Na_v1.5$ ($SCN5A$), appears to be widely expressed in mammalian ventricular

Fig. 1.2 Pore-forming (α) subunits of cardiac ion channels. Comparisons of primary sequences and the membrane topologies of the α subunits encoding voltage-gated Na^+ (Na_v) (a), voltage-gated Ca^{2+} (Ca_v) (b), voltage-gated K^+ (K_v) (c), and inwardly rectifying K^+ channels (Kir) (d) are illustrated

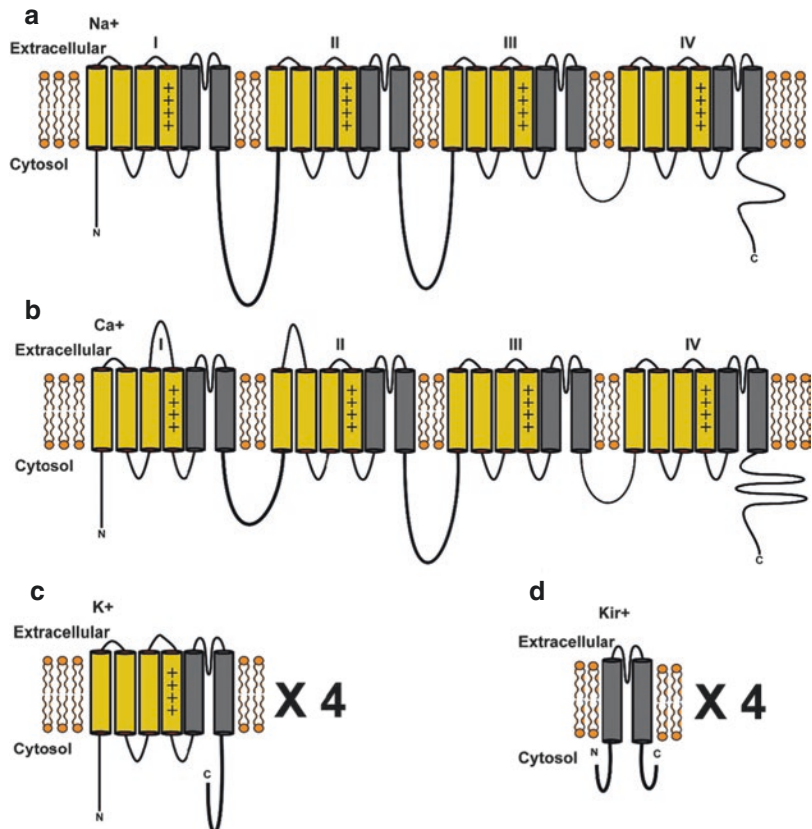


Table 1.2 Diversity of voltage-gated Na⁺ and Ca²⁺ α subunits

Subfamily	Protein	Gene	Locus			Cardiac current
			Homo	Mus	Rattus	
Na ⁺						
Na _v 1						
	Na_v1.1	<i>SCN1A</i>	2q24.3	2C1.3	3q21	
	Na _v 1.2	<i>SCN2A</i>	2q24.3	2C1.3	3q21	
	Na_v1.3	<i>SCN3A</i>	2q24.3	2C1.3	3q21	
	Na _v 1.4	<i>SCN4A</i>	17q23.3	11E1	10q32.1	
	Na_v1.5	<i>SCN5A</i>	3p22.2	9F3	8q32	<i>I_{Na}</i>
	Na _v 1.6	<i>SCN8A</i>	12q13.13	15F1	7q36	
	Na _v 1.7	<i>SCN9A</i>	2q24.3	2C1.3	3q21	
	Na _v 1.8	<i>SCN10A</i>	3p22.2	9F3	8q32	
	Na _v 1.9	<i>SCN11A</i>	3p22.2	9F3	8q32	
Na _x						
	Na_v2.1	<i>SCN7A</i>	2q24.3	2C1.3	3q21	
Ca ²⁺						
Ca _v 1						
	Ca _v 1.1	<i>CACNA1S</i>	1q32.1	1E4	13q13	
	Ca_v1.2	<i>CACNA1C</i>	12p13.33	6F1	4q42	<i>I_{Ca(L)}</i>
	Ca_v1.3	<i>CACNA1D</i>	3p21.1	14B	16p16	
	Ca _v 1.4	<i>CACNA1F</i>	Xp11.23	XA1.1	Xq12	
Ca _v 2						
	Ca_v2.1	<i>CACNA1A</i>	19p13.13	8C2	19q11	
	Ca _v 2.2	<i>CACNA1B</i>	9q34.3	2A3	3p13	
	Ca_v2.3	<i>CACNA1E</i>	1q25.3	1G3	13q21	<i>I_{Ca(R)}</i>
Ca _v 3						
	Ca_v3.1	<i>CACNA1G</i>	17q21.33	11D	10q26	
	Ca_v3.2	<i>CACNA1H</i>	16p13.3	17A3.3	10q12	
	Ca _v 3.3	<i>CACNA1I</i>	22q13.1	15E1	7q34	

Boxes denote cardiac expression

myocardium (Table 1.2) [36, 173–175]. Each Na_v α-subunit, which forms the ion-conducting pore and contains channel gating components, consists of four homologous domains (I to IV) (Fig. 1.2) [27, 176]. Each domain contains six α-helical transmembrane repeats (S1–S6), for which mutagenesis studies have revealed key functional roles [27, 36, 176]. The cytoplasmic linker between domains III and IV, for example, is an integral component underlying voltage-dependent inactivation [177], and a critical isoleucine, phenylalanine, and methionine (IFM) motif within this linker [27, 174, 178] has been

identified as the inactivation gate [179–181]. Na⁺ channel inactivation is due to rapid block of the inner mouth of the channel pore by the cytoplasmic linker between domains III and IV that occurs within milliseconds of membrane depolarization [182]. NMR analysis of this linker (gate) in solution has revealed a rigid helical structure that is positioned such that it can block the pore, providing a structural interpretation of the functional studies [183]. More recently, cryo-EM solved structures of Na_v1.4-β1 complex from a species of electric eel and from human has confirmed the predicted structural arrangement of

sodium channels and offered insight into the structure of $\text{Na}_v1.5$ [184, 185].

During the plateau phase of the ventricular action potential, more than 99% of the voltage-gated Na^+ channels are in an inactivated, nonconducting state in which the inactivation gate occludes the inner mouth of the conducting pore through specific interactions with sites on the S6 segment of domain IV [186] or the S4–S5 loop of domain IV [187]. Inherited mutations (i.e., ΔKPQ) in the linker between domains III and IV in *SCN5A* disrupt inactivation and cause one form of long QT syndrome, LQT3 [188]. The mutation-induced enhancement of sustained Na^+ current activity measured during prolonged depolarization is caused by altering modes of channel gating. In a gating mode in which sustained current is enhanced, single-channel recordings revealed that channels do not enter an absorbing inactivated state but instead reopen. Enhanced sustained current caused by bursting is sufficient to prolong cellular action potentials in theoretical models [189] and in genetically modified mice [190]. Subsequent analysis of additional *SNC5A* mutations, linked both to LQT-3 and another inherited arrhythmia, the Brugada syndrome, however, has revealed that this is not the only mechanism by which altered Na^+ channel function can prolong the cardiac action potential.

Several studies have revealed a critical role for the carboxy (C)-terminal tail of the Na_v channel α -subunit in the control of channel inactivation [28, 191–194]. Point mutations in the C-terminus, for example, can shift the voltage dependence of inactivation, promote sustained Na^+ channel activity, change the kinetics of both the onset of and recovery from inactivation, and alter drug-channel interactions [195–199]. In an investigation into the secondary structure of the Na^+ channel C-terminus and the roles of possible tail structures in the control of inactivation, single-channel data revealed that the C-terminus has pronounced effects on repetitive channel openings that occur in bursts during prolonged depolarization [200]. Homology modeling of the C-terminus, assuming similarity to the N-terminal domain of calmodulin, predicted that the C-terminus would adopt a predominantly

α -helical structure, a prediction verified by circular dichroism (CD) of a purified C-terminus fusion protein. Only the proximal region of the C-terminus, which contains all of the helical structure, markedly modulates channel inactivation, but not activation. The distal C-terminal tail, which is largely unstructured, does not affect channel gating but affects the density of functional Na^+ channels in the surface membrane. Taken together, these experiments suggest that interactions occur between the structured region of the C-terminus and other components of the channel protein and that these interactions function to stabilize the channel in a pore-blocked inactivated state during membrane depolarization.

The structural data also provide a framework to interpret the mechanistic basis of a large number of mutations linked either to LQT-3 or Brugada syndrome that occurs within the structured and charged proximal region of the C-terminus of the channel [201–204]. All inherited mutations linked to LQT-3, for example, alter Na^+ channel activity in a manner that prolongs the QT interval of the ECG in mutation carriers, but at least three different mutations, discovered by linkage to LQT-3, have now been reported that do not result in increased sustained inward Na^+ current. The first mutation, D1790G, was discovered in a large Israeli family [205]. Initial expression studies revealed that this mutation changed the voltage dependence and kinetics of inactivation of mutant channels but did not promote sustained current [206], a finding questioned by subsequent investigations [207]. Computer-based simulations suggest that this mutation may prolong action potential duration through an indirect effect on the control of cytoplasmic calcium concentrations [208], a result that awaits testing in animal models.

Another LQT-3 mutation has also been reported that does not appear to result in enhanced sustained current [209]. In this case, the mutation (E1295K) alters both activation and inactivation gating by causing small but significant shifts in the voltage dependence of gating. As a result, although there is no enhanced sustained Na^+ current, the voltage dependence of the “window” current is changed. The peak of the “window”

current is shifted in the positive direction such that the background currents against which it is expressed are different than in the case of wild-type channels [209]. As a result, window current of the same amplitude will have a greater effect on net membrane currents, and, because the currents flowing during the plateau phase are so small, the net result will be increased inward current and action potential prolongation [162, 210, 211]. More recently, a similar mechanism has been proposed to explain the cellular consequences of another Na⁺ channel mutation linked to sudden infant death syndrome [212].

Voltage-Gated Na⁺ Channel (Na) Accessory β Subunits

Functional voltage-gated Na⁺ channels appear to be multi-subunit complexes consisting of a central pore-forming α subunit (Fig. 1.2a) and one to two auxiliary β subunits [213]. There are at least four different β subunit genes encoding a total of five proteins. SCN1b encodes β 1 and β 1B [214–216]. SCN2b encodes β 2 [217, 218], and SCN3b encodes β 3 [219]. Additionally, SCN4A encodes β 4 protein [220] (Table 1.3). Structurally, most of the voltage-gated Na⁺ channel β subunits have a type I topology, meaning that they have an extracellular N-terminus and an intracellular C-terminus connected by a single pass through the membrane of their one amino acid chain [221]. The exception to this is β 1B that due to its incorporation of intron 3 in the SCN1b gene produces an alternate C-terminal region lacking a transmembrane domain. Thus, β 1B is a secreted cell adhesion protein [222, 223].

In the heart, the functional role of these subunits remains controversial. Most studies have focused on the role of SCN1b, which has relatively minor effects on channel gating in the heart compared with its effects on gating in the skeletal muscle [224]. Nevertheless, it has been shown that co-expression of SCN1b affects inactivation kinetics and current densities [206, 225]. Although relatively few functional effects have been reported for SCN2b [226], it has been reported that this subunit plays a role in control-

ling the Ca²⁺ permeability of voltage-gated Na⁺ channels [227]. Recently, SCN3b has been reported to also be expressed in the heart with predominant expression in the Purkinje fibers and ventricles but little expression in the atria [225]. In addition, like SCN1b, co-expression of SCN3b increases current density and may affect inactivation gating [225].

Voltage-Gated Ca²⁺ Channels, (CaV) Pore-Forming α Subunits

The α ₁ subunit of voltage-gated Ca²⁺ channels (VGCC) contains the channel pore and is the largest of the subunits [45, 47, 48, 228, 229]. Like Na_v channels, voltage-gated Ca²⁺ (Ca_v) channel pore-forming (α) subunits (Fig. 1.2b) belong to the “S4” superfamily of voltage-gated ion channel genes that also includes voltage-gated Na⁺ (Fig. 1.2a) and K⁺ (Fig. 1.2c) channel α subunits. Structurally, functional voltage-gated Ca²⁺ (Ca_v) channels consist of a Ca_v α ₁ subunit, with a predicted mass of 212–273 kDa, and auxiliary, Ca_v β and Ca_v α ₂ δ subunits (Fig. 1.3c). In most voltage-gated Ca²⁺ channels, the α ₁ subunit determines the properties of the resulting channels.

Also, like Na_v α ₁, Ca_v α ₁ subunits are comprised of four homologous domains (I–IV), each of which is made up of six putative transmembrane segments (S1–S6), one of which is the “S4” voltage-sensing domain, and a region between S5 and S6, known as the selectivity filter, that contributes to the Ca²⁺-selective pore (Fig. 1.2b) [4, 48, 229–231]. This schematic is supported by cryo-electron microscopy (cryo-EM) of a rabbit skeletal muscle voltage-gated calcium channel (Ca_v1.1) [232, 233]. Also supported by this cryo-EM is the assertion that, as also true in Na_v channels, Ca_v channel structurally adopts a “domain-swapped” conformation allowed by their long S4–S5 linker. In a domain-swapped conformation, the S5–S6 pore region is next to the S1–S4 region of the adjacent subunit [232, 233]. This is not, apparently, the case in channels with shorter S4–S5 linkers, such as hERG that will be discussed later [234, 235]. Similar to voltage-gated Na_v α ₁ subunits

Table 1.3 Diversity of Na⁺ and Ca²⁺ channel accessory subunits

Family	Gene	Locus			Subunit	Cardiac current
		Homo	Mus	Rattus		
Na ⁺						
β						
	<i>SCN1B</i>	19q13.11	7B1	1q21	β1	
					β1B	
	<i>SCN2B</i>	11q23.3	9A5.2	8q22	β2	INa
	<i>SCN3B</i>	11q24.1	9A5.1	8q22	β3	INa
	<i>SCN4B</i>	11q23.3	9A5.2	8q22	β4	
Ca ²⁺						
β						
	<i>CACNB1</i>	17q12	11B	10q31	β1a β1b	
	<i>CACNB2</i>	10p12.33-p12.31	2A2	17q12.3	β2	ICa _(L)
	<i>CACNB3</i>	12q13.12	15F1	7q36	β3	
	<i>CACNB4</i>	2q23.3	2C1.1	3q12	β4	
α2δ						
	<i>CACNA2D1</i>	7q21.11	5A2-A3	4q12	α2δ-1	ICa _(L)
	<i>CACNA2D2</i>	3p21.31	9F1	8q32	α2δ-2	ICa _(L)
	<i>CACNA2D3</i>	3p21.1-p14.3	14A3	16p16	α2δ-3	ICa _(L)
	<i>CACNA2D4</i>	12p13.33	6F1	4q42	α2δ-4	ICa _(L)
γ						
	<i>CACNG1</i>	17q24.2	11E1	10q32.1	γ1	
	<i>CACNG2</i>	22q12.3	15E1	7q34	γ2	
	<i>CACNG3</i>	16p12.1	7F2	1q36	γ3	
	<i>CACNG4</i>	17q24.2	11E1	10q32.1	γ4	ICa _(L)
	<i>CACNG5</i>	17q24.2	11E1	10q32.1	γ5	
	<i>CACNG6</i>	19q13.42	7A1	1q12	γ6	ICa _(L)
	<i>CACNG7</i>	19q13.42	7A1	1q12	γ7	ICa _(L)
	<i>CACNG8</i>	19q13.42	7A1	1q12	γ8	
γ like	<i>Tmem37</i>	2q14.2	1E2.3	13q11	TmEM37	

Boxes denote cardiac expression

(Fig. 1.2a), the N- and C-termini of Ca_vα₁ subunits are intracellular (Fig. 1.2b). The Ca_v channel N- and C-termini contain binding sites for a variety of proteins, including calmodulin and other calcium-binding proteins [48, 236, 237].

Supported by experimental evidence and molecular dynamics simulations of other voltage-gated channels, it is theorized that activation of

voltage-gated Ca²⁺ channels caused by the cellular depolarization triggered movement of the positively charged “S4” segment in each of the four domains [232, 233, 238].

To date, three distinct subfamilies of Ca_v channel pore-forming α₁ subunits, Cav1, Cav2, Cav3, have been identified, and in each case, there are many subfamily members [46]

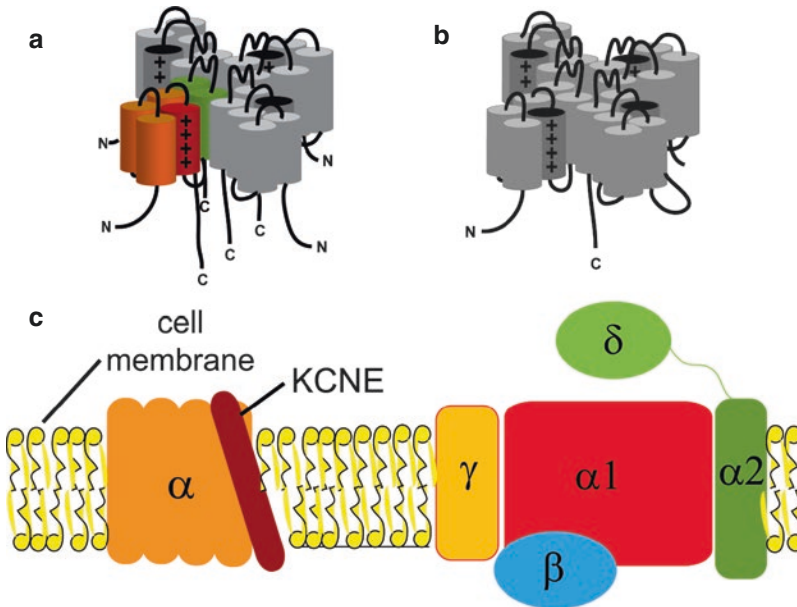


Fig. 1.3 Molecular comparison of assembly of cardiac voltage-gated channels. K_v channels assemble from four α subunits. (a) Each of these alpha subunits has an N-terminal region, a C-terminal region, and six transmembrane helices. The first four of these helices are the voltage-sensing domain (orange and red), where the fourth helix (red) contains charged residues for sensing voltage change. The last two helices (green) combine with their counterparts from the other three K_v α subunits to

form the pore. (b) In voltage-gated Na^+ and Ca^{2+} channels, there is one α subunit that is comprised of four similar repeats of six transmembrane helices, that fold into a similar structure as the four K_v channel α subunits, but is one continuous protein. (c) Voltage-gated channel complexes contain auxiliary subunits. (left) KCNQ1 contains a KCNE subunit in its functional complex. (right) An L-type voltage-gated Ca^{2+} channel complex contains an $\alpha 1$ subunit and may contain a β , $\alpha 2\delta$, and/or γ subunits

(Table 1.2). These numeric classifications represent the families of L-type, neuronal, and T-type Ca_v channels, respectively. The L-type and neuronal families are known to be high-voltage-activated (HVA) Ca^{2+} channels, and T-type are known to be low-voltage-activated (LVA) Ca^{2+} channels. The various $Ca_v\alpha_1$ subunits are differentially expressed, and heterologous expression studies have revealed that these genes encode voltage-gated Ca^{2+} channels with distinct time- and voltage-dependent properties and pharmacological sensitivities. As an example, functional expression of any one of the four members of the Ca_v1 subfamily, $Cav1.1$ (α_{1s}), $Cav1.2$ (α_{1c}), $Cav1.3$ (α_{1d}), or $Cav1.4$ (α_{1f}) (Table 1.2), reveals L-type Ca^{2+} channel currents, which are long-lasting when Ba^{2+} is the charge carrier. These channels activate at relative high voltages (~ -20 mV), and dihydropyridine (DHP) Ca^{2+} channel antagonists block these channels.

In the human heart, at different periods of development, there expressed both L-type (Ca_v1) and T-type (Ca_v3) voltage-gated calcium channels [239, 240]. Studies in rodents have suggested T-type channels (Ca_v3) play a role in development of the embryonic heart but are expressed less prominently in the adult human heart [241–244]. T-type channels appear to play a role in pacemaking and cardiac remodeling in the adult human myocardium [240, 245–248].

Two types of L-type calcium channels have been observed in the human cardiomyocytes: $Ca_v1.2$ (α_{1c}) and $Ca_v1.3$ (α_{1d}). These are expressed from embryonic stages onward [239]. $Ca_v1.2$ expression is throughout the heart, especially the atria and ventricles [47, 239]. It is widely accepted that the $Ca_v1.2$ (α_{1c}) is the most prevalent Ca_v expressed in the mammalian myocardium and is the major Ca_v involved in the Ca^{2+} -driven excitation-contraction coupling in

the heart [4, 231, 241, 249, 250]. Meanwhile, $\text{Ca}_v1.3$ is mainly found in the nonventricular regions: the pacemaking, sinoatrial node (SAN), the conductive Purkinje fibers and atrioventricular node (AVN), and the mechanical pumping atria [47, 239, 251, 252].

The human *CACNA1C* gene that encodes the α_{1c} subunit expansively stretches over 55 exons, 9 of which are subject to alternative splicing [253–256]. From these alternate exons, and many possible splice sites, many variations of α_{1c} result in many types of tissue-specific $\text{Ca}_v1.2$. Examples of these include $\text{Ca}_v1.2a$, $\text{Ca}_v1.2b$, and $\text{Ca}_v1.2c$ [4, 49, 253, 257, 258]. $\text{Ca}_v1.2$ is primarily represented by the smooth muscle isoform, $\text{Ca}_v1.2b$, and the cardiac-specific $\text{Ca}_v1.2a$ [256]. $\text{Ca}_v1.2a$ is encoded by 44 invariant and 6 alternative exons of the *CACNA1C* gene [257]. $\text{Ca}_v1.2a$ bears >95% amino acid sequence identity to the α_{1c} 's of $\text{Ca}_v1.2b$ and $\text{Ca}_v1.2c$ despite being expressed in different tissues [49, 259].

Ca_v Channel Accessory Subunits

Though it is the type of $\text{Ca}_v\alpha_1$ present that the variety of the channel is determined, there are usually other subunits present in the Ca_v channel complex. There are three major families of Ca_v channel accessory subunits [47, 48]. One major Ca_v auxiliary subunit is the $\text{Ca}_v\beta$ subunit [260, 261]. In the case of L-type calcium channels, such as $\text{Ca}_v1.2$ (α_{1c}) and $\text{Ca}_v1.3$ (α_{1d}), the $\text{Ca}_v\beta$ subunit is believed to be required for proper Ca_v channel trafficking [262–264]. The $\text{Ca}_v\alpha_2\delta$ subunit has been shown to increase the maximal Ca^{2+} current and increase inactivation rates of Ca_v channels [265]. A $\text{Ca}_v\gamma$ subunit may also be present in the Ca_v channel complex and is the least studied of the Ca_v accessory subunits with much of its role in the human myocardium still unknown [266].

Almost always found with the membrane-targeted α subunit is the β subunit [47, 48, 228, 262, 263, 267]. The β subunit is believed to be important in the trafficking and regulation of the α subunit to the membrane [262, 267]. Four different $\text{Ca}_v\beta$ subunit-encoding genes (and subunit coded for) have been identified: *CACNB1*

($\text{Ca}_v\beta_1$), *CACNB2* ($\text{Ca}_v\beta_2$), *CACNB3* ($\text{Ca}_v\beta_3$), and *CACNB4* ($\text{Ca}_v\beta_4$) [6, 260, 261, 268–270]. In these proteins amino acid sequence, there are three variable regions: the N-terminus, a small center HOOK region (~100 amino acids), and the C-terminus. Separating between the variable N-terminus and HOOK region is a highly conserved, hydrophobic SH3 domain. Between the HOOK region and the C-terminus is the highly conserved, guanylate kinase (GK) domain [271–275]. The variable regions are two conserved regions thought to mediate interaction with the $\text{Ca}_v\alpha_1$ subunit.

In heterologous expression systems, all four $\text{Ca}_v\beta$ subunits associate with $\text{Ca}_v\alpha_1$ subunits (Fig. 1.3c) and modify the time- and voltage-dependent properties, as well as the magnitude, of the expressed currents. It has been suggested that co-expression of $\text{Ca}_v\beta$ subunits with $\text{Ca}_v\alpha_1$ subunits increases the number of functional cell surface membrane channels, resulting in increases in Ca^{2+} current amplitudes and densities [276–279]. Alternatively, the association of $\text{Ca}_v\beta$ subunits and the resulting increases in current amplitudes/densities could reflect increased expression of the $\text{Ca}_v\alpha_1$ subunit, an increase in the channel open probability, [277] and/or the stabilization of channel complex in the cell membrane [264, 277, 280, 281]. In addition to increasing current amplitudes, co-expression of $\text{Ca}_v\beta$ subunits modifies the kinetics and the voltage dependences of current activation and inactivation [282–285].

Detailed analysis of different $\text{Ca}_v\alpha_1$ subunits has revealed that a highly conserved sequence motif, called the alpha subunit interaction domain (or AID), mediates the interaction(s) with $\text{Ca}_v\beta$ subunits [275]. The AID sequence, QqxExxLxGYxxWlxxxE, is located at 24 amino acids from the S6 transmembrane region of domain I (Fig. 1.2b) of the $\text{Ca}_v\alpha_1$ subunit [154, 173–175, 259, 286–288]. Regions outside of AID, including low-affinity binding sites in the C-termini of the $\text{Ca}_v\alpha_1$ subunits, have also been suggested to participate in the $\text{Ca}_v\beta$ - $\text{Ca}_v\alpha_1$ subunit-subunit interactions [289–291]. Nevertheless, it appears that these C-terminal regions in $\text{Ca}_v\alpha_1$ also interact specifically with

the second (internal) highly conserved domain of the $\text{Ca}_v\beta$ subunits to induce the observed modulatory effects [292, 293].

Another subunit that also may be present in the VGCC complex is the $\text{Ca}_v\alpha_2\delta$ subunit [48, 228, 262, 267, 294]. This disulfide-linked, transmembrane accessory subunit, was first cloned from the skeletal muscle [295], and, to date, five different isoforms of $\text{Ca}_v\alpha_2\delta$ -1 have been identified (Table 1.3). In addition, two homologous $\text{Ca}_v\alpha_2\delta$ genes, $\text{Ca}_v\alpha_2\delta$ -2 and $\text{Ca}_v\alpha_2\delta$ -3, have been identified in the brain [296]. $\text{Ca}_v\alpha_2\delta$ -4 is found in retinal neurons and some non-neuronal endocrine cells [267, 297, 298]. Sequence comparison revealed ~55% amino acid identity between $\text{Ca}_v\alpha_2\delta$ -1 and $\text{Ca}_v\alpha_2\delta$ -2 and ~30% identity between $\text{Ca}_v\alpha_2\delta$ -1 and $\text{Ca}_v\alpha_2\delta$ -3 [296]. The $\text{Ca}_v\alpha_2\delta$ subunits are heavily glycosylated proteins that are cleaved posttranslationally to yield disulfide-linked α_2 and δ proteins (Fig. 1.3c). The α_2 domain is located extracellularly, whereas the δ domain has a large hydrophobic region, which inserts into the membrane and serves as an anchor to secure the $\text{Ca}_v\alpha_2\delta$ complex [299–301].

In contrast to the accessory $\text{Ca}_v\beta$ subunits, the functional roles of $\text{Ca}_v\alpha_2\delta$ are somewhat variable and depend, at least in part, on the identities of the co-expressed $\text{Ca}_v\alpha_1$ and $\text{Ca}_v\beta$ subunits and the expression environment. In general, co-expression of $\text{Ca}_v\alpha_2\delta$ -1 shifts the voltage dependence of channel activation, accelerates the rates of current activation and inactivation, and increases current amplitudes, compared with the currents produced on expression of $\text{Ca}_v\alpha_1$ and $\text{Ca}_v\beta$ subunits alone [296, 300–304]. The increase in current density reflects improved targeting of $\text{Ca}_v\alpha_1$ subunits to the membrane [305]. This effect is attributed to α_2 , whereas the changes in channel kinetics reflect the expression of the δ protein [305].

Sometimes a Ca_v channel complex will also contain a $\text{Ca}_v\gamma$ subunit, of which there are eight human genes that code for these subunits. These subunits are named $\text{Ca}_v\gamma_1$ through $\text{Ca}_v\gamma_8$ and contain four transmembrane helices [306–309]. These eight proteins, believed to be members of the claudin superfamily of proteins [306, 309], have been grouped into two clusters: neuronal

and skeletal based on sequence similarity and tissue distribution [306]. The neuronal $\text{Ca}_v\gamma$ subunits contain $\text{Ca}_v\gamma_{2-5}$ and $\text{Ca}_v\gamma_{7-8}$ PDZ binding domain for binding AMPA receptors, and, thus, these $\text{Ca}_v\gamma$ subunits are classified as TARPs (transmembrane AMPA receptor regulatory proteins) [306, 310]. The skeletal $\text{Ca}_v\gamma$ s are $\text{Ca}_v\gamma_1$ and $\text{Ca}_v\gamma_6$ and are expressed in the skeletal muscle among other tissues. $\text{Ca}_v\gamma_4$, $\text{Ca}_v\gamma_6$, $\text{Ca}_v\gamma_7$, and $\text{Ca}_v\gamma_8$ are expressed in the human heart and associated with the cardiac $\text{Ca}_v\alpha_{1C}$ subunit [311].

Molecular Basis of Voltage-Gated K^+ Current Diversity in Mammalian Ventricle

Voltage-Gated K^+ (Kv) Channel Pore-Forming α Subunits

Voltage-gated K^+ channel (K_v) pore-forming (α) subunits are six transmembrane-spanning domain proteins (Fig. 1.2c) with a region between the fifth and sixth transmembrane domains that contributes to the K^+ -selective pore [11]. The positively charged fourth transmembrane domain in the K_v α -subunits (Figs. 1.2c and 1.3a) is homologous to the corresponding region in voltage-gated Na^+ (Figs. 1.2a and 1.3b) and Ca^{2+} (Figs. 1.2b and 1.3b) channel α -subunits, placing them in the “S4” superfamily of voltage-gated channels [312]. In contrast to voltage-gated Na^+ and Ca^{2+} channels, however, functional voltage-gated K^+ channels comprise four α -subunits (Fig. 1.3a, b). To an even greater degree than Na^+ and Ca^{2+} α subunits (Table 1.2), there is a great diversity of $\text{K}_v\alpha$ subunits (Table 1.4). Twelve homologous $\text{K}_v\alpha$ subunit subfamilies, $\text{K}_v1.x$, $\text{K}_v2.x$, $\text{K}_v3.x$, and $\text{K}_v4.x$, for example, have been identified, and many of these are expressed in mammalian ventricles (Table 1.4). In addition to the multiplicity of $\text{K}_v\alpha$ subunits (Table 1.4), further functional K^+ channel diversity can arise through alternative splicing of transcripts, as well as through the formation of heteromultimeric channels [313] between two or more K_v α -subunit proteins in the same K_v subfamily [11, 314].

Table 1.4 Diversity of K⁺ channel α subunits

Subfamily	Protein	Gene	Locus			Cardiac current	
			Homo	Mus	Rattus		
Kv1	Kv1.1	<i>KCNA1</i>	12p13.32	6F3	4q42	??	
	Kv1.2	<i>KCNA2</i>	1p13.3	3F2.3	2q34	$I_{k,slow(rat)}$ ($I_{k,DTX}$)	
	Kv1.3	<i>KCNA3</i>	1p13.3	3F2.3	2q34		
	Kv1.4	<i>KCNA4</i>	11p14.1	2E3	3q33	$I_{to,s}$	
	Kv1.5	<i>KCNA5</i>	12p13.32	6F3	4q42	$I_{Kur(human, rat)}$, $I_{k,slow(mousr)}$	
	Kv1.6	<i>KCNA6</i>	12p13.32	6F3	4q42		
	Kv1.7	<i>KCNA7</i>	19p13.33	7B3	1q22	??	
	Kv1.8	<i>KCNA10</i>	1p13.3	3F2	2q34	??	
	Kv2	Kv2.1	<i>KCNB1</i>	20q13.13	2H3	3q42	$I_{k,slow(mousr)}$
		Kv2.2	<i>KCNB2</i>	8q21.11	1A3	5q11	??
Kv3	Kv3.1	<i>KCNC1</i>	11p15.1	7B3	1q22	$I_{Kur(canine)}$	
	Kv3.2	<i>KCNC2</i>	12q21.1	10D2	7q22		
	Kv3.3	<i>KCNC3</i>	19q13.33	7B3	1q22		
	Kv3.4	<i>KCNC4</i>	1p13.3	3F2.3	2q34		
Kv4	Kv4.1	<i>KCND1</i>	Xp11.23	XA1.1	Xq12	??	
	Kv4.2	<i>KCND2</i>	7q31.31	6A2-A3.1	4q22	$I_{to,f}$	
	Kv4.3	<i>KCND3</i>	1p13.2	3F2.2	2q34	$I_{to,f}$	
Kv5	Kv5.1	<i>KCNF1</i>	2q25.1	12A1.1	6q16	??	
Kv6	Kv6.1	<i>KCNG1</i>	2q13.13	2H3	3q42	??	
	Kv6.2	<i>KCNG2</i>	18q23	18E3	18q12.3		
	Kv6.3	<i>KCNG3</i>	2p21	17E4	6q12		
	Kv6.4	<i>KCNG4</i>	16q24.1	8E1	19q12		
Kv7	Kv7.1	<i>KCNQ1</i>	11p15.5-p15.4	7F5	1q42	I_{Ks}	
	Kv7.2	<i>KCNQ2</i>	20q13.33	2H4	3q43	??	
	Kv7.3	<i>KCNQ3</i>	8q24.22	15D1	7q34		
	Kv7.4	<i>KCNQ4</i>	1q34.2	4D2.2	5q36		
	Kv7.5	<i>KCNQ5</i>	6q13	1A4	9q13		
Kv8	Kv8.1	<i>KCNV1</i>	8q23.22	15B3.3	7q31		
	Kv8.2	<i>KCNV2</i>	9q24.2	19C1	1q52		
Kv9							

Table 1.4 (continued)

Subfamily	Protein	Gene	Locus			Cardiac current
			Homo	Mus	Rattus	
	Kv9.1	<i>KCNS1</i>	20q13.12	2H3	3q42	
	Kv9.2	<i>KCNS2</i>	8q22.2	15B3.1	7q22	
	Kv9.3	<i>KCNS3</i>	2q24.2	12A1.1	6q15	??
Kv10						
	Kv10.1	<i>KCNH1</i>	1q32.2	1H6	13q27	
	Kv10.2	<i>KCNH5</i>	14q23.2	12C3	6q24	
Kv11						
	Kv11.1	<i>KCNH2</i>	7q36.1	5A3	4q11	I_{Kr}
	Kv11.2	<i>KCNH6</i>	17q23.3	11E1	10q32.1	
	Kv11.3	<i>KCNH7</i>	2q24.2	2C1.3	3q21	
Kv12						
	Kv12.1	<i>KCNH8</i>	3p24.3	17C	9q11	
	Kv12.2	<i>KCNH3</i>	12q13.12	15F1	7q36	
	Kv12.3	<i>KCNH4</i>	17q21.2	11D	10q31	

Boxes denote cardiac expression

In contrast to the $K_v1.x - K_v4.x$ α subunit subfamilies, heterologous expression of $K_v5.x - K_v9.x$ (Table 1.4) α subunits alone does not reveal functional voltage-gated K^+ channels, with the exception of $K_v7.1$, which is also known as *KCNQ1* [314–318]. Interestingly, however, co-expression of any of these ($K_v5.1$, $K_v6.1$, $K_v8.1$, or $K_v9.1$) subunits with *Shab* ($K_v2.x$) subfamily members attenuates the amplitudes of the *Shab* ($K_v2.x$) modulated currents [318]. These observations have been interpreted as suggesting that the $K_v5.x - K_v9.x$ subunits are regulatory K_v α subunits of the $K_v2.x$ subfamily [317], although the roles of these “silent” subunits in the generation of functional voltage-gated K^+ channels in cardiac cells remain to be determined.

The second subfamily of voltage-gated K^+ channel α -subunit gene was revealed with the cloning of the *Drosophila* ether-a-go-go (*eag*) locus [319]. Homology screening led to the identification of human *eag*, as well as another subfamily, the human *eag*-related gene, referred to as *hERG* [314, 320], which was subsequently identified as the locus of mutations leading to one form of familial long QT syndrome, *LQT2* [321]. Expression of *hERG* (human *ERG1*) in *Xenopus* oocytes revealed inwardly rectifying voltage-gated, K^+ -selective currents [322, 323] with properties similar to cardiac I_{Kr} (Table 1.4). Related

ERG genes, *ERG2* and *ERG3*, have also been identified (Table 1.4), although these appear to be nervous system specific and are not expressed in the mammalian heart [324]. Alternatively processed forms of *ERG1*, however, have been cloned from mouse and human heart cDNA libraries and postulated to contribute to cardiac I_{Kr} [325–327].

Another subfamily of voltage-gated K^+ channel α -subunits was revealed with the cloning of *KvLQTI* [328], the loci of mutations in another inherited form of long QT syndrome (*LQTI*) (Table 1.4). Although expression of *KvLQTI* (*KCNQI*) alone reveals rapidly activating and noninactivating K^+ currents, co-expression with the subunit *KCNE1* produces slowly activating K^+ currents that account for the slow component of cardiac delayed rectification, I_{Ks} [329, 330]. Additional *KCNQ* subfamily members, *KCNQ2* and *KCNQ3*, although not expressed in heart, have been identified [331–333]. Interestingly, however, *KCNQ2* and *KCNQ3* have been identified as loci of mutations leading to benign familial neonatal convulsions [331, 333]. Heterologous expression of *KCNQ2* or *KCNQ3* produces slowly activating, noninactivating K^+ -selective currents that deactivate very slowly on membrane repolarization [333, 334]. The unique kinetic and pharmacological properties of the expressed

currents suggest that functional neuronal M channels reflect the heteromeric assembly KCNQ2 and KCNQ3 [334].

Voltage-Gated K (Kv) Channel Accessory Subunits

A number of voltage-gated K⁺ (K_v) channel accessory subunits have now been identified

(Table 1.5). The first of these, KCNE1, encodes a small (130 amino acids) protein with a single membrane-spanning domain [335–337]. As expected for an accessory K_v channel subunit, KCNE1 does not produce functional voltage-gated K⁺ channels when expressed alone in heterologous systems [330]. Rather, it coassembles with KCNQ1 (Fig. 1.3c) to form functional I_{Ks} channels [329, 330]. KCNE1 homologues, MiRP1 (KCNE2), MiRP2 (KCNE3), MiRP3

Table 1.5 Diversity of K⁺ channel accessory subunits

Family	Gene	Locus			Subunit	Associates with	Cardiac current
		Homo	Mus	Rattus			
Kvβ	<i>KCNAB1</i>	3q25.31	3E1	2q31		Kv1.1-1.6, Kv4.3	<i>I_{to,f}</i> ?? <i>I_{Kur}</i> ??
					Kvβ1.1		
					Kvβ1.2		
					Kvβ1.3	Kv1.5	
	<i>KCNAB2</i>	1p36.31	4E2	5q36	Kvβ2.1	Kv1.1-1.6, Kv4.3	<i>I_{to,f}</i> ?? <i>I_{Kur}</i> ??
	<i>KCNAB3</i>	17p13.1	11B3	10q24	Kvβ3.1	Kv1.1-1.6	??
KCNE	<i>KCNE1</i>	21q22.12	16C4	11q11	Mink	KCNQ1	<i>I_{Ks}</i>
	<i>KCNE2</i>	21q22.11	16C4	11q11	MiRP1	KCNQ1,HERG	<i>I_{IKs}</i> , <i>I_{Kr}</i>
	<i>KCNE3</i>	11q13.4	7E2	1q32	MiRP2	HERG/Kv4,KCNQ1	<i>I_{Kr}</i> / <i>I_{to,f}</i> , <i>I_{Ks}</i>
	<i>KCNE4</i>	2q36.1	1C4	9q34	MiRP3		
	<i>KCNE5</i>	Xq23		Xq33	MiRP4	KCNQ1,Kv4	<i>I_{Ks}</i> , <i>I_{to,f}</i>
KChIP	<i>KCNIP1</i>	5q35.1	11A4	10q12	KchIP1	Kv4.1-4.3	
	<i>KCNIP2</i>	10q24.32	19C3	1q54	KchIP2	Kv4.1-4.3	<i>I_{to,f}</i>
	<i>KCNIP3</i>	2q11.1	2F1	3q36	KchIP3	Kv4.2	
	<i>KCNIP4</i>	4p15.31-p15.2	5B3	14q11	KchIP4	Kv4.2, Kv4.3	
KChAP ^a	<i>PIAS3</i>	1q21.1	3F2	2q34	KChAP		<i>I_{to,f}</i> ??, <i>I_K</i> ??
NCS	<i>NCS1</i>	9q34.11	2B	3p12	NCS 1		<i>I_{to,f}</i>
DPPLs	<i>DPP6</i>	7q36.2	5B1	4q11	DPP6	Kv4.2, Kv4.3	<i>I_{to,f}</i>
	<i>DPP10</i>	2q14.1	1E2	13q11-q12	DPP10	Kv4.2, Kv4.3	<i>I_{to,f}</i>

Boxes denote cardiac expression

^aKChAP only found interaction with Kv channels in rat

(KCNE4), and MiRP4 (KCNE5) have also been identified (Table 1.5), and it has been suggested that MiRP1 functions as an accessory subunit of ERG1 in the generation of (cardiac) I_{Kr} [338–340]. Although it is unclear whether KCNE1, MiRP1, or other KCNE subfamily members [338] contribute to the formation of voltage-gated K^+ channels in addition to I_{Ks} and I_{Kr} in the myocardium, it has been reported that MiRP2 assembles with $K_v3.4$ in mammalian skeletal muscle [341] and with $K_v4.x$ α -subunits in heterologous expression systems [342]. These observations suggest the interesting possibility that members of the KCNE subfamily of accessory subunits can assemble with multiple K_v α -subunits and contribute to the formation of multiple types of voltage-gated myocardial K^+ channels. Direct experimental support for this hypothesis, however, has not been provided to date, and the roles of the KCNE family of accessory subunits in the generation of functional ventricular K^+ channels need to be defined.

Another type of K_v accessory subunit was revealed with the identification of low molecular weight (~45 kD) cytosolic β subunits in the brain [343, 344]. Three homologous K_v β subunits, $K_v\beta1$, $K_v\beta2$, and $K_v\beta3$ (Table 1.5), as well as alternatively spliced transcripts, have been identified [345–350], and both $K_v\beta1$ and $K_v\beta2$ are expressed in the heart [350]. The K_v β subunits interact with the intracellular domains of the K_v α subunits of the K_v1 subfamily in assembled voltage-gated K^+ channels, and heterologous expression studies suggest that K_v β subunit co-expression affects the functional properties and the cell surface expression of K_v α subunit-encoded K^+ currents [345–349, 351–353]. Because K_v α and β subunits coassemble in the endoplasmic reticulum [354], the increase in functional channel expression suggests that the K_v β subunits affect channel assembly, processing, or stability or that they function as chaperon proteins.

Heterologous co-expression studies suggest that the effects of the K_v β subunits are subfamily specific, i.e., $K_v\beta1$, $K_v\beta2$, and $K_v\beta3$ interact only with the K_v1 subfamily of α subunits [355, 356],

whereas $K_v\beta4$ is specific for the K_v2 subfamily [357]. Nevertheless, it is not known which K_v α subunit(s), the $K_v\beta1$ and $K_v\beta2$ subunits, associate within the myocardium, and the roles of these (K_v β) subunits in the generation of functional cardiac K^+ channels remain to be determined.

Using a yeast two-hybrid screen, Wible and colleagues (1998) identified a novel voltage-gated K^+ channel regulatory protein, KChAP (K^+ channel accessory protein) (Table 1.5) [358]. Sequence analysis of ChAP revealed a 574 amino acid protein with no transmembrane domains and no homology to K_v α or K_v β subunits [358]. Co-expression of KChAP with $K_v2.1$ (or $K_v2.2$) in *Xenopus* oocytes, however, markedly increases functional $K_v2.x$ -induced current densities without measurably affecting the time- and/or the voltage-dependent properties of the currents [358] suggesting that KChAP functions as a chaperon protein. Yeast two-hybrid assays also revealed that KChAP interacts with the N-termini of $K_v1.x$ α subunits and with the C-termini of $K_v\beta1.x$ subunits [358].

Using the intracellular N-terminus (amino acids 1–180) of $K_v4.2$ as the “bait” in a yeast two-hybrid screen, An and colleagues (2000) identified three novel K_v channel interacting proteins, KChIP1, KChIP2, and KChIP3 (Table 1.5) [359]. Of these, only KChIP2 appears to be in the heart [359, 360], although there are several splice variants of KChIP2 expressed [360–362]. Sequence analysis revealed that the KChIPs belong to the recoverin family of neuronal Ca^{2+} -sensing (NCS) proteins, particularly in the “core” regions, which contain multiple EF-hand domains [363]. Unlike other NCS-1 proteins, however, KChIP2 and KChIP3 lack N-terminal myristoylation sites, and the N-termini of the KChIP proteins are unique [359]. Interestingly, KChIP3 is identical to the NCS protein calsenilin, a Ca^{2+} -binding protein that interacts with the presenilin proteins and regulates proteolytic processing [364]. In addition, the nucleotide sequence of KChIP3 is 99% identical to the Ca^{2+} -regulated transcriptional repressor, DREAM [365]. The expression of several genes has been shown to be regulated by downstream regulatory elements (DRE), and,

importantly, the DREAM protein binds to DRE elements in the absence of Ca^{2+} and dissociates when Ca^{2+} is elevated [365]. Thus, DREAM is thought to act as an activity-dependent regulator of gene expression [365]. It should be noted, however, that DREAM is predicted to have an alternative start codon resulting in a 20 amino acid N-terminal extension not present in KChIP3 [359, 365]. Nevertheless, these findings suggest the interesting possibility that the KChIP proteins may be expressed in different cellular compartments and may subserve multiple cellular functions.

When expressed in CHO cells with $\text{K}_{\text{v}}4.2$, the KChIPs increase the functional cell surface expression of $\text{K}_{\text{v}}4.2$ -encoded K^+ currents, slow current inactivation, speed recovery from inactivation, and shift the voltage-dependence of activation [359]. Similar effects are observed when $\text{K}_{\text{v}}4.2$ or $\text{K}_{\text{v}}4.3$ is expressed with the KChIPs in *Xenopus* oocytes [359] or HEK-293 cells [366, 367]. In contrast, KChIP expression does not affect the properties or the densities of $\text{K}_{\text{v}}1.4$ - or $\text{K}_{\text{v}}2.1$ -encoded K^+ currents, suggesting that the modulatory effects of the KChIP proteins are specific for *ex* subunits of the $\text{K}_{\text{v}}4$ subfamily [359]. In addition, although the binding of the KChIP proteins to $\text{K}_{\text{v}}4$ α subunits is not Ca^{2+} -dependent, mutations in EF-hand domains I, III, and IV eliminate the modulatory effects of KChIP1 on $\text{K}_{\text{v}}4.2$ -induced K^+ currents in CHO cells [359]. It has recently been shown that KChIP2 co-immunoprecipitates with $\text{K}_{\text{v}}4.2$ and $\text{K}_{\text{v}}4.3$ α subunits from adult mouse ventricles, consistent with a role for this subunit in the generation of $\text{K}_{\text{v}}4$ -encoded mouse ventricular $\text{I}_{\text{to},\text{f}}$ channels [366]. Interestingly, a gradient in KChIP2 message expression is observed through the thickness of the ventricular wall in canine and human heart, suggesting that KChIP2 underlies the observed differences in $\text{I}_{\text{to},\text{f}}$ densities in the epicardium and endocardium in human and canine ventricles [360]. In rat and mouse, however, there is no gradient in KChIP2 expression [360, 366], and it appears that differences in $\text{K}_{\text{v}}4.2$ underlie the regional variations in $\text{I}_{\text{to},\text{f}}$ densities in rodents [83, 366].

Relation Between K_{v} Subunits and Ventricular Transient Outward K^+ Channels

Considerable experimental evidence has accumulated documenting a role for K_{v} α subunits of the $\text{K}_{\text{v}}4$ subfamily in the generation of ventricular $\text{I}_{\text{to},\text{f}}$ channels. In rat ventricular myocytes exposed to antisense oligodeoxynucleotides (AsODNs) targeted against $\text{K}_{\text{v}}4.2$ or $\text{K}_{\text{v}}4.3$, for example, $\text{I}_{\text{to},\text{f}}$ density is reduced by $\sim 50\%$ [368]. Similar results have recently been obtained in studies on mouse ventricular $\text{I}_{\text{to},\text{f}}$ [366]. Reductions in rat ventricular $\text{I}_{\text{to},\text{f}}$ density are also seen in cells exposed to adenoviral constructs encoding a truncated $\text{K}_{\text{v}}4.2$ subunit ($\text{K}_{\text{v}}4.2\text{ST}$) that functions as a dominant negative [369]. In ventricular myocytes isolated from transgenic mice expressing a dominant negative pore mutant of $\text{K}_{\text{v}}4.2$ ($\text{K}_{\text{v}}4.2\text{W362F}$) in the myocardium, $\text{I}_{\text{to},\text{f}}$ is eliminated [370]. Taken together, these results demonstrate that members of the $\text{K}_{\text{v}}4$ subfamily underlie $\text{I}_{\text{to},\text{f}}$ in mouse and rat ventricles. In addition, biochemical and electrophysiological studies suggest that $\text{K}_{\text{v}}4.2$ and $\text{K}_{\text{v}}4.3$ are associated in adult mouse ventricles and that functional mouse ventricular $\text{I}_{\text{to},\text{f}}$ are heteromeric [366]. Given the similarities in the properties of $\text{I}_{\text{to},\text{f}}$ (Table 1.1), it seems reasonable to suggest that $\text{K}_{\text{v}}4$ α subunits also underlie $\text{I}_{\text{to},\text{f}}$ in other species. In dog and human, however, the candidate subunit is $\text{K}_{\text{v}}4.3$ because $\text{K}_{\text{v}}4.2$ appears not to be expressed [79]. Two splice variants of $\text{K}_{\text{v}}4.3$ have been identified in human [82] and rat [371, 372] heart. Although the longer version of $\text{K}_{\text{v}}4.3$, which contains a 19 amino acid insert in the carboxy tail, is the more abundant message [82, 371, 372], the expression levels of the two $\text{K}_{\text{v}}4.3$ proteins, as well as the roles of these subunits in the generation of functional cardiac $\text{I}_{\text{to},\text{f}}$ channels, have been determined.

The kinetic and pharmacological properties of the slow transient outward K^+ currents, $\text{I}_{\text{to},\text{s}}$, in ventricular myocytes are distinct from $\text{I}_{\text{to},\text{f}}$ (Table 1.1), suggesting the molecular correlates of ventricular $\text{I}_{\text{to},\text{s}}$ and $\text{I}_{\text{to},\text{f}}$ channels. Direct experimental support for this hypothesis has been

provided in studies completed on ventricular myocytes isolated from (C57BL6) mice with a targeted deletion in the $K_v1.4$ gene, $K_v1.4^{-/-}$ animals [373]. The waveforms of the outward K^+ currents in cells isolated from the RV or from the LV apex of $K_v1.4^{-/-}$ animals are indistinguishable from those recorded in wild-type (right ventricle and left ventricular apex) cells which lack $I_{to,s}$ [61]. In cells isolated from the septum of $K_v1.4^{-/-}$ animals, $I_{to,s}$ is undetectable, demonstrating that $K_v1.4$ underlies $I_{to,s}$ [61].

Interestingly, $I_{to,s}$ (and $K_v1.4$ protein) is upregulated in left ventricular apex and in right ventricular cells in the $K_v4.2W362F$ -expressing transgenics [62], suggesting that electrical remodeling occurs when $I_{to,f}$ is eliminated. When the dominant negative $K_v4.2W362F$ transgene is expressed in the $K_v1.4^{-/-}$ null background, both $I_{to,f}$ and $I_{to,s}$ are eliminated, although no further electrical remodeling is evident [62]. Indeed, electrophysiological recordings from $K_v4.2W362F$ -expressing $K_v1.4^{-/-}$ cells revealed that the waveforms of the outward K^+ currents in all right and left ventricular cells are indistinguishable [62]. Given the similarities in the time- and voltage-dependent properties of the slow transient outward K^+ currents in other species [59, 78], it seems reasonable to suggest that $K_v1.4$ also encodes $I_{to,s}$ in ferret, rabbit, and human left ventricular myocytes. Direct experimental support for this hypothesis, however, has not been provided to date.

Relation Between K_v Subunits and Ventricular Delayed Rectifier K^+ Channels

Human ERG1 was identified as the locus of one form of long QT syndrome, LQT2 [321], and heterologous expression of ERG1 in *Xenopus* oocytes revealed voltage-gated, inwardly rectifying K^+ -selective channels that are similar to cardiac I_{Kr} [322, 323]. Although these observations suggest that ERG1 encodes functional cardiac I_{Kr} channels [322], AsODNS targeted against KCNE1 attenuate I_{Kr} in AT-1 (an atrial tumor line) cells [374] and heterologously expressed

ERG1 and KCNE1 co-immunoprecipitate [375]. These observations might be interpreted as suggesting that I_{Kr} channels are multimeric, comprising of the protein products of KCNH2 and KCNE1 [374, 375].

Alternatively processed forms of HERG 1 and MERG1 with unique N- and C-termini have also been identified in mouse and human heart [325–327] and suggested to be important in the generation of functional I_{Kr} channels [325, 326]. Western blot analysis of ERG1 protein expression in the myocardium, however, revealed that only the full-length ERG1 proteins are detected in rat, mouse, and human ventricles, suggesting that alternatively spliced (ERG1) variants do not play a role in the generation of functional I_{Kr} channels [107].

Although heterologous expression of KCNQ1, the locus of mutations leading to LQT1 [328], reveals rapidly activating, noninactivating voltage-gated K^+ currents, co-expression with KCNE1 produces slowly activating K^+ currents similar to I_{Ks} [329, 330]. These observations, together with biochemical data demonstrating that heterologously expressed KCNQ1 and KCNE1 associate [329], have provided evidence KCNE1 coassembles with KCNQ1 to form functional cardiac I_{Ks} channels [329, 330]. In addition, the finding that mutations in the transmembrane domain of KCNE1 alter the properties of the resulting I_{Ks} channels suggests that the transmembrane segment of KCNE1 modifies to the I_{Ks} channel pore movement [376–379]. Also of interest, N-terminal truncated variants of KCNQ1 exert a dominant negative effect when co-expressed with full-length KCNQ1 [380].

Molecular Correlates of Other Ventricular K^+ Currents

Inwardly Rectifying Cardiac K^+ (I_{Kr}) Channel Pore-Forming α Subunits

Similar to the K_v channels, functionally distinct types of myocardial inwardly rectifying K^+ channels [381] are formed by the association of diverse

Table 1.6 Inward rectifier α subunits

Family	Subfamily	Protein	Gene	Location		Cardiac current	
				Human	Mouse		
Kir	Kir1						
		Kir1.1	KCNJ1	11q24.3	9 A4	??	
	Kir2						
		Kir2.1	KCNJ2	17q24.3	11 E2	IK1	
		Kir2.2	KCNJ12	17q11.2	11 B2	IK1	
		Kir2.3	KCNJ4	22q13.1	15 E1	IK1	
		Kir2.4	KCNJ14	9q13.33	7B3		
	Kir3						
		Kir3.1	KCNJ3	2q24.1	2	IKACH	
		Kir3.2	KCNJ6	21q22.13	16C4		
		Kir3.3	KCNJ9	1q23.2	1H3		
		Kir3.4	KCNJ5	11q24.3	9A4	IKACH	
	Kir4						
		Kir4.1	KCNJ10	1q23.2	1H3		
		Kir4.2	KCNJ15	21q22	16C4		
	Kir5						
		Kir5.1	KCNJ16	17q24.3	11 E2		
	Kir6						
		Kir6.1	KCNJ8	12p12.1	6G2		
		Kir6.2	KCNJ11	11p15.1	7B3	IKATP	
	Kir7						
Kir7.1		KCNJ13	2q37.1	1C5			

Boxes denote cardiac expression

inward rectifier K^+ (Kir) channel pore-forming α subunit genes (Fig 1.2d) [382]. Several Kir subunit subfamilies, Kir1 through Kir6, most with several members, have been identified (Table 1.6) and, like Kv α subunits, Kir α subunits also assemble as tetramers to form functional K^+ -selective channels. Also similar to Kv channel α subunits, a unifying terminology has been developed for naming the Kir α subunit proteins (Kir1.x – Kir7.x) and the genes (KCNJ1–KCNJ16) encoding these proteins [383, 384]. Potassium channels can be classified into three groups depending on their topological structures; two, four, or six transmembrane domains [385]. Kir α subunit are composed of one pore (P) domain and two transmembrane domains (M1–M2).

Based on the properties of heterologously expressed Kir subunits, it was suggested that α subunits of the Kir2 subfamily likely encode the strongly inwardly rectifying Kir channels, I_{K1} , in cardiac cells [381, 382]. Three members of the Kir2 subfamily Kir2.1, Kir2.2, and Kir2.3 (Table 1.6) are expressed in the myocardium [386, 387]. Kir 2.4 are predominantly expressed in motoneurons of cranial nerve motor nuclei within the general somatic and special visceral motor cell column [388]. Interestingly, the KCNJ2 gene, which encodes Kir2.1, has been identified as the locus of mutations in Andersen's syndrome [389, 390], an inherited disorder that is often life-threatening owing to QT prolongation and cardiac (ventricular) arrhythmias, also called

long QT syndrome type 7 (LQT7). Similar to Timothy's syndrome [391], however, Andersen's syndrome is actually a multisystem disorder involving the cardiovascular, skeletomuscular, and other systems, and typically, Andersen's syndrome patients present initially with developmental abnormalities [392]. The mutations in *KCNJ2* that are associated with Andersen's syndrome that have been described appear to result in mutant Kir2.1 protein that functions in a dominant negative fashion to suppress Kv2.x-encoded I_{K1} currents [393–395]. Individuals carrying Andersen's syndrome mutations in *KCNJ2* can display QT prolongation (long QT7), periodic paralysis, as well as craniofacial malformations [392, 393, 396, 397], alone or in combination. Because only the *KCNJ2* gene appears to be affected in Andersen's syndrome, the multisystem nature of this disorder likely reflects the fact that Kir2.x-encoded channels are expressed and are functional in a variety of cells/tissues. Myocardial I_{K1} (and other K^+ channels) have been shown to be regulated directly by phosphatidylinositol bisphosphate (PIP2) [398–401]. More than 33 mutations in *KCNJ2* have been linked to Andersen's syndrome [402]. Interestingly, many of Andersen's mutations are in the PIP2-binding region of Kir2.1 [403], suggesting that the regulation/modulation of I_{K1} channels by PIP2 is altered and that it is the alterations in the modulatory effects of PIP2 that underlie the phenotypic consequences of Andersen's syndrome mutations. It was reported that Kir2.1 gain-of-function mutations (V93I and D172N) are also associated with increased I_{K1} , short QT syndrome type 3, and familial atrial fibrillation [404–408]. The mutant of Kir2.1 channels showed larger outward currents than wild type. In addition to the short QT interval, absence of inward rectification in mutant can lead to familiar atrial fibrillation [408].

The first direct molecular evidence that Kir2 α subunits encode cardiac I_{K1} channels was provided in studies completed on myocytes isolated from mice bearing a targeted disruption of the coding region of Kir2.1 (Kir2.1 $^{-/-}$) or Kir 2.2 (Kir2.2 $^{-/-}$) [409, 410]. Although the Kir2.1 $^{-/-}$ mice have cleft palate and die shortly after birth,

thereby precluding electrophysiological studies on adult cells [410], experiments completed on isolated newborn Kir2.1 $^{-/-}$ ventricular myocytes revealed that I_{K1} is absent [409]. Interestingly, however, an inwardly rectifying current, with properties distinct from the wild-type I_{K1} , is evident in Kir2.1 $^{-/-}$ myocytes, suggesting either that an additional Kir current component is present, but difficult to resolve in wild-type cells in the presence of I_{K1} , or, alternatively, that a novel I_{K1} is upregulated in Kir2.1 $^{-/-}$ hearts. In contrast to the findings in Kir2.1 $^{-/-}$ cells, voltage-clamp recordings from adult Kir2.2 $^{-/-}$ ventricular myocytes revealed that I_{K1} densities are reduced, compared with I_{K1} densities in wild-type cells and that the properties of the residual I_{K1} currents (in Kir2.2 $^{-/-}$ cells) are indistinguishable from wild-type I_{K1} [409]. These results were interpreted as suggesting that both Kir2.1 and Kir2.2 contribute to (mouse) ventricular I_{K1} channels, and subsequent studies provided biochemical and molecular evidence to support this hypothesis [411, 412]. The observation that the inwardly rectifying channels remaining in the absence of Kir2.1 have properties distinct from the endogenous I_{K1} channels further suggests that functional cardiac I_{K1} channels are heteromeric. Consistent with this hypothesis, detailed comparisons of the properties of heterologously expressed Kir2.1, Kir2.2, and Kir2.3 α subunits and endogenous guinea pig and sheep atrial and ventricular myocytes suggest marked regional and cell type-specific differences in the molecular composition of I_{K1} channels [166]. Hetero-tetramerization of Kir2.1 channels with wild-type Kir2.2 and Kir2.3 channels in HEK cell or oocytes can present the molecular basis of the extraordinary pleiotropy of Andersen's syndrome [395]. Further studies focused on defining the molecular compositions of myocardial I_{K1} channels in different cell types and in different species, including humans, are needed to define the molecular diversity and the functioning of these channels.

K_{ATP} channels were first identified in cardiac myocytes [145] and later were also found in vascular smooth muscle [413], neuron [414], skeletal muscle, and β cells [415]. K_{ATP} channels

open spontaneously in inside-out patch-clamp experiments, and the opening can be inhibited by ATP and activated by NDP analogs such as ADP [416]. In the heart, weakly inwardly rectifying I_{KATP} channels are thought to play a role in both myocardial ischemia and preconditioning [145, 158, 163]. In heterologous systems, I_{KATP} channels can be reconstituted by co-expression of Kir6.x subunits with ATP-binding cassette proteins that encode the sulfonylurea receptors, SURx, composed with 4 Kir6.x subunits for pore and 4 SURx for auxiliary [417, 418]. Although previous pharmacological and molecular studies suggest that cardiac sarcolemmal I_{KATP} channels reflect the heteromeric assembly of Kir6.2 and SUR2A subunits, Kir6.1 is also expressed in the heart [419], and exposure of isolated (rat neonatal) ventricular myocytes to antisense oligodeoxynucleotides against SUR1 reduces I_{KATP} channel densities [420]. These observations suggest the interesting possibility that there may be some molecular heterogeneity among cardiac I_{KATP} channels. The absolute requirement for the Kir6.2 subunit in the generation of cardiac I_{KATP} channels, however, was unequivocally demonstrated in studies completed on mice in which the Kir6.2 gene was disrupted by homologous recombination [418, 421, 422]. Voltage-clamp recordings from ventricular myocytes isolated from these (Kir6.2^{-/-}) animals revealed no detectable I_{KATP} channel activity [421, 422]. These findings clearly suggest that Kir6.1 alone (i.e., in the absence of Kir6.2) cannot generate functional myocardial I_{KATP} channels. Nevertheless, it is certainly still possible that Kir6.1 coassembles with Kir6.2 to form Kir6.1/Kir 6.2 heteromeric cardiac I_{KATP} channels.

The suggestion that SUR2 plays a pivotal role in the generation of cardiac I_{KATP} channels is supported by the finding that I_{KATP} channel density is reduced in myocytes from animals (SUR2^{-/-}) in which SUR2 has been deleted [423]. In contrast, there are no measurable cardiac effects of the targeted disruption of SUR1 [418, 424]. Nevertheless, it is interesting to note that I_{KATP} channel density is reduced, i.e., the channels are not eliminated, in SUR2^{-/-} ventricular myocytes, and the proper-

ties of the residual I_{KATP} channels in SUR2^{-/-} ventricular myocytes are similar to those of the channels produced on heterologous co-expression of Kir6.2 and SUR1. These findings strongly suggest that SUR1 likely also coassembles with Kir6.2 in ventricular myocytes to produce functional I_{KATP} channels (at least in the absence of SUR2). Immunohistochemical studies suggest that Kir6.2 and SUR2A assemble to form plasma membrane cardiac I_{KATP} channels, whereas Kir6.1, Kir6.2, and SUR2A are expressed in mitochondria. These observations interpreted suggest that the molecular compositions of functional I_{K1} channels in different cellular compartments are distinct [425]. Similar to I_{K1} channels, myocardial I_{KATP} channels are also modulated by the binding of PIP2 and other membrane lipids [398, 400].

The waveforms of action potentials recorded from isolated Kir6.2^{-/-} ventricular myocytes are indistinguishable from those recorded from wild-type cells [422]. These observations clearly suggest that I_{KATP} channels do not play a role in shaping action potential waveforms (in mouse ventricles) under normal physiological conditions. The action potential shortening typically observed in wild-type ventricular cells during ischemia or metabolic blockade, however, is abolished in Kir6.2^{-/-} ventricular cells [422]. In addition, the protective effect of ischemic preconditioning is abolished in Kir6.2^{-/-} hearts [418, 426], and infarct size in Kir6.2^{-/-} animals, with and without preconditioning, is the same [426]. These observations are consistent with the hypothesis that cardiac I_{KATP} channels play an important role under pathophysiological conditions, particularly those involving metabolic stress [90, 427]. Interestingly, however, it has been demonstrated that action potential durations are also largely unaffected in transgenic animals expressing mutant I_{KATP} channels with markedly (40-fold) reduced ATP sensitivity [428]. The mutant I_{KATP} channels would be expected to be open (owing to the reduced sensitivity to closure by ATP) at rest and to markedly affect cardiac membrane excitability. The fact that action potentials are unaffected in ventricular myocytes expressing mutant I_{KATP} channels clearly suggests that additional inhibitory regulatory mechanisms play a role in

the physiological control of cardiac I_{KATP} channel activity in vivo [428]. Further studies focused on defining and characterizing these regulatory mechanisms will be of considerable interest.

Two Pore Domain K^+ Channels

In addition to the many voltage-gated K^+ (Kv) and the inwardly rectifying K^+ (Kir) (Tables 1.4

and 1.6) channel α subunits, a novel type of K^+ α subunit with four transmembrane-spanning domains and two pore domains was identified, with the cloning of TWIK-1, referred to as KCNK1 [429], the first member of the K2P family (Table 1.7). Studies in heterologous systems suggest that functional K2P channels, unlike Kv and Kir channels that assemble as tetramers, assemble as dimers. K2P channels possess three special characteristics compared

Table 1.7 Two-pore K^+ channel α subunits

Family	Subfamily	Protein	Location			Cardiac current
			Gene	Human	Mouse	
Two pore	TWIK		KCNK1	1q42.2	8 E2	??
		TWIK -1	KCNK6	19q13.2	7 B1	
		TWIK -2	TWIK-3	KCNK7	11q13.1	19A
	TREK		KCNK2	1q41	1 H6	Iss??
		TREK -1	KCNK10	14q31.3	12 E	
	TASK		KCNK3	2p23.3	5 B1	Ikp??
		TASK -1	KCNK9	8q24.3	15D3	
		TASK -3	KCNK15	20q13.12	2 H3	
		TASK -5				
	TALK		KCNK16	6p21.2	14	
		TALK -1	KCNK17	6p21.2	8	
		TALK -2	(TASK-4) ^a			
		TASK -2^b	KCNK5	6p21.2	14A3	
	TRAAK		KCNK4	11q13.1	19A	
		TRAAK -1				
	TRESK	TRESK-1	KCNK18	10q25.3	19D3	
	THIK		KCNK13	14q32	12 E	
		THIK -1	KCNK12	2p21	17 E4	
		THIK -2				

Boxes denote cardiac expression

^aTASK2 and TALK4 have been found to be the same protein

^bTASK2 has been found to actually be part of the TALK family

to other potassium channels. (1) Each subunit of K2P channels contributes with two pore-forming domains to the ion pore after being assembled as a dimer. The other potassium channels subunits have only one pore-forming domain. (2) The mechanisms of K2P channel regulation are multiple. Their activity can be regulated by pH, membrane stretch, temperature, or intracellular signaling pathway [430]. (3) K2P channels show a unique extracellular “helical cap” structure between the M1 and M2 domain. This structure could be a potential drug target to treat diseases related to K2P channel dysfunction [431, 432]. Heterologous expression of either of these subunits alone gives rise to instantaneous, noninactivating K^+ currents that display partly voltage dependence [430, 433]. These observations have led to suggestions that these subunits contribute to myocardial “background” or “leak” K^+ currents [434]. Interestingly, however, the properties of the currents produced on expression of TREK-1 or TASK-1 are similar to those of the current referred to as plateau current I_{Kp} identified in guinea pig ventricular myocytes [434, 435], as well as to I_{ss} in mouse ventricular myocytes [60, 436].

The K2P family has 15 members that are subdivided into 6 subfamilies, which are TWIK, TREK, TASK, TALK, THIK, and TWIK-related spinal cord K^+ channels (TRESK), and a subset of these appears to be expressed in the myocardium (Table 1.7). In 1996, the first K2P channel TWIK-1 was identified [429]. In the next 7 years (1996–2003), 14 other K2P members were identified [437]. Similar to the K_v and K_{ir} channels, a systematic terminology has been developed for naming the (KCNK) genes encoding K2P subunits.

Heterologous expression studies have demonstrated that the members of various K2P subunit subfamilies give rise to K^+ -selective currents with distinct time- and voltage-dependent properties and differential sensitivities to a variety of modulators, including pH, membrane stretch, fatty acids, and anesthetics and so on [430, 438]. It seems likely that K2P channels could be important in regulating the normal physiological func-

tioning of the adult mammalian heart, as well as influencing myocardial responses to pathophysiological stimuli. Direct experimental support for this hypothesis was provided with the demonstration that the pathophysiological effects of platelet-activating factor on the myocardium are directly linked to inhibition of KCNK3 (TASK-1)-encoded (or closely related) K^+ channels in ventricular myocytes [439]. The effects of both platelet-activating factor and TASK-1 are dependent on protein kinase C [439, 440]. Although it has been demonstrated that different KCNK-encoded K2P subunits can coassemble to form heterodimer channels [441, 442], it is presently unclear whether heterodimeric K2P subunit assembly is physiologically relevant in the myocardium. Similarly, there is very little information presently available about the role(s) of accessory subunits and/or other regulatory molecules in the generation of K2P subunit-encoded myocardial channels, looks like K2P channels do not need any accessory subunits.

The fact that there are so many K2P α subunits (Table 1.7), that some of them are ubiquitously expressed, and that the properties of K2P channels are regulated by a variety of potentially relevant physiological and pathophysiological stimuli suggests that K2P channels likely subserve a variety of important physiological functions. Experimental support for this hypothesis has been provided by the demonstration that mice bearing a targeted disruption of the KCNK2 gene (TREK-1, Table 1.7) display increased sensitivity to epilepsy and ischemia [443]. It is unclear, however, whether there is a cardiac phenotype in the KCNK2 $^{-/-}$ mice, primarily because this possibility appears not to have been addressed [443]. TREK-1, TALK-2, and TASK-1 are all expressed in the heart [444, 445]. We now know that TASK-1 channel modulation of TASK-1 can alter human atrial action potential duration, suggesting that this channel might be a drug target for the treatment of atrial fibrillation [446]. In our lab, we also discovered loss of function mutation in the KCNK3 gene (TASK-1) in patients with idiopathic and familial PAH [447]. TASK-4 (KCNK17, also named TALK-2) is also expressed in the atrioventricular node and cardiac Purkinje

fibers. Also, a gain of function by TASK-4 in the conduction system has suggested TASK-4 may be a novel arrhythmia gene [448].

Ca²⁺-Activated and Na⁺-Activated K⁺ Channels

Ca²⁺-activated K⁺ channels have three classifications based on their conductance. They are big conductance (BKCa), intermediate conductance (IKCa), and small conductance (SKCa) (Table 1.8) [449].

The first described K⁺ channel found to be sensitive to both Ca²⁺ and transmembrane voltage is a BKCa channel termed the BK channel (big conductance and Ca²⁺-dependent potassium channel). It is a tetramer of α subunit *slo1* (KCNMA1) gene products that assemble to form the channel pore [450, 451]. The BK channel is K_{Ca}1.1 in standard nomenclature [451, 452] and is expressed in cell membranes of most mammalian tissue types [450]. The BK channel may also be modulated by one of four (1–4) β or a γ subunit [450].

Following the discovery of K_{Ca}1.1 (BK), screening for *slo1*(*KCNMA1*) gene (K_{Ca}1.1), other Ca²⁺-dependent K⁺ channels with similar

sequences were discovered [451]. The next two classes were K_{Ca}2 and K_{Ca}3 and were found to be sensitive to Ca²⁺, but unlike K_{Ca}1.1, they are insensitive to membrane voltage. The K_{Ca}2 family has three members K_{Ca}2.1, (SK1) K_{Ca}2.2 (SK2), and K_{Ca}2.3 (SK3) [453]. The K_{Ca}3 family has one member, K_{Ca}3.1 [454, 455]. Two other families of channels, containing three total members, given names K_{Ca}4.1, K_{Ca}4.2, and K_{Ca}5.1, have been identified [451], but it has become evident that these channels are instead regulated by intracellular Na⁺ and Cl⁻ [451, 456–458].

A version of the BK channel known as mitoBKCa has been found to be present in the inner membrane of mitochondria in adult cardiomyocytes [449, 459]. BKCa channels are not believed to be present in the cell membrane of adult cardiomyocytes [449, 459]. The presence of the mitoBKCa channel in the cardiomyocyte mitochondrial inner membrane is believed to be cardioprotective [460]. NS1619, a potent BKCa opener, has been shown to cause a Ca²⁺-induced K⁺ flux that increases ROS production while maintaining membrane potential [461]. MitoBKCa-induced depolarization of the mitochondrial membrane potential has been reported to help stop mitochondrial Ca²⁺ overload, also cardioprotective [462].

Table 1.8 Calcium-activated potassium channel (Kca) pore-forming α subunits

Subfamily	Protein	Gene	Locus			Cardiac current
			Homo	Mus	Rattus	
K _{Ca} 1	K _{Ca} 1.1, BK	<i>KCNMA1</i>	10q22.3	14A3	15p16	
K _{Ca} 2		<i>KCNN1</i>	19p13.11	8B3.3	16p14	<i>I_{K(Ca)}</i>
	K_{Ca}2.1,SK1	<i>KCNN2</i>	5q22.3	18B3-C	18q11	<i>I_{K(Ca)}</i>
	K_{Ca}2.1,SK2	<i>KCNN3</i>	1q21.3	3F1	2q34	<i>I_{K(Ca)}</i>
	K_{Ca}2.1,SK3					
K _{Ca} 3	IK _{Ca} 1, IK	<i>KCNN4</i>	19q13.31	7A3	1q21	
K _{Ca} 4						
	K _{Ca} 4.1, Slack	<i>KCNT1</i>	9q34.3	2A3	3p13	
	K _{Ca} 4.2, Slick	<i>KCNT2</i>	1q31.3	1F	13q21	
K _{Ca} 5						
	K _{Ca} 5.1, Slo3	<i>KCNU1</i>	8p11.23	8A2	16q12.4	

Boxes denote cardiac expression

K_{Ca2} family channels are SKCas (small-conductance apamin-sensitive Ca^{2+} -activated K^+ channels) and have been shown to have a constitutively bound calmodulin that confers the Ca^{2+} sensitivity to the channel α subunit via the calmodulin's Ca^{2+} binding rather than direct Ca^{2+} binding to the α subunit [449, 463]. These channels have been found to be important to modulating cardiac action potential duration via this conferred Ca^{2+} sensitivity [464]. These channels, encoded by the KCNN gene, are responsible for the IKAS current found in cardiac cells, but most prominently in atrial, and not ventricular cells [451].

Demonstrated in mouse cardiomyocytes, SKCa channels are activated by increases in intracellular, cytosolic Ca^{2+} such as via ryanodine receptor 2 (RyR2) release of Ca^{2+} from the sarcoplasmic reticulum [465]. The hyperpolarization that occurs as a result of this Ca^{2+} -activated K^+ current inhibits and slows the firing frequency of repeated action potentials primarily in atrial cells.

Additionally, $K_{Ca4.2}$, also now known as $K_{Na1.2}$, is a Na^+ -sensitive channel found in cardiac cells, among other tissues [451]. It has been proposed that activation of this channel is cardioprotective in mouse [466]. There are no reported human mutations in $K_{Ca4.2}$ ($K_{Na1.2}$), so there is much unknown about its role in human physiology [451].

Summary and Conclusions

Electrophysiological studies have clearly identified multiple types of voltage-gated inward and outward currents that contribute to action potential repolarization in mammalian ventricular myocardium (Table 1.1). Interestingly, the outward currents are more numerous and more diverse than the inward currents, and mammalian ventricular myocytes express a repertoire of voltage-gated and inwardly rectifying K^+ channels (Table 1.1) that all contribute importantly to shaping the waveforms of action potentials, as well as influencing automaticity and refractoriness. Nevertheless, the voltage-gated inward Ca^{2+}

channel currents and the Na^+ channel “window” current [31, 32, 467] also contribute to ventricular repolarization. The pivotal role played by the Na^+ channel “window” current has been elegantly demonstrated in studies characterizing mutations in SCN5A that underlie long QT-3. These studies have revealed novel mechanisms whereby altered Na^+ channel function impacts ventricular action potential durations.

Computer-based simulations of cellular electrical activity have also been helpful in linking altered Na^+ (and other) channel functioning to possible/likely effects on action potential waveforms [190, 210, 211, 468]. The results of these studies demonstrate that subtle changes in Na^+ channel gating can have profound effects on repolarization because the plateau phase of the action potential is maintained by the balance of very small currents, a lesson learned more than 70 years ago from the elegant experiments of Silvio Weidmann [469]. The insights gleaned from the analysis of inherited Na^+ (and other) channel mutations also underscore the importance of the interplay of all of the ionic currents contributing to repolarization in determining ventricular action potential waveforms.

Molecular cloning studies have revealed an unexpected diversity of voltage-gated ion channel pore-forming α -subunits (Tables 1.2, 1.4, 1.6, 1.7, and 1.8) and accessory subunits (Tables 1.3 and 1.5) that contribute to the formation of the various inward and outward current channels (Table 1.1) identified electrophysiologically. Similar to the electrophysiological diversity of ventricular K^+ channels (Table 1.1), the molecular analyses have revealed that multiple voltage-gated (K_v) (Table 1.4) and inwardly rectifying (K_{ir}) (Table 1.6) K^+ channel pore-forming α -subunits, as well as the accessory subunits of these channels (Table 1.5), are expressed in the myocardium. A variety of *in vitro* and *in vivo* experimental approaches have been exploited to probe the relationship(s) between these subunits and functional ventricular K^+ channels. Important insights into these relationships have been provided through molecular genetics and the application of techniques that allow functional channel

expression to be manipulated *in vitro* and *in vivo*. The results of these efforts have led to the identification of the pore-forming α subunits contributing to the formation of most of the K^+ channels expressed in mammalian ventricular myocytes (Tables 1.4, 1.5, and 1.6). In contrast to the progress made in defining the Kv and the Kir α -subunits encoding the functional voltage-gated and inwardly rectifying K^+ currents expressed in mammalian ventricular myocytes, presently very little is known about the functional roles of the two-pore domain K^+ channel α -subunits (Table 1.7). In addition, the roles of the various accessory subunits (Table 1.5) in the generation of functional cardiac K^+ channels remain to be clarified.

It seems reasonable to suggest that defining the molecular correlates/compositions of the channels underlying ventricular action potential repolarization will facilitate future efforts focused on delineating the molecular mechanisms controlling the properties and the functional expression of these channels. Numerous studies have documented changes in functional ion channel expression during normal ventricular development, as well as in damaged or diseased ventricular myocardium. Importantly, it has also been shown that electrical remodeling occurs in the ventricles in response to changes in cardiac electrical activity or cardiac output, and most of the effects observed can be attributed to changes in the expression and/or the properties of the channels underlying ventricular repolarization.

Numerous possible (transcriptional, translational, and posttranslational) mechanisms could be involved in regulating the expression and the properties of the inward and outward current channels underlying repolarization. However, we are just beginning to learn about the underlying molecular mechanisms that are important in mediating the changes in channel expression evident during normal development, as well as in conjunction with myocardial damage, disease, and/or electrical remodeling. Clearly, a major focus of future research will be on exploring these mechanisms in detail.

References

1. Kanno S, Saffitz JE. The role of myocardial gap junctions in electrical conduction and arrhythmogenesis. *Cardiovasc Pathol.* 2001;10(4):169–77.
2. Saez JC, et al. Plasma membrane channels formed by connexins: their regulation and functions. *Physiol Rev.* 2003;83(4):1359–400.
3. Harris AL. Emerging issues of connexin channels: biophysics fills the gap. *Q Rev Biophys.* 2001;34(3):325–472.
4. Nerbonne JM, Kass RS. Molecular physiology of cardiac repolarization. *Physiol Rev.* 2005;85(4):1205–53.
5. Chen-Izu Y, et al. Na^+ channel function, regulation, structure, trafficking and sequestration. *J Physiol.* 2015;593(6):1347–60. PMC4376415.
6. Perez-Reyes E, et al. Cloning and expression of a cardiac/brain beta subunit of the L-type calcium channel. *J Biol Chem.* 1992;267(3):1792–7.
7. Santulli G, Marks AR. Essential roles of intracellular calcium release channels in muscle, brain, metabolism, and aging. *Curr Mol Pharmacol.* 2015;8(2):206–22.
8. Santana LF, Cheng EP, Lederer WJ. How does the shape of the cardiac action potential control calcium signaling and contraction in the heart? *J Mol Cell Cardiol.* 2010;49(6):901–3. PMC3623268.
9. Lodish HF. *Molecular cell biology.* 7th ed. New York: W.H. Freeman and Co; 2013. xxxiii, 1154, 58 p.
10. Page E, et al. The cardiovascular system. In: *The heart. Handbook of physiology, vol. 1.* New York: Published for the American Physiological Society by Oxford University Press; 2002. xi, 822 p.
11. Nerbonne JM. Molecular basis of functional voltage-gated K^+ channel diversity in the mammalian myocardium. *J Physiol.* 2000;525(Pt 2):285–98. PMC2269952.
12. Nerbonne JM, Guo W. Heterogeneous expression of voltage-gated potassium channels in the heart: roles in normal excitation and arrhythmias. *J Cardiovasc Electrophysiol.* 2002;13(4):406–9.
13. Barry DM, Nerbonne JM. Myocardial potassium channels: electrophysiological and molecular diversity. *Annu Rev Physiol.* 1996;58:363–94.
14. Yellen G. The moving parts of voltage-gated ion channels. *Q Rev Biophys.* 1998;31(3):239–95.
15. Hille B. *Ion channels of excitable membranes.* 3rd ed. Sunderland: Sinauer; 2001. xviii, 814 p.
16. DeMarco KR, Clancy CE. Cardiac Na channels: structure to function. *Curr Top Membr.* 2016;78:287–311. PMC5398315.
17. Wetzel GT, Klitzner TS. Developmental cardiac electrophysiology recent advances in cellular physiology. *Cardiovasc Res.* 1996;31 Spec No: E52–60.
18. Benitah JP, et al. Heterogeneity of the early outward current in ventricular cells isolated from normal and

- hypertrophied rat hearts. *J Physiol.* 1993;469:111–38. PMC1143864.
19. Nabauer M, Beuckelmann DJ, Erdmann E. Characteristics of transient outward current in human ventricular myocytes from patients with terminal heart failure. *Circ Res.* 1993;73(2):386–94.
 20. Beuckelmann DJ, Nabauer M, Erdmann E. Alterations of K⁺ currents in isolated human ventricular myocytes from patients with terminal heart failure. *Circ Res.* 1993;73(2):379–85.
 21. Kaab S, et al. Ionic mechanism of action potential prolongation in ventricular myocytes from dogs with pacing-induced heart failure. *Circ Res.* 1996;78(2):262–73.
 22. Potreau D, Gomez JP, Fares N. Depressed transient outward current in single hypertrophied cardiomyocytes isolated from the right ventricle of ferret heart. *Cardiovasc Res.* 1995;30(3):440–8.
 23. Bailly P, et al. Regional alteration of the transient outward current in human left ventricular septum during compensated hypertrophy. *Circulation.* 1997;96(4):1266–74.
 24. Freeman LC, et al. Decreased density of I_{to} in left ventricular myocytes from German shepherd dogs with inherited arrhythmias. *J Cardiovasc Electrophysiol.* 1997;8(8):872–83.
 25. Nabauer M, Kaab S. Potassium channel down-regulation in heart failure. *Cardiovasc Res.* 1998;37(2):324–34.
 26. Gomez AM, et al. Modulation of electrical heterogeneity by compensated hypertrophy in rat left ventricle. *Am J Phys.* 1997;272(3 Pt 2):H1078–86.
 27. Catterall WA. From ionic currents to molecular mechanisms: the structure and function of voltage-gated sodium channels. *Neuron.* 2000;26(1):13–25.
 28. Bennett PB. Long QT syndrome: biophysical and pharmacologic mechanisms in LQT3. *J Cardiovasc Electrophysiol.* 2000;11(7):819–22.
 29. Rivolta I, et al. A novel SCN5A mutation associated with long QT-3: altered inactivation kinetics and channel dysfunction. *Physiol Genomics.* 2002;10(3):191–7.
 30. Wang DW, et al. Characterization of human cardiac Na⁺ channel mutations in the congenital long QT syndrome. *Proc Natl Acad Sci U S A.* 1996;93(23):13200–5. PMC24070.
 31. Attwell D, et al. The steady state TTX-sensitive (“window”) sodium current in cardiac Purkinje fibres. *Pflugers Arch.* 1979;379(2):137–42.
 32. Salata JJ, Wasserstrom JA. Effects of quinidine on action potentials and ionic currents in isolated canine ventricular myocytes. *Circ Res.* 1988;62(2):324–37.
 33. Sakmann BF, et al. Distribution of a persistent sodium current across the ventricular wall in guinea pigs. *Circ Res.* 2000;87(10):910–4.
 34. Catterall WA. Voltage-gated sodium channels at 60: structure, function and pathophysiology. *J Physiol.* 2012;590(11):2577–89. PMC3424717.
 35. Mantegazza M, Catterall WA. Voltage-gated Na⁽⁺⁾ channels: structure, function, and pathophysiology. In: Noebels JL, et al., editors. *Jasper’s basic mechanisms of the epilepsies.* Bethesda: National Center for Biotechnology Information; 2012.
 36. Catterall WA, Goldin AL, Waxman SG. International Union of Pharmacology. XLVII. Nomenclature and structure-function relationships of voltage-gated sodium channels. *Pharmacol Rev.* 2005;57(4):397–409.
 37. Savio-Galimberti E, Gollob MH, Darbar D. Voltage-gated sodium channels: biophysics, pharmacology, and related channelopathies. *Front Pharmacol.* 2012;3:124. PMC3394224.
 38. Ogata N, Ohishi Y. Molecular diversity of structure and function of the voltage-gated Na⁺ channels. *Jpn J Pharmacol.* 2002;88(4):365–77.
 39. Patino GA, Isom LL. Electrophysiology and beyond: multiple roles of Na⁺ channel beta subunits in development and disease. *Neurosci Lett.* 2010;486(2):53–9. PMC2964441.
 40. Herren AW, Bers DM, Grandi E. Post-translational modifications of the cardiac Na channel: contribution of CaMKII-dependent phosphorylation to acquired arrhythmias. *Am J Physiol Heart Circ Physiol.* 2013;305(4):H431–45. PMC3891248.
 41. Marionneau C, Abriel H. Regulation of the cardiac Na⁺ channel Nav1.5 by post-translational modifications. *J Mol Cell Cardiol.* 2015;82:36–47.
 42. Rook MB, et al. Biology of cardiac sodium channel Nav1.5 expression. *Cardiovasc Res.* 2012;93(1):12–23.
 43. Tsien RW, et al. Multiple types of neuronal calcium channels and their selective modulation. *Trends Neurosci.* 1988;11(10):431–8.
 44. Snutch TP, et al. Rat brain expresses a heterogeneous family of calcium channels. *Proc Natl Acad Sci U S A.* 1990;87(9):3391–5. PMC53906.
 45. Birnbaumer L, et al. The naming of voltage-gated calcium channels. *Neuron.* 1994;13(3):505–6.
 46. Ertel EA, et al. Nomenclature of voltage-gated calcium channels. *Neuron.* 2000;25(3):533–5.
 47. Lacinova L. Voltage-dependent calcium channels. *Gen Physiol Biophys.* 2005;24(Suppl 1):1–78.
 48. Catterall WA. Voltage-gated calcium channels. *Cold Spring Harb Perspect Biol.* 2011;3(8):a003947. PMC3140680.
 49. Mikami A, et al. Primary structure and functional expression of the cardiac dihydropyridine-sensitive calcium channel. *Nature.* 1989;340(6230):230–3.
 50. Nowycky MC, Fox AP, Tsien RW. Three types of neuronal calcium channel with different calcium agonist sensitivity. *Nature.* 1985;316(6027):440–3.
 51. Shih HT. Anatomy of the action potential in the heart. *Tex Heart Inst J.* 1994;21(1):30–41. PMC325129.
 52. Niwa N, Nerbonne JM. Molecular determinants of cardiac transient outward potassium current (I_(to)) expression and regulation. *J Mol Cell Cardiol.* 2010;48(1):12–25. PMC2813406.
 53. Kenyon JL, Gibbons WR. Influence of chloride, potassium, and tetraethylammonium on the early outward current of sheep cardiac Purkinje fibers. *J Gen Physiol.* 1979;73(2):117–38. PMC2215241.

54. Coraboeuf E, Carmeliet E. Existence of two transient outward currents in sheep cardiac Purkinje fibers. *Pflugers Arch.* 1982;392(4):352–9.
55. Kenyon JL, Gibbons WR. 4-Aminopyridine and the early outward current of sheep cardiac Purkinje fibers. *J Gen Physiol.* 1979;73(2):139–57. PMC2215238.
56. Zygmunt AC, Gibbons WR. Calcium-activated chloride current in rabbit ventricular myocytes. *Circ Res.* 1991;68(2):424–37.
57. Campbell DL, et al. The calcium-independent transient outward potassium current in isolated ferret right ventricular myocytes. I. Basic characterization and kinetic analysis. *J Gen Physiol.* 1993;101(4):571–601. PMC2216777.
58. Nerbonne JM. Regulation of voltage-gated K⁺ channel expression in the developing mammalian myocardium. *J Neurobiol.* 1998;37(1):37–59.
59. Brahmajothi MV, et al. Distinct transient outward potassium current (I_{to}) phenotypes and distribution of fast-inactivating potassium channel alpha subunits in ferret left ventricular myocytes. *J Gen Physiol.* 1999;113(4):581–600. PMC2217167.
60. Xu H, Guo W, Nerbonne JM. Four kinetically distinct depolarization-activated K⁺ currents in adult mouse ventricular myocytes. *J Gen Physiol.* 1999;113(5):661–78. PMC2222908.
61. Guo W, et al. Molecular basis of transient outward K⁺ current diversity in mouse ventricular myocytes. *J Physiol.* 1999;521(Pt 3):587–99. PMC2269690.
62. Guo W, et al. Functional consequences of elimination of i_(to,f) and i_(to,s): early afterdepolarizations, atrioventricular block, and ventricular arrhythmias in mice lacking Kv1.4 and expressing a dominant-negative Kv4 alpha subunit. *Circ Res.* 2000;87(1):73–9.
63. Furukawa T, et al. Differences in transient outward currents of feline endocardial and epicardial myocytes. *Circ Res.* 1990;67(5):1287–91.
64. Litovsky SH, Antzelevitch C. Transient outward current prominent in canine ventricular epicardium but not endocardium. *Circ Res.* 1988;62(1):116–26.
65. Tseng GN, Hoffman BF. Two components of transient outward current in canine ventricular myocytes. *Circ Res.* 1989;64(4):633–47.
66. Wettwer E, et al. Transient outward current in human and rat ventricular myocytes. *Cardiovasc Res.* 1993;27(9):1662–9.
67. Wettwer E, et al. Transient outward current in human ventricular myocytes of subepicardial and subendocardial origin. *Circ Res.* 1994;75(3):473–82.
68. Konarzewska H, Peeters GA, Sanguinetti MC. Repolarizing K⁺ currents in nonfailing human hearts. Similarities between right septal subendocardial and left subepicardial ventricular myocytes. *Circulation.* 1995;92(5):1179–87.
69. Benndorf K, Markwardt F, Nilius B. Two types of transient outward currents in cardiac ventricular cells of mice. *Pflugers Arch.* 1987;409(6):641–3.
70. Benndorf K, Nilius B. Properties of an early outward current in single cells of the mouse ventricle. *Gen Physiol Biophys.* 1988;7(5):449–66.
71. Xu H, et al. Attenuation of the slow component of delayed rectification, action potential prolongation, and triggered activity in mice expressing a dominant-negative Kv2 alpha subunit. *Circ Res.* 1999;85(7):623–33.
72. Apkon M, Nerbonne JM. Characterization of two distinct depolarization-activated K⁺ currents in isolated adult rat ventricular myocytes. *J Gen Physiol.* 1991;97(5):973–1011. PMC2216507.
73. Inoue M, Imanaga I. Masking of A-type K⁺ channel in guinea pig cardiac cells by extracellular Ca²⁺. *Am J Phys.* 1993;264(6 Pt 1):C1434–8.
74. Yue L, et al. Transient outward and delayed rectifier currents in canine atrium: properties and role of isolation methods. *Am J Phys.* 1996;270(6 Pt 2):H2157–68.
75. Sanguinetti MC, et al. Heteropodatoxins: peptides isolated from spider venom that block Kv4.2 potassium channels. *Mol Pharmacol.* 1997;51(3):491–8.
76. Giles WR, Imaizumi Y. Comparison of potassium currents in rabbit atrial and ventricular cells. *J Physiol.* 1988;405:123–45. PMC1190968.
77. Fedida D, Giles WR. Regional variations in action potentials and transient outward current in myocytes isolated from rabbit left ventricle. *J Physiol.* 1991;442:191–209. PMC1179885.
78. Wang Z, et al. Potential molecular basis of different physiological properties of the transient outward K⁺ current in rabbit and human atrial myocytes. *Circ Res.* 1999;84(5):551–61.
79. Dixon JE, et al. Role of the Kv4.3 K⁺ channel in ventricular muscle. A molecular correlate for the transient outward current. *Circ Res.* 1996;79(4):659–68.
80. Gaborit N, et al. Regional and tissue specific transcript signatures of ion channel genes in the non-diseased human heart. *J Physiol.* 2007;582(Pt 2):675–93. PMC2075332.
81. Zhu XR, et al. Characterization of human Kv4.2 mediating a rapidly-inactivating transient voltage-sensitive K⁺ current. *Receptors Channels.* 1999;6(5):387–400.
82. Kong W, et al. Isolation and characterization of the human gene encoding I_{to}: further diversity by alternative mRNA splicing. *Am J Phys.* 1998;275(6 Pt 2):H1963–70.
83. Dixon JE, McKinnon D. Quantitative analysis of potassium channel mRNA expression in atrial and ventricular muscle of rats. *Circ Res.* 1994;75(2):252–60.
84. Marionneau C, et al. Specific pattern of ionic channel gene expression associated with pacemaker activity in the mouse heart. *J Physiol.* 2005;562(Pt 1):223–34. PMC1665484.
85. Wickenden AD, et al. Regional contributions of Kv1.4, Kv4.2, and Kv4.3 to transient outward K⁺ current in rat ventricle. *Am J Phys.* 1999;276(5 Pt 2):H1599–607.
86. Tseng-Crank JC, et al. Molecular cloning and functional expression of a potassium channel cDNA isolated from a rat cardiac library. *FEBS Lett.* 1990;268(1):63–8.

87. Comer MB, et al. Cloning and characterization of an Ito-like potassium channel from ferret ventricle. *Am J Phys.* 1994;267(4 Pt 2):H1383–95.
88. Po S, et al. Functional expression of an inactivating potassium channel cloned from human heart. *Circ Res.* 1992;71(3):732–6.
89. Liu DW, Antzelevitch C. Characteristics of the delayed rectifier current (IKr and IKs) in canine ventricular epicardial, midmyocardial, and endocardial myocytes. A weaker IKs contributes to the longer action potential of the M cell. *Circ Res.* 1995;76(3):351–65.
90. Yue L, et al. Characterization of an ultrarapid delayed rectifier potassium channel involved in canine atrial repolarization. *J Physiol.* 1996;496(Pt 3):647–62. PMC1160853.
91. Follmer CH, Colatsky TJ. Block of delayed rectifier potassium current, IK, by flecainide and E-4031 in cat ventricular myocytes. *Circulation.* 1990;82(1):289–93.
92. Furukawa T, et al. Potassium rectifier currents differ in myocytes of endocardial and epicardial origin. *Circ Res.* 1992;70(1):91–103.
93. Hume JR, Uehara A. Ionic basis of the different action potential configurations of single guinea-pig atrial and ventricular myocytes. *J Physiol.* 1985;368:525–44. PMC1192613.
94. Balsler JR, Bennett PB, Roden DM. Time-dependent outward current in guinea pig ventricular myocytes. Gating kinetics of the delayed rectifier. *J Gen Physiol.* 1990;96(4):835–63. PMC2229010.
95. Horie M, Hayashi S, Kawai C. Two types of delayed rectifying K⁺ channels in atrial cells of guinea pig heart. *Jpn J Physiol.* 1990;40(4):479–90.
96. Sanguinetti MC, Jurkiewicz NK. Delayed rectifier outward K⁺ current is composed of two currents in guinea pig atrial cells. *Am J Phys.* 1991;260(2 Pt 2):H393–9.
97. Walsh KB, et al. Delayed-rectifier potassium channel activity in isolated membrane patches of guinea pig ventricular myocytes. *Am J Phys.* 1991;260(4 Pt 2):H1390–3.
98. Anumonwo JM, et al. Delayed rectification in single cells isolated from guinea pig sinoatrial node. *Am J Phys.* 1992;262(3 Pt 2):H921–5.
99. Freeman LC, Kass RS. Delayed rectifier potassium channels in ventricle and sinoatrial node of the guinea pig: molecular and regulatory properties. *Cardiovasc Drugs Ther.* 1993;7(Suppl 3):627–35.
100. Wang Z, Fermi B, Nattel S. Rapid and slow components of delayed rectifier current in human atrial myocytes. *Cardiovasc Res.* 1994;28(10):1540–6.
101. Li GR, et al. Evidence for two components of delayed rectifier K⁺ current in human ventricular myocytes. *Circ Res.* 1996;78(4):689–96.
102. Fiset C, et al. A rapidly activating sustained K⁺ current modulates repolarization and excitation-contraction coupling in adult mouse ventricle. *J Physiol.* 1997;504(Pt 3):557–63. PMC1159960.
103. Zhou J, et al. Characterization of a slowly inactivating outward current in adult mouse ventricular myocytes. *Circ Res.* 1998;83(8):806–14.
104. Shibasaki T. Conductance and kinetics of delayed rectifier potassium channels in nodal cells of the rabbit heart. *J Physiol.* 1987;387:227–50. PMC1192502.
105. Veldkamp MW, van Ginneken AC, Bouman LN. Single delayed rectifier channels in the membrane of rabbit ventricular myocytes. *Circ Res.* 1993;72(4):865–78.
106. Boyle WA, Nerbonne JM. Two functionally distinct 4-aminopyridine-sensitive outward K⁺ currents in rat atrial myocytes. *J Gen Physiol.* 1992;100(6):1041–67. PMC2229143.
107. Pond AL, et al. Expression of distinct ERG proteins in rat, mouse, and human heart. Relation to functional I(Kr) channels. *J Biol Chem.* 2000;275(8):5997–6006.
108. Sanguinetti MC, Jurkiewicz NK. Two components of cardiac delayed rectifier K⁺ current. Differential sensitivity to block by class III antiarrhythmic agents. *J Gen Physiol.* 1990;96(1):195–215. PMC2228985.
109. Chen L, Sampson KJ, Kass RS. Cardiac delayed rectifier potassium channels in health and disease. *Card Electrophysiol Clin.* 2016;8(2):307–22. PMC4893812.
110. Busch AE, et al. The novel class III antiarrhythmics NE-10064 and NE-10133 inhibit I_{sK} channels expressed in *Xenopus* oocytes and I_{Ks} in guinea pig cardiac myocytes. *Biochem Biophys Res Commun.* 1994;202(1):265–70.
111. Wang Z, Fermi B, Nattel S. Sustained depolarization-induced outward current in human atrial myocytes. Evidence for a novel delayed rectifier K⁺ current similar to Kv1.5 cloned channel currents. *Circ Res.* 1993;73(6):1061–76.
112. Wang Z, Fermi B, Nattel S. Delayed rectifier outward current and repolarization in human atrial myocytes. *Circ Res.* 1993;73(2):276–85.
113. Salata JJ, et al. IK of rabbit ventricle is composed of two currents: evidence for I_{Ks}. *Am J Phys.* 1996;271(6 Pt 2):H2477–89.
114. Vandenberg JI, et al. hERG K(+) channels: structure, function, and clinical significance. *Physiol Rev.* 2012;92(3):1393–478.
115. Feng J, et al. Ultrarapid delayed rectifier current inactivation in human atrial myocytes: properties and consequences. *Am J Phys.* 1998;275(5 Pt 2):H1717–25.
116. Ravens U, Wettwer E. Ultra-rapid delayed rectifier channels: molecular basis and therapeutic implications. *Cardiovasc Res.* 2011;89(4):776–85.
117. Tamkun MM, et al. Molecular cloning and characterization of two voltage-gated K⁺ channel cDNAs from human ventricle. *FASEB J.* 1991;5(3):331–7.
118. Fedida D, et al. Identity of a novel delayed rectifier current from human heart with a cloned K⁺ channel current. *Circ Res.* 1993;73(1):210–6.
119. Wang J, et al. Hypoxia inhibits gene expression of voltage-gated K⁺ channel alpha subunits in

- pulmonary artery smooth muscle cells. *J Clin Invest.* 1997;100(9):2347–53. PMC508432.
120. Swanson R, et al. Cloning and expression of cDNA and genomic clones encoding three delayed rectifier potassium channels in rat brain. *Neuron.* 1990;4(6):929–39.
 121. Matsubara H, et al. Pretranslational mechanisms determine the type of potassium channels expressed in the rat skeletal and cardiac muscles. *J Biol Chem.* 1991;266(20):13324–8.
 122. Mays DJ, et al. Localization of the Kv1.5 K⁺ channel protein in explanted cardiac tissue. *J Clin Invest.* 1995;96(1):282–92. PMC185199.
 123. Xu H, et al. Developmental analysis reveals mismatches in the expression of K⁺ channel alpha subunits and voltage-gated K⁺ channel currents in rat ventricular myocytes. *J Gen Physiol.* 1996;108(5):405–19. PMC2229349.
 124. London B, et al. Long QT and ventricular arrhythmias in transgenic mice expressing the N terminus and first transmembrane segment of a voltage-gated potassium channel. *Proc Natl Acad Sci U S A.* 1998;95(6):2926–31. PMC19671.
 125. Kilborn MJ, Fedida D. A study of the developmental changes in outward currents of rat ventricular myocytes. *J Physiol.* 1990;430:37–60. PMC1181726.
 126. Jeck CD, Boyden PA. Age-related appearance of outward currents may contribute to developmental differences in ventricular repolarization. *Circ Res.* 1992;71(6):1390–403.
 127. Nuss HB, Marban E. Electrophysiological properties of neonatal mouse cardiac myocytes in primary culture. *J Physiol.* 1994;479(Pt 2):265–79. PMC1155745.
 128. Wahler GM, et al. Time course of postnatal changes in rat heart action potential and in transient outward current is different. *Am J Phys.* 1994;267(3 Pt 2):H1157–66.
 129. Sanchez-Chapula J, et al. Differences in outward currents between neonatal and adult rabbit ventricular cells. *Am J Phys.* 1994;266(3 Pt 2):H1184–94.
 130. Guo W, Kamiya K, Toyama J. Modulated expression of transient outward current in cultured neonatal rat ventricular myocytes: comparison with development in situ. *Cardiovasc Res.* 1996;32(3):524–33.
 131. Guo W, Kamiya K, Toyama J. Roles of the voltage-gated K⁺ channel subunits, Kv 1.5 and Kv 1.4, in the developmental changes of K⁺ currents in cultured neonatal rat ventricular cells. *Pflugers Arch.* 1997;434(2):206–8.
 132. Shimoni Y, et al. Thyroid hormone regulates postnatal expression of transient K⁺ channel isoforms in rat ventricle. *J Physiol.* 1997;500(Pt 1):65–73. PMC1159359.
 133. Wang L, Duff HJ. Developmental changes in transient outward current in mouse ventricle. *Circ Res.* 1997;81(1):120–7.
 134. Wickenden AD, et al. Effects of development and thyroid hormone on K⁺ currents and K⁺ channel gene expression in rat ventricle. *J Physiol.* 1997;504(Pt 2):271–86. PMC1159909.
 135. Petersen KR, Nerbonne JM. Expression environment determines K⁺ current properties: Kv1 and Kv4 alpha-subunit-induced K⁺ currents in mammalian cell lines and cardiac myocytes. *Pflugers Arch.* 1999;437(3):381–92.
 136. Fermini B, et al. Differences in rate dependence of transient outward current in rabbit and human atrium. *Am J Phys.* 1992;263(6 Pt 2):H1747–54.
 137. Davies MP, et al. Developmental changes in ionic channel activity in the embryonic murine heart. *Circ Res.* 1996;78(1):15–25.
 138. Wang L, et al. Developmental changes in the delayed rectifier K⁺ channels in mouse heart. *Circ Res.* 1996;79(1):79–85.
 139. Liu DW, Gintant GA, Antzelevitch C. Ionic bases for electrophysiological distinctions among epicardial, midmyocardial, and endocardial myocytes from the free wall of the canine left ventricle. *Circ Res.* 1993;72(3):671–87.
 140. Clark RB, et al. Heterogeneity of action potential waveforms and potassium currents in rat ventricle. *Cardiovasc Res.* 1993;27(10):1795–9.
 141. Bryant SM, et al. Regional differences in the delayed rectifier current (IKr and IKs) contribute to the differences in action potential duration in basal left ventricular myocytes in guinea-pig. *Cardiovasc Res.* 1998;40(2):322–31.
 142. Main MC, Bryant SM, Hart G. Regional differences in action potential characteristics and membrane currents of guinea-pig left ventricular myocytes. *Exp Physiol.* 1998;83(6):747–61.
 143. Lopatin AN, Nichols CG. Inward rectifiers in the heart: an update on I(K1). *J Mol Cell Cardiol.* 2001;33(4):625–38.
 144. Isomoto S, Kondo C, Kurachi Y. Inwardly rectifying potassium channels: their molecular heterogeneity and function. *Jpn J Physiol.* 1997;47(1):11–39.
 145. Noma A. ATP-regulated K⁺ channels in cardiac muscle. *Nature.* 1983;305(5930):147–8.
 146. Gu M, et al. Small-conductance Ca(2+)-activated K(+) channels: insights into their roles in cardiovascular disease. *Exp Mol Med.* 2018;50(4):23. PMC5938042.
 147. Schumacher MA, et al. Structure of the gating domain of a Ca2+-activated K+ channel complexed with Ca2+/calmodulin. *Nature.* 2001;410(6832):1120–4.
 148. Tuteja D, et al. Differential expression of small-conductance Ca2+-activated K+ channels SK1, SK2, and SK3 in mouse atrial and ventricular myocytes. *Am J Physiol Heart Circ Physiol.* 2005;289(6):H2714–23.
 149. Nattel S, Qi XY. Calcium-dependent potassium channels in the heart: clarity and confusion. *Cardiovasc Res.* 2014;101(2):185–6.
 150. Zipes DP, Jalife J, Stevenson WG. *Cardiac electrophysiology: from cell to bedside.* 7th ed. Philadelphia: Elsevier; 2018.
 151. Mahida S, et al. Overexpression of KCNN3 results in sudden cardiac death. *Cardiovasc Res.* 2014;101(2):326–34. PMC3896252.

152. Olesen MS, et al. Screening of KCNN3 in patients with early-onset lone atrial fibrillation. *Europace*. 2011;13(7):963–7.
153. Kurachi Y. G protein regulation of cardiac muscarinic potassium channel. *Am J Phys*. 1995;269(4 Pt 1):C821–30.
154. Yamada H, et al. Acetylcholine triggers L-glutamate exocytosis via nicotinic receptors and inhibits melatonin synthesis in rat pinealocytes. *J Neurosci*. 1998;18(13):4946–52.
155. Ravens U, Dobrev D. Cardiac sympathetic innervation and control of potassium channel function. *J Mol Cell Cardiol*. 2003;35(2):137–9.
156. Wickman K, et al. Abnormal heart rate regulation in GIRK4 knockout mice. *Neuron*. 1998;20(1):103–14.
157. Kovoor P, et al. Evaluation of the role of I(KACh) in atrial fibrillation using a mouse knockout model. *J Am Coll Cardiol*. 2001;37(8):2136–43.
158. Isomoto S, et al. Molecular aspects of ATP-sensitive K⁺ channels in the cardiovascular system. *Jpn J Physiol*. 1997;47(Suppl 1):S5–6.
159. Findlay I. The ATP sensitive potassium channel of cardiac muscle and action potential shortening during metabolic stress. *Cardiovasc Res*. 1994;28(6):760–1.
160. Downey JM. Ischemic preconditioning Nature's own cardioprotective intervention. *Trends Cardiovasc Med*. 1992;2(5):170–6.
161. Grover GJ, Garlid KD. ATP-sensitive potassium channels: a review of their cardioprotective pharmacology. *J Mol Cell Cardiol*. 2000;32(4):677–95.
162. Shaw RM, Rudy Y. Ionic mechanisms of propagation in cardiac tissue. Roles of the sodium and L-type calcium currents during reduced excitability and decreased gap junction coupling. *Circ Res*. 1997;81(5):727–41.
163. Nichols CG, Lopatin AN. Inward rectifier potassium channels. *Annu Rev Physiol*. 1997;59:171–91.
164. Heidbuchel H, Vereecke J, Carmeliet E. Three different potassium channels in human atrium. Contribution to the basal potassium conductance. *Circ Res*. 1990;66(5):1277–86.
165. Varro A, Nanasi PP, Lathrop DA. Potassium currents in isolated human atrial and ventricular cardiocytes. *Acta Physiol Scand*. 1993;149(2):133–42.
166. Dhamoon AS, et al. Unique Kir2.X properties determine regional and species differences in the cardiac inward rectifier K⁺ current. *Circ Res*. 2004;94(10):1332–9.
167. Noma A, et al. Resting K conductances in pacemaker and non-pacemaker heart cells of the rabbit. *Jpn J Physiol*. 1984;34(2):245–54.
168. Shimoni Y, Clark RB, Giles WR. Role of an inwardly rectifying potassium current in rabbit ventricular action potential. *J Physiol*. 1992;448:709–27. PMC1176224.
169. Vandenberg CA. Inward rectification of a potassium channel in cardiac ventricular cells depends on internal magnesium ions. *Proc Natl Acad Sci U S A*. 1987;84(8):2560–4. PMC304694.
170. Mazzanti M, DiFrancesco D. Intracellular Ca modulates K-inward rectification in cardiac myocytes. *Pflugers Arch*. 1989;413(3):322–4.
171. Ficker E, et al. Spermine and spermidine as gating molecules for inward rectifier K⁺ channels. *Science*. 1994;266(5187):1068–72.
172. Lopatin AN, Makhina EN, Nichols CG. Potassium channel block by cytoplasmic polyamines as the mechanism of intrinsic rectification. *Nature*. 1994;372(6504):366–9.
173. Zimmer T, Haufe V, Blechschmidt S. Voltage-gated sodium channels in the mammalian heart. *Glob Cardiol Sci Pract*. 2014;2014(4):449–63. PMC4355518.
174. Fozzard HA, Hanck DA. Structure and function of voltage-dependent sodium channels: comparison of brain II and cardiac isoforms. *Physiol Rev*. 1996;76(3):887–926.
175. Rogart RB, et al. Molecular cloning of a putative tetrodotoxin-resistant rat heart Na⁺ channel isoform. *Proc Natl Acad Sci U S A*. 1989;86(20):8170–4. PMC298237.
176. Guy HR, Seetharamulu P. Molecular model of the action potential sodium channel. *Proc Natl Acad Sci U S A*. 1986;83(2):508–12. PMC322889.
177. Patton DE, et al. Amino acid residues required for fast Na⁽⁺⁾-channel inactivation: charge neutralizations and deletions in the III-IV linker. *Proc Natl Acad Sci U S A*. 1992;89(22):10905–9. PMC50451.
178. Catterall WA. Molecular mechanisms of inactivation and modulation of sodium channels. *Ren Physiol Biochem*. 1994;17(3–4):121–5.
179. Vassilev PM, Scheuer T, Catterall WA. Identification of an intracellular peptide segment involved in sodium channel inactivation. *Science*. 1988;241(4873):1658–61.
180. Vassilev P, Scheuer T, Catterall WA. Inhibition of inactivation of single sodium channels by a site-directed antibody. *Proc Natl Acad Sci U S A*. 1989;86(20):8147–51. PMC298232.
181. West JW, et al. A cluster of hydrophobic amino acid residues required for fast Na⁽⁺⁾-channel inactivation. *Proc Natl Acad Sci U S A*. 1992;89(22):10910–4. PMC50452.
182. Stuhmer W, et al. Structural parts involved in activation and inactivation of the sodium channel. *Nature*. 1989;339(6226):597–603.
183. Rohl CA, et al. Solution structure of the sodium channel inactivation gate. *Biochemistry*. 1999;38(3):855–61.
184. Pan X, et al. Structure of the human voltage-gated sodium channel Nav1.4 in complex with beta1. *Science*. 2018;362(6412):eaau2486.
185. Yan Z, et al. Structure of the Nav1.4-beta1 complex from electric eel. *Cell*. 2017;170(3):470–482. e11.
186. McPhee JC, et al. A critical role for transmembrane segment IVS6 of the sodium channel alpha subunit in fast inactivation. *J Biol Chem*. 1995;270(20):12025–34.

187. McPhee JC, et al. A critical role for the S4-S5 intracellular loop in domain IV of the sodium channel alpha-subunit in fast inactivation. *J Biol Chem.* 1998;273(2):1121–9.
188. Bennett PB, et al. Molecular mechanism for an inherited cardiac arrhythmia. *Nature.* 1995;376(6542):683–5.
189. Clancy CE, Rudy Y. Linking a genetic defect to its cellular phenotype in a cardiac arrhythmia. *Nature.* 1999;400(6744):566–9.
190. Nuyens D, et al. Abrupt rate accelerations or premature beats cause life-threatening arrhythmias in mice with long-QT3 syndrome. *Nat Med.* 2001;7(9):1021–7.
191. Balser JR. Inherited sodium channelopathies: models for acquired arrhythmias? *Am J Physiol Heart Circ Physiol.* 2002;282(4):H1175–80.
192. Keating MT, Sanguinetti MC. Molecular and cellular mechanisms of cardiac arrhythmias. *Cell.* 2001;104(4):569–80.
193. Kambouris NG, et al. A revised view of cardiac sodium channel “blockade” in the long-QT syndrome. *J Clin Invest.* 2000;105(8):1133–40. PMC300835.
194. Viswanathan PC, et al. Gating-dependent mechanisms for flecainide action in SCN5A-linked arrhythmia syndromes. *Circulation.* 2001;104(10):1200–5.
195. Abriel H, et al. Molecular pharmacology of the sodium channel mutation D1790G linked to the long-QT syndrome. *Circulation.* 2000;102(8):921–5.
196. Benhorin J, et al. Effects of flecainide in patients with new SCN5A mutation: mutation-specific therapy for long-QT syndrome? *Circulation.* 2000;101(14):1698–706.
197. Liu H, et al. Channel openings are necessary but not sufficient for use-dependent block of cardiac Na(+) channels by flecainide: evidence from the analysis of disease-linked mutations. *J Gen Physiol.* 2002;120(1):39–51. PMC2311398.
198. Benhorin J, et al. Evidence of genetic heterogeneity in the long QT syndrome. *Science.* 1993;260(5116):1960–2.
199. Moss AJ, Robinson JL. The long-QT syndrome genetic considerations. *Trends Cardiovasc Med.* 1992;2(3):81–3.
200. Cormier JW, et al. Secondary structure of the human cardiac Na+ channel C terminus: evidence for a role of helical structures in modulation of channel inactivation. *J Biol Chem.* 2002;277(11):9233–41.
201. Bezzina C, et al. A single Na(+) channel mutation causing both long-QT and Brugada syndromes. *Circ Res.* 1999;85(12):1206–13.
202. Wei J, et al. Congenital long-QT syndrome caused by a novel mutation in a conserved acidic domain of the cardiac Na+ channel. *Circulation.* 1999;99(24):3165–71.
203. Veldkamp MW, et al. Two distinct congenital arrhythmias evoked by a multidysfunctional Na(+) channel. *Circ Res.* 2000;86(9):E91–7.
204. Rivolta I, et al. Inherited Brugada and long QT-3 syndrome mutations of a single residue of the cardiac sodium channel confer distinct channel and clinical phenotypes. *J Biol Chem.* 2001;276(33):30623–30.
205. Benhorin J, et al. Identification of a new SCN5A mutation, D1840G, associated with the long QT syndrome. Mutations in brief no. 153. *Online. Hum Mutat.* 1998;12(1):72.
206. An RH, et al. Novel LQT-3 mutation affects Na+ channel activity through interactions between alpha- and beta1-subunits. *Circ Res.* 1998;83(2):141–6.
207. Baroudi G, Chahine M. Biophysical phenotypes of SCN5A mutations causing long QT and Brugada syndromes. *FEBS Lett.* 2000;487(2):224–8.
208. Wehrens XH, et al. Arrhythmogenic mechanism of an LQT-3 mutation of the human heart Na(+) channel alpha-subunit: a computational analysis. *Circulation.* 2000;102(5):584–90.
209. Abriel H, et al. Novel arrhythmogenic mechanism revealed by a long-QT syndrome mutation in the cardiac Na(+) channel. *Circ Res.* 2001;88(7):740–5.
210. Luo CH, Rudy Y. A dynamic model of the cardiac ventricular action potential. I. Simulations of ionic currents and concentration changes. *Circ Res.* 1994;74(6):1071–96.
211. Luo CH, Rudy Y. A dynamic model of the cardiac ventricular action potential. II. Afterdepolarizations, triggered activity, and potentiation. *Circ Res.* 1994;74(6):1097–113.
212. Wedekind H, et al. De novo mutation in the SCN5A gene associated with early onset of sudden infant death. *Circulation.* 2001;104(10):1158–64.
213. Isom LL, De Jongh KS, Catterall WA. Auxiliary subunits of voltage-gated ion channels. *Neuron.* 1994;12(6):1183–94.
214. Isom LL, et al. Primary structure and functional expression of the beta 1 subunit of the rat brain sodium channel. *Science.* 1992;256(5058):839–42.
215. Makita N, et al. Genomic organization and chromosomal assignment of the human voltage-gated Na+ channel beta 1 subunit gene (SCN1B). *Genomics.* 1994;23(3):628–34.
216. Qin N, et al. Molecular cloning and functional expression of the human sodium channel beta1B subunit, a novel splicing variant of the beta1 subunit. *Eur J Biochem.* 2003;270(23):4762–70.
217. Isom LL, et al. Structure and function of the beta 2 subunit of brain sodium channels, a transmembrane glycoprotein with a CAM motif. *Cell.* 1995;83(3):433–42.
218. Jones JM, Meisler MH, Isom LL. Scn2b, a voltage-gated sodium channel beta2 gene on mouse chromosome 9. *Genomics.* 1996;34(2):258–9.
219. Morgan K, et al. beta 3: an additional auxiliary subunit of the voltage-sensitive sodium channel that modulates channel gating with distinct kinetics. *Proc Natl Acad Sci U S A.* 2000;97(5):2308–13. PMC15797.

220. Yu FH, et al. Sodium channel beta4, a new disulfide-linked auxiliary subunit with similarity to beta2. *J Neurosci.* 2003;23(20):7577–85.
221. O'Malley HA, Isom LL. Sodium channel beta subunits: emerging targets in channelopathies. *Annu Rev Physiol.* 2015;77:481–504. PMC4817109.
222. Kazen-Gillespie KA, et al. Cloning, localization, and functional expression of sodium channel beta1A subunits. *J Biol Chem.* 2000;275(2):1079–88.
223. Patino GA, et al. Voltage-gated Na⁺ channel beta1B: a secreted cell adhesion molecule involved in human epilepsy. *J Neurosci.* 2011;31(41):14577–91. PMC3212034.
224. Makita N, Bennett PB, George AL Jr. Molecular determinants of beta 1 subunit-induced gating modulation in voltage-dependent Na⁺ channels. *J Neurosci.* 1996;16(22):7117–27.
225. Fahmi AI, et al. The sodium channel beta-subunit SCN3b modulates the kinetics of SCN5a and is expressed heterogeneously in sheep heart. *J Physiol.* 2001;537(Pt 3):693–700. PMC2278985.
226. Dhar Malhotra J, et al. Characterization of sodium channel alpha- and beta-subunits in rat and mouse cardiac myocytes. *Circulation.* 2001;103(9):1303–10.
227. Santana LF, Gomez AM, Lederer WJ. Ca²⁺ flux through promiscuous cardiac Na⁺ channels: slip-mode conductance. *Science.* 1998;279(5353):1027–33.
228. Catterall WA. Functional subunit structure of voltage-gated calcium channels. *Science.* 1991;253(5027):1499–500.
229. Catterall WA. Structure and regulation of voltage-gated Ca²⁺ channels. *Annu Rev Cell Dev Biol.* 2000;16:521–55.
230. Perez-Reyes E, Schneider T. Calcium channels: structure, function, and classification. *Drug Dev Res.* 1994;33(3):295–318.
231. Hofmann F, et al. L-type Ca_v1.2 calcium channels: from in vitro findings to in vivo function. *Physiol Rev.* 2014;94(1):303–26.
232. Wu J, et al. Structure of the voltage-gated calcium channel Ca_v(v)1.1 at 3.6 Å resolution. *Nature.* 2016;537(7619):191–6.
233. Wu J, et al. Structure of the voltage-gated calcium channel Cav1.1 complex. *Science.* 2015;350(6267):aad2395.
234. Whicher JR, MacKinnon R. Structure of the voltage-gated K⁽⁺⁾ channel Eag1 reveals an alternative voltage sensing mechanism. *Science.* 2016;353(6300):664–9. PMC5477842.
235. Wang W, MacKinnon R. Cryo-EM structure of the open human ether-a-go-go-related K⁽⁺⁾ channel hERG. *Cell.* 2017;169(3):422–430. e10. PMC5484391.
236. Benarroch EE. Neuronal voltage-gated calcium channels: brief overview of their function and clinical implications in neurology. *Neurology.* 2010;74(16):1310–5.
237. Halling DB, Aracena-Parks P, Hamilton SL. Regulation of voltage-gated Ca²⁺ channels by calmodulin. *Sci STKE.* 2006;2006(318):er1.
238. Jensen MO, et al. Mechanism of voltage gating in potassium channels. *Science.* 2012;336(6078):229–33.
239. Mesirca P, Torrente AG, Mangoni ME. Functional role of voltage gated Ca(2+) channels in heart automaticity. *Front Physiol.* 2015;6:19. PMC4313592.
240. Ono K, Iijima T. Cardiac T-type Ca(2+) channels in the heart. *J Mol Cell Cardiol.* 2010;48(1):65–70.
241. Bohn G, et al. Expression of T- and L-type calcium channel mRNA in murine sinoatrial node. *FEBS Lett.* 2000;481(1):73–6.
242. Chandler NJ, et al. Molecular architecture of the human sinus node: insights into the function of the cardiac pacemaker. *Circulation.* 2009;119(12):1562–75.
243. Cribbs LL, et al. Cloning and characterization of alpha1H from human heart, a member of the T-type Ca²⁺ channel gene family. *Circ Res.* 1998;83(1):103–9.
244. Monteil A, et al. Molecular and functional properties of the human alpha(1G) subunit that forms T-type calcium channels. *J Biol Chem.* 2000;275(9):6090–100.
245. Hagiwara N, Irisawa H, Kameyama M. Contribution of two types of calcium currents to the pacemaker potentials of rabbit sino-atrial node cells. *J Physiol.* 1988;395:233–53. PMC1191991.
246. Lee JH, et al. Nickel block of three cloned T-type calcium channels: low concentrations selectively block alpha1H. *Biophys J.* 1999;77(6):3034–42. PMC1300574.
247. Doerr T, Denger R, Trautwein W. Calcium currents in single SA nodal cells of the rabbit heart studied with action potential clamp. *Pflugers Arch.* 1989;413(6):599–603.
248. Vassort G, Talavera K, Alvarez JL. Role of T-type Ca²⁺ channels in the heart. *Cell Calcium.* 2006;40(2):205–20.
249. Xu M, et al. Enhanced expression of L-type Cav1.3 calcium channels in murine embryonic hearts from Cav1.2-deficient mice. *J Biol Chem.* 2003;278(42):40837–41.
250. Catterall WA, et al. International Union of Pharmacology. XLVIII. Nomenclature and structure-function relationships of voltage-gated calcium channels. *Pharmacol Rev.* 2005;57(4):411–25.
251. James TN. Structure and function of the sinus node, AV node and his bundle of the human heart: part II--function. *Prog Cardiovasc Dis.* 2003;45(4):327–60.
252. Dobrzynski H, et al. Structure, function and clinical relevance of the cardiac conduction system, including the atrioventricular ring and outflow tract tissues. *Pharmacol Ther.* 2013;139(2):260–88.
253. Abernethy DR, Soldatov NM. Structure-functional diversity of human L-type Ca²⁺ channel: perspectives for new pharmacological targets. *J Pharmacol Exp Ther.* 2002;300(3):724–8.
254. Liao P, et al. Splicing for alternative structures of Cav1.2 Ca²⁺ channels in cardiac and smooth muscles. *Cardiovasc Res.* 2005;68(2):197–203.
255. Tang ZZ, et al. Transcript scanning reveals novel and extensive splice variations in human l-type voltage-

- gated calcium channel, Cav1.2 alpha1 subunit. *J Biol Chem.* 2004;279(43):44335–43.
256. Liao P, Soong TW. Understanding alternative splicing of Cav1.2 calcium channels for a new approach towards individualized medicine. *J Biomed Res.* 2010;24(3):181–6. PMC3596553.
 257. Soldatov NM. Genomic structure of human L-type Ca²⁺ channel. *Genomics.* 1994;22(1):77–87.
 258. Soldatov NM, et al. Molecular determinants of L-type Ca²⁺ channel inactivation. Segment exchange analysis of the carboxyl-terminal cytoplasmic motif encoded by exons 40–42 of the human alpha1C subunit gene. *J Biol Chem.* 1998;273(2):957–63.
 259. Biel M, et al. Primary structure and functional expression of a high voltage activated calcium channel from rabbit lung. *FEBS Lett.* 1990;269(2):409–12.
 260. Ruth P, et al. Primary structure of the beta subunit of the DHP-sensitive calcium channel from skeletal muscle. *Science.* 1989;245(4922):1115–8.
 261. Pragnell M, et al. Cloning and tissue-specific expression of the brain calcium channel beta-subunit. *FEBS Lett.* 1991;291(2):253–8.
 262. Arikath J, Campbell KP. Auxiliary subunits: essential components of the voltage-gated calcium channel complex. *Curr Opin Neurobiol.* 2003;13(3):298–307.
 263. Dolphin AC. Beta subunits of voltage-gated calcium channels. *J Bioenerg Biomembr.* 2003;35(6):599–620.
 264. Chien AJ, et al. Roles of a membrane-localized beta subunit in the formation and targeting of functional L-type Ca²⁺ channels. *J Biol Chem.* 1995;270(50):30036–44.
 265. Davies A, et al. The alpha2delta subunits of voltage-gated calcium channels form GPI-anchored proteins, a posttranslational modification essential for function. *Proc Natl Acad Sci U S A.* 2010;107(4):1654–9. PMC2824380.
 266. Shaw RM, Colecraft HM. L-type calcium channel targeting and local signalling in cardiac myocytes. *Cardiovasc Res.* 2013;98(2):177–86. PMC3633156.
 267. Dolphin AC. The alpha2delta subunits of voltage-gated calcium channels. *Biochim Biophys Acta.* 2013;1828(7):1541–9.
 268. Hullin R, et al. Calcium channel beta subunit heterogeneity: functional expression of cloned cDNA from heart, aorta and brain. *EMBO J.* 1992;11(3):885–90. PMC556528.
 269. Castellano A, et al. Cloning and expression of a neuronal calcium channel beta subunit. *J Biol Chem.* 1993;268(17):12359–66.
 270. Vance CL, et al. Differential expression and association of calcium channel alpha1B and beta subunits during rat brain ontogeny. *J Biol Chem.* 1998;273(23):14495–502.
 271. Chen YH, et al. Structural basis of the alpha1-beta subunit interaction of voltage-gated Ca²⁺ channels. *Nature.* 2004;429(6992):675–80.
 272. Van Petegem F, et al. Structure of a complex between a voltage-gated calcium channel beta-subunit and an alpha-subunit domain. *Nature.* 2004;429(6992):671–5. PMC3076333.
 273. Van Petegem F, et al. Alanine-scanning mutagenesis defines a conserved energetic hotspot in the CaValpha1 AID-CaVbeta interaction site that is critical for channel modulation. *Structure.* 2008;16(2):280–94. PMC3018278.
 274. Opatowsky Y, et al. Structural analysis of the voltage-dependent calcium channel beta subunit functional core and its complex with the alpha 1 interaction domain. *Neuron.* 2004;42(3):387–99.
 275. Pragnell M, et al. Calcium channel beta-subunit binds to a conserved motif in the I-II cytoplasmic linker of the alpha 1-subunit. *Nature.* 1994;368(6466):67–70.
 276. Gregg RG, et al. Absence of the beta subunit (cchb1) of the skeletal muscle dihydropyridine receptor alters expression of the alpha 1 subunit and eliminates excitation-contraction coupling. *Proc Natl Acad Sci U S A.* 1996;93(24):13961–6. PMC19477.
 277. Yamaguchi H, et al. Multiple modulation pathways of calcium channel activity by a beta subunit. Direct evidence of beta subunit participation in membrane trafficking of the alpha1C subunit. *J Biol Chem.* 1998;273(30):19348–56.
 278. Beurg M, et al. Recovery of Ca²⁺ current, charge movements, and Ca²⁺ transients in myotubes deficient in dihydropyridine receptor beta 1 subunit transfected with beta 1 cDNA. *Biophys J.* 1997;73(2):807–18. PMC1180977.
 279. Wei SK, et al. Ca(2+) channel modulation by recombinant auxiliary beta subunits expressed in young adult heart cells. *Circ Res.* 2000;86(2):175–84.
 280. Chien AJ, et al. Membrane targeting of L-type calcium channels. Role of palmitoylation in the subcellular localization of the beta2a subunit. *J Biol Chem.* 1998;273(36):23590–7.
 281. Brice NL, et al. Importance of the different beta subunits in the membrane expression of the alpha1A and alpha2 calcium channel subunits: studies using a depolarization-sensitive alpha1A antibody. *Eur J Neurosci.* 1997;9(4):749–59.
 282. Lacerda AE, et al. Normalization of current kinetics by interaction between the alpha 1 and beta subunits of the skeletal muscle dihydropyridine-sensitive Ca²⁺ channel. *Nature.* 1991;352(6335):527–30.
 283. Varadi G, et al. Acceleration of activation and inactivation by the beta subunit of the skeletal muscle calcium channel. *Nature.* 1991;352(6331):159–62.
 284. Bourinet E, et al. Voltage-dependent facilitation of a neuronal alpha 1C L-type calcium channel. *EMBO J.* 1994;13(21):5032–9. PMC395449.
 285. Jones LP, Wei SK, Yue DT. Mechanism of auxiliary subunit modulation of neuronal alpha1E calcium channels. *J Gen Physiol.* 1998;112(2):125–43. PMC2525748.
 286. De Waard M, et al. Properties of the alpha 1-beta anchoring site in voltage-dependent Ca²⁺ channels. *J Biol Chem.* 1995;270(20):12056–64.
 287. Hohaus A, et al. Modulation of the smooth-muscle L-type Ca²⁺ channel alpha1 subunit (alpha1C-b) by the beta2a subunit: a peptide which inhibits binding

- of beta to the I-II linker of alpha1 induces functional uncoupling. *Biochem J.* 2000;348(Pt 3):657–65. PMC1221110.
288. Bichet D, et al. Reversibility of the Ca(2+) channel alpha(1)-beta subunit interaction. *Biochem Biophys Res Commun.* 2000;277(3):729–35.
 289. Qin N, et al. Direct interaction of gbetagamma with a C-terminal gbetagamma-binding domain of the Ca2+ channel alpha1 subunit is responsible for channel inhibition by G protein-coupled receptors. *Proc Natl Acad Sci U S A.* 1997;94(16):8866–71. PMC23172.
 290. Tareilus E, et al. A Xenopus oocyte beta subunit: evidence for a role in the assembly/expression of voltage-gated calcium channels that is separate from its role as a regulatory subunit. *Proc Natl Acad Sci U S A.* 1997;94(5):1703–8. PMC19980.
 291. Walker D, et al. A beta 4 isoform-specific interaction site in the carboxyl-terminal region of the voltage-dependent Ca2+ channel alpha 1A subunit. *J Biol Chem.* 1998;273(4):2361–7.
 292. De Waard M, Pragnell M, Campbell KP. Ca2+ channel regulation by a conserved beta subunit domain. *Neuron.* 1994;13(2):495–503.
 293. Gao T, Chien AJ, Hosey MM. Complexes of the alpha1C and beta subunits generate the necessary signal for membrane targeting of class C L-type calcium channels. *J Biol Chem.* 1999;274(4):2137–44.
 294. Catterall WA, et al. International Union of Pharmacology. XL. Compendium of voltage-gated ion channels: calcium channels. *Pharmacol Rev.* 2003;55(4):579–81.
 295. Ellis SB, et al. Sequence and expression of mRNAs encoding the alpha 1 and alpha 2 subunits of a DHP-sensitive calcium channel. *Science.* 1988;241(4873):1661–4.
 296. Klugbauer N, et al. A T-type calcium channel from mouse brain. *Pflugers Arch.* 1999;437(5):710–5.
 297. Qin N, et al. Molecular cloning and characterization of the human voltage-gated calcium channel alpha(2) delta-4 subunit. *Mol Pharmacol.* 2002;62(3):485–96.
 298. Wycisk KA, et al. Mutation in the auxiliary calcium-channel subunit CACNA2D4 causes autosomal recessive cone dystrophy. *Am J Hum Genet.* 2006;79(5):973–7. PMC1698577.
 299. Gurnett CA, De Waard M, Campbell KP. Dual function of the voltage-dependent Ca2+ channel alpha 2 delta subunit in current stimulation and subunit interaction. *Neuron.* 1996;16(2):431–40.
 300. Gurnett CA, Felix R, Campbell KP. Extracellular interaction of the voltage-dependent Ca2+ channel alpha2delta and alpha1 subunits. *J Biol Chem.* 1997;272(29):18508–12.
 301. Wiser O, et al. The alpha 2/delta subunit of voltage sensitive Ca2+ channels is a single transmembrane extracellular protein which is involved in regulated secretion. *FEBS Lett.* 1996;379(1):15–20.
 302. Singer D, et al. The roles of the subunits in the function of the calcium channel. *Science.* 1991;253(5027):1553–7.
 303. Bangalore R, et al. Influence of L-type Ca channel alpha 2/delta-subunit on ionic and gating current in transiently transfected HEK 293 cells. *Am J Phys.* 1996;270(5 Pt 2):H1521–8.
 304. Felix R, et al. Dissection of functional domains of the voltage-dependent Ca2+ channel alpha2delta subunit. *J Neurosci.* 1997;17(18):6884–91.
 305. Shistik E, et al. Ca2+ current enhancement by alpha 2/delta and beta subunits in Xenopus oocytes: contribution of changes in channel gating and alpha 1 protein level. *J Physiol.* 1995;489(Pt 1):55–62. PMC1156791.
 306. Kang MG, Campbell KP. Gamma subunit of voltage-activated calcium channels. *J Biol Chem.* 2003;278(24):21315–8.
 307. Chen RS, et al. Calcium channel gamma subunits: a functionally diverse protein family. *Cell Biochem Biophys.* 2007;47(2):178–86.
 308. Chu PJ, Robertson HM, Best PM. Calcium channel gamma subunits provide insights into the evolution of this gene family. *Gene.* 2001;280(1–2):37–48.
 309. Burgess DL, et al. A cluster of three novel Ca2+ channel gamma subunit genes on chromosome 19q13.4: evolution and expression profile of the gamma subunit gene family. *Genomics.* 2001;71(3):339–50.
 310. Milstein AD, Nicoll RA. TARP modulation of synaptic AMPA receptor trafficking and gating depends on multiple intracellular domains. *Proc Natl Acad Sci U S A.* 2009;106(27):11348–51. PMC2708767.
 311. Yang L, et al. Cardiac L-type calcium channel (Cav1.2) associates with gamma subunits. *FASEB J.* 2011;25(3):928–36. PMC3042847.
 312. Pongs O. Molecular biology of voltage-dependent potassium channels. *Physiol Rev.* 1992;72(4 Suppl):S69–88.
 313. Covarrubias M, Wei AA, Salkoff L. Shaker, Shal, Shab, and Shaw express independent K+ current systems. *Neuron.* 1991;7(5):763–73.
 314. Gutman GA, et al. International Union of Pharmacology. LIII. Nomenclature and molecular relationships of voltage-gated potassium channels. *Pharmacol Rev.* 2005;57(4):473–508.
 315. Drewe JA, et al. Distinct spatial and temporal expression patterns of K+ channel mRNAs from different subfamilies. *J Neurosci.* 1992;12(2):538–48.
 316. Hugnot JP, et al. Kv8.1, a new neuronal potassium channel subunit with specific inhibitory properties towards Shab and Shaw channels. *EMBO J.* 1996;15(13):3322–31. PMC451895.
 317. Castellano A, et al. Identification and functional characterization of a K+ channel alpha-subunit with regulatory properties specific to brain. *J Neurosci.* 1997;17(12):4652–61.
 318. Salinas M, et al. New modulatory alpha subunits for mammalian Shab K+ channels. *J Biol Chem.* 1997;272(39):24371–9.
 319. Warmke J, Drysdale R, Ganetzky B. A distinct potassium channel polypeptide encoded by the *Drosophila* eag locus. *Science.* 1991;252(5012):1560–2.

320. Warmke JW, Ganetzky B. A family of potassium channel genes related to eag in *Drosophila* and mammals. *Proc Natl Acad Sci U S A*. 1994;91(8):3438–42. PMC43592.
321. Curran ME, et al. A molecular basis for cardiac arrhythmia: HERG mutations cause long QT syndrome. *Cell*. 1995;80(5):795–803.
322. Sanguinetti MC, et al. A mechanistic link between an inherited and an acquired cardiac arrhythmia: HERG encodes the IKr potassium channel. *Cell*. 1995;81(2):299–307.
323. Trudeau MC, et al. HERG, a human inward rectifier in the voltage-gated potassium channel family. *Science*. 1995;269(5220):92–5.
324. Shi W, et al. Identification of two nervous system-specific members of the erg potassium channel gene family. *J Neurosci*. 1997;17(24):9423–32.
325. Lees-Miller JP, et al. Electrophysiological characterization of an alternatively processed ERG K⁺ channel in mouse and human hearts. *Circ Res*. 1997;81(5):719–26.
326. London B, et al. Two isoforms of the mouse ether-a-go-go-related gene coassemble to form channels with properties similar to the rapidly activating component of the cardiac delayed rectifier K⁺ current. *Circ Res*. 1997;81(5):870–8.
327. Kupersmidt S, et al. A K⁺ channel splice variant common in human heart lacks a C-terminal domain required for expression of rapidly activating delayed rectifier current. *J Biol Chem*. 1998;273(42):27231–5.
328. Wang Q, et al. Positional cloning of a novel potassium channel gene: KVLQT1 mutations cause cardiac arrhythmias. *Nat Genet*. 1996;12(1):17–23.
329. Barhanin J, et al. K(V)LQT1 and IsK (minK) proteins associate to form the I(Ks) cardiac potassium current. *Nature*. 1996;384(6604):78–80.
330. Sanguinetti MC, et al. Coassembly of K(V)LQT1 and minK (IsK) proteins to form cardiac I(Ks) potassium channel. *Nature*. 1996;384(6604):80–3.
331. Biervert C, et al. A potassium channel mutation in neonatal human epilepsy. *Science*. 1998;279(5349):403–6.
332. Wang Z, et al. Differential distribution of inward rectifier potassium channel transcripts in human atrium versus ventricle. *Circulation*. 1998;98(22):2422–8.
333. Schroeder BC, et al. Moderate loss of function of cyclic-AMP-modulated KCNQ2/KCNQ3 K⁺ channels causes epilepsy. *Nature*. 1998;396(6712):687–90.
334. Wang HS, et al. KCNQ2 and KCNQ3 potassium channel subunits: molecular correlates of the M-channel. *Science*. 1998;282(5395):1890–3.
335. Murai T, et al. Molecular cloning and sequence analysis of human genomic DNA encoding a novel membrane protein which exhibits a slowly activating potassium channel activity. *Biochem Biophys Res Commun*. 1989;161(1):176–81.
336. Folander K, et al. Cloning and expression of the delayed-rectifier IsK channel from neonatal rat heart and diethylstilbestrol-primed rat uterus. *Proc Natl Acad Sci U S A*. 1990;87(8):2975–9. PMC53816.
337. Lesage F, et al. ISK, a slowly activating voltage-sensitive K⁺ channel. Characterization of multiple cDNAs and gene organization in the mouse. *FEBS Lett*. 1992;301(2):168–72.
338. Abbott GW, Goldstein SA. A superfamily of small potassium channel subunits: form and function of the MinK-related peptides (MiRPs). *Q Rev Biophys*. 1998;31(4):357–98.
339. Abbott GW, et al. MiRP1 forms IKr potassium channels with HERG and is associated with cardiac arrhythmia. *Cell*. 1999;97(2):175–87.
340. Abbott GW. KCNE4 and KCNE5: K(+) channel regulation and cardiac arrhythmogenesis. *Gene*. 2016;593(2):249–60. PMC5166581.
341. Abbott GW, et al. MiRP2 forms potassium channels in skeletal muscle with Kv3.4 and is associated with periodic paralysis. *Cell*. 2001;104(2):217–31.
342. Zhang M, Jiang M, Tseng GN. minK-related peptide 1 associates with Kv4.2 and modulates its gating function: potential role as beta subunit of cardiac transient outward channel? *Circ Res*. 2001;88(10):1012–9.
343. Muniz ZM, Parcej DN, Dolly JO. Characterization of monoclonal antibodies against voltage-dependent K⁺ channels raised using alpha-dendrotoxin acceptors purified from bovine brain. *Biochemistry*. 1992;31(49):12297–303.
344. Rettig J, et al. Inactivation properties of voltage-gated K⁺ channels altered by presence of beta-subunit. *Nature*. 1994;369(6478):289–94.
345. Castellino RC, et al. Time- and voltage-dependent modulation of a Kv1.4 channel by a beta-subunit (Kv beta 3) cloned from ferret ventricle. *Am J Phys*. 1995;269(1 Pt 2):H385–91.
346. England SK, et al. A novel K⁺ channel beta-subunit (hKv beta 1.3) is produced via alternative mRNA splicing. *J Biol Chem*. 1995;270(48):28531–4.
347. England SK, et al. Characterization of a voltage-gated K⁺ channel beta subunit expressed in human heart. *Proc Natl Acad Sci U S A*. 1995;92(14):6309–13. PMC41507.
348. Majumder K, et al. Molecular cloning and functional expression of a novel potassium channel beta-subunit from human atrium. *FEBS Lett*. 1995;361(1):13–6.
349. Morales MJ, et al. A novel beta subunit increases rate of inactivation of specific voltage-gated potassium channel alpha subunits. *J Biol Chem*. 1995;270(11):6272–7.
350. Deal KK, England SK, Tamkun MM. Molecular physiology of cardiac potassium channels. *Physiol Rev*. 1996;76(1):49–67.
351. Shi G, et al. Beta subunits promote K⁺ channel surface expression through effects early in biosynthesis. *Neuron*. 1996;16(4):843–52.
352. Accili EA, et al. Separable Kvbeta subunit domains alter expression and gating of potassium channels. *J Biol Chem*. 1997;272(41):25824–31.

353. Accili EA, et al. Interactions among inactivating and noninactivating Kv β subunits, and K α 1.2, produce potassium currents with intermediate inactivation. *J Biol Chem.* 1997;272(45):28232–6.
354. Nagaya N, Papazian DM. Potassium channel α and β subunits assemble in the endoplasmic reticulum. *J Biol Chem.* 1997;272(5):3022–7.
355. Nakahira K, et al. Selective interaction of voltage-gated K $^{+}$ channel β -subunits with α -subunits. *J Biol Chem.* 1996;271(12):7084–9.
356. Sewing S, Roeper J, Pongs O. Kv β 1 subunit binding specific for shaker-related potassium channel α subunits. *Neuron.* 1996;16(2):455–63.
357. Fink M, et al. A new K $^{+}$ channel β subunit to specifically enhance Kv2.2 (CDRK) expression. *J Biol Chem.* 1996;271(42):26341–8.
358. Wible BA, et al. Cloning and expression of a novel K $^{+}$ channel regulatory protein, KChAP. *J Biol Chem.* 1998;273(19):11745–51.
359. An WF, et al. Modulation of A-type potassium channels by a family of calcium sensors. *Nature.* 2000;403(6769):553–6.
360. Rosati B, et al. Regulation of KChIP2 potassium channel β subunit gene expression underlies the gradient of transient outward current in canine and human ventricle. *J Physiol.* 2001;533(Pt 1):119–25. PMC2278594.
361. Bähring R, et al. Conserved Kv4 N-terminal domain critical for effects of Kv channel-interacting protein 2.2 on channel expression and gating. *J Biol Chem.* 2001;276(26):23888–94.
362. Decher N, et al. hKChIP2 is a functional modifier of hKv4.3 potassium channels: cloning and expression of a short hKChIP2 splice variant. *Cardiovasc Res.* 2001;52(2):255–64.
363. Burgoyne RD, Weiss JL. The neuronal calcium sensor family of Ca $^{2+}$ -binding proteins. *Biochem J.* 2001;353(Pt 1):1–12. PMC1221537.
364. Buxbaum JD, et al. Calsenilin: a calcium-binding protein that interacts with the presenilins and regulates the levels of a presenilin fragment. *Nat Med.* 1998;4(10):1177–81.
365. Carrion AM, et al. DREAM is a Ca $^{2+}$ -regulated transcriptional repressor. *Nature.* 1999;398(6722):80–4.
366. Guo W, et al. Role of heteromultimers in the generation of myocardial transient outward K $^{+}$ currents. *Circ Res.* 2002;90(5):586–93.
367. Guo W, et al. Modulation of Kv4-encoded K $^{+}$ currents in the mammalian myocardium by neuronal calcium sensor-1. *J Biol Chem.* 2002;277(29):26436–43.
368. Fiset C, et al. Shal-type channels contribute to the Ca $^{2+}$ -independent transient outward K $^{+}$ current in rat ventricle. *J Physiol.* 1997;500(Pt 1):51–64. PMC1159358.
369. Johns DC, Nuss HB, Marban E. Suppression of neuronal and cardiac transient outward currents by viral gene transfer of dominant-negative Kv4.2 constructs. *J Biol Chem.* 1997;272(50):31598–603.
370. Barry DM, et al. Functional knockout of the transient outward current, long-QT syndrome, and cardiac remodeling in mice expressing a dominant-negative Kv4 α subunit. *Circ Res.* 1998;83(5):560–7.
371. Takimoto K, et al. Decreased expression of Kv4.2 and novel Kv4.3 K $^{+}$ channel subunit mRNAs in ventricles of renovascular hypertensive rats. *Circ Res.* 1997;81(4):533–9.
372. Ohya S, et al. Molecular cloning and tissue distribution of an alternatively spliced variant of an A-type K $^{+}$ channel α -subunit, Kv4.3 in the rat. *FEBS Lett.* 1997;420(1):47–53.
373. London B, et al. The transient outward current in mice lacking the potassium channel gene Kv1.4. *J Physiol.* 1998;509(Pt 1):171–82. PMC2230931.
374. Yang T, Kupersmidt S, Roden DM. Anti-minK antisense decreases the amplitude of the rapidly activating cardiac delayed rectifier K $^{+}$ current. *Circ Res.* 1995;77(6):1246–53.
375. McDonald TV, et al. A minK-HERG complex regulates the cardiac potassium current I(Kr). *Nature.* 1997;388(6639):289–92.
376. Goldstein SA, Miller C. Site-specific mutations in a minimal voltage-dependent K $^{+}$ channel alter ion selectivity and open-channel block. *Neuron.* 1991;7(3):403–8.
377. Takumi T, Ohkubo H, Nakanishi S. Cloning of a membrane protein that induces a slow voltage-gated potassium current. *Science.* 1988;242(4881):1042–5.
378. Wang KW, Tai KK, Goldstein SA. MinK residues line a potassium channel pore. *Neuron.* 1996;16(3):571–7.
379. Tai KK, Goldstein SA. The conduction pore of a cardiac potassium channel. *Nature.* 1998;391(6667):605–8.
380. Jiang M, Tseng-Crank J, Tseng GN. Suppression of slow delayed rectifier current by a truncated isoform of KvLQT1 cloned from normal human heart. *J Biol Chem.* 1997;272(39):24109–12.
381. Nichols CG, et al. Inward rectification and implications for cardiac excitability. *Circ Res.* 1996;78(1):1–7.
382. Doupnik CA, Davidson N, Lester HA. The inward rectifier potassium channel family. *Curr Opin Neurobiol.* 1995;5(3):268–77.
383. Gutman GA, et al. International Union of Pharmacology. XLI. Compendium of voltage-gated ion channels: potassium channels. *Pharmacol Rev.* 2003;55(4):583–6.
384. Hibino H, et al. Inwardly rectifying potassium channels: their structure, function, and physiological roles. *Physiol Rev.* 2010;90(1):291–366.
385. Zhong YS, et al. Potassium ion channels in retinal ganglion cells (review). *Mol Med Rep.* 2013;8(2):311–9.
386. Liu GX, et al. Comparison of cloned Kir2 channels with native inward rectifier K $^{+}$ channels from guinea-pig cardiomyocytes. *J Physiol.* 2001;532(Pt 1):115–26. PMC2278533.

387. Takahashi N, et al. Molecular cloning and functional expression of cDNA encoding a second class of inward rectifier potassium channels in the mouse brain. *J Biol Chem*. 1994;269(37):23274–9.
388. Topert C, et al. Kir2.4: a novel K⁺ inward rectifier channel associated with motoneurons of cranial nerve nuclei. *J Neurosci*. 1998;18(11):4096–105.
389. Jongsma HJ, Wilders R. Channelopathies: Kir2.1 mutations jeopardize many cell functions. *Curr Biol*. 2001;11(18):R747–50.
390. Plaster NM, et al. Mutations in Kir2.1 cause the developmental and episodic electrical phenotypes of Andersen's syndrome. *Cell*. 2001;105(4):511–9.
391. Splawski I, et al. Ca(V)₁2 calcium channel dysfunction causes a multisystem disorder including arrhythmia and autism. *Cell*. 2004;119(1):19–31.
392. Tawil R, et al. Andersen's syndrome: potassium-sensitive periodic paralysis, ventricular ectopy, and dysmorphic features. *Ann Neurol*. 1994;35(3):326–30.
393. Ai T, et al. Novel KCNJ2 mutation in familial periodic paralysis with ventricular dysrhythmia. *Circulation*. 2002;105(22):2592–4.
394. Lange PS, et al. Andersen mutations of KCNJ2 suppress the native inward rectifier current IK1 in a dominant-negative fashion. *Cardiovasc Res*. 2003;59(2):321–7.
395. Preisig-Muller R, et al. Heteromerization of Kir2.x potassium channels contributes to the phenotype of Andersen's syndrome. *Proc Natl Acad Sci U S A*. 2002;99(11):7774–9. PMC124349.
396. Andelfinger G, et al. KCNJ2 mutation results in Andersen syndrome with sex-specific cardiac and skeletal muscle phenotypes. *Am J Hum Genet*. 2002;71(3):663–8. PMC379203.
397. Tristani-Firouzi M, et al. Functional and clinical characterization of KCNJ2 mutations associated with LQT7 (Andersen syndrome). *J Clin Invest*. 2002;110(3):381–8. PMC151085.
398. Hilgemann DW, Feng S, Nasuhoglu C. The complex and intriguing lives of PIP2 with ion channels and transporters. *Sci STKE*. 2001;2001(111):re19.
399. Huang CL, Feng S, Hilgemann DW. Direct activation of inward rectifier potassium channels by PIP2 and its stabilization by Gbetagamma. *Nature*. 1998;391(6669):803–6.
400. Shyng SL, et al. Structural determinants of PIP(2) regulation of inward rectifier K(ATP) channels. *J Gen Physiol*. 2000;116(5):599–608. PMC2229479.
401. Takano M, Kuratomi S. Regulation of cardiac inwardly rectifying potassium channels by membrane lipid metabolism. *Prog Biophys Mol Biol*. 2003;81(1):67–79.
402. Anumonwo JM, Lopatin AN. Cardiac strong inward rectifier potassium channels. *J Mol Cell Cardiol*. 2010;48(1):45–54. PMC2813336.
403. Donaldson MR, et al. PIP2 binding residues of Kir2.1 are common targets of mutations causing Andersen syndrome. *Neurology*. 2003;60(11):1811–6.
404. Xia M, et al. A Kir2.1 gain-of-function mutation underlies familial atrial fibrillation. *Biochem Biophys Res Commun*. 2005;332(4):1012–9.
405. Priori SG, et al. A novel form of short QT syndrome (SQT3) is caused by a mutation in the KCNJ2 gene. *Circ Res*. 2005;96(7):800–7.
406. Ambrosini E, et al. Genetically induced dysfunctions of Kir2.1 channels: implications for short QT3 syndrome and autism-epilepsy phenotype. *Hum Mol Genet*. 2014;23(18):4875–86. PMC4140467.
407. Deo M, et al. KCNJ2 mutation in short QT syndrome 3 results in atrial fibrillation and ventricular proarrhythmia. *Proc Natl Acad Sci U S A*. 2013;110(11):4291–6. PMC3600465.
408. Hattori T, et al. A novel gain-of-function KCNJ2 mutation associated with short-QT syndrome impairs inward rectification of Kir2.1 currents. *Cardiovasc Res*. 2012;93(4):666–73.
409. Zaritsky JJ, et al. The consequences of disrupting cardiac inwardly rectifying K(+) current (I(K1)) as revealed by the targeted deletion of the murine Kir2.1 and Kir2.2 genes. *J Physiol*. 2001;533(Pt 3):697–710. PMC2278659.
410. Zaritsky JJ, et al. Targeted disruption of Kir2.1 and Kir2.2 genes reveals the essential role of the inwardly rectifying K(+) current in K(+)-mediated vasodilation. *Circ Res*. 2000;87(2):160–6.
411. McLerie M, Lopatin AN. Dominant-negative suppression of I(K1) in the mouse heart leads to altered cardiac excitability. *J Mol Cell Cardiol*. 2003;35(4):367–78.
412. Zobel C, et al. Molecular dissection of the inward rectifier potassium current (IK1) in rabbit cardiomyocytes: evidence for heteromeric co-assembly of Kir2.1 and Kir2.2. *J Physiol*. 2003;550(Pt 2):365–72. PMC2343053.
413. Beech DJ, et al. K channel activation by nucleotide diphosphates and its inhibition by glibenclamide in vascular smooth muscle cells. *Br J Pharmacol*. 1993;110(2):573–82. PMC2175936.
414. Ashford ML, Boden PR, Treherne JM. Tolbutamide excites rat glucoreceptive ventromedial hypothalamic neurones by indirect inhibition of ATP-K⁺ channels. *Br J Pharmacol*. 1990;101(3):531–40. PMC1917752.
415. Ashcroft FM, Harrison DE, Ashcroft SJ. Glucose induces closure of single potassium channels in isolated rat pancreatic beta-cells. *Nature*. 1984;312(5993):446–8.
416. Terzic A, Jahangir A, Kurachi Y. Cardiac ATP-sensitive K⁺ channels: regulation by intracellular nucleotides and K⁺ channel-opening drugs. *Am J Phys*. 1995;269(3 Pt 1):C525–45.
417. Babenko AP, Aguilar-Bryan L, Bryan J. A view of sur/KIR6.X, KATP channels. *Annu Rev Physiol*. 1998;60:667–87.
418. Seino S, Miki T. Gene targeting approach to clarification of ion channel function: studies of Kir6.x null mice. *J Physiol*. 2004;554(Pt 2):295–300. PMC1664767.

419. Pountney DJ, et al. Is the molecular composition of K(ATP) channels more complex than originally thought? *J Mol Cell Cardiol.* 2001;33(8):1541–6.
420. Yokoshiki H, et al. Antisense oligodeoxynucleotides of sulfonylurea receptors inhibit ATP-sensitive K⁺ channels in cultured neonatal rat ventricular cells. *Pflugers Arch.* 1999;437(3):400–8.
421. Li RA, et al. Molecular basis of electrocardiographic ST-segment elevation. *Circ Res.* 2000;87(10):837–9.
422. Suzuki M, et al. Functional roles of cardiac and vascular ATP-sensitive potassium channels clarified by Kir6.2-knockout mice. *Circ Res.* 2001;88(6):570–7.
423. Nerbonne JM. Molecular basis of functional myocardial potassium channel diversity. *Card Electrophysiol Clin.* 2016;8(2):257–73. PMC4893780.
424. Seghers V, et al. Sur1 knockout mice. A model for K(ATP) channel-independent regulation of insulin secretion. *J Biol Chem.* 2000;275(13):9270–7.
425. Singh H, et al. Distribution of Kir6.0 and SUR2 ATP-sensitive potassium channel subunits in isolated ventricular myocytes. *J Mol Cell Cardiol.* 2003;35(5):445–59.
426. Suzuki M, et al. Role of sarcolemmal K(ATP) channels in cardioprotection against ischemia/reperfusion injury in mice. *J Clin Invest.* 2002;109(4):509–16. PMC150878.
427. Boyle WA, Nerbonne JM. A novel type of depolarization-activated K⁺ current in isolated adult rat atrial myocytes. *Am J Phys.* 1991;260(4 Pt 2):H1236–47.
428. Koster JC, et al. Tolerance for ATP-insensitive K(ATP) channels in transgenic mice. *Circ Res.* 2001;89(11):1022–9.
429. Lesage F, et al. TWIK-1, a ubiquitous human weakly inward rectifying K⁺ channel with a novel structure. *EMBO J.* 1996;15(5):1004–11. PMC449995.
430. Goldstein SA, et al. International Union of Pharmacology. LV. Nomenclature and molecular relationships of two-P potassium channels. *Pharmacol Rev.* 2005;57(4):527–40.
431. Brohawn SG, del Marmol J, MacKinnon R. Crystal structure of the human K2P TRAAK, a lipid- and mechano-sensitive K⁺ ion channel. *Science.* 2012;335(6067):436–41. PMC3329120.
432. Miller AN, Long SB. Crystal structure of the human two-pore domain potassium channel K2P1. *Science.* 2012;335(6067):432–6.
433. Renigunta V, Schlichtorl G, Daut J. Much more than a leak: structure and function of K(2)p-channels. *Pflugers Arch.* 2015;467(5):867–94.
434. Backx PH, Marban E. Background potassium current active during the plateau of the action potential in guinea pig ventricular myocytes. *Circ Res.* 1993;72(4):890–900.
435. Yue DT, Marban E. A novel cardiac potassium channel that is active and conductive at depolarized potentials. *Pflugers Arch.* 1988;413(2):127–33.
436. Brunet S, et al. Heterogeneous expression of repolarizing, voltage-gated K⁺ currents in adult mouse ventricles. *J Physiol.* 2004;559(Pt 1):103–20. PMC1665075.
437. Enyedi P, Czirjak G. Molecular background of leak K⁺ currents: two-pore domain potassium channels. *Physiol Rev.* 2010;90(2):559–605.
438. Lesage F, Lazdunski M. Molecular and functional properties of two-pore-domain potassium channels. *Am J Physiol Renal Physiol.* 2000;279(5):F793–801.
439. Barbuti A, et al. Block of the background K(+) channel TASK-1 contributes to arrhythmogenic effects of platelet-activating factor. *Am J Physiol Heart Circ Physiol.* 2002;282(6):H2024–30.
440. Schiekel J, et al. The inhibition of the potassium channel TASK-1 in rat cardiac muscle by endothelin-1 is mediated by phospholipase C. *Cardiovasc Res.* 2013;97(1):97–105.
441. Berg AP, et al. Motoneurons express heteromeric TWIK-related acid-sensitive K⁺ (TASK) channels containing TASK-1 (KCNK3) and TASK-3 (KCNK9) subunits. *J Neurosci.* 2004;24(30):6693–702.
442. Kang D, et al. Functional expression of TASK-1/TASK-3 heteromers in cerebellar granule cells. *J Physiol.* 2004;554(Pt 1):64–77. PMC1664745.
443. Heurteaux C, et al. TREK-1, a K⁺ channel involved in neuroprotection and general anesthesia. *EMBO J.* 2004;23(13):2684–95. PMC449762.
444. Putzke C, et al. Differential effects of volatile and intravenous anesthetics on the activity of human TASK-1. *Am J Physiol Cell Physiol.* 2007;293(4):C1319–26.
445. Putzke C, et al. The acid-sensitive potassium channel TASK-1 in rat cardiac muscle. *Cardiovasc Res.* 2007;75(1):59–68.
446. Limberg SH, et al. TASK-1 channels may modulate action potential duration of human atrial cardiomyocytes. *Cell Physiol Biochem.* 2011;28(4):613–24. PMC3709183.
447. Bohnen MS, et al. The impact of heterozygous KCNK3 mutations associated with pulmonary arterial hypertension on channel function and pharmacological recovery. *J Am Heart Assoc.* 2017;6(9):PMC5634293.
448. Friedrich C, et al. Gain-of-function mutation in TASK-4 channels and severe cardiac conduction disorder. *EMBO Mol Med.* 2014;6(7):937–51. PMC4119356.
449. Dong DL, Bai YL, Cai BZ. Calcium-activated potassium channels: potential target for cardiovascular diseases. *Adv Protein Chem Struct Biol.* 2016;104:233–61.
450. Contreras GF, et al. A BK (Slo1) channel journey from molecule to physiology. *Channels (Austin).* 2013;7(6):442–58. PMC4042479.
451. Kaczmarek LK, et al. International Union of Basic and Clinical Pharmacology. C. Nomenclature and properties of calcium-activated and sodium-activated potassium channels. *Pharmacol Rev.* 2017;69(1):1–11.

452. Wei AD, et al. International Union of Pharmacology. LII. Nomenclature and molecular relationships of calcium-activated potassium channels. *Pharmacol Rev.* 2005;57(4):463–72.
453. Kohler M, et al. Small-conductance, calcium-activated potassium channels from mammalian brain. *Science.* 1996;273(5282):1709–14.
454. Ishii TM, et al. A human intermediate conductance calcium-activated potassium channel. *Proc Natl Acad Sci U S A.* 1997;94(21):11651–6. PMC23567.
455. Joiner WJ, et al. hSK4, a member of a novel subfamily of calcium-activated potassium channels. *Proc Natl Acad Sci U S A.* 1997;94(20):11013–8. PMC23566.
456. Bhattacharjee A, et al. Slick (Slo2.1), a rapidly-gating sodium-activated potassium channel inhibited by ATP. *J Neurosci.* 2003;23(37):11681–91.
457. Yuan A, et al. The sodium-activated potassium channel is encoded by a member of the Slo gene family. *Neuron.* 2003;37(5):765–73.
458. Kaczmarek LK. Slack, slick and sodium-activated potassium channels. *ISRN Neurosci.* 2013;2013(2013):1–14. PMC3850776.
459. Balderas E, et al. Mitochondrial BKCa channel. *Front Physiol.* 2015;6:104. PMC4379900.
460. Xu W, et al. Cytoprotective role of Ca²⁺-activated K⁺ channels in the cardiac inner mitochondrial membrane. *Science.* 2002;298(5595):1029–33.
461. Heinen A, et al. Reverse electron flow-induced ROS production is attenuated by activation of mitochondrial Ca²⁺-sensitive K⁺ channels. *Am J Physiol Heart Circ Physiol.* 2007;293(3):H1400–7.
462. Sato T, et al. Mitochondrial Ca²⁺-activated K⁺ channels in cardiac myocytes: a mechanism of the cardioprotective effect and modulation by protein kinase A. *Circulation.* 2005;111(2):198–203.
463. Xia XM, et al. Mechanism of calcium gating in small-conductance calcium-activated potassium channels. *Nature.* 1998;395(6701):503–7.
464. Grunnet M, et al. Cardiac ion channels and mechanisms for protection against atrial fibrillation. *Rev Physiol Biochem Pharmacol.* 2012;162:1–58.
465. Mu YH, et al. RyR2 modulates a Ca²⁺-activated K⁺ current in mouse cardiac myocytes. *PLoS One.* 2014;9(4):e94905. PMC3991633.
466. Wojtovich AP, et al. SLO-2 is cytoprotective and contributes to mitochondrial potassium transport. *PLoS One.* 2011;6(12):e28287. PMC3228735.
467. Wasserstrom JA, Salata JJ. Basis for tetrodotoxin and lidocaine effects on action potentials in dog ventricular myocytes. *Am J Phys.* 1988;254(6 Pt 2):H1157–66.
468. Clancy CE, Rudy Y. Na⁽⁺⁾ channel mutation that causes both Brugada and long-QT syndrome phenotypes: a simulation study of mechanism. *Circulation.* 2002;105(10):1208–13. PMC1997279.
469. Weidmann S. Effect of current flow on the membrane potential of cardiac muscle. *J Physiol.* 1951;115(2):227–36. PMC1391998.



Neuromodulation of Cardiac Repolarization and Arrhythmogenesis

2

Fabrice Extramiana and Pierre Maison-Blanche

Introduction

The relationship between neuropsychological influences and cardiac clinical symptoms has been long and consistently recognized. The most extreme illustration is being “scared to death” as demonstrated by the increase in sudden cardiac death (SCD) occurrence during intense psychological stress [1–6]. Physical stress and exercise are also classical triggers for SCD [7, 8]. But, on the other side of the same coin, SCD may also occur during sleep [9, 10]. These caricatures obviously point to autonomic factors precipitating ventricular fibrillation (VF) [11, 12]. Pioneer experimental studies have shown that sympathetic stimulation at different anatomical levels decreases the threshold for VF and that this effect is prevented by parasympathetic stimulation [12–16].

The classic Coumel’s triangle has raised awareness about the three ingredients required for the occurrence of a spontaneous clinical arrhythmia, an arrhythmogenic substrate, a trigger factor, and modulation factors of which the most common is the autonomic nervous system [17, 18].

There have been dramatic advances in the last decades in understanding the links between the

autonomic nervous system (ANS), arrhythmogenesis, and ventricular repolarization (VR). In the present chapter, we intend to synthesize current knowledge of the physiology and pathophysiology of autonomic influences on VR and the related clinical aspects of this interaction and finally to describe the current and potential future antiarrhythmic therapies based on neuromodulation of ventricular repolarization.

Physiology and Pathophysiology of Autonomic Nervous System (ANS) Influences on Ventricular Repolarization

A Short Description of the Neural Control of the Heart

Physiological cardiac properties are key determinants of blood pressure regulation and adaptation to stress and exercise, and their neural control has been long identified [19, 20].

The description of the complex anatomy of the ANS is beyond the scope of this chapter and not perfectly understood [21, 22]. It has been described as a three-component system with central, intrathoracic, and intrinsic cardiac components, each with a feedback loop resulting in a complex fine-tuning [23].

At the end-effector level, both sympathetic and parasympathetic autonomic receptors influence G proteins and, respectively, lead to an increase or a

F. Extramiana (✉) · P. Maison-Blanche
Arrhythmia Unit, Department of Cardiology, Bichat
Hospital, APHP, Paris University, Paris, France
e-mail: fabrice.extramiana@aphp.fr

decrease in PKA-dependent phosphorylation [24]. However, the two limbs of the ANS cannot be considered as independent from each other. A parasympathetic feedback will antagonize a sympathetic stimulation [25], and at the ventricular level, the effect of parasympathetic stimulation would be to antagonize any preexistent sympathetic stimulation but would be inefficient in the absence of sympathetic stimulation [14].

ANS Effects on Ventricular Repolarization (VR) Duration

The effects of the ANS on VR have been described at the channel, cellular, and organ levels.

Beta-1 adrenergic receptor stimulation is associated with a rate-independent increase of the slow calcium (ICaL) and slow component of the delayed potassium (IKs) currents [26–29]. In addition to these direct effects, IKs is also calcium-dependent and is also increased by the calcium concentration increase following adrenergic-dependent calcium channel phosphorylation.

Conversely, type 2 muscarinic receptor stimulation by acetylcholine will antagonize ICaL but only in the presence of β -adrenergic stimulation [29].

Adrenergic stimulation has been long recognized as increasing heart rate through affecting both the membrane and calcium clocks [20, 30]. The shortening of the cardiac cycle will impact the kinetics of ionic channels. Higher heart rates will be associated with less time for de-inactivation, thereby decreasing the INa, ICaL, and Ito1.

The global impact of heart rate-dependent and rate-independent effects of sympathetic stimulation is a shortening of ventricular APD and refractory periods [31–34].

Proarrhythmic Effects of Sympathetic Stimulation on Ventricular Repolarization

Although the link between sympathetic stimulation and ventricular arrhythmias is supported by overwhelming clinical data (see section “[Clinical](#)

[Syndromes](#)” of the present chapter), the underlying mechanisms are not fully understood.

Conduction properties [35–37] and calcium handling [38–40] are also influenced by sympathetic stimulation in a proarrhythmic manner. We will here schematically describe proarrhythmic effects mediated by changes in VR properties induced by sympathetic stimulation.

These effects might be summed up at cellular, tissue, and organ levels.

At the cellular level, early afterdepolarizations (EADs) may result in triggered activity arising from abnormal repolarization. Mathematical models show that EADs may result from secondary activation of the L-type Ca²⁺ current during the plateau of an action potential or from activation of sodium-calcium exchanger by increased intracellular calcium due to spontaneous Ca²⁺ release from the SR during the late repolarization phase [41, 42]. Increasing the L-type Ca²⁺ current and intracellular calcium by adrenergic stimulation promotes the occurrence of EADs via a complex kinetic mismatch of PKA targets [43]. This proarrhythmic effect at a cellular level seems to be particularly involved in case of decreased IKs current as seen in type 1 LQTS [44, 45].

Although triggered activities are critical for arrhythmia initiation, the maintenance of arrhythmias is related to self-sustained propagation of the depolarization front in a tissue structure. In most cases, the underlying mechanism is reentry which requires a match between propagation speed and refractory periods [46, 47]. Theoretically, the APD shortening induced by adrenergic stimulation [31–34] would decrease the wavelength of potential reentrant circuits (or the critical mass required for the reentry) and hence promote arrhythmia maintenance.

Beyond duration, VR heterogeneities, either spatial or temporal, have been recognized as key players in arrhythmogenesis.

Pioneer studies have shown the spatial heterogeneity of ventricular refractory periods and the potential role of increased spatial dispersion as a mechanism for transient (unidirectional) conduction block serving as the substrate for functional reentry [48, 49]. This arrhythmia mechanism has

been evidenced in experimental models of myocardial infarction, long QT syndrome, heart failure, Brugada syndrome, and short QT syndrome [50–57]. It is noteworthy that epicardial steep spatial ventricular repolarization gradient has been noninvasively evidenced (using ECG imaging) in the long QT syndrome when compared to normal subjects [58].

As discussed above, adrenergic stimulation is associated with a shortening of ventricular refractory periods. However, this effect is not spatially homogeneous due to (1) the spatial heterogeneities of ionic channel densities across the ventricular wall and different parts of the ventricles [59, 60] and (2) the heterogeneity in regional distribution and activity of sympathetic nerves [61]. And it has been shown that beta-adrenergic stimulation increases spatial VR heterogeneities in experimental models [51, 57] as well as in patients using invasive endocardial ventricular mapping in patients with myocardial infarction [62].

Finally, the spatial heterogeneity of ventricular repolarization not only may serve as a substrate for functional reentries. Steep local ventricular repolarization gradients may generate an electrotonic current leading to phase 3 EADs [63].

Temporal VR heterogeneities also play a critical role in arrhythmogenesis. VR duration is dependent on heart rate in steady-state condition but also on the duration of the preceding diastolic interval [64]. The former is named repolarization restitution and is displayed as a graphical curve which steepness would determine the evolution of the system [65]. Steep restitution curves (above 1) would induce APD alternans which when spatially discordant would lead to functional conduction blocks, hence promoting the transition from a stable to an unstable rhythm, ultimately to fibrillation [65–68]. The relationship between the ventricular restitution slope and the probability of inducing VF during premature ventricular stimulation has been found in patients with the Brugada syndrome [69].

Adrenergic stimulation has been shown to increase the steepness of the APD restitution in experimental models as well as in humans [70, 71]. Conversely, the steepness of the APD restitu-

tion is decreased by vagal nerve stimulation [71] in a muscarinic receptor-independent manner, through neuronal nitric oxide release [72, 73].

A very recent provocative study suggests, however, that APD alternans would be associated with a greater regional expression of calsequestrin and ryanodine receptor but not with restitution properties [74]. If this concept hold true, this mechanism would be a major link between adrenergic stimulation and arrhythmogenesis.

Finally, the proarrhythmic effect of sympathetic stimulation on VR at the organ level should not be overlooked.

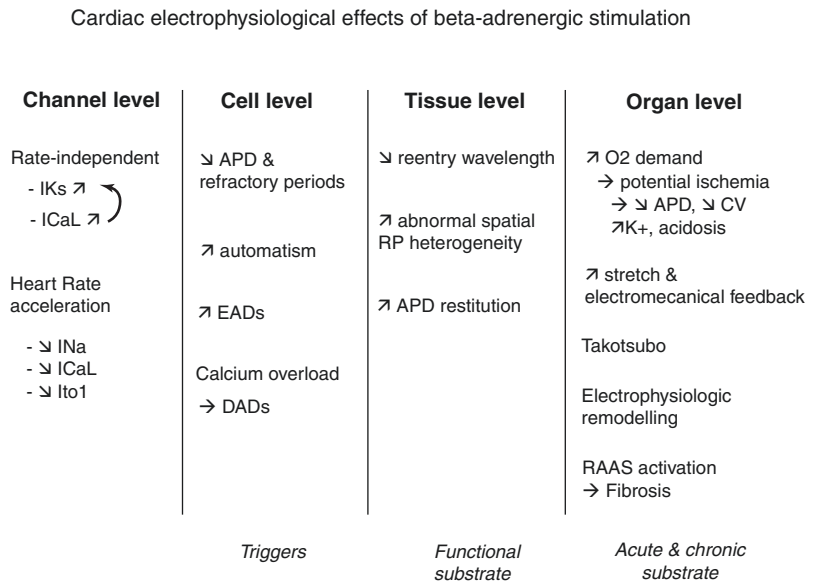
The adrenergic-induced increase in inotropy, chronotropy, dromotropy, and lusitropy is associated with a steep increase in myocardial oxygen demand potentially leading to ischemia defined as an imbalance in the supply and demand. Acute ischemia is associated with hyperkalemia and acidosis and will affect conduction velocity but also result in IKATP activation leading to APD shortening. Looking only to the consequences of altered repolarization, steep APD gradients at the ischemic border zone may promote triggered activity via phase 2 reentry and/or electrotonically triggered EADs [75, 76].

Although the pathophysiology of the Takotsubo cardiomyopathy is not fully understood and probably multifactorial, the common emotional stress before the event and the occurrence in patients with pheochromocytoma and after administration of catecholamines suggest an important role for adrenergic stimulation [77]. The Takotsubo cardiomyopathy is associated with profound surface ECG VR changes reflecting an increase in inhomogeneity and dispersion of ventricular repolarization and has been shown to lead to torsades de pointes [78, 79].

Last but not the least, chronic adrenergic stimulation has a profound impact on the myocardial structure as it promotes fibrosis [80] which in turn with cellular uncoupling will increase repolarization gradients, hence paving the way for an arrhythmogenic substrate [81–83].

Figure 2.1 provides a summary of the proarrhythmic effects of sympathetic stimulation effects on ventricular repolarization.

Fig. 2.1 Diagram of the electrophysiological effects of beta-adrenergic receptor stimulation at channel, cell, tissue, and organ levels. APD action potential duration, EADs early afterdepolarizations, DADs delayed afterdepolarization, RP refractory period, CV conduction velocity, RAAS renin-angiotensin-aldosterone system



Clinical Aspects

In the next paragraphs, We will first take a closer look into the interplay between body surface ECG markers of VR and ANS. Then, for the main ventricular arrhythmia syndromes, we will review the clinical features that provide evidence of the ANS influences.

Neuromodulation of ECG Correlates of Ventricular Repolarization

Availability of implantable cardiac defibrillators (ICDs) made precise cardiac arrhythmia risk assessment very useful. Reduced left ventricular ejection fraction (LVEF) is without question a strong predictor of the risk of SCD, but soon it was understood that LVEF has major drawbacks, mainly because the majority of SCD cases occur in patients with preserved or moderately reduced LVEF [84, 85]. Then a reduced LVEF is a risk factor for both sudden and non-sudden death. Currently, only relatively few patients with reduced LVEF will benefit from an ICD (most will never experience a threatening arrhythmic event).

Because of the direct relationship between VR abnormalities and arrhythmogenesis as reported

above, vast clinical research programs have been deployed to validate VR-based risk markers [86].

Due to length constraint, we will discuss only the role of global QT and T_{peak}-T_{end} ECG time intervals, QT hysteresis, and QT rate dependency. Pathophysiology of microvolt T wave alternans will be presented in another chapter.

Global QT Duration

Autonomic nervous system influences on QT/QTc interval in humans are poorly understood. In particular, the effects of an autonomic intervention, sympathetic stimulation, or parasympathetic blockade will impact both the heart rate and the QT interval. Therefore, any drugs that affect the ANS can modulate the QT interval directly or only by changing heart rate. Actually, autonomic modulation of QT interval has produced conflicting results, with among other methodological issues the limitations of any QT rate correction formula. In an elegant pioneer clinical study, Browne [87] compared QT intervals that had similar RR interval durations during sleep and awake states. At 60 beats per minute, the duration of the QT interval was longer during sleep in all 15 patients (19 ± 7 ms). In another study, Ahnve showed that in healthy subjects, when the heart rate was kept constant by cardiac pacing, propranolol did not induce any

Fig. 2.2 Circadian modulation of the QT intervals, a rate-independent approach. Using the rate-independent approach as introduced by Browne [88], the individual ECG waveforms collected at 60 beats per minute (RR = 1000 ms) separately at day and night were averaged. The ECG recording was a digital 24-hour recording with an orthogonal lead configuration (upper traces as X lead and bottom traces as Z lead). ECG intervals were manually measured using screen calipers

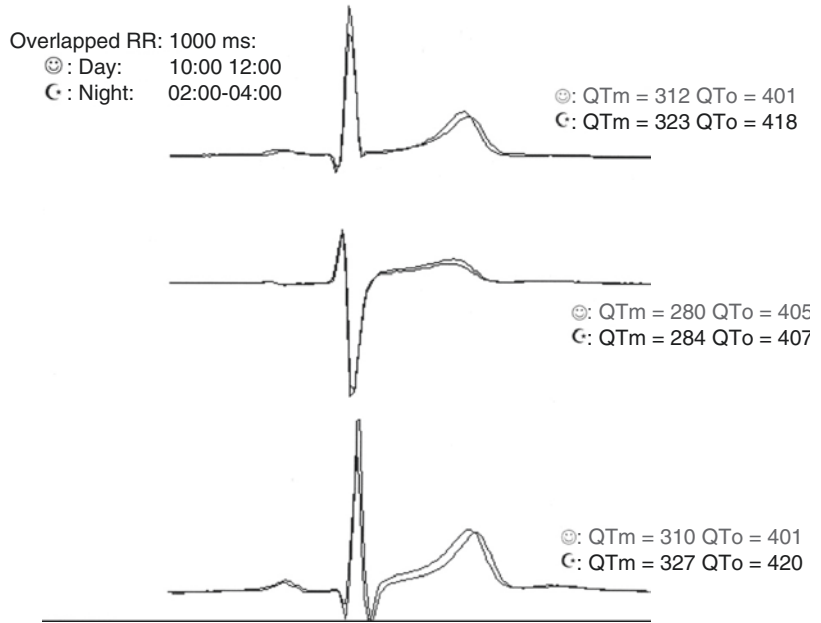
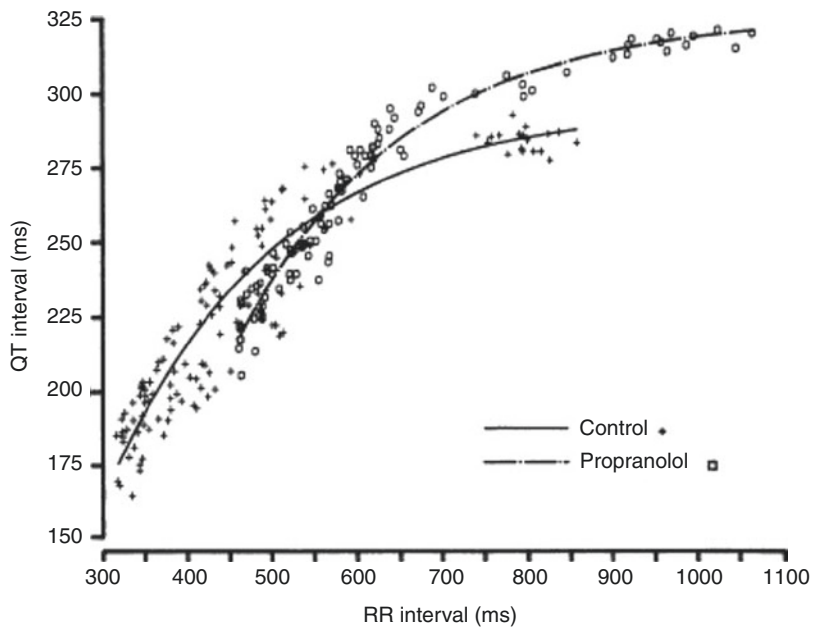


Fig. 2.3 Modulation of QT rate dependency by beta-blockers. In this study, the modulation of the QT/RR slope by a beta-blocker leads to a biphasic effect on the QT interval: a significant prolongation at longer cycle and a shortening at shorter cycle lengths. In this study, Bazett's formula did not show any significant effect when the same raw data were used. (Adapted from Sarma et al. [89])



significant change in the QT interval [88]. Figure 2.2 shows in a healthy individual two ECG waveforms collected at identical heart rate, but one during the day and the other at night. This figure provides a simple illustration of the QT circadian pattern. Using electrocardiograms continuously recorded, Sarma estimated the

effects of propranolol on the QT interval at three predefined RR intervals (400, 700, and 1000 ms). This study showed that the effect of propranolol on the QT intervals is biphasic (Fig. 2.3). It significantly prolonged the interval at longer cycle lengths but shortened it at shorter cycle lengths. It is noteworthy that Bazett's formula did not

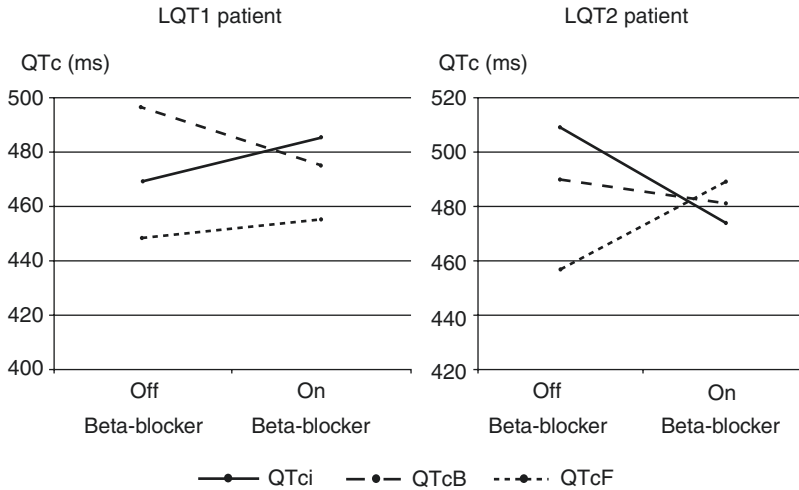


Fig. 2.4 The importance of the QT rate correction coefficient to determine the effects of pharmacologic beta-adrenergic blockade. QTc changes from baseline under beta-blocker treatment using different rate correction coefficients (individual, Bazett, or Fridericia) in a LQT1

(left) and a LQT2 patient (right). Depending on the mathematical factor, one can conclude in either QTc shortening or QTc lengthening after beta-blockade. (Adapted from Extramiana et al. [90]. Used with permission from John Wiley and Sons)

show any significant effect when the same raw data were used [89].

Therefore, it is likely that the QT rate correction formula is a confounding factor in clinical trials, but the use of a rate-independent QT approach based on continuous ECG recordings is not suitable in most patient populations (Fig. 2.4).

QT Interval and Risk Stratification in the General Population

Montanez and co-authors [91] conducted a literature search to identify all published prospective cohort studies evaluating the association between prolonged QTc interval and risks of total and cardiovascular mortality as well as sudden death. The seven prospective cohort studies identified included Framingham, Amsterdam, and two Rotterdam studies and the Zutphen, Finnish, and Danish studies. In this review article, there was no consistent association between prolonged QTc interval and total and cardiovascular mortality or morbidity, with the exception of patients with prior cardiovascular disease. Even in this subgroup, however, the data are not entirely consistent. This study outcome needs to be interpreted, keeping in mind the methodological limitations described above.

Inherited Arrhythmia Syndromes: Long and Short QT Syndromes

Mazzanti and co-authors recently reviewed database findings from 1710 patients affected by long QT syndrome (LQTS) and a follow-up time of 7.1 years. Based on QTc duration, the aim of the study was to estimate the 5-year risk of life-threatening arrhythmic events and to assess the antiarrhythmic efficacy of beta-blockers. The risk of arrhythmic events increased by 15% for every 10 ms increment of QTc duration for all genotypes. The risk for patients with LQT2 and LQT3 increased by 130% and 157% at any QTc duration versus patients with LQT1 [92].

Regarding LQT3 population, Wilde and co-authors analyzed electrocardiographic and genetic parameters accumulated by seven participating LQT3 registries. The study population included 406 LQT3 patients. In this study, the risk of a first cardiac event was also directly related to the degree of QTc prolongation. Each 10 ms increase in QTc duration up to 500 ms was associated with a 19% increase in cardiac events. Interestingly in this LQTS subgroup, beta-blocker therapy was associated with an 83% reduction in cardiac events in females but not in males [93]. In our LQT3 cohort of 111 genotyped

LQT3 patients (median follow-up 7 years, IQR 10.3) [7], beta-blockade was not associated with a decrease in severe rhythmic event occurrences (defined as documented polymorphic VT/VF or torsades de pointes, ACA, and SCD) but rather with a statistically nonsignificant increase (HR 3.87 95%CI 0.92–16.2, $p = 0.06$) [94].

Short QT syndrome (SQTS) is an inherited cardiac disease characterized by malignant ventricular tachyarrhythmias leading to syncope and sudden cardiac death [95]. Due to the low number of patients with SQTS, risk stratification represents the main current challenge in clinical characterization. So far, the only reliable predictor of cardiac arrest identified in SQTS population has been a previous history of cardiac arrest. In contrast with LQTS, a clear relationship between clinical risk and QT/QTc duration in patients with SQTS has not been proven. There are some trends in some studies toward increased events based on shorter absolute QT or QTc intervals. In a pediatric cohort of SQTS patients [96], Villafane reported that a Gollob score may be useful in identifying patients at higher risk for unexplained syncope or aborted SCD. QTc duration is embedded in the Gollob score (the shorter QTc rated a large number of points), and most symptomatic patients had high scores. However, Giustetto in a study with long-term follow-up of patients with SQTS did not report that the QTc values could differentiate between asymptomatic subjects and those with cardiac arrest [97].

QT Rate Dependency

The dynamic relationship between QT and RR intervals in humans includes two distinct phenomena: first, the so-called QT/RR dependency, representing the magnitude of QT interval variations at steady state following changes of RR intervals, and then the QT/RR hysteresis, i.e., the time course of the QT interval following an abrupt variation in RR interval and the time spent to reach steady state.

Many studies have assessed the effect of changes in heart rate on ventricular repolarization. Rather than using a rate correction formula and a “rate corrected” QT interval, the key clinical marker in those studies is the slope of the

QT/RR relationship. The magnitude of QT changes following changes in cardiac in cycle length is modulated by intrinsic factors that differ between subjects [98, 99]. QT-RR rate dependency varies among individuals, being not only population specific but patient specific. In addition, the lag adaptation times are also patient specific [100].

A neuromodulation of the QT rate dependency is demonstrated by many reports. When considering the analysis of the QT/RR slope separately at day- and nighttime, studies have shown that the slope is steeper during daytime [99]. This circadian pattern is blunted in diabetic patient with diabetic autonomic neuropathy [101]. The effects of beta-blockade on the rate dependency of the QT interval depend on the time of the day. In healthy subjects, at daytime, the QT rate dependency is reduced by atenolol, whereas during the night, the QT rate dependency remains unchanged [102, 103]. Oppositely, in healthy male volunteers, dobutamine increases the QT/RR slopes [104].

Not surprisingly, dynamic parameters of VR and expressed as the QT/RR slope have been used to identify patients with increased risk for ventricular arrhythmias. Steep QT/RR slopes, reflecting inadequate adaptation of ventricular repolarization to heart rate changes, and in particular both exaggerated lengthening of repolarization at long RR cycle lengths and shortened QT intervals at short RR cycle are frequently observed in patients at risk for sudden cardiac death [105–114].

Our group assessed QT/RR slopes in a group of 68 patients with a previous history of Q-wave myocardial infarction, including a VT subgroup of 34 patients who had a recent history of VT and a control group consisting of 34 patients with a previous Q-wave myocardial infarction but without a history of VT events, an arrhythmia-free survival for 3 years during follow-up [105]. From Holter recordings, QT/RR slopes were computed during three different periods, a diurnal period (eight consecutive daily hours with fastest heart rate (awake period), a sleep period (four consecutive sleeping hours with lowest heart rate), and finally the 2 hours around

the awakening heart rate acceleration (awakening period). A circadian pattern was observed in both groups; the lowest QT rate dependence was observed during sleep, whereas the awakening period was characterized by the steepest QT/RR slope. Interestingly, within the three circadian periods, QT/RR slopes were significantly stronger in the VT group, and the difference was more pronounced after awakening. In other words, the QT shortening with increasing heart rate is maximum during the awakening period and in patients prone to VTs (Fig. 2.5a). Interestingly, the QT/RR slopes were further increased in patients with VF when compared to patients with VT (Table 2.1). The higher incidence of arrhythmic events and sudden cardiac death in this period is well established (see section “[Neuromodulation of Cardiac Arrhythmias in Ischemic and Non-ischemic Cardiomyopathy](#)”).

Congenital long QT syndrome type 1 patients are at high risk for arrhythmic events during high adrenergic states such as exercise and emotion, and β -blockers are the first-line therapy for these patients (see section “[Congenital Long QT Syndrome](#)”). It has been shown that patients with missense mutations in the cytoplasmic loop (C-loops) regions had a higher risk for events than patients with mutations outside of the C-loop regions [116]. Furthermore (Fig. 2.5b), β -blockers were associated with greater benefit in patients

with mutations located in the C-loop regions. Analysis of the QT-RR dynamicity in 24-hour Holter recordings acquired in healthy individuals and LQT-1 patients with and without mutation in the C-loop region showed stronger QT adaptation to heart rate in non-C-loop mutation LQT-1 patients regardless of the period of the day, whereas C-loop mutation LQT-1 patients presented abnormal adaptation (flat slopes) during the day [115]. The lack of QT shortening leads to prolonged QT interval at elevated heart rate, and consequently one expects C-loop LQT-1 patients to be at higher risk for cardiac events during elevated heart rate.

QT Hysteresis

The QT-RR hysteresis during an exercise test has been previously described by Sarma and co-authors in 1985 [89]. In this setting, QT-RR hysteresis is a phenomenon marked by longer QT intervals at a given RR interval, while heart rates are increasing (RR intervals decreasing) during exercise and shorter QT intervals at the same RR interval when heart rates are decreasing (RR intervals increasing) during recovery. The ECG variable is the “ Δ QT” in milliseconds, an estimate of the difference between QT intervals measured at a predetermined RR observed both during rate acceleration and deceleration. Evaluation of this QT-RR relationship during

Fig. 2.5 Rate dependency in post-MI patients and in LQTS1 patients. (panel a) QT/RR slopes in the awakening period in post-myocardial infarction (MI) patients without (control group) or with ventricular tachycardia (VT group) during follow-up. For cardiac cycle lengths spanning from 740 to 960 ms RR intervals, QT intervals are not different between control and VT groups. At RR intervals >960 ms, QT intervals are significantly longer in the VT group. However, at RR intervals <740 ms, QT intervals are significantly shorter in the VT group (at RR intervals = 600 ms, the mean QT interval duration is 353 ms in the VT group versus 372 ms in the control

group, $p < 0.05$). (Adapted from Extramiana et al. [105]. Used with permission from Elsevier). (panel b) QT-RR slopes in LQTS1 patients off β -blocker and in controls. QT-RR lines describing the QT-interval duration for the controls (black dots), CL QT-1 (white dots), and NCL LQT-1 (squares) groups for the diurnal (lines) and nocturnal (dotted lines) periods. We superimposed the curve describing $QT_c = 500$ ms and grayed the areas corresponding to the range of RR and QT values associated with higher risk for cardiac events. CL C-loop LQT1 mutation, NCL non-C-loop LQT1 mutation. (Adapted from Couderc et al. [115])

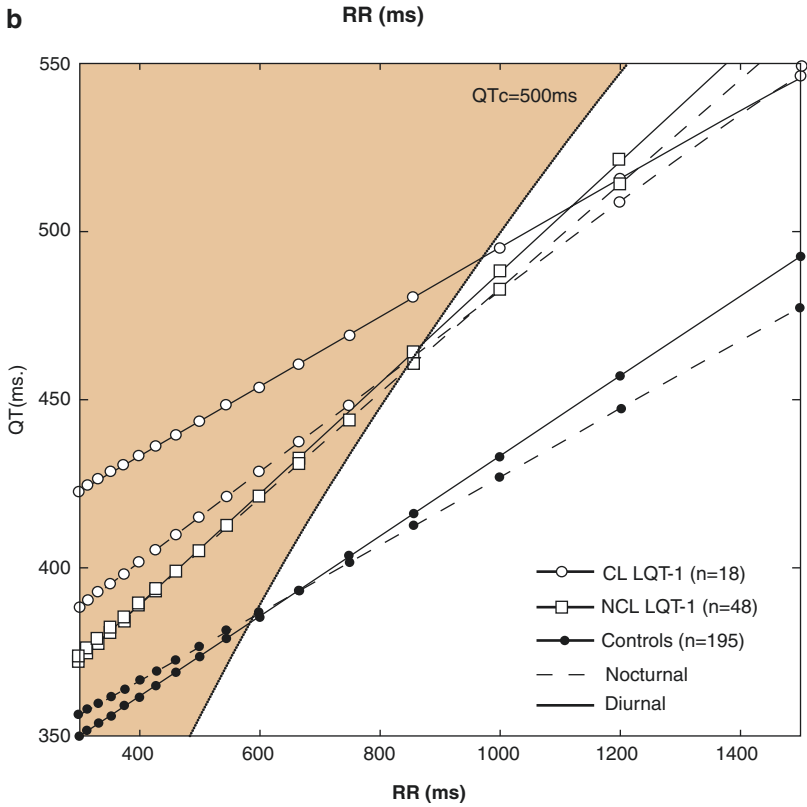
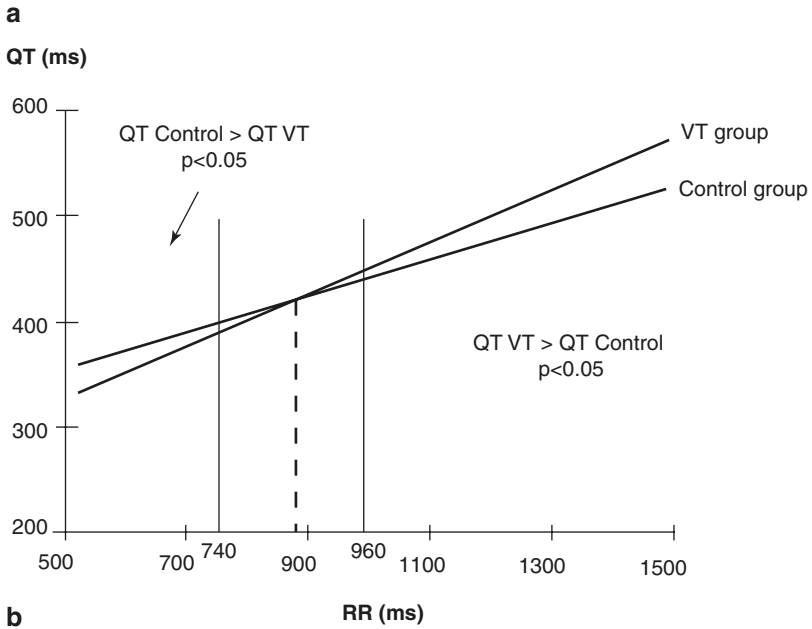


Table 2.1 QT/RR slopes in patients with VT or VF after myocardial infarction

	VT	VF	Difference [95% CI]
QT/RR	0.172	0.229	-0.057
During the day	[0.145; 0.199]	[0.193; 0.265]	[-0.101; -0.012]
QT/RR	0.175	0.188	-0.013
At night	[0.125; 0.226]	[0.143; 0.233]	[-0.081; 0.055]
QT/RR	0.180	0.338	-0.158
After awakening	[0.134; 0.226]	[0.292; 0.385]	[-0.224; -0.093]

Unpublished data from Ref. [105]

exercise and recovery has shown clinical value in certain situations, such as differentiating patients with long QT syndrome from patients with borderline QT duration [117, 118] and as a marker of myocardial ischemia [119, 120].

In long QT syndrome, Krahn showed that an exaggerated hysteresis of the QT interval was seen in patients with long QT syndrome at baseline compared with controls (46 ms vs. 19 ms). In this study, beta-blockers markedly reduced hysteresis [117]. In another study, this group reported that LQT2 patients had an exaggerated QT hysteresis compared with LQT1 and control subjects [118].

However, the mechanism of QT-RR hysteresis is not fully understood. It has been speculated that autonomic balance contributes to differences in repolarization during exercise and following recovery period. Specifically, late exercise is characterized by a shifted sympathovagal balance with enhanced sympathetic tone, whereas at early recovery, the parasympathetic tone quickly increases, while the sympathetic tone is declining. [117]. Pelchovitz evaluated QT-RR hysteresis in three groups of subjects, the first group consisted of normal subjects, the second group consisted of subjects with type 2 diabetes mellitus with no known cardiovascular disease, and the last group consisted of subjects with coronary artery disease. In this study protocol, subjects underwent exercise test with and without parasympathetic blockade [121]. The study demonstrates that parasympathetic blockade reverses the expected QT-RR hysteresis that would be due to directional changes in the RR interval, suggesting that differential parasympathetic inputs during exercise and recovery are responsible in large part for this phenomenon (for instance,

Δ QT intervals without parasympathetic blockade were 6.8 ms in the control, and after parasympathetic blockade, Δ QT intervals were - 19.1 ms).

Peak to Tend Interval

Tpeak to Tend (TpTe) interval has been found to be an independent risk factor for SCD. In the Oregon Sudden Unexpected Death Study, a population-based study of SCD, TpTe interval on the resting 12-lead ECG was prolonged in SCD cases compared to control subjects and was significantly associated with SCD independently of age, gender, QTc, QRS duration, and left ventricular dysfunction [122].

In 2017, Tse and co-authors performed a systematic review and a meta-analysis to evaluate the significance of the TpTe interval in predicting arrhythmic and/or mortality end points. A total of 33 observational studies involving 155,856 patients were included in the meta-analysis [123].

The main findings of this study were the following, supporting the Oregon study findings:

- A prolonged TpTe interval is associated with a 1.14-fold increased risk in VT/VF, SCD, cardiovascular death, or all-cause mortality when data from all pathological conditions were pooled with significant heterogeneity among studies.
- In the general population, a prolonged TpTe interval was also predictive of arrhythmic or mortality outcomes with an OR of 1.59.

The link from TpTe interval to mechanisms of ventricular arrhythmia has been investigated in many nonclinical trials. Using a canine myocardial wedge preparation model, Antzelevitch and co-workers have explored the genesis of TpTe.

In this study, TpTe corresponds to ventricular transmural dispersion of repolarization, a period during which the epicardium has repolarized and is fully excitable, but the M cells are still in the process of repolarization [124, 125]. According to this model, a prolonged TpTe corresponds to a vulnerable period during which EAD can lead to reentry and therefore could increase risk of ventricular arrhythmias. However, the surface ECG T wave also reflects other spatial heterogeneities, such as APD differences observed between the base and the apex of the heart [126].

Vaseghi showed that during sympathetic stimulation, there is an increase in dispersion of myocardial repolarization and increase in TpTe interval [127]. The global epicardial dispersion of repolarization as measured using activation recovery intervals (ARI) at baseline and during right stellate ganglion (RSG) and left stellate ganglion (LSG) stimulation correlated with TpTe interval. Vaseghi concludes that TpTe is a proarrhythmic ECG marker related to the underlying myocardial mechanisms that explain the proarrhythmia.

Recently, Srinivasan and co-authors also examined the association between intracardiac ventricular repolarization and the T wave on the body surface ECG. They positively concluded that the precordial ECG repolarization indices reflect regional repolarization differences between the right and left heart [128]. Interestingly, this article triggered a debate among the scientific community. On behalf of the e-Rhythm group of EHRA, a group of scientists stated that “Electrocardiography is certainly a very valuable tool and we believe that important information in ECG signals remains to be deciphered including assessment of repolarization heterogeneity in terms of both spatial and temporal dispersion. Nevertheless, it seems rather unlikely that obtaining such information could be based only on simple measurements made with the naked eye and ruler” [129].

We cannot conclude this paragraph without showing a superimposed view (“butterfly”) of a 12-lead ECG in a normal subject and in a subject with a long QT syndrome type 2. Figure 2.6

shows interlead variation of the Tpeak location supporting the concerns of the e-Rhythm group. It is also fair to recall an excellent editorial from Pentti Rautaharju “QT and dispersion of ventricular repolarization: the greatest fallacy in electrocardiography in the 1990s” [130].

Beat-to-Beat Evaluation

In 2014, the European Heart Rhythm Association (EHRA) together with the ESC Working Group on Cardiac Cellular Electrophysiology released a consensus guideline concerning the beat-to-beat QT interval variability (QTV) measurement, physiological background, and clinical utility [131].

From this consensus report, we have selected and quote the three main points related to neuromodulation of ventricular repolarization and arrhythmogenesis.

- Actually, there are many remaining technical issues: “While dedicated computer programs for QTV measurement are readily available, the current level QTV measurement standardization is insufficient. Data acquisition requirements, minimum signal-to-noise levels, recording duration, pre-processing modalities, and beat and artefact rejection techniques require further investigation.”
- Then regarding neuromodulation of QTV: “The physiological basis of QTV is currently insufficiently explored. Although evidence suggests that QTV may be useful for quantifying relative changes in sympathetic ventricular outflow during states of heightened activity, it remains to be established whether QTV indices can be used to infer absolute values of sympathetic activity in normal subjects or whether QTV magnitude correlates with changes of sympathetic activity only. Future investigations should differentiate neural control directed to the sinus node from that directed to ventricles and research how this regulation contributes to the coupling/decoupling between heart rate variability and QTV.”
- Finally, regarding clinical applications: “The pathophysiology of increased QTV is poorly understood, although reduced repolarization

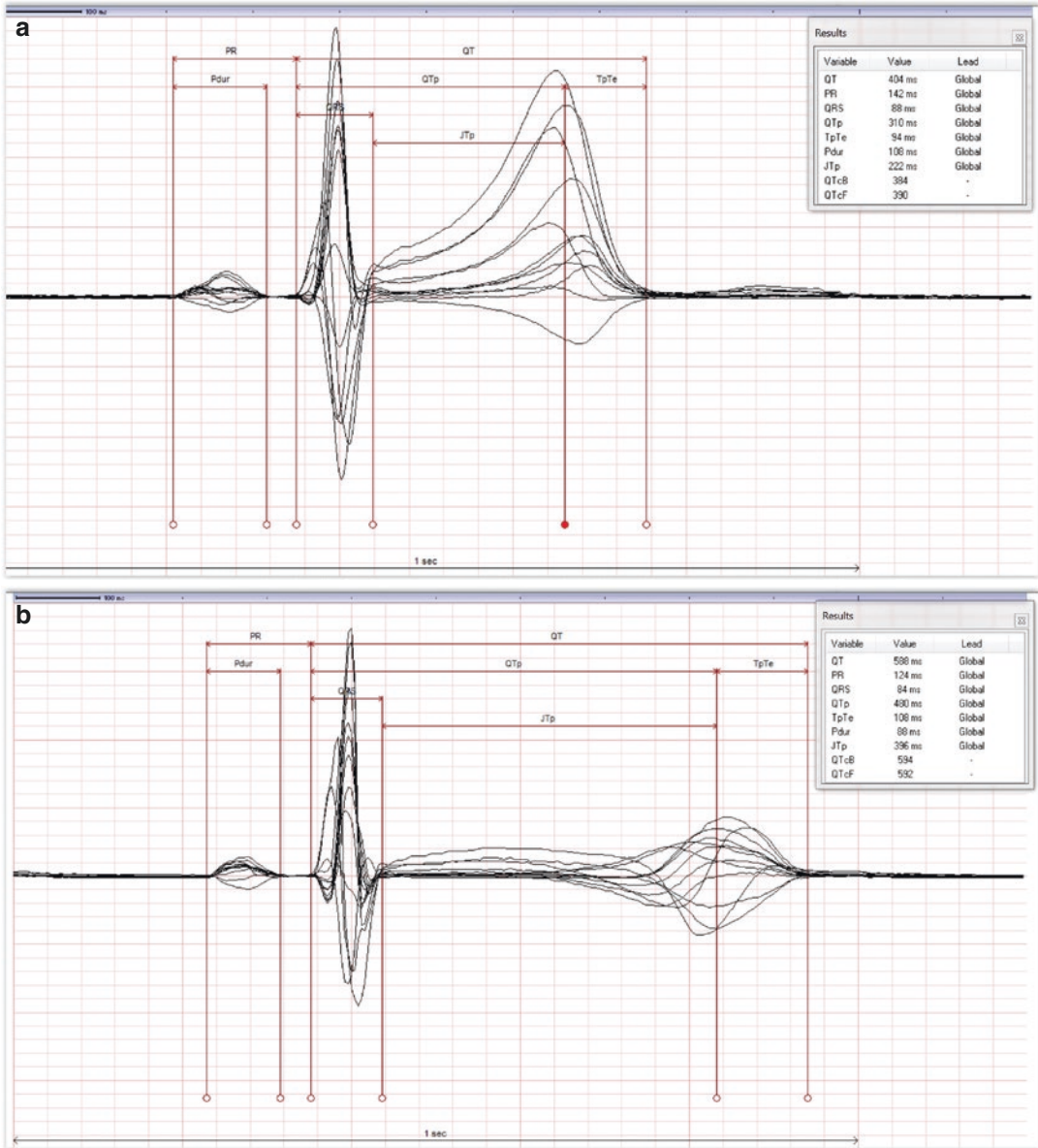


Fig. 2.6 The 12-lead superimposed view (“butterfly”) from two digital 10-second ECG. ECG collected in a normal subject (panel a) and in a LQTS patient (panel b).

Tables on the right show results calculated from the vertical cursor position. The interlead variation of the Tpeak position is large in B as well as in A

reserve, causing more variable regulation responses, may play a role. The relation between autonomic dysfunction and QTV in cardiac patients is not well established. The main clinical use of QTV may lie in SCD risk stratification. Although several studies have demonstrated independent predictive value of

QTV, most of the evidence is based on retrospective data analyze. Prospective trials are needed to prove the usefulness of QTV.”

To the best of our knowledge, the somewhat negative comment released in 2014 remains valid in 2019.

Clinical Syndromes

Several acquired cardiomyopathies and inherited channelopathies, including long QT syndrome (LQTS), catecholaminergic polymorphic ventricular cardiomyopathy (CPVT), hypertrophic cardiomyopathy (HCM), and arrhythmogenic right ventricular cardiomyopathy (ARVC), are associated with exercise-related sudden cardiac death. Syncope and cardiac arrest occur during exercise because of ventricular arrhythmias, which are mainly managed with oral β -blockade. The transvenous ICD has been in clinical use for >3 decades, and robust data from high-quality RCTs support its use in various patient populations including survivors of cardiac arrest, patients with VT and structural heart disease, and patients with significant LV dysfunction.

In this chapter, we will expose the main clinical data supporting neuromodulation of ventricular arrhythmias (Table 2.2). In particular, these are as follows:

- The mode of onset of spontaneous ventricular tachyarrhythmias and their circadian distribution, during the day, or at night, and during exercise, or at rest, at fast or low heart rates

- The daily timing of ICD therapy, early morning or at night, and the weekday peaks
- And finally, the effects of pharmacologic beta-blockade

Autonomic influences on arrhythmogenesis are not limited to VR changes. Calcium handling, DADs, conduction velocity, and rate-dependent conduction block are also modulated by ANS. But at bedside, there is no easy way of dealing with the respective contribution of each arrhythmic mechanism.

Neuromodulation of Cardiac Arrhythmias in Ischemic and Nonischemic Cardiomyopathy

There has been accumulating evidence that the sympathetic nervous system plays a considerable role in heart failure patients as well as in patients after myocardial infarction [132]. Because of their excellent safety profile and effectiveness in treating ventricular arrhythmias and reducing the risk of sudden cardiac death, beta-blockers are often the first-line antiarrhythmic therapy [84, 133–136]. Their antiarrhythmic efficacy is related to the effects of adrenergic-receptor blockade on sympathetically mediated triggering mechanisms.

Table 2.2 Neuromodulation of ventricular arrhythmias: clinical features

Clinical syndrome	Onset mode	Circadian pattern	Beta-blocker efficacy	Cardiac denervation
ICM, NICM	Exercise Mental stress Tachycardia HRV decrease	Early morning Monday	+++	+++ (electrical storm)
Type 1 LQTS	Exercise Stress Tachycardia Swimming	Unknown	+++	++
Type 2 LQTS	Exercise Stress Tachycardia Auditory stimulus	Unknown	++	++
Type 3 LQTS	Rest Bradycardia Pause	Nocturnal	±	–
Short QTS	None	None	±	–
Brugada syndrome	Bradycardia Meal Fever	Nocturnal	– Isoproterenol +	–
ERS	Bradycardia	Nocturnal	– Isoproterenol +	–

Sudden death and implantable cardioverter-defibrillator (ICD) shocks have been reported to occur with higher frequency in the early morning hours together with increased event rates on Mondays, in both ischemic and nonischemic cardiomyopathies. Mechanisms such as physical activity or mental stress that could stimulate sympathetic activity or cause ischemia were suggested to account for the morning peak and increase in events on Mondays. The higher risk for sudden death in the first hours after awakening may in part be due to the morning increase in blood pressure and heart rate, increased vascular tone, changes in heart rate variability, elevated blood viscosity, and platelet aggregability.

Analysis of the timing of ICD therapy for life-threatening ventricular arrhythmias in the Sudden Cardiac Death-Heart Failure Trial (SCD-HeFT) cohort also confirmed that the time distribution of ICD therapies shows an early morning nadir in occurrence of ventricular arrhythmia, but no overall typical morning peak or Monday increase in events. However, subjects not on beta-blocker therapy demonstrated an increased event rate on Mondays. These findings may indicate suppression of neurohormonal triggers with current cardiac therapies. This has also led to the hypothesis that a subset of episodes of ventricular arrhythmias and sudden cardiac death corresponding to these circadian surges may be aborted by treating patients with beta-blockers [137].

The Oregon SUDS is an ongoing, prospective community-based study of out-of-hospital SCA in the Portland, Oregon, metropolitan area. In brief, cases of SCA are identified prospectively from among all residents of the region. For this analysis, cases identified between February 1, 2002, and January 31, 2014, were included. The authors did not observe a morning peak in SCA in this community-based prospective observational study. Additionally, during the week, they did not observe any peak of SCA occurrence on Mondays. Instead, they found a nadir in SCA occurrence on Sundays. Although the exact mechanisms need further investigation, the authors speculated about a potential interference of the Internet and smartphones use, which allow any activities 24 hours a day, 7 days a week [138].

A direct temporal relationship has been established between sympathetic activity and spontaneous ventricular tachycardia using heart rate and as a surrogate of sympathetic tone. Results regarding heart rate variability are more conflicting. Shusterman reported that before the onset of VT recorded in Holter recordings, heart rate increases, whereas index of heart rate variability decreases [139]. The HAWAI registry evaluated the role of sinus tachycardia and heart rate variability in predicting the occurrence of ventricular tachycardia and fibrillation (VT/VF) in patients with an implantable cardioverter-defibrillator [140]. A significant decrease of the mean value of all RR intervals was observed in the period prior to VT. The standard deviation of RR intervals (SDNN) and the power at low frequency (LF) also showed significant changes prior to VT/VF. Au-Yeung explored the use of ICD data to automatically predict ventricular arrhythmia using heart rate variability in patients enrolled in the ICD arm of the Sudden Cardiac Death-Heart Failure Trial (SCD-HeFT). The AUC for the prediction models were above 0.8, and the authors conclude that moderate classification accuracy can be achieved to predict ventricular tachyarrhythmia with machine learning algorithms using HRV features from ICD data [141].

Finally, the results of sympathetic neural ablation procedures in patients with ventricular tachyarrhythmias. This will be discussed in the section “[Antiarrhythmic Neuromodulations of VR: beyond oral Beta-adrenergic blockade](#)”.

Congenital Long QT Syndrome

The diagnosis of LQTS is made clinically by combining patient and family history and the 12-lead ECG. The LQTS syndrome is caused by mutations in any of 17 LQTS genes, but the most common genotypes are LQT1, 2, and 3, and here we will only discuss the neuromodulation of those three genotypes. On the surface ECG, a prolonged QT interval is key [142–145].

LQT1 is the most common, representing 30–35% of all congenital LQTS. The hallmark of LQT1 is the failure of the QT interval to adapt to increases in heart rate, as often seen during diagnostic exercise stress testing [144, 145]. Cardiac

events in patients with IKs-associated LQTS are often triggered by stress and exercise [144, 145]. β -Blockers have been demonstrated as a particularly effective therapy for LQT1 patients, who are more sensitive to stress- and exercise-induced arrhythmia than other LQT subtypes [144–146]. The stronger the blockade, the stronger the clinical efficacy [147].

However, the efficacy of β -blockers is strongly genotype-specific. Adrenergic trigger seems less important in LQT2, and events more frequently occur during sleep or at rest in type 3 LQTS [148, 149]. Occurrence of arrhythmic events with bradycardia, as well as potential concomitant Brugada syndrome, has raised concerns about the use of β -blockers in LQT3 patients [148, 149]. β -Blockers produce greatest symptom relief and cardiac event reduction in LQT1 patients, followed by LQT2 patients, and are least effective in LQT3 patients [26, 148, 149]. The efficacy of beta-blockade in LQT1 and LQT2 is not related to the effects on QTc interval duration. Actually, we reported that the effect of beta-adrenergic blockade on QTc duration is different in LQT1 and LQT2 patients. In LQT1 patients, the beneficial effect of beta-blockade is associated with a prolongation of QTc duration, whereas beta-blockade therapy in LQT2 leads to QTc shortening [90].

In selected cases, left cervicothoracic sympathetic denervation (LCSD), which surgically interrupts adrenergic input to the heart, can be considered. This will be discussed in depth in section “[Vagus Nerve Stimulation](#)”.

Congenital Short QT Syndrome

Short QT syndrome (SQTS) is a rare disease known for less than 20 years. It is an inherited cardiac channelopathy characterized by an abnormally short QT interval and increased risk for atrial and ventricular arrhythmias. Diagnosis is based on the evaluation of symptoms (syncope or cardiac arrest), family history, and electrocardiogram (ECG) findings [150–152].

In SQTS, arrhythmic events occur both at rest and during effort, and as of today, it is not possible to identify a consistent trigger for those events. There is lack of data to support a clinically

significant neuromodulation of ventricular repolarization on SQTS patients [150–152]. In the study published by Mazzanti and co-authors [153], 20 patients experienced cardiac arrest, of whom 10 had multiple events. A total of 25 events occurred during rest, sleep, or quiet routine activities, 3 during emotional stress, and 2 during effort. The arrhythmic triggers in SQTS appear more similar to Brugada syndrome (see below).

Based on the family history of individuals with SQTS and their relatives, early studies of patients with SQTS suggested a very high risk of SCD. An ICD was considered the first-choice therapy, but alternative therapy was necessary, especially in small children [29, 153, 154]. The first clinical results of testing of hydroquinidine as a QT-prolonging drug and reducing arrhythmic events in patients with SQTS were reported as early as 2006 [155, 156]. So far, treatment with hydroquinidine remains to be associated with a lower incidence of arrhythmic events, and the therapy seems to be safe [153].

J-Wave Syndromes

Both Brugada syndrome (BrS) and early repolarization syndrome (ERS) are clinical syndromes occurring in subjects with no apparent structural heart disease but affected with severe ventricular arrhythmias, ventricular fibrillation (VF) and polymorphic ventricular tachycardia, and sudden cardiac death [145, 157, 158].

Among clinical similarities in BrS and ERS, there is a male predominance in both syndromes, with a peak incidence of VF or sudden cardiac death occurring in the third or fourth decade of life. Most interestingly for this review on neuromodulation of arrhythmogenesis, the accentuated J waves and ST-segment elevation are generally associated with bradycardia or pauses, and VF events have been proposed to occur mostly during sleep or at low levels of physical activity [145, 157, 158].

The pathophysiological mechanisms underlying the J-wave syndromes remain a matter of debate. Sympathovagal balance, among other factors, modulates not only ECG morphology in BrS but could also explain the development of ventricular arrhythmias under certain conditions [159]. Analysis of the mode of onset and

circadian distribution of spontaneous episodes of ventricular tachyarrhythmia indicates that the appearance of accentuated J waves and ST-segment elevation is generally associated with bradycardia or pauses. This can explain why VF in both syndromes often occurs during sleep or during a low level of physical activities [145, 157, 158].

Kamakura investigated the onset mode and circadian distribution of ventricular tachyarrhythmia episodes in ERS and BrS, respectively. They reported that most VTAs occurred nocturnally in patients with ERS and BrS [160, 161]. Kim reported similar findings in patients who underwent implantable cardioverter-defibrillator implantation. Circadian distribution of appropriate shocks showed a significant nocturnal peak in patients with ERS and a nonsignificant trend toward a nocturnal peak in patients with BrS [162]. Ikeda in patients with a Brugada-type ECG assessed 12-lead ECGs before and after a large meal (full stomach test). The full stomach test was positive in 17 of the study patients. A positive test outcome was characterized by a higher incidence of a history of life-threatening events [163]. Mizumaki evaluated the relationship between augmentation of J-wave elevation and changes in RR interval or autonomic nervous activities in patients with idiopathic VF. The authors concluded that J-wave elevation was more strongly augmented during bradycardia and was associated with an increase in vagal activity [164]. Aizawa assessed the circadian pattern of VF occurrence in 64 patients with idiopathic ventricular fibrillation, excluding Brugada syndrome. The overall distribution pattern of VF occurrence showed two peaks at approximately 6:00 AM and around 8:00 PM. Nocturnal VF was observed in 20 patients (31.3%), and J waves were present in 14 of these 20 individuals (70.0%), whereas J waves were less frequent in the 44 non-nocturnal patients with VF. The authors concluded that the presence of J waves may characterize a higher nocturnal incidence of VF and a higher acute and chronic risk of recurrence [165].

Catecholaminergic Polymorphic Ventricular Tachycardia (CPVT)

The CPVT is the most caricatural presentation of the link between exercise and/or mental stress and ventricular arrhythmias leading to syncope and SCD [166]. Key clinical features include 1) bidirectional ventricular premature beats or Tachycardia, 2) normal resting ECG, 3) structurally normal heart, 4) occurrence of arrhythmias and symptoms (syncope or cardiac arrest) under increased sympathetic activity conditions, 5) first symptoms during the 2 first decades of life [167]. CPVT is a genetic disease, and all the mutations found are located in genes coding for proteins involved in reticulum calcium handling [168, 169].

The mechanism of arrhythmias is believed to be related to diastolic calcium leakage from the sarcoplasmic reticulum, with a subsequent increase in the cytosolic calcium concentration leading to electrogenic sodium/calcium exchanger activation and DADs [170, 171]. Accordingly, VR is not a major player in arrhythmogenesis in CPVT. It was, however, difficult not to reference CPVT syndrome in this review.

Beta-blocker treatment is pivotal, although not fully effective, in CPVT management, but more recently sodium channel blockade has been shown to improve outcome [172–174].

Antiarrhythmic Neuromodulations of Ventricular Repolarization: Beyond Oral Beta-Adrenergic Blockade

Despite medications and ICD, a significant proportion of patients with heart disease continue to experience arrhythmias. Non-pharmacological intervention such as catheter ablation can be useful for reducing recurrent VT and ICD shocks [175]. Non-pharmacologic modulation of the autonomic nervous system for the purpose of preventing arrhythmias is an emerging new therapeutic modality [84].

Modulation of the Sympathetic Nervous System

The autonomic modulation can be achieved either through interruption of sympathetic outflow to the heart or through stimulation of the parasympathetic pathway [84]. Surgical autonomic modulation has proven efficacy for certain long QT syndrome and catecholaminergic polymorphic ventricular tachycardia [84].

Cardiac Sympathetic Denervation

Early studies in anginal patients treated with sympathectomy were highly successful in preventing anginal attacks and improving performance during an exercise stress test. But with the availability of oral β -blockers, sympathectomy became outdated despite its clear efficacy [176]. Interest for the antiarrhythmic potential has been rapidly expanding. The anti-fibrillatory effect of left cardiac sympathetic denervation (CSD) has clearly been demonstrated in LQTS patients and in patients with catecholaminergic polymorphic ventricular tachycardia [84, 145, 177–181]. Traditionally, a thoracotomy or cervical incision has been used as the standard surgical approach for performing left cardiac sympathetic denervation, but more recently video-assisted thoracoscopic surgery allows a minimally invasive technique [182].

Early studies demonstrated that only left stellate ganglion block increased the ventricular fibrillation threshold and protected against ischemic ventricular arrhythmia. Usually it has been admitted that blockade of the right stellate ganglion had a potentially arrhythmogenic effect. The different effects of left versus right cardiac sympathetic denervation were explained by the fact that the left-sided cardiac sympathetic nerves are quantitatively dominant at the ventricular level. However, bilateral cardiac sympathetic denervation does appear to be at least non-inferior and potentially superior to left CSD for treatment of ventricular arrhythmia in humans [183, 184].

For cardiovascular disease, CSD has been used primarily as a treatment modality in young adults and children with life-threatening arrhythmias due to inherited channelopathies, such as LQTS and CPVT [145]. Recent international guidelines recommend left CSD for LQTS and CPVT when ICD or beta-blocker therapy is not able to be implemented effectively [84]. The value of CSD for ventricular arrhythmias secondary to ischemia and ischemic cardiomyopathy is less well established, but more recently, a significant decrease in ICD shocks in patients with refractory ventricular arrhythmias following either left or bilateral CSD has been reported [185, 186]. Efficacy has also been demonstrated for general anesthesia in the acute management of refractory ventricular arrhythmias [187].

Cardiac Sympathetic Blockade

Cardiac sympathetic denervation is typically a surgical resection of the lower half of the stellate ganglion (thoracotomy or cervical incision and more recently video-assisted thoracoscopic surgery), but another approach of neuromodulation is stellate ganglion block, so-called stellate ganglion block (SGB), performed by injecting local anesthetic agents percutaneously to stellate ganglion, which is less invasive than CSD and can be performed at bedside in emergent setting in patients with hemodynamic instability [188–191]. To better understand the role of SGB in electrical storms, Meng and co-authors performed dedicated literature searches [189]. SGB was achieved by administering local anesthetic percutaneously to the SG. Most patients only had left SGB and in few of them both left and right SGB. The major findings of this review on the efficacy of SGB for electrical storm are threefold: GB is effective in reducing the number episodes and therapies for VA; this efficacy was independent of the subtype of ventricular arrhythmia, the presence or absence of cardiomyopathy, and the degree of LV dysfunction in the patients studied.

Vagus Nerve Stimulation

The finding that decreased vagal activity could be as important as increased sympathetic activity in jeopardizing cardiovascular morbidity and mortality drew attention to the possibility to implement the enhancement of vagal tone in clinical practice. However, it is fair to admit that there are few drugs that can be used for vagus nerve activation in the clinic.

Endurance exercise training is well established to modify autonomic nervous system balance, with a coupling effect, increase in cardiac parasympathetic tone and decrease in sympathetic activity [192, 193]. The effects of endurance exercise training exercise on ventricular repolarization abnormalities have not been extensively investigated. Some data suggest that endurance exercise training can reduce ischemically induced heterogeneities in repolarization and thereby could protect against ventricular fibrillation [192, 193].

By increasing parasympathetic drive, direct vagal nerve stimulation (VNS) has been shown to have beneficial cardiac effects. VNS reduces slope of APD restitution, lengthen ventricular refractory periods, and raise VF threshold in various animal models including rats, rabbits, pigs, cats, and dogs [194, 195]. A reduction in sudden cardiac death from ventricular arrhythmias has been demonstrated with vagal stimulation in a healed infarct canine model subjected to repeat ischemia. Vanoli showed that direct electrical vagal stimulation is feasible in conscious animals and that, when commenced shortly after the onset of an episode of acute myocardial ischemia, it provides significant protection from ventricular fibrillation [196].

Recently VNS was also shown to reduce ventricular tachyarrhythmia inducibility in the setting of chronic myocardial infarction. Kolman studied the effect of VNS upon ventricular vulnerability in 30 mongrel dogs subjected to varying levels of adrenergic stimulation [197]. Vulnerability was assessed both by determining the minimum current required to produce ventricular fibrillation (VF threshold). VNS was without significant effect on the VF threshold, but

during left SGS, however, VNS was associated with a 93% increase in VF threshold. After beta-adrenergic blockade with propranolol, VNS was without effect on VF threshold. Authors concluded that increased sympathetic tone is a precondition for a VNS-induced elevation in VF threshold. According to Kolman, the vagal effect is indirect and is expressed by opposing the effects of heightened adrenergic tone on ventricular vulnerability [197].

In another study, Yamaguchi reported that the electrophysiological and hemodynamic effects of bilateral VNS were not mitigated by CSD, involving bilateral stellectomy and removal of T2–T4 thoracic ganglia. The authors concluded that much of the beneficial effects of VNS are driven by activation of efferent vagal fibers acting directly at the neural-myocyte interface rather than through central sympathetic inhibition. Furthermore, CSD and VNS could have synergistic effects in the treatment of ventricular arrhythmias [198].

The first human cardiac application was described in eight patients for the indication of heart failure using CardioFit stimulators [199]. Subsequent human trials for heart failure have shown conflicting results. ANTHEM-HF, a nonblinded trial for NYHA II–III patients with EF <40%, showed improvements in NYHA class and EF [200]. NECTAR-HF was a randomized blinded study, which showed no improvements with VNS with respect to objective parameters, such as EF, but improved clinical parameters such as NYHA class [201]. INOVATE-HF was a randomized study that further showed no benefit of mortality or worsening HF in NYHA III patients with EF \leq 40% [202]. As mentioned above, the vago-sympathetic trunk contains both parasympathetic and sympathetic and afferent and efferent nerves. Different stimulation parameters can differentially engage these fibers, and the stimulation parameters used can significantly affect the outcomes of VNS and may account for the mixed human clinical trial results. With better characterization of the optimal dose of stimulation, VNS could remain a promising option to apply to reduce VT/VF.

A Black Cat Crossing the Path: Isoproterenol as Antiarrhythmic Drug

Although adrenergic stimulation is proarrhythmic in most cases, the antiarrhythmic effects of beta-adrenergic stimulation deserve to be described.

The chronotropic effect of beta-adrenergic stimulation has long been used to prevent ventricular arrhythmias arising during severe bradycardia [203]. Bradycardia-induced QT prolongation and drug-induced torsades de pointes are the hallmarks of the beneficial effects of adrenergic stimulation that can be found in any cardiology textbook. It is however important to underline that isoproterenol may promote torsades de pointes immediately after the start of the infusion, before heart rate acceleration, and when QT prolongation is related to a congenital form (specifically, type 1 LQTS).

More recently, the description of arrhythmia mechanisms related to abnormal epicardial ventricular repolarization in Brugada syndrome models has provided a rationale for the use of adrenergic stimulation in order to prevent arrhythmias [56]. Specifically, the adrenergic-induced increase in I_{CaL} will counterbalance the prominent I_{to} current, hence preventing the early repolarization at the base of both phase 2 reentry and increased spatial dispersion of ventricular repolarization duration.

The efficacy in clinical practice has been subsequently documented in patients with a Brugada syndrome during electrical storms [204, 205].

Isoproterenol infusion has also been shown to prevent VF recurrences during electrical storms in patients with the early repolarization syndrome (ERS) [206]. The efficacy of adrenergic stimulation in ERS patients supports a similar pathophysiological background with the Brugada syndrome and the so-called repolarization hypothesis as the underlying mechanism of arrhythmias in J-wave syndromes [207].

Finally, isoproterenol has been also reported to prevent ventricular arrhythmia recurrences in the short QT syndrome [208]. The underlying mechanism remains to be determined.

Future Aspects

Renal denervation has been proposed as a way to decrease central sympathetic activity, initially to decrease blood pressure in patients with refractory hypertension. It has also shown antiarrhythmic effects at the ventricular level in different animal models as well as in limited cases in patients [209–212]. This approach definitely warrants further validation.

Spinal cord stimulation reduces stellate ganglia activity and increases vagal tone. It has been shown to reduce regional myocardial sympathoexcitation, decrease ventricular arrhythmias, and improve myocardial function in a porcine model of acute ventricular ischemia [213]. Clinical evaluation in patients with reduced left ventricular ejection fraction heart failure showed however no improvement in ejection fraction [214].

Recent experimental studies have addressed the proarrhythmic consequences of heterogeneous spatial sympathetic innervation after myocardial infarction. Both innervation restoration [215] and homogenization by local denervation [216] have been shown to prevent ventricular arrhythmias. These innovative approaches underline the complexity of electrophysiologic effects of cardiac innervation [217], the gap in understanding but also the opportunity for future experimental research that will hopefully lead to clinical validation.

Conclusions

Adrenergic stimulation strongly influences ventricular repolarization with a proarrhythmic potential. Repolarization changes are not a single player, and changes in calcium handling induced by adrenergic stimulation are also potent proarrhythmic factors. However, as illustrated with action potential alternans mechanisms, these two determinants interact each other [218–220]. We still probably fail to reach a deep understanding of the complex relationship between repolarization dynamics and calcium handling, in the

search to elucidate the mechanisms and timing leading to ventricular fibrillation.

Despite the flaws in our understanding, counteracting adrenergic stimulation by using beta-blocking drugs has been one of the best success stories in cardiology. Indeed, as stated by Douglas Zipes: “the greatest reduction in cardiovascular mortality (including SCD) in patients with clinically manifest heart disease has resulted from the use of beta blockers and non-antiarrhythmic drugs” [38, 221].

The strong guideline recommendation and widespread use of beta-blockers in patients with cardiomyopathies do not mean that the proarrhythmic potential of adrenergic stimulation has been solved. Conversely, the concept of “the ‘adrenergic paradox’ that implies that “the more marked the autonomic nervous system dependence of tachyarrhythmias, the less obvious its evidence [222]” is strongly supported by the already proven efficacy of non-pharmacological reduction in sympathetic stimulation described above. Improving our understanding and ability to interfere with the complex tuning of the autonomic nervous system is most probably an avenue to further decrease the burden of sudden cardiac death.

References

- Engel GL. Sudden and rapid death during psychological stress. Folklore or folk wisdom? *Ann Intern Med.* 1971;74:771–82.
- Trichopoulos D, Katsouyanni K, Zavitsanos X, Tzonou A, Dalla-Vorgia P. Psychological stress and fatal heart attack: the Athens (1981) earthquake natural experiment. *Lancet.* 1983;1(8322):441–4.
- Meisel SR, Kutz I, Dayan KI, Pauzner H, Chetboun I, Arbel Y, David D. Effect of Iraqi missile war on incidence of acute myocardial infarction and sudden death in Israeli civilians. *Lancet.* 1991;338(8768):660–1.
- Leor J, Poole WK, Kloner RA. Sudden cardiac death triggered by an earthquake. *N Engl J Med.* 1996;334:413–9.
- Steinberg JS, Arshad A, Kowalski M, Kukar A, Suma V, Vloka M, et al. Increased incidence of life-threatening ventricular arrhythmias in implantable defibrillator patients after the World Trade Center attack. *J Am Coll Cardiol.* 2004;44:1261–4.
- Shedd OL, Sears SF Jr, Harvill JL, Arshad A, Conti JB, Steinberg JS, Curtis AB. The World Trade Center attack: increased frequency of defibrillator shocks for ventricular arrhythmias in patients living remotely from New York City. *J Am Coll Cardiol.* 2004 Sep 15;44:1265–7.
- Jokl E, McClellan JT. Exercise and cardiac death. *JAMA.* 1970;213:1489–91.
- Opie LH. Sudden death and sport. *Lancet.* 1975;1:263–6.
- Aponte G. The enigma of “Bangungut”. *Ann Intern Med.* 1960;52:1258–63.
- Baron RC, Thacker SB, Gorelkin L, Vernon AA, Taylor WR, Choi K. Sudden death among Southeast Asian refugees. An unexplained nocturnal phenomenon. *JAMA.* 1983;250:2947–51.
- Lown B, Verrier R, Corbalan R. Psychologic stress and threshold for repetitive ventricular response. *Science.* 1973;182:834–6.
- Brodsky MA, Sato DA, Iseri LT, Wolff LJ, Allen BJ. Ventricular tachyarrhythmia associated with psychological stress. The role of the sympathetic nervous system. *JAMA.* 1987;257:2064–7.
- Verrier RL, Thompson PL, Lown B. Ventricular vulnerability during sympathetic stimulation: role of heart rate and blood pressure. *Cardiovasc Res.* 1974;8:602–10.
- Lown B, Verrier RL. Neural activity and ventricular fibrillation. *N Engl J Med.* 1976;294:1165–70.
- Verrier RL, Calvert A, Lown B. Effect of posterior hypothalamic stimulation on ventricular fibrillation threshold. *Am J Phys.* 1975;228:923–7.
- Brooks WW, Verrier RL, Lown B. Influence of vagal tone on stellatectomy-induced changes in ventricular electrical stability. *Am J Phys.* 1978;234:H503–7.
- Coumel P, Rosengarten MD, Leclercq JF, Attuel P. Role of sympathetic nervous system in non-ischaemic ventricular arrhythmias. *Br Heart J.* 1982;47:137–47.
- Coumel P, Leenhardt A. Mental activity, adrenergic modulation, and cardiac arrhythmias in patients with heart disease. *Circulation.* 1991;83:II58–70.
- del Castillo J, Katz B. Production of membrane potential changes in the frog’s heart by inhibitory nerve impulses. *Nature.* 1955;175:1035.
- Hutter OF, Trautwein W. Vagal and sympathetic effects on the pacemaker fibers in the sinus venosus of the heart. *J Gen Physiol.* 1956;39:715–33.
- Kawashima T. The autonomic nervous system of the human heart with special reference to its origin, course, and peripheral distribution. *Anat Embryol.* 2005;209:425–38.
- Hanna P, Rajendran PS, Ajijola OA, Vaseghi M, Andrew Armour J, Ardell JL, Shivkumar K. Cardiac neuroanatomy – imaging nerves to define functional control. *Auton Neurosci.* 2017;207:48–58.
- Jänig W. Neurocardiology: a neurobiologist’s perspective. *J Physiol.* 2016;594:3955–62.
- Saucerman JJ, Brunton LL, Michailova AP, McCulloch AD. Modeling beta-adrenergic control of cardiac myocyte contractility in silico. *J Biol Chem.* 2003;278:47997–8003.

25. Levy MN. Sympathetic-parasympathetic interactions in the heart. *Circ Res.* 1971;29:437–45.
26. Reuter H. Calcium channel modulation by neurotransmitters, enzymes and drugs. *Nature.* 1983;301:569–74.
27. Tsien RW, Bean BP, Hess P, Lansman JB, Nilius B, Nowicky MC. Mechanisms of calcium channel modulation by beta-adrenergic agents and dihydropyridine calcium agonists. *J Mol Cell Cardiol.* 1986;18:691–710.
28. Bennett PB, Begenisich TB. Catecholamines modulate the delayed rectifying potassium current (IK) in guinea pig ventricular myocytes. *Pflugers Arch.* 1987;410:217–9.
29. Finlay M, Harmer SC, Tinker A. The control of cardiac ventricular excitability by autonomic pathways. *Pharmacol Ther.* 2017;174:97–111.
30. Choudhury M, Boyett MR, Morris GM. Biology of the sinus node and its disease. *Arrhythm Electrophysiol Rev.* 2015;4:28–34.
31. Carmeliet E. Repolarisation and frequency in cardiac cells. *J Physiol Paris.* 1977;73:903–23.
32. Nattel S, Euler DE, Spear JF, Moore EN. Autonomic control of ventricular refractoriness. *Am J Phys.* 1981;241:H878–82.
33. Viswanathan PC, Shaw RM, Rudy Y. Effects of IKr and IKs heterogeneity on action potential duration and its rate dependence: a simulation study. *Circulation.* 1999;99:2466–74.
34. Luo CH, Rudy Y. A model of the ventricular cardiac action potential. Depolarization, repolarization, and their interaction. *Circ Res.* 1991;68:1501–26.
35. Matsuda JJ, Lee H, Shibata EF. Enhancement of rabbit cardiac sodium channels by beta-adrenergic stimulation. *Circ Res.* 1992;70:199–207.
36. Hallaq H, Yang Z, Viswanathan PC, Fukuda K, Shen W, Wang DW, et al. Quantitation of protein kinase A-mediated trafficking of cardiac sodium channels in living cells. *Cardiovasc Res.* 2006;72:250–61.
37. Lambiase PD, Tinker A. Connexins in the heart. *Cell Tissue Res.* 2015;360:675–84.
38. Rubart M, Zipes DP. *J Clin Invest.* 2005;115:2305–15.
39. Brunello L, Slabaugh JL, Radwanski PB, Ho HT, Belevych AE, Lou Q, et al. Decreased RyR2 refractoriness determines myocardial synchronization of aberrant Ca²⁺ release in a genetic model of arrhythmia. *Proc Natl Acad Sci U S A.* 2013;110:10312–7.
40. Marx SO, Reiken S, Hisamatsu Y, Jayaraman T, Burkhoff D, Rosembli N, et al. PKA phosphorylation dissociates FKBP12.6 from the calcium release channel (ryanodine receptor): defective regulation in failing hearts. *Cell.* 2000;101:365–76.
41. Luo CH, Rudy Y. A dynamic model of the cardiac ventricular action potential. I. Simulations of ionic currents and concentration changes. *Circ Res.* 1994;74:1071–96.
42. Luo CH, Rudy Y. A dynamic model of the cardiac ventricular action potential. II. Afterdepolarizations, triggered activity, and potentiation. *Circ Res.* 1994;74:1097–113.
43. Xie Y, Grandi E, Puglisi JL, Sato D, Bers DM. β -adrenergic stimulation activates early afterdepolarizations transiently via kinetic mismatch of PKA targets. *J Mol Cell Cardiol.* 2013;58:153–61.
44. Burashnikov A, Antzelevitch C. Block of I_{Ks} does not induce early afterdepolarization activity but promotes beta-adrenergic agonist-induced delayed after depolarization activity. *J Cardiovasc Electrophysiol.* 2000;11:458–65.
45. Liu GX, Choi BR, Ziv O, Li W, de Lange E, Qu Z, Koren G. Differential conditions for early afterdepolarizations and triggered activity in cardiomyocytes derived from transgenic LQT1 and LQT2 rabbits. *J Physiol.* 2012;590:1171–80.
46. Mines GR. On dynamic equilibrium in the heart. *J Physiol.* 1913;46:349–83.
47. Kléber AG, Rudy Y. Basic mechanisms of cardiac impulse propagation and associated arrhythmias. *Physiol Rev.* 2004;84:431–88.
48. Han J, Moe GK. Nonuniform recovery of excitability in ventricular muscle. *Circ Res.* 1964;14:44–60.
49. Kuo CS, Munakata K, Reddy CP, Surawicz B. Characteristics and possible mechanism of ventricular arrhythmia dependent on the dispersion of action potential durations. *Circulation.* 1983;67:1356–67.
50. Gough WB, Mehra R, Restivo M, et al. Reentrant ventricular arrhythmias in the late myocardial infarction period. 13. Correlation of activation and refractory maps. *Circ Res.* 1985;57:432–42.
51. Shimizu W, Antzelevitch C. Cellular basis for the ECG features of the LQT1 form of the long-QT syndrome: effects of beta-adrenergic agonists and antagonists and sodium channel blockers on transmural dispersion of repolarization and torsade de pointes. *Circulation.* 1998;98:2314–22.
52. Lacroix D, Extramiana F, Delfaut P, Adamantidis M, Grandmougin D, Klug D, et al. Factors affecting epicardial dispersion of repolarization: a mapping study in the isolated porcine heart. *Cardiovasc Res.* 1999;41:563–74.
53. Chinushi M, Restivo M, Caref EB, El-Sherif N. Electrophysiological basis of arrhythmogenicity of QT/T alternans in the long-QT syndrome: tridimensional analysis of the kinetics of cardiac repolarization. *Circ Res.* 1998;83:614–28.
54. Akar FG, Yan GX, Antzelevitch C, Rosenbaum DS. Unique topographical distribution of M cells underlies reentrant mechanism of torsade de pointes in the long-QT syndrome. *Circulation.* 2002;105:1247–53.
55. Akar FG, Rosenbaum DS. Transmural electrophysiological heterogeneities underlying arrhythmogenesis in heart failure. *Circ Res.* 2003;93:638–45.
56. Yan GX, Antzelevitch C. Cellular basis for the Brugada syndrome and other mechanisms of arrhythmogenesis associated with ST-segment elevation. *Circulation.* 1999;100:1660–6.
57. Extramiana F, Antzelevitch C. Amplified transmural dispersion of repolarization as the basis for

- arrhythmogenesis in a canine ventricular wedge model of short QT. *Circulation*. 2004;110:3661–6.
58. Vijayakumar R, Silva JNA, Desouza KA, Abraham RL, Strom M, Sacher F, et al. Electrophysiologic substrate in congenital long QT syndrome: noninvasive mapping with electrocardiographic imaging (ECGI). *Circulation*. 2014;130:1936–43.
 59. Liu DW, Gintant GA, Antzelevitch C. Ionic bases for electrophysiological distinctions among epicardial, midmyocardial, and endocardial myocytes from the free wall of the canine left ventricle. *Circ Res*. 1993;72:671–87.
 60. Liu DW, Antzelevitch C. Characteristics of the delayed rectifier current (IKr and IKs) in canine ventricular epicardial, midmyocardial, and endocardial myocytes. A weaker IKs contributes to the longer action potential of the M cell. *Circ Res*. 1995;76:351–65.
 61. Angelakos ET, King MP, Millard RW. Regional distribution of catecholamines in the hearts of various species. *Ann NY Acad Sci*. 1969;156:219–40.
 62. Vaseghi M, Lux RL, Mahajan A, Shivkumar K. Sympathetic stimulation increases dispersion of repolarization in humans with myocardial infarction. *Am J Physiol Heart Circ Physiol*. 2012;302:H1838–46.
 63. Maruyama M, Lin SF, Xie Y, Chua SK, Joung B, Han S, et al. Genesis of phase 3 early afterdepolarizations and triggered activity in acquired long-QT syndrome. *Circ Arrhythm Electrophysiol*. 2011;4:103–11.
 64. Franz MR, Swerdlow CD, Liem LB, Schaefer J. Cycle length dependence of human action potential duration in vivo. Effects of single extrastimuli, sudden sustained rate acceleration and deceleration, and different steady-state frequencies. *J Clin Invest*. 1988;82:972–9.
 65. Nolasco JB, Dahlen RW. A graphic method for the study of alternation in cardiac action potentials. *J Appl Physiol*. 1968;25:191–6.
 66. Xie F, Qu Z, Yang J, Bahar A, Weiss JN, Garfinkel A. A simulation study of the effects of cardiac anatomy in ventricular fibrillation. *J Clin Invest*. 2004;113(5):686–93.
 67. Weiss JN, Qu Z, Chen PS, Lin SF, Karagueuzian HS, Hayashi H, et al. The dynamics of cardiac fibrillation. *Circulation*. 2005;112:1232–40.
 68. Engelman ZJ, Trew ML, Smaill BH. Structural heterogeneity alone is a sufficient substrate for dynamic instability and altered restitution. *Circ Arrhythm Electrophysiol*. 2010;3:195–203.
 69. Hayashi M, Takatsuki S, Maison-Blanche P, Messali A, Haggui A, Milliez P, et al. Ventricular repolarization restitution properties in patients exhibiting type 1 Brugada electrocardiogram with and without inducible ventricular fibrillation. *J Am Coll Cardiol*. 2008;51:1162–8.
 70. Taggart P, Sutton P, Chalabi Z, Boyett MR, Simon R, Elliott D, Gill JS. Effect of adrenergic stimulation on action potential duration restitution in humans. *Circulation*. 2003;107:285–9.
 71. Ng GA, Brack KE, Patel VH, Coote JH. Autonomic modulation of electrical restitution, alternans and ventricular fibrillation initiation in the isolated heart. *Cardiovasc Res*. 2007;73:750–60.
 72. Brack KE, Patel VH, Coote JH, Ng GA. Nitric oxide mediates the vagal protective effect on ventricular fibrillation via effects on action potential duration restitution in the rabbit heart. *J Physiol*. 2007;583:695–704.
 73. Brack KE, Coote JH, Ng GA. Vagus nerve stimulation protects against ventricular fibrillation independent of muscarinic receptor activation. *Cardiovasc Res*. 2011;91:437–46.
 74. Orini M, Yanni J, Taggart P, Hanson B, Hayward M, Smith A, et al. Mechanistic insights from targeted molecular profiling of repolarization alternans in the intact human heart. *Europace*. doi: <https://doi.org/10.1093/europace/euz007>. [Epub ahead of print].
 75. Lukas A, Antzelevitch C. Phase 2 reentry as a mechanism of initiation of circus movement reentry in canine epicardium exposed to simulated ischemia. *Cardiovasc Res*. 1996;32:593–603.
 76. Dutta S, Mincholé A, Quinn TA, Rodriguez B. Electrophysiological properties of computational human ventricular cell action potential models under acute ischemic conditions. *Prog Biophys Mol Biol*. 2017;129:40–52.
 77. Y-Hassan S, Tornvall P. Epidemiology, pathogenesis, and management of takotsubo syndrome. *Clin Auton Res*. 2018;28:53–65.
 78. Madias C, Fitzgibbons TP, Alsheikh-Ali AA, Bouchard JL, Kalsmith B, Garlitski AC, et al. Acquired long QT syndrome from stress cardiomyopathy is associated with ventricular arrhythmias and torsades de pointes. *Heart Rhythm*. 2011;8:555–61.
 79. Perazzolo Marra M, Zorzi A, Corbetti F, De Lazzari M, Migliore F, Tona F, et al. Apicobasal gradient of left ventricular myocardial edema underlies transient T-wave inversion and QT interval prolongation (Wellens' ECG pattern) in Tako-Tsubo cardiomyopathy. *Heart Rhythm*. 2013;10:70–7.
 80. Benjamin IJ, Jalil JE, Tan LB, Cho K, Weber KT, Clark WA. Isoproterenol-induced myocardial fibrosis in relation to myocyte necrosis. *Circ Res*. 1989;65:657–70.
 81. Gomez JF, Cardona K, Romero L, Ferrero JM Jr, Trenor B. Electrophysiological and structural remodeling in heart failure modulate arrhythmogenesis. 1D simulation study. *PLoS One*. 2014;9:e106602.
 82. Gomez JF, Cardona K, Martinez L, Saiz J, Trenor B. Electrophysiological and structural remodeling in heart failure modulate arrhythmogenesis. 2D simulation study. *PLoS One*. 2014;9:e103273.
 83. Gomez JF, Cardona K, Trenor B. Lessons learned from multi-scale modeling of the failing heart. *J Mol Cell Cardiol*. 2015;89:146–59.

84. Al-Khatib SM, Stevenson WG, Ackerman MJ, Bryant WJ, Callans DJ, Curtis AB, et al. 2017 AHA/ACC/HRS guideline for management of patients with ventricular arrhythmias and the prevention of sudden cardiac death: a report of the American College of Cardiology/American Heart Association Task Force on Clinical Practice Guidelines and the Heart Rhythm Society. *Heart Rhythm*. 2018;15:e73–e189.
85. Myerburg RJ, Goldberger JJ. Sudden cardiac arrest risk assessment: population science and the individual risk mandate. *JAMA Cardiol*. 2017;2:689–94.
86. Tse G, Yan BP. Traditional and novel electrocardiographic conduction and repolarization markers of sudden cardiac death. *Europace*. 2017;19:712–21.
87. Browne KF, Prystowsky E, Heger JJ, Chilson DA, Zipes DP. Prolongation of the Q-T interval in man during sleep. *Am J Cardiol*. 1983;52:55–9.
88. Ahnve S, Vallin H. Influence of heart rate and inhibition of autonomic tone on the QT interval. *Circulation*. 1982;65:435–9.
89. Sarma JS, Venkataraman K, Samant DR, Gadgil UG. Effect of propranolol on the QT intervals of normal individuals during exercise: a new method for studying interventions. *Br Heart J*. 1988;60:434–9.
90. Extramiana F, Maison-Blanche P, Denjoy I, De Jode P, Messali A, Labbé JP, Leenhardt A. Gene-specific effect of beta-adrenergic blockade on corrected QT interval in the long QT syndrome. *Ann Noninvasive Electrocardiol*. 2013;18:399–408.
91. Montanez A, Ruskin JN, Hebert PR, Lamas GA, Hennekens CH. Prolonged QTc interval and risks of total and cardiovascular mortality and sudden death in the general population: a review and qualitative overview of the prospective cohort studies. *Arch Intern Med*. 2004;164:943–8.
92. Mazzanti A, Maragna R, Vacanti G, Monteforte N, Bloise R, Marino M, et al. Interplay between genetic substrate, QTc duration, and arrhythmia risk in patients with long QT syndrome. *J Am Coll Cardiol*. 2018;71:1663–71.
93. Wilde AA, Moss AJ, Kaufman ES, Shimizu W, Peterson DR, Benhorin J, et al. Clinical aspects of type 3 long-QT syndrome: an international multicenter study. *Circulation*. 2016;134:872–82.
94. Hermida A, Extramiana F, Gourraud JB, Fressart V, Kyndt F, Maltret A, et al. Symptomatic LQT3 patients remain at risk of serious events despite treatment. *Heart Rhythm*. 2016;13:S536.
95. Campuzano O, Sarquella-Brugada G, Cesar S, Arbelo E, Brugada J, Brugada R. Recent advances in short QT syndrome. *Front Cardiovasc Med*. 2018;5:149.
96. Villafane J, Atallah J, Gollob MH, Maury P, Wolpert C, Gebauer R, et al. Long-term follow-up of a pediatric cohort with short QT syndrome. *J Am Coll Cardiol*. 2013;61:1183–91.
97. Giustetto C, Schimpf R, Mazzanti A, Scrocco C, Maury P, Anttonen O, et al. Long-term follow-up of patients with short QT syndrome. *J Am Coll Cardiol*. 2011;58:587–95.
98. Batchvarov VN, Ghuran A, Smetana P, Hnatkova K, Harries M, Dilaveris P, et al. QT-RR relationship in healthy subjects exhibits substantial intersubject variability and high intrasubject stability. *Am J Physiol Heart Circ Physiol*. 2002;282:H2356–63.
99. Extramiana F, Maison-Blanche P, Badilini F, Pinoteau J, Deseo T, Coumel P. Circadian modulation of QT rate dependence in healthy volunteers: gender and age differences. *J Electrocardiol*. 1999;32:33–43.
100. Malik M, Hnatkova K, Novotny T, Schmidt G. Subject-specific profiles of QT/RR hysteresis. *Am J Physiol Heart Circ Physiol*. 2008;295:H2356–63.
101. Valensi PE, Johnson NB, Maison-Blanche P, Extramiana F, Motte G, Coumel P. Influence of cardiac autonomic neuropathy on heart rate dependence of ventricular repolarization in diabetic patients. *Diabetes Care*. 2002;25:918–23.
102. Extramiana F, Maison-Blanche P, Tavernier R, Jordaens L, Leenhardt A, Coumel P. Cardiac effects of chronic oral beta-blockade: lack of agreement between heart rate and QT interval changes. *Ann Noninvasive Electrocardiol*. 2002;7:379–88.
103. Merri M, Moss AJ, Benhorin J, Locati EH, Alberti M, Badilini F. Relation between ventricular repolarization duration and cardiac cycle length during 24-hour Holter recordings. Findings in normal patients and patients with long QT syndrome. *Circulation*. 1992;85:1816–21.
104. Xhaët O, Argacha JF, Pathak A, Gujic M, Houssiere A, Najem B, et al. Sympathoexcitation increases the QT/RR slope in healthy men: differential effects of hypoxia, dobutamine, and phenylephrine. *Cardiovasc Electrophysiol*. 2008;19:178–84.
105. Extramiana F, Neyroud N, Huikuri HV, Koistinen MJ, Coumel P, Maison-Blanche P. QT interval and arrhythmic risk assessment after myocardial infarction. *Am J Cardiol*. 1999;83:266–9.
106. Järvenpää J, Oikarinen L, Korhonen P, Väänänen H, Toivonen L, Viitasalo M. Dynamic QT/RR relationship in post-myocardial infarction patients with and without cardiac arrest. *Scand Cardiovasc J*. 2010;44:352–8.
107. Szydło K, Trusz-Gluza M, Wita K, Filipecki A, Orszulak W, Urbanczyk D, et al. QT/RR relationship in patients after remote anterior myocardial infarction with left ventricular dysfunction and different types of ventricular arrhythmias. *Ann Noninvasive Electrocardiol*. 2008;13:61–6.
108. Jensen BT, Abildstrom SZ, Larroude CE, Agner E, Torp-Pedersen C, Nyvad O, et al. QT dynamics in risk stratification after myocardial infarction. *Heart Rhythm*. 2005;2:357–64.
109. Savelieva I, Yap YG, Yi G, Guo XH, Hnatkova K, Camm AJ, Malik M. Relation of ventricular repolarization to cardiac cycle length in normal subjects, hypertrophic cardiomyopathy, and patients with myocardial infarction. *Clin Cardiol*. 1999;22:649–54.

110. Bonnemeier H, Wiegand UK, Bode F, Hartmann F, Kurowski V, Katus HA, et al. Impact of infarct-related artery flow on QT dynamicity in patients undergoing direct percutaneous coronary intervention for acute myocardial infarction. *Circulation*. 2003;108:2979–86.
111. Chevalier P, Burri H, Adeleine P, Kirkorian G, Lopez M, Leizorovicz A, et al. QT dynamicity and sudden death after myocardial infarction: results of a long-term follow-up study. *Cardiovasc Electrophysiol*. 2003;14:227–33.
112. Smetana P, Pueyo E, Hnatkova K, Batchvarov V, Laguna P, Malik M. Individual patterns of dynamic QT/RR relationship in survivors of acute myocardial infarction and their relationship to antiarrhythmic efficacy of amiodarone. *J Cardiovasc Electrophysiol*. 2004;15:1147–54.
113. Iacoviello M, Forleo C, Guida P, Romito R, Sorgente A, Sorrentino S, et al. Ventricular repolarization dynamicity provides independent prognostic information toward major arrhythmic events in patients with idiopathic dilated cardiomyopathy. *J Am Coll Cardiol*. 2007;50:225–31.
114. Cygankiewicz I, Zareba W, Vazquez R, Almendral J, Bayes-Genis A, Fiol M, et al. Prognostic value of QT/RR slope in predicting mortality in patients with congestive heart failure. *J Cardiovasc Electrophysiol*. 2008;19:1066–72.
115. Couderc JP, Xia X, Denjoy I, Extramiana F, Maison-Blanche P, Moss AJ, Zareba W, Lopes CM, et al. Genotype- and sex-specific QT-RR relationship in the type-1 long-QT syndrome. *J Am Heart Assoc*. 2012;1:e000570.
116. Barsheshet A, Goldenberg I, O-Uchi J, Moss AJ, Jons C, Shimizu W, et al. Mutations in cytoplasmic loops of the KCNQ1 channel and the risk of life-threatening events: implications for mutation-specific response to β -blocker therapy in type 1 long-QT syndrome. *Circulation*. 2012;125:1988–96.
117. Krahn AD, Klein GJ, Yee R. Hysteresis of the RT interval with exercise: a new marker for the long-QT syndrome? *Circulation*. 1997;96:1551–6.
118. Wong JA, Gula LJ, Klein GJ, Yee R, Skanes AC, Krahn AD. Utility of treadmill testing in identification and genotype prediction in long-QT syndrome. *Circ Arrhythm Electrophysiol*. 2010;3:120–5.
119. Lauer MS, Pothier CE, Chernyak YB, Brunken R, Lieber M, Apperson-Hansen C, Starobin JM. Exercise-induced QT/R-R-interval hysteresis as a predictor of myocardial ischemia. *J Electrocardiol*. 2006;39:315–23.
120. Starobin JM, Cascio WE, Goldfarb AH, Varadarajan V, Starobin AJ, Danford CP, Johnson TA. Identifying coronary artery flow reduction and ischemia using quasi stationary QT/RR-interval hysteresis measurements. *J Electrocardiol*. 2007;40:S91–6.
121. Pelchovitz DJ, Ng J, Chicos AB, Bergner DW, Goldberger JJ. QT-RR hysteresis is caused by differential autonomic states during exercise and recovery. *Am J Physiol Heart Circ Physiol*. 2012;302:H2567–73.
122. Panikkath R, Reinier K, Uy-Evanado A, Teodorescu C, Hattenhauer J, Mariani R, et al. Prolonged Tpeak-to-tend interval on the resting ECG is associated with increased risk of sudden cardiac death. *Circ Arrhythm Electrophysiol*. 2011;4:441–7.
123. Tse G, Gong M, Wong WT, Georgopoulos S, Letsas KP, Vassiliou VS, et al. The Tpeak – tend interval as an electrocardiographic risk marker of arrhythmic and mortality outcomes: a systematic review and meta-analysis. *Heart Rhythm*. 2017;14:1131–7.
124. Antzelevitch C. Transmural dispersion of repolarization and the T wave. *Cardiovasc Res*. 2001;50:426–31.
125. Yan GX, Antzelevitch C. Cellular basis for the normal T wave and the electrocardiographic manifestations of the long QT syndrome. *Circulation*. 1998;98:1928–36.
126. Mines GR. On the functional analysis by the action of electrolytes. *J Physiol*. 1913;46:188–235.
127. Vaseghi M, Yamakawa K, Sinha A, So EL, Zhou W, Ajjjola OA, et al. Modulation of regional dispersion of repolarization and T-peak to T-end interval by the right and left stellate ganglia. *Am J Physiol Heart Circ Physiol*. 2013;305:H1020–30.
128. Srinivasan NT, Orini M, Providencia R, Simon R, Lowe M, Segal OR, et al. Differences in the upslope of the precordial body surface ECG T wave reflect right to left dispersion of repolarization in the intact human heart. *Heart Rhythm*. 2018. pii: S1547–5271(18)31261-X. <https://doi.org/10.1016/j.hrthm.2018.12.006>. [Epub ahead of print].
129. Malik M, Huikuri H, Lombardi F, Schmidt G, Zabel M. e-Rhythm Study Group of EHRA. Conundrum of the Tpeak-tend interval. *J Cardiovasc Electrophysiol*. 2018;29:767–70.
130. Rautaharju PM. QT and dispersion of ventricular repolarization: the greatest fallacy in electrocardiography in the 1990s. *Circulation*. 1999;99:2477–8.
131. Baumert M, Porta A, Vos MA, Malik M, Couderc JP, Laguna P, et al. QT interval variability in body surface ECG: measurement, physiological basis, and clinical value: position statement and consensus guidance endorsed by the European Heart Rhythm Association jointly with the ESC Working Group on Cardiac Cellular Electrophysiology. *Europace*. 2016;18:925–44.
132. Shen MJ, Zipes DP. Role of the autonomic nervous system in modulating cardiac arrhythmias. *Circ Res*. 2014;114:1004–21.
133. Solomon SD, Zelenkofske S, McMurray JJ, et al. Sudden death in patients with myocardial infarction and left ventricular dysfunction, heart failure, or both. *N Engl J Med*. 2005;352:2581–8.
134. Gula LJ, Klein GJ, Hellkamp AS, Massel D, Krahn AD, Skanes AC, et al. Ejection fraction assessment and survival: an analysis of the Sudden Cardiac Death in Heart Failure Trial (SCD-HeFT). *Am Heart J*. 2008;156:1196–200.

135. Ellison KE, Hafley GE, Hickey K, et al. Effect of beta-blocking therapy on outcome in the Multicenter UnSustained Tachycardia Trial (MUSTT). *Circulation*. 2002;106:2694–9.
136. Reiter MJ, Reiffel JA. Importance of beta blockade in the therapy of serious ventricular arrhythmias. *Am J Cardiol*. 1998;82:9I–19I.
137. Patton KK, Hellkamp AS, Lee KL, Mark DB, Johnson GW, Anderson J, et al. Unexpected deviation in circadian variation of ventricular arrhythmias: the SCD-HeFT (Sudden Cardiac Death in Heart Failure Trial). *J Am Coll Cardiol*. 2014;64:1968–9.
138. Ni YM, Rusinaru C, Reinier K, Uy-Evanado A, Chugh H, Stecker EC, et al. Unexpected shift in circadian and septadian variation of sudden cardiac arrest: the Oregon Sudden Unexpected Death Study. *Heart Rhythm*. 2018;pii: S1547–S5271.
139. Shusterman V, Aysin B, Gottipaty V, Weiss R, Brode S, Schwartzman D, Anderson KP. Autonomic nervous system activity and the spontaneous initiation of ventricular tachycardia. *ESVEM Investigators Electrophysiologic Study Versus Electrocardiographic Monitoring Trial*. *J Am Coll Cardiol*. 1998;32:1891–9.
140. Wollmann CG, Gradaus R, Böcker D, Fetsch T, Hintringer F, Hoh G, et al. Variations of heart rate variability parameters prior to the onset of ventricular tachyarrhythmia and sinus tachycardia in ICD patients. Results from the heart rate variability analysis with automated ICDs (HAWAI) registry. *Physiol Meas*. 2015;36:1047–61.
141. Au-Yeung WM, Reinhall PG, Bardy G, Brunton SL. Development and validation of warning system of ventricular tachyarrhythmia in patients with heart failure with heart rate variability data. *PLoS One*. 2018;13:e0207215.
142. Jervell A, Lange-Nielsen F. Congenital deaf-mutism, functional heart disease with prolongation of the Q-T interval and sudden death. *Am Heart J*. 1957;54:59–68.
143. Ward OC. A new familial cardiac syndrome in children. *J Irish Med Assoc*. 1964;54:103–6.
144. Ackerman MJ, Priori SG, Willems S, Berul C, Brugada R, Calkins H, et al. HRS/EHRA expert consensus statement on the state of genetic testing for the channelopathies and cardiomyopathies: this document was developed as a partnership between the Heart Rhythm Society (HRS) and the European Heart Rhythm Association (EHRA). *Europace*. 2011;13:1077–109.
145. Priori SG, Wilde AA, Horie M, Cho Y, Behr ER, Berul C, et al. HRS/EHRA/APHS expert consensus statement on the diagnosis and management of patients with inherited primary arrhythmia syndromes: document endorsed by HRS, EHRA, and APHS in May 2013 and by ACCF, AHA, PACES, and AEPC in June 2013. *Heart Rhythm*. 2013;10:1932–63.
146. Shimizu W, Antzelevitch C, Moss AJ, Zareba W, Hall WJ, Schwartz PJ, et al. Effectiveness and limitations of beta-blocker therapy in congenital long-QT syndrome. *Circulation*. 2000;101:616–23.
147. Abu-Zeitone A, Peterson DR, Polonsky B, McNitt S, Moss AJ. Efficacy of different beta-blockers in the treatment of long QT syndrome. *J Am Coll Cardiol*. 2014;64:1352–8.
148. Schwartz PJ, Priori SG, Spazzolini C, Moss AJ, Vincent GM, Napolitano C, et al. Genotype-phenotype correlation in the long-QT syndrome: gene-specific triggers for life-threatening arrhythmias. *Circulation*. 2001;103:89–95.
149. Waddell-Smith KE, Skinner JR. Members of the CSANZ Genetics Council Writing Group. Update on the diagnosis and management of familial long QT syndrome. *Heart Lung Circ*. 2016;25:769–76.
150. Gussak I, Brugada P, Brugada J, Wright S, Kopecky SL, Chaitman BR, Bjerregaard P. Idiopathic short QT interval: a new clinical syndrome? *Cardiology*. 2000;94:99–102.
151. Gaita F, Giustetto C, Bianchi F, Wolpert C, Schimpf R, Riccardi R, et al. Short QT syndrome: a familial cause of sudden death. *Circulation*. 2003;108:965–70.
152. Bjerregaard P. Diagnosis and management of short QT syndrome. *Heart Rhythm*. 2018;15:1261–7.
153. Mazzanti A, Kanthan A, Monteforte N, Memmi M, Bloise R, Novelli V, et al. Novel insight into the natural history of short QT syndrome. *J Am Coll Cardiol*. 2014;63:1300–8.
154. Giustetto C, Di Monte F, Wolpert C, Borggrefe M, Schimpf R, Sbragia P, et al. Short QT syndrome: clinical findings and diagnostic-therapeutic implications. *Eur Heart J*. 2006;27:2440–7.
155. Kaufman ES. Quinidine in short QT syndrome: an old drug for a new disease. *J Cardiovasc Electrophysiol*. 2007;18:665–6.
156. Gaita F, Giustetto C, Bianchi F, Schimpf R, Haissaguerre M, Calò L, et al. Short QT syndrome: pharmacological treatment. *J Am Coll Cardiol*. 2004;43:1494–9.
157. Antzelevitch C, Yan GX, Ackerman MJ, Borggrefe M, Corrado D, Guo J, et al. J-wave syndromes expert consensus conference report: emerging concepts and gaps in knowledge. *Heart Rhythm*. 2016;13:e295–324.
158. Macfarlane P, Antzelevitch C, Haissaguerre M, Huikuri HV, Potse M, Rosso R, et al. The early repolarization pattern: consensus paper. *J Am Coll Cardiol*. 2015;66:470–7.
159. Postema PG, Wolpert C, Amin AS, Probst V, Borggrefe M, Roden DM, et al. Drugs and Brugada syndrome patients: review of the literature, recommendations, and an up-to-date website. (www.brugadadrugs.org). *Heart Rhythm*. 2009;6:1335–41.
160. Nademane K, Veerakul G, Nimmannit S, Chaowakul V, Bhuripanyo K, Likittanasombat K, et al. Arrhythmogenic marker for the sudden unexplained death syndrome in Thai men. *Circulation*. 1997;96:2595–600.

161. Kamakura T, Wada M, Ishibashi K, Inoue YY, Miyamoto K, Okamura H, et al. Differences in the onset mode of ventricular tachyarrhythmia between patients with J wave in anterior leads and those with J wave in inferolateral leads. *Heart Rhythm*. 2017;14:553–61.
162. Kim SH, Nam GB, Baek S, Choi HO, Kim KH, Choi KJ, et al. Circadian and seasonal variations of ventricular tachyarrhythmias in patients with early repolarization syndrome and Brugada syndrome: analysis of patients with implantable cardioverter defibrillator. *J Cardiovasc Electrophysiol*. 2012;23:757–63.
163. Ikeda T, Abe A, Yusu S, Nakamura K, Ishiguro H, Mera H, et al. The full stomach test as a novel diagnostic technique for identifying patients at risk of Brugada syndrome. *J Cardiovasc Electrophysiol*. 2006;17:602–7.
164. Mizumaki K, Nishida K, Iwamoto J, Nakatani Y, Yamaguchi Y, Sakamoto T, et al. Vagal activity modulates spontaneous augmentation of J-wave elevation in patients with idiopathic ventricular fibrillation. *Heart Rhythm*. 2012;9:249–55.
165. Izawa Y, Sato M, Ohno S, Horie M, Takatsuki S, Fukuda K, et al. Circadian pattern of fibrillatory events in non-Brugada-type idiopathic ventricular fibrillation with a focus on J waves. *Heart Rhythm*. 2014;11:2261–6.
166. Leenhardt A, Lucet V, Denjoy I, Grau F, Ngoc DD, Coumel P. Catecholaminergic polymorphic ventricular tachycardia in children. A 7-year follow-up of 21 patients. *Circulation*. 1995;91:1512–9.
167. Hayashi M, Denjoy I, Extramiana F, Maltret A, Roux-Buisson N, Lupoglazoff J-M, et al. The role of stress test for predicting genetic mutations and future cardiac events in asymptomatic relatives of catecholaminergic polymorphic ventricular tachycardia probands. *Europace*. 2012;14:1344–51.
168. Roston TM, Yuchi Z, Kannankeril PJ, Hathaway J, Vinocur JM, Etheridge SP, et al. The clinical and genetic spectrum of catecholaminergic polymorphic ventricular tachycardia: findings from an international multi-centre registry. *Europace*. 2018;20:541–7.
169. Priori SG, Napolitano C, Tiso N, Memmi M, Vignati G, Bloise R, et al. Mutations in the cardiac ryanodine receptor gene (hRyR2) underlie catecholaminergic polymorphic ventricular tachycardia. *Circulation*. 2001;103:196–200.
170. Knollmann BC, Chopra N, Hlaing T, Akin B, Yang T, Etensohn K, et al. Casq2 deletion causes sarcoplasmic reticulum volume increase, premature Ca²⁺ release, and catecholaminergic polymorphic ventricular tachycardia. *J Clin Invest*. 2006;116:510–20.
171. Faggioni M, van der Werf C, Knollmann BC. Sinus node dysfunction in catecholaminergic polymorphic ventricular tachycardia: risk factor and potential therapeutic target? *Trends Cardiovasc Med*. 2014;24:273–8.
172. Hayashi M, Denjoy I, Extramiana F, Maltret A, Buisson NR, Lupoglazoff JM, et al. Incidence and risk factors of arrhythmic events in catecholaminergic polymorphic ventricular tachycardia. *Circulation*. 2009;119:2426–34.
173. van der Werf C, Kannankeril PJ, Sacher F, Krahn AD, Viskin S, Leenhardt A, et al. Flecainide therapy reduces exercise-induced ventricular arrhythmias in patients with catecholaminergic polymorphic ventricular tachycardia. *J Am Coll Cardiol*. 2011;57:2244–54.
174. Watanabe H, Chopra N, Laver D, Hwang HS, Davies SS, Roach DE, et al. Flecainide prevents catecholaminergic polymorphic ventricular tachycardia in mice and humans. *Nat Med*. 2009;15:380–3.
175. Aliot EM, Stevenson WG, Almendral-Garrote JM, et al. EHRA/HRS. Expert consensus on catheter ablation of ventricular arrhythmias: developed in a partnership with the European Heart Rhythm Association (EHRA), a Registered Branch of the European Society of Cardiology (ESC), and the Heart Rhythm Society (HRS); in collaboration with the American College of Cardiology (ACC) and the American Heart Association (AHA). *Heart Rhythm*. 2009;6:886–933.
176. Leriche R, Fontaine R. The surgical treatment of angina pectoris: what it is and what it should be. *Am Heart J*. 1928;3:649–71.
177. Hou Y, Zhou Q, Po SS. Neuromodulation for cardiac arrhythmia. *Heart Rhythm*. 2016;13:584–92.
178. Vaseghi M, Barwad P, Malavassi Corrales FJ, Tandri H, Mathuria N, Shah R, et al. Cardiac sympathetic denervation for refractory ventricular arrhythmias. *J Am Coll Cardiol*. 2017;69:3070–80.
179. Schwartz PJ. The rationale and the role of left stellectomy for the prevention of malignant arrhythmias. *Ann N Y Acad Sci*. 1984;427:199–221.
180. Schwartz PJ, Locati EH, Moss AJ, Crampton RS, Trazzi R, Ruberti U. Left cardiac sympathetic denervation in the therapy of congenital long QT syndrome. A worldwide report. *Circulation*. 1991;84:503–11.
181. Wilde AA, Bhuiyan ZA, Crotti L, Facchini M, De Ferrari GM, Paul T, Ferrandi C, et al. Left cardiac sympathetic denervation for catecholaminergic polymorphic ventricular tachycardia. *N Engl J Med*. 2008;358:2024–9.
182. Atallah J, Fynn-Thompson F, Cecchin F, DiBardino DJ, Walsh EP, Berul CI. Video-assisted thoracoscopic cardiac denervation: a potential novel therapeutic option for children with intractable ventricular arrhythmias. *Ann Thorac Surg*. 2008;86:1620–5.
183. Vaseghi M, Zhou W, Shi J, Ajijola OA, Hadaya J, Shivkumar K, et al. Sympathetic innervation of the anterior left ventricular wall by the right and left stellate ganglia. *Heart Rhythm*. 2012;9:1303–9.
184. Ajijola OA, Vaseghi M, Mahajan A, Shivkumar K. Bilateral cardiac sympathetic denervation: why, who and when? *Expert Rev Cardiovasc Ther*. 2012;10:947–9.
185. Vaseghi M, Gima J, Kanaan C, Ajijola OA, Marmureanu A, Mahajan A, et al. Cardiac sym-

- pathetic denervation in patients with refractory ventricular arrhythmias or electrical storm: intermediate and long-term follow-up. *Heart Rhythm*. 2014;11:360–6.
186. Ajjola OA, Lellouche N, Bourke T, Tung R, Ahn S, Mahajan A, Shivkumar K. Bilateral cardiac sympathetic denervation for the management of electrical storm. *J Am Coll Cardiol*. 2012;59:91–2.
 187. Bourke T, Vaseghi M, Michowitz Y, Sankhla V, Shah M, Swapna N, et al. Neuraxial modulation for refractory ventricular arrhythmias: value of thoracic epidural anaesthesia and surgical left cardiac sympathetic denervation. *Circulation*. 2010;121:2255–62.
 188. Tan AY, Abdi S, Buxton AE, Anter E. Percutaneous stellate ganglia block for acute control of refractory ventricular tachycardia. *Heart Rhythm*. 2012;9:2063–7.
 189. Meng L, Tseng CH, Shivkumar K, Ajjola O. Efficacy of stellate ganglion blockade in managing electrical storm: a systematic review. *JACC Clin Electrophysiol*. 2017;3:942–9.
 190. Fudim M, Boortz-Marx R, Ganesh A, Waldron NH, Qadri YJ, Patel CB, et al. Stellate ganglion blockade for the treatment of refractory ventricular arrhythmias: a systematic review and meta-analysis. *J Cardiovasc Electrophysiol*. 2017;28:1460–7.
 191. Hayase J, Patel J, Narayan SM, Krummen DE. Percutaneous stellate ganglion block suppressing VT and VF in a patient refractory to VT ablation. *J Cardiovasc Electrophysiol*. 2013;24:926–8.
 192. Genovesi S, Zaccaria D, Rossi E, Valsecchi MG, Stella A, Stramba-Badiale M. Effects of exercise training on heart rate and QT interval in healthy young individuals: are there gender differences? *Europace*. 2007;9:55–60.
 193. Billman GE. Aerobic exercise conditioning: a non-pharmacological antiarrhythmic intervention. *J Appl Physiol*. 2002;92:446–54.
 194. Such L, Alberola AM, Such-Miquel L, Lopez L, Trapero I, Pelechano F, et al. Effect of chronic exercise on myocardial refractoriness: a study on isolated rabbit heart. *Acta Physiol*. 2008;193:331–9.
 195. Ellenbogen KA, Smith ML, Eckberg DL. Increased vagal cardiac nerve traffic prolongs ventricular refractoriness in patients undergoing electrophysiology testing. *Am J Cardiol*. 1990;65:1345–50.
 196. Vanoli E, De Ferrari GM, Stramba-Badiale M, Hull SS Jr, Foreman RD, Schwartz PJ. Vagal stimulation and prevention of sudden death in conscious dogs with a healed myocardial infarction. *Circ Res*. 1991;68:1471–8.
 197. Kolman BS, Verrier RL, Lown B. The effect of vagus nerve stimulation upon vulnerability of the canine ventricle: role of sympathetic-parasympathetic interactions. *Circulation*. 1975;52:578–85.
 198. Yamaguchi N, Yamakawa K, Rajendran PS, Takamiya T, Vaseghi M. Antiarrhythmic effects of vagal nerve stimulation after cardiac sympathetic denervation in the setting of chronic myocardial infarction. *Heart Rhythm*. 2018;15:1214–22.
 199. Schwartz PJ, De Ferrari GM, Sanzo A, Landolina M, Rordorf R, Raineri C. Long term vagal stimulation in patients with advanced heart failure: first experience in man. *Eur J Heart Fail*. 2008;10:884–9.
 200. Premchand RK, Sharma K, Mittal S, Monteiro R, Dixit S, Libbus I, et al. Extended follow-up of patients with heart failure receiving autonomic regulation therapy in the ANTHEM-HF study. *J Card Fail*. 2016;22:639–42.
 201. Zannad F, De Ferrari GM, Tuinenburg AE, Wright D, Brugada J, Butter C, et al. Chronic vagal stimulation for the treatment of low ejection fraction heart failure: results of the NEural Cardiac TherApy foR Heart Failure (NECTAR-HF) randomized controlled trial. *Eur Heart J*. 2015;36:425–33.
 202. Gold MR, Van Veldhuisen DJ, Hauptman PJ, Borggrefe M, Kubo SH, Lieberman RA, et al. Vagus nerve stimulation for the treatment of heart failure: The INOVATE-HF Trial. *J Am Coll Cardiol*. 2016;68:149–58.
 203. Linenthal AJ, Zoll PM. Prevention of ventricular tachycardia and fibrillation by intravenous isoproterenol and epinephrine. *Circulation*. 1963 Jan;27:5–11.
 204. Tanaka H, Kinoshita O, Uchikawa S, Kasai H, Nakamura M, Izawa A, et al. Successful prevention of recurrent ventricular fibrillation by intravenous isoproterenol in a patient with Brugada syndrome. *Pacing Clin Electrophysiol*. 2001;24:1293–4.
 205. Maury P, Couderc P, Delay M, Boveda S, Brugada J. Electrical storm in Brugada syndrome successfully treated using isoprenaline. *Europace*. 2004;6:130–3.
 206. Haïssaguerre M, Sacher F, Nogami A, Komiya N, Bernard A, Probst V, et al. Characteristics of recurrent ventricular fibrillation associated with inferolateral early repolarization role of drug therapy. *J Am Coll Cardiol*. 2009;53:612–9.
 207. Koncz I, Gurabi Z, Patoeckai B, Panama BK, Szél T, Hu D, et al. Mechanisms underlying the development of the electrocardiographic and arrhythmic manifestations of early repolarization syndrome. *J Mol Cell Cardiol*. 2014;68:20–8.
 208. Bun SS, Maury P, Giustetto C, Deharo JC. Electrical storm in short-QT syndrome successfully treated with isoproterenol. *J Cardiovasc Electrophysiol*. 2012;23:1028–30.
 209. Linz D, Wirth K, Ukena C, Mahfoud F, Pöss J, Linz B, et al. Renal denervation suppresses ventricular arrhythmias during acute ventricular ischemia in pigs. *Heart Rhythm*. 2013;10:1525–30.
 210. Jackson N, Gizuraron S, Azam MA, King B, Ramadeen A, Zamiri N, et al. Effects of renal artery denervation on ventricular arrhythmias in a postinfarct model. *Circ Cardiovasc Interv*. 2017;10:e004172.
 211. Yu L, Huang B, Zhou X, Wang S, Wang Z, Wang M, et al. Renal sympathetic stimulation and ablation affect ventricular arrhythmia by modulating autonomic activity in a cesium-induced long QT canine model. *Heart Rhythm*. 2017;14:2–919.

212. Remo BF, Preminger M, Bradfield J, Mittal S, Boyle N, Gupta A, et al. Safety and efficacy of renal denervation as a novel treatment of ventricular tachycardia storm in patients with cardiomyopathy. *Heart Rhythm*. 2014;11:541–6.
213. Howard-Quijano K, Takamiya T, Dale EA, Kipke J, Kubo Y, Grogan T, et al. Spinal cord stimulation reduces ventricular arrhythmias during acute ischemia by attenuation of regional myocardial excitability. *Am J Physiol Heart Circ Physiol*. 2017;313:H421–31.
214. Zipes DP, Neuzil P, Theres H, Caraway D, Mann DL, Mannheimer C, et al. Determining the feasibility of spinal cord neuromodulation for the treatment of chronic systolic heart failure: The DEFEAT-HF Study. *JACC Heart Fail*. 2016;4:129–36.
215. Gardner RT, Wang L, Lang BT, Cregg JM, Dunbar CL, Woodward WR, et al. Targeting protein tyrosine phosphatase σ after myocardial infarction restores cardiac sympathetic innervation and prevents arrhythmias. *Nat Commun*. 2015;6:6235.
216. Liu X, Sun L, Chen J, Jin Y, Liu Q, Xia Z, et al. Effects of local cardiac denervation on cardiac innervation and ventricular arrhythmia after chronic myocardial infarction. *PLoS One*. 2017;12:e0181322.
217. Tomek J, Rodriguez B, Bub G, Heijman J. β -Adrenergic receptor stimulation inhibits proarrhythmic alternans in postinfarction border zone cardiomyocytes: a computational analysis. *Am J Physiol Heart Circ Physiol*. 2017;313:H338–53.
218. Goldhaber JJ, Xie LH, Duong T, Motter C, Khoo K, Weiss JN. Action potential duration restitution and alternans in rabbit ventricular myocytes: the key role of intracellular calcium cycling. *Circ Res*. 2005;96:459–66.
219. Jordan PN, Christini DJ. Characterizing the contribution of voltage- and calcium-dependent coupling to action potential stability: implications for repolarization alternans. *Am J Physiol Heart Circ Physiol*. 2007;293:H2109–18.
220. Kanaporis G, Blatter LA. Membrane potential determines calcium alternans through modulation of SR Ca^{2+} load and L-type Ca^{2+} current. *J Mol Cell Cardiol*. 2017;105:49–58.
221. Gottlieb SS, McCarter RJ, Vogel RA. Effect of beta-blockade on mortality among high-risk and low-risk patients after myocardial infarction. *N Engl J Med*. 1998;339:489–97.
222. Coumel P. Cardiac arrhythmias and the autonomic nervous system. *J Cardiovasc Electrophysiol*. 1993;4:338–55.



Repolarization Remodeling in Structural Heart Disease

3

Andreas S. Barth and Gordon F. Tomaselli

Introduction

Heart failure (HF) is highly prevalent, affecting 5.7 million adults in the United States alone, and the incidence and prevalence has continued to increase with the aging of the population [1]. Despite remarkable improvements in medical therapy, the prognosis of patients with heart failure remains poor with almost 50% of patients dying within 5 years of initial diagnosis. Of the deaths in patients with heart failure, up to 50% are sudden and unexpected. In the Framingham Study, HF was associated with a 2.6- to 6.2-fold increased risk of sudden cardiac death (SCD) [2].

Increased electrical instability of the failing heart is multifactorial, and, depending on etiology, different mechanisms including ischemia in coronary heart disease or structural alterations such as fibrosis or myocardial scarring after myocardial infarction may be prominent. However, one of the most important predictors of SCD is depressed left ventricular systolic function [3, 4], suggesting that, despite etiological heterogeneity, common mechanisms are involved in the propensity of failing myocardium to develop potentially fatal

arrhythmias. Altered intracellular and transmembrane calcium handling [5, 6], stretch-induced mechanisms due to altered ventricular loading conditions [7, 8], and changes in myocyte electrical [9, 10] and metabolic [11, 12] properties have been implicated in the increased electrical instability of the failing heart. Several lines of evidence indicate an important role of abnormalities in repolarization for the increased risk of SCD in HF. Prolongation of action potential duration (APD), one of the most consistent findings in myocytes from hypertrophied and failing hearts is associated with exaggerated lability of the repolarization process [10, 13]. In addition to alteration of individual currents, spatial and temporal inhomogeneity of repolarization, measured as dispersion of repolarization [14], has been described in patients with increased risk of SCD. This review is to give an overview on available evidence of alterations of ion currents that mediate cardiac repolarization in cardiac hypertrophy and heart failure.

Repolarization: A Labile Process

An elementary and distinctive signature of any given excitable tissue is its action potential profile. Myocardial cells possess a characteristically long action potential (Fig. 3.1). After an initial rapid upstroke, there is a plateau of maintained depolarization before repolarization occurs. APD prolongation in left ventricular hypertrophy or failure is caused by either a decrease in outward

A. S. Barth (✉)
Department of Cardiac Electrophysiology,
Johns Hopkins University, Baltimore, MD, USA
e-mail: Abarth3@jhmi.edu

G. F. Tomaselli (✉)
The Albert Einstein College of Medicine, Department
of Medicine, Bronx, NY, USA
e-mail: gordon.tomaselli@einstein.yu.edu

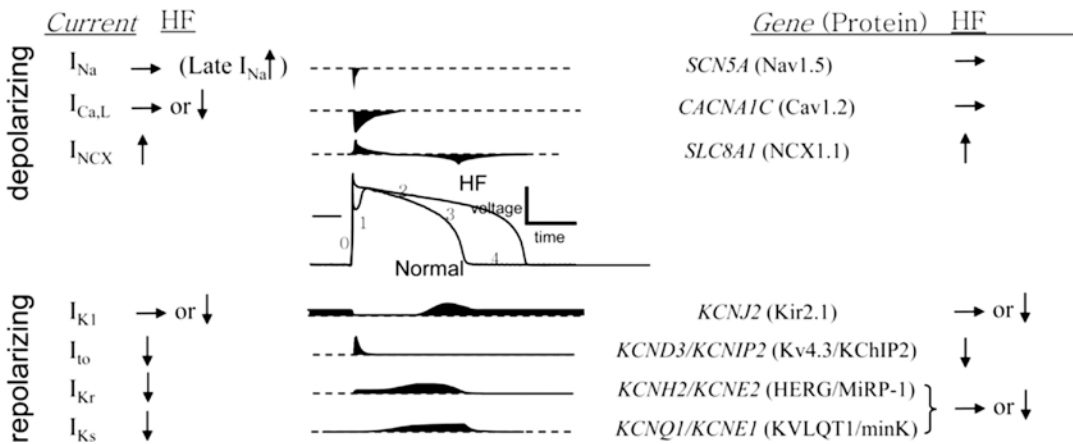


Fig. 3.1 Schematic of inward and outward currents, pumps, and exchanges which inscribed the ventricular action potential. A schematic of the time course of each current is shown on the left, while the gene product that

underlies the current is shown on the right. (Adapted from Tomaselli and Marban [9], by permission of Oxford University Press)

(mostly potassium) currents or an increase in depolarizing inward currents (sodium or calcium; Fig. 3.1). In animal models of pressure overload-induced HF, this prolongation is progressive and generally occurs in the absence of other electrophysiological abnormalities such as changes in resting membrane potential, action potential amplitude, or upstroke velocity [10]. The plateau phase of the action potential is known to be quite labile: this is a time of high membrane resistance during which small changes in current can easily tip the balance either toward repolarization or toward maintained depolarization. In general, the longer the action potential, the more labile is the repolarization process. This lability may be manifest as variability in duration and/or secondary depolarizations that interrupt action potential repolarization, including early afterdepolarizations (EADs) that can initiate torsade de pointes.

In addition to action potential prolongation on a cellular level, regional differences in the action potential duration represent an important aspect of arrhythmogenesis in hypertrophy and heart failure. Action potential durations vary across the myocardial wall [15–17] and in different regions [18] of the mammalian heart. Data from experimental animal models of hypertrophy and human heart failure suggest regional inhomogeneity in action potential prolongation [19, 20]. The finding

of enhanced spatial and temporal dispersion of APD, refractoriness, and electrocardiographic QT intervals in humans [21, 22] and animals with heart failure [23] is consistent with an exaggerated dispersion of action potential duration. Heterogeneous APD prolongation within the ventricular wall amplifies dispersion of repolarization, an established mechanism contributing to reentry.

Regional differences in electrical properties also play an important role in dyssynchronous heart failure and cardiac resynchronization therapy (CRT) [24]. In a large animal model of dyssynchronous heart failure (DHF), action potential durations were significantly prolonged in DHF, especially in late-activated lateral vs. early-activated anterior cells, and CRT abbreviated action potential duration in lateral as compared to anterior cells [24]. Early afterdepolarizations were more frequent in DHF than in control cells and were reduced with CRT [24].

Decrease in Outward Potassium Currents Leads to Prolongation of the Action Potential Duration

Downregulation of many repolarizing potassium currents during heart failure is well documented [9, 25]. While the major inward currents (sodium

and L-type calcium current) appear to be rather consistent among different species, a large diversity of potassium channels has been observed with expression of different potassium channel types and densities in different species and myocardial regions. Currently, more than 20 potassium channels are known to be expressed in the heart [26]. Thus, depending on the species studied, different channels may be involved in a similar phenotypic prolongation of the action potential in cardiac hypertrophy or failure. One of the potassium currents most consistently reduced in cardiac hypertrophy and heart failure is the transient outward potassium current (I_{to}).

Transient Outward Potassium Current (I_{to})

In ventricular myocytes and Purkinje fibers, the initial depolarization of the membrane potential is generated by Na^+ influx (I_{Na}) from coordinated opening of voltage-gated sodium channels. This depolarization rapidly activates the calcium-independent I_{to} which is primarily responsible for phase 1 or notch of the action potential. I_{to} then rapidly inactivates with a time constant of ~ 50 ms, thus, shaping the rapid phase 1 repolarization of the cardiac action potential and setting the height of the initial plateau (phase 2), thereby playing a key role in excitation-contraction (EC) coupling [27, 28], as well as in arrhythmogenesis [29].

Since I_{to} is an early transient current, it may not directly affect the ventricular APD in large mammalian hearts as it does in rodent ventricle. I_{to} downregulation is the most consistent change of any ion current in failing hearts [25, 30, 31]. I_{to} displays a large transmural gradient with a three to fivefold higher current density and faster recovery from inactivation kinetics in the subepicardium compared to the subendocardium [15]. In human myocardium, I_{to} is encoded by *KCND3* ($K_{v4.3}$) subunits in subepicardial and midmyocardial cell layers, while *KCNA4* encodes a slowly recovering current ($K_{v1.4}$) in the subendocardium, contributing to regional heterogeneities in action potential waveforms

[32]. In non-failing human hearts, the transmural gradient of I_{to} contributes to the slightly longer action potential duration in the subendocardium vs. subepicardium, which enables subendocardial myocytes to provide more coupling current to depolarize adjacent cells. As such, conduction of excitability is facilitated in the physiological direction of the endocardium to the epicardium but disfavored in the opposite direction [33]. Downregulation of I_{to} in cells isolated from terminally failing human hearts affects mostly *KCND3* ($K_{v4.3}$) [30, 31], leading to selective downregulation of the I_{to} in the subepicardium and midmyocardium and a diminished transmural gradient of I_{to} in HF. Therefore, the directional preference of conduction from the subendocardium to the subepicardium is blunted due to a HF-related decline in the transmural gradient of I_{to} . As conduction of abnormal impulses originating in the subepicardium is relatively facilitated, these changes may contribute to proarrhythmia [33].

The molecular mechanism of I_{to} downregulation in HF is likely to be multifactorial. Reduced steady-state levels of *KCND3* mRNA are highly correlated with functional downregulation of I_{to} in human HF [24, 30, 31, 34, 35]. In a canine HF model, tachycardia downregulates I_{to} expression, with the Ca^{2+} /calmodulin-dependent protein kinase II (CaMKII) and calcineurin/NFAT systems playing key Ca^{2+} -sensing and signal-transducing roles in rate-dependent I_{to} control [36].

Delayed Rectifier Currents (I_{Kr} and I_{Ks})

The delayed rectifier K^+ currents I_{Kr} and I_{Ks} (encoded by *KCNH2/KCNE2* and *KCNQ1/KCNE1*, respectively) play a prominent role in the late phase of repolarization [37]; therefore changes in either the slow (I_{Ks}) or fast (I_{Kr}) activating components of this current could contribute significantly to prolongation of the APD in HF. Reduced I_K density, slower activation, and faster deactivation kinetics have been observed in hypertrophied feline ventricles [38]. Downregulation of both I_{Kr} and I_{Ks} have

been reported in a rabbit model of rapid ventricular pacing HF [39], whereas I_{Ks} , but not I_{Kr} , was downregulated in all layers of the left ventricular myocardium in a canine model of tachypacing HF [40].

In human hearts, a greater inhibition of I_{Kr} by the specific inhibitor E-4031 indexed by greater APD prolongation in perfused left ventricular wedges was observed in non-failing compared with wedges isolated from failing hearts [41]. The reduced functional I_{Kr} expression was attributed to a shift in the ratio between the two protein isoforms of mammalian *KCNH2*/hERG1 channel subunits, hERG1a and hERG1b that conduct the I_{Kr} current in the heart, as no differences in steady-state mRNA levels of hERG1a or hERG1b were found between non-failing and failing human hearts [41].

There is increasing evidence to suggest that the neurohormonal dysregulation observed in HF contributes to downregulation of I_{Kr} , as angiotensin II (Ang II) has been shown to produce an inhibitory effect on I_{Kr} currents via angiotensin 1 receptors, linked to the PKC pathway in ventricular myocytes [42, 43]. Of note, Ang II has also been shown to inhibit I_{Ks} in a concentration-dependent manner in native guinea pig cardiomyocytes [44].

Importantly, K^+ current changes are often measured in nonphysiological conditions (voltage clamp, low pacing rates, cytosolic Ca^{2+} buffers). A recent study compared I_{Kr} , and I_{Ks} , and their Ca^{2+} - and β -adrenergic dependence in rabbit ventricular myocytes in chronic pressure/volume overload-induced HF (versus age-matched controls). Intriguingly, both I_{Kr} and I_{Ks} were significantly *upregulated* in HF under action potential clamp, but *only* when cytosolic Ca^{2+} was not buffered. CaMKII (Ca^{2+} /calmodulin-dependent protein kinase II) inhibition abolished I_{Ks} upregulation in HF, but it did not affect I_{Kr} . I_{Ks} response to β -adrenergic stimulation was also significantly diminished in HF. Thus, under β -adrenergic stimulation, reduced I_{Ks} responsiveness severely limits integrated repolarizing K^+ current and repolarization reserve in HF. This would increase arrhythmia propensity in HF, especially during adrenergic stress [45].

Inward Rectifier Current (I_{K1})

Reduced inward I_{K1} density in HF may contribute to prolongation of APD and enhanced susceptibility to spontaneous membrane depolarizations including delayed afterdepolarizations (DADs) [40, 45–47]. Changes in functional expression of I_{K1} are more variable than I_{to} and controversial. Even within the same experimental HF model (e.g., pacing-induced), inconsistencies have been observed across species: reduced I_{K1} density in canine [40, 48] and rabbit [45], whereas other investigators did not observe changes in rabbit [49]. In terminal human HF, I_{K1} is significantly reduced at negative voltages [30], but the underlying basis for such downregulation appears to be posttranscriptional in light of the absence of changes in the steady-state level of *KCNJ2*/*Kir2.1* mRNA [31].

Increase in Inward Current Leads to Prolongation of the APD

Late Inward Sodium Current

The cardiac voltage-dependent Na^+ channel (SCN5A) generates a large inward current (I_{Na}) within the first milliseconds of excitation and mediates the upstroke of the cardiac action potential in ventricular myocardium. Inactivation of I_{Na} has both fast and slow components, which range from several milliseconds to hundreds of milliseconds, respectively. The current associated with the slow inactivating phase has been referred to as late or persistent sodium current ($I_{Na,L}$) to distinguish it from the peak transient I_{Na} [50]. In non-failing hearts, the amplitude of late I_{Na} is less than 1% that of peak I_{Na} .

Whereas peak I_{Na} has been reported to be decreased [51], unchanged [48], or increased [52–54] in animal models of HF, changes in $I_{Na,L}$ are more consistent, as $I_{Na,L}$ as a percentage of peak I_{Na} can be significantly (up to tenfold) increased in HF due to a slower decay of $I_{Na,L}$ in failing canine and human hearts [55–57]. Therefore, increased $I_{Na,L}$ likely plays an important role in APD prolongation in heart failure and

may contribute to arrhythmogenesis. $I_{Na,L}$ inhibition decreased beat-to-beat AP variability and eliminated early afterdepolarizations in failing cardiomyocytes [57]. Likewise, dyssynchronous HF markedly increased $I_{Na,L}$ compared with non-failing hearts. CRT dramatically reduced DHF-induced enhanced $I_{Na,L}$, abbreviated the APD, and suppressed early afterdepolarizations. CRT was associated with a global reduction in phosphorylated Ca^{2+} /calmodulin protein kinase II, which has distinct effects on inactivation of cardiac Na^{+} channels [56].

Altered Ca^{2+} Currents and Calcium Homeostasis

Altered Ca^{2+} homeostasis underlies abnormalities in excitation-contraction coupling and arrhythmic risk in HF. Intracellular Ca^{2+} and APD are intricately linked by a variety of Ca^{2+} -mediated cell surface channels and transporters such as I_{Ca-L} , I_K , Ca^{2+} -activated Cl-current, and NCX. I_{Ca-L} density is unchanged or reduced in HF, the latter typically occurring in more advanced disease [38]. In human HF, baseline I_{Ca-L} density is consistently unchanged, although single channel studies suggest a reduction in channel number with an increase in open probability perhaps due to altered phosphorylation or subunit composition [58, 59].

The amplitude of the calcium transient (CaT) and its rate of decay are reduced in intact preparations and cells isolated from failing ventricles [60]. Systematic comparisons of the CaT profile and dynamics in cells isolated from different regions of the failing heart are limited. Sarcoplasmic reticulum Ca^{2+} -ATPase (*ATP2A2/SERCA2A*), its inhibitor phospholamban (PLN), and NCX are primary mediators of Ca^{2+} removal from the cytoplasm. In HF, ventricular myocytes exhibit a greater reliance on NCX for removal of Ca^{2+} from the cytosol and an increase in NCX function [61], which leads to defective sarcoplasmic Ca^{2+} loading. Altered NCX function in HF significantly influences CaT and AP dynamics [62]. Specifically, a sodium outward current through

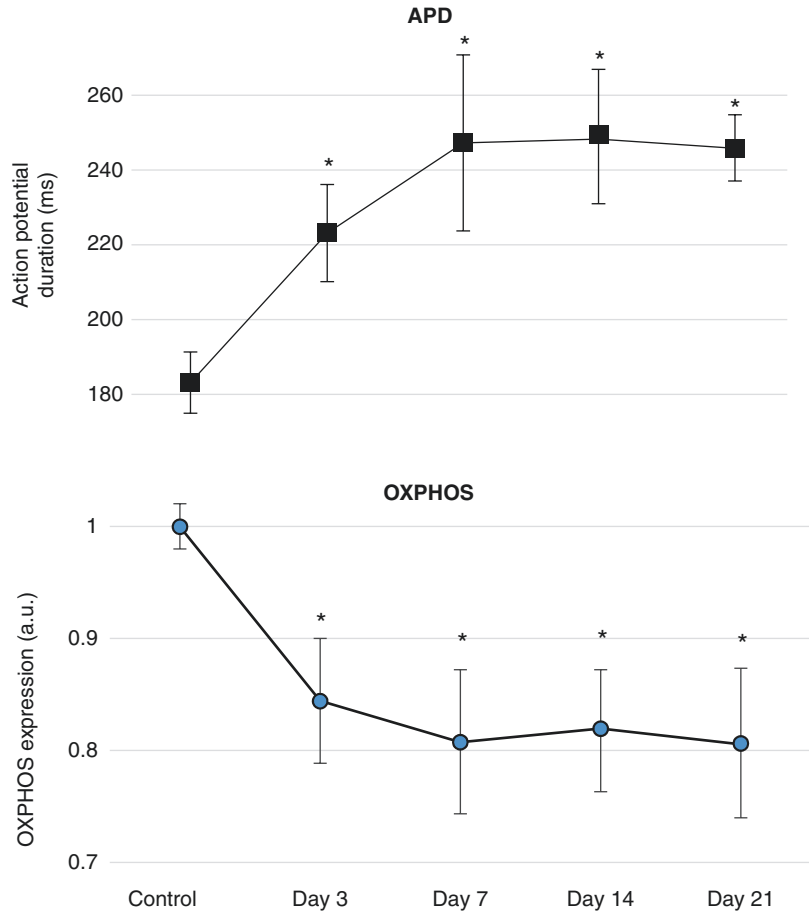
the Na^{+} - Ca^{2+} exchanger operating in reverse mode likely contributes to early repolarization. In canine hearts, administration of KB-R7943, a selective inhibitor of the reverse mode of the Na^{+}/Ca^{2+} exchanger, significantly increased QTc value and APD and lead to action potential alternans [63].

Repolarization: A Systems Biology View

Action potential prolongation, abnormal Ca^{2+} handling, fibrosis, and aberrant adrenergic signaling are hallmarks of left myocardial hypertrophy and failure. In a canine HF model (tachycardia-induced cardiomyopathy), we noted that the prolongation of the APD occurred early during the development of HF and coincided with profound transcriptional changes characterized by the downregulation of metabolic transcripts (Fig. 3.2) [64]. We then studied transcriptional co-expression patterns of >130 myocardial ion channels, transporters, and pumps across a whole range of physiological and pathophysiological conditions in order to test the hypothesis that altered expression of these ion channel transcripts occurs in the context of coordinated changes in metabolic gene expression. In human myocardium, we found that major repolarizing (e.g., *KCNH2*) ion channels were positively correlated with transcriptional activity of the oxidative phosphorylation pathway.

The coordinated transcriptional expression of metabolic and ion channel genes suggests that many ion channel genes expressed in the myocardium share common promoter regulatory regions with metabolic genes. Specifically, we found that transcription factor binding sites for estrogen-related receptor alpha (*ESRRA*, a key regulatory partner of PGC1 α , implicated in the downregulation of mitochondrial metabolic capacity in HF) and steroidogenic factor 1 (SF1 a member of the nuclear receptor family of intracellular transcription factors, encoded by the *NR5A1* gene) are shared by metabolic genes and major myocardial ion channel genes [65].

Fig. 3.2 Temporal correlation between APD prolongation (top) and expression of transcripts of oxidative phosphorylation (OXPHOS, bottom) during HF progression. * indicates $p < 0.05$ compared to control. (Adapted from data in [64])



Conclusion

Downregulation of potassium currents and upregulation of inward currents delay repolarization and can give rise to early afterdepolarizations and increased repolarization heterogeneity in different cell layers, thereby creating a substrate for ventricular tachyarrhythmia. A variety of extracardiac conditions (hypokalemia, antiarrhythmic drugs, autonomic tone) further reduce repolarization reserve and increase the arrhythmic risk in patients with organic heart disease. Antiarrhythmic pharmacotherapy targeting specific ion channel activity has shown promising antiarrhythmic effects in the basic science laboratory, but has not translated into clinical effectiveness due to proarrhythmia. Recent insights into complex mechanisms of electrical remodeling have raised the prospect of targeting disease-related events upstream of ion channels which

constitute the final common pathway of electrical activity. In fact, one of the most effective antiarrhythmic strategies so far has been targeting the early processes of the complex cascade leading to sudden arrhythmic death by non-antiarrhythmic drugs (i.e., beta-blockers, angiotensin-converting enzyme inhibitors, angiotensin receptor-blocker agents, and aldosterone antagonists). As our understanding of the role of the cellular context of cardiac repolarization continues to evolve, these advances are likely to lead to better treatment of ventricular arrhythmias.

References

1. Ziaieian B, Fonarow GC. Epidemiology and aetiology of heart failure. *Nat Rev Cardiol.* 2016;13:368–78.
2. Cupples LA, Gagnon DR, Kannel WB. Long- and short-term risk of sudden coronary death. *Circulation.* 1992;85:111–8.

3. Deyell MW, Krahn AD, Goldberger JJ. Sudden cardiac death risk stratification. *Circ Res.* 2015;116:1907–18.
4. Halliday BP, Cleland JGF, Goldberger JJ, Prasad SK. Personalizing risk stratification for sudden death in dilated cardiomyopathy. *Circulation.* 2017;136:215–31.
5. Gwathmey JK, Copelas L, MacKinnon R, Schoen FJ, Feldman MD, Grossman W, Morgan JP. Abnormal intracellular calcium handling in myocardium from patients with end-stage heart failure. *Circ Res.* 1987;61:70–6.
6. Luo M, Anderson ME. Mechanisms of altered Ca^{2+} handling in heart failure. *Circ Res.* 2013;113:690–708.
7. Crozatier B. Stretch-induced modifications of myocardial performance: from ventricular function to cellular and molecular mechanisms. *Cardiovasc Res.* 1996;32:25–37.
8. Schönleitner P, Schotten U, Antoons G. Mechano-sensitivity of microdomain calcium signalling in the heart. *Prog Biophys Mol Biol.* 2017;130:288–301.
9. Tomaselli GF, Marbán E. Electrophysiological remodeling in hypertrophy and heart failure. *Cardiovasc Res.* 1999;42:270–83.
10. Tomaselli GF, Beuckelmann DJ, Calkins HG, Berger RD, Kessler PD, Lawrence JH, et al. Sudden cardiac death in heart failure. The role of abnormal repolarization. *Circulation.* 1994;90:2534–9.
11. Dey S, DeMazumder D, Sidor A, Foster DB, O'Rourke B. Mitochondrial ROS drive sudden cardiac death and chronic proteome remodeling in heart failure. *Circ Res.* 2018;123:356–71.
12. Akar FG, Aon MA, Tomaselli GF, O'Rourke B. The mitochondrial origin of postischemic arrhythmias. *J Clin Invest.* 2005;115:3527–35.
13. Roden DM, Yang T. Protecting the heart against arrhythmias: potassium current physiology and repolarization reserve. *Circulation.* 2005;112:1376–8.
14. Misier AR, Ophof T, van Hemel NM, Vermeulen JT, de Bakker JM, Defauw JJ, et al. Dispersion of “refractoriness” in noninfarcted myocardium of patients with ventricular tachycardia or ventricular fibrillation after myocardial infarction. *Circulation.* 1995;91:2566–72.
15. Näbauer M, Beuckelmann DJ, Uberfuhr P, Steinbeck G. Regional differences in current density and rate-dependent properties of the transient outward current in subepicardial and subendocardial myocytes of human left ventricle. *Circulation.* 1996;93:168–77.
16. Litovsky SH, Antzelevitch C. Transient outward current prominent in canine ventricular epicardium but not endocardium. *Circ Res.* 1988;62:116–26.
17. Antzelevitch C, Sicouri S, Litovsky SH, Lukas A, Krishnan SC, Di Diego JM, et al. Heterogeneity within the ventricular wall. Electrophysiology and pharmacology of epicardial, endocardial, and M cells. *Circ Res.* 1991;69:1427–49.
18. Di Diego JM, Sun ZQ, Antzelevitch C. $\text{I}(\text{to})$ and action potential notch are smaller in left vs. right canine ventricular epicardium. *Am J Phys.* 1996;271:H548–61.
19. Bryant SM, Shipsey SJ, Hart G. Regional differences in electrical and mechanical properties of myocytes from guinea-pig hearts with mild left ventricular hypertrophy. *Cardiovasc Res.* 1997;35:315–23.
20. Johnson EK, Springer SJ, Wang W, Dranoff EJ, Zhang Y, Kanter EM, et al. Differential expression and remodeling of transient outward potassium currents in human left ventricles. *Circ Arrhythm Electrophysiol.* 2018;11:e005914.
21. Berger RD, Kasper EK, Baughman KL, Marban E, Calkins H, Tomaselli GF. Beat-to-beat QT interval variability: novel evidence for repolarization lability in ischemic and nonischemic dilated cardiomyopathy. *Circulation.* 1997;96:1557–65.
22. Barr CS, Naas A, Freeman M, Lang CC, Struthers AD. QT dispersion and sudden unexpected death in chronic heart failure. *Lancet.* 1994;343:327–9.
23. Pak PH, Nuss HB, Tunin RS, Kääb S, Tomaselli GF, Marban E, et al. Repolarization abnormalities, arrhythmia and sudden death in canine tachycardia-induced cardiomyopathy. *J Am Coll Cardiol.* 1997;30:576–84.
24. Aiba T, Hesketh GG, Barth AS, Liu T, Daya S, Chakir K, et al. Electrophysiological consequences of dyssynchronous heart failure and its restoration by resynchronization therapy. *Circulation.* 2009;119:1220–30.
25. Näbauer M, Kääb S. Potassium channel downregulation in heart failure. *Cardiovasc Res.* 1998;37:324–34.
26. Schmitt N, Grunnet M, Olesen S-P. Cardiac potassium channel subtypes: new roles in repolarization and arrhythmia. *Physiol Rev.* 2014;94:609–53.
27. Sah R, Ramirez RJ, Oudit GY, Gidrewicz D, Trivieri MG, Zobel C, et al. Regulation of cardiac excitation-contraction coupling by action potential repolarization: role of the transient outward potassium current ($\text{I}(\text{to})$). *J Physiol.* 2003;546:5–18.
28. Sah R, Ramirez RJ, Backx PH. Modulation of Ca^{2+} release in cardiac myocytes by changes in repolarization rate: role of phase-1 action potential repolarization in excitation-contraction coupling. *Circ Res.* 2002;90:165–73.
29. Calloe K, Cordeiro JM, Di Diego JM, Hansen RS, Grunnet M, Olesen SP, et al. A transient outward potassium current activator recapitulates the electrocardiographic manifestations of Brugada syndrome. *Cardiovasc Res.* 2009;81:686–94.
30. Beuckelmann DJ, Näbauer M, Erdmann E. Alterations of K^{+} currents in isolated human ventricular myocytes from patients with terminal heart failure. *Circ Res.* 1993;73:379–85.
31. Kääb S, Dixon J, Duc J, Ashen D, Näbauer M, Beuckelmann DJ, et al. Molecular basis of transient outward potassium current downregulation in human heart failure: a decrease in $\text{Kv}4.3$ mRNA correlates with a reduction in current density. *Circulation.* 1998;98:1383–93.
32. Niwa N, Nerbonne JM. Molecular determinants of cardiac transient outward potassium current ($\text{I}(\text{to})$) expression and regulation. *J Mol Cell Cardiol.* 2010;48:12–25.
33. Wang Y, Hill JA. Electrophysiological remodeling in heart failure. *J Mol Cell Cardiol.* 2010;48:619–32.

34. Zicha S, Xiao L, Stafford S, Cha TJ, Han W, Varro A, et al. Transmural expression of transient outward potassium current subunits in normal and failing canine and human hearts. *J Physiol*. 2004;561:735–48.
35. Akar FG, Wu RC, Juang GJ, Tian Y, Burysek M, DiSilvestre D, et al. Molecular mechanisms underlying K⁺ current downregulation in canine tachycardia-induced heart failure. *Am J Physiol Heart Circ Physiol*. 2005;288:H2887–96.
36. Xiao L, Coutu P, Villeneuve LR, Tadevosyan A, Maguy A, Le Bouter S, et al. Mechanisms underlying rate-dependent remodeling of transient outward potassium current in canine ventricular myocytes. *Circ Res*. 2008;103:733–42.
37. Liu DW, Antzelevitch C. Characteristics of the delayed rectifier current (IKr and IKs) in canine ventricular epicardial, midmyocardial, and endocardial myocytes. A weaker IKs contributes to the longer action potential of the M cell. *Circ Res*. 1995;76:351–65.
38. Furukawa T, Bassett AL, Furukawa N, Kimura S, Myerburg RJ. The ionic mechanism of reperfusion-induced early afterdepolarizations in feline left ventricular hypertrophy. *J Clin Invest*. 1993;91:1521–31.
39. Tsuji Y, Zicha S, Qi X-Y, Kodama I, Nattel S. Potassium channel subunit remodeling in rabbits exposed to long-term bradycardia or tachycardia: discrete arrhythmogenic consequences related to differential delayed-rectifier changes. *Circulation*. 2006;113:345–55.
40. Li G-R, Lau C-P, Ducharme A, Tardif J-C, Nattel S. Transmural action potential and ionic current remodeling in ventricles of failing canine hearts. *Am J Physiol Heart Circ Physiol*. 2002;283:H1031–41.
41. Holzem KM, Gomez JF, Glukhov AV, Madden EJ, Koppel AC, Ewald GA, et al. Reduced response to IKr blockade and altered hERG1a/1b stoichiometry in human heart failure. *J Mol Cell Cardiol*. 2016;96:82–92.
42. Wang YH, Shi CX, Dong F, Sheng JW, Xu YF. Inhibition of the rapid component of the delayed rectifier potassium current in ventricular myocytes by angiotensin II via the AT1 receptor. *Br J Pharmacol*. 2008;154:429–39.
43. Liu X, Wang Y, Zhang H, Shen L, Xu Y. Different protein kinase C isoenzymes mediate inhibition of cardiac rapidly activating delayed rectifier K⁺ current by different G-protein coupled receptors. *Br J Pharmacol*. 2017;174:4464–77.
44. Gou X, Wang W, Zou S, Qi Y, Xu Y. Protein kinase C epsilon mediates the inhibition of angiotensin II on the slowly activating delayed-rectifier potassium current through channel phosphorylation. *J Mol Cell Cardiol*. 2018;116:165–74.
45. Hegyi B, Bossuyt J, Ginsburg KS, Mendoza LM, Talken L, Ferrier WT, et al. Altered repolarization reserve in failing rabbit ventricular myocytes: calcium and β -adrenergic effects on delayed- and inward-rectifier potassium currents. *Circ Arrhythm Electrophysiol*. 2018;11:e005852.
46. Rose J, Aroundas AA, Tian Y, DiSilvestre D, Burysek M, Halperin V, et al. Molecular correlates of altered expression of potassium currents in failing rabbit myocardium. *Am J Physiol Heart Circ Physiol*. 2005;288:H2077–87.
47. Pogwizd SM, Schlotthauer K, Li L, Yuan W, Bers DM. Arrhythmogenesis and contractile dysfunction in heart failure: roles of sodium-calcium exchange, inward rectifier potassium current, and residual beta-adrenergic responsiveness. *Circ Res*. 2001;88:1159–67.
48. Käab S, Nuss HB, Chiamvimonvat N, O'Rourke B, Pak PH, Kass DA, et al. Ionic mechanism of action potential prolongation in ventricular myocytes from dogs with pacing-induced heart failure. *Circ Res*. 1996;78:262–73.
49. Rozanski GJ, Xu Z, Whitney RT, Murakami H, Zucker IH. Electrophysiology of rabbit ventricular myocytes following sustained rapid ventricular pacing. *J Mol Cell Cardiol*. 1997;29:721–32.
50. Clancy CE, Kass RS. Defective cardiac ion channels: from mutations to clinical syndromes. *J Clin Invest*. 2002;110:1075–7.
51. Maltsev VA, Sabbab HN, Undrovinas AI. Downregulation of sodium current in chronic heart failure: effect of long-term therapy with carvedilol. *Cell Mol Life Sci*. 2002;59:1561–8.
52. Huang B, El-Sherif T, Gidh-Jain M, Qin D, El-Sherif N. Alterations of sodium channel kinetics and gene expression in the postinfarction remodeled myocardium. *J Cardiovasc Electrophysiol*. 2001;12:218–25.
53. Jacques D, Bkaily G, Jasmin G, Ménard D, Proschek L. Early fetal like slow Na⁺ current in heart cells of cardiomyopathic hamster. *Mol Cell Biochem*. 1997;176:249–56.
54. Undrovinas AI, Maltsev VA, Sabbab HN. Repolarization abnormalities in cardiomyocytes of dogs with chronic heart failure: role of sustained inward current. *Cell Mol Life Sci*. 1999;55:494–505.
55. Valdivia CR, Chu WW, Pu J, Foell JD, Haworth RA, Wolff MR, et al. Increased late sodium current in myocytes from a canine heart failure model and from failing human heart. *J Mol Cell Cardiol*. 2005;38:475–83.
56. Aiba T, Barth AS, Hesketh GG, Hashambhoy YL, Chakir K, Tunin RS, et al. Cardiac resynchronization therapy improves altered Na channel gating in canine model of dyssynchronous heart failure. *Circ Arrhythm Electrophysiol*. 2013;6:546–54.
57. Maltsev VA, Silverman N, Sabbab HN, Undrovinas AI. Chronic heart failure slows late sodium current in human and canine ventricular myocytes: implications for repolarization variability. *Eur J Heart Fail*. 2007;9:219–27.
58. Chen X, Piacentino V, Furukawa S, Goldman B, Margulies KB, Houser SR. L-type Ca²⁺ channel density and regulation are altered in failing human ventricular myocytes and recover after support with mechanical assist devices. *Circ Res*. 2002;91:517–24.

59. Schröder F, Handrock R, Beuckelmann DJ, Hirt S, Hullin R, Priebe L, et al. Increased availability and open probability of single L-type calcium channels from failing compared with nonfailing human ventricle. *Circulation*. 1998;98:969–76.
60. O'Rourke B, Kass DA, Tomaselli GF, Kääh S, Tunin R, Marbán E. Mechanisms of altered excitation-contraction coupling in canine tachycardia-induced heart failure, I: experimental studies. *Circ Res*. 1999;84:562–70.
61. Hobai IA, O'Rourke B. Enhanced Ca(2+)-activated Na(+)-Ca(2+) exchange activity in canine pacing-induced heart failure. *Circ Res*. 2000;87:690–8.
62. Aroundas AA, Hobai IA, Tomaselli GF, Winslow RL, O'Rourke B. Role of sodium-calcium exchanger in modulating the action potential of ventricular myocytes from normal and failing hearts. *Circ Res*. 2003;93:46–53.
63. Shinada T, Hirayama Y, Maruyama M, Ohara T, Yashima M, Kobayashi Y, et al. Inhibition of the reverse mode of the Na⁺/Ca²⁺ exchange by KB-R7943 augments arrhythmogenicity in the canine heart during rapid heart rates. *J Electrocardiol*. 2005;38:218–25.
64. Gao Z, Barth AS, DiSilvestre D, Akar FG, Tian Y, Tanskanen A, et al. Key pathways associated with heart failure development revealed by gene networks correlated with cardiac remodeling. *Physiol Genomics*. 2008;35:222–30.
65. Barth AS, Kumordzie A, Tomaselli GF. Orchestrated regulation of energy supply and energy expenditure: transcriptional co-expression of metabolism, ion homeostasis and sarcomere genes in mammalian myocardium. *Heart Rhythm*. 2016;13:1131–9.



Cardiac Repolarization and Stem Cells: An Emerging Path Toward Precision Medicine

Massimiliano Gnechi, Luca Sala,
and Peter J. Schwartz

Introduction

The days when classic textbooks were sanctimoniously preaching that “the measurement of the QT interval has no clinical value” [1] are forever gone. The recognition that prolongation of the QT interval, as a marker of ventricular repolarization, is associated with an increased risk for sudden death—both in young patients with a genetic disorder [2, 3] and in patients surviving a myocardial infarction [4]—has determined the shift by which, during the last 40–50 years, studies of cardiac repolarization are endlessly growing.

Here, we review the progress made in these types of studies by using stem cells and their health-related implications for channelopathies, with a special focus on the relevance for the long QT syndrome (LQTS).

M. Gnechi
Coronary Care Unit, and Laboratory of Experimental
Cardiology for Cell and Molecular Therapy, IRCCS
Policlinico San Matteo Foundation, Pavia, Italy

Department of Molecular Medicine – Unit of
Cardiology, University of Pavia, Pavia, Italy

Department of Medicine, University of Cape Town,
Cape Town, South Africa

L. Sala · P. J. Schwartz (✉)
Center for Cardiac Arrhythmias of Genetic Origin –
Laboratory of Cardiovascular Genetics, Istituto
Auxologico Italiano, IRCCS, Milan, Italy
e-mail: peter.schwartz@unipv.it;
p.schwartz@auxologico.it

Classic Methods to Study Cardiac Repolarization

The study of cardiac repolarization is of fundamental importance to characterize the pathophysiology underlying cardiac arrhythmias. Even though significant progress has been made in the understanding of clinically relevant arrhythmias, there are still several unanswered questions in the field, and every experienced cardiologist recognizes the need for new and more targeted approaches. The major limitation that has hindered the study of cardiac arrhythmias at cellular level has been the lack of patient-specific cardiomyocytes (CMs) since biopsies cannot be easily obtained from patients. To circumvent this obstacle, complex experimental models have been introduced over the years, and they have contributed to improve our knowledge.

For instance, heterologous systems have been successfully used to model genetic repolarization disorders and channelopathies [5]. This technology consists in transfecting cancer cell lines with specific ion channels of interest to evaluate mutation-related changes in ion channel function and to predict the *in vivo* relevance of these changes. This approach is simple and inexpensive and has a potentially high yield, since heterologous systems are adaptable to robotic procedures [6]. However, these models lack important constituents of cardiac ion channel macromolecular complexes necessary to reproduce the molecular and electrophysiological

features investigated. Hence, the translational relevance of heterologous systems is often limited.

Animal models have also been used to model repolarization disorders, but their translational relevance is modest. The characteristics of the action potential (AP) of small animals, particularly the repolarization phase, are profoundly different from those of humans both in terms of duration and ion currents contribution [7, 8]. Consequently, drugs tested with positive results in small animal models often turned out ineffective in humans only in late stages of drug development, with huge losses in terms of costs and clinical advancement [9, 10]. Conversely, large animal models do show consistent similarities with humans [11] but also have important limitations that restrict their use only to more advanced stages of research and development [12]. Costs, particularly those associated with the generation, validation, and use of transgenic animals, represent a burden for laboratories and institutions, often caught between data reliability and budget limitations. Furthermore, growing ethical issues and the introduction of restrictive regulations are discouraging the use of animal models, with a profound negative impact on research.

Thus, methods that have allowed an undeniable amount of discoveries seem now limited and incapable of driving future innovation at a sustained pace.

Generation of Pluripotent Stem Cell-Derived Cardiomyocytes

Human stem cells as a tool in disease modeling and drug discovery represent a fairly recent concept, based on the hypothesis that cells of human origin may help to bridge the gap between pre-clinical research and clinical trials. In the late 1990s, the isolation of human embryonic stem cells (hESC) and the introduction of protocols to differentiate them into CMs (hESC-CMs) represented pivotal moments for the advancement of this novel approach. With time, the optimization of the differentiation protocols allowed to obtain spontaneously beating hESC-CMs that roughly recapitulated several typical human CM proper-

ties as cardiac ion currents expression and the presence of typical pharmacological responses [13–16]. Afterward, co-culturing systems with the mouse endoderm-like cell line (END2) and chemically driven protocols to induce cardiac differentiation were introduced and led to the reproducible generation of hESC-CMs resembling human CMs [17]. Since then, it became possible to generate ventricular-like CMs in virtually unlimited numbers. Even though this breakthrough was only partially embraced, particularly in Europe, due to ethical bans concerning the use of embryonic-derived material, this technology profoundly innovated the whole scientific field to a point that the core activity of multiple laboratories still relies on hESC-CMs for developmental studies, cardiac disease modeling, and drug testing.

The use of embryos as a source of pluripotent stem cells was made largely redundant by the discovery of induced pluripotent stem cells (iPSCs). It was in 2006 that Shinya Yamanaka, awarded with the Nobel Prize in Physiology or Medicine in 2012 for his discovery, identified four factors, *OCT4*, *SOX2*, *KLF4*, and *cMYC*—subsequently named *Yamanaka factors*—that, once transfected into somatic cells, are able to promote their reprogramming to a pluripotent state [18, 19]. Since iPSCs were initially obtained from skin dermal fibroblasts, thus not limited by ethical restrictions, their use literally exploded. Improvements in reprogramming methodologies have allowed the generation of iPSCs from even less invasive biological specimens as urine [20] or blood-derived mononuclear cells [21]. Furthermore, differently from hESCs, iPSCs can be generated from virtually any individual, opening the possibility to derive cell lines from healthy donors and patients to recreate *in vitro* more personalized approaches in disease modeling and therapy (Fig. 4.1) [22]. So far, iPSCs have been differentiated in multiple cell culture formats (Fig. 4.2) [23]: the generation of embryoid bodies (EBs) has been the first culture method used to generate iPSC-derived CMs (iPSC-CMs) and is still used in many laboratories, largely because these structures are easily formed. Subsequently, to reduce the workload and improve throughput and reproducibility, differentiation

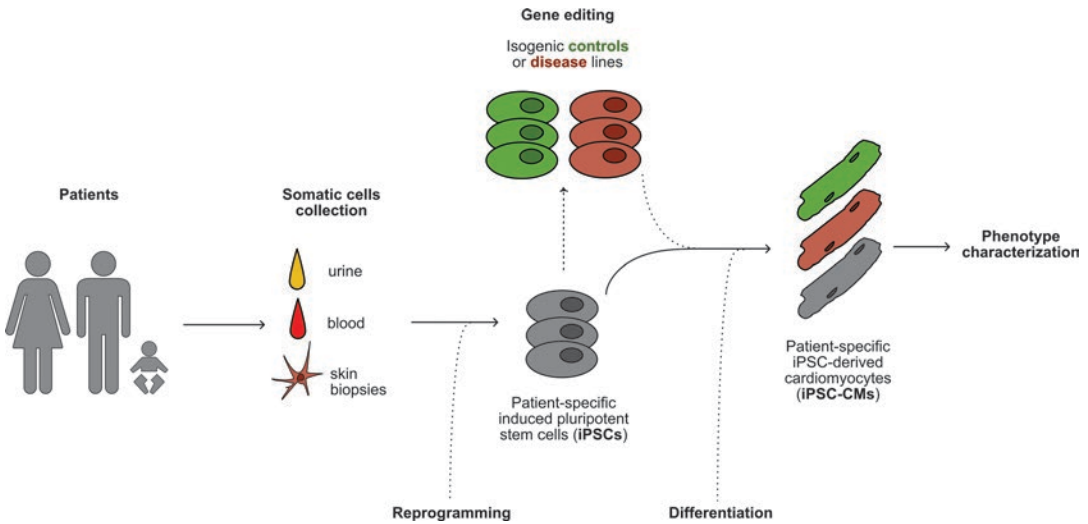


Fig. 4.1 iPSC generation. Somatic cells from multiple lineages can be collected from patients and reprogrammed to induced pluripotent stem cells (iPSCs) by a transfection with the Yamanaka factors. Patient-derived iPSCs can undergo gene editing approaches for the generation of the respective isogenic controls or isogenic mutated iPSC

line. iPSCs are then differentiated to iPSC-derived cardiomyocytes (iPSC-CMs) through multiple diverse differentiation protocols. iPSC-CMs, in different cellular formats, will be then used for phenotype characterization. Specific features of the phenotype of iPSC-derived cardiomyocytes (iPSC-CMs) will be then assessed and quantified

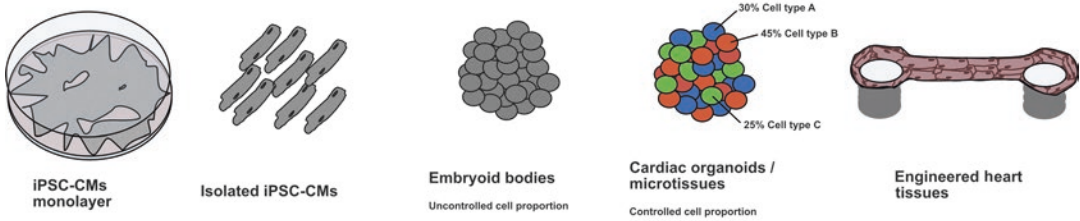
strategies based on supplementation of well-defined cytokine cocktails led to the generation of spontaneously beating monolayers of iPSC-CMs. However, these differentiation methods generate structures constituted by a variable and uncontrolled proportion of the different cell types, often exhibiting unpredictable line-to-line variability in differentiation efficiency. Accordingly, several groups are attempting to move toward standardized and controlled culture systems with the aim to generate monotypic cell cultures, constituted by a single cell type (i.e., CMs) embedded into extracellular matrix proteins or organoids [24–26]. This approach also allows to consciously mix different cell types (Fig. 4.2), for instance, CMs, endothelial cells, and fibroblasts, in fixed and reproducible ratios with consequent improvements in maturation and data reliability.

The Role of Pluripotent Stem Cells in Cardiac Arrhythmias

The field of cardiac repolarization disorders has been a pioneering playground for scientists

after the discovery of iPSCs [27, 28]. In particular, monogenic disorders as cardiac channelopathies were among the first to be modeled with iPSCs, given their generally straightforward disease mechanism and the fact that clear-cut phenotypes can be reproduced. Genetic mutations in ion channel genes may alter the ion channel biophysics and change key electrophysiological properties of the heart, with often devastating consequences for patients. The first iPSC line derived from a patient affected by LQTS was documented in 2010 by Alessandra Moretti and collaborators [29]. This seminal study opened the possibility to quantify the downstream effects of a specific ion channel mutation in terms of channel biophysics and allowed to determine complex and multiparametric features, typically restricted to primary CMs, such as AP, calcium transients, contraction, protein trafficking, protein-protein interaction, and pharmacological responses in cells having the same genotype of the patient. Multiple conditions were modeled in the following years using iPSC-CMs, with the main findings described below.

A) Common cell culture formats



B) Common maturation-enhancing strategies

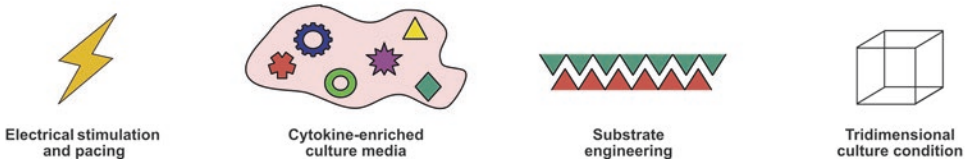


Fig. 4.2 Common cell culture formats and maturation strategies. **(a)** The most commonly used cell configurations for iPSC-CMs: (i) monolayers, (ii) isolated iPSC-CMs, (iii) embryoid bodies, (iv) cardiac organoids/microtissues, or (v) engineered heart tissues. **(b)** Strategies used to obtain more mature CMs generally simulate con-

ditions that do occur during development and include (i) electrical pacing, (ii) cytokine- or small molecules-enriched media, (iii) substrate engineering with more physiological strain or attachment properties, and (iv) tridimensional culture conditions

Cardiac Repolarization Disorders Modeled with Pluripotent Stem Cell-Derived Cardiomyocytes

Long QT Syndrome

Long QT syndrome is the best characterized arrhythmogenic disorder of genetic origin and a leading cause of sudden cardiac death (SCD) in young subjects [30, 31]. LQTS is a familial arrhythmogenic syndrome characterized by delayed repolarization that may lead to a life-threatening polymorphic ventricular tachycardia known as “torsades de pointes.” The congenital form of LQTS is caused by a mutation in one of at least 16 genes encoding for key cardiac ion channels or excitation-contraction coupling proteins [32], while the acquired form manifests QT interval prolongation mainly in response to pharmacological compounds blocking I_{Kr} , the rapid delayed rectifier potassium current [33–35]. LQTS was the first repolarization disorder linked to precise genetic bases [36–38], and this has markedly changed the approach to diagnosis, risk stratification, and management. Indeed, already in 1995, the first gene-specific therapy was pro-

posed based on the understanding that the genetic subtype caused by an increased sodium current (LQT3) could respond well to the sodium channel blocker mexiletine [32]. This has now become part of the standard therapy for LQTS [31, 39]. Recent data show that mexiletine can often shorten QTc also in LQT2 patients [40].

As said, Moretti et al. approached the disease modeling of LQTS with the iPSC technology, assuming that patient-specific cells, thus sharing the same genotype with the donor, should also reproduce the clinical phenotype *in vitro* [29]. They studied a patient with LQT1 caused by a heterozygous point mutation in the *KCNQ1* gene causing a loss of function of I_{Ks} . Skin fibroblasts were collected from the patient and from a healthy individual, expanded, reprogrammed to iPSCs using the four Yamanaka factors, and differentiated to iPSC-CMs with a chemically driven differentiation protocol. The APs of patient-specific iPSC-CMs were markedly prolonged (Fig. 4.3), and the magnitude of I_{Ks} was reduced compared to iPSC-CMs from the control. When they added catecholamines, a known arrhythmogenic trigger in LQT1 patients [41], arrhythmic activity (early afterdepolariza-

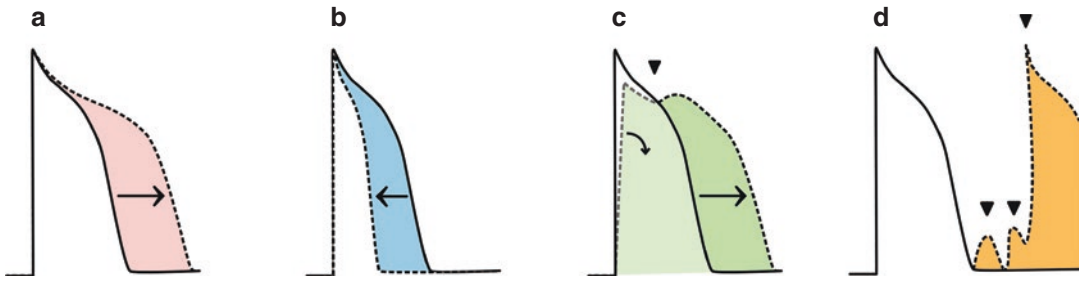


Fig. 4.3 Phenotype exhibited by repolarization disorders in iPSC-CMs. Normal (solid line) and diseased (dashed line) action potentials from (a) long QT syndrome, (b)

short QT syndrome, (c) Brugada syndrome, (d) catecholaminergic polymorphic ventricular tachycardia (CPVT)

tions) developed only in iPSC-CMs derived from the patient. These experiments demonstrated that a virtually unlimited source of patient-derived CMs could be generated to study disease traits and to validate targeted/personalized therapeutic approaches [28]. Subsequently, several iPSC lines were generated from patients with LQT1 [42–47], LQT2 [43, 45, 46, 48–59], LQT3 [60–65], LQT7 [66], LQT8 [67], LQT14 [68, 69], and LQT15 [68, 70, 71]. Phenotypic features as prolongation of AP were recapitulated as well as gain- or loss-of-function of ion currents, correctly reproducing the expected allelic stoichiometry (i.e., heterozygosity vs homozygosity).

A representative case to understand the importance of iPSC-CMs comes from the modeling of severe forms of LQTS (LQT14–16) caused by mutations in calmodulin [72], a ubiquitous and highly conserved protein that acts as calcium sensor within cells and is essential for the functioning of multiple organs, including the heart. Calmodulin is so important that identical proteins are encoded in humans by three different highly conserved genes (*CALM1–3*) [73] and a mutation in just one of the six alleles can cause life-threatening arrhythmias [72]. Heterologous overexpression of mutant calmodulin fails to preserve its native stoichiometry, while animal models are poorly predictive as the copy number and chromosomal localization of their calmodulin genes are different from those of humans. The only experimental model currently available in which gene stoichiometry can be conserved and reproduced is represented by iPSC-CMs [69]. Using patient-specific F142L iPSC-CMs we were able

not only to confirm a severe impairment in Ca^{2+} -dependent inactivation (CDI) of L-type calcium currents (LTCC) as the cause of the action potential prolongation but also to exclude other possible causes of LQTS and ventricular arrhythmia not previously predicted by heterologous systems [69]. For example, we found that alterations in the slowly activating delayed rectifier current or the late sodium current, both of which regulated by CaM, were not responsible for the prolonged action potentials of F142L iPSC-CMs. This iPSC-based approach, in parallel with the development of gene editing techniques, already allowed the first targeted studies to test novel therapeutic approaches with pharmacological [69] or biotechnological [70, 71] strategies that have already obtained preliminary translation to patients [74].

Short QT Syndrome

The key phenotypical manifestation of the short QT syndrome (SQTS) is an excessive shortening of ventricular repolarization due to gain- or loss-of-function mutations in genes encoding for ion channels carrying repolarizing or depolarizing currents, respectively [75]. SQTS type 1 (SQT1) is caused by mutations in the *KCNH2* gene, encoding for the voltage-gated potassium channel Kv11.1 (hERG) and conducting I_{K_r} . SQT1 has been modeled with iPSC-CMs, and patient-specific CMs exhibited a short AP duration (Fig. 4.3) as a consequence of an increased I_{K_r} magnitude, with pro-arrhythmic events recorded under baseline conditions and

pharmacological stimulation with carbachol [76]. The disease traits of SQTS were also recently reproduced at tissue level in iPSC-CMs monolayers, which further extends the capabilities of the iPSC technology to simulate complex arrhythmogenic patterns *in vitro* at both cellular and tissue levels [77].

Brugada Syndrome

The Brugada syndrome (BrS) is an autosomal dominant channelopathy with variable penetrance associated with premature APs in the right ventricular outflow tract which may result in SCD. ECG patterns are characterized by incomplete right bundle-branch block and ST-segment elevations in the anterior precordial leads V1-V3 [78].

The BrS type 1 (BrS1), the first type modeled with iPSC-CMs, may arise as a consequence of mutations in the *SCN5A* gene, encoding for the voltage-gated cardiac sodium channel $\text{Na}_v1.5$, causing a loss of function in the peak sodium current (I_{Na}) and a delay in the cardiac electrical impulse conduction. Approximately 20% of patients affected by BrS carry mutations in the *SCN5A* gene [33, 79]. Patient-specific iPSC-CMs reproduced the decreased I_{Na} magnitude and exhibited short APs (Fig. 4.3) and arrhythmogenic features as sustained triggered activity with incomplete and asynchronous Ca^{2+} transients [80]. The use of gene-edited isogenic controls confirmed that such peculiar features were inherent of iPSC-CMs from BrS donors and indicated that iPSC-CMs are suitable experimental models for BrS [80]. Importantly, iPSC-CMs proved useful to identify novel disease mechanisms. For instance, Veerman and coworkers identified three patients with a BrS type 1 ECG pattern who tested negative for the known BrS-related genes [81]. Their iPSC-CMs did not exhibit functional alterations in the I_{Na} , transient outward potassium current (I_{to}), or the L-type calcium current (I_{CaL}), suggesting the existence of a still unveiled disease mechanism underlying BrS, likely attributable to genetic modifiers or to external factors (e.g., fibrosis, structural defects, age, etc.) diffi-

cult to reproduce in iPSC-CMs at the present state of technology [82]. Moreover, although an attempted pharmacological rescue strategy, based on innovative read-through compounds, failed to revert disease traits in iPSC-CMs from *SCN5A* nonsense mutation carriers with a mixed LQT3/BrS phenotype [83], it contributed to demonstrate the plethora of applications for iPSC-CM models to study repolarization disorders. Importantly, Okata et al., through a refined gene knockout targeting strategy, demonstrated that embryonal or neonatal isoforms of the sodium channel, absent in human adult CMs but expressed in iPSC-CMs, can mask the effect of BrS mutations present in the adult isoform of the gene [64]. This raises warning signs for the modeling of certain diseases with immature iPSC-CMs.

Catecholaminergic Polymorphic Ventricular Tachycardia (CPVT)

Catecholaminergic polymorphic ventricular tachycardia (CPVT) is another genetic arrhythmogenic condition characterized by ventricular tachycardia induced by beta-adrenergic activation [84, 85]. Multiple forms exist and all relate to mechanisms controlling intracellular Ca^{2+} homeostasis. Mutations in the *RyR2* gene, encoding for the cardiac ryanodine receptors, the first to be linked with CPVT, are associated with the CPVT type 1 (CPVT1) [86, 87]. Mutations in *CASQ2*, encoding for calsequestrin 2, an important protein that acts as Ca^{2+} buffer within the SR, have been associated with CPVT type 2 (CPVT2) [88]. The majority of CPVT cases are caused by these two genotypes, but minor genes have been identified and linked, respectively, to CPVT3–5. The immaturity of iPSCs-CMs may profoundly hinder the disease modeling of CPVT, since the absence of a properly formed T-tubules network, the lack of sarcomere organization, and the differential expression levels of ion channels and Ca^{2+} handling proteins could represent a hurdle difficult to circumvent. Nonetheless, several laboratories attempted to model CPVT with iPSC-CMs, surprisingly recapitulating multiple clinical

features observed in patients as aberrant Ca^{2+} transients, altered Ca^{2+} -store stability, arrhythmic APs (Fig. 4.3), and beta-adrenergic sensitization [89–92]. Drug screening strategies were also attempted using these models, and, in addition to the validation of current treatments, they also opened new possibilities for innovative pharmacological therapies [93–97]. Of note, iPSC-CMs allowed the identification of a novel gene (*TECRL*), which mutations are associated to a mixed LQTS/CPVT phenotype and provided an efficient platform for a pharmacological rescue of the phenotype [98].

Techniques to Quantify the Phenotype

Along with gold standard and established techniques, the use of stem cell-derived CMs for the study of cardiac disease allowed the introduction of innovative tools or technologies for the investigation of the functional phenotype. The leading and more widespread techniques are presented below.

Patch Clamp

After almost 50 years, the patch clamp technique remains the gold standard for single-cell electrophysiology studies. A pulled glass capillary filled with a high potassium solution resembling the ionic composition of the cytosol allows the recording of ionic currents flowing across the cell membrane (Fig. 4.4) [99]. Two main modes can be used to assess a pathological phenotype: in **current clamp**, a controlled current square pulse is used to trigger APs from isolated CMs. Depending on the characteristics of the glass pipettes and intracellular solutions, this mode can be used to record APs from multicellular structures. In the **voltage clamp** mode, the operator controls the membrane potential to take advantage of the voltage-gated kinetics of ion channels and to investigate changes in their biophysical properties due to ion channel mutations. This mode can also be used in the **AP clamp** configuration to simulate the kinetics of specific ion cur-

rents during one AP and has been extremely useful to gather biophysical data from specific ion currents to be incorporated later into computational models [45, 100, 101].

Multielectrode Array

The multielectrode array (MEA) technology has gained an amazing momentum after iPSC-CMs became of routine use. Unlike primary CMs, iPSC-CMs can spontaneously contract, have a high attachment capacity, can effectively form functional syncytia, and tolerate well long-term culturing conditions. This high flexibility allowed iPSC-CMs to access platforms usually considered a prerogative for immature cell types (e.g., chicken embryos CMs or murine neonatal CMs) or neurons. The MEA technology allows the recording of extracellular signals, called field potentials (FP), from excitable cells plated on extracellular microelectrode arrays. The FP is the net result of extracellular ion fluxes acquired by the tiny electrodes, and its trajectory is also affected by cell distance from the electrode, vector direction of the electrical signal, and spatial organization of the cells; the main quantitative parameters of the MEA technology applied to iPSC-CMs are FPD and beating frequency, respectively, rough equivalents of the QT and RR intervals [102] (Fig. 4.4). Although MEA data need a careful interpretation because of the high number of variables that can influence these measurements, their high-throughput predictive potential in cardiac disease modeling has been clearly established, to the point that pharma companies have begun to use this technology for their preclinical drug screening pipelines [45, 102–104]. Recent technological improvements also allowed the combined measurement of impedance and FPs [105], the recording of intracellular signals through grids of sharp nanoelectrodes [106], and the investigation of the effect of strain with stretchable MEAs [107]. Finally, MEAs can be easily combined to pacing technologies as stimulators [108] or optogenetics [109] to improve their predictivity for cardiac disease modeling and drug screening.

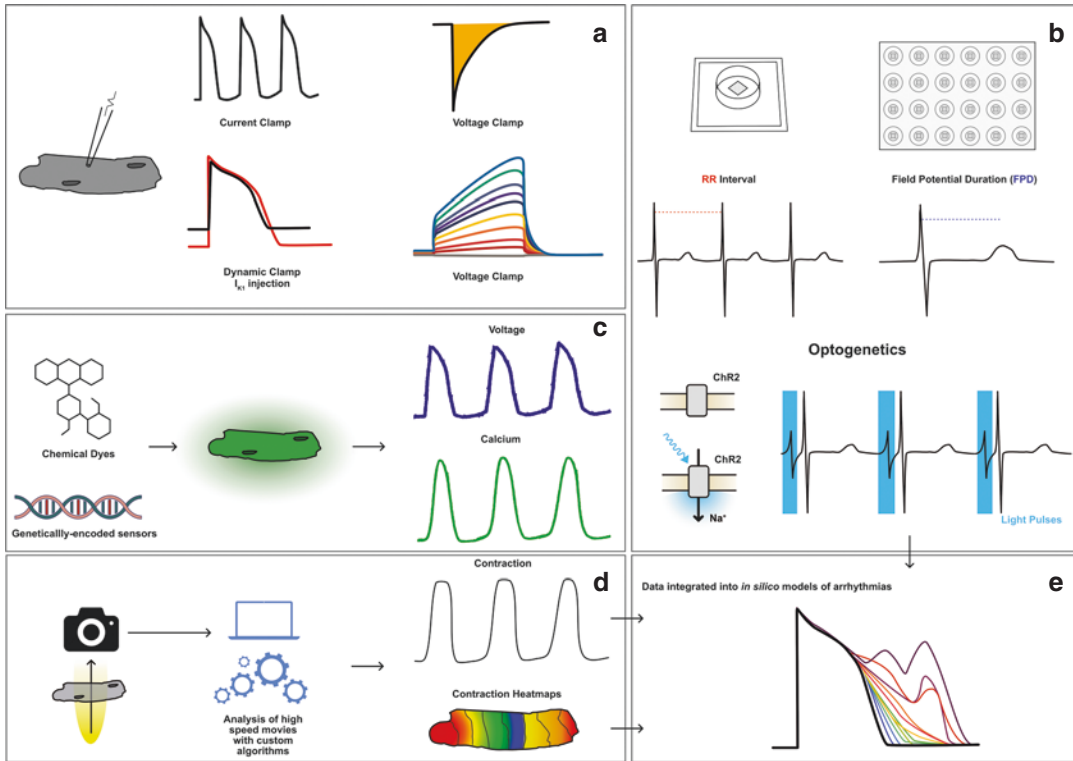


Fig. 4.4 Technologies used for phenotype evaluation. **(a)** *Patch clamp electrophysiology*: a glass capillary allows the recording of action potentials (current clamp mode) in native conditions or with the injection of a computer-simulated current (I_{K1} , in the example; dynamic clamp mode) and ionic currents (voltage clamp mode) in iPSC-CMs. **(b)** *Multielectrode arrays*: iPSC-CMs are plated on single-well (top, left) or multi-well MEA chips (top, right). The recorded signals, called field potentials (FP), remind an electrocardiographic recording; the beating frequency (RR interval, mid-left) and the FP duration (FPD, mid-right) are the most relevant parameters that can be extracted and quantified with this platform. The MEA technology can be easily coupled with optogenetic actuators such as the channelrhodopsin 2 (ChR2, bottom left). This light-sensitive ion channel opens when hit by blue light, and this allows an inward flow of Na^+ ions to depolarize the membrane potential and trigger an action potential, recorded by the MEA as FP (bottom, right). **(c)**

Fluorescent reporters: iPSC-CMs can be incubated with chemical dyes or transfected with genetically encoded voltage or ion sensors. These will allow the recording of multiple parameters such as voltage profiles or calcium transients in medium-high-throughput formats. **(d)** *Optical methods*: bright-field movies of contracting cells are recorded through high-speed digital cameras and analyzed by custom-made algorithms. These software tools, through different mathematical strategies, will output quantitative contraction profiles or heat maps that can be used to quantify and estimate the effect of a repolarization disorder on cardiac contraction. **(e)** *Computational approaches*: data recorded from the aforementioned techniques are combined and integrated into mathematical in silico models of arrhythmias; these models will offer tools to predict the effect of disease mutations on the phenotype of iPSC-CMs and will contribute to the generation of more accurate models of repolarization disorders

Fluorescent Dyes

The abundant availability of iPSC-CMs boosted their integration into large-scale analysis platforms, with increasing demand from industry and academia for high-throughput technologies to quantify pharmacological effects and disease

phenotypes. Technical advancements in imaging, fluorescent dyes synthesis, and genetic engineering have led to a fast optimization of chemical and genetically encoded fluorescent indicators capable to track membrane potential and intracellular ion concentrations with sufficiently rapid kinetics (Fig. 4.4) [110]. Incubation with chemi-

cal dyes is cheaper and easier than the stable integration in the genome of plasmids carrying voltage- or cation-sensitive probes; on the other hand, chemical dyes cannot be used in long-term repeated recordings and carry the inherent disadvantage of a higher phototoxicity. The relatively low signal-to-noise ratio and the low sensitivity to changes in fluorescence upon rapid voltage- or ion-concentration shifts represent general limitations of fluorescent dyes; this is why more efficient and brighter probes have been recently developed [111, 112]. The benefits offered by the high-throughput capabilities of these platforms and by the possibility to perform multiparametric measurements [113] significantly outweigh their lower accuracy. This has enhanced the diffusion of fluorescent dyes for the automated

characterization of diseased cell lines and for drug testing performed using large screening platforms [114–116].

Video-Based Analyses

Recent advancements in image acquisition and processing allowed the generation of platforms capable to extract quantitative information of cardiac repolarization from movies recorded with high-speed cameras. These techniques quantify properties associated with CM contraction and relaxation such as amplitude, force, speed, and duration (Figs. 4.4 and 4.5); these measurements are possible due to the combination of sophisticated recording devices [117–119] and analysis

Precision Medicine

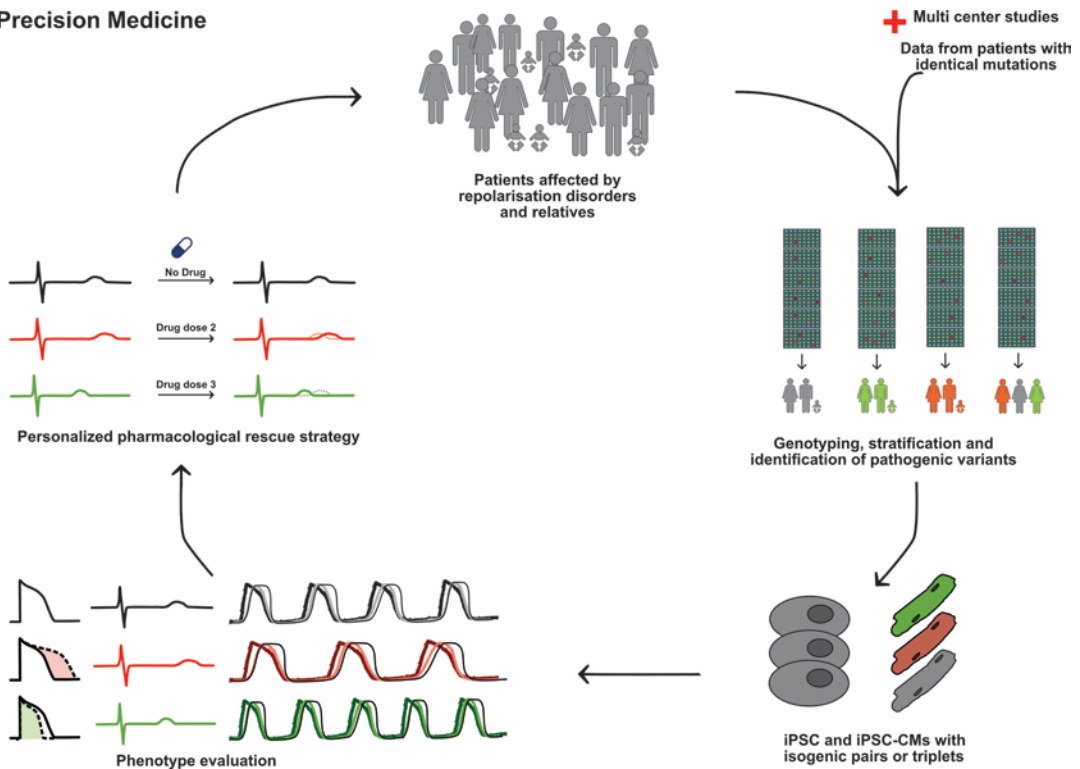


Fig. 4.5 Precision medicine. Patients with repolarization disorders are genetically screened to evaluate the presence of disease-causing mutations or polymorphisms, and they are stratified according to their genotype or other key features as ethnicity, gender, age, etc. iPSC lines are generated from these cohorts of subjects and differentiated towards iPSC-CMs. Functional *in vitro* evaluations on

patient-derived iPSC-CMs will prove the putative pathogenic role of the identified variants and will contribute to stratify patients according to the *in vitro* phenotypes. *In vitro* individual drug tests are performed, and specific patterns of response are identified and correlated to clinical features to deliver the most effective treatment to each patient

algorithms [120, 121]. Although some of these platforms may be limited by costs or by their low flexibility toward different cell configurations or substrates, the most recent ones offer open-source solutions to counterbalance the costs of proprietary systems and advanced algorithms to cope with multiple cell formats and attachment conditions [120, 121]. Of relevance, the latest trend is to move toward the determination of multiple parameters within a single measurement; e.g., quantification of contraction in combination with MEA, patch clamp, or fluorescence analyses allows simultaneous insights from multiple aspects of cardiac repolarization as contraction, membrane potential, or calcium handling [121], which is quite important for gathering insights from disorders of cardiac repolarization or pharmacological responses.

Technological Improvements

Current differentiation strategies have approached maturation from different angles, but, despite the recent great progress, standardized protocols for large production of fully mature iPSC-CMs are not yet available. The exponential success of iPSC-CMs for disease modeling and drug testing has promoted the convergence of multiple disciplines, with some of the most representative technological advancements harnessed to obtain CMs with a more mature electrophysiological phenotype or to generate genetically engineered cell lines. Moreover, advancements in substrate engineering and computational power ensured the possibility to generate and analyze large amount of data at high throughput or to simulate consequences of disease or pharmacological challenges *in silico*. We report here some of the most recent applications.

Dynamic Clamp

The electrophysiological phenotype immaturity of iPSC-CMs can be mitigated with an elegant computational approach known as dynamic clamp [122]. This technique allows the injection

of a simulated ion current of interest in the cell to compensate the lack of the endogenous counterpart (Fig. 4.4). This requires the real-time coupling of an *in silico* mathematical model of ion currents with the *in vitro* measurement in patched cells. The voltage contour of the AP recorded in the cell is processed by a mathematical model, and the generated ion current profile is outputted and reinjected into the cell. Examples in adult CMs include the simulation of pathogenic conditions in I_{Kr} [101], I_{to} [100], and I_{Na} [123]. Specifically for hESC- and iPSC-CMs, the efforts so far aimed to counterbalance their low I_{K1} magnitude that is typical of immature CMs [69, 124, 125]. Recently, this technology has been implemented in high-throughput systems on automated patch clamp platforms [126], and, once optimized, this strategy will allow drug tests on stem cell-derived CMs in more physiological conditions.

Optogenetics

The possibility to derive CMs from cultured iPSCs has eased the generation of cell lines carrying the insertion of stable constructs, and one of the most promising application is the use of optogenetic sensors, i.e., light-sensitive ion channels whose characteristics can be exploited to control CM's behavior [127]. The most widespread sensor is the channelrhodopsin 2 (ChR2), which encodes for an ion channel equipped with a photoreceptor unit (Fig. 4.4). Stimulation with blue light modifies the ion channel structure triggering a depolarizing current and a consequent AP [128]. Human iPSC-CMs expressing ChR2 have been generated, and they exhibit a normal cardiac phenotype with the exception that their beating frequency can be controlled by precisely triggered light pulses. As demonstrated by Sala and coworkers [45], the frequency dependence of iPSC-CMs appears, conversely to adult CMs, to be cell line specific regardless of the formulae used for rate correction; this impacts the reliability of disease phenotype assessment and pharmacological effect quantification. Algorithms partially mitigate this limitation [129], but they

often require complex stimulation platforms that are sometimes poorly compatible with many of the most used recording technologies. These limitations are circumvented through optogenetics, which can be promptly integrated into current platforms for drug screening and cardiac safety pharmacology [109].

Computational Approaches

The exponential increase in computational capabilities of bioinformatic tools has significantly empowered these systems and their usage as predictive systems for *in silico* mathematical modeling of disease phenotypes, pharmacological responses, and clinical trials [130, 131]. These tools should be used in combination with experimental methodologies and will likely evolve, in the near future, into more sophisticated multiscale human models capable to simulate single cells [132–136] or even the whole heart [137] that could be used as ethical, safe, and cost-effective platform to integrate, or replace where possible, current animal or *in vitro* studies (Fig. 4.4). *In silico* models of stem cell-derived CMs have allowed the recapitulation of key features of healthy and diseased cells as APs [132, 133, 136], ion currents [134], phenotypic variability [135], and pharmacological responses. Computational approaches have shown an enormous potential especially when they were integrated into data analysis procedures. The ability of artificial neural networks to identify complex patterns, invisible to the human eye, has been harnessed for the classification of cell morphology [138], pharmacological responses [139], or disease patterns. Machine learning approaches have recently demonstrated the ability to automatically discriminate, with a remarkable accuracy (78–88%), cardiac disorders such as LQTS, CPVT, or hypertrophic cardiomyopathy by the profile and kinetics of Ca^{2+} transients of patient-specific iPSC-CMs [140]. Computational-based strategies have been also proposed as one of the key pillars of the Comprehensive *In Vitro* Proarrhythmia Assay (CiPA) initiative [141], a

joint effort of academia, regulatory agencies, and pharmaceutical companies which aims to overcome current guidelines of safety pharmacology and drug testing through a multilevel approach including iPSC-CMs and computational models.

Genome Editing

Shortly after the first investigation of cardiac disease phenotypes, it emerged that iPSC-CMs from different human donors, regardless of the presence of pathogenic mutations, may exhibit different, sometimes opposite, electrophysiological phenotypes. This has been related to variations in the genetic background of each donor which may influence the *in vitro* phenotype of iPSC-CMs. These variations can be attributed to unique allelic variants among individuals and epigenetic variability, on top of which relies the experimental variability associated to clonal selection and culturing conditions [142]. Thus, iPSC-CMs suffer from cell line-dependent variation which may influence their functionality and hamper the reproducibility of the results. This heterogeneity may be markedly visible when studying repolarization disorders and, specifically, the interline variations of APD and FPD, two parameters investigated during the characterization of LQTS or SQTs mutations and pivotal for safety pharmacology. As previously demonstrated [143], it is often difficult to cluster cell lines into specific disease types by relying only on APD. One solution to partially reduce background genetic variation is to generate, when feasible, a control line from a first-degree relative. Although the concept behind this approach is reasonable, its effectiveness compared to a random control selection has still to be experimentally validated. Genetic engineering now offers a smart, albeit complex, solution to this problem: the generation of *isogenic controls*. These cell lines are obtained by gene editing technologies that allow the precise insertion of point mutation in the genome without altering the overall background (Fig. 4.1). Currently, the CRISPR/Cas9 gene editing approach is the most

widely used [144], albeit its remarkable activity has also the downside to potentially leave off-target “scars” in the host DNA and might restrict the implementation of this technology to *in vitro* or *ex vivo* applications. Gene editing techniques allow the derivation of isogenic pairs or isogenic triplets to investigate disease phenotypes in an identical genetic background environment and with the additional key contribution of gene stoichiometry. They proved essential for the characterization of disease phenotypes [42, 43, 52, 70] and drug discovery approaches [45], even though their use becomes challenging when insertions or corrections of heterozygous mutations, rather than gene knockouts, are required. Although too complex to be performed by non-experts, inefficient, time-consuming, and expensive to achieve at present state of technology, which restricts their benefits to a minority of laboratories worldwide, these strategies do offer undeniable advantages in terms of results reproducibility and data reliability.

Limitations

Cell Maturity

The level of maturation is the main limitation of iPSC-CMs, but it represents an acceptable trade-off between reliability of results and the massive amount of information that can be obtained with high-throughput systems. Due to technical limitations, high-throughput electrophysiology screenings can be used mostly with immature CMs, similar to those derived from stem cells, because these cells are relatively easy to generate and handle, and can be adaptable to robotic procedures. Conversely, mature primary CMs are rod shaped, do not form monolayers *in vitro*, cannot be processed with fluorescence-activated cell sorting, and tend to rapidly dedifferentiate while in culture [145]. In the last few years, the characterization of iPSC-CMs has demonstrated that their phenotype resembles that of CMs at an early stage of development [146] and this aspect must be kept into consideration when analyzing the results of disease modeling studies. Several strat-

egies, aimed to recreate conditions that occur during embryogenesis, have been attempted over the years to increase the maturation of iPSC-CMs and generate more predictive systems for disease modeling, drug screening, and cardiac toxicity (Fig. 4.2). Those include prolonged time in culture [147]; electrical stimulation [148]; media enriched with cytokines or growth factors [149]; the presence of physical stimuli as shear stress and mechanical stretch [148, 150, 151]; the presence of substrates of different stiffness, composition, and pattern [152]; or the assembly into more physiological tridimensional structures [24, 25, 153, 154]. All these techniques dramatically increase the costs, but the generation of more mature iPSC-CMs will guarantee more reproducible and predictive results.

Translational Perspective

The translational capabilities of iPSC-CMs have still to be fully explored. Unlike what happens in human hearts, repolarization duration in iPSC-CMs is highly variable and often may not reflect a pathological manifestation per se. Even in the presence of putatively healthy genotypes, repolarization duration may span across values that can be considered pathological [143]. Thus, the use of appropriate controls is absolutely mandatory to avoid misinterpretations (Fig. 4.1). Differentiation conditions play a major role in such a high variability, and only the use of very strict culture conditions can guarantee homogeneous results across different research centers [103, 104], although an individual susceptibility to growth factors and cytokines exists across different cell lines [155]. The generation of paired transgenic and iPSC mouse, canine, or human models [156] to study the *in vivo* relevance of *in vitro* observations will identify the presence of recurrent patterns of similarity between preclinical and clinical observations and clarify the boundaries of iPSC-CM technology. In particular, efforts are needed to better correlate the baseline parameters of pharmacological responses recorded *in vitro* to their *in vivo* counterparts and to validate whether the observed *in vitro* values

can be sufficiently predictive and representative of the *in vivo* condition.

A Glimpse of the Future

One of the most intriguing uses of iPSC-CMs is the possibility to generate experimental models for personalized approaches to disease modeling and therapy. Although the dream of personalized medicine might be still considered overambitious and cannot be pursued at the present state of technology, precision medicine approaches will be pushed forward thanks to the availability of patient-specific and isogenic iPSC-CM lines [157]. In agreement with the goals of precision medicine, individuals are clustered according to specific population classifiers as age, gender, ethnicity, disease conditions, etc., to identify genetic or molecular targets and mechanisms of disease through a combination of large-scale population data with *in vitro* experimental models tailored on precise population characteristics. These, in combination to a scrutinized clinical history and multiple population-specific iPSC lines, can be used to identify molecular or functional differences in disease severity, to better stratify the population, or to detect specific patterns of response to therapy, with potential implications on drug discovery and development. As a representative example of precision medicine, Burridge and coworkers were able to reproduce, in patient-derived iPSC-CMs, the different grades of cardiotoxicity observed in patients treated with doxorubicin [158]. The high similarity between the clinical phenotype and that recreated in iPSC-CMs allowed to identify new genetic causes underlying doxorubicin-induced cardiotoxicity with immediate implications for clinical handling of cancer patients. If extended, this strategy holds promises for the identification of novel compounds tailored on specific population classifiers and will allow the determination of patterns of drug response in populations previously considered identical and thus being wrongly administered identical therapies.

In this line of thought, new therapeutic possibilities are emerging through drug repurposing

strategies, i.e., the identification of new clinical applications for compounds already approved for commercialization [159]. Since the safety profiles of these compounds have already been assessed, the long and expensive final stages of preclinical drug development could be skipped, allowing these drugs, once they give positive results *in vitro*, to be validated in patients within few months. This certainly represents a revolution that guarantees fast feedbacks compared to classical drug discovery approaches. The first example of application of iPSCs to drug repurposing came from amyotrophic lateral sclerosis. Wainger and coworkers reproduced the patient features *in vitro* using neurons derived from iPSCs and were able to demonstrate that retigabine, approved on the market for the treatment of epilepsy, reverted the pathological phenotype of amyotrophic lateral sclerosis *in vitro*. Based on these results, shortly after this discovery, a phase II randomized clinical trial (NCT02450552) including ~ 200 patients was launched [160, 161].

A similar approach recently emerged also for repolarization disorders; our group has demonstrated that lumacaftor, a drug approved for the treatment of a cystic fibrosis subtype, can rescue hERG trafficking defect and decrease the arrhythmogenic activity of iPSC-CMs derived from patients affected by a specific LQT2 mutation class [51]. This finding opens new possibilities for the management of LQT2 patients not fully protected by the current therapies. Also in this case, the feasibility of a clinical trial to assess the therapeutic efficacy of lumacaftor in LQTS patients will be greatly facilitated by the fact that the safety of this drug has already been proven [162, 163]. Indeed, very recently we very rapidly translated this drug repurposing strategy by treating the two LQT2 patients whose iPSC-CMs were previously tested *in vitro* and proved that, besides the expected discrepancies between the clinical and *in vitro* conditions, the data obtained in patient-specific iPSC-CMs may offer a reasonable degree of predictability in the clinical setting [164]. Time will tell us if this approach will decrease the overall duration and costs of research and development in pharmacology.

The concept of precision medicine can be also extended to the identification of new polymorphisms or variants able to shape the phenotype and the clinical severity of a disease. Several research groups have demonstrated that mutations or polymorphisms in specific genes, defined *modifier genes*, can profoundly impact the severity of cardiac arrhythmias [165–172]. Unfortunately, this kind of clinical studies require the enrollment of a high number of patients in order to reach a statistically relevant power, which might be challenging as these are often rare diseases. iPSC-CMs may then offer an easier way to investigate, in more controlled experimental conditions, the putative contribution of these genetic modifiers. A recent work from Chai and coworkers [171], by combining innovative approaches as whole exome sequencing and gene editing of iPSC-CMs derived from LQT2 patients with different clinical phenotype despite an identical disease-causing mutation, identified two novel gene variants able to exacerbate a preexisting repolarization deficiency. This study significantly improved the current knowledge on the limitations and applicability of the iPSC-CMs technology to cardiac disease modeling and also proved that genotype-phenotype discordance (i.e., minimal vs severe disease phenotype), unlike any other experimental model, can be reproduced *in vitro* with iPSC-CMs. Furthermore, the dramatic reduction in costs for whole genome sequence data has led to the identification of a plethora of rare variants of unknown significance (VUS) that have been linked to a certain degree of pathogenicity for multiple disorders. As recently demonstrated by Ma and coworkers in the case of cardiomyopathies [173], a VUS can be inserted into a healthy iPSC line to define its level of pathogenicity through a phenotypic characterization (Fig. 4.5). As the number of VUSs is rapidly increasing, we anticipate that this approach will be quickly extended to other diseases and will soon embrace repolarization disorders.

In conclusion, few years after the publication of the first study describing the discovery of iPSC-CMs, it is now clear that the road leading to an unlimited source of mature adult human CMs is and will be very demanding. Novel and prom-

ising technologies in biomaterials and organs-on-chip will certainly facilitate this path by generating better and more physiological environments for CMs, likely including the contribution of multiple cell types and the presence of metabolic byproducts or physiological stimuli. On the other side, more innovative platforms for data acquisition and phenotype characterization will be implemented due to technological leaps in bioengineering, computational power, and artificial intelligence that will lead, in the near future, to more integrative and predictive techniques to comprehensively model and study repolarization disorders at high-throughput level. The exciting times are not over.

Acknowledgments This work was facilitated by the Leducq Foundation for Cardiovascular Research grant 18CVD05 “Towards Precision Medicine with Human iPSCs for Cardiac Channelopathies”; by a grant of the Italian Ministry of Education, University and Research (MIUR) to the Department of Molecular Medicine of the University of Pavia under the initiative Dipartimenti di Eccellenza (2018–2022) to Massimiliano Gnecci; and by a Marie Skłodowska-Curie Individual Fellowship (H2020-MSCA-IF-2017 No. 795209) to Luca Sala.

References

1. Grant RP. Clinical electrocardiography. New York: McGraw-Hill; 1957.
2. Jervell A, Lange-Nielsen F. Congenital deaf-mutism, functional heart disease with prolongation of the Q-T interval, and sudden death. *Am Heart J.* 1957;54:59–68.
3. Schwartz PJ, Periti M, Malliani A. The long Q-T syndrome. *Am Heart J.* 1975;89:378–90.
4. Schwartz PJ, Wolf S. QT interval prolongation as predictor of sudden death in patients with myocardial infarction. *Circulation.* 1978;57:1074–7.
5. Campuzano O, Allegue C, Fernandez A, Iglesias A, Brugada R. Determining the pathogenicity of genetic variants associated with cardiac channelopathies. *Sci Rep.* 2015;5:7953.
6. Conforti L. Patch-clamp techniques. In: Cell physiology source book. Fourth Edition, Cambridge: Academic Press; 2012. p. 369–81. <https://doi.org/10.1016/B978-0-12-387738-3.00020-2>.
7. London B. Cardiac arrhythmias: from (transgenic) mice to men. *J Cardiovasc Electrophysiol.* 2001;12:1089–91.
8. Milan DJ, MacRae CA. Animal models for arrhythmias. *Cardiovasc Res.* 2005;67:426–37.

9. Kola I, Landis J. Can the pharmaceutical industry reduce attrition rates? *Nat Rev Drug Discov.* 2004;3:711–6.
10. Hay M, Thomas DW, Craighead JL, Economides C, Rosenthal J. Clinical development success rates for investigational drugs. *Nat Biotechnol.* 2014;32:40–51.
11. Hasenfuss G. Animal models of human cardiovascular disease, heart failure and hypertrophy. *Cardiovasc Res.* 1998;39:60–76.
12. Tsang HG, Rashdan NA, Whitelaw CBA, Corcoran BM, Summers KM, MacRae VE. Large animal models of cardiovascular disease. *Cell Biochem Funct.* 2016;34:113–32.
13. Maltsev VA, Wobus AM, Rohwedel J, Bader M, Hescheler J. Cardiomyocytes differentiated in vitro from embryonic stem cells developmentally express cardiac-specific genes and ionic currents. *Circ Res.* 1994;75:233–44.
14. Maltsev VA, Rohwedel J, Hescheler J, Wobus AM. Embryonic stem cells differentiate in vitro into cardiomyocytes representing sinusnodal, atrial and ventricular cell types. *Mech Dev.* 1993;44:41–50.
15. Wobus AM, Wallukat G, Hescheler J. Pluripotent mouse embryonic stem cells are able to differentiate into cardiomyocytes expressing chronotropic responses to adrenergic and cholinergic agents and Ca²⁺ channel blockers. *Differentiation.* 1991;48:173–82.
16. Itskovitz-Eldor J, Schuldiner M, Karsenti D, Eden A, Yanuka O, Amit M, et al. Differentiation of human embryonic stem cells into embryoid bodies compromising the three embryonic germ layers. *Mol Med.* 2000;6:88–95.
17. Mummery C, Ward-van Oostwaard D, Doevendans P, Spijker R, van den Brink S, Hassink R, et al. Differentiation of human embryonic stem cells to cardiomyocytes: role of coculture with visceral endoderm-like cells. *Circulation.* 2003;107:2733–40.
18. Takahashi K, Yamanaka S. Induction of pluripotent stem cells from mouse embryonic and adult fibroblast cultures by defined factors. *Cell.* 2006;126:663–76.
19. Takahashi K, Tanabe K, Ohnuki M, Narita M, Ichisaka T, Tomoda K, et al. Induction of pluripotent stem cells from adult human fibroblasts by defined factors. *Cell.* 2007;131:861–72.
20. Zhou T, Benda C, Dünzinger S, Huang Y, Ho JC, Yang J, et al. Generation of human induced pluripotent stem cells from urine samples. *Nat Protoc.* 2012;7:2080–9.
21. Loh Y-H, Agarwal S, Park I-H, Urbach A, Huo H, Heffner GC, et al. Generation of induced pluripotent stem cells from human blood. *Blood.* 2009;113:5476–9.
22. Chun YS, Byun K, Lee B. Induced pluripotent stem cells and personalized medicine: current progress and future perspectives. *Anat Cell Biol.* 2011;44:245–55.
23. Denning C, Borgdorff V, Crutchley J, Firth KSA, George V, Kalra S, et al. Cardiomyocytes from human pluripotent stem cells: from laboratory curiosity to industrial biomedical platform. *Biochim Biophys Acta.* 2016;1863:1728–48.
24. Eder A, Vollert I, Hansen A, Eschenhagen T. Human engineered heart tissue as a model system for drug testing. *Adv Drug Deliv Rev.* 2016;96:214–24.
25. Giacomelli E, Bellin M, Sala L, van Meer BJ, Tertoolen LGJ, Orlova VV, et al. Three-dimensional cardiac microtissues composed of cardiomyocytes and endothelial cells co-differentiated from human pluripotent stem cells. *Development.* 2017;144:1008–17.
26. Nunes SS, Miklas JW, Liu J, Aschar-Sobbi R, Xiao Y, Zhang B, et al. Biowire: a platform for maturation of human pluripotent stem cell-derived cardiomyocytes. *Nat Methods.* 2013;10:781–7.
27. Gneccchi M, Stefanello M, Mura M. Induced pluripotent stem cell technology: toward the future of cardiac arrhythmias. *Int J Cardiol.* 2017;237:49–52.
28. Sala L, Gneccchi M, Schwartz PJ. Long QT syndrome modelling with cardiomyocytes derived from human-induced pluripotent stem cells. *Arrhythm Electrophysiol Rev.* 2019;8:105–10.
29. Moretti A, Bellin M, Welling A, Jung CB, Lam JT, Bott-Flügel L, et al. Patient-specific induced pluripotent stem-cell models for long-QT syndrome. *N Engl J Med.* 2010;363:1397–409.
30. Schwartz PJ, Crotti L, Insolia R. Long-QT syndrome: from genetics to management. *Circ Arrhythm Electrophysiol.* 2012;5:868–77.
31. Schwartz PJ, Ackerman MJ. The long QT syndrome: a transatlantic clinical approach to diagnosis and therapy. *Eur Heart J.* 2013;34:3109–16.
32. Schwartz PJ, Ackerman MJ, George AL, Wilde AAM. Impact of genetics on the clinical management of channelopathies. *J Am Coll Cardiol.* 2013;62:169–80.
33. Roden DM. Drug-induced prolongation of the QT interval. *N Engl J Med.* 2004;350:1013–22.
34. Schwartz PJ, Woolsley RL. Predicting the unpredictable: drug-induced QT prolongation and torsades de pointes. *J Am Coll Cardiol.* 2016;67:1639–50.
35. Itoh H, Crotti L, Aiba T, Spazzolini C, Denjoy I, Fressart V, et al. The genetics underlying acquired long QT syndrome: impact for genetic screening. *Eur Heart J.* 2016;37:1456–64.
36. Wang Q, Shen J, Splawski I, Atkinson D, Li Z, Robinson JL, et al. SCN5A mutations associated with an inherited cardiac arrhythmia, long QT syndrome. *Cell.* 1995;80:805–11.
37. Curran ME, Splawski I, Timothy KW, Vincen GM, Green ED, Keating MT. A molecular basis for cardiac arrhythmia: HERG mutations cause long QT syndrome. *Cell.* 1995;80:795–803.
38. Wang Q, Curran ME, Splawski I, Burn TC, Millholland JM, VanRaay TJ, et al. Positional cloning of a novel potassium channel gene: KVLQT1 mutations cause cardiac arrhythmias. *Nat Genet.* 1996;12:17–23.

39. Priori SG, Wilde AA, Horie M, Cho Y, Behr ER, Berul C, et al. HRS/EHRA/APHR expert consensus statement on the diagnosis and management of patients with inherited primary arrhythmia syndromes. *J Arrhythm.* 2014;30:1–28.
40. Bos JM, Crotti L, Rohatgi RK, Castelletti S, Dagradi F, Schwartz PJ, Ackerman MJ. Mexiletine shortens the QT interval in patients with potassium channel-mediated type 2 long QT syndrome. *Circ Arrhythm Electrophysiol.* 2019;12:e007280.
41. Schwartz PJ, Priori SG, Spazzolini C, Moss AJ. Genotype-phenotype correlation in the long-QT syndrome gene-specific triggers for life-threatening arrhythmias. *Circulation.* 2001;103:89–95.
42. Zhang M, D’Aniello C, Verkerk AO, Wrobel E, Frank S, Ward-van Oostwaard D, et al. Recessive cardiac phenotypes in induced pluripotent stem cell models of Jervell and Lange-Nielsen syndrome: disease mechanisms and pharmacological rescue. *Proc Natl Acad Sci U S A.* 2014;111:E5383–92.
43. Wang Y, Liang P, Lan F, Wu H, Lisowski L, Gu M, et al. Genome editing of isogenic human induced pluripotent stem cells recapitulates long QT phenotype for drug testing. *J Am Coll Cardiol.* 2014;64:451–9.
44. Ma D, Wei H, Lu J, Huang D, Liu Z, Loh LJ, et al. Characterization of a novel KCNQ1 mutation for type 1 long QT syndrome and assessment of the therapeutic potential of a novel IKs activator using patient-specific induced pluripotent stem cell-derived cardiomyocytes. *Stem Cell Res Ther.* 2015;6:39.
45. Sala L, Yu Z, Ward-van Oostwaard D, van Veldhoven JP, Moretti A, Laugwitz K-L, et al. A new hERG allosteric modulator rescues genetic and drug-induced long-QT syndrome phenotypes in cardiomyocytes from isogenic pairs of patient induced pluripotent stem cells. *EMBO Mol Med.* 2016;8:1065–81.
46. Kuusela J, Kujala VJ, Kiviahio A, Ojala M, Swan H, Kontula K, et al. Effects of cardioactive drugs on human induced pluripotent stem cell derived long QT syndrome cardiomyocytes. *Springerplus.* 2016;5:276.
47. Wei H, Wu J, Liu Z. Studying KCNQ1 mutation and drug response in type 1 long QT syndrome using patient-specific induced pluripotent stem cell-derived cardiomyocytes. *Potassium Channels, New York, NY: Springer New York; 2017. p. 7–28.*
48. Liu Q, Trudeau MC. Eag domains regulate LQT mutant hERG channels in human induced pluripotent stem cell-derived cardiomyocytes. *PLoS One.* 2015;10:e0123951.
49. Fatima A, Ivanyuk D, Herms S, Heilmann-Heimbach S, O’Shea O, Chapman C, et al. Generation of human induced pluripotent stem cell line from a patient with a long QT syndrome type 2. *Stem Cell Res.* 2016;16:304–7.
50. Mura M, Mehta A, Ramachandra CJ, Zappatore R, Pisano F, Ciuffreda MC, et al. The KCNH2-IVS9-28A/G mutation causes aberrant isoform expression and hERG trafficking defect in cardiomyocytes derived from patients affected by long QT syndrome type 2. *Int J Cardiol.* 2017;240:367–71.
51. Mehta A, Ramachandra CJA, Singh P, Chitre A, Lua CH, Mura M, et al. Identification of a targeted and testable antiarrhythmic therapy for long-QT syndrome type 2 using a patient-specific cellular model. *Eur Heart J.* 2018;39:1446–55.
52. Bellin M, Casini S, Davis RP, D’Aniello C, Haas J, Ward-van Oostwaard D, et al. Isogenic human pluripotent stem cell pairs reveal the role of a KCNH2 mutation in long-QT syndrome. *EMBO J.* 2013;32:3161–75.
53. Matsa E, Rajamohan D, Dick E, Young L, Mellor I, Staniforth A, et al. Drug evaluation in cardiomyocytes derived from human induced pluripotent stem cells carrying a long QT syndrome type 2 mutation. *Eur Heart J.* 2011;32:952–62.
54. Lahti AL, Kujala VJ, Chapman H, Koivisto A-P, Pekkanen-Mattila M, Kerkelä E, et al. Model for long QT syndrome type 2 using human iPS cells demonstrates arrhythmogenic characteristics in cell culture. *Dis Model Mech.* 2012;5:220–30.
55. Okata S, Yuasa S, Yamane T, Furukawa T, Fukuda K. The generation of induced pluripotent stem cells from a patient with KCNH2 G603D, without LQT2 disease associated symptom. *J Med Dent Sci.* 2013;60:17–22.
56. Terrenoire C, Wang K, Chan Tung KW, Chung WK, Pass RH, Lu JT, et al. Induced pluripotent stem cells used to reveal drug actions in a long QT syndrome family with complex genetics. *J Gen Physiol.* 2012;141:61–72.
57. Mehta A, Sequiera GL, Ramachandra CJA, Sudibyo Y, Chung Y, Sheng J, et al. Re-trafficking of hERG reverses long QT syndrome 2 phenotype in human iPS-derived cardiomyocytes. *Cardiovasc Res.* 2014;102:497–506.
58. Matsa E, Dixon JE, Medway C, Georgiou O, Patel MJ, Morgan K, et al. Allele-specific RNA interference rescues the long-QT syndrome phenotype in human-induced pluripotency stem cell cardiomyocytes. *Eur Heart J.* 2013;35:1078–87.
59. Jouni M, Si-Tayeb K, Es-Salah-Lamoureux Z, Latypova X, Champon B, Caillaud A, et al. Toward personalized medicine: using cardiomyocytes differentiated from urine-derived pluripotent stem cells to recapitulate electrophysiological characteristics of type 2 long QT syndrome. *J Am Heart Assoc.* 2015;4:e002159.
60. Malan D, Friedrichs S, Fleischmann BK, Sasse P. Cardiomyocytes obtained from induced pluripotent stem cells with long-QT syndrome 3 recapitulate typical disease-specific features in vitro. *Circ Res.* 2011;109:841–7.
61. Fatima A, Kaifeng S, Dittmann S, Xu G, Gupta MK, Linke M, et al. The disease-specific phenotype in cardiomyocytes derived from induced pluripotent stem cells of two long QT syndrome type 3 patients. *PLoS One.* 2013;8:e83005.

62. Ma D, Wei H, Zhao Y, Lu J, Li G, Sahib NBE, et al. Modeling type 3 long QT syndrome with cardiomyocytes derived from patient-specific induced pluripotent stem cells. *Int J Cardiol.* 2013;168:5277–86.
63. Spencer CI, Baba S, Nakamura K, Hua EA, Sears MAF, Fu C, et al. Calcium transients closely reflect prolonged action potentials in iPSC models of inherited cardiac arrhythmia. *Stem Cell Reports.* 2014;3:269–81.
64. Okata S, Yuasa S, Suzuki T, Ito S, Makita N, Yoshida T, et al. Embryonic type Na⁺ channel β -subunit, SCN3B masks the disease phenotype of Brugada syndrome. *Sci Rep.* 2016;6:34198.
65. Malan D, Zhang M, Stallmeyer B, Müller J, Fleischmann BK, Schulze-Bahr E, et al. Human iPSC cell model of type 3 long QT syndrome recapitulates drug-based phenotype correction. *Basic Res Cardiol.* 2016;111:11–4.
66. Gélinas R, El Khoury N, Chaix M-A, Beauchamp C, Alikashani A, Ethier N, et al. Characterization of a human induced pluripotent stem cell-derived cardiomyocyte model for the study of variant pathogenicity: validation of a KCNJ2 mutation. *Circ Cardiovasc Genet.* 2017;10:e001755.
67. Yazawa M, Hsueh B, Jia X, Pasca AM, Bernstein JA, Hallmayer J, et al. Using induced pluripotent stem cells to investigate cardiac phenotypes in Timothy syndrome. *Nature.* 2011;471:230–4.
68. Pipilas DC, Johnson CN, Webster G, Schlaepfer J, Fellmann F, Sekarski N, et al. Novel calmodulin mutations associated with congenital long QT syndrome affect calcium current in human cardiomyocytes. *Heart Rhythm.* 2016;13:2012–9.
69. Rocchetti M, Sala L, Dreizehnter L, Crotti L, Sinnecker D, Mura M, et al. Elucidating arrhythmogenic mechanisms of long-QT syndrome CALM1-F142L mutation in patient-specific induced pluripotent stem cell-derived cardiomyocytes. *Cardiovasc Res.* 2017;113:531–41.
70. Limpitikul WB, Dick IE, Tester DJ, Boczek NJ, Limphong P, Yang W, et al. A precision medicine approach to the rescue of function on malignant calmodulinopathic long-QT syndrome. *Circ Res.* 2017;120:39–48.
71. Yamamoto Y, Makiyama T, Harita T, Sasaki K, Wuriyanghai Y, Hayano M, et al. Allele-specific ablation rescues electrophysiological abnormalities in a human iPSC cell model of long-QT syndrome with a CALM2 mutation. *Hum Mol Genet.* 2017;26:1670–7.
72. Crotti L, Johnson CN, Graf E, De Ferrari GM, Cuneo BF, Ovidia M, et al. Calmodulin mutations associated with recurrent cardiac arrest in infants. *Circulation.* 2013;127:1009–17.
73. Fischer R, Koller M, Flura M, Mathews S, Strehler-Page MA, Krebs J, et al. Multiple divergent mRNAs code for a single human calmodulin. *J Biol Chem.* 1988;263:17055–62.
74. Webster G, Schoppen ZJ, George AL. Treatment of calmodulinopathy with verapamil. *BMJ Case Rep.* 2017;2017:pii: bcr-2017-220568.
75. Antzelevitch C, Pollevick GD, Cordeiro JM, Casis O, Sanguinetti MC, Aizawa Y, et al. Loss-of-function mutations in the cardiac calcium channel underlie a new clinical entity characterized by ST-segment elevation, short QT intervals, and sudden cardiac death. *Circulation.* 2007;115:442–9.
76. El Battrawy I, Lan H, Cyganek L, Zhao Z, Li X, Buljubasic F, et al. Modeling short QT syndrome using human-induced pluripotent stem cell-derived cardiomyocytes. *J Am Heart Assoc.* 2018;7:e007394.
77. Shinnawi R, Shaheen N, Huber I, Shiti A, Arbel G, Gepstein A, Ballan N, et al. Modeling reentry in the short QT syndrome with human-induced pluripotent stem cell-derived cardiac cell sheets. *J Am Coll Cardiol.* 2019;73:2310–24.
78. Brugada P, Brugada J. Right bundle branch block, persistent ST segment elevation and sudden cardiac death: a distinct clinical and electrocardiographic syndrome: a multicenter report. *J Am Coll Cardiol.* 1992;20(6):1391–6.
79. Horie M, Ohno S. Genetic basis of Brugada syndrome. *J Arrhythm.* 2013;29:71–6.
80. Liang P, Sallam K, Wu H, Li Y, Itzhaki I, Garg P, et al. Patient-specific and genome-edited induced pluripotent stem cell-derived cardiomyocytes elucidate single cell phenotype of Brugada syndrome. *J Am Coll Cardiol.* 2017;68:2086–96.
81. Veerman CC, Mengarelli I, Guan K, Stauske M, Barc J, Tan HL, et al. HiPSC-derived cardiomyocytes from Brugada syndrome patients without identified mutations do not exhibit clear cellular electrophysiological abnormalities. *Sci Rep.* 2016;6:1391.
82. Miller DC, Harmer SC, Poliandri A, Nobles M, Edwards EC, Ware JS, et al. Ajmaline blocks I_{Na} and I_{Kr} without eliciting differences between Brugada syndrome patient and control human pluripotent stem cell-derived cardiac clusters. *Stem Cell Res.* 2017;25:233–44.
83. Kosmidis G, Veerman CC, Casini S, Verkerk AO, Van De Pas S, Bellin M, et al. Readthrough-promoting drugs gentamicin and PTC124 Fail to Rescue Na^v1.5 function of human-induced pluripotent stem cell-derived cardiomyocytes carrying nonsense mutations in the sodium channel gene SCN5A. *Circ Arrhythm Electrophysiol.* 2016;9:e004227.
84. Hayashi M, Denjoy I, Extramiana F, Maltret A, Buisson NR, Lupoglazoff JM, et al. Incidence and risk factors of arrhythmic events in catecholaminergic polymorphic ventricular tachycardia. *Circulation.* 2009;119:2426–34.
85. De Ferrari GM, Dusi V, Spazzolini C, Bos JM, Abrams DJ, Berul CI, et al. Clinical management of catecholaminergic polymorphic ventricular tachycardia the role of left cardiac sympathetic denervation. *Circulation.* 2015;131:2185–93.
86. Priori SG, Napolitano C, Memmi M, Colombi B, Drago F, Gasparini M, et al. Clinical and molecular

- characterization of patients with catecholaminergic polymorphic ventricular tachycardia. *Circulation*. 2002;106:69–74.
87. Marks AR, Priori S, Memmi M, Kontula K, Laitinen PJ. Involvement of the cardiac ryanodine receptor/calcium release channel in catecholaminergic polymorphic ventricular tachycardia. *J Cell Physiol*. 2002;190:1–6.
 88. Lahat H, Pras E, Eldar M. RYR2 and CASQ2 mutations in patients suffering from catecholaminergic polymorphic ventricular tachycardia. *Circulation*. 2003;107:e29.
 89. Fatima A, Xu G, Shao K, Papadopoulos S, Lehmann M, Arnáiz-Cot JJ, et al. In vitro modeling of ryanodine receptor 2 dysfunction using human induced pluripotent stem cells. *Cell Physiol Biochem*. 2011;28:579–92.
 90. Kujala K, Paavola J, Lahti A, Larsson K, Pekkanen-Mattila M, Viitasalo M, et al. Cell model of catecholaminergic polymorphic ventricular tachycardia reveals early and delayed afterdepolarizations. *PLoS One*. 2012;7:e44660.
 91. Itzhaki I, Maizels L, Huber I, Gepstein A, Arbel G, Caspi O, et al. Modeling of catecholaminergic polymorphic ventricular tachycardia with patient-specific human-induced pluripotent stem cells. *J Am Coll Cardiol*. 2012;60:990–1000.
 92. Zhang X-H, Haviland S, Wei H, Sarić T, Fatima A, Hescheler J, et al. Ca²⁺ signaling in human induced pluripotent stem cell-derived cardiomyocytes (iPSC-M) from normal and catecholaminergic polymorphic ventricular tachycardia (CPVT)-afflicted subjects. *Cell Calcium*. 2013;54:57–70.
 93. Jung CB, Moretti A, Mederos Y, Schnitzler M, Iop L, Storch U, Bellin M, et al. Dantrolene rescues arrhythmogenic RYR2 defect in a patient-specific stem cell model of catecholaminergic polymorphic ventricular tachycardia. *EMBO Mol Med*. 2012;4:180–91.
 94. Di Pasquale E, Lodola F, Miragoli M, Denegri M, Avelino-Cruz JE, Buonocore M, et al. CaMKII inhibition rectifies arrhythmic phenotype in a patient-specific model of catecholaminergic polymorphic ventricular tachycardia. *Cell Death Dis*. 2013;4:e843.
 95. Penttinen K, Swan H, Vanninen S, Paavola J, Lahtinen AM, Kontula K, et al. Antiarrhythmic effects of dantrolene in patients with catecholaminergic polymorphic ventricular tachycardia and replication of the responses using iPSC models. *PLoS One*. 2015;10:e0125366.
 96. Preininger MK, Jha R, Maxwell JT, Wu Q, Singh M, Wang B, et al. A human pluripotent stem cell model of catecholaminergic polymorphic ventricular tachycardia recapitulates patient-specific drug responses. *Dis Model Mech*. 2016;9:927–39.
 97. Sasaki K, Makiyama T, Yoshida Y, Wuriyanghai Y, Kamakura T, Nishiuchi S, et al. Patient-specific human induced pluripotent stem cell model assessed with electrical pacing validates S107 as a potential therapeutic agent for catecholaminergic polymorphic ventricular tachycardia. *PLoS One*. 2016;11:e0164795.
 98. Devalla HD, Gélinas R, Aburawi EH, Beqqali A, Goyette P, Freund C, et al. *TECRL*, a new life-threatening inherited arrhythmia gene associated with overlapping clinical features of both LQTS and CPVT. *EMBO Mol Med*. 2016;8:1390–408.
 99. Neher E, Sakmann B. The patch clamp technique. *Sci Am*. 1992;266:44–51.
 100. Sala L, Hegyi B, Bartolucci C, Altomare C, Rocchetti M, Váczi K, et al. Action potential contour contributes to species differences in repolarization response to β -adrenergic stimulation. *Europace*. 2018;20:1543–52.
 101. Altomare C, Bartolucci C, Sala L, Bernardi J, Mostacciolo G, Rocchetti M, et al. IKr impact on repolarization and its variability assessed by dynamic clamp. *Circ Arrhythm Electrophysiol*. 2015;8:1265–75.
 102. Sala L, Ward-van Oostwaard D, Tertoolen LGJ, Mummery CL, Bellin M. Electrophysiological analysis of human pluripotent stem cell-derived cardiomyocytes (hPSC-CMs) using multi-electrode arrays (MEAs). *J Vis Exp*. 2017(123):e55587.
 103. Nozaki Y, Honda Y, Watanabe H, Saiki S, Koyabu K, Itoh T, et al. CSAHi study-2: validation of multi-electrode array systems (MEA60/2100) for prediction of drug-induced proarrhythmia using human iPSC cell-derived cardiomyocytes: assessment of reference compounds and comparison with non-clinical studies and clinical information. *Regul Toxicol Pharmacol*. 2017;88:238–51.
 104. Kitaguchi T, Moriyama Y, Taniguchi T, Ojima A, Ando H, Uda T, et al. CSAHi study: evaluation of multi-electrode array in combination with human iPSC cell-derived cardiomyocytes to predict drug-induced QT prolongation and arrhythmia – effects of 7 reference compounds at 10 facilities. *J Pharmacol Toxicol Methods*. 2016;78:93–102.
 105. Obergrussberger A, Juhasz K, Thomas U, Stölzle-Feix S, Becker N, Dörr L, et al. Safety pharmacology studies using EFP and impedance. *J Pharmacol Toxicol Methods*. 2016;81:223–32.
 106. Lin ZC, McGuire AF, Burridge PW, Matsa E, Lou H-Y, Wu JC, et al. Accurate nanoelectrode recording of human pluripotent stem cell-derived cardiomyocytes for assaying drugs and modeling disease. *Microsyst Nanoeng*. 2017;3:16080.
 107. Khoshfetrat Pakazad S, Savov A, van de Stolpe A, Dekker R. A novel stretchable micro-electrode array (SMEA) design for directional stretching of cells. *J Micromech Microeng*. 2014;24:34003.
 108. Asakura K, Hayashi S, Ojima A, Taniguchi T, Miyamoto N, Nakamori C, et al. Improvement of acquisition and analysis methods in multi-electrode array experiments with iPSC cell-derived cardiomyocytes. *J Pharmacol Toxicol Methods*. 2015;75:17–26.
 109. Lapp H, Bruegmann T, Malan D, Friedrichs S, Kilgus C, Heidsieck A, et al. Frequency-dependent drug screening using optogenetic stimulation of

- human iPSC-derived cardiomyocytes. *Sci Rep*. 2017;7:9629.
110. Shinnawi R, Huber I, Maizels L, Shaheen N, Gepstein A, Arbel G, et al. Monitoring human-induced pluripotent stem cell-derived cardiomyocytes with genetically encoded calcium and voltage fluorescent reporters. *Stem Cell Reports*. 2015;5:582–96.
 111. Yang Y, Liu N, He Y, Liu Y, Ge L, Zou L, et al. Improved calcium sensor GCaMP-X overcomes the calcium channel perturbations induced by the calmodulin in GCaMP. *Nat Commun*. 2018;9:1504.
 112. St-Pierre F, Marshall JD, Yang Y, Gong Y, Schnitzer MJ, Lin MZ. High-fidelity optical reporting of neuronal electrical activity with an ultrafast fluorescent voltage sensor. *Nat Neurosci*. 2014;17:884–9.
 113. Song L, Awari DW, Han EY, Uche-Anya E, Park S-HE, Yabe YA, et al. Dual optical recordings for action potentials and calcium handling in induced pluripotent stem cell models of cardiac arrhythmias using genetically encoded fluorescent indicators. *Stem Cells Transl Med*. 2015;4:468–75.
 114. Hortigon-Vinagre MP, Zamora V, Burton FL, Green J, Gintant GA, Smith GL. The use of ratiometric fluorescence measurements of the voltage sensitive dye Di-4-ANEPPS to examine action potential characteristics and drug effects on human induced pluripotent stem cell-derived cardiomyocytes. *Toxicol Sci*. 2016;154:320–31.
 115. Shaheen N, Shiti A, Huber I, Shinnawi R, Arbel G, Gepstein A, et al. Human induced pluripotent stem cell-derived cardiac cell sheets expressing genetically encoded voltage indicator for pharmacological and arrhythmia studies. *Stem Cell Reports*. 2018;10:1879–94.
 116. Leyton-Mange JS, Mills RW, Macri VS, Jang MY, Butte FN, Ellinor PT, et al. Rapid cellular phenotyping of human pluripotent stem cell-derived cardiomyocytes using a genetically encoded fluorescent voltage sensor. *Stem Cell Reports*. 2014;2:163–70.
 117. Hortigon-Vinagre MP, Zamora V, de Korte T, Vlaming M, Braam S, Burton F, et al. Characterization of electrical and mechanical functions of Pluricyte® hiPSC-derived cardiomyocytes using the optical platform CelloPTIQ®. *J Pharmacol Toxicol Methods*. 2017;88:238–9.
 118. Zamora V, Hortigon-Vinagre MP, Burton F, Taylor A, Anson B, Craig MA, et al. Medium throughput electrophysiological and inotropic studies on iCell 2 hiPSC-derived cardiomyocytes using the CelloPTIQ® platform. *J Pharmacol Toxicol Methods*. 2017;88:243.
 119. Matsa E, Burrige PW, Yu K-H, Ahrens JH, Termglinchan V, Wu H, et al. Transcriptome profiling of patient-specific human iPSC-cardiomyocytes predicts individual drug safety and efficacy responses in vitro. *Cell Stem Cell*. 2016;19:311–25.
 120. Kijlstra JD, Hu D, Mittal N, Kausel E, van der Meer P, Garakani A, et al. Integrated analysis of contractile kinetics, force generation, and electrical activity in single human stem cell-derived cardiomyocytes. *Stem Cell Reports*. 2015;5:1226–38.
 121. Sala L, van Meer BJ, Tertoolen LGJ, Bakkers J, Bellin M, Davis RP, et al. MUSCLEMOTION: a versatile open software tool to quantify cardiomyocyte and cardiac muscle contraction in vitro and in vivo. *Circ Res*. 2018;122:e5–16.
 122. Wilders R. Dynamic clamp: a powerful tool in cardiac electrophysiology. *J Physiol*. 2006;576:349–59.
 123. Berecki G, Zegers JG, Bhuiyan ZA, Verkerk AO, Wilders R, van Ginneken ACG. Long-QT syndrome-related sodium channel mutations probed by the dynamic action potential clamp technique. *J Physiol*. 2006;570:237–50.
 124. Meijer van Putten RME, Mengarelli I, Guan K, Zegers JG, van Ginneken ACG, Verkerk AO, et al. Ion channelopathies in human induced pluripotent stem cell derived cardiomyocytes: a dynamic clamp study with virtual IK1. *Front Physiol*. 2015;6:7.
 125. Verkerk AO, Veerman CC, Zegers JG, Mengarelli I, Bezzina CR, Wilders R. Patch-clamp recording from human induced pluripotent stem cell-derived cardiomyocytes: improving action potential characteristics through dynamic clamp. *Int J Mol Sci*. 2017;18:1873.
 126. Goversen B, Becker N, Stoelzle-Feix S, Obergrussberger A, Vos MA, van Veen TAB, et al. A hybrid model for safety pharmacology on an automated patch clamp platform: using dynamic clamp to join iPSC-derived cardiomyocytes and simulations of Ik1 ion channels in real-time. *Front Physiol*. 2017;8:1094.
 127. Bruegmann T, Malan D, Hesse M, Beiert T. Optogenetic control of heart muscle in vitro and in vivo. *Nat Methods*. 2010;7:897–900.
 128. Nussinovitch U, Shinnawi R, Gepstein L. Modulation of cardiac tissue electrophysiological properties with light-sensitive proteins. *Cardiovasc Res*. 2014;102:176–87.
 129. Izumi-Nakaseko H, Kanda Y, Nakamura Y, Hagiwara-Nagasawa M, Wada T, Ando K, et al. Development of correction formula for field potential duration of human induced pluripotent stem cell-derived cardiomyocytes sheets. *J Pharmacol Sci*. 2017;135:44–50.
 130. Lei CL, Wang K, Clerx M, Johnstone RH, Hortigon-Vinagre MP, Zamora V, et al. Tailoring mathematical models to stem-cell derived cardiomyocyte lines can improve predictions of drug-induced changes to their electrophysiology. *Front Physiol*. 2017;8:986.
 131. Rodriguez B, Carusi A, Abi-Gerges N, Ariga R, Britton O, Bub G, et al. Human-based approaches to pharmacology and cardiology: an interdisciplinary and intersectorial workshop. *Europace*. 2016;18:1287–98.
 132. Paci M, Sartiani L, Del Lungo M, Jaconi M, Mugelli A, Cerbai E, et al. Mathematical modeling of the action potential of human embryonic stem cell derived cardiomyocytes. *Biomed Eng Online*. 2012;11:61.

133. Paci M, Hyttinen J, Aalto-Setälä K, Severi S. Computational models of ventricular- and atrial-like human induced pluripotent stem cell derived cardiomyocytes. *Ann Biomed Eng.* 2013;41:2334–48.
134. Paci M, Hyttinen J, Rodriguez B, Severi S. Human induced pluripotent stem cell-derived versus adult cardiomyocytes: an in silico electrophysiological study on effects of ionic current block. *Br J Pharmacol.* 2015;172:5147–60.
135. Passini E, Severi S, Hyttinen J, Rodriguez B. Phenotypic variability in LQT3 human induced pluripotent stem cell-derived cardiomyocytes and their response to antiarrhythmic pharmacologic therapy: an in silico approach. *Heart Rhythm.* 2017;14:1704–12.
136. Passini E, Britton OJ, Lu HR, Rohrbacher J, Hermans AN, Gallacher DJ, et al. Human in silico drug trials demonstrate higher accuracy than animal models in predicting clinical pro-arrhythmic cardiotoxicity. *Front Physiol.* 2017;8:15–88.
137. Trayanova NA. Whole-heart modeling: applications to cardiac electrophysiology and electromechanics. *Circ Res.* 2011;108:113–28.
138. Fan K, Zhang S, Zhang Y, Lu J, Holcombe M, Zhang X. A machine learning assisted, label-free, non-invasive approach for somatic reprogramming in induced pluripotent stem cell colony formation detection and prediction. *Sci Rep.* 2017;7:13496.
139. Lee EK, Tran DD, Keung W, Chan P, Wong G, Chan CW, et al. Machine learning of human pluripotent stem cell-derived engineered cardiac tissue contractility for automated drug classification. *Stem Cell Reports.* 2017;9:1560–72.
140. Juhola M, Joutsijoki H, Penttinen K, Aalto-Setälä K. Detection of genetic cardiac diseases by Ca²⁺ transient profiles using machine learning methods. *Sci Rep.* 2018;8:861.
141. Fermi B, Hancox JC, Abi-Gerges N, Bridgland-Taylor M, Chaudhary KW, Colatsky T, et al. A new perspective in the field of cardiac safety testing through the comprehensive in vitro proarrhythmia assay paradigm. *J Biomol Screen.* 2016;21:1–11.
142. Liang G, Zhang Y. Genetic and epigenetic variations in iPSCs: potential causes and implications for application. *Cell Stem Cell.* 2013;13:149–59.
143. Sala L, Bellin M, Mummery CL. Integrating cardiomyocytes from human pluripotent stem cells in safety pharmacology: has the time come? *Br J Pharmacol.* 2017;174:3749–65.
144. Sander JD, Joung JK. CRISPR-Cas systems for editing, regulating and targeting genomes. *Nat Biotechnol.* 2014;32:347–55.
145. Wang WE, Li L, Xia X, Fu W, Liao Q, Lan C, et al. Dedifferentiation, proliferation, and redifferentiation of adult mammalian cardiomyocytes after ischemic injury. *Circulation.* 2017;136:834–48.
146. Veerman CC, Kosmidis G, Mummery CL, Casini S, Verkerk AO, Bellin M. Immaturity of human stem-cell-derived cardiomyocytes in culture: fatal flaw or soluble problem? *Stem Cells Dev.* 2015;24:1035–52.
147. Paavilainen T, Pelkonen A, Mäkinen ME-L, Peltola M, Huhtala H, Fayuk D, et al. Effect of prolonged differentiation on functional maturation of human pluripotent stem cell-derived neuronal cultures. *Stem Cell Res.* 2018;27:151–61.
148. Ruan J-L, Tulloch NL, Razumova MV, Saiget M, Muskheli V, Pabon L, et al. Mechanical stress conditioning and electrical stimulation promote contractility and force maturation of induced pluripotent stem cell-derived human cardiac tissue. *Circulation.* 2016;134:1557–67.
149. Minami I, Yamada K, Otsuji TG, Yamamoto T, Shen Y, Otsuka S, et al. A small molecule that promotes cardiac differentiation of human pluripotent stem cells under defined, cytokine- and xeno-free conditions. *Cell Rep.* 2012;2:1448–60.
150. Yang X, Pabon L, Murry CE. Engineering adolescence: maturation of human pluripotent stem cell-derived cardiomyocytes. *Circ Res.* 2014;114:511–23.
151. Sun X, Nunes SS. Bioengineering approaches to mature human pluripotent stem cell-derived cardiomyocytes. *Front Cell Dev Biol.* 2017;5:19.
152. Patel AK, Celiz AD, Rajamohan D, Anderson DG, Langer R, Davies MC, et al. A defined synthetic substrate for serum-free culture of human stem cell derived cardiomyocytes with improved functional maturity identified using combinatorial materials microarrays. *Biomaterials.* 2015;61:257–65.
153. Hirt MN, Boeddinghaus J, Mitchell A, Schaaf S, Börnchen C, Müller C, et al. Functional improvement and maturation of rat and human engineered heart tissue by chronic electrical stimulation. *J Mol Cell Cardiol.* 2014;74:151–61.
154. Mannhardt I, Breckwoldt K, Letuffe-Brenière D, Schaaf S, Schulz H, Neuber C, et al. Human engineered heart tissue: analysis of contractile force. *Stem Cell Reports.* 2016;7:29–42.
155. Cahan P, Daley GQ. Origins and implications of pluripotent stem cell variability and heterogeneity. *Nat Rev Mol Cell Biol.* 2013;14:357–68.
156. Betts DH, Tobias IC. Canine pluripotent stem cells: are they ready for clinical applications? *Front Vet Sci.* 2015;2:298.
157. Chen IY, Matsa E, Wu JC. Induced pluripotent stem cells: at the heart of cardiovascular precision medicine. *Nat Rev Cardiol.* 2016;13:333–49.
158. Burridge PW, Li YF, Matsa E, Wu H, Ong S-G, Sharma A, et al. Human induced pluripotent stem cell-derived cardiomyocytes recapitulate the predilection of breast cancer patients to doxorubicin-induced cardiotoxicity. *Nat Med.* 2016;22:547–56.
159. Sleigh SH, Barton CL. Repurposing strategies for therapeutics. *Pharmaceut Med.* 2012;24:151–9.
160. Wainger BJ, Kiskinis E, Mellin C, Wiskow O, Han SSW, Sandoe J, et al. Intrinsic membrane hyperexcitability of amyotrophic lateral sclerosis patient-derived motor neurons. *Cell Rep.* 2014;7:1–11.
161. McNeish J, Gardner JP, Wainger BJ, Woolf CJ, Eggan K. From dish to bedside: lessons learned while translating findings from a stem cell model of disease to a clinical trial. *Cell Stem Cell.* 2015;17:8–10.

162. Milla CE, Ratjen F, Marigowda G, Liu F, Waltz D, Rosenfeld M, et al. Lumacaftor/ivacaftor in patients aged 6-11 years with cystic fibrosis and homozygous for F508del-CFTR. *Am J Respir Crit Care Med.* 2017;195:912–20.
163. Boyle MP, Bell SC, Konstan MW, McColley SA, Rowe SM, Rietschel E, et al. A CFTR corrector (lumacaftor) and a CFTR potentiator (ivacaftor) for treatment of patients with cystic fibrosis who have a phe508del CFTR mutation: a phase 2 randomised controlled trial. *Lancet Respir Med.* 2014;2: 527–38.
164. Schwartz PJ, Gneocchi M, Dagradi F, Castelletti S, Parati G, Spazzolini C, et al. From patient-specific induced pluripotent stem cells to clinical translation in long QT syndrome type 2. *Eur Heart J.* 2019;40:1832–6.
165. Crotti L, Monti MC, Insolia R, Peljto A, Goosen A, Brink PA, et al. NOS1AP is a genetic modifier of the long-QT syndrome. *Circulation.* 2009;120: 1657–63.
166. Duchatelet S, Crotti L, Peat RA, Denjoy I, Itoh H, Berthet M, et al. Identification of a KCNQ1 polymorphism acting as a protective modifier against arrhythmic risk in long-QT syndrome. *Circ Cardiovasc Genet.* 2013;6:354–61.
167. Earle N, Yeo Han D, Pilbrow A, Crawford J, Smith W, Shelling AN, et al. Single nucleotide polymorphisms in arrhythmia genes modify the risk of cardiac events and sudden death in long QT syndrome. *Heart Rhythm.* 2014;11:76–82.
168. Kolder ICRM, Tanck MWT, Postema PG, Barc J, Sinner MF, Zumhagen S, et al. Analysis for genetic modifiers of disease severity in patients with long-QT syndrome type 2. *Circ Cardiovasc Genet.* 2015;8:447–56.
169. Pollak MR. Modifiers of cardiac phenotypes. *Circ Cardiovasc Genet.* 2015;8:425–6.
170. Ter Bekke RMA, Isaacs A, Barysenka A, Hoos MB, Jongbloed JDH, Hoomtje JCA, et al. Heritability in a SCN5A-mutation founder population with increased female susceptibility to non-nocturnal ventricular tachyarrhythmia and sudden cardiac death. *Heart Rhythm.* 2017;14(12):1873–81.
171. Chai S, Wan X, Ramirez-Navarro A, Tesar PJ, Kaufman ES, Ficker E, et al. Physiological genomics identifies genetic modifiers of long QT syndrome type 2 severity. *J Clin Invest.* 2018;128:1043–56.
172. Schwartz PJ, Crotti L, George AL. Modifier genes for sudden cardiac death. *Eur Heart J.* 2018;39:3925–31.
173. Ma N, Zhang J, Itzhaki I, Zhang SL, Chen H, Haddad F, et al. Determining the pathogenicity of a genomic variant of uncertain significance using CRISPR/Cas9 and human-induced pluripotent stem cells. *Circulation.* 2018;138:2666–81.



Role of Late Sodium Current During Repolarization and Its Pathophysiology

Mohamed Chahine

Introduction

The heart is a rhythmic electromechanical pump that requires optimal action potential (AP) generation and propagation through the myocardium to work properly. The electrical functioning of individual cardiomyocytes is distinct and coordinated, reflecting differences in the expression levels, biophysical properties, and distribution of various types of voltage-gated ion channels in the myocardium. These ion channels underlie the different phases of APs. Changes in their densities or in their function can lead to AP prolongation, dispersion of ventricular repolarization, and early afterdepolarizations (EADs), which are substrates for polymorphic ventricular tachycardia.

Voltage-gated sodium channels are a critical determinant of cardiac excitability and play a central role in the initiation and propagation of cardiac APs. They are also involved in determining the duration of APs. In functional terms, these channels are minimally characterized by three processes: closing, activation, and inactivation. There is much evidence for the existence of additional channel conformations, modal gating, for

instance, which may underlie the persistent activity of these channels. Slow cycling of the channels between the different modes over a period of many seconds is a characteristic of modal gating and is seen in many different voltage-gated channel families, including those in cardiac myocytes [1–4]. These findings were confirmed using single channel recordings of skeletal muscle and cardiac sodium channels [4, 5]. Modal gating is thought to underlie the persistent or late sodium current, which is an intrinsic property of sodium channels and, when exacerbated, causes an increase in intracellular sodium and may result in calcium overload, a precipitator of myocyte abnormal electrical activity [1–4].

These mechanisms are involved in several inherited (e.g., type 3 long QT syndrome) and acquired (e.g., associated with heart failure) cardiac arrhythmic disorders. The dysfunction of sodium channels in these disorders has profound physiological consequences, including the development of life-threatening cardiac arrhythmias and even sudden death.

In this chapter, we review basic cardiac electrophysiology, with a focus on the role of voltage-gated sodium channels, their biophysical properties, and their pathophysiology, in particular the role that the late sodium current plays in cardiac repolarization. An increase in the late sodium current is a major cause of AP duration (APD) prolongation and EADs. We also review the pharmacology of persistent currents as a potential target for treating cardiac arrhythmogenesis in failing

M. Chahine (✉)
CERVO Research Center, Institut Universitaire en
Santé Mentale de Québec, Québec City, QC, Canada

Department of Medicine, Université Laval,
Québec City, QC, Canada
e-mail: mohamed.chahine@phc.ulaval.ca

hearts. In this regard, ranolazine, which is an anti-anginal drug that specifically targets persistent sodium currents, shortens APDs and eliminates EADs. We review several clinical trials that established the beneficial role this drug plays in managing several related ischemic heart diseases.

Cardiac Action Potential

Following threshold depolarization, sodium channel opening causes a large and rapid influx of sodium ions (I_{Na}) that depolarizes the myocardial membrane (phase 0) (Fig. 5.1). This is followed by a rapid repolarization due to the efflux of potassium ions through outward potassium channels (e.g., I_{to}). In *phase 1*, sodium channels remain inactivated, and I_{to} is transiently activated. Membrane depolarization also activates voltage-gated calcium inward currents (L-type, I_{Ca-L} and T-type, I_{Ca-T}). I_{Ca-T} plays an important role in automaticity, while I_{Ca-L} is essential for the contraction of myocardial cells by triggering the excitation-contraction coupling mechanism during phase 2. In *phase 2*, also known as the plateau phase, there is a delicate balance between inward (I_{Ca-L}) and outward (I_{Kr} and I_{Ks}) currents. In this phase, three

sodium ions move into the cell for each calcium ion that moves out. This occurs via the sodium-calcium exchanger. In *phase 3*, sustained repolarization occurs via delayed rectifier currents (I_{Ks} and I_{Kr}). Calcium channels become inactivated during this phase. Lastly, in *phase 4*, the I_{K1} inward potassium current ends the repolarization phase, and the net potassium efflux restores the resting intracellular gradient to $-80/90$ mV. The sodium channel makes a major contribution to two phases of the AP, that is, the period of rapid depolarization (phase 0) and the AP plateau (phase 2) and thus to the repolarization of APs. The height of APs increases with each increment in the extracellular concentration of sodium ions. A dysfunction of depolarization during phase 2 can trigger arrhythmia, which is maintained by a reentry mechanism, leading to a regenerative circuit of electrical activity around relatively unexcitable tissue (Fig. 5.1) [6].

Voltage-Gated Sodium Channels (Structure)

Given that the focus of this chapter is sodium channels, we will briefly review their structure and function.

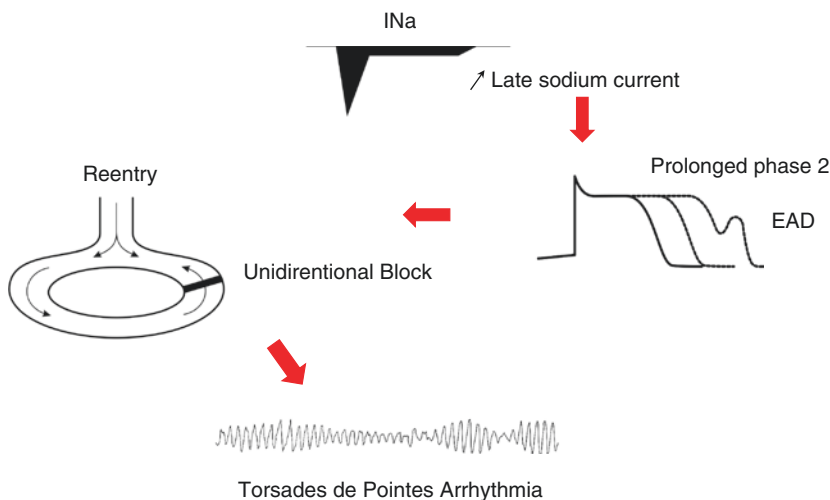


Fig. 5.1 A sodium current activity during action potential. Incomplete inactivation gate (top panel) resulting in late sodium current activity during action potential duration. A cardiac action potential comprising phase 0

through phase 4 (top). Late sodium current may delay cardiac repolarization and QT-interval prolongation, triggering ventricular tachycardia or ventricular fibrillation (torsades de pointes) through phase 2 reentry mechanism

The *SCN5A* gene encodes the pore-forming α -subunit of the human cardiac voltage-dependent sodium channel now known as $\text{Na}_v1.5$, which activates the production of a depolarizing inward current I_{Na} , with prompt inactivation within milliseconds [7, 8]. The gene locus, which has been mapped to chromosome 3p21, consists of 28 exons and spans 80 kbp. It encodes a 2016-amino-acid protein and has a putative structure comprised of four homologous domains (DI–DIV), each containing six transmembrane-spanning segments (S1–S6) [7]. Transmembrane segments S1–S4 form the voltage sensor domain (VSD), and S5–S6 constitute the pore permeation pathway or pore domain. $\text{Na}_v1.5$ VSD is characterized by its S4 segment, which contains highly conserved positively charged residues (arginine or lysine) and several highly conserved acidic residues on the S2 and S3 segments.

Voltage-Gated Sodium Channels (Function)

Voltage-gated sodium channels pass through many conformational states during the time course of their activity (open and activated states, fast and slow inactivated states, recovery from inactivation, etc.). Other conformations have been reported also. In sodium channels, transitions between fast and slow conformations have been referred to as modal gating. Excessive residency times in slow conformations lead to channel malfunction and, as a consequence, type 3 long QT syndrome (LQTS3), heart failure (HF), and cardiac arrhythmias.

At almost the same time as activation, depolarization initiates fast or N-type inactivation. Sodium influx gradually comes to a halt during this process. With inactivation disabled, sodium currents exhibit a plateau of a persistent inward current during sustained depolarization. A fast inactivation process prevents channels from reopening until they have had enough time to recover. The fast inactivation of voltage-gated sodium channels is also linked to the outward movement of an S4 segment and a ball-and-chain or hinged lid mechanism. The III–IV linker acts

as a lid, in which the inactivation particle (IFM) occludes the inner pore by binding to the docking site like a latch. The docking site consists of several regions, including the cytoplasmic linkers connecting S4–S5 in DIII and DIV and the cytoplasmic end of S6 in DIV.

Sodium channels also enter a slow inactivated state with prolonged depolarization, which is also called C-type inactivation. Previous studies have shown that the structural basis for slow inactivation involves the P-segment and the III–IV linker [9–11]. The duration of this more stable and non-conducting state ranges from hundreds of milliseconds up to several seconds. A dysfunction of this process contributes to pathophysiologic events associated with reduced cellular excitability, prolonged membrane depolarization, and cardiac arrhythmias.

The overlap of steady-state activation and inactivation of sodium channels defines a range of voltages (i.e., window) where the likelihood of sodium channels being open is significant, which could result in an inward sodium current that could potentially depolarize the resting membrane potential and increase myocyte excitability [12]. This is a time-independent current that can contribute to increasing excitability.

Several studies have shown that late sodium currents play an important role during the time course of APs. Low concentrations of TTX, a specific sodium channel blocker, reduce the duration of APs without affecting the V_{max} [2, 13, 14], highlighting the role of the persistent activity of sodium channels during AP repolarization.

Molecular Mechanisms and Pathophysiology of the Late Sodium Current

When the transmembrane potential reaches a certain voltage, the activation and inactivation states of the sodium channel overlap. Following the rapid depolarization of a myocyte, the sodium current does not recover as a small portion of sodium channels is inactivated slowly during the plateau phase. Although, under normal conditions, this current is very small

(0.5–1%) compared to the transient sodium current, it can contribute to delaying AP repolarization. Reactive oxygen species (ROS) are generated in ischemic hearts and contribute to left ventricular remodeling, cardiac myocyte disarray, and abnormal cardiac electrical activity. It has been shown that ROS can activate the Ca/calmodulin-dependent protein kinase II δ via oxidation and that this may enhance late I_{Na}, causing a cellular sodium and calcium overload [15]. In this regard, H₂O₂ (50–200 μ M), which is one of the ROS products, has been shown to induce a large late sodium current and yield a marked prolongation of the AP [16]. Furthermore, sodium entry during the few-hundred-millisecond duration of the plateau phase may cause an elevation of intracellular sodium, a condition that predisposes to calcium overload and cardiac arrhythmogenesis.

This flimsy persistent current opposes repolarizing potassium currents, delaying repolarization. Excessive residency time in abnormal conformations leads to channel malfunction and, as a consequence, severe pathologies known as channelopathies, in particular LQTS3 or HF. In certain cardiovascular pathologies, including HF, and in some genetic dysfunctions such as LQTS, this increase in the persistent sodium current may lead to the failure of repolarization. When certain repolarizing ionic currents compensate for the increase in depolarizing currents, there is a slight decrease in the repolarization reserve that, however, does not delay repolarization. However, if the magnitude of the late sodium current is substantial, a significant prolongation of repolarization can occur and can trigger abnormal impulses such as EADs.

Although the main properties of cardiac sodium channels can be expressed by the α -subunit, they are also associated with multi-protein complexes composed of auxiliary subunits such as SCN_B4, cytoskeletal proteins, and caveolin-3 (CAV3). In particular, dysfunctional interacting proteins can exacerbate the magnitude of the persistent current. In this regard, mutations in SCN_B4 and CAV3 have been reported to exacerbate the persistent sodium current [17–19].

Several mechanisms have recently been proposed to explain the pathophysiological role of sodium channels.

Channelopathies Associated with Sodium Channels

Normal cardiac cellular excitation and relaxation depend on normal depolarization and repolarization processes. Defective genes and structural abnormalities can influence these two processes, leading to a variety of clinical manifestations ranging from asymptomatic to symptomatic. Many inheritable cardiac diseases involve a dysfunction of, for example, potassium, sodium, and calcium channels, leading to LQTS, BrS, progressive cardiac conduction disorders (PCCD), and overlap syndrome. LQTS is an inherited cardiac disease that can cause syncope and even sudden cardiac death associated with polymorphic ventricular tachycardia (torsades de pointes). Patients with LQTS present with an increase in the QT_c value over 0.460 s for men and 0.470 for women s on a 12-lead ECG.

LQTS3 is caused by mutations in *SCN5A* genes mapped to chromosome 3q21–24, which encodes the α -subunits of the cardiac sodium channel [20]. *SCN5A* mutations have been identified in approximately 10% of genotyped LQTS patients. In many cases, the development of arrhythmias is often associated with bradycardia during sleep or relaxation when the QT_c value increases.

LQTS3 is considered an inherited disorder due to abnormal myocardial repolarization. As mentioned above, cardiac repolarization is a delicately balanced process between inward currents (I_{Na} and I_{Ca-L}) and outward potassium currents (I_{Kr} and I_{Ks}) during phase 2 of the APs. Shifts in the balance of these inward and outward currents can either increase or decrease the duration of APs, resulting in QT interval prolongation or shortening, respectively. The most common cause of QT interval prolongation in LQTS3 is a late sodium current leading to AP prolongation in phase 2. During

the kinetic gating process, fast inactivation is disrupted, which causes incomplete closure of the inactivation gate during sustained depolarization. This induces a small but persistent sodium current during the plateau that delays myocyte repolarization, leading to QT interval prolongation on ECGs at slow heart rates. This kinetic gating phenomenon is thus called a gain-of-sodium function [21, 22]. This sustained inward current is extremely small, accounting for 1–2% of the peak inward sodium current. However, the relationship between this sustained current and AP prolongation has been confirmed in computational modeling by a highly nonlinear relationship between sodium channel function and cardiac excitability [21]. Although most mutations cause LQTS3 by a persistent inward current, there are other mechanisms associated with QT interval prolongation. These include faster recovery from inactivation due to the destabilization of the inactivation state, with shifts in the voltage dependence of activation and inactivation [21, 23, 24]. These kinetic gating abnormalities may lead to a loss of the delicate balance between the inward and outward currents that is required to maintain the plateau of the AP, provoking QT interval prolongation.

Late Sodium Current and Heart Failure

HF is a major public health problem in industrialized countries, in particular because of its frequency and its consequences in terms of morbidity and mortality [25, 26]. Cardiomyocytes isolated from failing human hearts and animal models of HF both display a prolonged AP duration [27, 28]. In elegant work using a cell-attached macropatch technique in post-MI rat cardiomyocytes, Huang et al. showed that sodium current bursting activity increases during sustained depolarization, resulting in a large slow component of the sodium current decay [29]. The authors also reported an increase in nervous system sodium channel subtypes in post-MI myocytes, with a reversion of the fetal to the adult variant of the

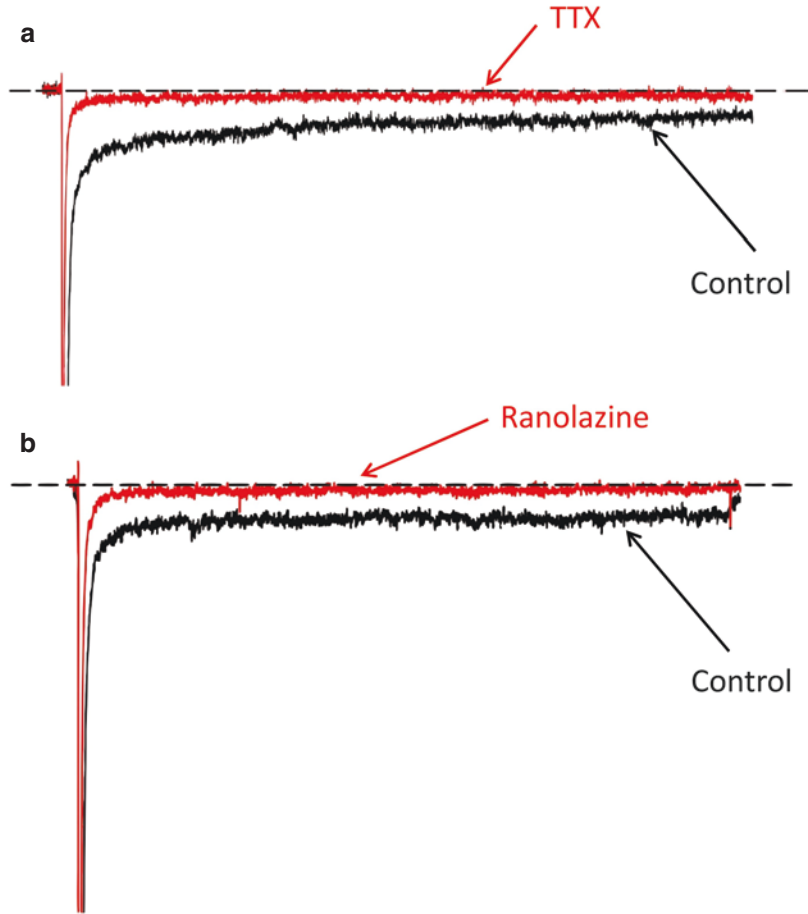
sodium channel. One of the mechanisms proposed to explain the slow kinetics of the sodium channel is the increase in a late sodium current flowing through dysfunctional sodium channels. This would have two main consequences: (1) a delay in repolarization, leading to EADs and the initiation of torsades de pointes arrhythmia, and (2) an increase in intracellular sodium, favoring a calcium overload, oscillatory calcium release, and the initiation of late (delayed) afterdepolarizations generated by the sodium-calcium exchange mechanism. We and others confirmed the involvement of these two mechanisms using computer model simulations [30, 31].

Pharmacology of the Late Sodium Current

Class 1 Antiarrhythmic Drugs

Because of the central role sodium channels play in initiating and propagating cardiac APs, these channels have proved to be effective targets for antiarrhythmic (AA) drug therapy. Inhibiting these channels using AAs reduces the rate of myocardial depolarization and intracardiac conduction velocity, properties that have proved beneficial in the treatment of cardiac arrhythmias. Several studies [32, 33] have shown that class IAAs are effective inhibitors of late sodium currents associated with LQTS3 mutations and have proved beneficial in the treatment of patients carrying these mutations (Fig. 5.2). We have investigated and compared the effects of ranolazine and class IAAs on the Y1767C mutation, which is associated with QT prolongation and sudden death in a family. We found differential effects of the Y1767C mutation on ranolazine, quinidine, mexiletine, and flecainide, with ranolazine exhibiting a more potent effect [34]. Our data suggest that ranolazine primarily inhibits $\text{Na}_v1.5$ channels via an open-channel blocking mechanism. This contrasts with conventional class IAAs, which inhibit sodium channels by preferentially binding with high affinity to inactivated states of the channel [35].

Fig. 5.2 Effects of tetrodotoxin (TTX, 10 μM) and ranolazine (50 μM) on the cardiac late sodium currents. Sodium currents were elicited at -10 mV from -140 mV holding potential. **(a)** Effects on late sodium current of channels treated with 10 μM TTX a sodium channel blocker. **(b)** Effects on late sodium current of channels treated with ranolazine. In both cases, both TTX and ranolazine were efficient in inhibiting the late sodium current



Ranolazine

Ranolazine is an antianginal agent that shares a similar structure with class I AAs [36] and is an effective inhibitor of late sodium currents of both LQTS3 mutant and native cardiac sodium channels [37, 38]. Increases in late I_{Na} due to the progression of ischemia contribute to the elevation of intracellular sodium concentrations in cardiomyocytes, which in turn activates the cell membrane sodium-calcium exchanger in an attempt to correct the sodium overload at the expense of a calcium overload [39, 40]. Prolonged activation of the sodium-calcium exchanger leads to an intracellular $[\text{Ca}^{2+}]_i$ overload and induces further ischemia [40]. It has been suggested that ranolazine inhibits and reverses the deleterious effects of late I_{Na} . Sea anemone toxin ATX-II (ATX-II) was used as an enhancer of late I_{Na} in a prelini-

cal study [41] because it mimics the effect of ischemia by increasing intracellular $[\text{Na}^+]_i$ [41] and intracellular $[\text{Ca}^{2+}]_i$ [42]. This study showed that ranolazine is able to attenuate the ATX-II-induced increase in late I_{Na} [41] and $[\text{Na}^+]_i$ -dependent calcium overload [42]. Ranolazine has also been reported to reversibly shorten the AP duration of ventricular myocytes isolated from canine failing hearts and to be more potent than lidocaine and amiodarone [37].

Although research in animal models has demonstrated that ranolazine could potentially be used to treat arrhythmias and HF, it is important that the beneficial effect of ranolazine be confirmed in clinical trials. Several clinical trials have assessed ranolazine use in patients with coronary artery diseases. In the Monotherapy Assessment of Ranolazine in Stable Angina (MARISA) trial [43], the authors showed that

ranolazine significantly improves exercise performance and delays or prevents the symptoms and ECG evidence of myocardial ischemia during exercise. In the Combination Assessment of Ranolazine in Stable Angina (CARISA) randomized trial [44], the authors showed that ranolazine increases exercise capacity and provides additional antianginal relief to symptomatic patients with severe chronic angina taking standard doses of atenolol, amlodipine, or diltiazem, without evident adverse long-term survival consequences over 1–2 years. In the Observational Study in Patients with Chronic Angina Under Ranolazine Treatment in Greece (OSCAR-GR) study [45], the authors investigated the relationship between ranolazine therapy and patient satisfaction, quality of life, physicians' assessment of therapy, and safety in patients with chronic stable angina (CSA) treated in a routine clinical setting. They concluded that ranolazine was associated with decreased angina frequency and severity and improved the quality of life. In the TERISA randomized clinical trial (Type 2 Diabetes Evaluation of Ranolazine in Subjects With Chronic Stable Angina) [46], the authors reported that ranolazine significantly reduces angina frequency among patients with type 2 diabetes, coronary artery disease, and persistent chronic angina despite a treatment with 1–2 antianginals. In the ERICA (Efficacy of Ranolazine in Chronic Angina) trial [47], the investigators reported that ranolazine significantly reduces the frequency of angina and nitroglycerin consumption when combined with amlodipine.

By inhibiting late I_{Na} using ranolazine, sodium accumulation can be reduced. Hence, ranolazine would be expected to prevent calcium accumulation that may originate from the sodium/calcium exchanger mechanism and thus improve diastolic pressure and relaxation. Using an HF dog model, the authors showed that ranolazine preserves left ventricular (LV) function and attenuates LV remodeling [48]. The authors also reported that ranolazine, when combined with an ACE inhibitor or a β -blocker, improves LV systolic and diastolic function and that the reversal of LV remodeling is superior than ranolazine alone. In a recent proof-of-concept trial, the

authors reported that ranolazine improves diastolic function in HF and preserves the ejection fraction [49]. However, based on echocardiography findings, no improvements in relaxation parameters were observed. Further studies are warranted to determine whether ranolazine is beneficial for patients with diastolic heart failure.

Based on the studies described above, it seems reasonable to prescribe ranolazine to patients with chronic angina. It could also be considered a first-line drug because of its low hemodynamic effects.

Conclusion

Persistent sodium channel currents exacerbated by different pathologies such as LQT3 syndrome or HF can delay repolarization which per se can lead to intracellular sodium overload and EADs. These EADs if of sufficient amplitude can provide the trigger for initiation of ventricular arrhythmias such as torsades de pointes and sudden cardiac death. Ranolazine demonstrated some beneficial effects in reducing late sodium channel currents in animal models. Based on the clinical trials described above, it seems reasonable to prescribe ranolazine to patients with chronic angina. It could also be considered a first-line drug because of its well tolerance and low hemodynamic effects.

Acknowledgments Supported by the Canadian Institutes of Health Research (MOP-111072 and MOP-130373 to MC). Association Française contre les Myopathies (AFM) – Téléthon (Research Grant AFM19962 to MC).

References

1. Kirsch GE, Brown AM. Kinetic properties of single sodium channels in rat heart and rat brain. *J Gen Physiol.* 1989;93(1):85–99.
2. Kiyosue T, Arita M. Late sodium current and its contribution to action potential configuration in guinea pig ventricular myocytes. *Circ Res.* 1989;64(2):389–97.
3. Nilius B. Modal gating behavior of cardiac sodium channels in cell-free membrane patches. *Biophys J.* 1988;53(6):857–62.

4. Patlak JB, Ortiz M. Slow currents through single sodium channels of the adult rat heart. *J Gen Physiol.* 1985;86:89–104.
5. Patlak JB, Ortiz M. Two modes of gating during late Na⁺ channel currents in frog sartorius muscle. *J Gen Physiol.* 1986;87(2):305–26.
6. Grant AO. Electrophysiological basis and genetics of Brugada syndrome. *J Cardiovasc Electrophysiol.* 2005;16(Suppl 1):S3–7.
7. Gellens ME, George AL Jr, Chen LQ, Chahine M, Horn R, Barchi RL, et al. Primary structure and functional expression of the human cardiac tetrodotoxin-insensitive voltage-dependent sodium channel. *Proc Natl Acad Sci U S A.* 1992;89(2):554–8.
8. Wang Q, Li Z, Shen J, Keating MT. Genomic organization of the human *SCN5A* gene encoding the cardiac sodium channel. *Genomics.* 1996;34(1):9–16.
9. Hilber K, Sandtner W, Kudlacek O, Schreiner B, Glaaser I, Schutz W, et al. Interaction between fast and ultra-slow inactivation in the voltage-gated sodium channel. Does the inactivation gate stabilize the channel structure? *J Biol Chem.* 2002;277(40):37105–15.
10. Townsend C, Horn R. Interaction between the pore and a fast gate of the cardiac sodium channel. *J Gen Physiol.* 1999;113(2):321–32.
11. Balsler JR, Nuss HB, Chiamvimonvat N, Pérez-garcía MT, Marban E, Tomaselli GF. External pore residue mediates slow inactivation in m1 rat skeletal muscle sodium channels. *J Physiol.* 1996;494(Pt 2):431–42.
12. Attwell D, Cohen I, Eisner D, Ohba M, Ojeda C. The steady state TTX-sensitive (“window”) sodium current in cardiac Purkinje fibres. *Pflügers Arch.* 1979;379(2):137–42.
13. Coraboeuf E, Deroubaix E, Coulombe A. Effect of tetrodotoxin on action potentials of the conducting system in the dog heart. *Am J Phys.* 1979;236(4):H561–H7.
14. Coraboeuf E, Deroubaix E. Shortening effect of tetrodotoxin on action potentials of the conducting system in the dog heart. *J Physiol.* 1978;280:24P.
15. Wagner S, Ruff HM, Weber SL, Bellmann S, Sowa T, Schulte T, et al. Reactive oxygen species-activated Ca/calmodulin kinase IIdelta is required for late I(Na) augmentation leading to cellular Na and Ca overload. *Circ Res.* 2011;108(5):555–65.
16. Ward CA, Giles WR. Ionic mechanism of the effects of hydrogen peroxide in rat ventricular myocytes. *J Physiol.* 1997;500(Pt 3):631–42.
17. Medeiros-Domingo A, Kaku T, Tester DJ, Iturralde-Torres P, Ity A, Ye B, et al. SCN4B-encoded sodium channel beta4 subunit in congenital long-QT syndrome. *Circulation.* 2007;116(2):134–42.
18. Vatta M, Ackerman MJ, Ye B, Makielski JC, Ughanze EE, Taylor EW, et al. Mutant caveolin-3 induces persistent late sodium current and is associated with long-QT syndrome. *Circulation.* 2006;114(20):2104–12.
19. Cronk LB, Ye B, Kaku T, Tester DJ, Vatta M, Makielski JC, et al. Novel mechanism for sudden infant death syndrome: persistent late sodium current secondary to mutations in caveolin-3. *Heart Rhythm.* 2007;4(2):161–6.
20. George AL Jr, Varkony TA, Drabkin HA, Han J, Knops JF, Finley WH, et al. Assignment of the human heart tetrodotoxin-resistant voltage-gated Na⁺ channel α -subunit gene (*SCN5A*) to band 3p21. *Cytogenet Cell Genet.* 1995;68(1–2):67–70.
21. Bennett PB, Yazawa K, Makita N, George AL Jr. Molecular mechanism for an inherited cardiac arrhythmia. *Nature.* 1995;376(6542):683–5.
22. Tan HL, Bezzina CR, Smits JPP, Verkerk AO, Wilde AAM. Genetic control of sodium channel function. *Cardiovasc Res.* 2003;57(4):961–73.
23. Wattanasirichaigoon D, Vesely MR, Duggal P, Levine JC, Blume ED, Wolff GS, et al. Sodium channel abnormalities are infrequent in patients with long QT syndrome: identification of two novel *SCN5A* mutations. *Am J Med Genet.* 1999;86(5):470–6.
24. Dumaine R, Wang Q, Keating MT, Hartmann HA, Schwartz PJ, Brown AM, et al. Multiple mechanisms of Na⁺ channel-linked long-QT syndrome. *Circ Res.* 1996;78(5):916–24.
25. Estes NA 3rd. Predicting and preventing sudden cardiac death. *Circulation.* 2011;124(5):651–6.
26. Savarese G, Lund LH. Global public health burden of heart failure. *Card Fail Rev.* 2017;3(1):7–11.
27. Valdivia CR, Chu WW, Pu J, Foell JD, Haworth RA, Wolff MR, et al. Increased late sodium current in myocytes from a canine heart failure model and from failing human heart. *J Mol Cell Cardiol.* 2005;38(3):475–83.
28. Maltsev VA, Sabbah HN, Higgins RS, Silverman N, Lesch M, Undrovinas AI. Novel, ultraslow inactivating sodium current in human ventricular cardiomyocytes. *Circulation.* 1998;98(23):2545–52.
29. Huang B, El-Sherif T, Gidh-Jain M, Qin D, El-Sherif N. Alterations of sodium channel kinetics and gene expression in the postinfarction remodeled myocardium. *J Cardiovasc Electrophysiol.* 2001;12(2):218–25.
30. Noble D, Noble PJ. Late sodium current in the pathophysiology of cardiovascular disease: consequences of sodium-calcium overload. *Heart.* 2006;92(Suppl 4):iv1–5.
31. Christophe G, Chahine M, Chevalier P, Pasek M. Changes in action potentials and intracellular ionic homeostasis in a ventricular cell model related to a persistent sodium current in *SCN5A* mutations underlying LQT3. *Prog Biophys Mol Biol.* 2008;96(1–3):281–93.
32. Schwartz PJ, Priori SG, Locati EH, Napolitano C, Cantù F, Towbin JA, et al. Long QT syndrome patients with mutations of the *SCN5A* and *HERG* genes have differential responses to Na⁺ channel blockade and to increases in heart rate. Implications for gene-specific therapy. *Circulation.* 1995;92(12):3381–6.
33. Benhorin J, Taub R, Goldmit M, Kerem B, Kass RS, Windman I, et al. Effects of flecainide in patients with new *SCN5A* mutation: mutation-specific therapy for long-QT syndrome? *Circulation.* 2000;101(14):1698–706.

34. Huang H, Priori SG, Napolitano C, O'Leary ME, Chahine M. Y1767C, a novel SCN5A mutation, induces a persistent Na⁺ current and potentiates ranolazine inhibition of Nav1.5 channels. *Am J Physiol Heart Circ Physiol*. 2011;300(1):H288–H99.
35. O'Leary ME, Chahine M. Mechanisms of drug binding to voltage-gated sodium channels. *Handb Exp Pharmacol*. 2018;246:209–31.
36. Fredj S, Sampson KJ, Liu H, Kass RS. Molecular basis of ranolazine block of LQT-3 mutant sodium channels: evidence for site of action. *Br J Pharmacol*. 2006;148(1):16–24.
37. Undrovinas AI, Belardinelli L, Undrovinas NA, Sabbah HN. Ranolazine improves abnormal repolarization and contraction in left ventricular myocytes of dogs with heart failure by inhibiting late sodium current. *J Cardiovasc Electrophysiol*. 2006;17(Suppl 1):S169–s77.
38. Pepine CJ, Wolff AA. A controlled trial with a novel anti-ischemic agent, ranolazine, in chronic stable angina pectoris that is responsive to conventional antianginal agents. Ranolazine Study Group. *Am J Cardiol*. 1999;84(1):46–50.
39. Ju YK, Saint DA, Gage PW. Hypoxia increases persistent sodium current in rat ventricular myocytes. *J Physiol*. 1996;497(Pt 2):337–47.
40. Murphy E, Perlman M, London RE, Steenbergen C. Amiloride delays the ischemia-induced rise in cytosolic free calcium. *Circ Res*. 1991;68(5):1250–8.
41. Song Y, Shryock JC, Wu L, Belardinelli L. Antagonism by ranolazine of the pro-arrhythmic effects of increasing late I_{Na} in guinea pig ventricular myocytes. *J Cardiovasc Pharmacol*. 2004;44(2):192–9.
42. Belardinelli L, Shryock JC, Fraser H. Inhibition of the late sodium current as a potential cardioprotective principle: effects of the late sodium current inhibitor ranolazine. *Heart*. 2006;92(Suppl 4):iv6–iv14.
43. Chaitman BR, Skettino SL, Parker JO, Hanley P, Meluzin J, Kuch J, et al. Anti-ischemic effects and long-term survival during ranolazine monotherapy in patients with chronic severe angina. *J Am Coll Cardiol*. 2004;43(8):1375–82.
44. Chaitman BR, Pepine CJ, Parker JO, Skopal J, Chumakova G, Kuch J, et al. Effects of ranolazine with atenolol, amlodipine, or diltiazem on exercise tolerance and angina frequency in patients with severe chronic angina: a randomized controlled trial. *JAMA*. 2004;291(3):309–16.
45. Alexopoulos D, Kochiadakis G, Afthonidis D, Barbetseas J, Kelembekoglou P, Limberi S, et al. Ranolazine reduces angina frequency and severity and improves quality of life: observational study in patients with chronic angina under ranolazine treatment in Greece (OSCAR-GR). *Int J Cardiol*. 2016;205:111–6.
46. Kosiborod M, Arnold SV, Spertus JA, McGuire DK, Li Y, Yue P, et al. Evaluation of ranolazine in patients with type 2 diabetes mellitus and chronic stable angina: results from the TERISA randomized clinical trial (type 2 diabetes evaluation of ranolazine in subjects with chronic stable angina). *J Am Coll Cardiol*. 2013;61(20):2038–45.
47. Stone PH, Gratsiansky NA, Blokhin A, Huang IZ, Meng L. Antianginal efficacy of ranolazine when added to treatment with amlodipine: the ERICA (efficacy of ranolazine in chronic angina) trial. *J Am Coll Cardiol*. 2006;48(3):566–75.
48. Rastogi S, Sharov VG, Mishra S, Gupta RC, Blackburn B, Belardinelli L, et al. Ranolazine combined with enalapril or metoprolol prevents progressive LV dysfunction and remodeling in dogs with moderate heart failure. *Am J Physiol Heart Circ Physiol*. 2008;295(5):H2149–55.
49. Maier LS, Layug B, Karwatowska-Prokopczuk E, Belardinelli L, Lee S, Sander J, et al. RANoLazIne for the treatment of diastolic heart failure in patients with preserved ejection fraction: the RALI-DHF proof-of-concept study. *JACC Heart Fail*. 2013;1(2):115–22.



Age, Sex and Racial Differences in Cardiac Repolarization and Arrhythmogenesis

Arja Suzanne Vink, Sally-Ann B. Clur, Pieter G. Postema, Nico A. Blom, and Arthur A. M. Wilde

Introduction

Willem Einthoven recorded the first electrocardiogram (ECG) in a healthy man in 1905, long before the understanding of the role of ion channels and the cardiac action potential. Over the last decades, extensive progress has been made in our understanding of the relationship between structure and

function of the cardiac ion channels and the effects of changes in expression and gating of these channels on the electrical substrate and the ECG. The function of ion channels is significantly modified by the subunit assembly and environmental conditions (i.e. hormones, electrolyte concentrations and pH), which have substantial effects on the cardiac depolarization and repolarization. Profound ECG changes in individuals with primary arrhythmia syndromes have helped to discover the role of subunits of ion channels in causing different types of cardiac channelopathies. Indeed, pathogenic mutations in the genes encoding these subunits are causal to some of these rare arrhythmia syndromes. However, despite this improved understanding of the physiology of the cardiac ion channels, there is still a lack of knowledge on age, sex and racial differences seen in the human ECG especially regarding the QTc-interval. This is due to incomplete and controversial information on age, sex and racial differences in the expression and properties of ion channels and the regulation of ion channels, i.e. by sex hormones.

This chapter outlines the recent developments in the study of age, sex and racial differences in QTc-interval in healthy individuals.

A. S. Vink (✉)

Department of Clinical and Experimental Cardiology, Amsterdam UMC, University of Amsterdam, Heart Center, Amsterdam, The Netherlands

Department of Pediatric Cardiology, Emma Children's Hospital, Amsterdam UMC, University of Amsterdam, Amsterdam, The Netherlands
e-mail: a.s.vink@amsterdamumc.nl

S.-A. B. Clur

Department of Pediatric Cardiology, Emma Children's Hospital, Amsterdam UMC, University of Amsterdam, Amsterdam, The Netherlands
e-mail: s.a.clur@amsterdamumc.nl

P. G. Postema · A. A. M. Wilde

Department of Clinical and Experimental Cardiology, Amsterdam UMC, University of Amsterdam, Heart Center, Amsterdam, The Netherlands
e-mail: p.g.postema@amsterdamumc.nl;
a.a.wilde@amsterdamumc.nl

N. A. Blom

Department of Pediatric Cardiology, Emma Children's Hospital, Amsterdam UMC, University of Amsterdam, Amsterdam, The Netherlands

Department of Paediatric Cardiology, Willem-Alexander Children's Hospital, Leiden University Medical Centre, Leiden, The Netherlands
e-mail: n.a.blom@amsterdamumc.nl

General Aspects of Cardiac Repolarization

The role of cardiac ion channels in the generation of the ventricular cardiac action potential is

Ventricular action potential

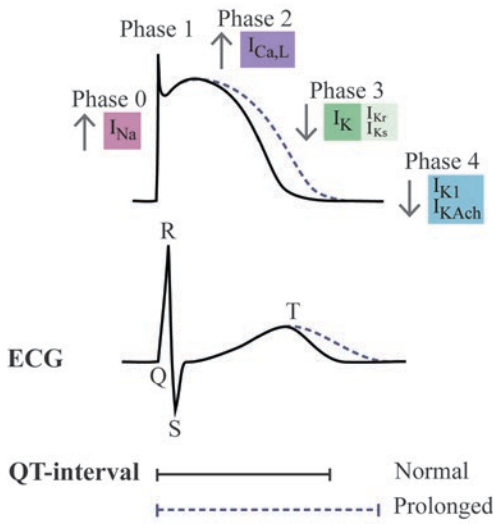


Fig. 6.1 Electrophysiological basis of the ventricular action potential and prolongation of the QT-interval. See text for explanation

outlined in depth in Chap. 1. In short, the rapid depolarization (phase 0) is caused by the influx of sodium ions into the cell through voltage-gated sodium channels (I_{Na}) (Fig. 6.1). Phase 1 repolarization is mainly caused by activation of the transient outward potassium currents (I_{to}) together with a corresponding rapid decay of the sodium current, which is followed by phase 2. In this plateau phase, continued L-type late calcium ($I_{Ca,L}$) and a small amplitude late sodium current into the cell balance the effect of potassium currents out of the cell. The decay of the calcium current and the increase in delayed rectifier potassium current (I_{Ks}), in the rapid activation component of the delayed rectifier potassium current (I_{Kr}), and particularly the late activation of the inward rectifier potassium current (I_{K1}), are together responsible for the repolarization (phase 3) with ultimate return to the resting potential (phase 4).

The vectorial sum of the complex interactions of these different electrical currents in all the cardiomyocytes results in the physical manifestation of the cardiac waveform morphologies on the ECG that consist of a QRS complex and a T-wave.

The QT-interval is measured from the beginning of the QRS complex to the end of the T-wave and represents the duration of activation and recovery of the ventricular myocardium. The QT-interval is most affected by alterations in phase 2 and phase 3 of the ventricular action potential [1]. Upregulation of the $I_{Ca,L}$ channel currents prolongs the QT-interval, whereas downregulation shortens the QT-interval. During phases 2 and 3, upregulation of I_{Ks} , I_{Kr} and I_{K1} channel currents shorten the QT-interval, and downregulation prolong the QT-interval. Finally, an increased amplitude of the late sodium current lengthens the action potential and thus the QT-interval.

In the normal heart, the QT-interval shortens with an increase in heart rate and lengthens with a decrease in heart rate. Since the QT-interval adapts to the heart rate, the QT-interval should be corrected for heart rate using the preceding RR-interval (QTc-interval), which can be done using several formulas [2]. None of these formulas gives an optimal correction, but the Bazett correction formula is most frequently used in daily practice [3]. A prolonged QTc-interval is a marker for an increased risk of torsades de pointes (TdP), a malignant polymorphic ventricular tachyarrhythmia that precipitates syncope, sudden cardiac arrest (SCA) or sudden cardiac death (SCD) [4, 5].

Age-Related QTc-Interval Changes in Healthy Individuals

The QTc-interval is remarkably long after birth, in both males and females [6–8]. The QTc-interval then decreases during the first weeks after birth in both sexes [6–8] and then remains relatively consistent over the years until the age of approximately 16 years [6, 8–14]. However, when individual age trends are taking into account, both males and females have longer QTc-intervals at the age of 12 years compared to the ages of 6 and 15 years [15, 16]. After puberty, the QTc-interval shortens in males but not in females [6, 17–21]. During adulthood, the QTc-interval gradually increases with age [11, 22–33]

in both sexes [17–20, 22, 34–45]. In contradiction, there is one study that showed QTc-interval shortening in older age groups (>60 years) [46].

Sex Differences in QTc-Interval in Healthy Individuals

Nearly 100 years ago in the early ECG recordings by Bazett [3], differences in QTc-interval were described between healthy adult males and females. Decades later, it became clear that these sex differences are not present during the first month of life [6, 8, 47, 48] but arise at a later age. At the age of 1–3 months, females have a slightly longer QTc-interval compared to males [6, 13, 14]. Thereafter, no sex difference is seen until approximately the onset of puberty [6, 9, 10, 12–14, 16, 18, 20, 49, 50]. Fukushima et al. [15] described a shorter QTc-interval in 6-year-old females compared to males, but this difference was very small (384 ms versus 386 ms; $P < 0.05$). After puberty, females have a longer QTc-interval compared to males [6, 9, 14–17, 20, 21, 50–59]. This difference has also been reported in adulthood by several studies [3, 15, 17, 19, 20, 22–27, 29–33, 35–46, 57, 60–74], although some other studies found no difference [34, 66] or even a longer QTc-interval in males [75]. The difference in QTc-interval between males and females decreases with age [25] because the QTc-interval increases more in time in males compared to females [37]. As a result, no clear sex differences are present in the highest age groups of approximately >60 years [19, 20, 27, 34, 37].

Racial Differences in QTc-Interval in Healthy Individuals

The presence of racial differences in QTc-interval still requires clarification as the effect of race has been looked at in only a limited number of studies. Most studies report no clear racial differences [29, 48, 70, 76], although some small differences may be present. Blacks tend to have slightly shorter QTc-intervals compared to Caucasians [8, 31, 32, 74], and Asians, especially females [31,

62, 72, 73, 77], have slightly longer QTc-intervals compared to Caucasians [30, 48, 72, 78]. In addition, collective consideration of available pharmacogenetic and clinical information suggests that there may be inter-race differences in QT-prolonging effects of drugs and that Caucasians may be more sensitive than other populations [79]. These possible differences are most likely the result of the presence of considerable heterogeneity among race/ethnicity for multiple genetic loci that have an impact on the QT-interval. Some of these loci show a striking difference (i.e. order of magnitude 40–50%) between the highest and lowest frequencies between ethnicities [80]. Unfortunately, there is no data on racial-specific age-related sex differences.

Possible Role of Sex Hormones on the QTc-Interval and Arrhythmogenesis

The age- and sex-related differences in QTc-interval, especially the change post-puberty, most likely are due to changes in sex hormones levels. The mechanisms underlying the influence of sex hormones on the repolarization are complex and still unresolved; however, mechanistic studies suggest that sex hormone has varying effects on the I_{CaL} , I_{Kr} , I_{Ks} and I_{K1} channel currents. Testosterone decreases the I_{CaL} current and increases the potassium channel currents, resulting in a shorter QTc-interval observed in both animal and human studies [81]. Progesterone decreases the I_{CaL} current and increases the I_{Ks} current and may therefore shorten the QTc-interval [81]. Conflicting results of endogenous oestrogen on the QTc-interval have been described. Oestrogen lengthens the QTc-interval in animals; however, this has not been supported by human studies. In animal studies, oestrogen decreases the potassium channel currents and may lengthen the QT-interval through this mechanism [81].

In children, concentrations of sex hormones are influenced by the activity of the hypothalamic-pituitary-gonadal (HPG) axis. The HPG axis is active during the (I) mid-gestational period in the

foetus, (II) first months of life and (III) pubertal period [82], and therefore higher concentrations of testosterone and oestrogen are found during these periods. As a consequence, during periods of sudden changes in sex hormone concentrations (i.e. the first months of life and the onset of puberty), a marked QTc-interval shortening in males would be expected based on the higher level of testosterone compared to females. This could explain the shorter QTc-intervals in males between 1 and 3 months and after the onset of puberty compared to females.

In adulthood, the level of testosterone gradually decreases with age in males [83], potentially explaining why with ageing, the QTc-interval in males gradually lengthens and approximates that of females. Changes in sex hormone levels in females are more complex due to the influence of the menstrual cycle, pregnancy and the menopause.

Menstrual Cycle

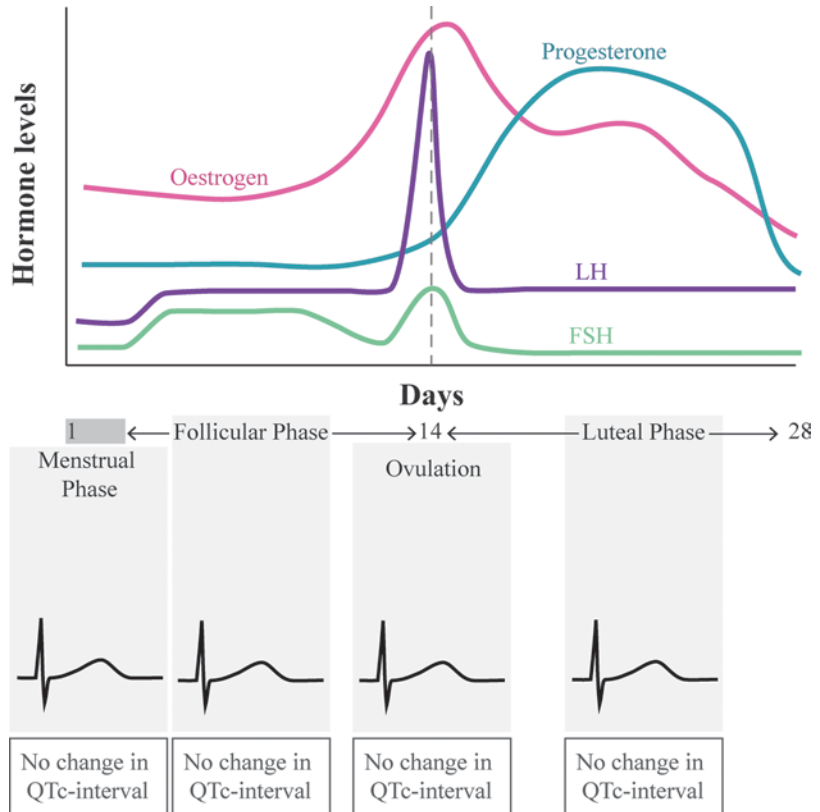
Oestrogen and progesterone levels fluctuate during the menstrual cycle and are lowest at the onset of menses (menstrual phase). After the cessation of the menstrual flow, there is a gradual increase in oestrogen (follicular phase). Oestrogen levels peak in the middle of the menstrual phase during the ovulation (ovulation phase), and after the ovulation, the oestrogen levels gradually decrease during the luteal phase. Progesterone levels, in contrast, are low during the menstrual and follicular phase and increase after the ovulation through the luteal phase (Fig. 6.2).

In females, there are no clear QTc-interval differences between the different phases of the menstrual cycle [84–89]. In addition, there are also no distinct differences in heart rate [86, 87, 89–92], so there is probably no effect of the method chosen to correct the QT-interval for the heart rate. Hulot et al. [84] found no relationship between the level of oestrogen and the length of the QTc-interval ($P = 0.92$). In the study by Nakagawa et al. [85], the uncorrected QT-interval was shorter in the luteal phase compared to the follicular phase, although no difference in QTc-interval

was seen. They found no statistically significant difference in oestrogen level between the luteal and follicular phase, while progesterone ($P < 0.001$) and noradrenaline levels ($P < 0.05$) were higher in the luteal phase suggesting the role of progesterone and/or autonomic tone on the uncorrected QT-interval. When double autonomic blockade was given, e.g. atropine and propranolol administration, QTc-interval differences between the phases of the menstrual cycle were seen. Under these circumstances, Burke et al. [86] found a shorter QTc-interval in the luteal phase compared to the menstrual and follicular phase, whereas Endres et al. [87] observed a significantly longer QTc-interval during the follicular phase compared to the menstrual and luteal phase. Both studies indicate the important role of autonomic tone in alternations in the QTc-interval during the menstrual cycle. Rodriguez et al. [88] showed that ibutilide infusion, a known I_{Kr} blocker mimicking long QT syndrome (LQTS), causes differences in QTc-interval between the phases of the menstrual cycle, whereas the luteal phase seemed to be protective against the drug-induced QTc-interval prolongation. Hence, since there is an effect of the menstrual cycle on the QTc-interval during administration of QTc-interval prolonging medication, it could be argued that this effect is also present in patients with LQTS.

Despite the unclear changes in the QTc-interval between the phases of the menstrual cycle in the normal situation, there seems to be a cyclic variation in the occurrence of episodes of arrhythmia with the menstrual cycle. During the luteal phase, an increase in the number and duration of paroxysmal supraventricular tachycardia (SVT) has been reported compared to other phases of the menstrual cycle [93, 94], with a correlation with plasma concentrations of progesterone and an inverse correlation with plasma concentrations of oestradiol [93]. Also ventricular ectopic beats seems to be more frequent during the luteal phase of the menstrual cycle [93]. So it seems that there can be significant changes in the arrhythmogenic substrate of the heart throughout the menstrual cycle without dramatic changes in the QTc-interval. As we know, there is no simple relationship between absolute QTc-

Fig. 6.2 Oestrogen, progesterone, luteinizing hormone (LH) and follicle-stimulating hormone (FSH) levels over a single menstrual cycle in females together with a schematic representation of the QTc-intervals during the phases of the menstrual cycle (i.e. menstrual phase, follicular phase, ovulation and luteal phase). See text for explanation. (Derived from data in: Sedlak et al. [81])



interval and arrhythmogenic potential or SCD [63, 88, 95], so perhaps the autonomic tone also plays an important role which is influenced by sex hormones [85, 96].

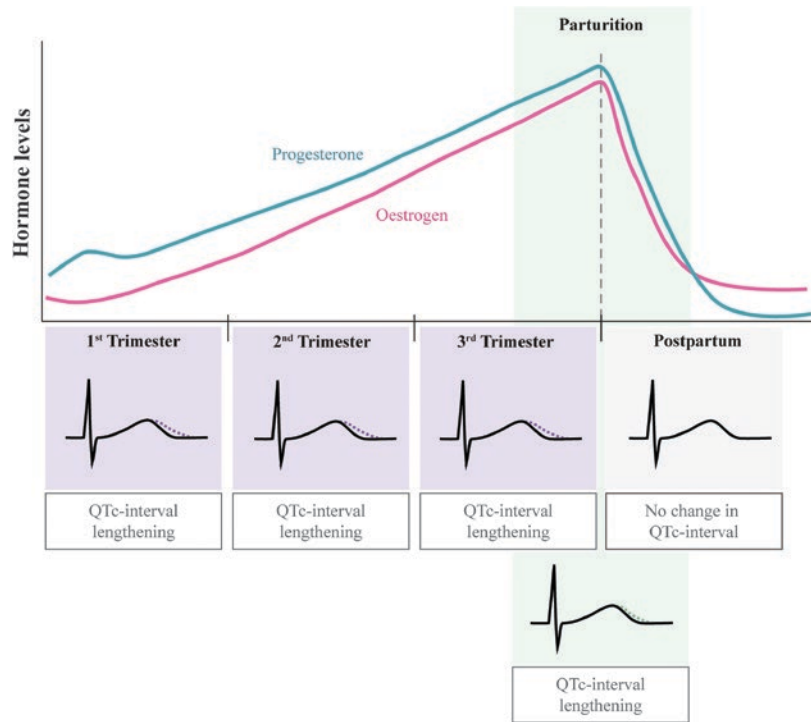
The fluctuations of oestrogen and progesterone levels during the menstrual cycle are controlled by the gonadotropin hormones, e.g. luteinizing hormone (LH) and follicle-stimulating hormone (FSH). A peak in LH and FSH is seen prior to ovulation in the normal menstrual cycle which is recognizable by an increase in body temperature (Fig. 6.2). Abehsira et al. [97] showed recently that the QTc-interval is probably influenced by a complex interaction between sex hormones and gonadotropins. In both males and females, FSH was positively correlated to QTc-interval ($r = 0.39$ and $r = 0.38$, respectively, in males and females), while free testosterone in males ($r = -0.34$) and progesterone/oestrogen ratio in women ($r = -0.38$) were negatively correlated. LH was only correlated in females to the QTc-interval ($r = 0.30$).

Pregnancy

During gestation, there is a complex and varying combination of sex hormones. Oestrogen and progesterone levels gradually increase during pregnancy until labour when the levels drop sharply reaching pregravid levels by the fifth postpartum day (Fig. 6.3) [98–102].

Studies regarding changes in QT/QTc-interval during pregnancy used either longitudinal data during pregnancy [103], the postpartum state as a control [104] or a control group of non-pregnant women [105, 106]. There is a longer QTc-interval during the first trimester and late pregnancy, with a shortening of the QTc-interval after delivery [104–106]. The QTc-interval just after delivery is however longer compared to the postpartum period [104]. The heart rate is, on the contrary, higher during pregnancy and delivery compared to the control group [104–106] and seems to increase with gestation [103]. Due to these changes in heart rate, it is not unlikely that the

Fig. 6.3 Oestrogen and progesterone levels during pregnancy and after parturition together with a schematic representation of the QTc-intervals during the trimesters, parturition and the postpartum period. See text for explanation. (Derived from data in: Bett [115])



observed differences in the QTc-interval are influenced by the correction method used to correct the QT-interval for the heart rate [107]. Anneken et al. [108] recently studied five healthy women who became pregnant after stimulation by clomiphene citrate therapy for infertility, observing shorter QTc-intervals during higher oestrogen levels. Progesterone did not affect the QTc-interval significantly in that study.

The gestational prolongation of the QTc-interval does not precipitate widespread fatal cardiac arrhythmias in pregnant women. However, there is a slight increase in arrhythmias during pregnancy regarding SVTs and even ventricular tachycardia (VT) compared to the postpartum period or non-pregnant controls [109, 110]. Although the occurrence of VT is usually uncommon, their presence should raise a suspicion of underlying cardiovascular disease.

Menopausal Period

The menopause is defined as the permanent cessation of menstrual periods, determined retrospectively after a woman has experienced 12 months of

amenorrhoea without any other obvious pathological or physiological cause. The menopause is a reflection of complete, or near-complete, ovarian follicular depletion resulting in very low levels of oestrogen and progesterone and high levels of FSH concentrations (Fig. 6.4). The menopausal transition, or perimenopause, occurs after the reproductive years and before the menopause. This period is characterized by irregular menstrual cycles and significant hormonal variability [111, 112].

Two studies comparing premenopausal females to postmenopausal females showed no differences in QTc-interval and heart rate [113, 114]. One of the studies also measured the hormone levels and found no difference in oestrogen levels but a lower level of progesterone in the postmenopausal phase compared to the premenopausal phase [114].

The data regarding postmenopausal arrhythmogenesis is lacking; however the autonomic tone may also play a role in the peri-/postmenopausal period. Hence, the QTc-interval is shorter in women with hot flushes compared to those without, and the absence of menopausal hot flushes is associated with an elevated activity of the sympathetic nervous system.

Fig. 6.4 Menstrual cycle patterns during menopause. FMP = Final menstrual period. See text for explanation. (Reprinted by permission from Springer Nature: Deecher and Dorries [116])

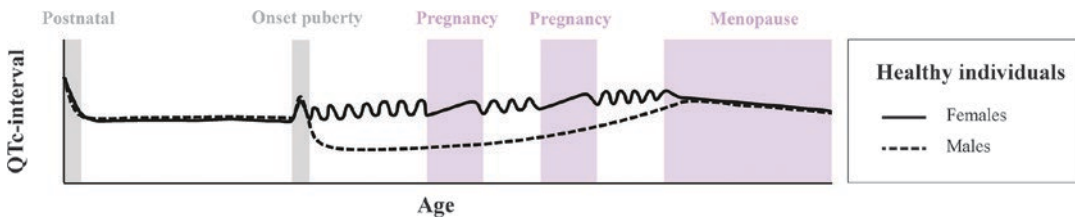
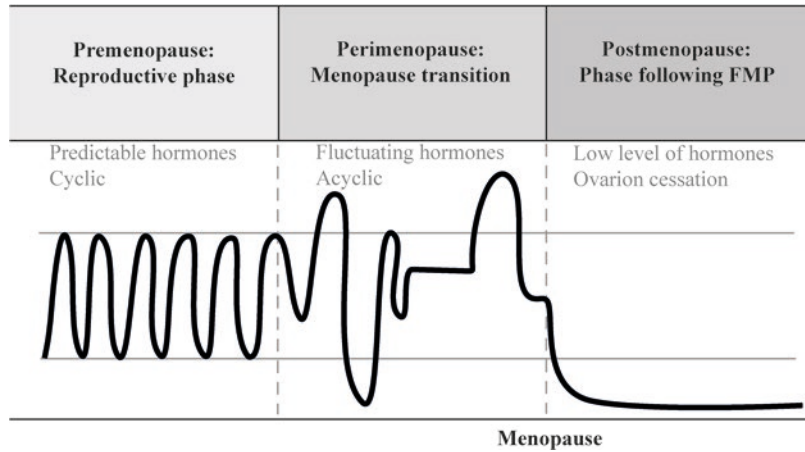


Fig. 6.5 Schematic representation of hypothetical changes in QTc-interval in healthy individuals

Conclusion

Age, sex and race have an influence on the QTc-interval. Although data regarding racial differences is lacking, the small differences seen are probably the result of the presence of considerable heterogeneity among race/ethnicity for multiple genetic loci that influence the QT-interval. Age- and sex-related differences in QTc-interval (Fig. 6.5) are most likely the result of changes in sex-specific hormones. Although the exact mechanisms and pathophysiology of the effect of sex hormones on the QTc-interval and the arrhythmogenesis are not known, testosterone appears to shorten the QTc-interval in males. In females, however, there is a more complex interaction between progesterone and oestrogen. In addition, the autonomic nervous system and gonadotropins may play an important part in this complex interaction.

Acknowledgements The authors are indebted to Larissa Groot and Jacqueline Limpens for their support.

References

1. James AF, Choisy SC, Hancox JC. Recent advances in understanding sex differences in cardiac repolarization. *Prog Biophys Mol Biol.* 2007;94(3): 265–319.
2. Funck-Brentano C, Jaillon P. Rate-corrected QT interval: techniques and limitations. *Am J Cardiol.* 1993;72(6):17b–22b.
3. Bazett HC. An analysis of the time-relations of electrocardiograms. *Heart.* 1920;7:353–70.
4. van Noord C, Eijgelsheim M, Stricker BH. Drug- and non-drug-associated QT interval prolongation. *Br J Clin Pharmacol.* 2010;70(1):16–23.
5. Nachimuthu S, Assar MD, Schussler JM. Drug-induced QT interval prolongation: mechanisms and clinical management. *Ther Adv Drug Saf.* 2012;3(5):241–53.
6. Semizel E, Ozturk B, Bostan OM, Cil E, Ediz B. The effect of age and gender on the electrocardiogram in children. *Cardiol Young.* 2008;18(1):26–40.
7. Walsh SZ. Electrocardiographic intervals during the first week of life. *Am Heart J.* 1963;66:36–41.
8. Schaffer MS, Trippel DL, Buckles DS, Young RH, Dolan PL, Gillette PC. The longitudinal time course of QTc in early infancy. Preliminary results of a prospective sudden infant death syndrome surveillance program. *J Perinatol.* 1991;11(1):57–62.

9. Benatar A, Feenstra A. QT correction methods in infants and children: effects of age and gender. *Ann Noninvasive Electrocardiol.* 2015;20(2):119–25.
10. Dilaveris P, Roussos D, Giannopoulos G, Katinakis S, Maragiannis D, Raftopoulos L, et al. Clinical determinants of electrocardiographic and spatial vectorcardiographic descriptors of ventricular repolarization in healthy children. *Ann Noninvasive Electrocardiol.* 2011;16(1):49–55.
11. Braschi A, Abrignani MG, Francavilla VC, Abrignani V, Francavilla G. Age- and sex-based reference ranges for non-invasive ventricular repolarisation parameters. *Int J Clin Pract.* 2017;71(5).
12. Molinari G, Brunetti ND. Electrocardiograms of children and adolescents practicing non-competitive sports: normal limits and abnormal findings in a large European cohort evaluated by telecardiology. *Sports Med.* 2017;47(3):555–63.
13. Rijnbeek PR, Witsenburg M, Schrama E, Hess J, Kors JA. New normal limits for the paediatric electrocardiogram. *Eur Heart J.* 2001;22(8):702–11.
14. Yoshinaga M, Iwamoto M, Horigome H, Sumitomo N, Ushinohama H, Izumida N, et al. Standard values and characteristics of electrocardiographic findings in children and adolescents. *Circ J.* 2018;82(3):831–9.
15. Fukushige T, Yoshinaga M, Shimago A, Nishi J, Kono Y, Nomura Y, et al. Effect of age and overweight on the QT interval and the prevalence of long QT syndrome in children. *Am J Cardiol.* 2002;89(4):395–8.
16. Hazeki D, Yoshinaga M, Takahashi H, Tanaka Y, Haraguchi Y, Abe M, et al. Cut-offs for screening prolonged QT intervals from Fridericia's formula in children and adolescents. *Circ J.* 2010;74(8):1663–9.
17. Mason JW, Ramseth DJ, Chanter DO, Moon TE, Goodman DB, Mendzelevski B. Electrocardiographic reference ranges derived from 79,743 ambulatory subjects. *J Electrocardiol.* 2007;40(3):228–34.
18. Rautaharju PM, Mason JW, Akiyama T. New age- and sex-specific criteria for QT prolongation based on rate correction formulas that minimize bias at the upper normal limits. [Erratum appears in *Int J Cardiol.* 2015;178:299; PMID: 25639760]. *Int J Cardiol.* 2014;174(3):535–40.
19. Rijnbeek PR, van Herpen G, Bots ML, Man S, Verweij N, Hofman A, Hillege H, Numans ME, Swenne CA, Witteman JC, Kors JA. Normal values of the electrocardiogram for ages 16-90 years. *J Electrocardiol.* 2014;47(6):914–21.
20. Surawicz B, Parikh SR. Prevalence of male and female patterns of early ventricular repolarization in the normal ECG of males and females from childhood to old age. *J Am Coll Cardiol.* 2002;40(10):1870–6.
21. Santini M, Di Fusco SA, Colivicchi F, Gargaro A. Electrocardiographic characteristics, anthropometric features, and cardiovascular risk factors in a large cohort of adolescents. *Europace.* 2018;20(11):1833–40. <https://doi.org/10.1093/europace/euy073>.
22. Macfarlane PW, Lloyd SM, Singh D, Hamde S, Clark E, Devine B, et al. Normal limits of the electrocardiogram in Indians. *J Electrocardiol.* 2015;48(4):652–68.
23. de Bruyne MC, Hoes AW, Kors JA, Hofman A, van Bommel JH, Grobbee DE. Prolonged QT interval predicts cardiac and all-cause mortality in the elderly. The Rotterdam Study. *Eur Heart J.* 1999;20(4):278–84.
24. Dewhurst MJ, Di Marco LY, Dewhurst F, Adams PC, Murray A, Orega GP, et al. Electrocardiographic reference values for a population of older adults in sub-Saharan Africa. *Ann Noninvasive Electrocardiol.* 2014;19(1):34–42.
25. Rabkin SW, Cheng XJ, Thompson DJ. Detailed analysis of the impact of age on the QT interval. *J Geriatr Cardiol.* 2016;13(9):740–8.
26. Chen CY, Chiang BN, Macfarlane PW. Normal limits of the electrocardiogram in a Chinese population. *J Electrocardiol.* 1989;22(1):1–15.
27. Mangoni AA, Kinirons MT, Swift CG, Jackson SH. Impact of age on QT interval and QT dispersion in healthy subjects: a regression analysis. *Age Ageing.* 2003;32(3):326–31.
28. Baumert M, Czipelova B, Porta A, Javorka M. Decoupling of QT interval variability from heart rate variability with ageing. *Physiol Meas.* 2013;34(11):1435–48.
29. Benoit SR, Mendelsohn AB, Nourjah P, Staffa JA, Graham DJ. Risk factors for prolonged QTc among US adults: Third National Health and Nutrition Examination Survey. *Eur J Cardiovasc Prev Rehabil.* 2005;12(4):363–8.
30. Macfarlane PW, McLaughlin SC, Devine B, Yang TF. Effects of age, sex, and race on ECG interval measurements. *J Electrocardiol.* 1994;27 Suppl:14–9.
31. Macfarlane PW, Katibi IA, Hamde ST, Singh D, Clark E, Devine B, Francq BG, Lloyd S, Kumar V. Racial differences in the ECG-selected aspects. *J Electrocardiol.* 2014;47(6):809–14.
32. Ramirez AH, Schildcrout JS, Blakemore DL, Masys DR, Pulley JM, Basford MA, Roden DM, Denny JC. Modulators of normal electrocardiographic intervals identified in a large electronic medical record. *Heart Rhythm.* 2011;8(2):271–7.
33. Zerkiebel N, Perret F, Bovet P, Abel M, Jaggy C, Paccaud F, Kappenberger L. Electrocardiographic findings in a middle-aged African population in the Seychelles islands. *J Electrocardiol.* 2000;33(1):1–15.
34. Reardon M, Malik M. QT interval change with age in an overtly healthy older population. *Clin Cardiol.* 1996;19(12):949–52.
35. Katibi I, Clark EN, Devine B, Lloyd SM, Macfarlane PW. Normal limits of the electrocardiogram in Nigerians. *J Electrocardiol.* 2013;46(4):289–95.

36. Tran H, White CM, Chow MS, Kluger J. An evaluation of the impact of gender and age on QT dispersion in healthy subjects. *Ann Noninvasive Electrocardiol.* 2001;6(2):129–33.
37. Vicente J, Johannesen L, Galeotti L, Strauss DG. Mechanisms of sex and age differences in ventricular repolarization in humans. *Am Heart J.* 2014;168(5):749–56.
38. Wu J, Kors JA, Rijnbeek PR, van Herpen G, Lu Z, Xu C. Normal limits of the electrocardiogram in Chinese subjects. *Int J Cardiol.* 2003;87(1):37–51.
39. Tan ES, Yap J, Xu CF, Feng L, Nyunt SZ, Santhanakrishnan R, et al. Association of age, sex, body size and ethnicity with electrocardiographic values in community-based older Asian adults. *Heart Lung Circ.* 2016;25(7):705–11.
40. Sugao M, Fujiki A, Sakabe M, Nishida K, Tsuneda T, Iwamoto J, et al. New quantitative methods for evaluation of dynamic changes in QT interval on 24 hour Holter ECG recordings: QT interval in idiopathic ventricular fibrillation and long QT syndrome. *Heart.* 2006;92(2):201–7.
41. van der Ende MY, Siland JE, Snieder H, van der Harst P, Rienstra M. Population-based values and abnormalities of the electrocardiogram in the general Dutch population: The LifeLines Cohort Study. *Clin Cardiol.* 2017;40(10):865–72.
42. Heemskerk CPM, Pereboom M, van Stralen K, Berger FA, van den Bemt P, Kuijper AFM, et al. Risk factors for QTc interval prolongation. *Eur J Clin Pharmacol.* 2018;74(2):183–91.
43. Khumrin P, Srisuwan P, Lertprayoonmit W, Leelarphat L, Phumphuang C. Effective ECG reference ranges for Northern Thai people. *Heart Asia.* 2015;7(1):32–40.
44. Rautaharju PM, Zhou SH, Wong S, Calhoun HP, Berenson GS, Prineas R, Davignon A. Sex differences in the evolution of the electrocardiographic QT interval with age. *Can J Cardiol.* 1992;8(7):690–5.
45. Mizuno Y. Normal limits and variability of electrocardiographic items of the Japanese. *Jpn Circ J.* 1966;30(4):357–78.
46. Shinmura K, Ebihara Y, Kawamura M, Tani M, Nakamura Y. [Changes in electrocardiographic findings with aging in a longitudinal study of 500 apparently healthy persons aged 60 years and older]. *Nihon Ronen Igakkai Zasshi Jpn J Geriatr.* 1994;31(5):366–73.
47. Stramba-Badiale M, Spagnolo D, Bosi G, Schwartz PJ. Are gender differences in QTc present at birth? MISNES Investigators. Multicenter Italian Study on Neonatal Electrocardiography and Sudden Infant Death Syndrome. *Am J Cardiol.* 1995;75(17):1277–8.
48. Marti-Almor J, Berruero R, Garcia-Algar O, Mur A, Bazan V, Recasens L, Pérez-Rodón J, Bruguera J. QT interval in newborns of different ethnic origin: usefulness of neonatal ECG screening. *Rev Esp Cardiol.* 2008;61(9):980–2.
49. Eberle T, Hessling G, Ulmer HE, Brockmeier K. Prediction of normal QT intervals in children. *J Electrocardiol.* 1998;31(Suppl):121–5.
50. Pearl W. Effects of gender, age, and heart rate on QT intervals in children. *Pediatr Cardiol.* 1996;17(3):135–6.
51. Griffet V, Finet G, Di Filippo S, Lantelme P, Caignault JR, Guerard S. [Athlete's heart in the young: electrocardiographic and echocardiographic patterns in 107 French athletes]. *Ann Cardiol Angeiol (Paris).* 2013;62(2):116–21.
52. Kumar N, Saini D, Froelicher V. A gender-based analysis of high school athletes using computerized electrocardiogram measurements. *PLoS One.* 2013;8(1):e53365.
53. Arai K, Nakagawa Y, Iwata T, Horiguchi H, Murata K. Relationships between QT interval and heart rate variability at rest and the covariates in healthy young adults. *Auton Neurosci.* 2013;173(1–2):53–7.
54. Bessem BB, de Bruijn MM, Nieuwland WW. Gender differences in the electrocardiogram screening of athletes. *J Sci Med Sport.* 2017;20(2):213–7.
55. Mandic S, Fonda H, Dewey F, Le VV, Stein R, Wheeler M, et al. Effect of gender on computerized electrocardiogram measurements in college athletes. *Phys Sportsmed.* 2010;38(2):156–64.
56. Omiya K, Sekizuka H, Kida K, Suzuki K, Akashi YJ, Ohba H, Musha H. Influence of gender and types of sports training on QT variables in young elite athletes. *Eur J Sport Sci.* 2014;14 Suppl 1:S32–8.
57. Merri M, Benhorin J, Alberti M, Locati E, Moss AJ. Electrocardiographic quantitation of ventricular repolarization. *Circulation.* 1989;80(5):1301–8.
58. Tutar HE, Ocal B, Imamoglu A, Atalay S. Dispersion of QT and QTc interval in healthy children, and effects of sinus arrhythmia on QT dispersion. *Heart.* 1998;80(1):77–9.
59. Misigoj-Durakovic M, Durakovic Z, Prskalo I. Heart rate-corrected QT and JT intervals in electrocardiograms in physically fit students and student athletes. *Ann Noninvasive Electrocardiol.* 2016;21(6):595–603.
60. Haarmark C, Graff C, Andersen MP, Hardahl T, Struijk JJ, Toft E, et al. Reference values of electrocardiogram repolarization variables in a healthy population. *J Electrocardiol.* 2010;43(1):31–9.
61. Rautaharju PM, Zhang ZM, Haisty WK Jr, Gregg RE, Warren J, Horacek MB, et al. Race- and sex-associated differences in rate-adjusted QT, QTpeak, ST elevation and other regional measures of repolarization: the Atherosclerosis Risk in Communities (ARIC) Study. *J Electrocardiol.* 2014;47(3):342–50.
62. Santhanakrishnan R, Wang N, Larson MG, Magnani JM, Vasani RS, Wang TJ, et al. Racial differences in electrocardiographic characteristics and prognostic significance in whites versus Asians. *J Am Heart Assoc.* 2016;5(3):e002956.
63. Goldberg RJ, Bengtson J, Chen ZY, Anderson KM, Locati E, Levy D. Duration of the QT interval and

- total and cardiovascular mortality in healthy persons (The Framingham Heart Study experience). *Am J Cardiol.* 1991;67(1):55–8.
64. Extramiana F, Maisson-Blanche P, Badilini F, Pinoteau J, Deseo T, Coumel P. Circadian modulation of QT rate dependence in healthy volunteers: gender and age differences. *J Electrocardiol.* 1999;32(1):33–43.
 65. Zhang Y, Ouyang P, Post WS, Dalal D, Vaidya D, Blasco-Colmenares E, et al. Sex-steroid hormones and electrocardiographic QT-interval duration: findings from the third National Health and Nutrition Examination Survey and the Multi-Ethnic Study of Atherosclerosis. *Am J Epidemiol.* 2011;174(4):403–11.
 66. Sliwa K, Lee GA, Carrington MJ, Obel P, Okreglicki A, Stewart S. Redefining the ECG in urban South Africans: electrocardiographic findings in heart disease-free Africans. *Int J Cardiol.* 2013;167(5):2204–9.
 67. Akyzbekova EL, Crow RS, Johnson WD, Buxbaum SG, Njemanze S, Fox E, et al. Clinical correlates and heritability of QT interval duration in blacks: the Jackson Heart Study. *Circ Arrhythm Electrophysiol.* 2009;2(4):427–32.
 68. Kassotis J, Costeas C, Bedi AK, Tolat A, Reiffel J. Effects of aging and gender on QT dispersion in an overtly healthy population. *Pacing Clin Electrophysiol.* 2000;23(7):1121–6.
 69. Marjamaa A, Salomaa V, Newton-Cheh C, Porthan K, Reunanen A, Karanko H, et al. High prevalence of four long QT syndrome founder mutations in the Finnish population. *Ann Med.* 2009;41(3):234–40.
 70. Bonny A, Bika Lele EC, Mandengue S, Larrazet F, Amara W. [Ethnic differences in electrocardiogram between a black African and a white European young adult population under 35 years]. *Presse Med.* 2013;42(4 Pt 1):e96–105.
 71. Brink AJ. The normal electrocardiogram in the adult South African Bantu. *S Afr J Lab Clin Med.* 1956;2(2):97–123.
 72. Grandinetti A, Seifried S, Mor J, Chang HK, Theriault AG. Prevalence and risk factors for prolonged QTc in a multiethnic cohort in rural Hawaii. *Clin Biochem.* 2005;38(2):116–22.
 73. Mansi IA, Nash IS. Ethnic differences in electrocardiographic intervals and axes. *J Electrocardiol.* 2001;34(4):303–7.
 74. Vitelli LL, Crow RS, Shahar E, Hutchinson RG, Rautaharju PM, Folsom AR. Electrocardiographic findings in a healthy biracial population. Atherosclerosis Risk in Communities (ARIC) Study Investigators. *Am J Cardiol.* 1998;81(4):453–9.
 75. Woods JB, Laurie W. The electrocardiogram of the South African Bantu. *Circulation.* 1959;19(2):251–6.
 76. Sgarbossa EB, Pinski SL, Williams D, Pavlovic-Surjancev B, Tang J, Trohman RG. Comparison of QT intervals in African-Americans versus Caucasians. *Am J Cardiol.* 2000;86(8):880–2.
 77. Rautaharju PM, Prineas RJ, Kadish A, Larson JC, Hsia J, Lund B. Normal standards for QT and QT subintervals derived from a large ethnically diverse population of women aged 50 to 79 years (the Women's Health Initiative [WHI]). *Am J Cardiol.* 2006;97(5):730–7.
 78. Munger RG, Prineas RJ, Crow RS, Changbumrung S, Keane V, Wangsuphachart V, et al. Prolonged QT interval and risk of sudden death in South-East Asian men. *Lancet.* 1991;338(8762):280–1.
 79. Shah RR. Drug-induced QT interval prolongation: does ethnicity of the thorough QT study population matter? *Br J Clin Pharmacol.* 2013;75(2):347–58.
 80. Seyerle AA, Young AM, Jeff JM, Melton PE, Jorgensen NW, Lin Y, Carty CL, et al. Evidence of heterogeneity by race/ethnicity in genetic determinants of QT interval. *Epidemiology.* 2014;25(6):790–8.
 81. Sedlak T, Shufelt C, Iribarren C, Merz CN. Sex hormones and the QT interval: a review. *J Womens Health (Larchmt).* 2012;21(9):933–41.
 82. Kuiri-Hanninen T, Sankilampi U, Dunkel L. Activation of the hypothalamic-pituitary-gonadal axis in infancy: minipuberty. *Horm Res Paediatr.* 2014;82(2):73–80.
 83. Harman SM, Metter EJ, Tobin JD, Pearson J, Blackman MR. Longitudinal effects of aging on serum total and free testosterone levels in healthy men. Baltimore Longitudinal Study of Aging. *J Clin Endocrinol Metab.* 2001;86(2):724–31.
 84. Hulot JS, Demolis JL, Riviere R, Strabach S, Christin-Maitre S, Funck-Brentano C. Influence of endogenous oestrogens on QT interval duration. *Eur Heart J.* 2003;24(18):1663–7.
 85. Nakagawa M, Ooie T, Takahashi N, Taniguchi Y, Anan F, Yonemochi H, Saikawa T. Influence of menstrual cycle on QT interval dynamics. *Pacing Clin Electrophysiol.* 2006;29(6):607–13.
 86. Burke JH, Ehlert FA, Kruse JT, Parker MA, Goldberger JJ, Kadish AH. Gender-specific differences in the QT interval and the effect of autonomic tone and menstrual cycle in healthy adults. *Am J Cardiol.* 1997;79(2):178–81.
 87. Endres S, Mayuga KA, Cristofaro A, Taneja T, Goldberger JJ, Kadish AH. Menstrual cycle and ST height. *Ann Noninvasive Electrocardiol.* 2004;9(2):121–6.
 88. Rodriguez I, Kilborn MJ, Liu XK, Pezzullo JC, Woosley RL. Drug-induced QT prolongation in women during the menstrual cycle. *JAMA.* 2001;285(10):1322–6.
 89. Dogan M, Yiginer O, Uz O, Kucuk U, Degirmencioglu G, Isilak Z, et al. The effects of female sex hormones on ventricular premature beats and repolarization parameters in physiological menstrual cycle. *Pacing Clin Electrophysiol.* 2016;39(5):418–26.
 90. Yildirim A, Kabakci G, Akgul E, Tokgozoglu L, Oto A. Effects of menstrual cycle on cardiac autonomic innervation as assessed by heart rate variability. *Ann Noninvasive Electrocardiol.* 2002;7(1):60–3.

91. Sato N, Miyake S, Akatsu J, Kumashiro M. Power spectral analysis of heart rate variability in healthy young women during the normal menstrual cycle. *Psychosom Med.* 1995;57(4):331–5.
92. Claydon VE, Younis NR, Hainsworth R. Phase of the menstrual cycle does not affect orthostatic tolerance in healthy women. *Clin Auton Res.* 2006;16(2):98–104.
93. Rosano GM, Leonardo F, Sarrel PM, Beale CM, De Luca F, Collins P. Cyclical variation in paroxysmal supraventricular tachycardia in women. *Lancet.* 1996;347(9004):786–8.
94. Myerburg RJ, Cox MM, Interian A Jr, Mitrani R, Gargis I, Dylewski J, Castellanos A. Cycling of inducibility of paroxysmal supraventricular tachycardia in women and its implications for timing of electrophysiologic procedures. *Am J Cardiol.* 1999;83(7):1049–54.
95. Roden DM. Drug-induced prolongation of the QT interval. *N Engl J Med.* 2004;350(10):1013–22.
96. Du XJ, Riemersma RA, Dart AM. Cardiovascular protection by oestrogen is partly mediated through modulation of autonomic nervous function. *Cardiovasc Res.* 1995;30(2):161–5.
97. Abehsira G, Bachelot A, Badilini F, Koehl L, Lebot M, Favet C, et al. Complex influence of gonadotropins and sex steroid hormones on QT interval duration. *J Clin Endocrinol Metab.* 2016;101(7):2776–84.
98. Boroditsky RS, Reyes FI, Winter JS, Faiman C. Maternal serum estrogen and progesterone concentrations preceding normal labor. *Obstet Gynecol.* 1978;51(6):686–91.
99. Tulchinsky D, Hobel CJ, Yeager E, Marshall JR. Plasma estrone, estradiol, estriol, progesterone, and 17-hydroxyprogesterone in human pregnancy. I. Normal pregnancy. *Am J Obstet Gynecol.* 1972;112(8):1095–100.
100. Dorr HG, Heller A, Versmold HT, Sippell WG, Herrmann M, Bidlingmaier F, Knorr D. Longitudinal study of progestins, mineralocorticoids, and glucocorticoids throughout human pregnancy. *J Clin Endocrinol Metab.* 1989;68(5):863–8.
101. Johansson ED. Plasma levels of progesterone in pregnancy measured by a rapid competitive protein binding technique. *Acta Endocrinol.* 1969;61(4):607–17.
102. Yannone ME, McCurdy JR, Goldfien A. Plasma progesterone levels in normal pregnancy, labor, and the puerperium. II. Clinical data. *Am J Obstet Gynecol.* 1968;101(8):1058–61.
103. Baumert M, Javorka M, Seeck A, Faber R, Sanders P, Voss A. Multiscale entropy and detrended fluctuation analysis of QT interval and heart rate variability during normal pregnancy. *Comput Biol Med.* 2012;42(3):347–52.
104. Lechmanova M, Kittnar O, Mlcek M, Slavicek J, Dohnalova A, Havranek S, et al. QT dispersion and T-loop morphology in late pregnancy and after delivery. *Physiol Res.* 2002;51(2):121–9.
105. Tanindi A, Akgun N, Pabuccu EG, Gursoy AY, Yuce E, Tore HF, Duvan CI. Electrocardiographic P-wave duration, QT interval, T peak to end interval and Tp-e/QT ratio in pregnancy with respect to trimesters. *Ann Noninvasive Electrocardiol.* 2016;21(2):169–74.
106. Carpenter RE, D’Silva LA, Emery SJ, Uzun O, Rassi D, Lewis MJ. Changes in heart rate variability and QT variability during the first trimester of pregnancy. *Physiol Meas.* 2015;36(3):531–45.
107. Luo S, Michler K, Johnston P, Macfarlane PW. A comparison of commonly used QT correction formulae: the effect of heart rate on the QTc of normal ECGs. *J Electrocardiol.* 2004;37 Suppl:81–90.
108. Anneken L, Baumann S, Vigneault P, Biliczki P, Friedrich C, Xiao L, et al. Estradiol regulates human QT-interval: acceleration of cardiac repolarization by enhanced KCNH2 membrane trafficking. *Eur Heart J.* 2016;37(7):640–50.
109. Gowda RM, Khan IA, Mehta NJ, Vasavada BC, Sacchi TJ. Cardiac arrhythmias in pregnancy: clinical and therapeutic considerations. *Int J Cardiol.* 2003;88(2–3):129–33.
110. Shotan A, Ostrzega E, Mehra A, Johnson JV, Elkayam U. Incidence of arrhythmias in normal pregnancy and relation to palpitations, dizziness, and syncope. *Am J Cardiol.* 1997;79(8):1061–4.
111. Buckler H. The menopause transition: endocrine changes and clinical symptoms. *J Br Menopause Soc.* 2005;11(2):61–5.
112. Hee J, MacNaughton J, Bangah M, Burger HG. Perimenopausal patterns of gonadotrophins, immunoreactive inhibin, oestradiol and progesterone. *Maturitas.* 1993;18(1):9–20.
113. Dogan U, Dogan NU, Basarir AO, Yildirim S, Celik C, Incesu F, Ozdemir K. P-wave parameters and cardiac repolarization indices: does menopausal status matter? *J Cardiol.* 2012;60(4):333–7.
114. Lavi S, Nevo O, Thaler I, Rosenfeld R, Dayan L, Hirshoren N, et al. Effect of aging on the cardiovascular regulatory systems in healthy women. *Am J Physiol Regul Integr Comp Physiol.* 2007;292(2):R788–93.
115. Bett GC. Hormones and sex differences: changes in cardiac electrophysiology with pregnancy. *Clin Sci (Lond).* 2016;130(10):747–59.
116. Deecher DC, Dorries K. Understanding the pathophysiology of vasomotor symptoms (hot flushes and night sweats) that occur in perimenopause, menopause, and postmenopause life stages. *Arch Womens Ment Health.* 2007;10(6):247–57.



ECG-Derived Evaluation of Cardiac Repolarization

7

Gioia Turitto and Nabil El-Sherif

Introduction

The resting 12-lead electrocardiogram (ECG) is the oldest tool and the most widely adopted clinical test for detection of heart disease. Today, it is still one of the most useful methods for risk stratification for sudden cardiac death and arrhythmic events. This is based on a large body of experimental and clinical data, which support the contention that both depolarization and repolarization analyses on the 12-lead ECG and its derivatives can provide a measure of arrhythmic risk.

Repolarization is the summation of the intrinsic characteristics of the individual cells ensuing from ion channel properties, channel density and distribution, autonomic modulation, and cell-cell coupling effects. The differences observed in ventricular cells mediate the distinct repolarization times of varying regions in the myocardium, which affect the electrocardiographic T wave [1]. The left ventricle exhibits gradients in repolarization time in both transmural and apicobasal

directions. These gradients, caused by the varying strengths of cellular ionic currents in the different regions, affect the morphology of the electrocardiographic T wave. Abnormal gradients, observed clinically by alterations in the ECG, can increase susceptibility to arrhythmias.

A number of ECG repolarization measures have been identified and assessed in large population studies, as well as in research focused on high-risk cohorts, and will be discussed in this chapter. They include static parameters, such as QT interval duration, as well as dynamic markers, such as QT variability, and computationally derived variables, such as T-wave alternans. The reader is also advised to consult other chapter of this book, for additional discussion of specific methods to assess cardiac repolarization, as well as clinical syndromes associated with cardiac repolarization abnormalities.

QT Interval Duration

In clinical practice, studies on QT and corrected QT (QTc) interval represent archetypal examples of research on abnormal repolarization for the purpose of risk stratification for sudden cardiac death [2]. Since the QT interval shortens with an increasing heart rate, its interpretation requires correction, which can be made using different formulae (Table 7.1). The most popular method is the Bazett's formula, which is given by the QT interval divided by the square root of the RR

G. Turitto (✉)

Cardiac Electrophysiology Services, Department of Medicine, New York-Presbyterian Brooklyn Methodist Hospital, Brooklyn, NY, USA
e-mail: git9006@nyp.org

N. El-Sherif

Department of Medicine and Physiology, State University of New York Downstate Medical Center, VA New York Harbor Healthcare Center, Brooklyn, NY, USA

Table 7.1 Commonly utilized formulae for QT correction

Author	Formula
Bazett	$QT/RR^{1/2}$
Fridericia	$QT/RR^{1/3}$
Framingham	$QT + 0.154 (1000 - RR)$
Hodges	$QT + 105 (1/RR - 1)$

interval. The disadvantage of this method is that QT interval is overestimated at high heart rates and underestimated at low heart rates. Fridericia's formula divides the QT interval by the cubic root of the RR interval and is preferred for slow heart rates. The ESC Guidelines published in 2015 propose an upper normal limit for the QTc interval of 480 msec and a lower limit of 340 msec for both genders [3]. The risk of developing malignant ventricular arrhythmias increases at either extreme of the QT interval, as exemplified by the long and short QT syndromes.

Different genetic types of the long QT syndrome (LQTS) are associated with distinct ECG manifestations, which relate to the type and magnitude of ion channel dysfunction. The QTc duration does not differentiate LQTS types, and therefore other static and dynamic ECG parameters reflecting changes in T-wave morphology are used to describe phenotypic expression of different LQTS genotypes. LQT1 carriers usually have broad-based T waves, LQT2 carriers show low-amplitude T waves with high incidence of notches, and LQT3 carriers frequently have extended ST segment, with relatively narrow peaked T wave [4]. QTc duration was found to predict cardiac events in LQTS. A QTc greater than 470 msec, but especially a QTc greater than 500 msec, was associated with a significant increase in the risk of cardiac events. When analyzing the predictive value of QTc by genotype, there were no differences in risk associated with QTc prolongation among patients with LQT1, LQT2, and LQT3. Furthermore, stratifying this analysis by age, sex, and genotype confirmed that QTc is uniformly predictive for cardiac events and does not have different prognostic significance in tested subgroups [4].

The diagnostic hallmark for the short QT syndrome (SQTS) is a short ECG QT interval on the

12-lead ECG; however, consensus on an appropriate cutoff value and diagnostic criteria sufficient to establish a diagnosis of SQTS have yet to emerge in the literature. The diagnosis of SQTS is further complicated by the presence of an overlapping range of QT intervals between affected cases and apparently healthy subjects. This concept is highlighted in a long-term follow-up study of healthy Finnish individuals with short (<340 msec) and very short (<320 msec) QTc values, who had no documented arrhythmic events after an average follow-up of 29 years [5]. Additional studies examining subjects with short QT intervals from the general population have revealed similarly benign outcomes with no evidence of increased arrhythmic risk. These findings suggest that the presence of a short QT interval in isolation is not always predictive of an increased arrhythmic risk and therefore should not invariably lead to a diagnosis of SQTS [6]. On the other hand, an abnormal QTc interval on a resting 12-lead ECG has not been found to be independently correlated with mortality or arrhythmic outcomes in patients with myocardial infarction or with left ventricular dysfunction [7].

Beyond QT Interval Duration

Several novel indices of abnormal repolarization have been proposed during the past two decades (Table 7.2). While some have been validated in clinical practice, only a handful of data is available on the clinical usefulness of other parameters. The impetus for this research stemmed from the recognition that QTc provided no information on the heterogeneity of repolarization across the heart, yet the presence of such heterogeneity in repolarization may elevate arrhythmic risk. This can occur when prolongation of the action potential duration is nonuniform across the myocardium. These limitations of QTc in predicting malignant ventricular arrhythmias and sudden cardiac death have led to the development of additional markers, such as QT dispersion (QTD), the interval from the peak to the end of the T-wave (Tpeak-Tend), and Tpeak-Tend/QT ratio, among others [2].

Table 7.2 Commonly used variables to quantify cardiac repolarization abnormalities

Variable	Definition	Experimental correlate
Corrected QT interval	QT interval duration corrected for heart rate	Action potential duration (APD)
QT dispersion	Difference between the maximum and minimum QT intervals measured on all 12 ECG leads	Spatial differences in APD values
Tpeak-Tend	Interval from the peak of the T wave to its offset	Spatial dispersion of repolarization (DR)
Tpeak-Tend/QT	Interval from the peak to the end of the T wave divided by QT interval	DR divided by APD
QT dynamicity	Slope of the linear regression of QT/RR	Temporal APD variations
QT variability	$SDQT$ standard deviation of QT intervals	Temporal APD variations
T-wave alternans	T-wave duration difference between alternate beats at the microvolt level	APD alternans

Experimental work has suggested that QTD showed a significant correlation with dispersion of monophasic action potential. QTD is calculated as the difference between the maximum and minimum QT intervals measured on all 12 leads of the ECG. Reported values of QTD vary widely, with studies showing normal values between 10 and 71 msec, with a mean value of 33 msec. In otherwise healthy individuals, QTD values >58 and >80 msec were shown to increase the risk of cardiovascular mortality by three- and fourfold, respectively, when compared with subjects with QTD values <30 msec [2]. Other authors have argued, however, that elevated values for QTD may largely be due to the unreliable localization of the T-wave offset in patients with abnormal T waves [8].

Tpeak-Tend is calculated by measuring the interval from the peak of the T wave to its offset. The offset of the T wave is frequently defined as the intersection of the tangent to the steepest portion of the terminal portion of the T wave and the

isoelectric line [2, 8]. It was initially suggested as a marker for transmural dispersion of repolarization, based on observations in coronary-perfused canine wedge preparations that the end of repolarization at the epicardium coincided with the Tpeak and at the M-cells coincided with Tend. Subsequent experiments showed that Tpeak coincided not with full epicardial repolarization but rather with the earliest end of repolarization, whereas Tend coincided with the latest end of repolarization rather than full M-cell repolarization. In other words, Tpeak-Tend may be a marker for global, rather than transmural, dispersion of repolarization [2]. Validation of Tpeak-Tend as a direct measure of transmural dispersion of repolarization is still debated, but most studies agree that Tpeak-Tend provides at least some measure of spatial dispersion or repolarization heterogeneity. A prolonged Tpeak-Tend may be seen in patients with LQTS1 and LQTS2, as well as in patients with SQTS and Brugada syndrome. Furthermore, Tpeak-Tend predicted mortality in both ST elevation and non-ST elevation myocardial infarction [2]. Additionally, repolarization heterogeneity, as measured by Tpeak-Tend, may be associated with adverse outcomes, including mortality, in the general population [8]. Other investigators have proposed dividing Tpeak-Tend by the QT interval. This yields the Tpeak-Tend/QT ratio, which has a relatively constant normal range between 0.17 and 0.23. Theoretically, an increased ratio represents a higher dispersion of repolarization, which should be proarrhythmic; its predictive value for arrhythmic events remains controversial [9].

Dynamic Changes in QT Interval

An important component of arrhythmogenesis relates to dynamic changes in cardiac repolarization, which may lead to increased vulnerability to ventricular arrhythmias. Several kinds of software have been developed in order to continuously analyze the QT interval from 24-hour ECG recordings. Compared to the ECG static evaluation, dynamic assessment of ventricular repolarization allows the analysis of the relationship between the duration of the QT interval and heart

rate changes [10]. The most studied dynamic measures of abnormal repolarization on 24-hour ECG are QT dynamicity and QT variability [2, 7, 11]. The automatic assessment of QT dynamicity is based on the measure of: QT apex (QTa, the interval between the Q wave start and the T wave apex), and QT end (QTe, the interval between the Q wave start and the T wave end). QT dynamicity is generally assessed on 24-hour ECG recordings, which are analyzed by a specific software able to automatically calculate, in a template of 30 sec, the QTa, the QTe, and the corresponding RR interval. By interpolating each measure, the software also computes the slopes of the linear regressions between QTe and QTa and the corresponding RR interval. QT-RR slope is considered an index of QT dynamicity related to arrhythmic events.

Whereas QT dynamicity is based on the analysis of QT/RR relationship, QT variability is based on the analysis of beat-to-beat changes in duration and morphology of ventricular repolarization. QT variability can be measured during a short recording (256 sec or 30 beats) or over a 24-hour period, distinguishing short-term from long-term variability. Dedicated QT variability measurement techniques match complete or partial ECG waveforms with one or several templates, either user defined or automatically computed [11]. Several studies have demonstrated the independent predictive value of QT variability for risk stratification for sudden cardiac death; however, most of the evidence is based on retrospective data analyses. Prospective trials are needed to prove the usefulness of QT variability. Additionally, cutoff values or hazard ratios need to be defined for QT variability to become an integral part of risk stratification strategies [7, 11].

Periodic repolarization dynamics is a novel ECG phenomenon that refers to previously unknown oscillations of cardiac repolarization instability. Those oscillations take place in the low-frequency range (< 0.1 Hz), occur independently from underlying heart rate variability, and can be assessed by means of a multipolar high-resolution resting ECG. Although the exact mechanisms still need to be identified, electro-

physiological and other studies indicated that periodic repolarization dynamics most likely reflects the effect of phasic sympathetic activation on the myocardial cells. Periodic repolarization dynamics has been shown to be a significant predictor of mortality in cohorts of postinfarction patients with either preserved or reduced left ventricular ejection fraction [12].

The most recent electrocardiographic marker for cardiac repolarization abnormalities, T-wave area dispersion, is a measure of repolarization heterogeneity, obtained by assessing interlead T-wave areas during a single cardiac cycle. The ability of this marker to identify patients at risk for sudden cardiac death in the general population was recently tested. Low T-wave area dispersion, reflecting increased heterogeneity of repolarization, in standard 12-lead resting ECGs, was shown to be a powerful and independent predictor of sudden cardiac death in the adult general population, when assessed in the Health 2000 Study—an epidemiological survey representative of the Finnish adult population. Independent replication was performed in 3831 participants of the KORA S4 Study (Cooperative Health Research in the Region of Augsburg) [13].

According to the American Heart Association/American College of Cardiology Foundation/Heart Rhythm Society Scientific Statement on Noninvasive Risk Stratification Techniques for Identifying Patients at Risk for Sudden Cardiac Death, the present data do not support the use of QT interval, QT dispersion, or QT-interval variability for risk stratification for sudden cardiac death in patients without the long QT syndrome. This statement may not apply to the more recent risk stratification techniques based on cardiac repolarization analysis, but there is no definite conclusion about the usefulness of such techniques for screening of the general population or cohorts at high risk [14].

T-Wave Alternans

Microvolt T-wave alternans (TWA) was deemed to be a promising measure of dynamic electrical instability. The value of TWA in estimating risk

for cardiovascular mortality and sudden cardiac death is based on the assessment of the degree of heterogeneity of repolarization and of abnormalities in intracellular calcium cycling, which provoke a beat-to-beat alternation of action potential duration culminating in alternating changes in the size and shape of the T wave. TWA can be either spatially concordant, when action potentials in neighboring cell regions alternate in phase, or discordant, when they are out of phase. The transition from concordant to discordant TWA is likely a harbinger of increased risk for malignant arrhythmias [15]. The association of TWA with spatiotemporal heterogeneity of repolarization (i.e., transient or lasting repolarization differences among neighboring myocardial regions) is supported by a number of investigations, including in vitro optical mapping, intact large animal experimental laboratory studies, computer simulations, and clinical studies [16].

Two main techniques have been commercialized to measure microvolt levels of TWA for risk stratification for sudden cardiac death: the spectral method and the modified moving average (MMA) method [15, 16]. TWA is a rate-dependent phenomenon that can be assessed by exercise testing or by evaluating spontaneous changes during 24-hour ECG recording. In the spectral method, which requires the patient to achieve a target heart rate of 105–110/min, a composite power spectrum of the ST–T segment amplitude fluctuations is formed by applying fast Fourier transform technique to the beat-to-beat series of amplitude measurements along the JT interval in 128 consecutive QRS-aligned ECG complexes [17]. The alternans voltage is defined as the square root of the spectral power occurring at the alternans frequency (0.5 cycles/beat) after noise reduction, which corresponds to the difference in voltage between the overall average beat and either the averaged even or odd-numbered beat (i.e., half of the difference between the averaged even and odd beats). A TWA level $\geq 1.9 \mu\text{V}$ with sufficient signal-to-noise ratio for >2 min is defined as a positive test result, while a TWA level $< 1.9 \mu\text{V}$ is considered negative. However, as the spectral method requires a stable target

heart rate to be achieved, a relatively large proportion (approximately 20–40%) of tests are classified as “indeterminate,” either due to patient-related factors such as failure to achieve the target heart rate, excessive ventricular ectopy, atrial fibrillation, or non-sustained TWA or technical problems such as noise in the recording.

The MMA method is time-domain based and employs recursive averaging. The algorithm continuously streams odd and even beats into separate bins and creates averaged complexes for both bins. These complexes are then superimposed, and the maximum difference between the odd and even complexes at any point within the JT-segment is averaged for every 10 or 15 seconds and reported as the TWA value. The MMA method allows TWA analysis during routine exercise stress testing and also during 24-hour ECG recordings. Risk stratification is based on the peak TWA value using the MMA; cutoff levels of $\geq 47 \mu\text{V}$ and $\geq 60 \mu\text{V}$ have been most commonly used to define abnormal and severely abnormal TWA, respectively [18]. The four- to tenfold difference in TWA voltage output between the two methods can be accounted for largely by differences in the degree of signal averaging and filtering. Another factor accounting for the lower values reported by the spectral method as compared to MMA is that with the former, the average TWA value across the ST–T wave is calculated, whereas with the latter, the peak TWA value is provided.

Microvolt TWA has been associated with cardiovascular mortality and sudden cardiac death in several clinical studies involving several thousand subjects with reduced as well as preserved left ventricular function. Although TWA appears to be a useful marker of susceptibility for lethal ventricular arrhythmias and cardiovascular death, so far there is no sufficient evidence from randomized clinical trials to support its use in guiding therapy. In particular, the use of TWA was proposed to select patients with a reduced left ventricular ejection fraction, who may be unlikely to benefit from implantation of a cardioverter-defibrillator, in the presence of a negative TWA, but this has not been validated [15, 16, 18].

J-Wave Syndromes: ECG Characteristics

Early repolarization, Brugada syndrome, and pathologic J waves have been described for decades, but only recently experimental and clinical data have allowed reconciliation of Brugada and early repolarization under the common definition of J-wave syndromes [19]. The J-wave syndromes are so named because they involve accentuation of the electrocardiographic J wave. Experimental evidence indicates that the J wave is inscribed as a consequence of a transmural voltage gradient caused by the manifestation of an action potential notch in the epicardium but not in the endocardium, due to a heterogeneous transmural distribution of the Ito current. The region generally most affected in Brugada syndrome is the anterior right ventricular outflow tract; in early repolarization, it is the inferior region of the left ventricle. As a consequence, Brugada syndrome is characterized by accentuated J waves appearing as a coved-type ST-segment elevation in the right precordial leads V1-V3, whereas early repolarization is characterized by J waves, notch or slur of the terminal part of the QRS, and ST-segment or Jp elevation >0.1 mV in ≥ 2 contiguous leads, in the lateral (type I), inferolateral (type II), or inferolateral + anterior or right ventricular leads (type III), with the peak of an end QRS notch and/or the onset of an end QRS slur being designated as Jp [19, 20]. An early repolarization pattern is often encountered in ostensibly healthy individuals, particularly in young males, black individuals, and athletes. Such pattern may also be observed in acquired conditions, including hypothermia and ischemia. When associated with malignant ventricular arrhythmias in the absence of organic heart disease, the early repolarization pattern is referred to as early repolarization syndrome.

According to the 2013 Consensus statement on inherited cardiac arrhythmias and the 2015 Guidelines for the management of patients with ventricular arrhythmias and prevention of sudden cardiac death, Brugada syndrome is diagnosed in patients with type 1 ECG features, i.e., coved

ST-segment elevation ≥ 2 mm in ≥ 1 lead among the right precordial leads V1 and V2, positioned in the 2nd, 3rd, or fourth intercostal space, occurring either spontaneously or after provocative drug test with intravenous administration of Class I antiarrhythmic drugs [19]. Brugada syndrome is diagnosed in patients with type 2 or type 3 ECG features, only when a provocative drug test with intravenous administration of Class I antiarrhythmic drugs induces a type 1 ECG morphology. Type 2 is characterized by ST-segment elevation of ≥ 0.5 mm (generally ≥ 2 mm in V2) in ≥ 1 right precordial lead (V1-V3), followed by a convex ST. The ST segment is followed by a positive T wave in V2 and variable morphology V1. Type 3 is characterized by either a saddleback or coved appearance with an ST-segment elevation of <1 mm. The placement of the right precordial leads in more cranial positions (in the third or second intercostal space) in a 12-lead resting ECG or 12-lead Holter ECG increases the sensitivity of the ECG. It is recommended that ECG recordings be obtained in standard and superior positions for the V1 and V2 leads.

The cellular mechanisms underlying the J-wave syndrome have long been a matter of debate. In the case of Brugada syndrome, two principal hypotheses have been advanced: (1) the repolarization hypothesis, proposing that an outward shift in the balance of currents in right ventricular epicardium can lead to repolarization abnormalities resulting in the development of phase 2 reentry, which generates closely coupled premature beats capable of precipitating polymorphic ventricular tachycardia/fibrillation, and (2) the depolarization hypothesis, suggesting that slow conduction in the right ventricular outflow tract, secondary to fibrosis, plays a primary role in the development of the electrocardiographic and arrhythmic manifestations of the syndrome [19].

Conclusion

The standard ECG is a potentially attractive tool for large-scale screening and risk assessment,

due to its relative low cost and ubiquitous availability [7]. It is increasingly apparent that repolarization heterogeneity is present in a variety of cardiovascular diseases and syndromes and may also be predictive of sudden cardiac death in the general population [8]. However, at the present time, there is no consensus on how to best measure repolarization heterogeneity in human subjects. Currently available ECG techniques are still seldom used in clinical practice, partly due to their unclear diagnostic accuracy, as well as to the lack of consensus about the appropriate computational signal processing implementation [8, 21, 22].

References

1. Antzelevitch C. Transmural dispersion of repolarization and the T wave. *Cardiovasc Res.* 2001;50(3):426–31.
2. Tse G, Yan BP. Traditional and novel electrocardiographic conduction and repolarization markers of sudden cardiac death. *Europace.* 2017;19(5):712–21.
3. Priori SG, Blomström-Lundqvist C, Mazzanti A, Blom N, Borggrefe M, Camm J, et al. 2015 ESC Guidelines for the management of patients with ventricular arrhythmias and the prevention of sudden cardiac death: The Task Force for the Management of Patients with Ventricular Arrhythmias and the Prevention of Sudden Cardiac Death of the European Society of Cardiology (ESC) Endorsed by: Association for European Paediatric and Congenital Cardiology (AEPC). *Europace.* 2015;17(11):1601–87.
4. Zareba W. Genotype-specific ECG patterns in long QT syndrome. *J Electrocardiol.* 2006;39(4 Suppl):S101–6.
5. Anttonen O, Junttila MJ, Rissanen H, Reunanen A, Viitasalo M, Huikuri HV. Prevalence and prognostic significance of short QT interval in a middle-aged Finnish population. *Circulation.* 2007;116(7):714–20.
6. Gollob MH, Redpath CJ, Roberts JD. The short QT syndrome: proposed diagnostic criteria. *J Am Coll Cardiol.* 2011;57(7):802–12.
7. Deyell MV, Krahn AD, Goldberger JJ. Sudden cardiac death risk stratification. *Circ Res.* 2015;116(12):1907–18.
8. Prener SB, Shah SJ, Goldberger JJ, Sauer AJ. Repolarization heterogeneity: beyond the QT interval. *J Am Heart Assoc.* 2016;5(5):e003607.
9. TSE G, Wong CW, Gong M-Q, Meng L, Letsas KP, Li G-P, et al. Meta-analysis of T-wave indices for risk stratification in myocardial infarction. *J Geriatr Cardiol.* 2017;14(12):776–9.
10. Monitillo F, Leone M, Rizzo C, Passantino A, Iacoviello M. Ventricular repolarization measures for arrhythmic risk stratification. *World J Cardiol.* 2016;8(1):57–73.
11. Baumert M, Porta A, Vos MA, Malik M, Couderc JP, Laguna P, et al. QT interval variability in body surface ECG: measurement, physiological basis, and clinical value: position statement and consensus guidance endorsed by the European Heart Rhythm Association jointly with the ESC Working Group on Cardiac Cellular Electrophysiology. *Europace.* 2016;18(6):925–44.
12. Rizas KD, McNitt S, Hamm W, Massberg S, Kääh S, Zareba W, Couderc JP, et al. Prediction of sudden and non-sudden cardiac death in post-infarction patients with reduced left ventricular ejection fraction by periodic repolarization dynamics: MADIT-II substudy. *Eur Heart J.* 2017;38(27):2110–8.
13. Kenttä TV, Sinner MF, Nearing BD, Freudling R, Porthan K, Tikkanen JT, et al. Repolarization heterogeneity measured with T-wave area dispersion in standard 12-lead ECG predicts sudden cardiac death in general population. *Circ Arrhythm Electrophysiol.* 2018;11(2):e005762.
14. Goldberger JJ, Cain ME, Hohnloser SH, Kadish AH, Knight BP, Lauer MS, et al. American Heart Association/American College of Cardiology Foundation/Heart Rhythm Society Scientific Statement on Noninvasive Risk Stratification Techniques for Identifying Patients at Risk for Sudden Cardiac Death. A scientific statement from the American Heart Association Council on Clinical Cardiology Committee on Electrocardiography and Arrhythmias and Council on Epidemiology and Prevention. *J Am Coll Cardiol.* 2008;52(14):1179–99.
15. Verrier RL, Malik M. Quantitative T-wave alternans analysis for guiding medical therapy: an under-exploited opportunity. *Trends Cardiovasc Med.* 2015;25(3):201–13.
16. Verrier RL, Klingenhoben T, Malik M, El-Sherif N, Exner D, Hohnloser SH, et al. Microvolt T-wave alternans: physiologic basis, methods of measurement, and clinical utility. Consensus guideline by the International Society for Holter and Noninvasive Electrocardiology. *J Am Coll Cardiol.* 2011;58(13):1309–24.
17. Turitto G, Caref EB, El-Attar G, Helal M, Mohamed A, Pedalino RP, et al. Optimal target heart rate for exercise-induced T-wave alternans. *Ann Noninv Electrocardiol.* 2001;6(2):123–8.
18. Aro AL, Kenttä TV, Huikuri HV. Microvolt T-wave alternans: where are we now? *Arrhythm Electrophysiol Rev.* 2016;5(1):37–40.
19. Antzelevitch C, Yan GX, Ackerman MJ, Borggrefe M, Corrado D, Guo J, et al. J-wave syndromes expert consensus conference report: emerging concepts and gaps in knowledge. *Europace.* 2017;19(4):665–94.

20. Patton KK, Ellinor PT, Ezekowitz M, Kowey P, Lubitz SA, Perez M, et al. Electrocardiographic early repolarization. A scientific statement from the American Heart Association. *Circulation*. 2016;133(15):1520–9.
21. Gimeno-Blanes FJ, Blanco-Velasco M, Barquero-Perez O, Garcia-Alberola A, Rojo-Alvarez JL. Sudden cardiac risk stratification with electrocardiographic indices -a review on computational processing, technology transfer, and scientific evidence. *Front Physiol*. 2016;7:82.
22. El-Sherif N, Boutjdir M, Turitto G. Sudden cardiac death in ischemic heart disease: pathophysiology and risk stratification. *Card Electrophysiol Clin*. 2017;9(4):681–91.

Part II

Pathophysiology, Molecular Biology, and Clinical Aspects of Long QT Syndromes



Genotype-Phenotype Correlation in Congenital LQTS: Implications for Diagnosis and Risk Stratification

Ilan Goldenberg

Overview

The hereditary long QT syndrome (LQTS) is a genetic channelopathy with variable penetrance and expressivity. Clinically, LQTS is recognized by abnormal QT interval prolongation on the ECG and is associated with increased risk of polymorphic ventricular tachycardia, syncope, and sudden cardiac death (SCD). It has an estimated prevalence of 1:2000 to 1:5000 [1, 2]. Mutations in the three genes *KCNQ1*, *KCNH2*, and *SCN5A* underlying LQT1, LQT2, and LQT3, respectively, account for about 95% of patients with an identified genetic cause, although mutations in a total of 17 genes have been reported to cause LQTS [1–4]. Prior studies by our group and others have investigated the phenotype-genotype relationship regarding clinical presentation, electrocardiogram (ECG) patterns, risk stratification for cardiac events, and therapy [1, 3, 5–10]. LQT1 and LQT2 genotypes caused by potassium ion-channel dysfunction account for about 80–85% of the reported LQTS cases, whereas LQT3, caused by impaired closing of the cardiac sodium channel, accounts for about 5–13% of LQTS patients [2, 4]. In 1995 [10], we provided the first evidence for a significant phenotype-genotype relationship in LQT1,

LQT2, and LQT3 patients of ECG repolarization morphology describing a normal broad-based T-wave morphology in LQT1 patients, flat and frequently notched T waves in LQT2 patients, and a delayed and peaked T wave in LQT3 patients. Subsequently, we have shown a significant relationship between LQTS genotype and risk of cardiac events in LQT1–3 patients, with the lethality of cardiac events (likelihood of dying suddenly during the first syncopal episode) being fivefold higher in LQT3 than in LQT1 and LQT2 patients [1]. Accordingly, an understanding of the relationship between the genotype and phenotype characteristics of LQTS can lead to improved risk stratification and management of this hereditary arrhythmogenic disorder. However, there is substantial variation within LQT subtypes even within families segregating the same variants in penetrance and expression of disease and important sex differences in the clinical course of the disease, prompting a search for disease-modifying factors.

Genetics and Molecular Mechanisms

Genetic Forms of LQTS

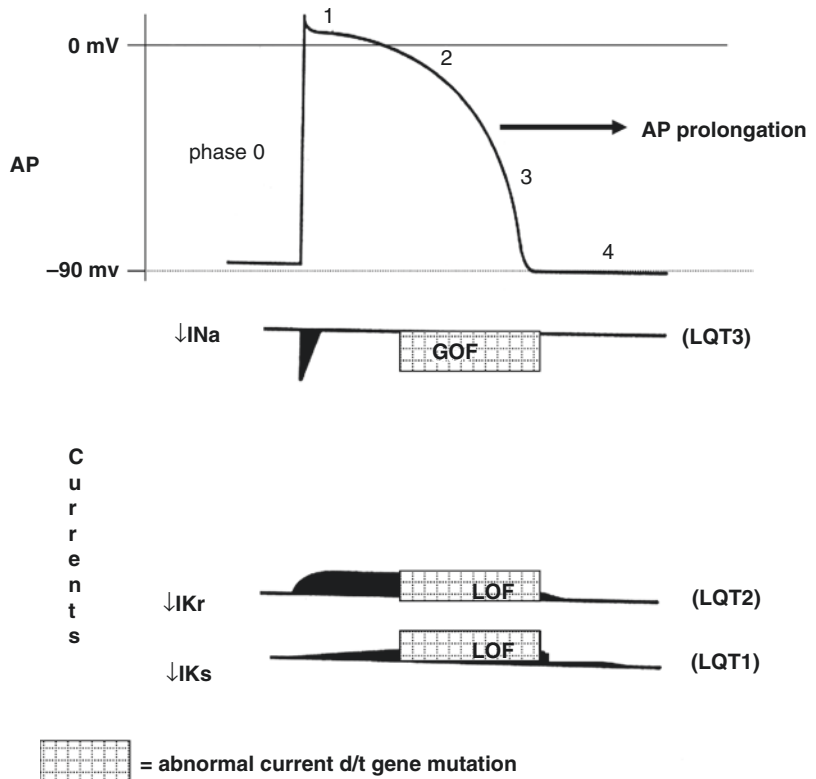
To date, more than 600 mutations have been identified in 17 LQTS genes. The LQT1, LQT2, and LQT3 genotypes comprise more than 95% of the patients with genotype-positive LQTS and

I. Goldenberg (✉)
Cardiology Division, Clinical Cardiovascular
Research Center, University of Rochester Medical
Center, Rochester, NY, USA
e-mail: Ilan.Goldenberg@heart.rochester.edu

Table 8.1 Mutations in ion-channel genes causing the main types long QT syndrome

Genotype	Chromosome	Affected gene	Channel protein	Ion-channel current	Frequency in mutation-identified LQTS patients
LQT1	11	KCNQ1 (Kv7.1)	4 α -subunits each with 6 membrane-spanning segments	$\downarrow I_{Ks}$	45%
LQT2	7	KCNH2 (hERG) (Kv11.1)	4 α -subunits each with 6 membrane-spanning segments	$\downarrow I_{Kr}$	45%
LQT3	3	SCN5A (Na _v 1.5)	1 α -subunit with 24-membrane spanning segments	\uparrow late I _{Na}	7%

Fig. 8.1 Schematic diagram of the influence of altered ion-channel currents on the action potential duration in LQTS. Inward currents are indicated below the line and outward currents above the line. The hatched rectangles denote the timing location of the effect of mutations in LQT1, LQT2, and LQT3 genes on sodium and potassium ion-channel currents. The action potential is prolonged (horizontal arrow) when there is inappropriate gain of function (GOF) in late sodium current I_{Na} or loss of function (LOF) in slowly (I_{Ks}) or rapidly (I_{Kr}) acting repolarizing potassium currents



approximately 75% of all patients with LQTS (Table 8.1) [4, 11]. The most common pattern of inheritance of LQTS is autosomal dominant (Romano-Ward syndrome), but there is also an autosomal recessive form of inheritance. The presence of two mutations in either the KCNQ1 (LQT1) or KCNE1 (LQT5) gene results in the Jervell and Lange-Nielsen syndrome, a severe form of LQTS with sensory hearing loss. Mutations in LQTS genes affect different ion channels and produce gain or loss of function that determine phenotypic manifestations of the disease. Most commonly, QT prolongation arises from either a decrease in repolarizing potassium

current during phase 3 of the action potential (“loss of function”) or a prolonged depolarization due to late inward entry into the myocyte sodium or calcium current (“gain of function”) (Fig. 8.1) [11].

LQTS type 1 (LQT1) is caused by a mutation in the KCNQ1 gene leading to dysfunction of the KvLQT1 potassium channel and reduction in the slowly repolarizing cardiac potassium current (I_{Ks}) (Fig. 8.1). The mutations associated with the KCNQ1 genes act mainly through a dominant-negative mechanism when the normal and mutant subunits create the defective channel protein resulting in dysfunctional channel with more

than 50% reduction in the channel current. The other common biophysical mechanism leading to decreased potassium current is haploinsufficiency in which potassium channel mutant subunits are incapable in co-assembling with the normal subunits to form a tetramer channel. Therefore, only subunits encoded by a normal allele form a functional channel resulting in 50% or less reduction in channel function [4].

In LQTS type 2 (LQT2), a mutation in the *KCNH2* gene leads to dysfunction of the hERG potassium channel and reduction in the rapidly repolarizing cardiac potassium current (I_{Kr}) (Fig. 8.1).

LQTS type 3 (LQT3) is caused by a mutation in the *SCN5A* gene leading to dysfunction of the Nav1.5 protein, increasing the cardiac sodium current influx (I_{Na}) (Fig. 8.1). Reduced repolarizing potassium current or increase in the late sodium current leads to prolongation of the ventricular action potential and early afterdepolarizations, which are the potential triggers for ventricular tachyarrhythmias [11].

LQTS types 4–17 are rare, representing less than 5% of patients with genotype-positive LQTS (Table 8.2). These include (1) mutation in the *KCNJ2* gene results in a reduction in Kir2.1 current, QT prolongation, and a phenotype dominated by skeletal abnormalities (Andersen-Tawil syndrome) (LQT7) [12]; (2) mutation in the *CACNA1C* gene results in an increase in $Ca_v1.2$ current, QT prolongation, and a phenotype characterized by syndactyly in both hands and feet and multiorgan dysfunction (Timothy syndrome)

(LQT8) [13]; and (3) mutation in the *SCN4B* gene (LQT10), one of the β -subunits of *SCN5A*, results in an increase late entry of sodium current into the cell with associated QT prolongation [14].

It is now appreciated that mutations in non-ion-channel genes can affect ion-channel currents with resultant prolongation in ventricular repolarization and the QT interval. LQT4 is caused by mutations in the ankyrin-B gene [15] that produces a protein that functions as a cytoskeletal membrane adapter and is involved in the cellular organization of the sodium pump, the sodium/calcium exchanger, and the inositol-1,4,5-triphosphate receptors [16]. Mutations in caveolin-3 have been labeled LQT9 [17]. Electrophysiologic studies have revealed altered gating kinetics in the cardiac sodium channel with resultant increase in sustained late sodium current ($Na_v1.5$) probably due to direct protein-protein interactions [18]. Thus, LQT4 and LQT9 may be considered “channelopathy-related disorders” (Table 8.2), and it is likely that mutations in other channelopathy-related genes will be identified in the future to account for some of the 25% or so LQTS patients who are negative for mutations in the eight classical channelopathy genes.

Ion-Channel Structure and Function

Ion channels are formed by transcription of exonic DNA from the gene into mRNA with translation into a sequence of amino acids that make up channel protein subunits [4, 11]. The subunits are co-assembled into a structural channel protein that is transported to the cell surface through a process called trafficking. The protein is then anchored into the myocyte membrane so it can function as an ion channel. The protein channel undergoes controlled degradation and appropriate replacement. Thus, a mutation in the genetic DNA can produce an abnormal or deficient ion channel through a variety of processes that may include altered subunit assembly, trafficking deficiencies, impaired anchoring of the channel in the myocyte membrane, abnormal amino acid sequence in the protein channel, or an imbalance in the degradation-formation rates of

Table 8.2 Mutations in ion-channel genes causing the rare types of long QT syndrome

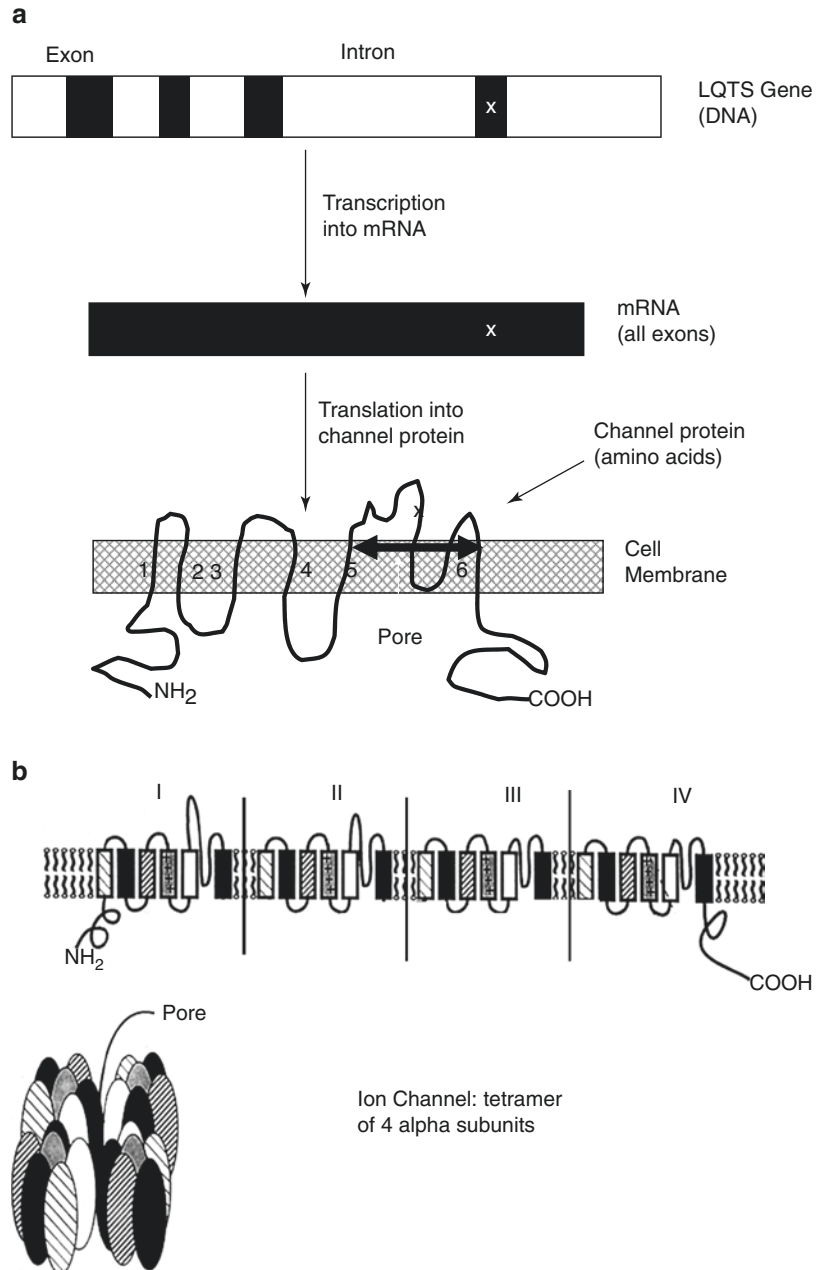
Gene ^{1,2,3}	LQTS phenotype	Comments
<i>AKAP9</i>	LQTS type 11	Limited
<i>ANK2</i>	LQTS type 4	<1%
<i>CACNA1C</i>	LQTS type 8	<1%
<i>CALM1</i>	LQTS type 14	<1%
<i>CALM2</i>	LQTS type 15	<1%
<i>CAV3</i>	LQTS type 9	<1%
<i>KCNE1</i>	LQTS type 5	<1%
<i>KCNE2</i>	LQTS type 6	<1%
<i>KCNJ2</i>	LQTS type 7	<1%
<i>KCNJ5</i>	LQTS type 13	<1%
<i>SCN4B</i>	LQTS type 10	Limited
<i>SNTA1</i>	LQTS type 12	<1%

the channel protein [4, 11]. Trafficking deficiencies are especially common in LQTS patients with mutations in the *KCNH2* (*LQT2*) gene [19].

The putative topology of each voltage-gated cardiac ion channel consists of a pore-forming α -subunit and one or more attached β -subunits. The protein structures of the α -subunits of the *LQT1* and *LQT2* potassium channels (*KCNQ1*,

KCNH2) are similar and consist of a series of amino acids with an N-terminus region, six membrane-spanning segments (S1–S6) with connecting intracellular cytoplasmic loops (S2–S3 and S4–S5) and a pore area (S5-loop-S6), and a C-terminus region (Fig. 8.2a). Four α -subunits join together to form a tetrameric potassium channel around a central pore (Fig. 8.2b). The

Fig. 8.2 (a) Schematic diagram of ion-channel formation. Exons (black) are transcribed into messenger RNA (mRNA) that translates the information into a channel protein involving a chain of amino acids consisting of an N-terminus region, six membrane-spanning segments, and a C-terminus region. The pore area is located between the fifth and sixth membrane-spanning segments. The X in the *LQTS* gene denotes a DNA mutation that appears as an altered amino acid sequence in the channel protein. (b) Schematic topology of a prototypic α -subunit of a potassium channel with six membrane-spanning segments. Four α -subunits (I–IV) join together to form a tetrameric potassium channel around a central pore



LQT3 sodium channel (SCN5A) consists of a single protein involving four conjoined, homologous repeat α -subunits (24 membrane-spanning segments) assembled around a central permeation pathway plus one β -subunit. The LQT7 potassium channel (KCNJ2) is a simpler channel with just two transmembrane segments that embrace a pore region. The LQT8 calcium channel (CACNA1C) consists of α_1 -subunit (24 membrane-spanning segments) plus four subunits. The voltage gating, selectivity filter, inactivation plugging of the pore, role of the N- and C-terminus regions, and the modifying function of the attached subunits vary among and between the potassium, sodium, and calcium ion channels resulting in their unique and specific functional characteristics. Resolution X-ray crystallographic analysis of the ion channels has provided unique insight into the structural alterations associated with specific ion-channel mutations. It is clear from the complexity of the structure of the individual ion channels that LQTS mutations that result in altered amino acid sequences in various portions of the structural ion-channel protein can have a spectrum of effects on the channel function with mild to severe alterations in ion-channel kinetics and the phenotypic manifestations of the disorder.

Diagnosing LQTS Patients

QTc Duration in Standard 12-Lead ECG

An LQTS patient may present with a QTc interval duration that is in the normal range, borderline, or prolonged, following the criteria proposed by Moss and Robinson [5, 20]: normal QTc (<440 ms in children 1–15 years old, <430 ms in adult males, and <450 ms in adult females); borderline QTc (440–460 ms in children 1–15 years old, 430–450 ms in adult males, and 450–470 ms in adult females); and prolonged QTc (>460 ms in children 1–15 years old, >450 ms in adult males, and >470 ms in adult females). The values of QTc (corrected using Bazett's formula) are gender and age dependent with adult women and

children showing longer values than male adults [20]. Rautaharju et al. [21] studied over 13,000 subjects representing both males and females across ages from birth till elderly, and they demonstrated that heart rate decreasing with age in males at the time of puberty contributes to gender-related difference in QTc values. The changes in heart rate (and consequently in QTc) were observed between ages 17 and 55 years, whereas in younger individuals and in individuals >55 years of age, both heart rate and QTc values were similar in both males and females, indicating the potential underlying role of sex hormones.

The major challenge of LQTS diagnosis is related to the substantial overlap observed in genetically affected and unaffected individuals. In 1991, Vincent et al. [22] demonstrated that QTc durations ranging from 410 to 470 ms may be observed among both carriers and noncarriers in LQT1 families. This substantial overlap relates to a number of factors, including varying penetrance of genes, possible effect of modifying genes, and inadequacy of the Bazett's correction formula that overcorrects QTc duration during slower heart rates that are frequently observed in LQTS patients. With increasing knowledge regarding the genetic types of LQTS, we are learning that about 50% of carriers and noncarriers may present with QTc in the gray-zone range. These patients are particularly difficult to diagnose. Such patients may benefit from analyses of multiple ECG recordings (if available), for they may show consistency of QTc prolongation or clear evidence of QTc prolongation at somewhat faster heart rates.

The diagnosis of LQTS based on QTc duration is particularly difficult in newborns. The question whether a newborn child inherited the disease is crucial for parents and for physicians taking care of LQTS families. As demonstrated by Schwartz et al. [23], healthy newborns up to about 1 month of age frequently show a QTc interval duration that exceeds 470 ms, partially due to immaturity of the ion channels but also because Bazett's formula may overestimate QTc at fast heart rates in the newborn. Fridericia's formula works somewhat better at fast heart rates.

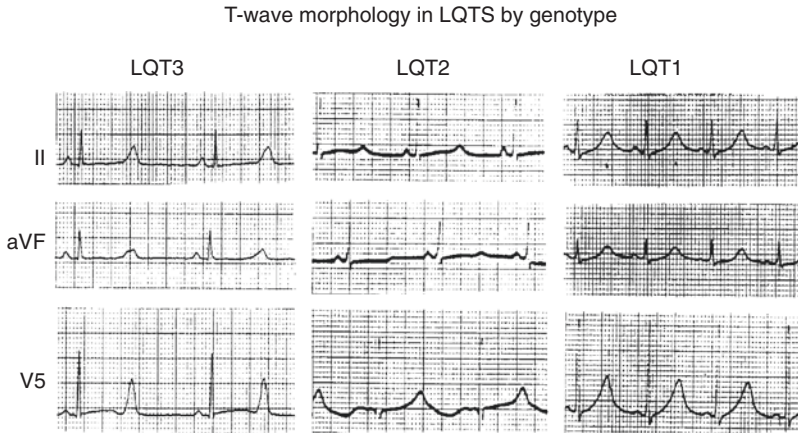


Fig. 8.3 ECG recordings from leads II, aVF, and V5 from patients with LQT1, LQT2, and LQT3. The three LQTS genotypes are each associated with QT prolongation, yet the morphologic patterns are distinctively different. LQT1 is associated with a broad-based prominent T

wave, LQT2 with low-amplitude T wave, and LQT3 with a prolonged isoelectric ST segment before the inscription of a large, somewhat peaked, T wave. (Reproduced with permission from Moss et al. [10])

T-Wave Morphology

In 1995, Moss et al. [10] evaluated the relationship between T-wave morphology and genotype and, as shown in Fig. 8.3, specific patterns were associated with distinct genetic types of the disorder. LQT1 was found to be associated with wide, broad-based T waves, LQT2 patients usually had low-amplitude and frequently notched T waves, and LQT3 patients were categorized with a relatively long ST segment followed by a peaked, frequently tall, T wave. These initial observations were confirmed and further expanded on by Zhang and coworkers [24] who emphasized that LQT1 patients may present with normally looking T waves. Following these findings, the identification of T-wave morphology has been used to predict genotype in the era of limited genetic testing. The genotype suggested by the T-wave morphology may provide useful information to laboratories involved in screening genes for LQTS mutations, for it could save time and effort in the genetic screening process. Currently, most laboratories favor sequential testing of all major LQTS genes.

LQTS patients frequently show abnormal T-wave morphology, and careful evaluation of all 12 leads is recommended to determine the presence or absence of even subtle changes in T-wave

shape. This is particularly important and useful in patients with QTc durations in the gray zone of 420–470 ms, where the diagnosis is uncertain based on just QTc. In patients with QTc <440 ms (which is considered as normal by clinicians), abnormal T-wave morphology may provide an important hint regarding the possibility of LQTS. Abnormal, mostly flat, and notched T waves are the most pathognomonic for LQT2, especially in adolescents and adults. However, it is worth stressing that T-wave notches can occur in unaffected young children. Similar to the point made regarding QTc duration, access to multiple ECGs and careful evaluation of T-wave morphology in these ECGs may help in the diagnosis of suspected individuals.

LQTS Score

The above changes in QTc duration and T-wave morphology should be analyzed in light of the clinical history of the evaluated individual. The meaning of a QTc duration of 460 ms will be different if there is a history of frequent syncopal episodes in the past or if there is sudden death at young age in the family. This clinical approach is reflected by a LQTS diagnostic score published by Schwartz, Moss and colleagues in pre-genetic

Table 8.3 Diagnostic criteria for long QT syndrome^a

Findings	Score
<i>Electrocardiographic^b</i>	
Corrected QT interval, ms	
≥480	3
460–470	2
450 (in males)	1
Torsade de pointes ^c	2
T-wave alternans	1
Notched T-wave in 3 leads	1
Low heart rate for age ^d	0.5
<i>Clinical history</i>	
Syncope ^e	
With stress	2
Without stress	1
Congenital deafness	0.5
<i>Family history^e</i>	
Family members with definite LQTS	1
Unexplained SCD in immediate family members <30 years	0.5

^aReprinted with permission from Schwartz et al. [25]. Scoring ≤1 point, low probability of LQTS; 2 to 3 points, intermediate probability of LQTS; and ≥4 points, high probability of LQTS

^bFindings in the absence of medications or disorders known to affect these electrocardiographic findings. The corrected QT interval (QTc) is calculated by Bazett's formula: $QT/RR^{1/2}$

^cTorsade de pointes and syncope are mutually exclusive

^dResting heart rate below the second percentile for age

^eThe same family member cannot be counted in both categories

era of LQTS diagnosis [25]. The score, shown in Table 8.3, proposes that a high probability of LQTS diagnosis is present if it reaches a value of at least 4, whereas in the case of score values of 2–3, the likelihood of diagnosis is lower. It is important to stress that the score not only relies on QTc duration but also accounts for documented torsade de pointes, T-wave alternans, T-wave notches, as well as for bradycardia, findings frequently seen in LQTS patients. A personal history of cardiac events, diagnosis of LQTS in first-degree family members, as well as a sudden unexpected death <30 years of age further enrich the system based on ECG findings.

Tester et al. [26] studied the correlation between the LQTS score and results of genetic testing in 541 patients. In patients with a score >4, indicating a high probability of LQTS diagnosis, 72% of patients were found to be genotype

positive, whereas among patients with a score <4, indicating lower probability of the diagnosis, 44% were positive by genetic testing. These data emphasize important limitations of phenotypic evaluation using the LQTS score.

Other ECG Modalities for the Diagnosis of LQTS

In the case of clear-cut QTc prolongation >500 ms, usually there is not much doubt regarding the diagnosis. However, individuals with QTc <500 ms are frequently referred for exercise ECG testing, 24-hour Holter monitoring, or sometimes event monitoring. The diagnostic value of these modalities in borderline cases is still controversial. Krahn et al. [27] demonstrated that QT hysteresis, evaluation based on a response of QT to changing heart rate during exercise testing, may be helpful in the diagnosis of suspected cases. A distinct adaptation to increased heart rate on the upslope of exercise activity compared with the early recovery period at a similar heart rate was found useful. The authors postulated that a difference in QT >21 ms between 1 minute into recovery and early exercise measured in matched heart rates may be indicative of LQTS.

Takenaka et al. [28] analyzed exercise induced repolarization changes in a cohort of 51 LQT1 and 31 LQT2 patients. The QTc and TpTc (the interval between the peak and the end of the T wave) were 510 ± 68 ms and 143 ± 53 ms in LQT1 and 520 ± 61 ms and 195 ± 69 ms in LQT2, respectively, at baseline. These measures were both significantly larger than those observed in control subjects (402 ± 36 ms and 99 ± 36 ms). Both QTc and TpTc were significantly prolonged during exercise in LQT1 patients (599 ± 54 ms and 215 ± 46 ms) in whom a morphological change into a broad-based T-wave pattern was observed. In contrast, in LQT2 patients, exercise produced a prominent notch on the descending limb of the T wave, with no significant changes in the QTc and TpTc (502 ± 82 ms and 163 ± 86 ms). QT adaptation to changing heart rate was recognized as another method indicative of LQTS. As shown by Takenaka et al. [28], LQT2 patients

have steeper QT-RR slope than LQT1 patients during exercise. In addition, TpTe dynamics were shown to be different among subgroups. In LQT2 patients and controls, the TpTe was reduced in response to shortening of the R-R interval, thereby producing a positive TpTe/R-R slope; among LQT1 patients, the TpTe significantly prolonged when the R-R interval shortened, resulting in a negative TpTe/R-R slope [28].

For diagnostic purposes, it is believed that the presence of QTc >500 ms at heart rates <100 beats per minute during exercise testing or Holter recordings may be indicative of LQTS, whereas values below 500 ms are within physiologic range (again using Bazett's formula which is inadequate at faster heart rates).

Holter recordings may also provide information regarding adaptation of T-wave amplitude morphology with changing heart rates. Nemeč et al. [29] studied the heart rate dependence of the QT interval duration in different LQTS genotypes and control subjects using computerized QT measurements obtained from Holter recordings. The dependence of the QT duration on heart rate was steeper in LQTS than in control subjects (0.347 ± 0.263 vs. 0.162 ± 0.083 at a heart rate of 100 beats/min; $p < 0.05$). In addition, the QT interval was significantly longer in LQT2 and LQT3 patients than in those with the LQT1 genotype at slow (533 ± 23 ms vs. 468 ± 30 ms at heart rate 60 beats/min; $p < 0.0001$), but not at rapid, heart rates. The heart rate dependence of QT interval was steeper in LQT2 and LQT3 than in LQT1 (0.623 ± 0.245 vs. 0.19 ± 0.079 at a heart rate of 100 beats/min; $p < 0.05$). For a given heart rate, the QT intervals varied more in LQT2 and LQT3 patients than in LQT1 patients (25.98 ± 11.18 ms vs. 14.39 ± 1.55 ms; $p < 0.01$).

In a study by Couderc et al. [30], the T-amplitude/RR slope was significantly flatter in LQT2 patients ($0.31 \pm 0.27 \mu\text{V}/\text{ms}$) than in both LQT1 patients ($0.62 \pm 0.40 \mu\text{V}/\text{ms}$) and healthy individuals ($0.55 \pm 0.29 \mu\text{V}/\text{ms}$). The above tests evaluating dynamics of repolarization are still considered more useful as research tools than in clinical practice. Nevertheless, the additive information obtained from these tests is valuable when diagnosing patients with LQTS.

Kaufman et al. [31] studied a series of ECG parameters including exercise-induced T-wave alternans in a cohort of LQTS gene carriers and healthy controls. Standard resting QTc duration was found to be most predictive among individuals with a genotype-positive status; however, there was a 78% overlap between gene carriers and noncarriers. A T-wave alternans test did not contribute to improve LQTS diagnosis.

Epinephrine testing is considered as another test in the diagnosis of LQTS. Experimental studies using pharmacological models of LQTS tests in perfused wedge preparations by Antzelevitch and Shimizu [32] demonstrated a differential response of repolarization to epinephrine in different types of LQTS. Clinical evidence subsequently came from studies by Noda et al. [33] and Ackerman et al. [34]. The study of Noda et al. [33] showed that in LQT1 patients, QTc was prolonged remarkably (477 ± 42 to 631 ± 59 ms; $P < 0.0005$, % delta prolongation = +32%) as the RR was maximally decreased (at peak of epinephrine) and remained prolonged at steady-state conditions of epinephrine infusion (556 ± 56 ms; $P < 0.0005$ vs. baseline, +17%). In LQT2 patients, epinephrine also prolonged the QTc dramatically (502 ± 23 to 620 ± 39 ms; $P < 0.0005$, +24%) at peak epinephrine, but this shortened to baseline levels at steady state (531 ± 25 ms; $P = \text{ns}$ vs. baseline, +6%). The QTc was much less prolonged at peak epinephrine infusion in LQT3 patients (478 ± 44 to 532 ± 41 ms; $P < 0.05$, +11%) and controls (394 ± 21 to 456 ± 18 ms; $P < 0.0005$, +16%) than in LQT1 and LQT2 patients and shortened to baseline levels (LQT3: 466 ± 49 ms, -3%; controls: 397 ± 16 ms, +1%; $P = \text{ns}$ vs. baseline) at steady state.

Shimizu reported the responses of 12-lead ECG parameters to epinephrine examined in 31 LQT1, 23 LQT2, 6 LQT3, and 30 control subjects. The sensitivity by ECG diagnostic criteria was lower in LQT1 (68%) than in LQT2 (83%) or LQT3 (83%) before epinephrine and improved with steady-state epinephrine in LQT1 (87%) and LQT2 (91%) but not in LQT3 (83%), without the expense of specificity (100%) [35].

The above findings indicate that epinephrine testing may be useful, particularly in differentiating borderline cases of LQTS. However, responses to epinephrine infusion must be interpreted with caution in view of the limited amount of data available involving normal controls.

Genetic Testing for LQTS Diagnosis

Genetic testing adds significantly to the diagnosis of LQTS. The diagnosis may be straightforward in patients showing QTc >500 ms, and one could argue that genetic testing may offer little diagnostic or prognostic value in such clearly affected individuals. Nevertheless, there are data indicating that the clinical course is different by genotype [1, 3] and the effectiveness of therapy with beta-blockers also differs in LQT1 than LQT2 and LQT3 patients [36]. Furthermore, knowing the genetic type (mutation) in a proband provides an opportunity to conduct genotyping of family members who frequently cannot be diagnosed just based on ECG findings. Genetic testing of a proband is excessively costly, and these high cost and reimbursement issues are factors limiting much wider application of the testing in clinical practice. Testing of family members for mutation(s) found in a proband should become routine to diminish overall costs of unnecessary multiple clinical testing frequently used for diagnosing individuals.

Genetic testing of individuals suspected for LQTS with QTc <500 ms is particularly useful since an overlap between affected and unaffected individuals in this category of patients is very substantial. Standard genotyping usually focuses on the most frequent LQTS genes, LQT1, LQT2, LQT3, LQT5, and LQT6, whereas the remaining genes (LQT4, LQT 7–17) are tested less frequently since mutations of these genes are very infrequent. Current state of genotyping LQTS patients leads to identification of gene mutations in about three quarters of those tested. The fact that a majority of patients can be identified with specific mutation(s) should be encouraging to both physicians and patients who should pursue this testing. Splawski et al. [4] reported that

among genotyped patients, about 45% of tested patients were identified with LQT1, another 45% of patients were identified with LQT2, and about 5–8% of patients were identified with LQT3; the remaining 1–3% percent were in LQT5 and LQT6 genes. Napolitano et al. [37] evaluated the yield of genetic testing in 430 consecutive patients, with 310 (72%) patients having 235 different mutations, 138 of which were novel. The distribution of detected LQTS genotypes was as follows: 49% LQT1, 39% LQT2, 10% LQT3, 1.7% LQT5, and 0.7% LQT6. Importantly, they showed that by using the sex-based cutoff values for QTc, 40% of affected individuals (i.e., carriers of a genetic defect) were not identified by clinical assessment, further reinforcing the need for genetic testing.

Recent data from Taggart et al. [38] demonstrate that genetic testing supported by expert clinical evaluation may improve the diagnostic strategy of identifying LQTS patients. The authors have found that about 40% of individuals referred as having LQTS were found to be unaffected based on miscalculation of QTc or misinterpretation of symptoms. Again, genetic testing may be helpful in avoiding misdiagnoses, which carry lifelong consequences for LQTS-labeled individuals.

An additional benefit of comprehensive genetic testing may come from testing other non-LQTS genes of interest in suspected individuals. Tester et al. [39] found ryanodine receptor gene mutations responsible for the catecholaminergic polymorphic ventricular tachycardia in 17 (6.3%) of 269 patients with negative LQTS genetic testing.

The cost-effectiveness of genetic testing for LQTS is of concern. Philips et al. [40] found that genetic testing is more cost-effective than not testing for symptomatic index cases at an estimated cost of \$2500 US dollar per life-year saved.

Genotype-Phenotype Correlations in LQTS

LQTS genes affect different ion-current mechanisms; thus, the type of ion-channel mutation can affect phenotypic expression. As described

above, distinct genotype-phenotype correlations have been recognized in LQTS (Fig. 8.3) [10]. ST-T-wave patterns on the ECG and the triggers for cardiac events vary between the three genotypes. In addition, gene-specific differences in risk for cardiac events have also been described, with the genotype-specific risk factors including the type of trigger for cardiac event, age, gender, resting heart rate, mutation location, and response to beta-blockers. It has been shown that life-threatening arrhythmias in LQTS patients occur under specific circumstances (Fig. 8.4). In a study of 670 symptomatic LQTS patients with one of the three main LQTS genotypes [41], LQT1 patients were shown to experience 62% of cardiac events (including syncope, aborted cardiac arrest [ACA], and SCD) during exercise and only 3% during rest/sleep. By contrast, LQT3 patients experienced 13% of the events during exercise and 39% occurred at sleep/rest. LQT2 patients had an intermediate pattern, with only 13% occurring during exercise and most of the remainder (43%) occurring with emotional stress (i.e., fear, anger, startle, or sudden noise during sleep/rest). Similar trigger distribution pattern was found for the lethal cardiac events (ACA and SCD) (Fig. 8.4). This study and others [41–44] have shown that patients with the LQT1 genotype are at a higher

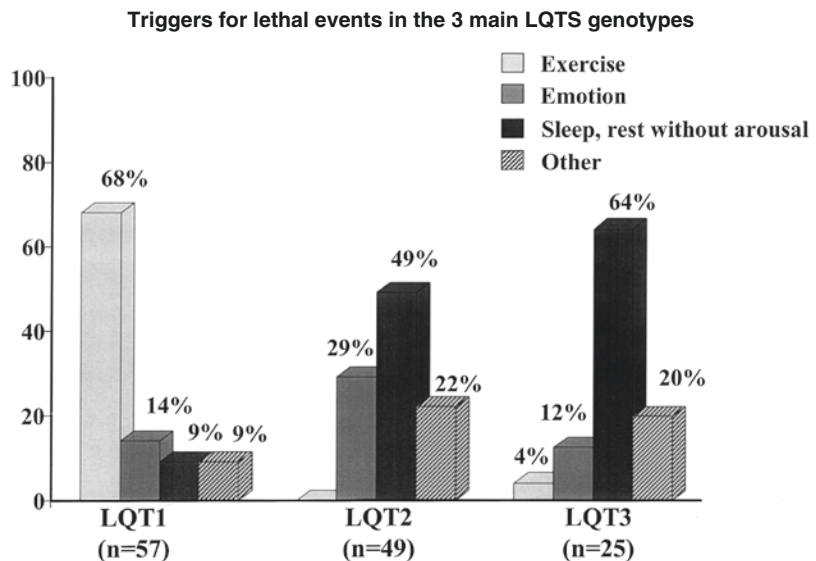
risk for arrhythmic events triggered by sympathetic activation induced by exercise. Among the different types of exercise, swimming was shown to be a specific trigger for LQT1 patients [42, 43]. In contrast, patients with the LQT2 genotype experience cardiac events associated with sudden loud noise, whereas patients with the LQT3 genotype experience events during sleep or at rest without emotional arousal [42, 43, 45].

Clinical Course of LQTS Patients

We assessed the clinical course of 3779 LQTS patients enrolled in the registry, of whom 2319 patients (60%) were females. The cumulative probability of a first cardiac event (comprising syncope, aborted cardiac arrest [ACA], and sudden cardiac death [SCD]) from age 1 to 75 years and the corresponding probability of a first life-threatening cardiac event (comprising ACA and SCD) by sex are shown in Fig. 8.5a, b, respectively. Data from previous and ongoing registry analyses regarding sex differences in the risk of the two end points, by age-groups, are shown in Tables 8.4a–c.

The results of these analyses consistently demonstrate that during childhood, male patients

Fig. 8.4 Triggers for lethal cardiac events according to three genotypes. Numbers in parentheses indicate number of triggers, not number of patients. (Reproduced with permission from Schwartz et al. [41])



respectively; $P < 0.0001$) and affected family members (20% vs. 16%, respectively; $P < 0.01$). A similar pattern was present also in 181 family members with unexplained sudden death, in whom the death rate before age 15 years was twice as high in males as in females (57% vs.

29%, respectively; $P < 0.0001$). In multivariate analysis, male gender was independently associated with a significant 85% and 72% increase in the risk of cardiac events before age 15 years among probands and affected family members, respectively (Table 8.4a).

Table 8.4 Data from the International LQTS Registry regarding gender-related risk of cardiac events by age groups

Population	N	Age range, (yrs)	End point	Male-female adjusted HR ^b (95% CI)	Data source
A. Pre-adolescence period					
Probands	479	0–14	Any cardiac event	1.85 (1.59–2.70)	Locati et al. [46]
Affected family members	1041	0–14	Any cardiac event	1.72 (1.23–2.39)	Locati et al. [46]
LQT1	247	0–15	Any cardiac event	1.72 (1.19–2.33)	Zareba et al. [6]
LQT2	209	0–15	Any cardiac event	1.37 (0.80–2.33)	Zareba et al. [6]
LQT3	81	0–15	Any cardiac event	0.54 (0.14–2.13)	Zareba et al. [6]
Registry pts diagnosed by QTc criteria or genetic testing	3015	1–12	ACA or SCD	3.03 (1.80–5.12)	Goldenberg et al. [47]
Registry pts diagnosed by genetic testing ^a	805	1–12	ACA or SCD	4.31 (1.14–20.50)	Goldenberg et al. [47]
Registry pts diagnosed by QTc criteria or genetic testing	2772	10–12	ACA or SCD	4.0 (1.8–9.2)	Hobbs et al. [48]
Registry pts diagnosed by QTc criteria or genetic testing	2772	10–12	SCD	11.6 (1.4–94.2)	Hobbs et al. [48]
B. Adolescence through age 40 years					
Probands	479	15–40	Any cardiac event	0.53 (0.27–1.06)	Locati et al. [46]
Affected family members	1041	15–40	Any cardiac event	0.31 (0.17–0.56)	Locati et al. [46]
LQT1	247	16–40	Any cardiac event	0.30 (0.12–0.71)	Zareba et al. [6]
LQT2	209	16–40	Any cardiac event	0.27 (0.09–0.73)	Zareba et al. [6]
LQT3	81	16–40	Any cardiac event	1.11 (0.35–3.45)	Zareba et al. [6]
Registry pts diagnosed by QTc criteria or genetic testing	2772	13–20	SCD	1.6 (0.2–0.8)	Hobbs et al. [48]
Registry pts diagnosed by genetic testing	812	18–40	Any cardiac event	3.05 (2.13–4.38)	Sauer et al. [49]
Registry pts diagnosed by genetic testing	812	18–40	ACA or SCD	2.77 (1.66–4.62)	Sauer et al. [49]
C. After the fourth decade of life					
Registry pts diagnosed by QTc criteria	540	41–75	Any cardiac event	0.54 (0.28–0.87)	LQTS registry analyses
Registry pts with QTc ≥ 470 msec.	860	41–60	All-cause mortality	0.97 (0.52–1.81)	LQTS registry analyses
Registry pts with QTc ≥ 470 ms	314	61–75	All-cause mortality	0.69 (0.37–1.26)	LQTS registry analyses

ACA aborted cardiac arrest, LQT1, LQT2, and LQT3 long QT syndrome types 1, 2, and 3, respectively, SCD sudden cardiac death

^aSubgroup of the 3015 patients in the previous row

^bFindings adjusted for QTc duration, time-dependent beta-blocker therapy; for the end point of ACA or SCD, findings were also adjusted for a history of time-dependent syncope

Zareba et al. [6] studied 533 registry patients who were genetically tested and found to be carriers of the LQT1 ($n = 243$), LQT2 ($n = 209$), and LQT3 ($n = 81$) genotypes. During childhood, the rate of cardiac events was significantly higher in LQT1 males than in LQT1 females (56% vs. 44%, respectively), corresponding to a 71% increase in the risk of a first cardiac event during childhood in males (Table 8.4a), whereas there was no significant gender-related difference in the risk of cardiac events among LQT2 and LQT3 carriers during the same time period.

In a comprehensive analysis from the International LQTS Registry, we assessed the end point of ACA or SCD in 3015 LQTS children (1893 males and 1122 females) from proband identified families who were diagnosed by QTc criteria [47]. In this study population, the cumulative probability of a first life-threatening cardiac event from age 1 through 12 years was 5% in males as compared with only 1% among females ($P < 0.001$). Accordingly, multivariate analysis showed that male gender was associated with a threefold increase in the risk of ACA or SCD during childhood, and with more than a fourfold increase in the risk of this end point in a subgroup of 803 genotype-positive LQTS children (Table 8.4a).

Clinical Course of LQTS Patients from Adolescence Through Age 40 Years

In the registry analysis of 479 probands and 1041 affected family members carried out by Locati et al. [46], a sex-related risk reversal was shown to occur after age 14 years when the end point of a first cardiac event of any type was assessed. Thus, in the age range of 15–40 years, females had an 87% increase in the risk of cardiac events as compared with males among probands and a 3.3-fold increase in the risk among affected family members (Table 8.4b). Consistently, Zareba et al. [6] showed that in the age range of 16 through 40 years, the risk of cardiac events of any type was more than threefold higher among both LQT1 and LQT2 females as compared with the

respective males (Table 8.4b), whereas among LQT3 genotype carriers, no significant gender difference in the risk was detected.

As noted above, when the end point of ACA or SCD is considered, sex-related risk reversal occurs at a later stage than the age shown for the less severe cardiac event end point that includes also syncope (Fig. 8.5). In a recent study of 2772 registry patients that were followed between the ages of 10 and 20 years, Hobbs et al. [48] showed that in the age range of 10–12 years, males had a fourfold increase in the risk of ACA or SCD and an 11-fold increase in the risk of SCD compared with females (Table 8.4a), whereas in the age range of 12–20 years, no significant gender difference in the risk of life-threatening cardiac events was shown (Table 8.4b). Subsequently, Sauer et al. [49], in an analysis of 812 mutation-confirmed LQTS patients from the registry who were followed up between the ages of 18 and 40 years, showed that during adulthood females have nearly a threefold increase in the risk of ACA or SCD as compared with males (Table 8.4b). In this study, the cumulative probability of ACA or SCD at age 40 years was 11% among females as compared with only 2% among males ($P < 0.001$). The two latter studies further demonstrate that gender risk reversal occurs at a later age when the end point of life-threatening cardiac events is considered.

Clinical Course of LQTS Patients after the Fourth Decade of Life

Published studies on the clinical course of LQTS patients are limited to the first 4 decades of life due to lack of appropriate follow-up information in the older age-group. The International LQTS Registry has recently expanded the duration of follow-up in enrolled subjects, and current updated data facilitates now a comprehensive analysis of the clinical course of affected patients beyond the age of 40 years.

We assessed the end point of a first cardiac event of any type after age 40 years in 540 LQTS patients. In this analysis, the cumulative probability of LQTS-related cardiac events at age

75 years was 32% in females as compared with 18% in males ($P = 0.005$), corresponding to an 85% increase in the adjusted risk of cardiac event in females compared with males (Table 8.4c). Since in the older age-group the competing risks cardiovascular comorbidities are higher among males, and may counterbalance the higher risk of LQTS-related cardiac events in females, we also assessed the end point of all-cause mortality in affected subjects after age 40 years. In an analysis of 2759 LQTS patients, the cumulative probability of all-cause mortality from age 41 years through 75 years was 27% among females as compared with 32% in males ($P = 0.37$) [50]. Consistently, the risk associated with female sex was not significant when the end point of all-cause mortality was assessed in age ranges of 41–60 years and 61–75 years (Table 8.4c). Thus, it appears that LQTS continues to confer a high risk of arrhythmic events among females even after the fourth decade of life that counterbalances the higher risk of acquired cardiovascular morbidity and mortality of males in this age-group. These age-specific risk interactions lead to a neutral effect of gender on the end point of all-cause mortality in the older age-group.

LQTS and Sex Hormones

The pronounced difference in the clinical course of LQTS males and females suggests that sex hormones may affect arrhythmic risk in LQTs patients.

As described above, this increased risk in cardiac events is more pronounced in LQT2 women. LQT2 women experience a significant increase in the risk of cardiac events after the onset of adolescence [48, 49]. Female sex is associated with a longer baseline QTc and is an independent risk factor for development of torsade de pointes in acquired LQTS (affecting the I_{Kr} current) [51, 52]. After the onset of adolescence, women with LQTS experience hormonal changes (during menstrual cycle or associated with pregnancy and peripartum period) that may favor QT prolongation and vulnerability to arrhythmias [53]. These data suggest that hormonal factors affect the clinical course of LQTS males and females.

The possible relationship between female sex hormones and a more pronounced arrhythmic risk in I_{Kr} mutation carriers is also supported by a study from our registry that showed a significant increase in the risk of cardiac events in the 9-month postpartum period, mainly among women who were LQT2 genotype carriers (Fig. 8.6) [54]. Similarly,

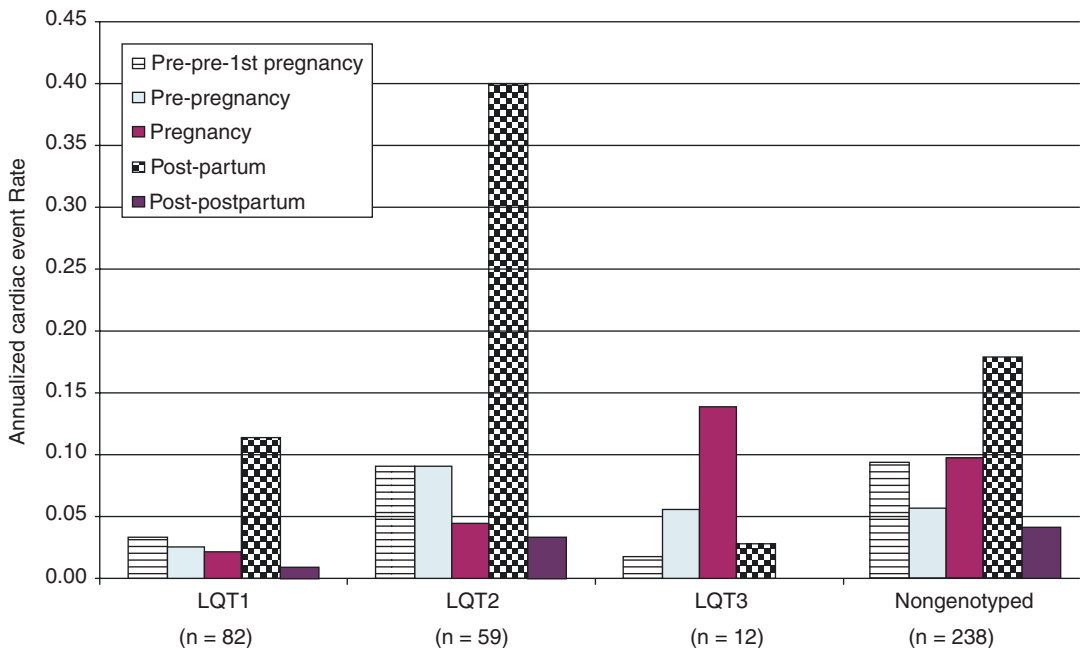


Fig. 8.6 Rate (in patient years) of cardiac events among LQTS women by pregnancy periods. (Reproduced with permission from Seth et al. [54])

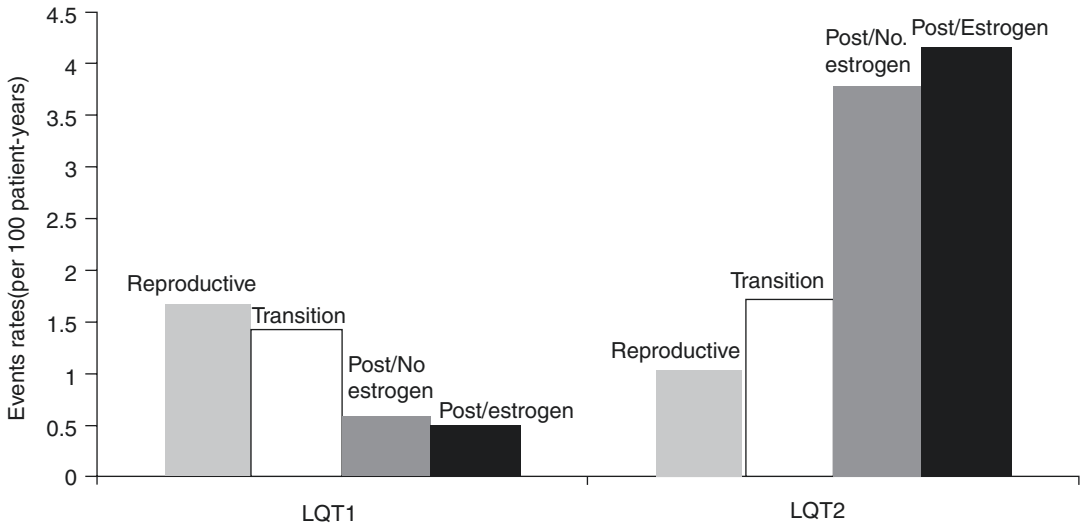


Fig. 8.7 Rate (in patient years) of cardiac events among LQT1 and LQT2 women by menstrual stage and estrogen therapy. (Reproduced with permission from Buber et al. [55])

we have shown that LQT2 women experience a significant increase in the risk of recurrent cardiac events after the onset of menopause (Fig. 8.7) [55].

There is also an unexplained sex imbalance among patients referred to the LQTS Registry. We have shown that among the enrolled registry patients, there is a higher frequency of females (approximately 60%) than males [1–3, 5–8], consistent with data by Imboden et al. [56] who showed that LQTS alleles were transmitted more often to females than to males in 484 LQT1 and 269 LQT2 families.

Risk Stratification for Cardiac Events in LQTS Patients

Risk stratification relies on a combined assessment of clinical information, ECG, and mutation-specific factors. Based on existing data among non-genotyped patients, LQTS patients may be classified into three main risk categories (Fig. 8.8): very high risk, high risk, and low risk (5-year Kaplan-Meier cumulative estimate rate of ACA/SCD is 14%, 3%, and 0.5%, respectively) [2]. The patients in the very-high-risk group are those with a history of ACA and/or spontaneous torsade de pointes; these patients

require an ICD implantation for secondary prevention of SCD. The high-risk group includes subjects with history of prior syncope or QTc of over 500 ms, and the low-risk group includes those with QTc duration of 500 ms or less and without prior syncopal event.

Genotype-Specific Risk Stratification

Multiple studies have shown that there are genotype-specific factors affecting the phenotypic expression in patients with LQTS; those risk factors include age, gender, postpartum time period, menopause, resting heart rate, prior syncope, mutation location, type of mutation (missense/non-missense), the biophysical function of the mutation, and response to beta-blockers. In addition cardiac events triggered by exercise, arousal, or rest/sleep are associated with distinctive clinical and genetic risk factors.

Risk stratification in LQTS type 1: Our data indicate that the location, type, and biophysical function of the KCNQ1 mutation are important independent risk factors influencing the clinical course of patients with LQT1. Moss et al. [6] have demonstrated, among 600 patients with 77 different KCNQ1 mutations, that patients with

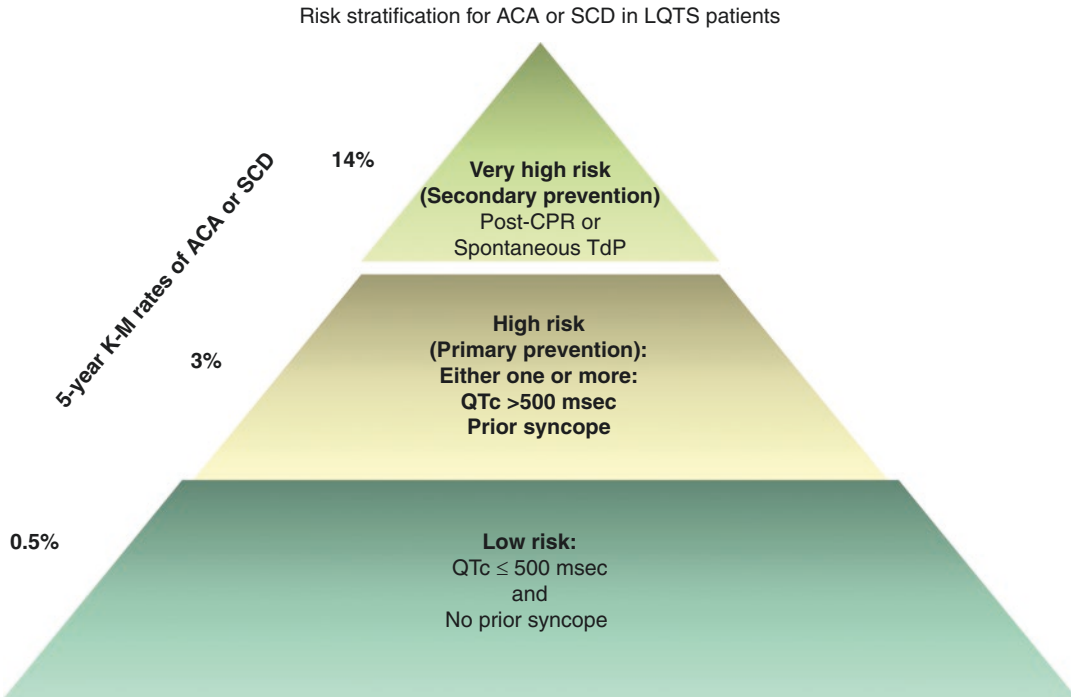


Fig. 8.8 Risk stratification categories for LQTS patients based on published event rates. Kaplan-Meier estimates are based on a series of 869 long QT syndrome patients

[2]. CPR cardiopulmonary resuscitation, TdP torsade de pointes. (Reproduced with permission from Goldenberg and Moss [2])

mutations in the transmembrane region (including the cytoplasmic loops [C-loops] domains) compared to mutations in the C-terminus of the KCNQ1 channel had a twofold ($p < 0.001$) increased risk for syncope, ACA, or SCD. Similarly, patients with dominant negative ion-current effects ($>50\%$ reduction in channel current) had a 2.2-fold increase ($p < 0.001$) in the risk of cardiac events compared with those who had mutations with haploinsufficiency effect ($\leq 50\%$ reduction in channel current). Furthermore, this study has shown that patients with missense mutations had a significantly higher risk of cardiac events compared to those with non-missense mutations. Subsequently, we have analyzed data on 860 patients with a KCNQ1 mutation from the International LQTS Registry [57]. Patients were categorized into carriers of missense mutations located in the S2–S3 and S4–S5 C-loops, membrane-spanning domain, C-/N-terminus, and non-missense mutations. There were 27 ACA and 78 SCD events from birth through age 40 years. The presence of

C-loop mutations was associated with the longest QTc on the ECG and with highest risk for ACA or SCD (hazard ratio [HR] 2.75, $P = 0.009$ compared with non-missense mutations (Fig. 8.9)). It is known that C-loops play an important role in the sympathetic regulation of the KCNQ1 channel [58]. Based on results from cellular expression studies [58], we have suggested that a combination of decrease in basal function and altered adrenergic regulation of the I_{Ks} channel underlies the increased cardiac risk in this subgroup of patients [56].

There are accumulating data showing that the risk for cardiac events in LQT1 is affected by sex and age. Zareba et al. [6] have shown in 243 subjects with LQT1 that during childhood (age-group: 0–15 years), there was a 1.7-fold ($p = 0.005$) increased risk for cardiac events (syncope, ACA, or SCD) among males compared with females, whereas during adulthood, LQT1 females had a 3.3-fold ($p = 0.007$) higher risk for cardiac events compared with males. We have further assessed the sex-specific risk factors for

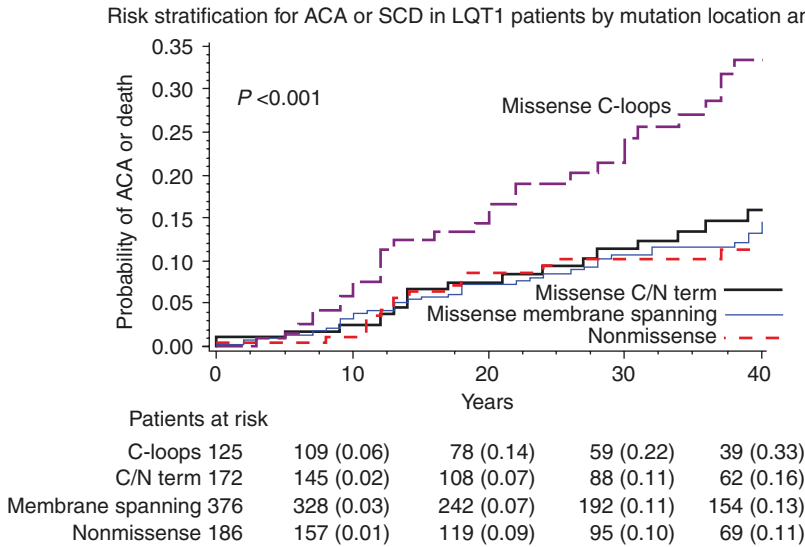


Fig. 8.9 Kaplan-Meier estimates of cumulative probability of life-threatening cardiac events by mutation location and type in LQT1 patients. The numbers in parentheses reflect the cumulative event rate at that point in time. ACA

indicates aborted cardiac arrest; LQTS long QT syndrome. (Reproduced with permission from Barsheshet et al. [57])

life-threatening cardiac events (ACA/SCD) in a large population of 1051 genetically confirmed patients with LQT1 from the US portion of the International LQTS Registry [59]. We have found that during childhood (age-group: 0–13 years), males had >twofold ($P = 0.003$) increased risk for ACA/SCD than females, whereas after the onset of adolescence, the risk for ACA/SCD was similar between men and women ($HR = 0.89$; $P = 0.64$). Importantly, mutation location showed a sex-specific association with the risk for ACA or SCD. The presence of C-loop domains (S2–S3 and S4–S5) mutations was associated with a 2.7-fold ($P < 0.001$) increased risk for ACA/SCD among women, whereas the risk for ACA/SCD among men with LQT1 was high, predominantly during the childhood period, regardless of mutation location/type. Additional risk factors for ACA or SCD among both men and women included a prolonged QTc (>500 ms) and the occurrence of time-dependent syncope [59]. Time-dependent syncope was associated with a more pronounced risk increase among men than women (HR 4.73; [$P < 0.001$] and 2.43 [$P = 0.02$], respectively), whereas a prolonged corrected QT interval (≥ 500 ms) was associated with a higher

risk among women than men. The proposed risk stratification scheme for ACA or SCD in LQT1 based on these findings is presented in Fig. 8.10.

In LQT1, the majority of events are triggered by exercise activity, and a lower proportion of events are associated with acute arousal or sleep/rest. In a study carried out among 721 genetically confirmed patients with LQT1 from the US portion of the International LQTS Registry [44], we have analyzed the independent contribution of clinical and genetic risk factors to the first occurrence of trigger-specific cardiac events, categorized as exercise-induced, arousal, and nonarousal/nonexercise. This study showed that age and sex have a distinct association with exercise-, arousal-, and sleep-/rest-triggered events in patients with LQT1. During childhood (age <13 years), males had a 2.8-fold ($P < 0.001$) increase in the risk for exercise-triggered events, whereas females >13 years showed a 3.5-fold ($P = 0.002$) increase in the risk for sleep/rest nonarousal events. Mutations located in the C-loops portion of the KCNQ1 channel were associated with an increased risk for cardiac events triggered by both exercise- and arousal-triggered events (i.e., sympathetic stimulation,

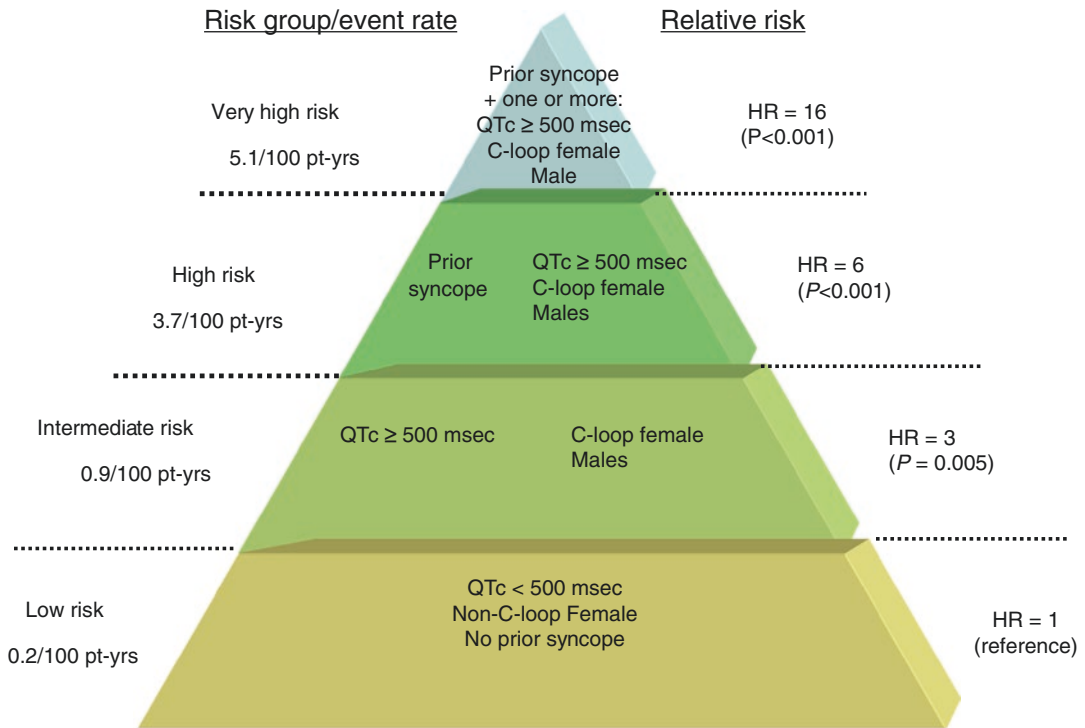


Fig. 8.10 Proposed scheme for risk stratification for the end point of ACA or SCD in LQT1 patients by gender, mutation location, QTc, and a history of prior syncope. *Hazard ratios and score estimates were obtained from a multivariate Cox model that included interactions among the identified risk factors (categorized by QTc duration, time-dependent syncope, gender, and mutation location); decimal points in HRs are rounded to the nearest whole number; event rates per 100 person-years were calculated

by dividing the number of life-threatening cardiac events (comprising ACA or SCD) in each risk category by the total follow-up time in the category (with follow-up censored after the occurrence of a ACA) and multiplying the result by 100. ACA aborted cardiac arrest, HR hazard ratio, LQT2 long QT syndrome type 2, SCD sudden cardiac death, QTc corrected QT. (Data based on event rates estimated provided in Ref. [59])

HR = 6.19 [$P < 0.001$] and HR = 4.99 [$P < 0.001$], respectively) but were not related to sleep/rest nonarousal events (HR = 0.72; $p = 0.46$).

Finally, it has been shown that faster resting heart rates are associated with increased risk for cardiac events in LQT1 patients and that resting heart rate provides incremental prognostic information to mere assessment of QTc in LQT1 but not in LQT2 patients [60–62]. Thus, we have suggested that risk stratification for life-threatening cardiac events in LQTS patients may be improved by incorporating a genotype-specific correction of the QT interval for heart rate with a greater degree of QT correction for heart rate in LQT1 (improved QTc = $QT/RR^{0.8}$) than in LQT2 patients (improved QTc = $QT/RR^{0.2}$) [62].

Risk stratification in LQTS type 2: Similar to LQT1, the type and location of KCNH2 mutations were shown to be linked to the risk of cardiac events in patients with LQT2. In a study of 858 subjects with 162 different KCNH2 mutations, Shimizu et al. [8] have reported that patients with missense mutations located in the transmembrane pore region (S5-loop-S6 region) are associated with the greatest risk for cardiac events. Furthermore, mutations located in the alpha-helical domain of the KCNH2 channel were associated with a significantly higher risk compared with mutations in either the beta-sheet domains or other uncategorized locations.

With regard to the effect of sex and age on the phenotypic expression in LQT2 patients, Zareba

et al. [6] assessed the risk of cardiac events in 209 carriers of KCNH2 mutations and found that females >15 years old had a 3.7-fold ($p = 0.01$) increased risk for cardiac events as compared with males >15 years old, but there was no significant difference between female and male carriers ≤ 15 years old ($HR = 0.73, p = 0.3$).

Migdalovich et al. [63] have investigated the relationship between mutation location in the KCNH2 channel and gender-specific risk for life-threatening cardiac events (ACA/SCD). This study among 1166 patients with LQT2 showed that the risk for life-threatening cardiac events from birth through age 40 years was significantly higher among women than men, with a cumulative probability of life-threatening cardiac events of 26% and 14% among women and

men, respectively ($P < 0.001$). The increased risk for ACA/SCD among LQT2 females was pronounced after the age of 13 years. The risk for life-threatening cardiac events was not significantly different between women with and without pore-loop mutations ($HR 1.20; P = 0.3$). In contrast, men with pore-loop mutations displayed a significant >twofold higher risk of a first ACA/SCD as compared with those with non-pore-loop mutations ($HR = 2.18; P = 0.01$). Figure 8.11 shows a proposed risk stratification scheme for ACA or SCD in LQT2 patients.

As mentioned earlier, most of cardiac event stimuli in LQT2 patients are sudden arousal triggers, whereas a lower proportion of events are associated with exercise activity. We have

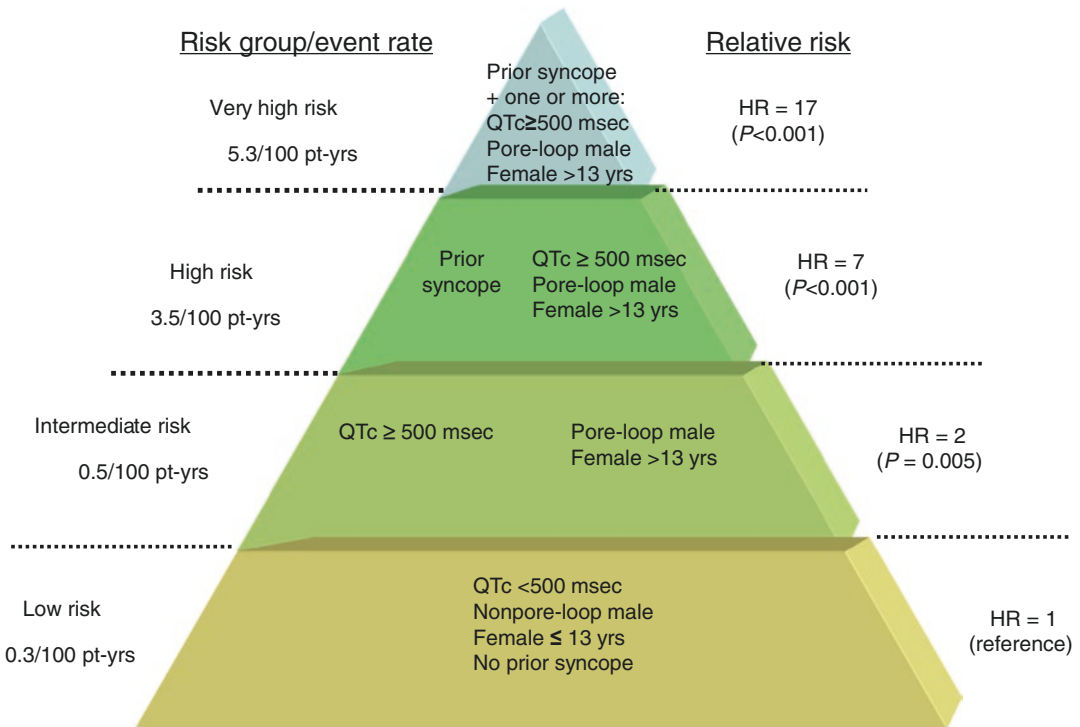


Fig. 8.11 Proposed scheme for risk stratification for the end point of ACA or SCD in LQT2 patients by gender, mutation location, QTc, and a history of prior syncope. *Hazard ratios and score estimates were obtained from a multivariate Cox model that included interactions among the identified risk factors (categorized by QTc duration, time-dependent syncope, gender, and mutation location); decimal points in HRs are rounded to the nearest whole number; event rates per 100 person-years were calculated

by dividing the number of life-threatening cardiac events (comprising ACA or SCD) in each risk category by the total follow-up time in the category (with follow-up censored after the occurrence of a ACA) and multiplying the result by 100. ACA aborted cardiac arrest, HR hazard ratio, LQT2 long QT syndrome type 2, SCD sudden cardiac death, QTc corrected QT. (Reproduced with permission from Migdalovich et al. [63])

recently carried out a study among 634 genetically confirmed LQT2 patients [6] investigating the clinical and genetic factors associated with trigger-specific risk for cardiac events. Females >13 years as compared with males >13 years had a ninefold ($p < 0.001$) increased risk for arousal-triggered cardiac events, and patients with pore-loop mutations had a >twofold increased risk for this end point ($P = 0.009$). In contrast, non-pore-loop transmembrane mutations were associated with a 6.8-fold ($p < 0.001$) increased risk for exercise-triggered events, whereas gender was not a significant risk factor for this end point. Risk factors for nonexercise/nonarousal events included female gender, mutation location and type, and prolonged QTc (>500 ms).

Thus, in both LQT1 and LQT2, risk factors for cardiac events showed a trigger-specific association with arrhythmic cardiac events.

Risk stratification in LQTS type 3: As described above, a gain of function mutation in the cardiac sodium channel SCN5A leads to LQT3. The SCN5A channels open quickly in response to depolarization, but within a few milliseconds the channels undergo fast inactivation. The mutations leading to LQT3 produce gain of function defects by disrupting this inactivation causing late persistent sodium currents, window sodium currents, or both.

Preliminary findings from data of LQT3 patients enrolled in the US portion of the Registry show that mutations involving two functional defects (i.e., mutations leading to both late sodium currents and window sodium currents) had a 2.5-fold ($p = 0.001$) increased risk for ACA/SCD as compared with mutations involving only one functional defect. The international LQT3 research group showed no significant difference in the risk of cardiac events among patients with mutations in transmembrane versus C-terminus segments of the SCN5A channel.

Liu et al. [64] investigated the clinical course of patients with two relatively common LQT3 mutations. The study population involved 50

patients with the Δ KPQ mutation and 35 patients with the missense D1790G mutation of the SCN5A gene. Patients with the Δ KPQ mutation had a 2.4-fold ($p < 0.001$) higher risk for cardiac events from birth through age 40 years compared to patients with the D1790G mutation, demonstrating the importance of knowing the specific mutation in risk stratification of LQT3 patients (Fig. 8.12).

Zareba et al. [6] assessed the risk of cardiac events in 81 carriers of SCN5A mutations and found no trend toward age and sex dependency of the risk for cardiac events in patients with LQT3. The lethality of cardiac events in males and females with LQT3 was similar but was significantly higher than in LQT1 and LQT2 patients. In a more recent study comprising 406 LQTS patients, we have shown no statistically significant differences in the clinical course of LQT3 males and females [9]. Independent risk factors for cardiac events in this study include a history of prior syncope and baseline QTc. The rate of sudden cardiac death at 40 years in this LQT3 cohort was 14% (Fig. 8.13) [9].

Summary

Genotype-phenotype correlation in the LQTS has been the most active line of research among the genetic diseases associated with life-threatening ventricular arrhythmias. The discovery that genes responsible for LQTS encode different ion channels involved in the control of the cardiomyocyte repolarization has led to important advancements in current knowledge regarding the relationship between basic causal mechanisms and clinical aspects of LQTS. It has been shown that life-threatening arrhythmias in LQTS patients occur under specific circumstances and in a gene-specific manner. The interplay between the genetic defect, QT duration, age, and sex can provide an algorithm for risk stratification in LQTS. Most importantly, an understanding of the genotype-phenotype relationship can lead to improved management of LQTS.

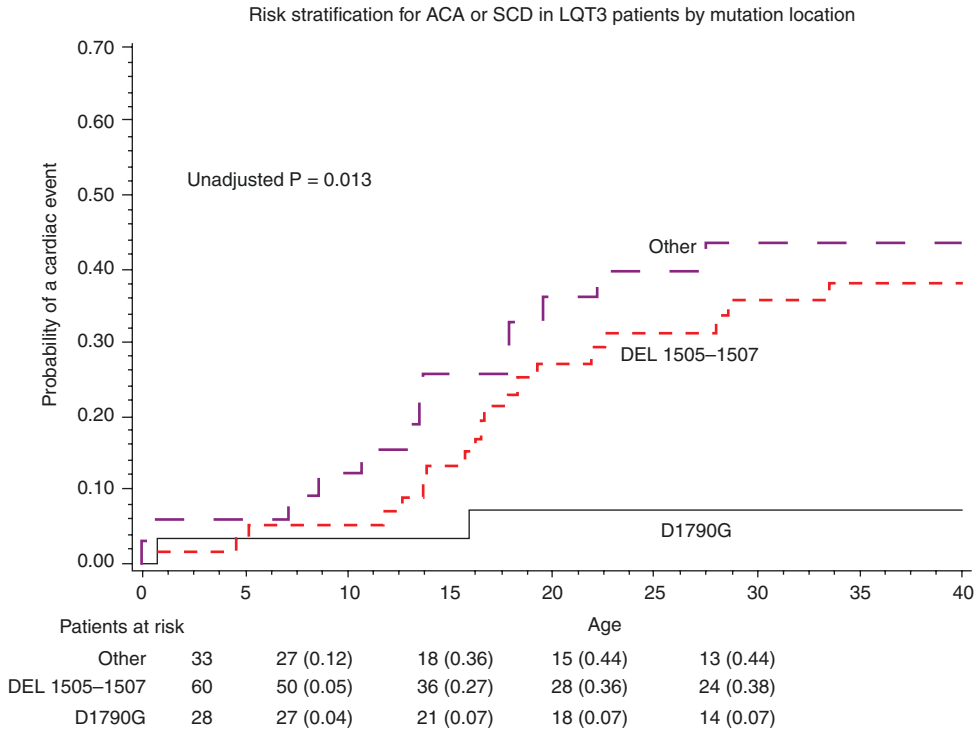


Fig. 8.12 Kaplan-Meier estimates of cumulative probability of life-threatening cardiac events by mutation location in LQT3 patients. The numbers in parentheses reflect the cumulative event rate at that point in time. (Reproduced with permission from Liu et al. [64])

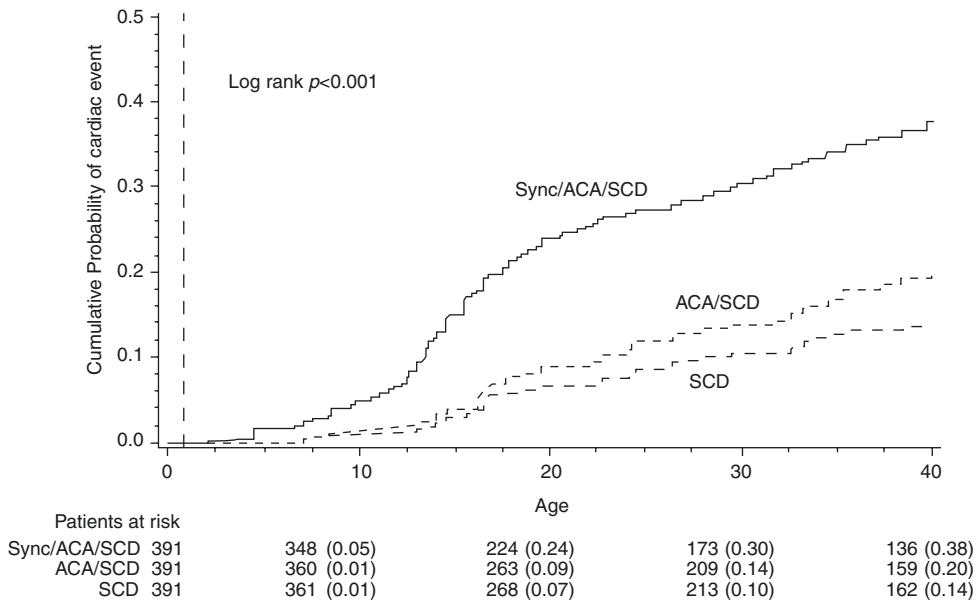


Fig. 8.13 Kaplan-Meier cumulative probability of first LQT3-triggered cardiac event for combinations of syncope, ACA, and SCD, conditional on event-free survival to age 1 year. ACA indicates aborted cardiac arrest, LQT3 type 3 long QT syndrome, SCD sudden cardiac death. (Reproduced with permission from Wilde et al. [9])

References

- Zareba W, Moss AJ, Schwartz PJ, Vincent GM, Robinson JL, Priori SG, et al. Influence of the genotype on the clinical course of the long-QT syndrome. International Long-QT Syndrome Registry Research Group. *N Engl J Med.* 1998;339:960–5.
- Goldenberg I, Moss AJ. Long QT syndrome. *J Am Coll Cardiol.* 2008;51:2291–300.
- Priori SG, Schwartz PJ, Napolitano C, Bloise R, Ronchetti E, Grillo M, et al. Risk stratification in the long-QT syndrome. *N Engl J Med.* 2003;348:1866–74.
- Splawski I, Shen J, Timothy KW, Lehmann MH, Priori S, Robinson JL, et al. Spectrum of mutations in long-QT syndrome genes. KVLQT1, HERG, SCN5A, KCNE1, and KCNE2. *Circulation.* 2000;102:1178–85.
- Moss AJ, Schwartz PJ, Crampton RS, Tzivoni D, Locati EH, MacCluer J, et al. The long QT syndrome. Prospective longitudinal study of 328 families. *Circulation.* 1991;84:1136–44.
- Zareba W, Moss AJ, Locati EH, Lehmann MH, Peterson DR, Hall WJ, et al. Modulating effects of age and gender on the clinical course of long QT syndrome by genotype. *J Am Coll Cardiol.* 2003;42:103–9.
- Moss AJ, Shimizu W, Wilde AA, Towbin JA, Zareba W, Robinson JL, et al. Clinical aspects of type-1 long-QT syndrome by location, coding type, and biophysical function of mutations involving the KCNQ1 gene. *Circulation.* 2007;115:2481–9.
- Shimizu W, Moss AJ, Wilde AA, Towbin JA, Ackerman MJ, January CT, et al. Genotype-phenotype aspects of type 2 long QT syndrome. *J Am Coll Cardiol.* 2009;54:2052–62.
- Wilde AA, Moss AJ, Kaufman ES, Shimizu W, Peterson DR, Benhorin J, et al. Clinical aspects of type 3 long-QT syndrome: an International Multicenter Study. *Circulation.* 2016;134:872–82.
- Moss AJ, Zareba W, Benhorin J, Locati EH, Hall WJ, Robinson JL, et al. ECG T-wave patterns in genetically distinct forms of the hereditary long QT syndrome. *Circulation.* 1995;92:2929–34.
- Moss AJ, Kass RS. Long QT syndrome: from channels to cardiac arrhythmias. *J Clin Invest.* 2005;115:2018–24.
- Plaster NM, Tawil R, Tristani-Firouzi M, et al. Mutations in Kir2.1 cause the developmental and episodic electrical phenotypes of Andersen's syndrome. *Cell.* 2001;105:511–9.
- Splawski I, Timothy KW, Sharpe LM, et al. Ca(V)1.2 calcium channel dysfunction causes a multisystem disorder including arrhythmia and autism. *Cell.* 2004;119:19–31.
- Medeiros-Domingo A, Kaku T, Tester DJ, et al. SCN4B-encoded sodium channel beta4 subunit in congenital long-QT syndrome. *Circulation.* 2007;116:134–42.
- Schott J-J MP, Gramolini AO. Mutation in the ankyrin-B gene causes Long QT syndrome and sinus node dysfunction. *Circulation.* 2002;106:II–308.
- Mohler PJ, Schott JJ, Gramolini AO, et al. Ankyrin-B mutation causes type 4 long-QT cardiac arrhythmia and sudden cardiac death. *Nature.* 2003;421:634–9.
- Vatta M, Ackerman MJ, Ye B, et al. Mutant caveolin-3 induces persistent late sodium current and is associated with long-QT syndrome. *Circulation.* 2006;114:2104–12.
- Cronk LB, Ye B, Kaku T, et al. Novel mechanism for sudden infant death syndrome: persistent late sodium current secondary to mutations in caveolin-3. *Heart Rhythm.* 2007;4:161–6.
- Anderson CL, Delisle BP, Anson BD, et al. Most LQT2 mutations reduce Kv11.1 (hERG) current by a class 2 (trafficking-deficient) mechanism. *Circulation.* 2006;113:365–73.
- Moss AJ, Robinson JL. Long QT syndrome. *Heart Dis Stroke.* 1992;1:309–14.
- Rautaharju PM, Zhou SH, Wong S, et al. Sex differences in the evolution of the electrocardiographic QT interval with age. *Can J Cardiol.* 1992;8:690–5.
- Vincent GM, Jaiswal D, Timothy KW. Effects of exercise on heart rate, QT, QTc and QT/QS2 in the Romano-Ward inherited long QT syndrome. *Am J Cardiol.* 1991;68:498–503.
- Schwartz PJ, Stramba-Badiale M, Segantini A, et al. Prolongation of the QT interval and the sudden infant death syndrome. *N Engl J Med.* 1998;338:1709–14.
- Zhang L, Timothy KW, Vincent GM, et al. Spectrum of ST-T-wave patterns and repolarization parameters in congenital long-QT syndrome: ECG findings identify genotypes. *Circulation.* 2000;102:2849–55.
- Schwartz PJ, Moss AJ, Vincent GM, Crampton RS. Diagnostic criteria for the long QT syndrome: an update. *Circulation.* 1993;88:782–4.
- Tester DJ, Will ML, Haglund CM, Ackerman MJ. Effect of clinical phenotype on yield of long QT syndrome genetic testing. *J Am Coll Cardiol.* 2006;47:764–8.
- Krahn AD, Klein GJ, Yee R. Hysteresis of the RT interval with exercise: a new marker for the long-QT syndrome? *Circulation.* 1997;96:1551–6.
- Takenaka K, Tomohiko A, Shimizu W, et al. Exercise stress test amplifies genotype-phenotype correlation in the LQT1 and LQT2 forms of the long-QT syndrome. *Circulation.* 2003;107:838–44.
- Nemec J, Buncova M, Bulkova V, et al. Heart rate dependence of the QT interval duration: differences among congenital long QT syndrome subtypes. *J Cardiovasc Electrophysiol.* 2004;15:550–6.
- Couderc JP, Vaglio M, Cia X, et al. Impaired T-amplitude adaptation to heart rate characterizes IKr inhibition in the congenital and acquired forms of the long QT syndrome. *J Cardiovasc Electrophysiol.* 2007;18:1299–305.
- Kaufman ES, Priori SG, Napolitano C, et al. Electrocardiographic prediction of abnormal genotype in congenital long QT syndrome: experience in 101 related family members. *J Cardiovasc Electrophysiol.* 2001;12(4):455–61.

32. Antzelevitch C, Shimizu W. Cellular mechanisms underlying the long-QT syndrome. *Curr Opin Cardiol.* 2002;17:43–51.
33. Noda T, Takaki H, Kurita T, et al. Gene-specific response of dynamic ventricular repolarization to sympathetic stimulation in LQT1, LQT2 and LQT3 forms of congenital long QT syndrome. *Eur Heart J.* 2002;23:975–83.
34. Ackerman MJ, Khositseth A, Tester DJ, Hejlik J, Shen WK, Porter CJ. Epinephrine-induced QT interval prolongation: a gene-specific paradoxical response in congenital long QT syndrome. *Mayo Clin Proc.* 2002;77:413–21.
35. Shimizu W, Noda T, Takaki H, et al. Diagnostic value of epinephrine test for genotyping LQT1, LQT2, and LQT3 forms of congenital long QT syndrome. *Heart Rhythm.* 2004;1:276–83.
36. Priori SG, Napolitano C, Schwartz PJ, et al. Association of long QT syndrome loci and cardiac events among patients treated with β -blockers. *JAMA.* 2004;292:1341–4.
37. Napolitano C, Priori SG, Schwartz PJ, et al. Genetic testing in the long QT syndrome. Development and validation of an efficient approach to genotyping in clinical practice. *JAMA.* 2005;294:2975–80.
38. Taggart NW, Haglund CM, Tester DJ, Ackerman MJ. Diagnostic miscues in congenital long-QT syndrome. *Circulation.* 2007;115:2613–20.
39. Tester DJ, Kopplin LJ, Will ML, Ackerman MJ. Spectrum and prevalence of cardiac ryanodine receptor (RyR2) mutations in a cohort of unrelated patients referred explicitly for long QT syndrome genetic testing. *Heart Rhythm.* 2005;2:1099–105.
40. Phillips KA, Ackerman MJ, Sakiwski J, Berul CI. Cost-effectiveness analysis of genetic testing for familial long QT syndrome in symptomatic index cases. *Heart Rhythm.* 2005;2:1294–300.
41. Schwartz PJ, Priori SG, Spazzolini C, et al. Genotype-phenotype correlation in the long-QT syndrome: gene-specific triggers for life-threatening arrhythmias. *Circulation.* 2001;103(1):89–95.
42. Ackerman MJ, Tester DJ, Porter CJ. Swimming, a gene-specific arrhythmogenic trigger for inherited long QT syndrome. *Mayo Clin Proc.* 1999;74(11):1088–94.
43. Moss AJ, Robinson JL, Gessman L, et al. Comparison of clinical and genetic variables of cardiac events associated with loud noise versus swimming among subjects with the long QT syndrome. *Am J Cardiol.* 1999;84(8):876–9.
44. Goldenberg I, Thottathil P, Lopes CM, et al. Trigger-specific ion-channel mechanisms, risk factors, and response to therapy in type 1 long QT syndrome. *Heart Rhythm.* 2012;9(1):49–56.
45. Kim JA, Lopes CM, Moss AJ, et al. Trigger-specific risk factors and response to therapy in long QT syndrome type 2. *Heart Rhythm.* 2010;7(12):1797–805.
46. Locati EH, Zareba W, Moss AJ, et al. Age- and sex-related differences in clinical manifestations in patients with congenital long-QT syndrome: findings from the International LQTS Registry. *Circulation.* 1998;97:2237–44.
47. Goldenberg I, Moss AJ, Peterson DR, McNitt S, Zareba W, Andrews ML, et al. Risk factors for aborted cardiac arrest and sudden cardiac death in children with the congenital long-QT syndrome. *Circulation.* 2008;117:2184–91.
48. Hobbs JB, Peterson DR, Moss AJ, et al. Risk of aborted cardiac arrest or sudden cardiac death during adolescence in the long-QT syndrome. *JAMA.* 2006;296:1249–54.
49. Sauer AJ, Moss AJ, McNitt S, et al. Long QT syndrome in adults. *J Am Coll Cardiol.* 2007;49:329–37.
50. Goldenberg I, Moss AJ, Bradley J, Polonsky S, Peterson DR, McNitt S, et al. Long-QT syndrome after age 40. *Circulation.* 2008;117:2192–201.
51. Drici MD, Burklow TR, Haridasse V, Glazer RI, Woosley RL. Sex hormones prolong the QT interval and downregulate potassium channel expression in the rabbit heart. *Circulation.* 1996;94:1471–4.
52. Bidoggia H, Maciel JP, Capalozza N, Mosca S, Blaksley EJ, Valverde E, et al. Sex differences on the electrocardiographic pattern of cardiac repolarization: possible role of testosterone. *Am Heart J.* 2000;140:678–83.
53. Liu XK, Katchman A, Drici MD, et al. Gender difference in the cycle length-dependent QT and potassium currents in rabbits. *J Pharmacol Exp Ther.* 1998;285:672–9.
54. Seth R, Moss AJ, McNitt S, et al. Long QT syndrome and pregnancy. *J Am Col Cardiol.* 2007;49:1092–8.
55. Buber J, Mathew J, Moss AJ, Hall WJ, Barsheshet A, McNitt S, et al. Risk of recurrent cardiac events after onset of menopause in women with congenital long-QT syndrome types 1 and 2. *Circulation.* 2011;123:2784–91.
56. Imboden M, Swan H, Denjoy I, Van Langen IM, Latinen-Forsblom PJ, Napolitano C, et al. Female predominance and transmission distortion in the long-QT syndrome. *N Engl J Med.* 2006;355:2744–5.
57. Barsheshet A, Goldenberg I, O-Uchi J, et al. Mutations in cytoplasmic loops of the KCNQ1 channel and the risk of life-threatening events: implications for mutation-specific response to beta-blocker therapy in type 1 long-QT syndrome. *Circulation.* 2012;125:1988–96.
58. Matavel A, Medei E, Lopes CM. PKA and PKC partially rescue long QT type 1 phenotype by restoring channel-PIP(2) interactions. *Channels (Austin).* 2010;4(1):3–11.
59. Costa J, Lopes CM, Barsheshet A, et al. Combined assessment of sex- and mutation-specific information for risk stratification in type 1 long QT syndrome. *Heart Rhythm.* 2012;9(6):892–8.
60. Schwartz PJ, Vanoli E, Crotti L, et al. Neural control of heart rate is an arrhythmia risk modifier in long QT syndrome. *J Am Coll Cardiol.* 2008;51(9):920–9.

61. Brink PA, Crotti L, Corfield V, et al. Phenotypic variability and unusual clinical severity of congenital long-QT syndrome in a founder population. *Circulation*. 2005;112(17):2602–10.
62. Barsheshet A, Peterson DR, Moss AJ, et al. Genotype-specific QT correction for heart rate and the risk of life-threatening cardiac events in adolescents with congenital long-QT syndrome. *Heart Rhythm*. 2011;8(8):1207–13.
63. Migdalovich D, Moss AJ, Lopes CM, et al. Mutation and gender-specific risk in type 2 long QT syndrome: implications for risk stratification for life-threatening cardiac events in patients with long QT syndrome. *Heart Rhythm*. 2011;8(10):1537–43.
64. Liu JF, Moss AJ, Jons C, et al. Mutation-specific risk in two genetic forms of type 3 long QT syndrome. *Am J Cardiol*. 2010;105(2):210–3.



Clinical Management of LQTS Patients

9

Wojciech Zareba

Overall Management of Patients with LQTS

The long QT syndrome (LQTS) is an inherited channelopathy characterized by QT prolongation and propensity to syncope, cardiac arrest, or sudden death in association with torsade de pointes polymorphic ventricular tachycardia or ventricular fibrillation [1–5]. Management of patients with LQTS aims to decrease the risk of arrhythmic cardiac events and sudden cardiac death in usually young, otherwise healthy individuals [6]. Goals of this therapy are to (1) minimize adrenergic response, (2) shorten QTc, (3) decrease dispersion of refractoriness, and (4) improve function of dysfunctional ion channel, all of them leading to decreasing the risk of ventricular tachyarrhythmias [4, 6]. The risk of arrhythmic events could be significantly diminished by lifestyle modifications and antiadrenergic therapy, decreasing the probability of catecholaminergic response to triggers of arrhythmias [7]. Protection in the case of the recurrent ventricular tachycardia/fibrillation is provided by implantable cardioverter-defibrillator (ICD) usually reserved for high-risk patients and left cardiac sympathetic denervation usually exercised in patients with recurrent arrhythmic events documented on

ICD [8–10]. The QTc shortening is a desired treatment of choice, but the therapeutic options are limited mostly to sodium channel blockers used in patients with LQT3 including mexiletine and ranolazine [11, 12]. A better understanding of the mechanisms of ion channel dysfunction or inappropriate trafficking of channel proteins might lead to pharmacotherapy, correcting the underlying ion channel abnormalities [4]. Gene therapy is an ultimate future of treatment of inherited arrhythmia disorders, but it is not yet available for clinical trials.

Preventive Measures in LQTS Patients

The LQTS patients frequently have their arrhythmic events triggered by stress, exercise, or sudden awakening [13–15]. Several precautions and preventive measures should be implemented in patients with LQTS (Table 9.1). Patients and their family members should be advised to remove or blunt ringing clocks and silent the phones and other devices creating sudden noise. Any conditions resulting in a startle, arousal, or stress should be avoided. Patients should avoid getting involved in competitive sports and especially water sports because swimming and sudden immersion in water might trigger ventricular tachyarrhythmias [15, 16]. The triggers of arrhythmic events are predominantly gene-specific (swimming in LQT1, loud noise in LQT2), but in general, they

W. Zareba (✉)
Cardiology Division, Clinical Cardiovascular
Research Center, University of Rochester Medical
Center, Rochester, NY, USA
e-mail: wojciech_zareba@urmc.rochester.edu

Table 9.1 Preventive management in LQTS patients

Diminish the risk of stress and arousal situations triggering cardiac events including phone rings, alarm clocks, and other sudden startle conditions.
Avoid competitive sports and strenuous exercises.
Increase awareness of the risks associated with water activities including jumping into water and swimming.
Avoid QT-prolonging drugs.
Monitor adherence to beta-blocker treatment.
Use automatic external defibrillator to protect patients.

should be avoided by all LQTS patients [15, 17, 18]. Refraining from competitive sports including swimming or jumping into water is difficult to accomplish in adolescents and young adults who are motivated to participate in competitive sport activities at schools [19]. Prospect of sport-based scholarships when considering admission to a college is a strong incentive, and LQTS patients and their parents sometimes refuse to accept advice that participation in competitive sports should be abandoned. This advice should be applied to all types of LQTS patients; however, some patients with LQT3 pursue their athletic activities since their QTc shortens with exercise and they mostly have their events during sleep at night. In the case LQTS patients still pursue athletic activities, one needs to consider extra precautions including automatic external defibrillators at trainings [20] and competitions, and in high-risk patients, an ICD could be considered on case-by-case basis [19].

LQTS patients and their family members must be informed about drugs that might prolong QT interval because a number of cardiac and noncardiac medications might cause drug-induced QT prolongation and torsade de pointes [21]. Updated list of drugs that might have QT-prolonging properties is provided at www.crediblemeds.org, and a mobile app is available to immediately access online QTdrugs database [22]. In 2018, the CredibleMeds added another list called QTFactors, describing clinical conditions/diseases associated with prolonged QTc and/or TdP ventricular tachycardia. Clinical factors predisposing to QT prolongation and TdP may include female sex, older age, hypokalemia, hypomagnesemia, bradycardia, pheochromocytoma, and Takotsubo cardiomyopathy. These two databases

are maintained by the nonprofit Arizona Center for Education and Research on Therapeutics (AZCERT) and made available at no cost to researchers, healthcare providers, and patients [22].

Beta-Blocker Therapy

Moss et al. [23] introduced left cervicothoracic sympathetic ganglionectomy in 1971 to effectively treat high-risk patients with LQTS. From this point on, the concept of antiadrenergic therapy with left cardiac sympathetic denervation stlectomy was subsequently translated into broad use of beta-blockers in LQTS patients [24, 25]. Schwartz et al. [25] demonstrated significant effect of beta-blocker therapy in preventing cardiac events in a large cohort of over 200 patients with a 15-year follow-up. Since then beta-blockers remain the therapy of choice in patients with LQTS. In 2000, Moss et al. [26] evaluated the effectiveness of beta-blockers in 896 LQTS patients from the Rochester-Based International LQTS Registry. After initiation of beta-blockers, there was a significant ($p < 0.001$) reduction in the rate of cardiac events in probands (0.97 ± 1.42 to 0.31 ± 0.86 events per year) and in affected family members (0.26 ± 0.84 to 0.15 ± 0.69 events per year) during 5-year matched periods. Interestingly, when effects of beta-blockers on QTc duration was evaluated, patients with aborted cardiac arrest or death had no significant change in QTc before vs. after beta-blocker therapy, whereas patients free of events had a 20-millisecond QTc shortening after initiation of beta-blocker therapy. Cardiac event rates were more effectively reduced with beta-blockers in LQT1 than in LQT2 patients. The analysis of dose dependency of response to beta-blockers showed that lower and higher doses of beta-blockers had similar effects on cardiac event rates. Among 33 patients who died on beta-blockers, 8 stopped beta-blockers and 3 were not known whether they continued therapy with beta-blockers.

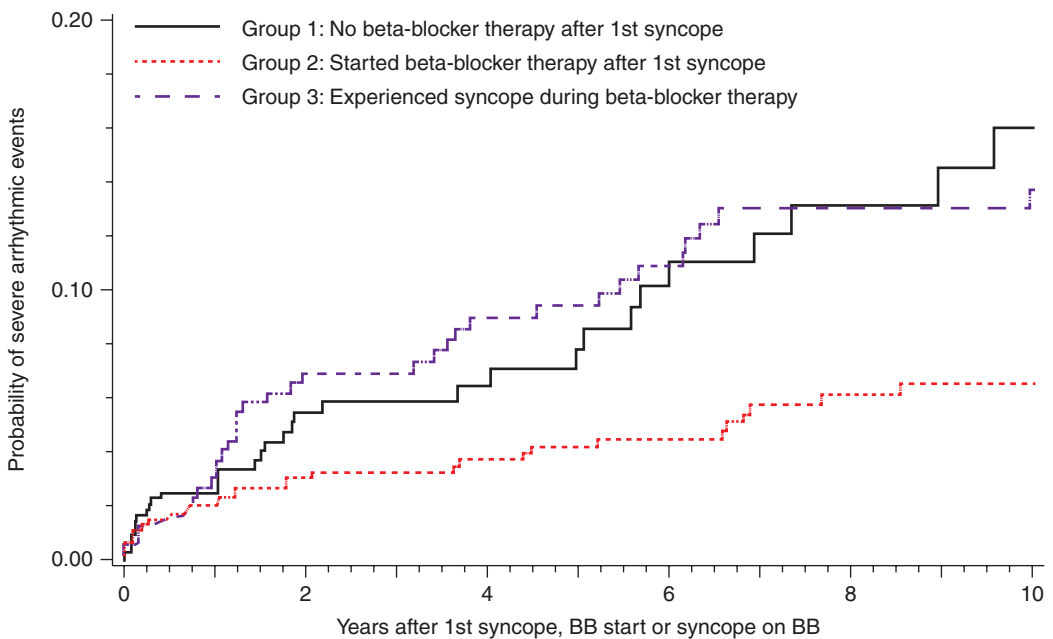
In 2004, Priori et al. [27] evaluated effects of beta-blockers in 335 LQTS patients. Cardiac

events occurred in 19 of 187 (10%) LQT1 patients, 27 of 120 (23%) LQT2 patients, and 9 of 28 (32%) LQT3 patients ($p < 0.001$). The risk of cardiac events was higher among LQT2 and LQT3 patients than among LQT1 patients, suggesting inadequate protection from beta-blocker therapy in LQT2 and LQT3 patients.

In a Rochester LQTS Registry study of high-risk adolescents with LQTS and history of syncope in the past 2 years [28], beta-blockers were associated with a 64% reduced risk (hazard ratio, 0.36; 95% CI: 0.18–0.72; $p = 0.01$). Figure 9.1 shows cumulative probability of aborted cardiac arrest in a large cohort LQTS patients from Rochester LQTS Registry who experienced syncope, which is one of the key risk factors in relationship to beta-blocker treatment [29]. Patients who started beta-blockers after first syncope had a 7% risk of life-threatening arrhythmic events at

10-year follow-up in comparison to 16% for those who did not start beta-blocker after first event and 14% for those who had syncope during beta-blocker therapy.

Vincent et al. [30] studied cardiac events in 216 LQT1 patients treated with beta-blocker and followed up for a median time of 10 years. Before beta-blockers, 157 (73%) patients had cardiac events, and after beta-blocker, 75% were asymptomatic, and cardiac events were significantly reduced ($p < 0.001$). Twelve patients suffered cardiac arrest or sudden death, but 11 of 12 were non-compliant. This study further confirmed high effectiveness of beta-blockers in LQT1 patients. However, as it was shown by the study of Barsheshet et al. from 2012 [31], LQT1 patients with mutations located in the cytoplasmic loop of the KCNQ1 channel had significantly higher risk of cardiac events than patients with other mutation



Patients at risk

Group 1	975	247 (0.05)	145 (0.06)	103 (0.10)	77 (0.13)	53 (0.16)
Group 2	746	526 (0.03)	410 (0.04)	315 (0.04)	235 (0.06)	173 (0.07)
Group 3	314	250 (0.07)	211 (0.09)	175 (0.11)	143 (0.13)	119 (0.14)

Fig. 9.1 The cumulative risk of severe arrhythmic events and beta-blocker therapy. The solid black line represents all patients after the first syncopal event until start of beta-blocker (BB) therapy. After the start of beta-blocker

therapy, patients are represented by the red dashed line. Patients with a syncopal event occurring while off beta-blocker therapy are represented by the purple dashed line. (Reproduced with permission from Jons et al. [29])

locations. Interestingly, those with cytoplasmic loop mutations had about 88% reduction in aborted cardiac arrest or sudden death with beta-blockers, whereas those with other mutations did not have benefit of beta-blockers. This important observation implies that when physicians plan treatment of LQT1 patients, they should identify location of mutation.

In 2014, Abu-Zeitone et al. [32] published data from 1530 LQTS patients from the Rochester LQTS Registry who were prescribed common beta-blockers (atenolol, metoprolol, propranolol, or nadolol). Time-dependent Cox regression analyses were used to compare the efficacy of different beta-blockers with the risk of cardiac events in LQTS. There were 346 cardiac events defined as syncope, aborted cardiac arrest, or sudden cardiac death among 1319 patients who continuously were taking beta-blockers, and in overall, any beta-blocker treatment was associated with a 37% reduction in the risk of first cardiac events (HR = 0.63; 95% CI: 0.47–0.86; $p = 0.004$). Nadolol was associated with the most pronounced reduction of these events (HR = 0.51; 95% CI: 0.35–0.74; $p < 0.001$), propranolol showed HR = 0.65 (95% CI: 0.46–0.90; $p = 0.01$), atenolol showed hazard ratio = 0.71 (95% CI: 0.50–1.01; $p = 0.06$), and metoprolol showed with hazard ratio = 0.70 (95% CI: 0.43–1.15; $p = 0.16$). When the analysis was focused on

more severe life-threatening events consisting of aborted cardiac arrest or sudden cardiac death, which were observed in 73 patients, there was a 63% overall reduction with any beta-blockers, and there was no significant difference among different beta-blockers. As shown in Table 9.2 for LQT1 and LQT2 patients, the analysis of the effectiveness of beta-blockers by genotype was powered for cardiac events that included syncope. In LQT1 patients, all beta-blockers had a similar effect (although there were too few patients and too few events on metoprolol). However, in LQT2 patients, nadolol was the only beta-blocker showing significant efficacy.

Mazzanti et al. [33] evaluated efficacy of beta-blockers in reducing the risk of life-threatening arrhythmic events in 1710 LQTS patients, and they found that nadolol was associated with a significant 62% risk reduction (HR: 0.38; 95% CI: 0.15–0.93; $p = 0.03$) compared with no treatment. Propranolol was not associated with significant reduction in events (HR: 0.74; 95% CI: 0.32–1.68; $p = 0.47$). The selective beta-blockers combined (including metoprolol, atenolol, bisoprolol, carvedilol, and nebivolol) were not associated with reduction in events (HR: 0.79; 95% CI: 0.35–1.77; $p = 0.56$).

They also evaluated whether the difference in efficacy in favor of nadolol could be confirmed in the subgroup of patients treated with therapeutic

Table 9.2 Genotype- and drug-specific first cardiac event rates on beta-blocker therapy and covariate-adjusted hazard ratios. Relative to discontinuing beta-blockers in patients with LQT1 and LQT2

Time-dependent variable	LQT1 ($n = 379$) Total number of CE = 87			LQT2 ($n = 406$) Total number of CE = 85		
	First CE	Hazard ratio (95% CI)	P value	First CE	Hazard ratio (95% CI)	P value
Atenolol	21/105 (20.0%)	0.43 (0.22–0.86)	0.02	28/114 (24.6%)	1.04 (0.48–2.27)	0.92
Metoprolol	3/20 (15.0%)	0.44 (0.13–1.54)	0.2	10/46 (21.7%)	0.82 (0.32–2.09)	0.67
Propranolol	26/72 (36.1%)	0.38 (0.19–0.73)	0.004	28/100 (28.0%)	0.65 (0.29–1.42)	0.28
Nadolol	22/125 (17.6%)	0.50 (0.25–0.98)	0.04	10/109 (9.2%)	0.40 (0.16–0.98)	0.04
Test of equality of 4 drug specific			0.83			0.04

Reproduced with permission from Abu-Zeitone et al. [32]

CE denotes cardiac events (syncope or aborted cardiac arrest or death)

CI confidence interval

doses of nadolol, metoprolol, and propranolol, corresponding to 50% or more of the recommended daily dose (i.e., nadolol 0.5 mg/kg, metoprolol 1.0 mg/kg, and propranolol 1.5 mg/kg).

Patients treated with therapeutic doses of propranolol or metoprolol were at greater risk of events than patients treated with high doses of nadolol (HR for propranolol/metoprolol vs. nadolol: 2.77; 95% CI: 1.11–6.94; $p = 0.03$).

In the Abu-Zeitone’s analysis [32], patients experiencing cardiac events while receiving beta-blocker therapy were at high risk for subsequent life-threatening cardiac events, and propranolol was the least effective agent when comparing with nadolol, metoprolol, and atenolol in preventing recurrent cardiac events in these high-risk patients (Fig. 9.2). Although nadolol remains the beta-blocker of choice based on the above data, the fact that atenolol and metoprolol might similarly reduce the risk of recurrent event is

important for clinical practice when patients might not tolerate given beta-blockers.

In another study by Chockalingam et al. [34], cardiac events were analyzed in 281 previously asymptomatic patients and no differences in cardiac event occurrence was observed among patients using metoprolol, propranolol, and nadolol. They found a higher rate of cardiac events among symptomatic patients receiving metoprolol compared with those taking propranolol and nadolol.

Lower effect of propranolol and metoprolol might be related to their additional action on potassium ion channels. Kawakami et al. [35] evaluated the effect of beta-blockers on the hERG channel, and they found that the rapid component of the cardiac potassium channel (IKr) was blocked by high concentrations of propranolol, but not by atenolol or metoprolol within the therapeutic concentration range. In contrast, carvedilol directly inhibited HERG channels at clinically

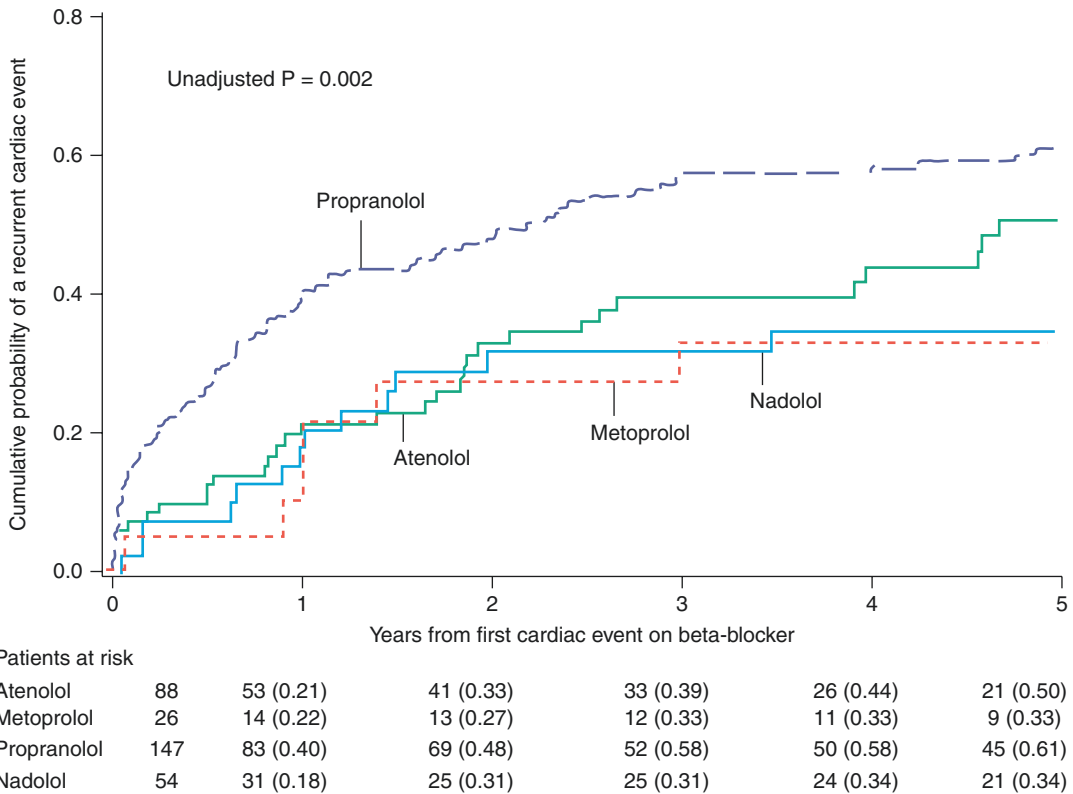


Fig. 9.2 Cumulative probability of a subsequent cardiac event among patients with first cardiac event while taking beta-blocker therapy. (Reproduced with permission from Abu-Zeitone et al. [32])

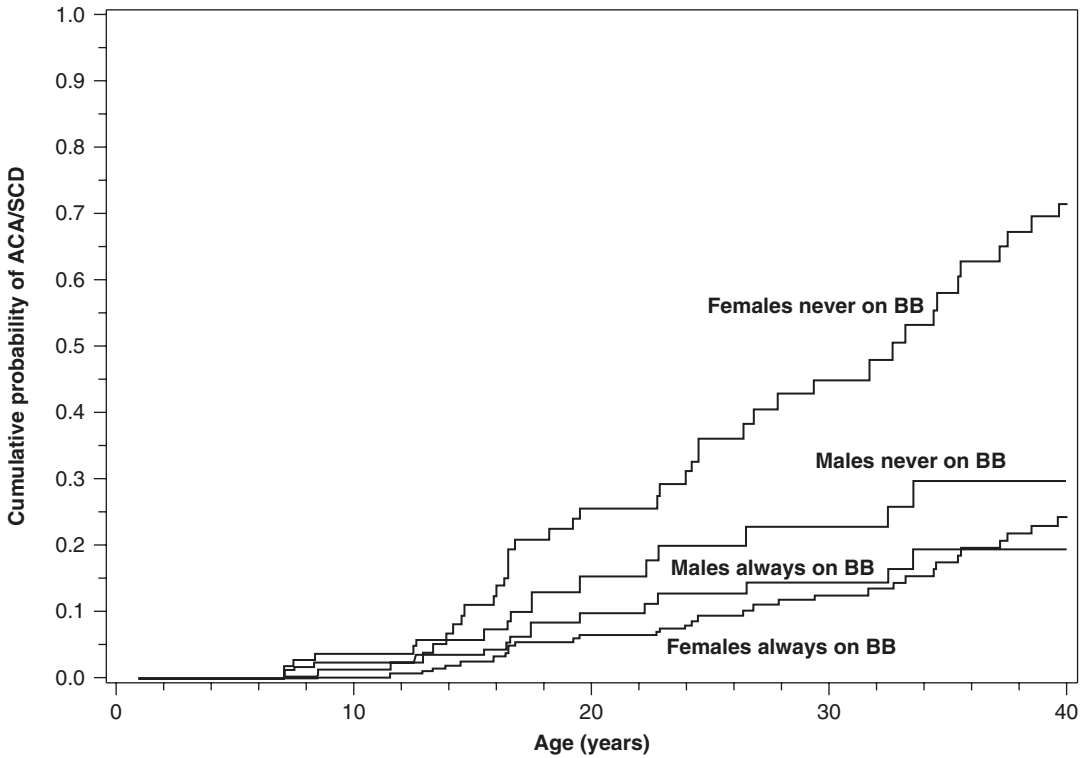


Fig. 9.3 Cox model-based predicted distributions of the age at first ACA or SCD. The analysis is conditional on event-free survival to age 1 year, by BB and sex for asymptomatic patients (no prior syncope) born in 1971

(median) with a QTc ≥ 500 ms and neither lower-risk mutation (neither E1784K nor D1790G). (Reproduced with permission from Wilde et al. [38])

relevant concentrations. Thus, carvedilol might not be recommended in the treatment of LQTS patients. High-risk LQTS patients might be more sensitive to HERG-blocking action of propranolol, and possibly this is why they are less effective in LQTS patients with prior events.

The use of beta-blockers in LQTS patients has always been controversial since these patients tend to have more pronounced QT prolongation and events during bradycardia than tachycardia [17, 27, 36]. Calvillo et al. [36] demonstrated in the LQT3 transgenic mice that propranolol was effective in reducing life-threatening arrhythmias despite prior experimental and clinical data warning against use of beta-blockers [27, 37]. In the largest to date analysis of 391 LQT3 patients by Wilde et al. [38], 118 (30%) patients had cardiac event including syncope and 24 (20%) had aborted cardiac arrest or sudden cardiac death. Females had significantly higher risk of cardiac events than males in univariate analysis, 44% vs.

28%, respectively ($p = 0.036$), and the effect of beta-blockers on reducing cardiac events was significant in females but not in males (Fig. 9.3). Cox regression analysis revealed that time-dependent beta-blocker therapy was associated with an 83% reduction in cardiac events in females (HR = 0.17; 95% CI: 0.04–0.70; $p = 0.014$) but not in males (HR = 0.94; 95% CI: 0.40–2.21; $p = 0.895$), with a significant sex-beta-blocker interaction ($p = 0.04$). When analyzing life-threatening events defined as aborted cardiac arrest or sudden cardiac death, beta-blockers reduced these events by 80% among women (HR = 0.20; 95% CI: 0.05–0.87; $p = 0.032$) and by 49% although nonsignificantly in males (HR = 0.51; 95% CI: 0.13–1.88; $p = 0.308$). There is no good explanation why there is different efficacy of beta-blockers in LQTS females than males, but these data have proven no evidence of proarrhythmia by beta-blockers even in LQTS males.

Table 9.3 2017 AHA/ACC/HRS guideline for therapeutic management of patients with long QT syndrome

Class of recommendation	Recommendations
I	In patients with LQTS and SCA, an ICD is recommended if meaningful survival of greater than 1 year is expected
I	In patients with LQTS with a resting QTc greater than 470 ms, a beta-blocker is recommended
I	In high-risk patients with symptomatic LQTS in whom a beta-blocker is ineffective or not tolerated, intensification of therapy with additional medications (guided by consideration of the particular long QT syndrome type), left cardiac sympathetic denervation, and/or an ICD is recommended
I	In patients with LQTS and recurrent appropriate ICD shocks despite maximum tolerated doses of a beta-blocker, intensification of medical therapy with additional medications (guided by consideration of the particular long QT syndrome type) or left cardiac sympathetic denervation is recommended
II a	In asymptomatic patients with LQTS and a resting QTc less than 470 ms, chronic therapy with a beta-blocker is reasonable
II b	In asymptomatic patients with long QT syndrome and a resting QTc greater than 500 ms while receiving a beta-blocker, intensification of therapy with medications (guided by consideration of the particular long QT syndrome type), left cardiac sympathetic denervation, or an ICD may be considered

Based on data in Al-Khatib et al. [40]. For all these recommendations, there is a level of evidence B without data from randomized trials

As indicated by study of Vincent et al. [30] for LQT1 patients, nonadherence to prescribed beta-blockers is of major consequences. In a study from New Zealand [39], half of studied LQT1 and LQT2 patients showed suboptimal adherence indicating that significant education of LQTS patients is needed especially since a number of them are adolescents or young adults.

Table 9.3 summarizes the “2017 AHA/ACC/HRS Guideline for Management of Patients With Ventricular Arrhythmias and the Prevention of Sudden Cardiac Death” specifically focusing on the LQTS patients [40]. In patients with LQTS with a resting QTc greater than 470 ms, a beta-blocker is recommended with class I indication regardless of genotype. Class IIa indication is given to asymptomatic patients with LQTS and a resting QTc less than 470 ms, in whom chronic therapy with a beta-blocker is reasonable.

Pharmacotherapy Targeting Ion Channel Dysfunction

During the last over two decades since first identification of specific LQTS gene mutations affecting ion channel function, there were substantial advances in the understanding of the pathophysiology of inherited arrhythmia syndromes with

LQTS serving as a paradigm disease [41]. These advances may open opportunities to develop gene-specific therapy for LQTS patients.

Sodium Channel Mutations

The LQT3 is caused by an excessive inflow of sodium current during phase 3 of the action potential caused by mutations in the SCN5A gene [4, 42]. Schwartz et al. [43] published first clinical experience with Na⁺ channel blockade with mexiletine in 6 LQT3 patients in whom a significant QTc interval shortening was observed from 535 ± 32 to 445 ± 31 ms, $p < 0.005$. Administration of mexiletine in 7 LQT2 patients did not change significantly QTc duration in that study. Benhorin et al. [44] evaluated effects of flecainide in 8 LQT3 patients with D1790G mutation carriers in whom a significant QTc shortening was observed from 517 ± 45 to 468 ± 36 ms, $p = 0.011$. These effects were observed during long-term (9–17 months) follow-up with no adverse effects. Windle et al. [45] evaluated effects of 48-hour administration of flecainide in 5 LQT3 patients with delta-KPQ mutation. After the oral dose of 50 mg twice a day, the QTc interval decreased on average by 104 ms, from a baseline value of 565 ± 60 ms to

461 ± 23 ms ($p < 0.04$) with normalization of T-wave morphology. This study was followed by a long-term crossover design (6 months on and 6 months off the drug for 2 years) with low-dose flecainide administration study, which showed an average reduction of QTc interval by 27 ms without major side effects [46]. Priori et al. [47] evaluated the effects of intravenous bolus of flecainide used for diagnosing Brugada syndrome in 13 LQT3 patients, and 6 of them developed significant ST elevation raising concerns about flecainide therapy in LQT3 patients. Flecainide has been used in LQT3 patients with atrial fibrillation, and most likely it could be safely used with a low-dose regimen [46].

The most comprehensive study regarding the use of mexiletine in LQT3 patients was published by Mazzanti et al. [11]. The study population consisted of 34 LQT3 patients, including 19 males and 15 females at the median age of 22 years and median QTc interval before therapy of 509 ms. Before starting mexiletine, 21 of 34 (62%) individuals were asymptomatic. Among the symptomatic patients, 7 had experienced cardiac arrest: 4 while on beta-blockers and 3 while off therapy. At the time of mexiletine initiation, 21 of 34 (62%) patients were on chronic beta-blocker therapy. Mexiletine was administered at the average daily dose of 8 ± 0.5 mg/kg for a median duration of 36 months. Mexiletine significantly shortened QTc by 63 ± 6 ms ($p < 0.0001$) and reduced the percentage of patients with arrhythmic events from 22% to 3% ($p = 0.031$). As shown in Fig. 9.4, the mean number of arrhythmic events per patient was reduced from 0.43 ± 0.17 to 0.03 ± 0.03 ($p = 0.027$), and the annual rate of arrhythmic events from 10.3% to 0.7% ($p = 0.0097$). This study demonstrated in a convincing way that LQT3 patients should be treated with mexiletine with therapeutic goal of reducing QTc <500 ms. Knowing high lethality of cardiac events in the LQT3 patients [3, 5], mexiletine should be considered as the first-line therapy. The question of concomitant administration of beta-blockers together with mexiletine is not fully resolved, but since data from Wilde et al. [38] showed no effectiveness of beta-blockers in LQT3 males, mexiletine should be routinely used

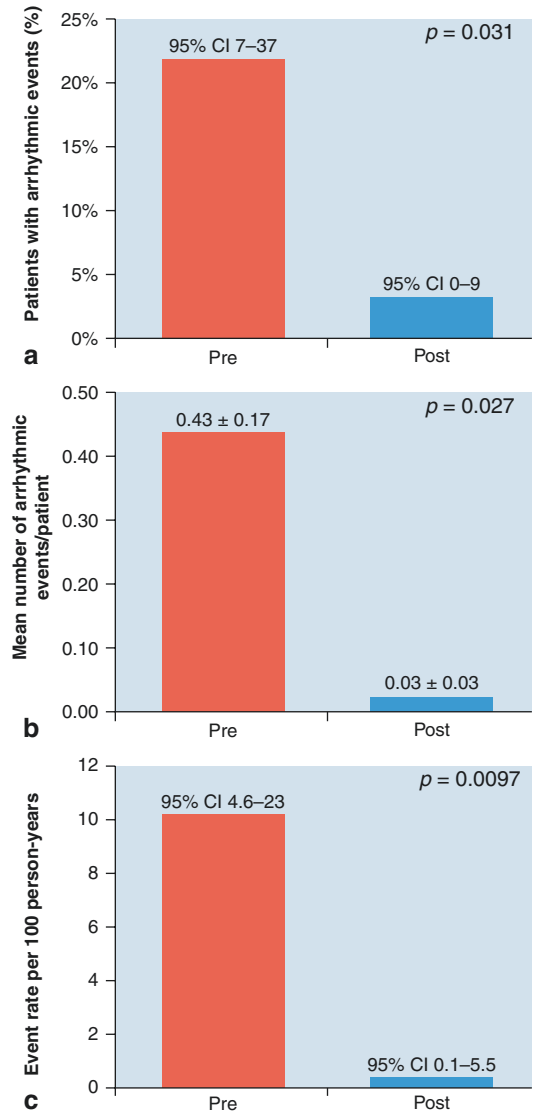


Fig. 9.4 Reduction of arrhythmic events during treatment with mexiletine in patients with LQT3. (Reproduced with permission from Mazzanti et al. [11])

in such patients. Although Wilde et al. [38] showed very significant reduction of cardiac events in LQT3 women with beta-blockers, mexiletine should be considered too in LQT3 women especially if QTc >500 ms, who show high lethality of cardiac events [5]. Mexiletine was well tolerated in the study by Mazzanti et al. [11] without evidence for Brugada ST elevation.

Ranolazine, a late sodium current inhibitor, has been first tested by Moss et al. [48] in LQT3

patients with del-KPQ mutations showing significant reduction in QTc duration after intravenous administration. Subsequently, Chorin et al. [12] conducted a long-term clinical evaluation of ranolazine administration in eight LQT3 patients carrying the D1790G mutation in whom the QTc shortened from 509 ± 41 to 451 ± 26 ms, a mean decrease of 56 ± 52 ms ($p = 0.012$), which was maintained over a period of 22.8 ± 12.8 months of follow-up. Ranolazine reduced the QTc at all heart rates but less so during extreme nocturnal bradycardia. There was no evidence for Brugada ST elevation after ranolazine.

Flecainide blocks the open state of the channel and does not depend on channels entering the inactivated state [49, 50]. An open-state block mechanism underlies the use-dependent blocking effect of flecainide [51]. Ranolazine also is an open-state blocker that unbinds rapidly from the closed state of the sodium channel but is trapped when the channel is in the inactivated state [52]. Flecainide and ranolazine both reduce peak I_{Na} and late I_{Na} , but in the ventricular myocardium, ranolazine more selectively blocks late I_{Na} . The greater selectivity for late I_{Na} , rather than peak I_{Na} , makes ranolazine a better choice than flecainide. Recent data indicates that mexiletine acts via an interaction with the Domain III of the cardiac Na^+ channel voltage-sensing domain, in contrary or in addition to binding effects to the channel pore [53].

The above advances in the gene-specific pharmacotherapy of the LQT3 serve as a paradigm for future of gene-specific therapies in other forms of LQTS. The LQT3 therapeutic options could rely on the existence of several sodium channel blockers, which is not the case for LQT1 and LQT2 forms of the disease since no effective drugs correcting their channel dysfunction exist.

Potassium Channel Mutations

Experimental data shown that an increase in extracellular potassium can limit the development of an arrhythmogenic substrate under long QT conditions, due principally to its action to increase I_{Kr} and I_{K1} and limit the potency of I_{Kr}

blockers [37]. Compton et al. [54] demonstrated that administered potassium corrects repolarization abnormalities in LQT2 patients with I_{Kr} defects. Potassium chloride and spironolactone were administered to 8 LQT2 patients for 4 weeks. The average daily potassium dose was 3.3 ± 1.5 mEq/kg and spironolactone dose was 3.5 ± 1.2 mg/kg, and this regimen resulted in an increase in serum potassium levels from 4.0 ± 0.3 to 5.2 ± 0.3 mEq/l. There were no serious complications associated with therapy. The increase in serum potassium resulted in a decrease in the corrected QT interval from 526 ± 94 to 423 ± 36 ms. These results were encouraging, but long-term supplementation of potassium and administration of spironolactone were proven to be difficult to achieve; therefore, this approach did not get tested in longer event-oriented trials.

Potassium channel openers were also considered based on the observation that administration of nicorandil reduces epinephrine-induced prolongation of the QT interval in LQT1 patients [55]. Oral dosing of nicorandil leads to blood levels in the range of 0.2–0.3 $\mu\text{mol/L}$, whereas intravenous injection can raise plasma levels to 4 $\mu\text{mol/L}$. Therefore, intravenously but not orally administered nicorandil may be of therapeutic value in suppressing repetitive episodes of TdP in patients with LQT1 and LQT2 syndromes; however, it will not be an option for long-term oral therapy.

LQT2 mutations might be caused by hERG-trafficking defects [4]. Lumacaftor is a drug acting on channel trafficking which was tested as safe medication and is used in cystic fibrosis patients [56]. In a study by Mehta et al. [57], induced pluripotent stem cell-derived cardiomyocytes harboring mutations from eight LQT2 patients were tested, and they showed a prolonged corrected field potential durations (equivalent of QTc interval) and increased arrhythmias. Lumacaftor significantly shortened corrected field potential duration by correcting the hERG-trafficking defect, and also it seemed to act on calcium handling by reducing RyR2S2808 phosphorylation in studied cardiomyocytes. The authors concluded that lumacaftor, a drug already in use, can rescue the pathological phenotype of

LQT2-induced pluripotent stem cell-derived cardiomyocytes and might be an option for treating select LQT2 patients, pending proofs of safety and efficacy in clinical trials.

Left Cardiac Sympathetic Denervation (LCSD)

LQTS patients who experience cardiac events while taking beta-blockers are at increased risk for sudden cardiac death, and such patients may benefit from non-pharmacological antiadrenergic therapies such as left cardiac sympathetic denervation [10, 24, 58]. First reported case of such denervation was performed in 1970 by Moss and McDonald [23] in a 39-year-old LQTS patient with recurrent syncope in whom they first tried an injection of lidocaine into the region of left stellate ganglion, which resulted in dramatic QT shortening from 0.64 to 0.46 seconds. Based on this pharmacological testing 2 days later, they performed cervicothoracic sympathetic gangliectomy of left seventh cervical through left second thoracic ganglion, and patients remained free of symptoms for decades. In 1985, Moss et al. [24] reported first data from the International LQTS Registry of 196 patients of whom 16 patients (8%) had undergone left stellate gangliectomy for refractory ventricular arrhythmias showing a 75% reduction in the relative risk of cardiac events. Subsequently, in 1991, Schwartz et al. [10] identified 85 symptomatic LQTS patients worldwide who underwent LCSD and 55% did not have events during about 6-year follow-up after the surgery. This series was further expanded to 147 patients reported in 2004 [58], of whom 99% were symptomatic and 48% experienced prior aborted cardiac arrest, with follow-up over a mean period of 8 years after surgery. During long-term follow-up, 46% of patients became asymptomatic; syncope occurred in 31%, aborted cardiac arrest in 16%, and sudden cardiac death in 7% (Fig. 9.5). The mean yearly number of cardiac events decreased by 91% from 1.32 to 0.19 events per person per year ($p < 0.001$). There was an average QTc shortening by 39 ms

after LCSD in comparison to ECGs before surgery. This study demonstrated that LCSD is associated with a significant, long-term reduction in the frequency of aborted cardiac arrest and syncope. However, the procedure is not entirely effective in preventing sudden death. This therapy should be considered in LQTS patients who experience syncope despite beta-blocker therapy and in those who have arrhythmia storms and shocks with an ICD. In 2009, Collura et al. [59] shared their experience with LCSD performed using minimally invasive video-assisted thoracic surgery in 18 LQTS patients. Subsequent long-term analyses from Mayo Clinic of 52 LQTS patients (18 with minimally invasive surgery) showed that 23% of them had cardiac events after denervation. The authors concluded that LCSD must not be viewed as curative or as an alternative in implantable cardioverter-defibrillator for high-risk patients [60].

Cardiac Pacing

Nowadays, cardiac pacing alone without a defibrillator is rarely used in LQTS patients with exception for significant bradycardia and pauses that contributed to significant QTc prolongation and might lead to bradycardia-dependent TdP [61–63]. Moss et al. [61] demonstrated in a pre-ICD era that pacing is effective in reducing risk of cardiac events and in reducing QTc duration, especially when pacing rate exceeded intrinsic atrial rate. Very similar results were published by Eldar et al. [62]. Since development of atrioventricular blocks is infrequent in LQTS patients (with exception for infants), atrial-only pacing might be exercised. However, experimental data indicate that although atrial pacing shortens repolarization, this effect is diminished during sympathetic activation [64]. Currently, LQTS patients with bradycardia might be offered an ICD, but on individual basis, pacemaker therapy with atrial or dual-chamber pacing might be still considered. In young children with 2:1 atrioventricular block associated with extreme QT prolongation, pacing might be used to enable beta-blocker treatment [65].

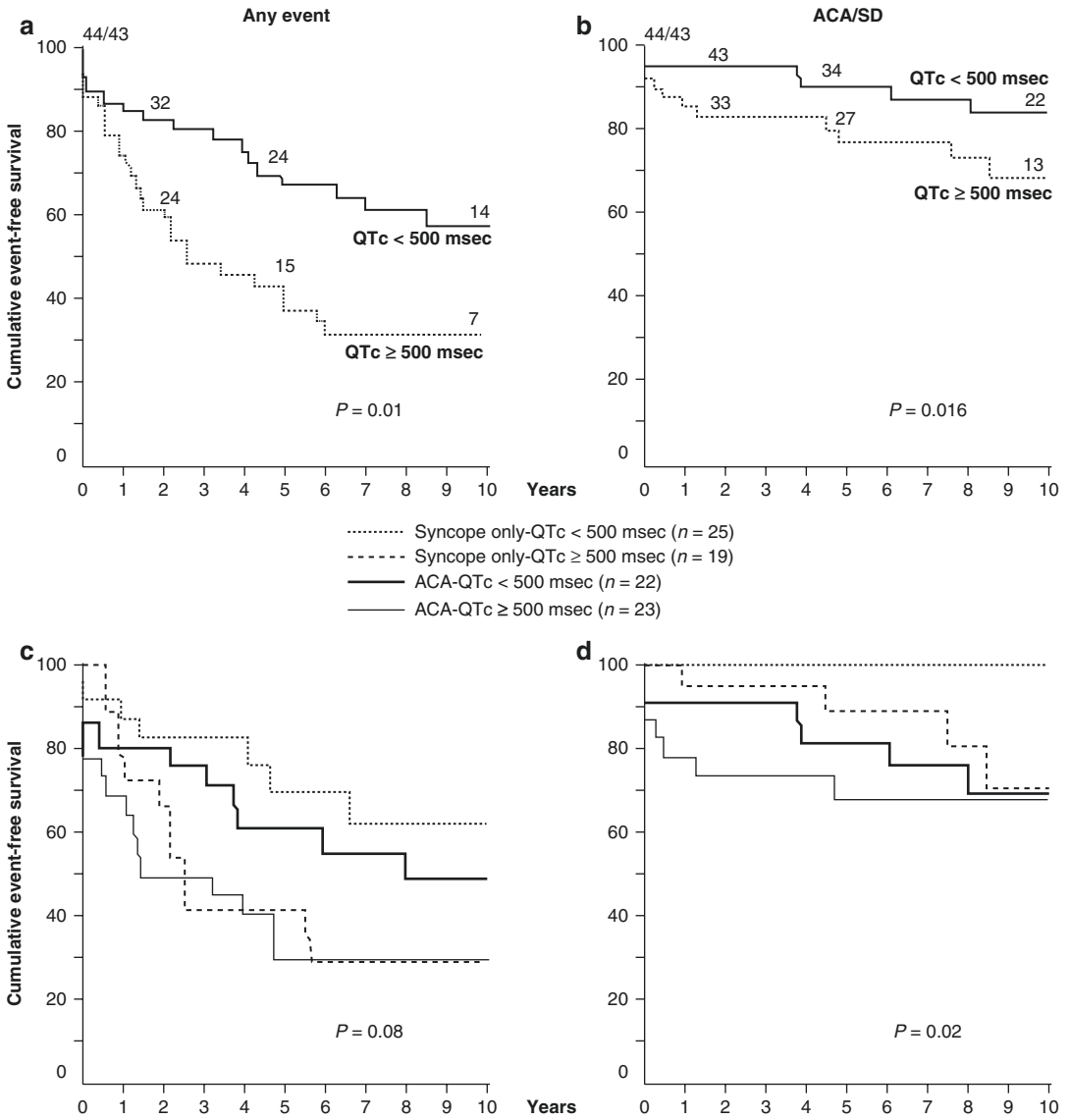


Fig. 9.5 Kaplan-Meier curves of event-free survival and survival according to post-LCSD and QTc in entire population (a, b) and in patients with only syncope or ACA

before LCSD (c, d). (Reproduced with permission from Schwartz et al. [58])

Implantable Cardioverter-Defibrillator in LQTS

Implanted cardioverter-defibrillator (ICD) is indicated for secondary prevention in LQTS patients and for primary prevention in high-risk patients who remain symptomatic despite beta-blocker therapy [40]. Table 9.3 summarizes the “2017 AHA/ACC/HRS Guideline for Management of

Patients With Ventricular Arrhythmias and the Prevention of Sudden Cardiac Death” specifically focusing on the LQTS patients [40]. In patients with LQTS and sudden cardiac arrest, there is class I recommendation for an ICD if meaningful survival of greater than 1 year is expected (level of evidence B with no randomized trials). Similarly, class I indication includes high-risk patients with symptomatic LQTS in whom a

beta-blocker is ineffective (usually syncope on beta-blocker) or not tolerated, in whom intensification of therapy with additional medications (guided by consideration of the particular long QT syndrome type, which is relevant only for LQT3 patients that could be treated with mexiletine, flecainide, or ranolazine), left cardiac sympathetic denervation, and/or an ICD is recommended. There is no clear evidence whether in such high-risk cases LCSD or ICD should be exercised as the first therapy. Knowing limited worldwide accessibility to the LCSD surgery, most frequently an ICD is implanted in such cases.

Figure 9.6 further elaborates on currently proposed strategies regarding prevention of sudden death in LQTS patients [40]. In patients with cardiac events despite beta-blockers, the following risk factors would favor an ICD: QTc >500 ms, genotypes LQT2 and LQT3, females with genotype LQT2, <40 years of age, onset of symptoms

at <10 years of age, and patients with recurrent syncope. Asymptomatic LQTS patients with QTc >500 on beta-blocker therapy have class IIb indication for an ICD [40]. However, there are individual asymptomatic LQT2 and LQT3 patients that might be at high 6% 5-year risk of lethal cardiac events with QTc above 500 or 550 ms [33].

The above recommendations are based on a series of observational papers showing effectiveness of ICD therapy in LQTS patients with primary and secondary prevention of sudden cardiac death. In 1996, Groh et al. [66] reported the use of the ICD in 35 patients with LQTS of whom 75% had aborted cardiac arrest, and during a mean 31-month follow-up, there was no death and 21 patients experienced one or more appropriate ICD therapies. Zareba et al. [8] described ICD therapy in 125 LQTS patients from Rochester LQTS ICD Registry of whom 73 were considered high risk due to either prior aborted cardiac arrest (*n* = 54) or prior syncope despite

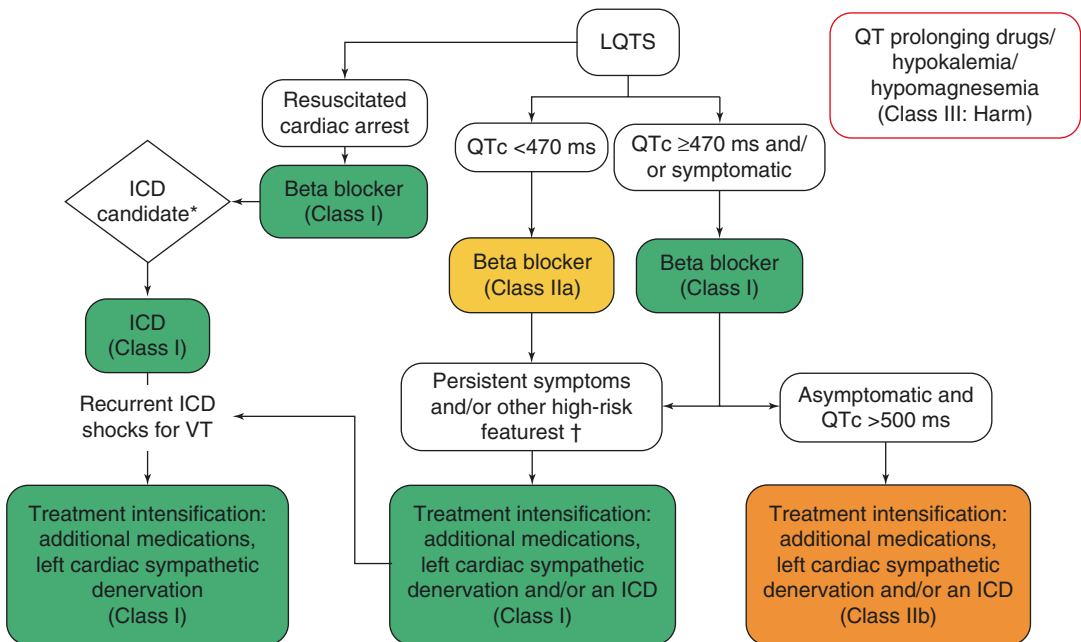


Fig. 9.6 Prevention of SCD in patients with long QT syndrome. Colors correspond to class of recommendation in Table 9.2. (Reproduced with permission from [40])

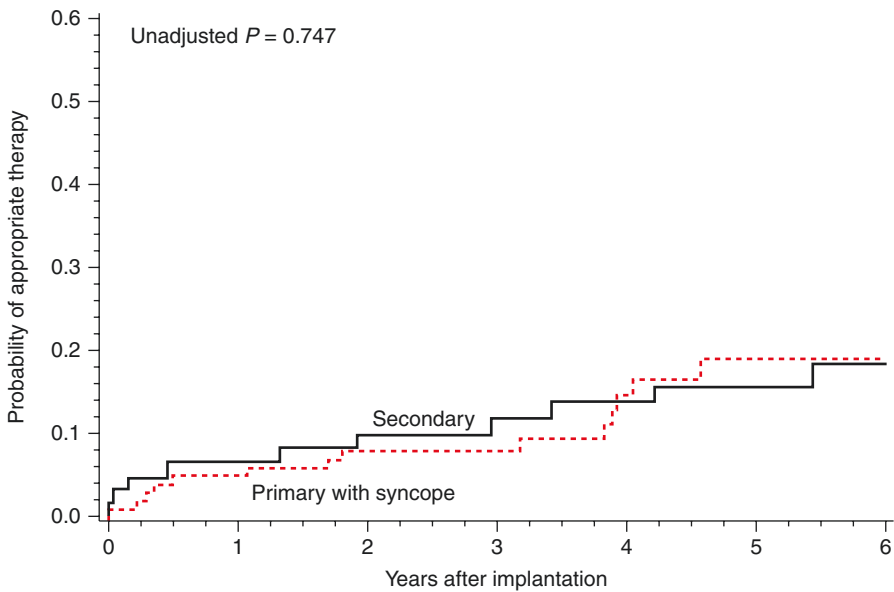
*ICD candidacy as determined by functional status, life expectancy, or patient preference

†High-risk patients with LQTS include those with QTc >500 ms, genotypes LQT2 and LQT3, females with genotype LQT2, <40 years of age, onset of symptoms at <10 years of age, and patients with recurrent syncope ICD indicates implantable cardioverter-defibrillator, LQTS long QT syndrome, VT ventricular tachycardia

beta-blocker therapy ($n = 19$). These 73 ICD patients were matched to 161 LQTS patients who met identical criteria for ICD implantation but were managed medically without an ICD because of patient or physician preference. In the 73 high-risk ICD-treated patients, one death (1.3%) occurred during an average follow-up of 3 years, whereas in the non-ICD patients, 26 deaths (16%) occurred over a follow-up of 8 years. Beta-blockers were used in nearly all the ICD patients. However, despite consistent medical therapy with beta-blockers, treated patients were shown to experience a 4% annual rate of ICD shocks [67]. Additional analyses of Rochester LQTS ICD Registry of 64 patients with secondary indications for ICD due to aborted cardiac arrest vs. 109 ICD patients with primary prevention with syncope showed a similar risk of appropriate ICD therapy at 5 years: 16% and 19%, respectively (Fig. 9.7).

Horner et al. [68] analyzed 51 LQTS patients with an ICD from the Mayo Clinic among whom 12 patients (24%) experienced an appropriate, VF-terminating therapy and 15 (29%) patients experienced an inappropriate shock with an average follow-up of 7.3 years. Secondary prevention indications, non-LQT3 genotype, $QTc \geq 500$ ms, documented syncope, documented torsade de pointes, and a negative family history were most predictive of an appropriate therapy. Potentially lifesaving therapies were rendered at a 5–6% per year rate among those selected for ICD therapy.

In 2010, Schwartz et al. [69] reported data on 233 patients from the European LQTS ICD Registry of whom 44% had a history of aborted cardiac arrest. During a mean 4.6-year follow-up, appropriate ICD therapy was observed in 28% of patients with a 4-year risk at about 30%, higher than risks observed in the Rochester LQTS ICD



	Patients at risk							
Secondary	64	57 (0.06)	50 (0.10)	46 (0.12)	44 (0.14)	36 (0.16)	28 (0.18)	
Primary with Syncope	109	95 (0.05)	86 (0.08)	66 (0.08)	46 (0.15)	27 (0.19)	20 (0.19)	

Fig. 9.7 Probability of appropriate ICD therapy in LQTS patients by indications: 64 patients with secondary indications due to aborted cardiac arrest and 109 patients with primary indications with syncope. The rates of

appropriate ICD therapy at 5 years are 16% in secondary prevention patients and 19% in primary prevention patients with syncope

Registry [8] despite similar mean QTc and similar proportion of patients with aborted cardiac arrest and syncope in both cohorts. In the study by Schwartz et al. [69], appropriate ICD therapies were predicted by age <20 years at implantation, a QTc >500 ms, prior cardiac arrest, and cardiac events despite therapy. These authors have developed the M-FACT score to further risk stratify LQTS patients for an ICD therapy with 1 point given for QTc >500–550 and 2 points for QTc >550 ms, 1 point for prior aborted cardiac arrest, 1 for events on therapy, and 1 point for age ≤20 years, but a negative 1 point was considered if a patient was event-free for >10 years. Cumulative score of 2–3 observed in 103 patients was associated with a 65% event-free survival, whereas score of 4–5 observed in 34 patients was associated with a 35% event-free survival indicating that these two groups were benefiting from an ICD. When analyzing 124 patients without aborted cardiac arrest, those with score of at least 2 (64 patients; 52%) had a 40% event rate, i.e., 60% event-free survival over a mean 7-year follow-up. This risk stratification approach might help in identifying patients that might benefit from an ICD therapy.

Biton et al. [70] analyzed data from Rochester LQTS ICD Registry with 212 LQTS patients that had ICD implantation for primary prevention while excluding patients with prior aborted cardiac arrest who without doubt qualify for ICD. During a median follow-up of 9.2 ± 4.9 years, 42 patients experienced at least one appropriate ICD shock with the 22% cumulative probability of appropriate shock at 8 years. QTc ≥550 ms and prior syncope on beta-blockers were significantly associated with increased risk of appropriate shocks. LQT2 mutation and multiple mutations were associated with 2–three-fold higher risk for recurrent ICD shocks as compared with LQT1 (there was not enough data to assess LQT3 patients in this cohort).

Table 9.4 shows the risk score, which was developed based on these 212 LQTS patients without aborted cardiac arrest, with 1 point given

Table 9.4 Rochester ICD risk score when assessing risk of appropriate ICD shocks in LQTS patients without history of aborted cardiac arrest

Risk variables	0 points	1 point	2 points
QTc	≤499 ms	500–549 ms	≥550 ms
Prior syncope on beta-blocker	No	Yes	
LQT2	No	Yes	
Multiple mutations	No	Yes	

The calculated score is the sum of the points of all four risk variables categories. Reproduced with permission from Biton et al. [70]

for QTc of 500–549, 2 points for QTc ≥550 ms, and 1 point given for history of syncope on beta-blocker, LQT2 mutation, and multiple mutations. As shown in Fig. 9.8, among 137 patients with available genotype data, there were 19 (14%) patients with score of 0, 47 (34%) patients with score of 1, 36 (26%) patients with score of 2, and 35 (26%) patients with score of ≥3. The cumulative probabilities of the first appropriate shock were 0%, 11%, 23%, and 46%, respectively at 6 years of follow-up where more data were available, p -value <0.001. Consistently, the risk score was highly predictive of the rate of appropriate shocks per 100 patient years, p <0.001 (Fig. 9.9), with scores 2–3 identifying high-risk patients. We believe that this Rochester score will help identify LQTS patients without prior aborted cardiac arrest who might benefit from an ICD therapy.

LQTS patients who receive an ICD are generally young and may experience complications of the device for many years [71–73]. These include inappropriate shocks, multiple shocks during a ventricular tachycardia/ventricular fibrillation storm, lead-related complications, the need for device replacement, infection, and psychological adjustment due to device therapy in general [73].

Among the 228 patients from a large study by Schwartz et al. [67], 103 patients (45%) underwent at least 1 revision of the ICD mostly due to battery depletion, and 58 patients (25%) suffered from at least 1 acute and/or chronic adverse event

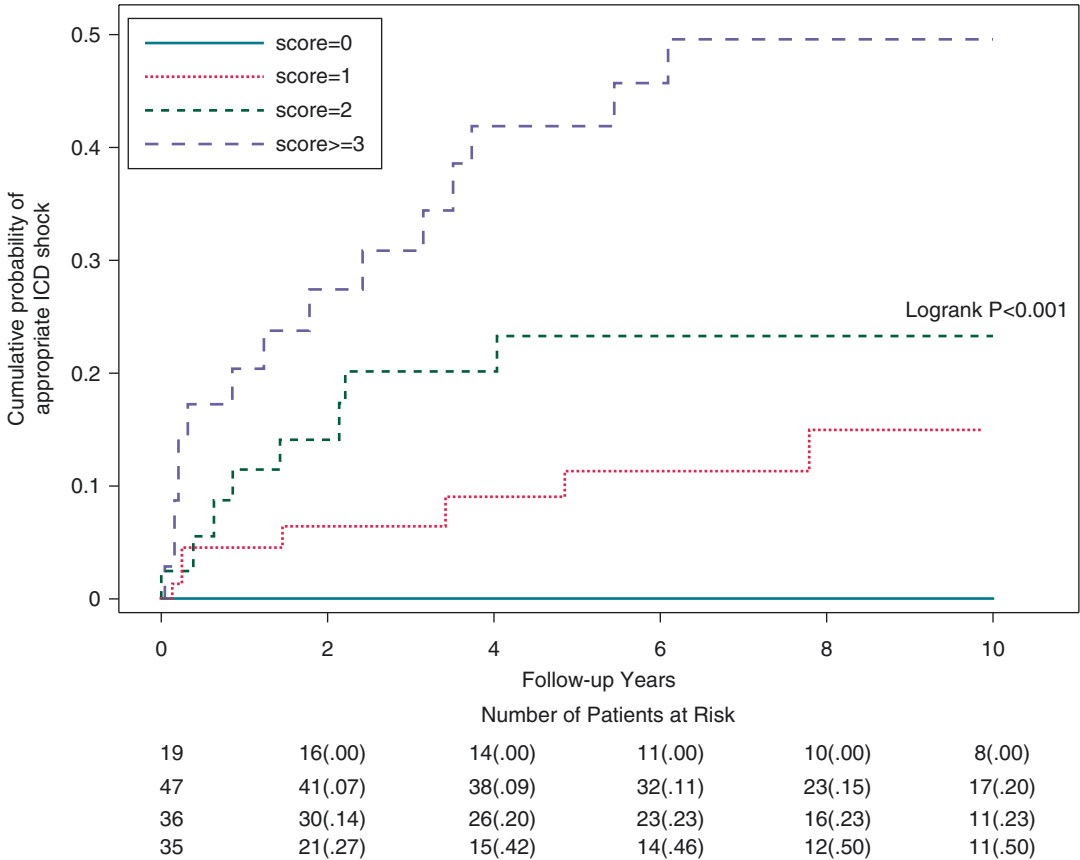
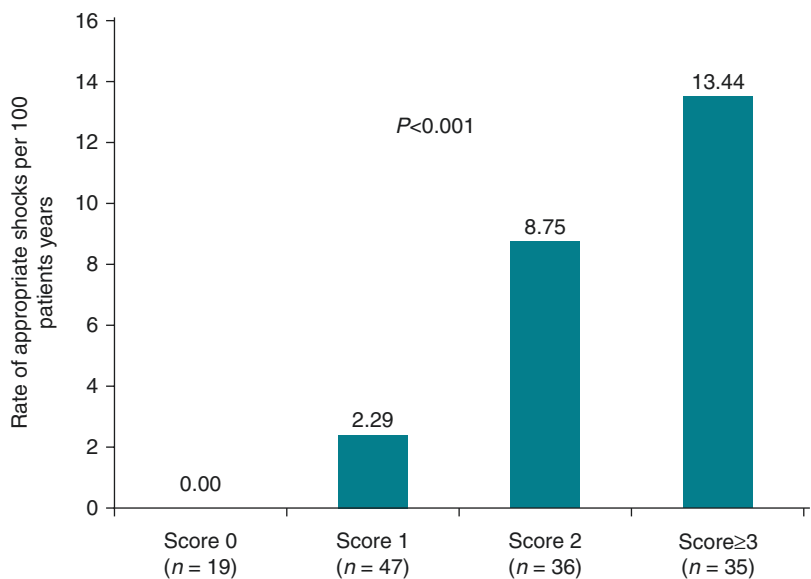


Fig. 9.8 The Kaplan-Meier curves of appropriate ICD shocks by Rochester ICD risk score. (Reproduced with permission from Biton et al. [70])

Fig. 9.9 Event rate of appropriate ICD-rendered shocks (including recurrent) by the Rochester ICD risk score. Event rates of all the appropriate shocks (including recurrent) per 100 patients-years were calculated by dividing the total number of appropriate shocks during the period of follow-up by person-years and multiplying the results by 100. (Reproduced with permission from Biton et al. [70])



associated with the surgical procedure of ICD implantation and/or with both lead and generator functioning.

In the recent analyses of Biton et al. [68], there were 88 inappropriate ICD shocks, 41% were caused due to T-wave oversensing, 14% due to atrial flutter/fibrillation, 22% due to supraventricular tachyarrhythmias, and 20% were caused by electromagnetic interference. Most of the inappropriate shocks ended without further consequences. Two patients (2%) had

appropriate shocks preceded by inappropriate shocks.

Inappropriate therapies tend to occur more often in younger patients [70], and concomitant medical therapy with beta-blockers at higher doses is recommended to minimize the incidence of shocks due to sinus tachycardia or supraventricular arrhythmias. T-wave oversensing, especially in LQT3 or LQT1 patients with larger T waves, remain a challenge requiring further innovation from device manufacturers.

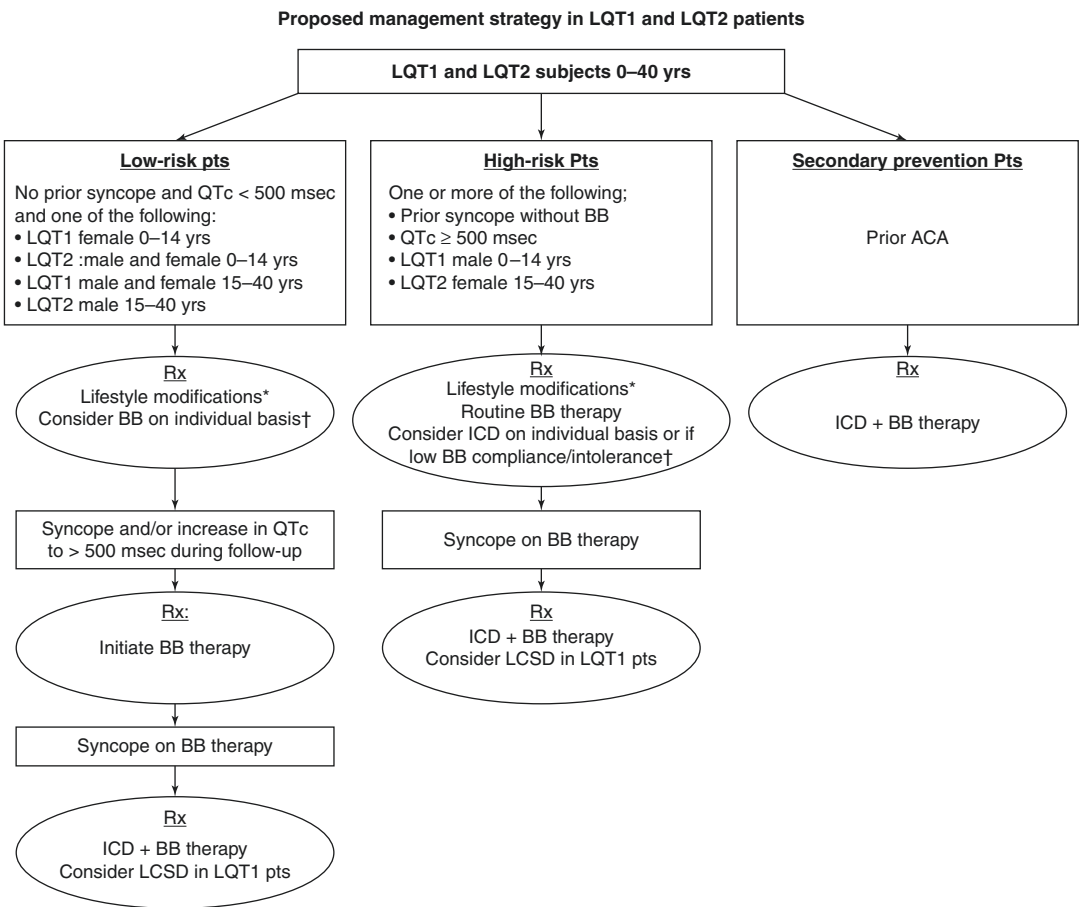


Fig. 9.10 Proposed strategy for the management of LQT1 and LQT2 patients

BB beta-blockers, ICD implantable cardioverter-defibrillator, LCSD left cardiac sympathetic denervation, Rx treatment

*Lifestyle modifications include restriction from competitive sports and swimming in patients with both genotypes and avoidance of unexpected auditory stimuli in the

bedroom (especially during rest or sleep) and potassium supplements (to levels >4 mEq/L) in LQT2 patients. (Reproduced with permission from Goldenberg et al. [75])

†Some authorities recommend different therapeutic approaches, including routine administration of beta-blocker therapy to low-risk patients and primary ICD therapy to high-risk patients with ≥2 risk factors

Avoiding inappropriate or appropriate unnecessary ICD shocks is of major importance in LQTS patients whose catecholaminergic response to initial shock may lead to arrhythmia storm. When programming the device, the duration of detection may be set longer than usual 30 out of 40 to prevent an intervention for a nonsustained TdP that would have terminated spontaneously. VT zone rate also tends to be programmed nowadays at 200 bpm or higher up to 240–250 bpm.

Subcutaneous ICD is increasingly used, and patients with inherited arrhythmia disorders might benefit from this less invasive implantation [74]. Rudic et al. reported data on 62 patients with inherited arrhythmia disorders implanted with subcutaneous ICD for both primary and secondary prevention of sudden death. This cohort included 6 LQTS patients. A total of 20 spontaneous ventricular tachyarrhythmias requiring shock intervention occurred in 10 patients during a mean 31-month follow-up, none in LQTS patients. Averaged delay was 19 seconds, and in 55% of patients, single zone at >240 bpm was used; and in the remaining 24% dual zones, 190–240 and >240 were programmed. All episodes were terminated within the first ICD shock delivery with 80 J. Two patients had inappropriate therapies caused by oversensing. These data support the use of subcutaneous ICD in inherited arrhythmia patients.

Conclusions

Decades of basic and clinical research focused on a better understanding of etiology, mechanisms, and clinical course of the LQTS have led to significantly improved management and therapies resulting in a better survival. Increasing availability of genetic testing provides opportunity to apply more personalized gene-specific management and therapy. LQTS treatment should begin with lifestyle modification and beta-blockers, unless there are valid contraindications. If the patient has one or more syncope despite full-dose beta-blockers, LCSD and ICD should be considered with the final decision based on the individual patient characteristics including age, sex,

previous history, and genetic subgroup including sometime mutation-specific features. Figure 9.10 summarizes management of LQT1 and LQT2 patients dependent on their risk profile. Gene-specific pharmacotherapy is available for LQT3 patients with mexiletine, ranolazine, and flecainide as therapeutic options usually administered together with beta-blockers. This therapy should be administered to decrease QTc duration to values below 500 ms. In high-risk patients with QTc >500 ms despite such therapy or those with prior syncope, an ICD should be considered.

References

1. Moss AJ, Schwartz PJ, Crampton RS, Tzivoni D, Locati EH, MacCluer J, et al. The long QT syndrome. Prospective longitudinal study of 328 families. *Circulation*. 1991;84:1136–44.
2. Schwartz PJ, Moss AJ, Vincent GM, Crampton RS. Diagnostic criteria for the long QT syndrome. An update. *Circulation*. 1993;88:782–4.
3. Zareba W, Moss AJ, Schwartz PJ, Vincent GM, Robinson JL, Priori SG, et al. Influence of the genotype on the clinical course of the long-QT syndrome. International Long-QT Syndrome Registry Research Group. *N Engl J Med*. 1998;339:960–5.
4. El-Sherif N, Turitto G, Boutjdir M. Congenital Long QT syndrome and torsade de pointes. *Ann Noninvasive Electrocardiol*. 2017;22(6).
5. Zareba W, Moss AJ, Locati EH, Lehmann MH, Peterson DR, Hall WJ, et al. Modulating effects of age and gender on the clinical course of long QT syndrome by genotype. *J Am Coll Cardiol*. 2003;42:103–9.
6. Schwartz PJ, Crotti L, Insolia R. Long-QT syndrome: from genetics to management. *Circ Arrhythm Electrophysiol*. 2012;5:868–77.
7. Schwartz PJ. Idiopathic long QT syndrome: progress and questions. *Am Heart J*. 1985;109:399–411.
8. Zareba W, Moss AJ, Daubert JP, Hall WJ, Robinson JL, Andrews M. Implantable cardioverter defibrillator in high-risk long QT syndrome patients. *J Cardiovasc Electrophysiol*. 2003;14:337–41.
9. Sundstrom E, Jensen SM, Diamant UB, Rydberg A. Implantable cardioverter defibrillator treatment in long QT syndrome patients: a national study on adherence to international guidelines. *Scand Cardiovasc J*. 2017;51:88–94.
10. Schwartz PJ, Locati EH, Moss AJ, Crampton RS, Trazzi R, Ruberti U. Left cardiac sympathetic denervation in the therapy of congenital long QT syndrome. A worldwide report. *Circulation*. 1991;84:503–11.
11. Mazzanti A, Maragna R, Faragli A, Monteforte N, Bloise R, Memmi M, et al. Gene-specific therapy

- with mexiletine reduces arrhythmic events in patients with long QT syndrome type 3. *J Am Coll Cardiol*. 2016;67:1053–8.
12. Chorin E, Hu D, Antzelevitch C, Hochstadt A, Belardinelli L, Zeltser D, et al. Ranolazine for congenital long-QT syndrome type III: experimental and long-term clinical data. *Circ Arrhythm Electrophysiol*. 2016;9(10).
 13. Schwartz PJ, Zaza A, Locati E, Moss AJ. Stress and sudden death. The case of the long QT syndrome. *Circulation*. 1991;83:1171–80.
 14. Goldenberg I, Zareba W, Moss AJ. Long QT syndrome. *Curr Probl Cardiol*. 2008;33:629–94.
 15. Ali RH, Zareba W, Moss AJ, Schwartz PJ, Benhorin J, Vincent GM, et al. Clinical and genetic variables associated with acute arousal and nonarousal-related cardiac events among subjects with long QT syndrome. *Am J Cardiol*. 2000;85:457–61.
 16. Moss AJ, Robinson JL, Gessman L, Gillespie R, Zareba W, Schwartz PJ, et al. Comparison of clinical and genetic variables of cardiac events associated with loud noise versus swimming among subjects with the long QT syndrome. *Am J Cardiol*. 1999;84:876–9.
 17. Schwartz PJ, Priori SG, Spazzolini C, Moss AJ, Vincent GM, Napolitano C, et al. Genotype-phenotype correlation in the long-QT syndrome: gene-specific triggers for life-threatening arrhythmias. *Circulation*. 2001;103:89–95.
 18. Goldenberg I, Thottathil P, Lopes CM, Moss AJ, McNitt S, O-Uchi J, et al. Trigger-specific ion-channel mechanisms, risk factors, and response to therapy in type 1 long QT syndrome. *Heart Rhythm*. 2012;9:49–56.
 19. Schnell F, Behar N, Carre F. Long-QT syndrome and competitive sports. *Arrhythm Electrophysiol Rev*. 2018;7:187–92.
 20. Pundi KN, Bos JM, Cannon BC, Ackerman MJ. Automated external defibrillator rescues among children with diagnosed and treated long QT syndrome. *Heart Rhythm*. 2015;12:776–81.
 21. Zareba W. Drug induced QT prolongation. *Cardiol J*. 2007;14:523–33.
 22. Woosley RL, Heise CW, Romero KA. www.crediblemeds.org, QTdrugs List; 2019.
 23. Moss AJ, McDonald J. Unilateral cervicothoracic sympathetic ganglionectomy for the treatment of long QT interval syndrome. *N Engl J Med*. 1971;285:903–4.
 24. Moss AJ, Schwartz PJ, Crampton RS, Locati E, Carleen E. The long QT syndrome: a prospective international study. *Circulation*. 1985;71:17–21.
 25. Schwartz PJ, Locati E. The idiopathic long QT syndrome: pathogenetic mechanisms and therapy. *Eur Heart J*. 1985;6 Suppl D:103–14.
 26. Moss AJ, Zareba W, Hall WJ, Schwartz PJ, Crampton RS, Benhorin J, et al. Effectiveness and limitations of beta-blocker therapy in congenital long-QT syndrome. *Circulation*. 2000;101:616–23.
 27. Priori SG, Napolitano C, Schwartz PJ, Grillo M, Bloise R, Ronchetti E, et al. Association of long QT syndrome loci and cardiac events among patients treated with beta-blockers. *JAMA*. 2004;292:1341–4.
 28. Hobbs JB, Peterson DR, Moss AJ, McNitt S, Zareba W, Goldenberg I, et al. Risk of aborted cardiac arrest or sudden cardiac death during adolescence in the long-QT syndrome. *JAMA*. 2006;296:1249–54.
 29. Jons C, Moss AJ, Goldenberg I, Liu J, McNitt S, Zareba W, et al. Risk of fatal arrhythmic events in long QT syndrome patients after syncope. *J Am Coll Cardiol*. 2010;55:783–8.
 30. Vincent GM, Schwartz PJ, Denjoy I, Swan H, Bithell C, Spazzolini C, et al. High efficacy of beta-blockers in long-QT syndrome type 1: contribution of noncompliance and QT-prolonging drugs to the occurrence of beta-blocker treatment “failures”. *Circulation*. 2009;119:215–21.
 31. Barsheshet A, Goldenberg I, O-Uchi J, Moss AJ, Jons C, Shimizu W, et al. Mutations in cytoplasmic loops of the KCNQ1 channel and the risk of life-threatening events: implications for mutation-specific response to beta-blocker therapy in type 1 long-QT syndrome. *Circulation*. 2012;125:1988–96.
 32. Abu-Zeitone A, Peterson DR, Polonsky B, McNitt S, Moss AJ. Efficacy of different beta-blockers in the treatment of long QT syndrome. *J Am Coll Cardiol*. 2014;64:1352–8.
 33. Mazzanti A, Maragna R, Vacanti G, Monteforte N, Bloise R, Marino M, et al. Interplay between genetic substrate, QTc duration, and arrhythmia risk in patients with long QT syndrome. *J Am Coll Cardiol*. 2018;71:1663–71.
 34. Chockalingam P, Crotti L, Girardengo G, Johnson JN, Harris KM, van der Heijden JF, et al. Not all beta-blockers are equal in the management of long QT syndrome types 1 and 2: higher recurrence of events under metoprolol. *J Am Coll Cardiol*. 2012;60:2092–9.
 35. Kawakami K, Nagatomo T, Abe H, Kikuchi K, Takemasa H, Anson BD, et al. Comparison of HERG channel blocking effects of various beta-blockers—implication for clinical strategy. *Br J Pharmacol*. 2006;147:642–52.
 36. Calvillo L, Spazzolini C, Vullo E, Insolia R, Crotti L, Schwartz PJ. Propranolol prevents life-threatening arrhythmias in LQT3 transgenic mice: implications for the clinical management of LQT3 patients. *Heart Rhythm*. 2014;11:126–32.
 37. Yan GX, Antzelevitch C. Cellular basis for the normal T wave and the electrocardiographic manifestations of the long-QT syndrome. *Circulation*. 1998;98:1928–36.
 38. Wilde AA, Moss AJ, Kaufman ES, Shimizu W, Peterson DR, Benhorin J, et al. Clinical aspects of type 3 long-QT syndrome: an International Multicenter Study. *Circulation*. 2016;134:872–82.
 39. Waddell-Smith KE, Li J, Smith W, Crawford J, Skinner JR. Beta-blocker adherence in familial long QT syndrome. *Circ Arrhythm Electrophysiol*. 2016;9(8).
 40. Al-Khatib SM, Stevenson WG, Ackerman MJ, Bryant WJ, Callans DJ, Curtis AB, et al. 2017 AHA/ACC/HRS guideline for management of patients with ventricular arrhythmias and the prevention of sudden

- cardiac death: executive summary. *Heart Rhythm*. 2018;15:e190–252.
41. El-Sherif N, Boutjdir M. Role of pharmacotherapy in cardiac ion channelopathies. *Pharmacol Ther*. 2015;155:132–42.
 42. Moss AJ, Kass RS. Long QT syndrome: from channels to cardiac arrhythmias. *J Clin Invest*. 2005;115:2018–24.
 43. Schwartz PJ, Priori SG, Locati EH, Napolitano C, Cantu F, Towbin JA, et al. Long QT syndrome patients with mutations of the SCN5A and HERG genes have differential responses to Na⁺ channel blockade and to increases in heart rate. Implications for gene-specific therapy. *Circulation*. 1995;92:3381–6.
 44. Benhorin J, Taub R, Goldmit M, Kerem B, Kass RS, Windman I, et al. Effects of flecainide in patients with new SCN5A mutation: mutation-specific therapy for long-QT syndrome? *Circulation*. 2000;101:1698–706.
 45. Windle JR, Geletka RC, Moss AJ, Zareba W, Atkins DL. Normalization of ventricular repolarization with flecainide in long QT syndrome patients with SCN5A:DeltaKPQ mutation. *Ann Noninvasive Electrocardiol*. 2001;6:153–8.
 46. Moss AJ, Windle JR, Hall WJ, Zareba W, Robinson JL, McNitt S, et al. Safety and efficacy of flecainide in subjects with Long QT-3 syndrome (DeltaKPQ mutation): a randomized, double-blind, placebo-controlled clinical trial. *Ann Noninvasive Electrocardiol*. 2005;10:59–66.
 47. Priori SG, Napolitano C, Schwartz PJ, Bloise R, Crotti L, Ronchetti E. The elusive link between LQT3 and Brugada syndrome: the role of flecainide challenge. *Circulation*. 2000;102:945–7.
 48. Moss AJ, Zareba W, Schwarz KQ, Rosero S, McNitt S, Robinson JL. Ranolazine shortens repolarization in patients with sustained inward sodium current due to type-3 long-QT syndrome. *J Cardiovasc Electrophysiol*. 2008;19:1289–93.
 49. Ragsdale DS, McPhee JC, Scheuer T, Catterall WA. Common molecular determinants of local anesthetic, antiarrhythmic, and anticonvulsant block of voltage-gated Na⁺ channels. *Proc Natl Acad Sci U S A*. 1996;93:9270–5.
 50. Anno T, Hondeghem LM. Interactions of flecainide with guinea pig cardiac sodium channels. Importance of activation unblocking to the voltage dependence of recovery. *Circ Res*. 1990;66:789–803.
 51. Zhu Y, Kyle JW, Lee PJ. Flecainide sensitivity of a Na channel long QT mutation shows an open-channel blocking mechanism for use-dependent block. *Am J Physiol Heart Circ Physiol*. 2006;291:H29–37.
 52. Zygmunt AC, Nesterenko VV, Rajamani S, Hu D, Barajas-Martinez H, Belardinelli L, et al. Mechanisms of atrial-selective block of Na⁽⁺⁾ channels by ranolazine: I. Experimental analysis of the use-dependent block. *Am J Physiol Heart Circ Physiol*. 2011;301:H1606–14.
 53. Zhu W, Mazzanti A, Voelker TL, Hou P, Moreno JD, Angsutararux P, et al. Predicting patient response to the antiarrhythmic mexiletine based on genetic variation. *Circ Res*. 2019;124:539–52.
 54. Compton SJ, Lux RL, Ramsey MR, Strelch KR, Sanguinetti MC, Green LS, et al. Genetically defined therapy of inherited long-QT syndrome. Correction of abnormal repolarization by potassium. *Circulation*. 1996;94:1018–22.
 55. Shimizu W, Kurita T, Matsuo K, Suyama K, Aihara N, Kamakura S, et al. Improvement of repolarization abnormalities by a K⁺ channel opener in the LQT1 form of congenital long-QT syndrome. *Circulation*. 1998;97:1581–8.
 56. Wainwright CE, Elborn JS, Ramsey BW, Marigowda G, Huang X, Cipolli M, et al. Lumacaftor-Ivacaftor in patients with cystic fibrosis homozygous for Phe508del CFTR. *N Engl J Med*. 2015;373:220–31.
 57. Mehta A, Ramachandra CJA, Singh P, Chitre A, Lua CH, Mura M, et al. Identification of a targeted and testable antiarrhythmic therapy for long-QT syndrome type 2 using a patient-specific cellular model. *Eur Heart J*. 2018;39:1446–55.
 58. Schwartz PJ, Priori SG, Cerrone M, Spazzolini C, Odero A, Napolitano C, et al. Left cardiac sympathetic denervation in the management of high-risk patients affected by the long-QT syndrome. *Circulation*. 2004;109:1826–33.
 59. Collura CA, Johnson JN, Moir C, Ackerman MJ. Left cardiac sympathetic denervation for the treatment of long QT syndrome and catecholaminergic polymorphic ventricular tachycardia using video-assisted thoracic surgery. *Heart Rhythm*. 2009;6:752–9.
 60. Bos JM, Bos KM, Johnson JN, Moir C, Ackerman MJ. Left cardiac sympathetic denervation in long QT syndrome: analysis of therapeutic nonresponders. *Circ Arrhythm Electrophysiol*. 2013;6:705–11.
 61. Moss AJ, Liu JE, Gottlieb S, Locati EH, Schwartz PJ, Robinson JL. Efficacy of permanent pacing in the management of high-risk patients with long QT syndrome. *Circulation*. 1991;84:1524–9.
 62. Eldar M, Griffin JC, Van Hare GF, Witherell C, Bhandari A, Benditt D, et al. Combined use of beta-adrenergic blocking agents and long-term cardiac pacing for patients with the long QT syndrome. *J Am Coll Cardiol*. 1992;20:830–7.
 63. van den Berg MP, Wilde AA, Viersma TJW, Brouwer J, Haaksma J, van der Hout AH, et al. Possible bradycardic mode of death and successful pacemaker treatment in a large family with features of long QT syndrome type 3 and Brugada syndrome. *J Cardiovasc Electrophysiol*. 2001;12:630–6.
 64. Hirao H, Shimizu W, Kurita T, Suyama K, Aihara N, Kamakura S, et al. Frequency-dependent electrophysiologic properties of ventricular repolarization in patients with congenital long QT syndrome. *J Am Coll Cardiol*. 1996;28:1269–77.
 65. Fruh A, Siem G, Holmstrom H, Dohlen G, Haugaa KH. The Jervell and Lange-Nielsen syndrome: atrial pacing combined with ss-blocker therapy, a favorable approach in young high-risk patients with long QT syndrome? *Heart Rhythm*. 2016;13:2186–92.

66. Groh WJ, Silka MJ, Oliver RP, Halperin BD, McNulty JH, Kron J. Use of implantable cardioverter-defibrillators in the congenital long QT syndrome. *Am J Cardiol.* 1996;78:703–6.
67. Daubert JP, Zareba W, Rosero SZ, Budzikowski A, Robinson JL, Moss AJ. Role of implantable cardioverter defibrillator therapy in patients with long QT syndrome. *Am Heart J.* 2007;153:53–8.
68. Horner JM, Kinoshita M, Webster TL, Haglund CM, Friedman PA, Ackerman MJ. Implantable cardioverter defibrillator therapy for congenital long QT syndrome: a single-center experience. *Heart Rhythm.* 2010;7:1616–22.
69. Schwartz PJ, Spazzolini C, Priori SG, Crotti L, Vicentini A, Landolina M, et al. Who are the long-QT syndrome patients who receive an implantable cardioverter-defibrillator and what happens to them?: data from the European Long-QT Syndrome Implantable Cardioverter-Defibrillator (LQTS ICD) Registry. *Circulation.* 2010;122:1272–82.
70. Biton Y, Rosero S, Moss AJ, Goldenberg I, Kutiyafa V, McNitt S, et al. Primary prevention with the implantable cardioverter-defibrillator in high-risk long-QT syndrome patients. *Europace.* 2019;21:339–46.
71. Gaba P, Bos JM, Cannon BC, Cha YM, Friedman PA, Asirvatham SJ, et al. Implantable cardioverter-defibrillator explantation for overdiagnosed or over-treated congenital long QT syndrome. *Heart Rhythm.* 2016;13:879–85.
72. Olde Nordkamp LR, Wilde AA, Tijssen JG, Knops RE, van Dessel PF, de Groot JR. The ICD for primary prevention in patients with inherited cardiac diseases: indications, use, and outcome: a comparison with secondary prevention. *Circ Arrhythm Electrophysiol.* 2013;6:91–100.
73. Olde Nordkamp LR, Postema PG, Knops RE, van Dijk N, Limpens J, Wilde AA, et al. Implantable cardioverter-defibrillator harm in young patients with inherited arrhythmia syndromes: a systematic review and meta-analysis of inappropriate shocks and complications. *Heart Rhythm.* 2016;13:443–54.
74. Rudic B, Tulumen E, Berlin V, Roger S, Stach K, Liebe V, et al. Low prevalence of inappropriate shocks in patients with inherited arrhythmia syndromes with the subcutaneous implantable defibrillator single center experience and long-term follow-up. *J Am Heart Assoc.* 2017;6(10).
75. Goldenberg I, Bradley J, Moss A, McNitt S, Polonsky S, Robinson JL, et al. Beta-blocker efficacy in high-risk patients with the congenital long-QT syndrome types 1 and 2: implications for patient management. *J Cardiovasc Electrophysiol.* 2010;21:893–901.



Drug-Induced Long QT Syndrome and Torsades de Pointes

10

Raymond L. Woosley and Peter J. Schwartz

Recognition and Diagnosis of Drug-Induced Long QT Syndrome (diLQTS)

In the 1990s, a previously obscure adverse drug reaction, drug-induced long QT syndrome (diLQTS), achieved notoriety and set in place changes that have dramatically altered the practice of medicine [1]. This syndrome is the clinical association of (1) the administration of a drug(s) that delays cardiac repolarization, (2) resultant prolongation of the QTc (heart rate-corrected) to values ≥ 500 ms, and (3) the development of an unusual type of ventricular tachycardia known as torsades de pointes (TdP). The diagnosis of diLQTS requires all three features be present and should be distinguished from congenital long QT syndrome (cLQTS) [2] or “short-coupled TdP” [3–5] which have very different pathogenesis and clinical management.

Before the recognition of diLQTS as a syndrome, TdP had been recognized as a distinct type of arrhythmia and named TdP by the French

cardiologist Dessertenne because of its characteristic “twisting of the points” pattern in which the ventricular complexes rotate around the electrical axis of the heart (Fig. 10.1) [2, 6, 7]. Subsequently, TdP has been subdivided into two types. The classic form has antecedent QT prolongation and is most often initiated by a long-short series of cardiac depolarizations [3]. A second form is “short-coupled” TdP, which is a polymorphic ventricular tachycardia that occurs in the absence of QT prolongation [4, 5, 8]. This chapter will focus on the classic type of TdP which is most often the result of drug-induced prolongation of repolarization [9] or is the arrhythmia naturally seen in patients with the congenital long QT syndrome (cLQTS) [2].

International Impact of diLQTS

What initially appeared to be tragic but rare anecdotes of TdP and deaths associated with commonly prescribed drugs such as antihistamines [10] turned out to be a not uncommon clinical entity with far-reaching ramifications. Regulatory agencies responded relatively quickly to develop new guidelines for drug testing to identify the drugs with a risk of diLQTS [11]. Testing for in vitro effects of drugs on measures of cardiac repolarization and of QT prolongation in normal volunteers and/or patients has become standard for new drug development. These requirements prompted many pharmaceutical

R. L. Woosley (✉)
Department of Medicine, Division of Clinical Data
Analytics and Decision Support, University of
Arizona, College of Medicine-Phoenix,
Phoenix, AZ, USA
e-mail: rwoosley@azcert.org

P. J. Schwartz
Center for Cardiac Arrhythmias of Genetic Origin –
Laboratory of Cardiovascular Genetics, Istituto
Auxologico Italiano IRCCS, Milan, Italy

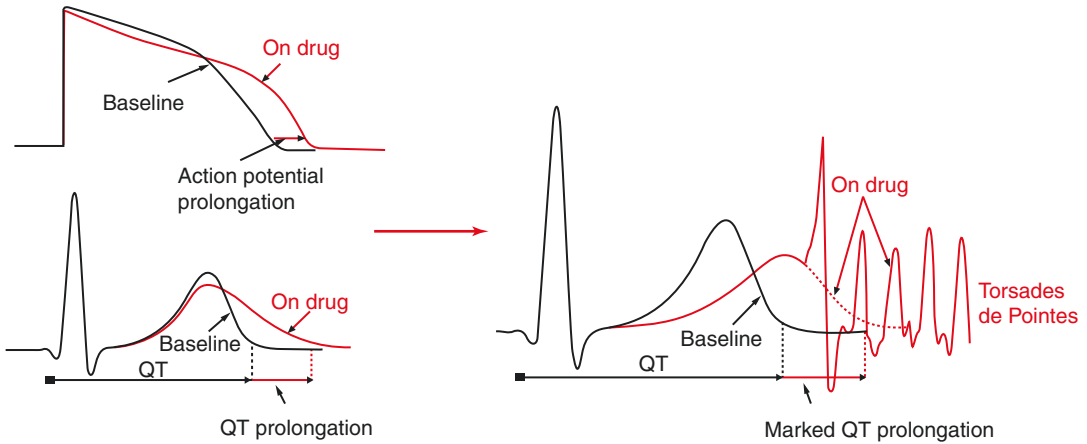


Fig. 10.1 Pathophysiology of diLQTS. The left side of the figure shows the relationship between the surface ECG (bottom) and a typical ventricular action potential (top) in black. The “on drug” tracings in red show the concomitant prolongation of action potential (top) and the QT interval (bottom) caused by drugs that have the ability to block the

hERG channel which reduces the rapid component of the delayed rectifier current, I_{Kr} . The right side of the figure demonstrates that as the QT prolongation becomes more marked, spontaneous early afterdepolarizations occur which can initiate the arrhythmia torsades de pointes (red)

companies to withdraw over 14 highly profitable products from the market and many to halt the development of numerous promising new agents [12]. In recent years, we have come to realize that a large number of drugs can precipitate this syndrome and an even larger number of drugs can prolong QT.

Historical Background

In retrospect, diLQTS was most likely the culprit in cases of quinidine syncope first reported in the 1920s [13]. More than 40 years later, Dessertenne described TdP as an arrhythmia associated with QT prolongation [6] and Selzer and Wray reported cases of quinidine syncope and “paroxysmal ventricular fibrillation” with the typical TdP pattern on their ECG [14]. Subsequently cardiologists recognized that these dramatic episodes of quinidine syncope had two key features: prolongation of the QT interval and the occurrence of TdP arrhythmia. TdP and di-LQTS gained greater recognition in 1982 when Moss and Schwartz advanced the hypothesis that these drug-induced events could represent a “forme fruste” of the congenital long QT syndrome (cLQTS) [15].

Since most of the first cases of TdP reported in the 1970s and 1980s were observed in patients being treated for cardiac arrhythmias, it was initially assumed that this relatively rare form of proarrhythmic event was mainly confined to antiarrhythmic drugs that prolong the QT interval, such as quinidine [16], disopyramide [17, 18], and procainamide [19]. However, in the early 1990s, the medical community’s attitude toward TdP changed dramatically when it became apparent that popular non-cardiac drugs, such as the non-sedating antihistamine terfenadine, could also cause QT prolongation, TdP, and death [10]. Shortly thereafter, reports of TdP emerged with another antihistamine, astemizole [20], followed by the gastrointestinal drug cisapride [21], the antibiotic erythromycin [22], the opiates levomethadyl [23] and methadone [24], probucol for hypercholesterolemia [25], and many other non-antiarrhythmic drugs, including antifungal agents and anticancer drugs [9]. It soon became clear that TdP could occur with drugs in any therapeutic class and, despite its uncommon occurrence, the incidence for many drugs became unacceptable, prompting their removal from the market [26]. Since 1989, 14 clinically important drugs have been removed from the market due to TdP [26], and an unknown number have been stopped

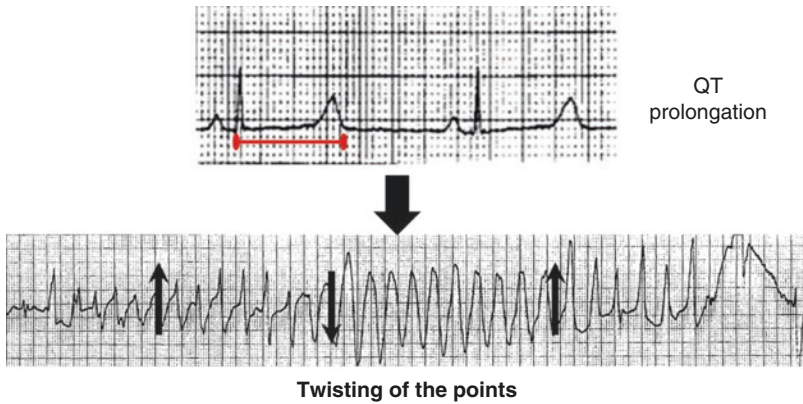


Fig. 10.2 An example of drug-induced torsades de pointes. The top tracing shows a markedly prolonged QTc (approximately 592 ms corrected by Bazett and 620 ms by Fridericia), and the bottom is a tracing of TdP

that developed subsequently in this patient shortly after initiation of sotalol therapy. The alternating black arrows show the twisting nature of the R waves during the tachycardia

in development due to evidence that they cause QT prolongation and therefore might have a risk of TdP. Although many drugs may have been discarded, many have also received FDA approval in spite of evidence that they can prolong QT and, for some, even that they can clearly cause TdP. In the last 18 years, the number of marketed drugs known to cause diLQTS has approximately doubled to total 47 and the number of drugs associated with QT prolongation alone has quadrupled from 25 to 105. The rapid increase in the number of drugs in both categories can be seen in Fig. 10.2 [27]. These drugs have reached the market because their risk of TdP is acceptably small and/or their clinical benefit is substantial, for example, drugs like arsenic trioxide which is used exclusively to treat cancer [28]. When there are no safe alternatives, clinicians, drug developers, drug regulators, and even patients, such as those with congenital long QT, must develop ways to minimize the risk of harm associated with a growing number of these medicines.

Cellular Mechanism of diLQTS

Like many adverse drug reactions, diLQTS was initially considered to be idiosyncratic [16, 29]. As the electrophysiologic and molecular basis for diLQTS has been unraveled, it is no longer considered to be idiosyncratic [29, 30]. It has

been studied extensively, and its mechanism is understood to the point that it can be replicated in animal and cellular models such as human stem cells induced to become spontaneously beating cardiac myocytes [31]. These studies are described in Chap. 4. The rich scientific basis for the mechanisms underlying TdP is well defined and described in Chap. 11 [8, 32, 33]. Much of our understanding of TdP comes from similarities found between the ion channel defects responsible for cLQTS [2] (discussed in Chap. 8) and the cellular actions of the drugs that cause diLQTS, i.e., primarily their actions that prolong repolarization by either reduction of I_{Kr} [34], a major outward cardiac potassium current that is missing in patients with cLQTS type 2, or enhancement of late inward sodium currents as seen in cLQTS type 3 [35]. Other well-known causes of acquired QT prolongation include electrolyte abnormalities (hypokalemia, hypomagnesemia, and hypocalcemia), hypothyroidism, hypothermia, and extreme bradycardia, any of which can contribute to the risk of drug-induced TdP or, in extreme cases, cause TdP on their own [8]. Over 65 clinical and biochemical factors have been associated with QT prolongation and are summarized on the CredibleMeds.org website at QTFactors.org. The website includes an assessment of the quality of the evidence and the strength of the associations and is updated monthly.

There is an increased risk of TdP whenever a patient's QTc exceeds 500 ms or increases by more than 60–70 ms, especially when the increase occurs rapidly [8]. QT interval prolongation is particularly proarrhythmic when associated with increased dispersion in the recovery of excitability [36]. Although QT prolongation is an essential first step in TdP, it is not considered sufficient to induce TdP [8]. Additional electrophysiologic changes are required for TdP to occur; specifically, early afterdepolarizations that are calcium-mediated have been identified as an important element in *in vitro* models of TdP [33]. A common feature of drugs that induce diLQTS is the ability to block or disrupt the hERG potassium channel, thereby reducing I_{Kr} and prolonging the QT interval [8]. However, Yang et al. recently reported that some I_{Kr} blocking drugs known to cause TdP (dofetilide, E-4031, d-sotalol, thioridazine, and erythromycin) also increase the late sodium current which also may contribute to their proarrhythmic effect [35].

Clinical Sequelae of diLQTS

While QT prolongation is not symptomatic, excessive prolongation above 500 ms can facilitate bursts of TdP that are often self-limited but cause symptoms of palpitations, light headedness, dizziness, presyncope, and syncope. If the arrhythmia persists, diLQTS can have a lethal outcome. Most patients survive the initial bursts of arrhythmia, especially if it is recognized and treated appropriately [8]. TdP can progress to ventricular fibrillation and death if not diagnosed as TdP and if the QT prolonging medicines are not discontinued and/or other precipitating factors such as hypokalemia or bradycardia not reversed. As an indication of the potential severity of diLQTS, many of the drugs that cause diLQTS have been associated with a higher than expected incidence of sudden cardiac death [37–41].

The fact that only a subset of patients who develop drug-induced QT prolongation experience TdP or death suggests that QT prolongation alone is not a perfect biomarker for predicting

TdP [40]. To have true clinical utility, it must be combined with other known risk factors for TdP [42]. Several of these approaches to augment screening for risk of diLQTS are discussed below. Be that as it may, the prolonged QTc interval remains one of the most readily available and clinically useful early warning signals to alert for the possible occurrence of diLQTS [8]. According to the CredibleMeds website, for at least 100 drugs, the FDA-approved label includes a recommendation for monitoring the QT interval before or during therapy.

CredibleMeds Risk Categorization of Drugs Associated with diLQTS

In the late 1990s, upon recognition that non-cardiac drugs such as terfenadine or cisapride could cause diLQTS and even death, the questions arose: *Which of the other over 3000 prescription drugs on the market might also carry this risk? How can they best be identified?* In 1999, the Agency for Healthcare Research and Quality (AHRQ) awarded funds to the University of Arizona's Center for Education and Research on Therapeutics (AZCERT), to develop a process to analyze evidence and establish criteria to identify drugs that prolong QT and have a risk of TdP [27]. This process, now known as the Adverse Drug Event Causality Analysis, has evolved and the risk categories expanded and validated by clinical investigations using large healthcare databases [43, 44]. For almost two decades, the AZCERT has conducted an independent analysis of evidence, placed drugs in risk categories, and made the information freely available to the public, healthcare providers, and research scientists [27]. In recent years, funded by a contract with the US FDA's Safe Use Initiative, AZCERT has been able to develop additional platforms such as smartphone apps in multiple languages and decision support tools to expand access to the information [45]. The lists of drugs were initially known as the QTdrugs lists, and the website can still be reached at www.QTdrugs.org [46]. More recently, they are also available on the CredibleMeds website

(www.crediblemeds.org) and as of 2018 were regularly accessed by over 112,000 registered visitors from 193 countries. AZCERT has developed an application program interface (API) that enables health information technology systems to have online, open-source access to the lists of drugs. To prevent real or perceived conflicts of interest and to assure independence in the decision-making process, AZCERT has been only supported by peer-reviewed federal awards and charitable contributions from the public and philanthropic foundations.

The methods that AZCERT uses to analyze evidence and assess TdP causality are described on the CredibleMeds website (<https://www.crediblemeds.org/research-scientists/why-lists/>) and in peer-reviewed publications [27, 45]. Because the available evidence frequently has limitations or gaps and is often of variable quality, AZCERT has developed a systematic, in-depth process to analyze all available data and to assess causality [27]. Since the QTdrugs list was created in 1999 with only 29 drugs in 1 category, over 194 new drugs have been added in 4 categories, and many have been moved among categories or removed. Beginning in 2012, AZCERT extended its analysis to include drugs marketed outside the United

States, especially those in Europe, Australia, and Canada.

The analysis of evidence includes a thorough review of published studies (PubMed search using standardized search terms) and reports of adverse events in the FDA's Adverse Event Reporting System (AERS) or WHO's Vigibase. AZCERT uses the data-mining statistical software developed for the FDA (Empirica Signal Software, Oracle Health Sciences, Redwood Shores, California) [27]. Today, AZCERT places drugs in four categories of TdP risk (Fig. 10.3). The main category of interest, "Known Risk of TdP," are drugs found to have convincing clinical evidence that they can cause TdP, even when used as recommended in the drug's FDA-approved label. Those drugs that prolong the QT interval during routine clinical use, but do not at this time have convincing evidence of TdP causality, are placed in the "Possible Risk of TdP" category. Beginning in 2006, the "Conditional Risk" category was created and includes drugs for which there is a documented association with TdP but only under certain specific conditions, such as overdose, hypokalemia, hypomagnesemia, and bradycardia, or when there is an interaction with another drug(s). This category also

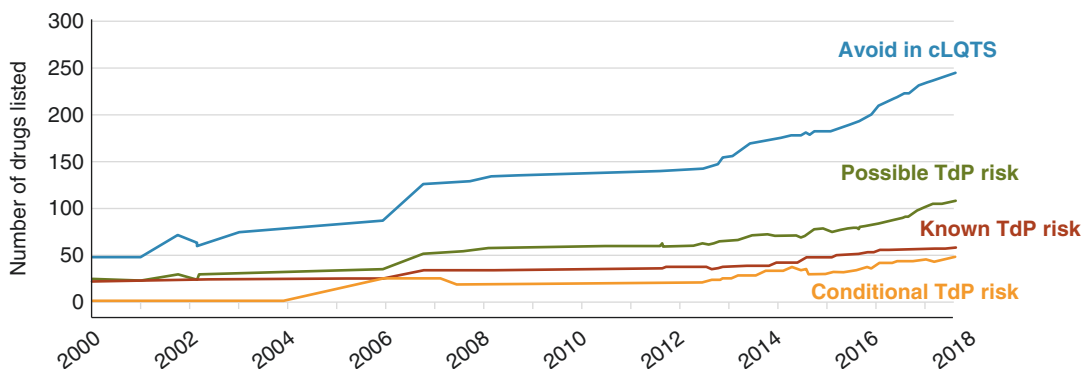
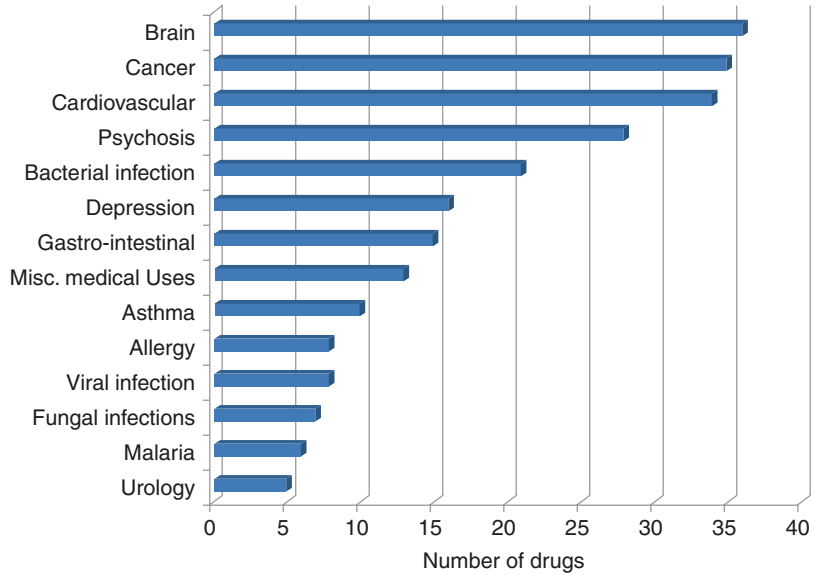


Fig. 10.3 The number of drugs in each of the four categories of TdP risk on the CredibleMeds website from 1999 to July 2018. The graph displays the changing number of drugs in each of the four categories of TdP risk at www.CredibleMeds.org between 1999 and July 2018. The number of drugs on the list with Known Risk of TdP at any point in time is shown as a red line. The number of drugs with Possible Risk of TdP is shown in green. The number of drugs with Conditional Risk of TdP (i.e., associated

with TdP under certain conditions) is shown in orange. The number of drugs on the list of Drugs to Avoid in patients with congenital long QT syndrome is shown in blue. The latter list includes all of the drugs listed in the other three risk categories plus additional drugs that do not prolong QT, per se, but have actions known to place some patients with cLQTS at increased risk of diLQTS (e.g., adrenergic drugs). cLQTS = congenital long QT syndrome, TdP = torsades de pointes

Fig. 10.4 Spectrum of therapeutic areas for drugs with known risk of TdP, possible risk of TdP, and conditional risk of TdP. The X-axis displays the number of drugs that were in each of the therapeutic categories listed on the Y-axis as of July 2018. Each drug's therapeutic area is based on its primary clinical indication. ADHD = attention deficit hyperactivity disorder, Misc. = miscellaneous, TdP = torsades de pointes



includes drugs that are associated with TdP because they have the ability to create the conditions that enable other drugs to cause TdP (e.g., loop diuretic agents that induce hypokalemia or drugs that are metabolic inhibitors of a QT prolonging drug). The website also posts a fourth list of drugs that AZCERT recommends are “Drugs to be Avoided by patients with congenital LQTS, if clinically feasible.” For maximum safety, this list includes all of the drugs in the other three risk categories plus the adrenergic drugs that are considered to place some cLQTS patients at high risk of sudden death [27]. The process for evaluating drugs and decisions regarding their inclusion on lists is overseen by an international Advisory Board of clinical and pharmacological experts. The Board's advice is sought whenever conflicting evidence must be resolved or when any Board member has a concern about placement of a drug in a category. The drugs on all four lists are monitored continuously for new evidence, and, in recent years, the lists have been revised every 4–8 weeks. As of July 2018, 58 medications are on the list of drugs known to cause TdP (including 10 removed from the US market, but which may still be available in some countries). Another 108 are on the list for possible risk of TdP and 48 are on the list for conditional TdP risk. Figure 10.4 shows the broad range of therapeutic areas

impacted by the drugs on the QTdrugs lists and demonstrates their ubiquitous use in medicine.

CredibleMeds has become an invaluable tool for the clinical management of patients affected by cLQTS [2]. Experienced centers dealing with these patients refer them to the public portal of CredibleMeds where they and their families can obtain an updated list of drugs to avoid or to take only under specific monitored circumstances [2]. As most general practitioners and many cardiologists are unaware of the QT prolonging potential of many cardiac and non-cardiac drugs [47, 48], this practice has become an essential part of the proper management of patients with channelopathies [2].

Epidemiology of diLQTS and Death Associated with QT Prolonging Drugs

For most drugs, the incidence of diLQTS is difficult to quantify due to its rarity. Estimates appear to vary greatly from drug to drug [49] and range from extremely low for drugs such as the macrolide antibiotics [50], 1.5–3% for quinidine [3, 51], and 3–9% for drugs such as ibutilide [52], sotalol [53], and azimilide [54]. Estimates for drugs such as sotalol or ibutilide are likely to be

more accurate because the FDA required more extensive premarket research on the incidence of TdP with their use. The overall incidence of TdP in a given population will depend on the relative risk of the drugs prescribed and the frequency of their use in the population. For example, a cardiac care unit (CCU) population is more likely to be prescribed antiarrhythmic drugs and will likely have a much higher frequency of TdP than would be seen in a routine hospital population treated mostly with non-cardiac drugs. A mental health population prescribed methadone, antidepressants, and/or antipsychotics may have a higher incidence than a younger healthy population such as the military.

Estimating the incidence of diLQTS in a given population is difficult, partly because the arrhythmia can be transient or may be unrecognized. An accurate diagnosis requires that an ECG be taken during an arrhythmic episode to document the presence of QT prolongation and the characteristic twisting pattern of the ventricular tachycardia. Without an ECG, diLQTS may be diagnosed as syncope, seizures, or sudden cardiac death. Reporting diLQTS is hindered by the fact that the International Classification of Diseases, tenth Revision (ICD-10), that is used to record diagnoses in medical records lacks a specific code for drug-induced TdP or excessive QT prolongation. diLQTS and TdP tend to be reported under codes for VT, VF, or SCD [55]. One study estimated that between 5% and 7% of reports of VT, VF, or SCD were, in fact, diLQTS [55]. Acknowledging the probable impact of under-reporting, European pharmacovigilance centers in Sweden [56], Germany [49], France, and Italy [57] have found an annual reporting rate for diLQTS of approximately 0.8–1.2 per million person-years [55]. In an epidemiological study, Sarganas et al. [49] reviewed patient records, looking for episodes of TdP or cases of “symptomatic QT prolongation” (defined as QTc >450 ms for men and >470 for women associated with ECG evidence of TdP, successful cardiac resuscitation, syncope, or severe dizziness) in Berlin and found the reporting rate to be 2.5 per million person-years for men and 4.0 for women. Vandael et al. found the incidence of diLQTS in the University Hospital

in Leuven to be 0.16 per thousand/year, and they estimated that would extrapolate to 173 possibly lethal cases of TdP in Belgian hospitals each year [58].

The frequency of death due to diLQTS is also difficult to estimate because if a patient dies without having an ECG recorded, TdP may not be recognized as the cause of death. Perhaps this explains why reports of death are not a dominant feature in most case series of TdP [51, 59, 60]. Yet, even with these potentially confounded diagnoses, many of the drugs that prolong the QT interval have still been associated with a significantly higher risk of sudden cardiac death in some studies [37–41, 61–63]. In a population-based, case-control study in the Netherlands, Straus et al. [62] examined all-cause mortality associated with non-cardiac drugs that prolong the QT interval (drugs listed on the CredibleMeds.org website) and found an approximately three-fold greater risk of death (95% CI, 1.6–47). On this basis, they estimated that the use of these non-cardiac drugs causes >15,000 deaths annually in the United States and Europe. Because many of these drugs, especially the antibiotics, have therapeutic alternatives that lack QT prolonging activity, it is possible that many of these deaths may have been preventable. Levofloxacin, erythromycin, clarithromycin, and azithromycin are among the most commonly prescribed antibiotics in the world, and all have been associated with QT prolongation, a risk of TdP, and an increased risk of sudden death [37–41, 61–65]. TdP and related deaths due to these antibiotics are a special concern, made more serious because of their widespread and often inappropriate use. In 2013, the FDA issued warnings and expressed concern regarding the overuse of antibiotics, especially citing the excess numbers of deaths associated with levofloxacin, azithromycin, and other macrolides [38, 39, 63, 64]. It was noted that in 2011, 40 million people took azithromycin and, on the basis of the study by Ray et al. [38], which found 1 excess death for every 21,000 prescriptions compared with amoxicillin, this would result in an estimated 1900 excess deaths with this drug in the United States alone. In 2014, another study from the US Veterans Health

System estimated that 4560 people die each year due to azithromycin when amoxicillin would have been a safe alternative [63]. A recent meta-analysis of 33 studies involving 20,779,963 patients taking macrolides compared outcomes with those of patients who took no macrolides and found an increased risk of developing SCD or ventricular tachyarrhythmias (RR, 2.42; 95% CI, 1.61–3.63), SCD (RR, 2.52; 95% CI, 1.91–3.31), and cardiovascular death (RR, 1.31; 95% CI, 1.06–1.62) [50]. The authors concluded that treatment with macrolides is associated with an absolute risk increase of 118.1 additional SCDs or ventricular tachyarrhythmias and 38.2 additional cardiovascular deaths per one million treatment courses. Because of the magnitude of TdP associated with these antibiotics, the FDA's Safe Use Initiative has focused on the safe use of antibiotics and funded efforts to reduce their risk of TdP [66]. It is important to note that some studies that focussed on relatively healthy populations [67] have not observed an increased mortality with these antibiotics which emphasizes the need for targeting risk mitigation strategies such as CDSS.

Prevention of diLQTS

In 2010, a panel of experts published a thorough and thoughtful consensus paper on the prevention of diLQTS in the hospital setting and described an approach for monitoring the QT interval as part of a prevention strategy [8]. For most drugs that have demonstrated the potential for causing diLQTS, the cost and inconvenience of routine, untargeted screening for QT prolongation is difficult to justify because of the relatively low number of patients expected to develop clinically significant QT prolongation (>500 ms or >60–70 ms change) [8]. Furthermore, the number of patients who develop diLQTS is usually only a relatively small subset of those with increased QTc. On the other hand, for some drugs, such as dofetilide, the frequency of TdP can exceed 2% [68], and the FDA recommends hospital admission and ECG monitoring of the QT interval when initiating or re-initiating therapy [69]. It is important to note that, at this point in time, no strategy has been shown to prevent or reduce the incidence of TdP.

Identifying Risk Factors for diLQTS

It has become apparent that the QT interval alone, despite its primary role, is but one of several risk factors that must be considered in order to reliably identify patients at highest risk for developing diLQTS. Numerous studies suggest that in order for a strategy for prevention to have an acceptable level of predictive accuracy and be cost-effective, it must include consideration of those risk factors in three general categories: (1) patient specific, (2) drug specific, and (3) clinical scenario specific [8].

Patient-Specific Risk Factors: Patient-specific risk factors for diLQTS include the same factors that are known to be clinically associated with an increase in the QT interval, that is, female sex, bradycardia, hypokalemia, hypomagnesemia, hypocalcemia, diuretic agent use, hypothermia, and history of heart disease [42]. Additional factors associated with QT prolongation were found by Haugaa et al. [70] by extracting patient-specific information from the electronic medical record (EMR) of Mayo Clinic Health System. These factors included diabetes, cardiomyopathy, pheochromocytoma, hypoglycemia, anorexia, congenital long QT, renal dialysis, and status after conversion from atrial fibrillation. These investigators have developed a system that calculates what they have termed a “pro-QTc” risk score that is based on the presence of these risk factors and the use of drugs on the Known Risk list at the CredibleMeds.org website. They found that the pro-QTc risk score could identify hospitalized patients that have a fourfold higher mortality than that of the overall population. This system generates alerts that are part of a clinical decision support system (CDSS) that has been implemented across the institution [70, 71]. Using this CDSS, Sorita et al. were able to reduce the prescribing of many of the QT prolonging medications for high-risk patients [71].

Similarly, for a Coronary Care Unit (CCU) population, Tisdale et al. developed a CDSS and QT risk score that they found could identify patients with excessive QT interval prolongation [72]. Tisdale et al. found that their CDSS was

able to reduce the overall incidence of excessive QTc prolongation and reduce the overall prescribing of QT prolonging drugs, especially for patients who had baseline QT prolongation [73].

In Belgium, Vandael et al. have made extensive progress in developing a CDSS to help reduce the harm from QT prolonging drugs. First, they reviewed the medical literature and identified risk factors for QT prolongation [74]. They then analyzed the medical records of patients in the University Hospitals Leuven to confirm the association of risk factors in their patient population [75]. In addition to the risk factors found at Mayo Clinic and by Tisdale in the CCU, Vandael et al. found additional risk factors such as C reactive protein, body mass index, smoking, diabetes, and liver failure [75]. These investigators have used these factors and the CredibleMeds drugs lists to compute a RISQ-PATH score as part of a CDSS that has been implemented and tested in six Belgian psychiatric hospitals [58, 76]. They have used this CDSS to estimate the incidence of diLQTS in their hospital population [58] and, in a psychiatric population, to identify those patients most likely to develop excessive QT prolongation [76].

There is some overlap in the patient-specific QT risk factors used in these three CDSS, but there are also some significant differences. In addition to the risk factors utilized in the pro-QT score of Haugaa et al. [70], the Tisdale score for CCU patients identified sepsis and assigned greater weight to the patients' use of multiple QT prolonging drugs. Unlike Tisdale's score and the Mayo pro-QT score, the RISQ-PATH score included scoring for drugs on the Possible Risk and Conditional Risk lists. These differences in risk factors and in their assigned weights in these three CDSS most likely reflect the fact that they were developed using different patient populations and for slightly different purposes. This suggests that healthcare institutions will most likely have to determine which elements of QT risk scores are most appropriate for their specific clinical environment(s). The posted list of QT risk factors at CredibleMeds' website (QTFactors.org) was created to provide a resource for investigators

and healthcare providers wishing to develop risk scores for evaluation and incorporation in their decision support tools.

Drug-Specific Risk Factors: As discussed above, the common feature of drugs that cause TdP is their ability to block hERG channels and thereby to prolong the QT interval [77]. In theory, efforts to prevent TdP might incorporate a ranking of drugs by their in vitro hERG potency or degree of QT prolongation in humans. However, attempts to find useful correlations have not had much success [78]. Most likely, the inter-individual variability in drug sensitivity and the variable influence of factors that affect each patient's drug exposure (e.g., dose, drug metabolism, route of administration) reduce the predictive accuracy of such ranking to levels that lack clinical utility. For example, terfenadine and astemizole have very high hERG blocking potency but are extensively metabolized in most people so that it is unusual for them to attain blood levels that can cause TdP [60].

Prevention strategies must not only consider the drug's toxic potential but also its route and rate of administration and the dose and interactions with any concomitant medicines. The contribution of these factors is not always well defined for a given drug. For some drugs, like sotalol, the FDA required extensive testing during its clinical development to characterize the relationship between dose and QT prolongation and even TdP frequency. In this case, investigators found a positive dose-response relationship for sotalol-induced TdP [79]. In contrast, the risk of TdP with quinidine appears to have little relationship to dose and may be influenced more by the patient's clinical sensitivity, such as the presence of atrial fibrillation, which can cause long cardiac pauses that facilitate TdP [3]. For many drugs, like haloperidol or papaverine, the available data suggest that the risk of TdP is markedly influenced by the route of administration, with a larger proportion of cases occurring after rapid intravenous injection of haloperidol [80] or intracoronary injection of papaverine [81].

Table 10.1 Clinical scenarios for risk of diLQTS

Concomitant therapy with two or more QT prolonging drugs
Concomitant therapy with a QT prolonging drug and a potassium-wasting diuretic
Concomitant therapy with a drug that blocks the metabolism of a QT prolonging drug
Development of renal failure in a patient treated with a QT prolonging drug that requires renal elimination (e.g., sotalolol)
Development of liver failure in a patient treated with a QT prolonging drug that requires hepatic metabolism for clearance (e.g., methadone)
Development of vomiting or diarrhea resulting in electrolyte disturbances that potentiate the QT prolonging effects of drugs such as antiemetic agents or antibiotics
Taking a QT prolonging drug concomitant with extended therapy with a proton-pump inhibitor that produces hypomagnesemia and/or hypokalemia to further prolong the QT
Taking a QT prolonging drug concomitant with a beta-blocker or ivabradine that slows heart rate and thereby further prolongs the QT interval
Excessive dose titration of a QT prolonging drug due to lack of desired clinical response or development of tolerance (e.g., methadone)
Depression causing attempted suicide with toxic doses of QT prolonging drugs (e.g., antipsychotics, antidepressants, among others)

Scenario-Specific Risk: Analyses of case series of TdP caused by a specific drug reveal that the great majority of cases fall into certain categories of drug use that are influenced by the patients' medical condition [51, 59, 60, 82]. Many of these reports were of patients who had been successfully treated with the offending drug for extended periods of time but who developed TdP shortly after a change had occurred in their clinical condition or in the way it was being managed. For example, patients with heart failure may tolerate QT prolonging drugs until their medical condition deteriorates and a loop diuretic agent is prescribed and induces hypokalemia. Initially well-tolerated antibiotics that prolong the QT interval may later eradicate normal bowel flora, causing diarrhea, and result in electrolyte disturbances that can potentiate a patient's risk of TdP. A partial list of scenarios that, like these, can accentuate the TdP risk of a medication is in Table 10.1.

Genetic Factors Contributing to diLQTS

The fact that the life-threatening arrhythmia in patients with diLQTS and those with cLQTS are the same (i.e., TdP) and that both conditions are associated with extreme prolongation of the QT interval (often with bizarre morphology of the T-wave) should have raised immediately the issue of a potential relationship between the two conditions [15].

A key component here was the realization that the second most frequent type of cLQTS, LQT2, is due to mutations in the hERG gene, which encodes the protein that mediates the I_{Kr} current. When it became clear that a key mechanism for the development of diLQTS is the block, even partial, of I_{Kr} , the connection to cLQTS became obvious. In this regard, another critical step was the development of the concept of *repolarization reserve* by Roden [1]. This concept maintains that every person has a physiological *cardiac repolarization reserve*, which is genetically determined and can usually compensate for factors (e.g., drugs, hypokalemia, bradycardia, etc.) that might either decrease repolarizing or increase depolarizing currents during the action potential. People with reduced repolarization reserve are more likely to develop QT prolongation and TdP when exposed to I_{Kr} blocking drugs. It follows that patients with cLQTS who, by definition, have a reduced repolarization reserve will be more likely than normal subjects to develop diLQTS. In theory, depending on the magnitude of genetically related deficiency of repolarizing currents, it should influence sensitivity to drugs, and smaller or higher doses of I_{Kr} blocking drugs will trigger TdP.

In 2002, the report by Yang et al. [83] on 92 diLQTS patients suggested that cLQTS mutations could be found in 10–15% of diLQTS cases. Several studies have since followed, with mixed results [84–88]. For example, whereas the *KCNE1*-D85N polymorphism was found to be associated with an increased risk for diLQTS [85], three other studies suggested that rare variants play a prominent role [86–88]. The most recent data on 188 diLQTS patients compared

with over 1000 cLQTS patients [89] provide a different and more positive set of findings. The first is that disease-causing mutations for cLQTS were found in 28% of these patients; the second is that in baseline conditions, the QTc of diLQTS patients (453 ± 39 ms), although shorter than that of cLQTS patients (478 ± 46 ms), is significantly longer than that of control subjects (406 ± 26 ms). It is likely that some of the minor cLQTS genes [90], usually not tested, may be involved in some cases of diLQTS, thus further increasing the contribution of one syndrome to the other.

Just as genes that control expression of ion channels could directly increase risk of diLQTS, genes that control the rate of a drug's metabolism or elimination can also affect its ability to cause diLQTS by either limiting or increasing the amount of drug that reaches the heart tissue [91]. Genetic defects in drug metabolism have been shown to accentuate the ability of some drugs to cause diLQTS in affected patients [91]. Because some drugs that cause TdP, such as thioridazine or methadone [91], are strongly influenced by genetic variability in drug metabolism and others, such as the renally cleared sotalol [79], are not, the same genetic associations cannot be expected to have predictive ability for all drugs. Furthermore, genetic variability in the response receptor for drugs such as the mu receptor serves for methadone can result in reduced sensitivity to methadone and the need to titrate dosages to those that could precipitate diLQTS [92]. These examples may at least partially explain why efforts to identify gene variants associated with diLQTS have had limited success when lumping together cases caused by a diverse group of drugs that have dissimilar pharmacodynamics and pharmacokinetic disposition [86, 87].

Opportunities for TdP Prevention: Potential Role of Genomics and CDSS

One can hope that a combination of rapid genetic screening, risk profiling, and monitoring of the QT interval during the first days of treatment with I_{Kr} blocking drugs may result in a decrease

of the number of patients manifesting TdP in response to a drug treatment. The massive amount of information that must be considered for the safe use of medicines has prompted the development of decision support tools to help physicians and other members of the healthcare team to reach optimal medical and therapeutic decisions. To support better prescribing of medicines, most CDSS described to date have issued alerts that warn of potential harm from a prescribing decision [73, 93, 94]. As discussed earlier, investigators at the Mayo Clinic [70], the University of Indiana [73], and Leuven, Belgium [75], have developed CDSSs to reduce the risk of QT prolongation in hospitalized patients. Unfortunately, the beneficial impact of these CDSS has been limited because in 75–95% of cases, physicians and pharmacists override or ignore the alerts [71, 73, 95] and no CDSS has yet been found to have sufficient impact on prescribing to effectively reduce the incidence of TdP. For improved acceptance of alerts and the effectiveness of CDSS overall, an expert panel has recommended that CDSS should provide clinically relevant and essential information at the time when a decision is being made, without overwhelming the decision-makers with more information than they need or can manage [96].

As an alternative to the use of interruptive alerts to signal prescribing errors, the concept of “medical autopilots” has been suggested as a potential preferred approach for CDSS [66]. Just as autopilots assist the pilot by capturing data and displaying only relevant warnings to the pilot, these programs can monitor the EMR and send signals to guide prescribers to make decisions that result in maximum benefit to patients and minimal risk of TdP. Hopefully, in the near future, a CDSS with these characteristics will be shown to prevent TdP.

A very recent attempt to identify potential genetic loci and risk factors causally associated with sudden cardiac death provides relevant suggestions. In the largest exploration of the genomics of sudden death to date, 9000 cases and 48,000 controls from 9 genome-wide association studies were analyzed by a meta-analysis in a discovery and in a replication stage [97]. Ashar et al. [97]

exploited the power of Mendelian randomization [98] by exploring causal relations underlying sudden cardiac death and relevant risk factors. Indeed, those factors which are causally associated with increased sudden death risk could represent a novel rational target for prevention. Their finding that QT interval prolongation increases risk not only after a myocardial infarction [99] but also in the general population may shift the current paradigm by which the use of I_{Kr} blockers must be avoided in patients with the cLQTS [2] as it may be reasonable to consider that, whenever possible and medically appropriate, drugs without I_{Kr} -blocking activity should always be preferred in order to reduce TdP and sudden death [98].

Conclusions

Most of the etiologic factors involved in diLQTS have been identified, as well as the major clinical risk factors for TdP. The relative contribution of each in specific populations is being defined. Also, for the most part, the drugs most likely to prolong the QT interval and to trigger TdP are being identified. Nonetheless, there is a considerable gap between the increased level of understanding of TdP and our current ability to effectively prevent diLQTS. This gap is being closed through the use of new technologies and standards in information management, machine learning, and system inter-operability [100].

The advances in genetics, including not only the clear evidence that genetic variants causing or favoring cLQTS play a major role in diLQTS but also the shortened turnaround time due to faster genetic testing methods, can open new options. For example, they allow the possibility of pre-emptive testing to screen the patients before they need to receive drugs, to rule out at least the presence of the most common variants associated with this life-threatening arrhythmia [101].

Finally, device technology such as the use of simple handheld ECG devices connected to smartphones is capable of screening for long QT and monitoring QT changes and may allow the early identification of those subjects more prone to development of a significant QT prolongation

[102]. Another potentially useful approach to reduce the risk of TdP when patients cannot avoid taking an I_{Kr} blocking drug has been recently described [103]. A wearable monitor can reliably assess the QT interval independently of whether it is normal, as in healthy controls, or prolonged as in patients affected by the congenital LQTS. This implies the possibility of administering I_{Kr} blocking drugs while remotely monitoring the QTc for 5–7 days or more to assess whether the patient manifests a prolongation of the QT interval that could predispose to TdP and, in case of risk detection, to interrupt a therapy that might become dangerous. This type of ECG patch monitors could prove useful to detect and/or track QT interval changes and could help overcome traditional barriers in addressing the mythical unpredictability of drug-induced TdP [104]. Newer technologies such as these should make diLQTS an even more rare event in the near future.

References

1. Roden DM. Drug-induced prolongation of the QT interval. *N Engl J Med*. 2004;350:1013–22.
2. Schwartz PJ, Ackerman MJ. The long QT syndrome: a transatlantic clinical approach to diagnosis and therapy. *Eur Heart J*. 2013;34:3109–16.
3. Kay GN, Plumb VJ, Arciniegas JG, Henthorn RW, Waldo AL. Torsades de pointes: the long-short initiating sequence and other clinical features: observations in 32 patients. *J Am Coll Cardiol*. 1983;2:806–17.
4. Leenhardt A, Glaser E, Burguera M, Nurnberg M, Maison-Blanche P, Coumel P. Short-coupled variant of torsade de pointes. A new electrocardiographic entity in the spectrum of idiopathic ventricular tachyarrhythmias. *Circulation*. 1994;89:206–15.
5. Fujii Y, Itoh H, Ohno S, et al. A type 2 ryanodine receptor variant associated with reduced Ca(2+) release and short-coupled torsades de pointes ventricular arrhythmia. *Heart Rhythm*. 2017;14:98–107.
6. Dessertenne F. Ventricular tachycardia with 2 variable opposing foci. *Arch Mal Coeur Vaiss*. 1966;59:263–72.
7. Roden DM. Predicting drug-induced QT prolongation and torsades de pointes. *J Physiol*. 2016;594:2459–68.
8. Drew BJ, Ackerman MJ, Funk M, et al. Prevention of torsade de pointes in hospital settings: a scientific statement from the American Heart Association and the American College of Cardiology Foundation. *Circulation*. 2010;121:1047–60.

9. Schwartz PJ, Woosley RL. Predicting the unpredictable: drug-induced QT prolongation and torsades de pointes. *J Am Coll Cardiol.* 2016;67:1639–50.
10. Monahan BP, Ferguson CL, Killeavy ES, Lloyd BK, Troy J, Cantilena LR Jr. Torsades de pointes occurring in association with terfenadine use. *JAMA.* 1990;264:2788–90.
11. Harmonisation ICo. International conference on harmonisation; guidance on E14 clinical evaluation of QT/QTc interval prolongation and proarrhythmic potential for non-antiarrhythmic drugs; availability. Notice. *Fed Regist.* 2005;70:61134–5.
12. Darpo B, Garnett C, Keirns J, Stockbridge N. Implications of the IQ-CSRC prospective study: time to revise ICH E14. *Drug Saf.* 2015;38(9):773–80.
13. Clark-Kennedy AE. Discussion on the action of quinidine in cases of cardiac disease. *Proc R Soc Med.* 1923;16:32–8.
14. Selzer A, Wray HW. Quinidine syncope: paroxysmal ventricular fibrillation occurring during treatment of chronic atrial arrhythmias. *Circulation.* 1964;30:17–26.
15. Moss AJ, Schwartz PJ. Delayed repolarization (QT or QTU prolongation) and malignant ventricular arrhythmias. *Mod Concepts Cardiovasc Dis.* 1982;51:85–90.
16. Reynolds EW, Vander Ark CR. Quinidine syncope and the delayed repolarization syndromes. *Mod Concepts Cardiovasc Dis.* 1976;45:117–22.
17. Schweitzer P, Mark H. Torsades de pointes caused by disopyramide and hypokalemia. *Mt Sinai J Med.* 1982;49:110–4.
18. Aarskog D, Reikvam A. Torsades de pointes ventricular tachycardia induced by disopyramide at therapeutic serum concentration. *Tidsskr Nor Laegeforen.* 1992;112:2511–3.
19. Vlasses PH, Ferguson RK, Rocci ML Jr, Raja RM, Porter RS, Greenspan AM. Lethal accumulation of procainamide metabolite in severe renal insufficiency. *Am J Nephrol.* 1986;6:112–6.
20. Woosley RL. Do H1 blockers astemizole (Hismanal) and terfenadine (Seldane) cause torsades de pointes? *Eur J Cardiac Pac Elect.* 1994;4:15.
21. Ahmad S, Wolfe S. Cisapride and torsades de pointes. *Lancet.* 1995;345:508.
22. Oberg KC, Bauman JL. QT interval prolongation and torsades de pointes due to erythromycin lactobionate. *Pharmacotherapy.* 1995;15:687–92.
23. Deamer RL, Wilson DR, Clark DS, Prichard JG. Torsades de pointes associated with high dose levomethadyl acetate (ORLAAM). *J Addict Dis.* 2001;20:7–14.
24. Krantz MJ, Lewkowicz L, Hays H, Woodroffe MA, Robertson AD, Mehler PS. Torsade de pointes associated with very-high-dose methadone. *Ann Intern Med.* 2002;137:501–4.
25. Gohn DC, Simmons TW. Polymorphic ventricular tachycardia (Torsade de Pointes) associated with the use of probucof. *N Engl J Med.* 1992;326:1435–6.
26. Ninan B, Wertheimer A. Withdrawing drugs in the US versus other countries. *Innov Pharm.* 2012;3:1–4.
27. Woosley R, Romero K, Heise C, et al. Adverse drug event causality analysis: a process for evaluating evidence and assigning drugs to risk categories for sudden death. *Drug Saf.* 2017;40:465–74.
28. Barbey JT, Soignet S. Prolongation of the QT interval and ventricular tachycardia in patients treated with arsenic trioxide for acute promyelocytic leukemia. *Ann Intern Med.* 2001;135:842–3.
29. Roden DM. Taking the “idio” out of “idiosyncratic”: predicting torsades de pointes. *Pacing Clin Electrophysiol.* 1998;21:1029–34.
30. Roden DM, Anderson ME. Proarrhythmia. *Handb Exp Pharmacol.* 2006;171:73–97.
31. Vicente J, Zusterzeel R, Johannesen L, et al. Mechanistic model-informed proarrhythmic risk assessment of drugs: review of the “CiPA” initiative and design of a prospective clinical validation study. *Clin Pharmacol Ther.* 2018;103(1):54–66.
32. Antzelevitch C, Zhang Z-Q, Sun Z-Q, Yan G-X. Cellular and ionic mechanisms underlying erythromycin-induced Long QT intervals and torsade de pointes. *J Am Coll Cardiol.* 1996;28:1836–48.
33. Jackman WM, Friday KJ, Anderson JL, Aliot EM, Clark M, Lazzara R. The Long QT Syndromes: a critical review, new clinical observations and a unifying hypothesis. *Prog Cardiovasc Dis.* 1988;31:115–72.
34. Roden DM. Cellular basis of drug-induced torsades de pointes. *Br J Pharmacol.* 2008;154:1502–7.
35. Yang T, Chun YW, Stroud DM, et al. Screening for acute IKr block is insufficient to detect torsades de pointes liability: role of late sodium current. *Circulation.* 2014;130:224–34.
36. Han J, Moe GK. Nonuniform recovery of excitability in ventricular muscle. *Circ Res.* 1964;14:44–60.
37. Ray WA, Chung CP, Murray KT, Cooper WO, Hall K, Stein CM. Out-of-hospital mortality among patients receiving methadone for noncancer pain. *JAMA Intern Med.* 2015;175:420–7.
38. Ray WA, Murray KT, Hall K, Arbogast PG, Stein CM. Azithromycin and the risk of cardiovascular death. *N Engl J Med.* 2012;366:1881–90.
39. Ray WA, Murray KT, Meredith S, Narasimhulu SS, Hall K, Stein CM. Oral erythromycin and the risk of sudden death from cardiac causes. *N Engl J Med.* 2004;351:1089–96.
40. Leonard CE, Freeman CP, Newcomb CW, et al. Antipsychotics and the risks of sudden cardiac death and all-cause death: cohort studies in medicaid and dually-eligible medicaid-medicare beneficiaries of five states. *J Clin Exp Cardiol.* 2013;Suppl 10:1–9.
41. Holmgren CM, Abdon NJ, Bergfeldt LB, et al. Changes in medication preceding out-of-hospital cardiac arrest where resuscitation was attempted. *J Cardiovasc Pharmacol.* 2014;63:497–503.
42. Zeltser D, Justo D, Halkin A, Prokhorov V, Heller K, Viskin S. Torsade de pointes due to noncardiac

- drugs: most patients have easily identifiable risk factors. *Medicine*. 2003;82:282–90.
43. Meid AD, von Medem A, Heider D, et al. Investigating the additive interaction of QT-prolonging drugs in older people using claims data. *Drug Saf*. 2017;40:133–44.
 44. Meid AD, Bighelli I, Machler S, et al. Combinations of QTc-prolonging drugs: towards disentangling pharmacokinetic and pharmacodynamic effects in their potentially additive nature. *Ther Adv Psychopharmacol*. 2017;7:251–64.
 45. Woosley RL, Black K, Heise CW, Romero K. CredibleMeds.org: what does it offer? *Trends Cardiovasc Med*. 2018;28(2):94–9.
 46. Romero K, Woosley RL. Clarification to the www.qtdrugs.org updated lists. *Pharmacoepidemiol Drug Saf*. 2009;18:423–4.
 47. Viskin S, Rosovski U, Sands AJ, et al. Inaccurate electrocardiographic interpretation of long QT: the majority of physicians cannot recognize a long QT when they see one. *Heart Rhythm*. 2005;2:569–74.
 48. LaPointe NM, Al-Khatib SM, Kramer JM, Califf RM. Knowledge deficits related to the QT interval could affect patient safety. *Ann Noninvasive Electrocardiol*. 2003;8:157–60.
 49. Sarganas G, Garbe E, Klimpel A, Hering RC, Bronder E, Haverkamp W. Epidemiology of symptomatic drug-induced long QT syndrome and Torsade de Pointes in Germany. *Europace*. 2014;16:101–8.
 50. Cheng YJ, Nie XY, Chen XM, et al. The role of macrolide antibiotics in increasing cardiovascular risk. *J Am Coll Cardiol*. 2015;66:2173–84.
 51. Roden DM, Woosley RL, Primm RK. Incidence and clinical features of the quinidine-associated long QT syndrome: implications for patient care. *Am Heart J*. 1986;111:1088–93.
 52. Gowda RM, Khan IA, Punukollu G, Vasavada BC, Sacchi TJ, Wilbur SL. Female preponderance in ibutilide-induced torsade de pointes. *Int J Cardiol*. 2004;95:219–22.
 53. Roden DM. Usefulness of sotalol for life-threatening ventricular arrhythmias. *Am J Cardiol*. 1993;72:51A–5A.
 54. Pratt CM, Al-Khalidi HR, Brum JM, et al. Cumulative experience of azimilide-associated torsades de pointes ventricular tachycardia in the 19 clinical studies comprising the azimilide database. *J Am Coll Cardiol*. 2006;48:471–7.
 55. Molokhia M, Pathak A, Lapeyre-Mestre M, Caturla L, Montastruc JL, McKeigue P. Case ascertainment and estimated incidence of drug-induced long-QT syndrome: study in Southwest France. *Br J Clin Pharmacol*. 2008;66:386–95.
 56. Astrom-Lilja C, Odeberg JM, Ekman E, Hagg S. Drug-induced torsades de pointes: a review of the Swedish pharmacovigilance database. *Pharmacoepidemiol Drug Saf*. 2008;17:587–92.
 57. Raschi E, Poluzzi E, Salvo F, et al. The contribution of national spontaneous reporting systems to detect signals of torsadogenicity: issues emerging from the ARITMO project. *Drug Saf*. 2016;39:59–68.
 58. Vandael E, Vandenberk B, Vandenberghe J, Pince H, Willems R, Foulon V. Incidence of Torsade de Pointes in a tertiary hospital population. *Int J Cardiol*. 2017;243:511–5.
 59. Pearson EC, Woosley RL. QT prolongation and torsades de pointes among methadone users: reports to the FDA spontaneous reporting system. *Pharmacoepidemiol Drug Saf*. 2005;14:747–53.
 60. Woosley RL, Chen Y, Freiman JP, Gillis RA. Mechanism of the cardiotoxic actions of terfenadine. *JAMA*. 1993;269:1532–6.
 61. Hennessy S, Bilker WB, Knauss JS, et al. Cardiac arrest and ventricular arrhythmia in patients taking antipsychotic drugs: cohort study using administrative data. *BMJ*. 2002;325:1070.
 62. Straus SM, Sturkenboom MC, Bleumink GS, et al. Non-cardiac QTc-prolonging drugs and the risk of sudden cardiac death. *Eur Heart J*. 2005;26:2007–12.
 63. Rao GA, Mann JR, Shoaibi A, et al. Azithromycin and levofloxacin use and increased risk of cardiac arrhythmia and death. *Ann Fam Med*. 2014;12:121–7.
 64. Mosholder AD, Mathew J, Alexander JJ, Smith H, Nambiar S. Cardiovascular risks with azithromycin and other antibacterial drugs. *N Engl J Med*. 2013;368:1665–8.
 65. Svanstrom H, Pasternak B, Hviid A. Use of clarithromycin and roxithromycin and risk of cardiac death: cohort study. *BMJ*. 2014;349:g4930.
 66. Woosley RL, Whyte J, Mohamadi A, Romero K. Medical decision support systems and therapeutics: the role of autopilots. *Clin Pharmacol Ther*. 2016;99:161–4.
 67. Trac MH, McArthur E, Jandoc R, et al. Macrolide antibiotics and the risk of ventricular arrhythmia in older adults. *CMAJ*. 2016;188:E120–9.
 68. Pedersen HS, Elming H, Seibaek M, et al. Risk factors and predictors of Torsade de pointes ventricular tachycardia in patients with left ventricular systolic dysfunction receiving Dofetilide. *Am J Cardiol*. 2007;100:876–80.
 69. Allen LaPointe NM, Chen A, Hammill B, DeLong E, Kramer JM, Califf RM. Evaluation of the dofetilide risk-management program. *Am Heart J*. 2003;146:894–901.
 70. Haugaa KH, Bos JM, Tarrell RF, Morlan BW, Caraballo PJ, Ackerman MJ. Institution-wide QT alert system identifies patients with a high risk of mortality. *Mayo Clin Proc*. 2013;88:315–25.
 71. Sorita A, Bos JM, Morlan BW, Tarrell RF, Ackerman MJ, Caraballo PJ. Impact of clinical decision support preventing the use of QT-prolonging medications for patients at risk for torsade de pointes. *J Am Med Inform Assoc*. 2015;22:e21–7.
 72. Tisdale JE, Jaynes HA, Kingery JR, et al. Development and validation of a risk score to predict QT interval prolongation in hospitalized patients. *Circ Cardiovasc Qual Outcomes*. 2013;6:479–87.

73. Tisdale JE, Jaynes HA, Kingery JR, et al. Effectiveness of a clinical decision support system for reducing the risk of QT interval prolongation in hospitalized patients. *Circ Cardiovasc Qual Outcomes*. 2014;7:381–90.
74. Vandael E, Vandenberg B, Vandenberghe J, Willems R, Foulon V. Risk factors for QTc-prolongation: systematic review of the evidence. *Int J Clin Pharm*. 2017;39:16–25.
75. Vandael E, Vandenberg B, Vandenberghe J, Spriet I, Willems R, Foulon V. Development of a risk score for QTc-prolongation: the RISQ-PATH study. *Int J Clin Pharm*. 2017;39:424–32.
76. Vandael E, Vandenberg B, Willems R, Reyntens J, Vandenberghe J, Foulon V. Risk management of hospitalized psychiatric patients taking multiple QTc-prolonging drugs. *J Clin Psychopharmacol*. 2017;37:540–5.
77. Redfern WS, Carlsson L, Davis AS, et al. Relationships between preclinical cardiac electrophysiology, clinical QT interval prolongation and torsade de pointes for a broad range of drugs: evidence for a provisional safety margin in drug development. *Cardiovasc Res*. 2003;58:32–45.
78. Kongsamut S, Kang J, Chen XL, Roehr J, Rampe D. A comparison of the receptor binding and HERG channel affinities for a series of antipsychotic drugs. *Eur J Pharmacol*. 2002;450:37–41.
79. Soyka LF, Wirtz C, Spangenberg RB. Clinical safety profile of sotalol in patients with arrhythmias. *Am J Cardiol*. 1990;65:74A–81A.
80. Meyer-Massetti C, Cheng CM, Sharpe BA, Meier CR, Guglielmo BJ. The FDA extended warning for intravenous haloperidol and torsades de pointes: how should institutions respond? *J Hosp Med*. 2010;5:E8–16.
81. Okabe Y, Otowa K, Mitamura Y, et al. Evaluation of the risk factors for ventricular arrhythmias secondary to QT prolongation induced by papaverine injection during coronary flow reserve studies using a 4 Fr angio-catheter. *Heart Vessel*. 2018;33(11):1358–64.
82. Hancox JC, Hasnain M, Vieweg WV, Gysel M, Methot M, Baranchuk A. Erythromycin, QTc interval prolongation, and torsade de pointes: case reports, major risk factors and illness severity. *Ther Adv Infect Dis*. 2014;2:47–59.
83. Yang P, Kanki H, Drolet B, et al. Allelic variants in long-QT disease genes in patients with drug-associated torsades de pointes. *Circulation*. 2002;105:1943–8.
84. Crotti L, Schwartz PJ. Drug-induced long QT syndrome and exome sequencing: Chinese shadows link past and future. *J Am Coll Cardiol*. 2014;63:1438–40.
85. Kaab S, Crawford DC, Sinner MF, et al. A large candidate gene survey identifies the KCNE1 D85N polymorphism as a possible modulator of drug-induced torsades de pointes. *Circ Cardiovasc Genet*. 2012;5:91–9.
86. Behr ER, Ritchie MD, Tanaka T, et al. Genome wide analysis of drug-induced torsades de pointes: lack of common variants with large effect sizes. *PLoS One*. 2013;8:e78511.
87. Ramirez AH, Shaffer CM, Delaney JT, et al. Novel rare variants in congenital cardiac arrhythmia genes are frequent in drug-induced torsades de pointes. *Pharmacogenomics J*. 2013;13:325–9.
88. Weeke P, Mosley JD, Hanna D, et al. Exome sequencing implicates an increased burden of rare potassium channel variants in the risk of drug-induced long QT interval syndrome. *J Am Coll Cardiol*. 2014;63:1430–7.
89. Itoh H, Crotti L, Aiba T, et al. The genetics underlying acquired long QT syndrome: impact for genetic screening. *Eur Heart J*. 2016;37:1456–64.
90. Schwartz PJ, Ackerman MJ, George AL Jr, Wilde AAM. Impact of genetics on the clinical management of channelopathies. *J Am Coll Cardiol*. 2013;62:169–80.
91. Niemeijer MN, van den Berg ME, Eijgelsheim M, Rijnbeek PR, Stricker BH. Pharmacogenetics of drug-induced QT interval prolongation: an update. *Drug Saf*. 2015;38(10):855–67.
92. Levran O, Peles E, Randesi M, et al. Association of genetic variation in pharmacodynamic factors with methadone dose required for effective treatment of opioid addiction. *Pharmacogenomics*. 2013;14:755–68.
93. Tamblyn R, Egale T, Buckeridge DL, et al. The effectiveness of a new generation of computerized drug alerts in reducing the risk of injury from drug side effects: a cluster randomized trial. *J Am Med Inform Assoc*. 2012;19:635–43.
94. Seidling HM, Klein U, Schaiër M, et al. What, if all alerts were specific - estimating the potential impact on drug interaction alert burden. *Int J Med Inform*. 2014;83:285–91.
95. Bryant AD, Fletcher GS, Payne TH. Drug interaction alert override rates in the meaningful use era: no evidence of progress. *Appl Clin Inform*. 2014;5:802–13.
96. Payne TH, Hines LE, Chan RC, et al. Recommendations to improve the usability of drug-drug interaction clinical decision support alerts. *J Am Med Inform Assoc*. 2015;22:1243–50.
97. Ashar FN, Mitchell RN, Albert CM, et al. A comprehensive evaluation of the genetic architecture of sudden cardiac arrest. *Eur Heart J*. 2018;39(44):3961–9.
98. Schwartz PJ, Gentilini D. Can genetics predict risk for sudden cardiac death? The relentless search for the holy grail. *Eur Heart J*. 2018;39(44):3970–2.
99. Schwartz PJ, Wolf S. QT interval prolongation as predictor of sudden death in patients with myocardial infarction. *Circulation*. 1978;57:1074–7.
100. Bloomfield RA Jr, Polo-Wood F, Mandel JC, Mandl KD. Opening the Duke electronic health record to apps: implementing SMART on FHIR. *Int J Med Inform*. 2017;99:1–10.
101. Roden DM, Van Driest SL, Mosley JD, et al. Benefit of pre-emptive pharmacogenetic information on clinical outcome. *Clin Pharmacol Ther*. 2018;103(5):787–94.

102. Chung EH, Guise KD. QTC intervals can be assessed with the AliveCor heart monitor in patients on dofetilide for atrial fibrillation. *J Electrocardiol.* 2015;48:8–9.
103. Castelletti S, Dagradi F, Goulene K, et al. A wearable remote monitoring system for the identification of subjects with a prolonged QT interval or at risk for drug-induced long QT syndrome. *Int J Cardiol.* 2018;266:89–94.
104. Verrier RL. The power of the patch: a smart way to track risk for Torsades de pointes in congenital and drug-induced long QT syndromes? *Int J Cardiol.* 2018;266:145–6.



Acquired Long QT Syndrome and Electrophysiology of Torsade de Pointes

11

Nabil El-Sherif, Gioia Turitto,
and Mohamed Boutjdir

Abbreviations

AP-A	Anthopleurin-A
APD	Action potential duration
CL	Cycle length
DAD	Delayed afterdepolarization
DR	Dispersion of repolarization
EAD	Early afterdepolarization
ECG	Electrocardiogram
END	Endocardial cell
EPI	Epicardial cell

GWAS	Genome-wide association studies
hERG	Human Ether-à-go-go-Related Gene
LQTS	Long QT syndrome
M	Mid-myocardial cell
Na	Sodium
NST	nonself-terminating
QTc	Corrected QT interval
SCD	Sudden cardiac death
ST	Self-terminating
TdP	Torsade de pointes
TWA	T-wave alternans
VF	Ventricular fibrillation
VT	Ventricular tachyarrhythmia

Supported in part by Cardiovascular Research Program, the Narrows Institute for Biomedical Research and Education and a MERIT Award Number I01 BX002137 from Biomedical Laboratory Research & Development Service of the Veterans Affairs Office of Research and Development.

N. El-Sherif (✉)
Department of Medicine and Physiology, State
University of New York Downstate Medical Center,
VA New York Harbor Healthcare Center,
Brooklyn, NY, USA

G. Turitto
Cardiac Electrophysiology Services, Department of
Medicine, New York-Presbyterian Brooklyn
Methodist Hospital, Brooklyn, NY, USA

M. Boutjdir
Department of Medicine and Physiology, SUNY
Downstate Medical Center, Brooklyn, NY, USA

State University of New York Downstate Medical
Center, New York, NY, USA

NYU School of Medicine, New York, NY, USA

Introduction

Since its initial description by Jervell and Lange-Nielsen in 1957 [1], the congenital long QT syndrome (LQTS) has been the most investigated cardiac ion channelopathy. A prolonged QT interval on the surface electrocardiogram (ECG) is a surrogate measure of prolonged ventricular action potential duration (APD). Congenital as well as acquired alterations in certain cardiac ion channels can affect their currents in such a way as to increase the APD and hence the QT interval. The inhomogeneous lengthening of the APD across the ventricular wall results in dispersion of APD, i.e., dispersion of repolarization (DR). This, together with the tendency of prolonged APD to be associated with oscillations at the plateau level,

termed early afterdepolarizations (EADs), provides the substrate of ventricular tachyarrhythmia (VT) associated with LQTS, usually referred to as torsade de pointes (TdP) VT [2].

Acquired LQTS is by far more prevalent than congenital LQTS. The vast majority of acquired LQTS is the result of the adverse effect of drugs [3] and/or electrolyte abnormalities [4], which, in the majority of cases, interact with the human Ether-à-go-go-Related Gene (hERG) encoding the pore-forming subunits (Kv11.1) of the rapidly activating delayed rectifier current, I_{Kr} . However, recent reports suggest that some drugs can also increase the late sodium current, which may contribute to their proarrhythmic effect [5].

This chapter is divided into three sections: Section “Acquired LQTS” will review the electrophysiological mechanisms, electrocardiographic (ECG) characteristics, clinical presentation, and management of acquired LQTS. Section “Comprehensive Electrophysiological Mechanisms of TdP” will provide a comprehensive review of the electrophysiological mechanisms of TdP. Section “Future Directions” is a brief discussion of future direction in the field.

Acquired LQTS

ECG Characteristics of TdP

In an analysis of 150 different episodes of sustained VT obtained from 62 patients with the acquired LQTS, the arrhythmia ranged in length from 3 beats (the definition of nonsustained VT) up to 117 beats (Fig. 11.1, panel a), with an average length of 16 ± 8 beats [2]. The cycle length (CL) of these episodes ranged from 193 to 364 ms, with an average of 279 ± 47 ms. The VT was frequently preceded by a variable period of bigeminal rhythm due to one or two premature ventricular beats coupled to the prolonged QT segment of the preceding basic beat (Fig. 11.1, panels a and c). This so called short-long cardiac sequence is seen in both the acquired and congenital LQTS, and the arrhythmogenic mechanism may be related to increased dispersion of repolarization (DR) [6].

Following termination of an episode of fast VT, it is not uncommon to see one or more

ectopic beats of variable configuration occurring at much longer CL compared to that of the VT (see beats marked by stars in Fig. 11.2). The change in QRS configuration during VT can take several forms. During a very fast VT, periodic decrease in the amplitude of the entire QRS-T complex is seen with less distinct shifts in QRS axis (Fig. 11.1a). In VTs with slower rates, the classic twisting of the QRS axis from a predominantly positive to a predominantly negative configuration with a variable number of transitional complexes and vice versa is commonly seen as originally described by Dessertenne [7] (Fig. 11.1b). Sometimes, a polymorphic QRS configuration is seen without any of the two previously characteristic patterns (as verified in multiple simultaneous leads, Fig. 11.2c, middle recording). Different patterns can be seen in different VT episodes from the same patient (Fig. 11.1c).

QT/T Wave Alternans and TdP

It has long been known that tachycardia-dependent T wave alternans (TWA) occurs in patients with the congenital or acquired form of the LQTS and may presage the onset of TdP (Fig. 11.2) [2, 8].

In analysis of 1103 LQTS patients with QTc interval > 0.44 seconds from the International LQTS Registry, TWA was recorded in 30 patients [8]. The frequency of occurrence of TWA was directly proportional to the length of the QTc interval on the enrollment ECG. TWA occurred in one or more occasions during an average 4-year follow-up in 21% of the patients with QTc > 0.60 seconds, but in $< 0.2\%$ of the patients with QTc < 0.50 seconds. Patients with advanced forms of TWA (those with bidirectional beat-to-beat changes in T wave polarity; $n = 21$) were younger, had longer QTc values, had a higher incidence of complex VT, and were more likely to experience a cardiac event (syncope or cardiac arrest) than those with less advanced forms of TWA (those without bidirectional beat-to-beat changes in T wave polarity; $n = 9$).

In contrast to TWA in congenital LQTS, the incidence of TWA in acquired LQTS is unknown.

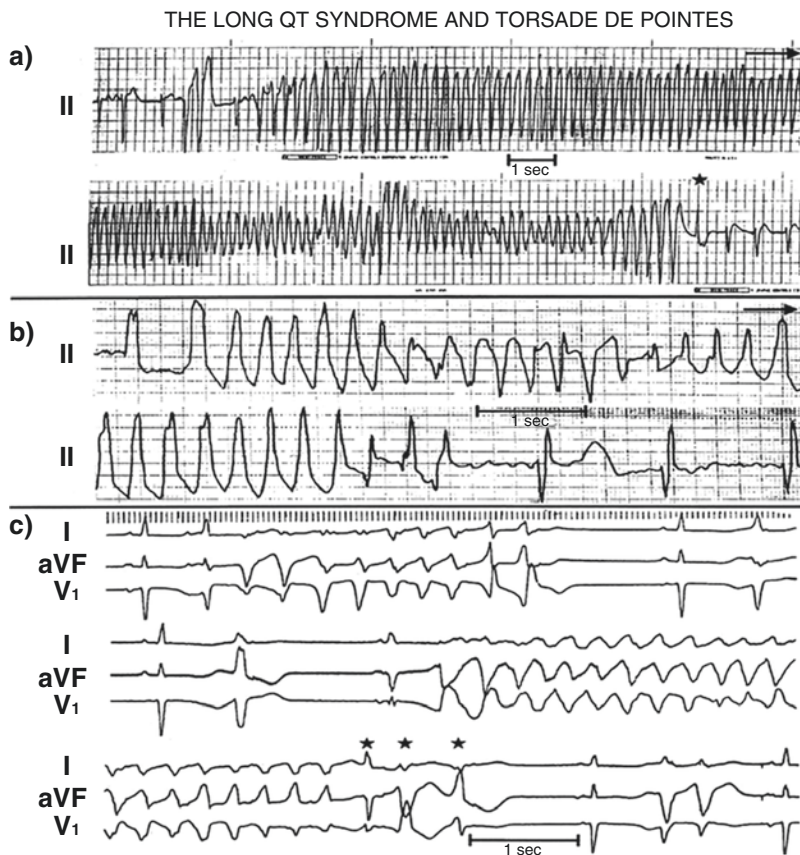


Fig. 11.1 Three electrocardiographic examples of acquired long QT syndrome (LQTS) and torsade de pointes (TdP). (a) was obtained from a 23-year-old woman who was human immunodeficiency virus (HIV) positive and was receiving pentamidine. The patient was admitted with severe diarrhea and hypokalemia. (b) was recorded from a 62-year-old man with hypertension and chronic atrial fibrillation who was receiving digoxin and hydrochlorothiazide and had a potassium level of 3.2 mEq/L. The TdP tachycardia developed 12 hours after

the patient received a total of four tablets of quinidine gluconate in an attempt to restore normal sinus rhythm. (c) was obtained from a 64-year-old man who was receiving procainamide for suppression of very frequent ventricular premature complexes. N.B. pentamidine, quinidine, and procainamide are considered drugs with high risk of drug-induced acquired QT syndrome and their use is currently curtailed. (Reproduced El-Sherif and Turitto [2]. Used with permission of John Wiley and Sons)

It has been reported in acquired LQTS due to hypokalemia and hypomagnesemia (Fig. 11.3) [4] as well as in association with medications that prolong the QT interval (Fig. 11.3) [9]. Patients with acquired LQTS and TWA are likely to develop TdP (Figs. 11.2 and 11.3).

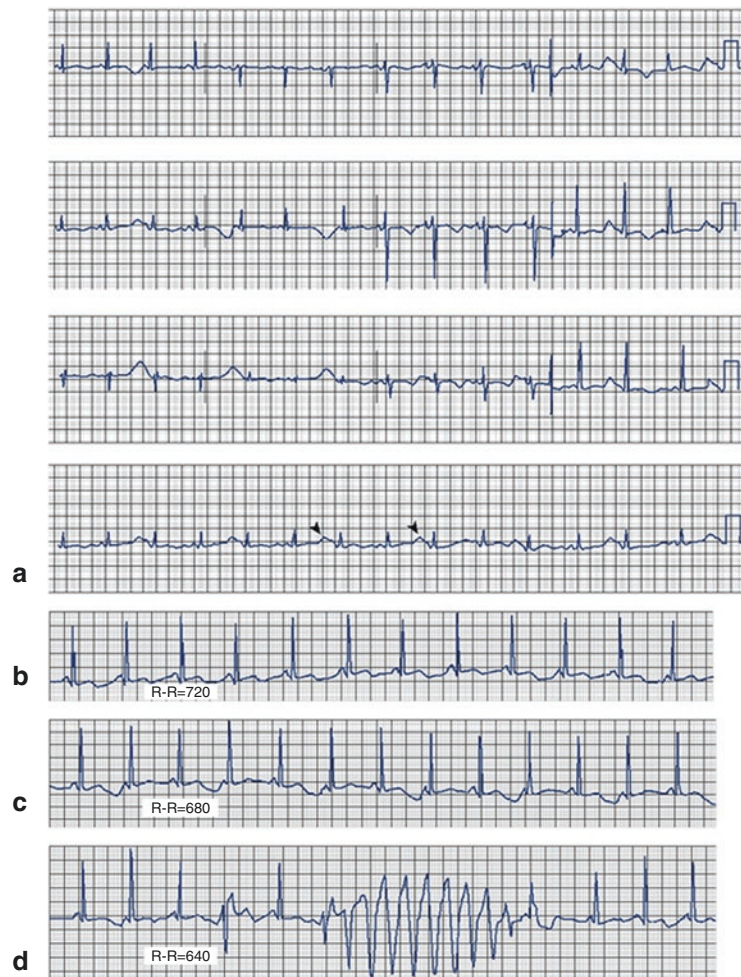
Although overt TWA in the ECG is not common, in recent years, digital signal processing techniques have made it possible to detect subtle degrees of TWA [10]. This suggests that the phenomenon may be more prevalent than previously recognized and may represent an important marker of vulnerability to VT. A recent report

confirms this view by showing that microvolt TWA is far more prevalent in LQTS patients than previously reported and is strongly associated with TdP history [11]. Interest in TWA is attributed to the hypothesis that it reflects a greater degree of underlying DR [12].

Etiology of Acquired LQTS

The vast majority of acquired LQTS is the result of adverse effects of drugs that interact with the hERG gene and the I_{Kr} . However, although most

Fig. 11.2 (a) Twelve-lead ECG from a patient with hypokalemia and hypomagnesemia showing marked QTU prolongation and QTU alternans (marked by arrowheads). (b–d) Representative rhythm strips from the same patient, showing tachycardia-dependent QTU alternans and torsade de pointes. (Reproduced from El-Sherif and Turitto [4], 233–245; an Open Access journal)



drugs that cause TdP do so via hERG channel blockade, TdP is not necessarily a potential consequence of all drugs blocking the hERG pathway. Milberg et al. [13] compared the TdP induction ability of two hERG blocking drugs, DL-sotalol and amiodarone. While both drugs can increase the QT interval, the former causes transmural DR and triangulation of the action potential by prolonging phase 3 and triggers both EADs and TdP. On the other hand, amiodarone does not usually cause DR, EADs, or TdP and by prolonging phase 2 results in a square-shaped action potential. While square-shaped action potentials are considered to be antiarrhythmic, triangulated action potentials are considered to

be proarrhythmic [14]. Several authors have suggested that DR, attributed to preferential prolongation of the APD of midmyocardial (M) cells, is a preclinical marker of drug-induced proarrhythmia [15]. However, the existence, location, and clinical contribution of M cells have been a matter of debate [16].

Recent studies have shown that some drugs designated as arrhythmogenic I_{Kr} blocker can generate arrhythmias by augmenting I_{Na-L} through the PI3K pathway [5]. For example, while acute exposure of flecainide to adult mouse cardiomyocyte which lacks I_{Kr} produced no change in ion currents and action potential duration, extended exposure up to 48 hours of the



Fig. 11.3 Representative ECG recordings from a 63-year-old female with HIV who developed efavirenz-related QT prolongation and TdP arrhythmia. Panel **a** shows sinus rhythm at 95 bpm and QT alternans. Panel **b** shows sinus bradycardia, marked QT interval prolongation, and the onset of a TdP arrhythmia that required cardioversion for termination. Panel **c** shows that the arrhythmia could be suppressed by overdrive ventricular

pacing at a rate of 100 bpm. For a number of days it was noted that QT prolongation and nonsustained TdP episodes developed when the pacing rate was lowered to <100 bpm. The QT returned to normal several days after discontinuation of the long-acting efavirenz. (Reproduced with permission from: Castillo et al. [9]. Used with permission of SAGE Publications)

drug generated up to 15-fold increase in I_{Na-L} and resulted in arrhythmogenic EADs. However, not all I_{Kr} blockers modulate I_{Na-L} and this diversity of effects, in return, may contribute to the apparent difference in TdP frequency across culprit drugs [5]. A major implication of these data has to be, that relying on an assay to assess acute block of I_{Kr} may not provide a comprehensive assessment of a candidate drug arrhythmogenic potential.

Other causes of acquired LQTS include electrolyte abnormalities (hypokalemia, hypomagnesemia, and hypocalcemia; see Fig. 11.3), hypothyroidism, hypothermia, and marked bradycardia (sinus bradycardia as in Fig. 11.4 or atrioventricular block [17]). Any of these factors can cause acquired LQTS or contribute to the risk of drug-induced LQTS. In addition, there is recent evidence of the high prevalence of QTc interval prolongation in patients with anti-SSA/Ro antibodies, as well as autoimmune and inflammatory diseases [18–20]. A recent report from this laboratory provided strong evidence for a pathogenic role of anti-SSA/Ro antibodies in the development of QTc prolongation. Anti-Ro antibodies from patients with autoimmune disease

were shown to inhibit I_{Kr} by directly cross-reacting with the hERG channel, likely at the pore region where homology between 52Ro antigen and hERG channel was demonstrated [21]. In addition, an animal model of autoimmune-associated QTc prolongation was established, for the first time, whereby induction of anti-SSA/Ro antibodies by immunization resulted in QTc prolongation on the surface ECG [21].

Pharmacogenetics of Acquired LQTS

The susceptibility to acquired QT interval prolongation can be influenced by genetic variations [22]. This is supported by the fact that the heritability of QT interval duration in the general population (excluding congenital LQTS patients) is estimated to be around 35% [23, 24]. Further, first-degree relatives of patients with congenital LQTS have a higher risk of drug-induced QT prolongation than non-related individuals [25]. In genome-wide association studies (GWAS), a large number of genes associated with QT interval duration

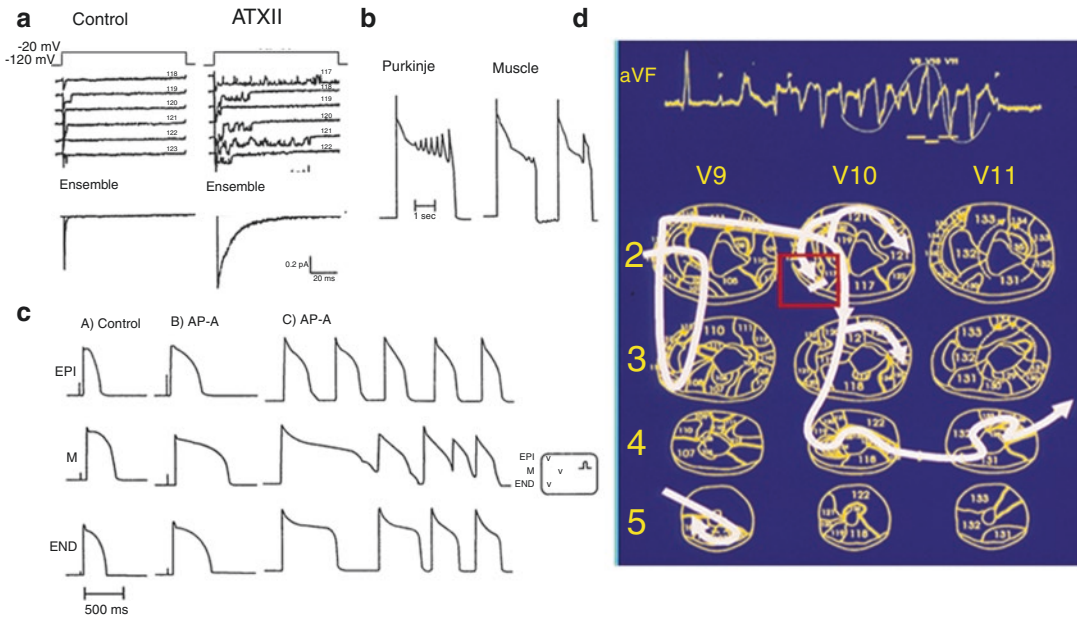


Fig. 11.4 Composite figure that illustrates the correlation between the specific molecular changes of the Na channel in the canine surrogate model of LQT3, the electrophysiological consequence, and the final phenotype presentation of LQTS and TdP. **(a)** Cell-attached patch clamp recordings of the Na channel during control and following superfusion with sea anemone toxin ATXII. This neurotoxin faithfully reproduces the molecular changes associated with the clinical mutations of the Na channel in patients with LQT3. It illustrates sequential recordings of single Na channel current responses during depolarizing steps from -120 to -20 mV from rabbit cardiomyocytes. The left panel shows control recordings and the right panel shows recordings from a patch exposed to 100 nM of ATXII that resulted in long-lasting bursts consisting of repetitive long opening interrupted by brief closures. The ensemble current from this patch shows markedly slowed relaxation. **(b)** Action potential recordings from a Purkinje fiber (PF) and a mid-myocardial (M) cell, both isolated from a 10-week-old puppy and placed in the same chamber perfused with 50 mg/l anisoleurine-A (AP-A) and stimulated at 3000 ms. The PF shows a series of early afterdepolarizations (EADs) that increased gradually in amplitude before final repolarization. **(c)** Simultaneous recordings from a subepicardial cell (EPI), M cell, and a

subendocardial cell (END) from a transmural strip isolated from the left ventricle of a 12-week-old puppy and transfused with 50 mg/l AP-A and stimulated at 4000 ms. Because of the different ionic characteristics of different myocardial fibers, AP-A resulted in marked differential prolongation of the action potential of the M cell resulting in asynchronous activation in the preparation, which is a substrate of reentrant excitation. **(d)** Tridimensional activation maps of a 12-beat run of TdP from the in vivo canine surrogate AP-A model of LQT3 which helps to summarize the final electrophysiological mechanism of TdP in the LQTS. The first beat of a TdP is due to an EAD-triggered beat from the subendocardial Purkinje network that acts on the transmural dispersion of myocardial repolarization to induce reentrant excitation in the form of circulating tridimensional wavefronts (the thick continuous line that traces the activation wavefront from one beat to the next). The twisting QRS pattern of the classic TdP is attributed in this example to transient bifurcation of a predominantly single rotating wavefront into two separate simultaneous wavefronts rotating around the left and right ventricular cavities. (Reproduced from: El-Sherif and Boutjdir [62]. Used with permission of Elsevier)

have been identified [26]. The gene with the strongest signal related to QT interval duration is the nitric oxide synthase 1 adaptor protein gene (NOS1AP), located on chromosome 1 (1q23.3) [26, 27], which inhibits the L-type calcium channel and influences impulse propaga-

tion [28]. Other findings from GWAS included polymorphisms within genes known to be mutated in congenital LQTS, genes associated with intracellular calcium handling, as well as genes previously not known to influence cardiac repolarization [29]. A recent study that

compared 188 patients with drug-induced LQTS and more than 1000 patients with congenital LQTS found disease-causing mutations in 28% of patients with drug-induced LQTS [30]. Of interest, under basal conditions, the QTc of drug-induced LQTS patients (453 ± 39 ms) was significantly longer than that of control subjects (406 ± 26 ms) [30].

It is important to consider pharmacogenetics of drug-induced LQTS as related to both pharmacokinetic and pharmacodynamic properties [22, 29]. Pharmacokinetics constitute the effect of the body on the drug, which is usually categorized into effect on absorption, distribution, metabolism, and elimination of the drug. Pharmacokinetic genetic susceptibility is mainly characterized by variation in genes encoding drug-metabolizing cytochrome P450 or drug transporter, like the P-glycoprotein. On the other hand, the pharmacodynamic component of genetic susceptibility is mainly characterized by genes known to be associated with QT prolongation in the general population and genes in which the causal mutations of congenital LQTS are located [30].

Incidence of Drug-Induced LQTS

The overall incidence of drug-induced LQTS in a given population is difficult to estimate. One study estimated that between 5% and 7% of reports of VT, VF, or SCD were in fact drug-induced LQTS and TdP [31]. European pharmacovigilance centers in Sweden, Germany, and Italy have found an annual reporting rate of drug-induced LQTS or TdP of approximately 0.8 to 1.2 per million person-years [31]. An epidemiological study of drug-induced LQTS in Germany found the reporting rate for symptomatic acquired LQTS to be 2.5% per million person-years for men and 4.0% per million person-years for women, with 60% attributed to drugs [32].

QT prolongation is one of the most common reasons for drug withdrawal from the market, despite the fact that these drugs may be benefi-

cial for certain patients and not harmful in every patient [29]. Since 1989, 14 clinically important drugs have been removed from the market due to TdP [33], and development of an unknown number has been stopped, due to concerns that these might pose a risk of causing QT prolongation and TdP [33]. In the 1990s, the US Food and Drug Administration (FDA) and the European Medicine Agency (EMA) began requiring routine preclinical and clinical testing to determine whether drugs have the potential to cause QT prolongation [34]. According to the CredibleMeds website, which has become the standard reference for drug-induced TdP, 38 marketed drugs are recognized for their potential to cause TdP and another 72 to cause QT prolongation [35].

In the past decade, hERG channel-mediated cardiac toxicity, manifested as QT interval prolongation, has become a major safety issue in drug development, superseding liver injury as the main cause of drug withdrawals. *In vitro* electrophysiological testing of the drug's effects on the function of the hERG channel may be cheaper, faster, and potentially more sensitive than other current surrogates for TdP risk, such as *in vivo* QT prolongation and action potential prolongation in cardiomyocytes [36].

Ethnicity and Gender Differences in Drug-Induced LQTS

As ethnic differences ultimately reflect genetic variation, it is useful to study ethnicity with regard to susceptibility to drug-induced QT interval prolongation and TdP. However, the role of ethnic differences has not been well established in published studies on drug-induced QT interval prolongation. In 20 QT/QTc studies, only 10% of the total study population was African American and only 7% was Asian [37]. Nevertheless, the frequency of polymorphisms in genes known from congenital LQTS showed varying distribution among ethnic groups [38]. African Americans had the highest risk of prolonged QT interval after

acute overdose of QT-prolonging drugs, while Hispanics had the lowest risk compared to all other ethnic groups [39].

Females with inherited LQTS demonstrate pronounced sex difference in cardiac repolarization and arrhythmic risk. Adult women with LQT1 and LQT2 have longer QT intervals, a more pronounced transmural QT dispersion, and a higher risk of TdP and SCD than men [40, 41]. Interestingly, in female patients with LQT2, the arrhythmogenic risk remains elevated after menopause, suggesting that other gender-related factors besides sex hormones may contribute to gender difference in arrhythmogenesis [42].

Gender is a risk factor for adverse drug reactions [43, 44]. The concept of reduced repolarization reserve in females compared to males has been used to explain sex differences in arrhythmia risk in acquired LQTS [45]. The reduced repolarization reserve of the female heart is attributed to lower repolarizing K^+ currents. This difference was thought to be primarily due to testosterone-mediated increase in I_{Kr} and I_{K1} resulting in shorter APD and QTc interval in male hearts. However, in a recent review, the effects of sex hormones go well beyond their modulation of K^+ currents [46]. The underlying mechanisms could be summarized as follows [47]: (1) an estradiol-induced decrease in I_{Kr} as well as increase of I_{CaL} , sodium calcium exchange (NCX) expression and activity, RyR2 leakiness, Ca^{2+} transient amplitude, and $\alpha 1$ - and $\beta 2$ -adrenoreceptor responsiveness; (2) a testosterone-induced increase in I_{Kr} , I_{Ks} , and I_{K1} , increased SERCA activity, and shortened Ca^{2+} transient; and (3) a progesterone-induced increase in I_{Ks} , increased SERCA expression and activity, and increased I_{CaL} current sensitivities with reduced Ca^{2+} oscillations upon sympathetic stimulation. In a recent study, we have shown that modulation of voltage- Ca^{2+} uncoupling [48] may provide one more attractive electrophysiological mechanism for the increased vulnerability of females to drug-induced LQTS.

Acute and Long-Term Management of Acquired LQTS

The American College of Cardiology (ACC), American Heart Association (AHA), and European Society of Cardiology (ESC) published guidelines for management of ventricular arrhythmias, including drug-induced TdP [49], in 2006 and the key recommendations have been endorsed in a more recent ACC/AHA statement [50].

When monitoring for drug-induced prolonged QT interval, a baseline QTc should be obtained. If any one of the following conditions is observed during QT interval monitoring, the patient should be admitted to the hospital for telemetry: (1) QTc > 500 ms, (2) QTc increase > 60 ms above baseline, (3) QT prolongation accompanied by syncope, and (4) any evidence of ECG instability, specially TWA, AV block, QRS widening, or ventricular ectopy. The offending drug should be discontinued, electrolyte abnormalities corrected, and a defibrillator placed at bedside [50].

Nonself-terminating TdP with hemodynamic collapse should obviously be cardioverted with adequate post-cardioversion management. More typical TdP occurs as recurrent self-terminating episodes. In these cases, the first line of management is intravenous administration of magnesium sulfate as a single 2g (8 mmol) dose over 1–2 min followed by a second dose if necessary. Magnesium sulfate is effective in suppressing TdP without reducing the QT interval [67]. The mechanism of action may be related to suppression of late calcium influx via L-type calcium current and reduction in the amplitude of EADs [51]. If magnesium sulfate fails to suppress TdP, the next step is to increase the heart rate, typically by transvenous pacing. In the interim if necessary, isoproterenol administration could promptly increase the heart rate while waiting for insertion of pacing electrode. Increasing the heart rate is associated with shortening of the QT interval and suppression of TdP. At the same time, the culprit drug should be discontinued and acid-base and electrolytes should be corrected as necessary.

There are novel experimental drugs that can enhance the delayed rectifier conductance [52] or activate the cardiac ATP-sensitive potassium channel [53], which may have future value for the treatment of acquired LQTS.

Long-term management of acquired LQTS is important. All patients with previous drug-induced prolongation of the QT interval should be instructed about the importance of subsequent avoidance of QT-prolonging drugs and should have a list of QT-prolonging medications provided by their physicians. In patients with acquired LQTS, the risk of further episodes of TdP is reduced once the culprit drug is removed and other aggravating situations such as electrolyte abnormalities or marked bradycardia are corrected. This should result in normalization of the QTc interval. If it does not, the patient and symptomatic first-degree family members should be considered for genetic testing for the presence of LQTS-associated mutations [50, 54]. This is especially important for relatives of patients with drug-induced case fatality.

Comprehensive Electrophysiological Mechanisms of TdP

Experimental Models of LQTS

Both drug-induced and genetically modified animal models of various species have been generated and utilized to investigate the electrophysiological mechanisms of arrhythmogenesis in LQTS and potential pro- and antiarrhythmic agents. However, due to species differences in features of cardiac electrical function, particularly in repolarization currents, these models do not completely recapitulate all aspects of the electrophysiology of the human disease. Genetically modified animal models, such as mice and rabbits, are commonly used to investigate the arrhythmogenicity of LQTS. Current transgenic LQTS rabbit models have already been instrumental in increasing our understand-

ing of the role of spatial and temporal dispersion of repolarization to provide an arrhythmogenic substrate, genotype differences in the mechanisms for EAD formation and arrhythmia maintenance, and mechanisms of hormonal modification of arrhythmogenesis [55].

On the other hand, two dog models of LQTS and TdP have been extensively investigated. One model is the dog with induced complete atrioventricular conduction block (AVB). Complete AVB results within few weeks in hypertrophy and remodeling of the left ventricle associated with prolongation of the QT interval, APD, as well as spatial DR [56]. When the animal is challenged with a drug that blocks the I_{Kr} , like dofetilide, it results in further prolongation of the QT interval and creation of a drug-induced model of acquired LQTS and TdP [57].

The other dog model of LQTS and TdP is the anthopleurin-A (AP-A) canine surrogate model of LQT3 that was developed in this laboratory [58]. The model is created by the neurotoxin anthopleurin-A or ATX II [59] that faithfully reproduces the molecular changes associated with clinical mutations of the Na channel in patients with LQT3 [60]. Of interest, the experimental surrogate model of LQT3 anticipated the first description of the clinical LQT3 by 7 years [61]. Figure 11.4 is a representative composite of the salient experimental techniques that were utilized to investigate the model and illustrate the correlation between the modulation of a cardiac ion current, its electrophysiological consequence, and the final phenotype presentation as LQTS and TdP.

Electrophysiological Mechanisms of the Trigger of TdP in the LQTS

There is an almost complete agreement that initiating one or two beats of TdP is due to EAD-triggered focal activity from the subendocardial Purkinje network [57, 63–65]. A study by Caref and associates has confirmed beyond reasonable doubt the subendocardial origin of the trigger of TdP [66]. In this study the canine surrogate

model of LQT3 was placed on cardiopulmonary bypass and chemical ablation of the endocardial Purkinje network was obtained using Lugol's iodine following which spontaneous TdP was no longer observed. However, a properly timed premature stimulus induced reentrant ventricular arrhythmias (VA) based on the underlying marked DR. On the other hand, the perpetuation of TdP remains controversial and could be attributed to focal activity, reentrant excitation, or a combination of both mechanisms.

The ionic mechanism(s) that underlie the generation of EADs have been widely investigated. The central hypothesis on the generation of EADs suggests that a spontaneous release of calcium from the sarcoplasmic reticulum would temporarily increase cytosolic calcium concentration with a subsequent sudden activation of the NCX. This inward current could "re-depolarize" the sarcolemmal membrane to a potential from which sodium or calcium currents become reactivated, triggering an afterdepolarization [67]. Although this model has been primarily discussed to explain delayed afterdepolarizations, there is also evidence that this mechanism may be the trigger for EADs [68]. This hypothesis is also supported by studies that showed that inhibition of the NCX suppresses TdP in the intact heart model of LQTS2 and LQTS3 [69].

Electrophysiological Mechanism(s) of Perpetuation of TdP

Contrary to the established mechanism of the trigger of TdP, the perpetuation of TdP remains controversial and could be attributed to focal activity, reentrant excitation, or a combination of both mechanisms [70, 71]. Both reentrant and focal activity are assumed to be nonstationary. For reentrant excitation, this could be a heterogeneity-induced drift of a reentrant circuit [72] or a meandering reentrant spiral wave (see Fig. 11.1, panel d) [73]. Alternatively, ectopic beats originating from different locations may explain the perpetuation of TdP. The original description of TdP by Dessertenne attributed the

pattern to two variable opposing foci (deux foyers) [7]. In computational modelling as well as experimental observation of the canine chronic AVB model, both multiple competing foci and reentrant excitation could develop depending on heterogeneity of repolarization in comparison to the surrounding tissue [70]. Large heterogeneities can produce ectopic TdP, while smaller heterogeneities will produce reentrant type TdP. An experimental study in the same model reported that short-lasting episodes of TdP had a focal mechanism while long-lasting episodes were maintained by reentrant excitation [71]. However, the results were criticized because of the controversial definition of focal versus reentrant excitation [74].

However, it remains an open question why and how ectopic beats emerge and compete; and what their relationship to the observed EAD activity. EADs arising from the subendocardial Purkinje network conducted to overlying myocardium through Purkinje-muscle junctions (PMJ). Electrotonic interactions across PMJs can modulate APD locally. A recent study has proposed that, dependent on resistive properties across PMJs, large spatial gradient of APD can develop at the endocardium and the transmural plane [75]. This may provide a better explanation compared to the concept of M cells with different ionic characteristics [76].

One of the problems of sustained fast EAD-induced focal activity, is that the short cycle length will be associated with short APD that would suppress further EAD generation unless there is some form of protected islands of prolonged APD with EADs capable of conduction across PMJs to activate the ventricular myocardium. In a study, combined computational simulation and experimental observations in isolated myocytes, showed that in electrically homogeneous tissue models, chaotic EADs synchronize globally when the tissue is smaller than a critical size. However, when the tissue exceeds the critical size, electronic coupling can no longer globally synchronize EADs, resulting in regions of partial synchronization that shift in time and space. These regional, partially synchronized EADs then form

premature ventricular complexes that propagate into recovered tissue without EADs, thus creating “shifting” foci that resemble polymorphic VT [77].

Delayed Afterdepolarization (DAD)-Triggered Activity Contributes to VA in the LQTS

The electrophysiologic mechanism of VT in LQTS is somewhat more complex than that described earlier. Figure 11.5, panel a, was obtained from one of the classic reviews of cellular mechanisms of cardiac arrhythmias by Hoffman and Rosen [78]. It shows transmembrane AP recording from a canine Purkinje fiber superfused with 20 mM cesium chloride (a surrogate experimental model for LQT2). The recording illustrates the classic bradycardia-dependent prolongation of APD associated with membrane oscillation on late phase 2/early phase 3 of the repolarization phase characteristic of EADs. But it also shows that complete repolarization of the AP is followed by a subthreshold delayed afterdepolarization (DAD). The latter is simply explained on the basis of increased intra-

cellular Ca^{2+} associated with the prolonged AP duration triggering a transient inward current. This, almost forgotten, observation strongly suggests that some VT and ectopic beats in LQTS could be secondary to DADs.

Figure 11.5, panel b, shows a corroboration of this observation from the canine surrogate model of LQT3 [79]. The top ECG tracing was obtained 10 minutes after infusion of AP-A and shows moderate prolongation of the QT interval and a run of nonsustained monomorphic VT at a rate of 150 beats/min. The VT starts with a late coupled beat that is well beyond the end of the QT interval of the preceding sinus beat. Tridimensional mapping of activation showed that the VT arose as a focal discharge (F) from the same subendocardial site. For all practical purposes, the focal discharge could be attributed to DAD-triggered activity.

The bottom ECG tracing was obtained from the same experiment 10 minutes later and shows further prolongation of the QT interval. The ectopic beats labeled F now seem to be coupled to the end of the prolonged QT interval of the preceding sinus beats. The middle of the tracing illustrates a six-beat run of polymorphic VT. Tridimensional mapping shows that the first beat arose from a

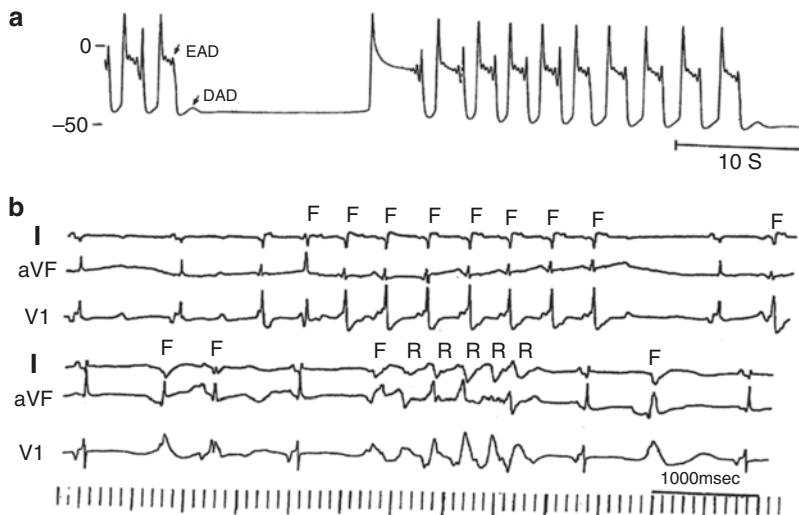


Fig. 11.5 Transmembrane action potential recording from a Purkinje fiber superfused with 20 mM cesium chloride showing both early and delayed afterdepolarizations. (b) ECG recording from an *in vivo* canine antho-

pleurin-A surrogate model of LQT3. See text for details. F focal discharge, R reentrant excitation. (Reproduced from: El-Sherif [79]. Used with permission of John Wiley and Sons)

subendocardial focal site and could be safely attributed to EAD-triggered activity, whereas subsequent beats were due to reentrant excitation in the form of continuously varying scroll waves.

Electrophysiological Mechanisms of Self-Terminating (ST) Versus Nonself-Terminating (NST) TdP VT

The majority of TdP episodes terminate spontaneously (self-terminating, ST) (see Fig. 11.1). However, a minority can degenerate in VF (nonself-terminating, NST). The electrophysio-

logical mechanisms of the NST episodes of TdP have never been elucidated. Obviously, this is a more important issue than the “twisting and turning” to see if perpetuation of TdP VT is due to focal or reentrant activation [74]. Figures 11.6 and 11.7, obtained from the canine surrogate model of LQT3, provide one possible electrophysiological mechanism [79]. The lesson gained from this example is that subtle changes in underlying spatial DR and conduction characteristics can result in fractionation of activation wavefronts and VF. It also demonstrates clearly the difficulty in predicting which TdP episodes will be ST or NST.

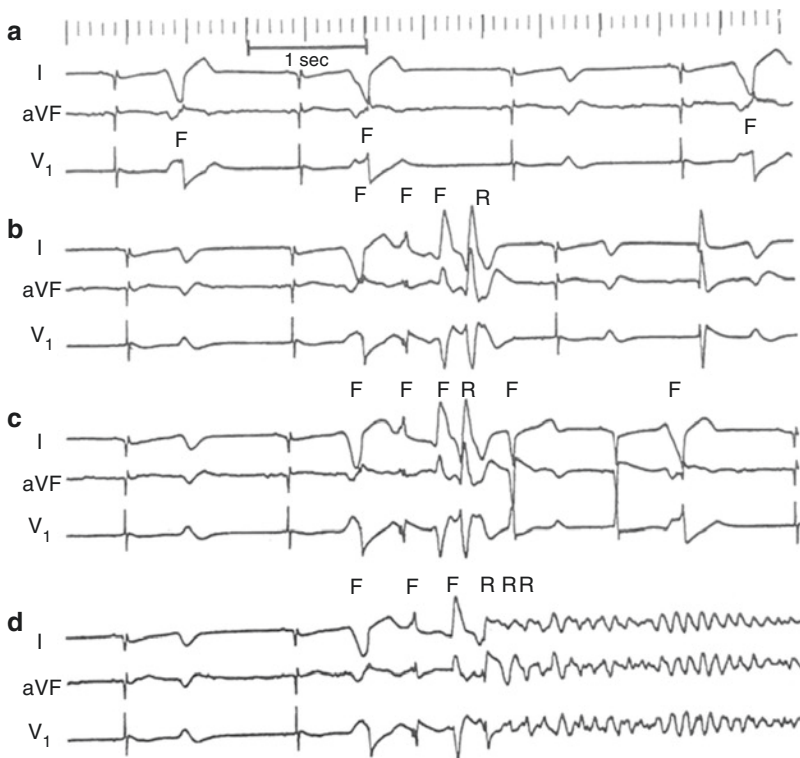


Fig. 11.6 ECG recordings from an *in vivo* canine AP-A surrogate model of LQT3. The recordings are arranged chronologically, a few minutes apart. Panel **a** shows a stable bigeminal and trigeminal rhythm due to subendocardial discharge attributed to EAD-triggered activity from the same focus. This was followed several minutes later by runs of four- or five-beat polymorphic VT with remarkable repetition of the same QRS morphology. The first beat of each run arose from the same site of the bigeminal/trigeminal beats in panel **a**. The second and third beats of each run arose from two different

subendocardial focal sites; the fourth beat was reentrant in origin. The fifth beat in a five-beat run again was focal in origin and arose well after the end of the reentrant excitation and could be attributed to DAD-triggered activity. After approximately 10 minutes of repetitive nonsustained VT, the same three initial focal beats were followed by reentrant excitation that degenerated into ventricular fibrillation (VF) (panel **d**). F = focal discharge; R = reentrant excitation. (Reproduced from: El-Sherif [79]. Used with permission of John Wiley and Sons)

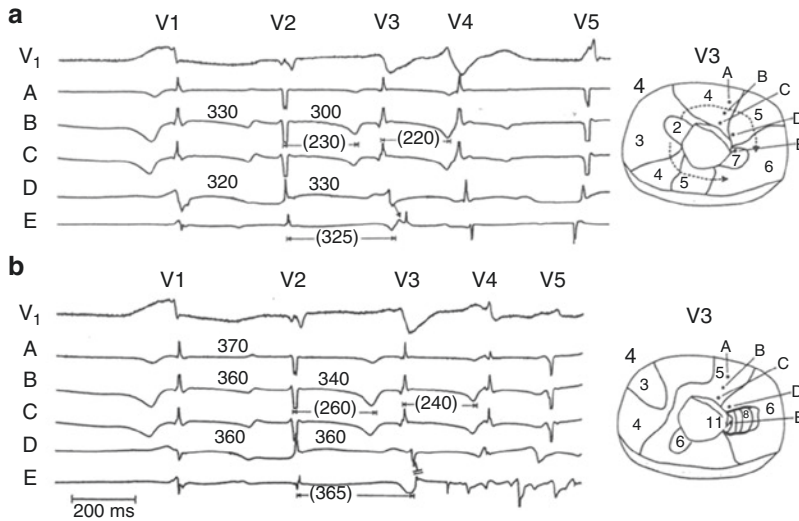


Fig. 11.7 Selected electrograms of the five-beat nonsustained VT shown in Fig. 11.6c (V1 to V5) and the first five beats of the VT that degenerated into ventricular fibrillation shown in Fig. 11.6d (V1 to V5). Also shown is a limited activation map of both V3 beats. The figure shows the electrophysiological mechanism of the different consequences of the same V3 ectopic beat in the two episodes. It shows that the inter-ectopic intervals V1-V2 and V2-V3 increased by approximately 30–40 msec in the second episode compared with the first episode (the equivalent of a slight slowing of the discharge of the focal activity). This resulted in lengthening of local repolarization fol-

lowing the V2 beat by 30–40 msec. However, the degree of lengthening of repolarization was disparate at contiguous sites, resulting in functional conduction block and the initiation of a more complex reentrant wavefront. One such site where new conduction block developed during the NST TdP is shown in the electrograms between sites D and E, as well as in the isochronal maps on the right side of the figure. The numbers without brackets represent cycle lengths in milliseconds, and the numbers in brackets represent activation-recovery intervals. (Reproduced from: El-Sherif [79]. Used with permission of John Wiley and Sons)

Future Directions

Although congenital LQTS continues to remain the domain of cardiologists, cardiac electrophysiologists, and specialized centers, the by far more frequent acquired drug-induced LQTS is the domain of all physicians and other members of the healthcare team who are required to make therapeutic decisions. To support better prescribing of medicines, clinical decision support systems to date have issued alerts that warn of potential harm from a prescribing decision [80]. However, the impact of these systems has been limited. Moving away from the use of alerts to signal prescribing errors, the concept of “medical autopilots” has been suggested as a preferred approach [81]. These programs will monitor the electronic medical record and send signals to guide prescribers toward decisions that result in maximum benefit and minimal risk of TdP.

References

1. Jervell A, Lange-Nielsen F. Congenital deaf-mutism, functional heart disease with prolongation of the QT interval and sudden death. *Am Heart J.* 1957;54:59–68.
2. El-Sherif N, Turitto G. The long QT syndrome and torsade de pointes. *Pacing Clin Electrophysiol.* 1999;22:91–110.
3. Kannankeril P, Roden DM, Darbar D. Drug-induced long QT syndrome. *Pharmacol Rev.* 2010;62:760–81.
4. El-Sherif N, Turitto G. Electrolyte disorders and arrhythmogenesis. *Cardiol J.* 2011;18:1–13.
5. Yang T, Chun YW, Stroud DM, Mosley JD, Knollman BC, Hong C, et al. Screening for acute IKr block is insufficient to detect torsade de pointes liability: role of late sodium current. *Circulation.* 2014;130:224–34.
6. El-Sherif N, Caref EB, Chinushi M, Restivo M. Mechanism of arrhythmogenicity of the short-long cardiac sequence that precedes ventricular tachyarrhythmias in the long QT syndrome. *J Am Coll Cardiol.* 1999;33:1415–23.
7. Dessertenne F. Ventricular tachycardia with two variable opposing foci. *Arch Mal Coeur Vaiss.* 1966;59:263–72.

8. Moss AJ, Long QT syndrome. In: Podrid PJ, Kowey PR, editors. *Cardiac arrhythmias. mechanisms, diagnosis, and management*. Baltimore: Williams & Wilkins; 1995. p. 1110–20.
9. Castillo R, Pedalino R, El-Sherif N, Turitto G. Efavirenz-associated QT prolongation and Torsade de Pointes arrhythmia. *Ann Pharmacother*. 2002;36:1006–8.
10. Verrier RL, Klungenheben T, Malik M, El-Sherif N, Exner DV, Hohnloser SH, et al. Microvolt T-wave alternans: physiological basis, methods of assessment, and clinical utility- consensus guideline by International Society of Holter and Noninvasive Electrocardiology. *J Am Coll Cardiol*. 2011;58:1309–24.
11. Takasugi N, Goto H, Takasugi M, Verrier RL, Kuwahara T, Kubota T, et al. Prevalence of microvolt T-wave alternans in patients with long QT syndrome and its association with torsade de pointes. *Circ Arrhythm Electrophysiol*. 2016;9:e003206.
12. Chinushi M, Restivo M, Caref EB, El-Sherif N. Electrophysiological basis of the arrhythmogenicity of QT/T alternans in the long QT syndrome: Tridimensional analysis of the kinetics of cardiac repolarization. *Circ Res*. 1998;83:614–28.
13. Milberg P, Ramtin S, Monnig G, Osada N, Wasmer K, Breithardt G, et al. Comparison of the in vitro electrophysiologic and proarrhythmic effects of amiodarone and sotalol in a rabbit model of acute atrioventricular block. *J Cardiovasc Pharmacol*. 2004;44:278–86.
14. Hondenghem LM, Carlsson L, Duker G. Instability and triangulation of the action potential predict serious proarrhythmia, but action potential duration prolongation is antiarrhythmic. *Circulation*. 2001;103:2004–13.
15. Said TH, Lance DW, Jeyaraj D, Fossa AA, Rosenbaum DS. Transmural dispersion of repolarization as a pre-clinical marker of drug-induced proarrhythmia. *J Cardiovasc Pharmacol*. 2012;60:165–71.
16. Nattel S, Antzelevich C, Noble D. Resolving the M-cell debate: why and how. *Heart Rhythm*. 2011;8:1293–5.
17. Cho MS, Nam GB, Kim YG, Hwang KW, Kim YR, Choi H, et al. Electrocardiographic predictors of bradycardia-induced torsades de pointes in patients with acquired atrioventricular block. *Heart Rhythm*. 2015;12:498–505.
18. Lazzzerini PE, Capecchi PL, Laghi-Pasini F. Long QT syndrome: an emerging role for inflammation and immunity. *Front Cardiovasc Med*. 2015;2:1–17.
19. Boutjdir M, Lazzzerini PE, Capecchi PL, Capecchi PL, Laghi-Pasini F, El-Sherif N. Potassium channel block and novel autoimmune-associated long QT syndrome. *Card Electrophysiol Clin*. 2016;8:373–84.
20. Lazzzerini PE, Yue Y, Srivastava U, Fabris F, Capecchi PL, Bertolozzi I, et al. Arrhythmogenicity of anti Ro/SSA antibodies in patients with torsade de pointes. *Circ Arrhythm Electrophysiol*. 2016;9:e003419.
21. Yue Y, Castrichini M, Srivastava U, Fabris F, Shah K, Li Z, et al. Pathogenesis of the novel autoimmune-associated long-QT syndrome. *Circulation*. 2015;132:230–40.
22. Mahida S, Hogarth AJ, Cowan C, Tayebjee MH, Graham LN, Pepper CB. Genetics of congenital and drug-induced long QT syndromes: current evidence and future research perspectives. *J Interv Card Electrophysiol*. 2013;37:9–19.
23. Hong Y, Rautaharju PM, Hopkins PN, Arnett DK, Djousse L, Pankow JS, et al. Familial aggregation of QT-interval variability in a general population: results from the NHLBI Family Heart Study. *Clin Genet*. 2001;59:171–7.
24. Newton-Cheh C, Larson MG, Corey DC, Benjamin EJ, Herbert AG, Levy D, et al. QT interval is a heritable quantitative trait with evidence of linkage to chromosome 3 in a genome-wide linkage analysis: the Framingham Heart Study. *Heart Rhythm*. 2005;2:277–84.
25. Kannankeril PJ, Roden DM, Norris KJ, Whalen SP, George AL Jr, Murray KT, et al. Genetic susceptibility to acquired long QT syndrome: pharmacologic challenge in first-degree relatives. *Heart Rhythm*. 2005;2:134–40.
26. Pfeufer A, Sanna S, Arking DE, Müller M, Gateva V, Fuchsberger C, et al. Common variants at ten loci modulate the QT interval duration in the QTSCD Study. *Nat Genet*. 2009;41:407–14.
27. Jamshidi Y, Nolte IM, Dalageorgou C, Zheng D, Johnson T, Bastiaenen R, et al. Common variation in the NOS1AP gene is associated with drug-induced QT prolongation and ventricular arrhythmia. *J Am Coll Cardiol*. 2012;60:841–50.
28. Kapoor A, Sekar RB, Hansen NF, Fox-Talbot K, Morley M, Pihur V, et al. An enhancer polymorphism at the cardiomyocyte intercalated disc protein NOS1AP locus is a major regulator of the QT interval. *Am J Hum Genet*. 2014;94:854–69.
29. Niemeijer MN, van den Berg ME, Eijgelsheim M, Rijnbeek PR, Stricker BH. Pharmacogenetics of drug-induced QT interval prolongation: an update. *Drug Saf*. 2015;38:855–67.
30. Ito H, Crotti L, Aiba T, Spazzolini C, Denjoy I, Fressart V, et al. The genetics underlying acquired long QT syndrome: impact for genetic screening. *Eur Heart J*. 2016;37:1456–64.
31. Molokhia M, Pathak A, Lapeyre-Mestre M, Caturla L, Montastruc JL, McKeigue P. Case ascertainment and estimated incidence of drug-induced long-QT syndrome: study in Southwest France. *Br J Clin Pharmacol*. 2008;66:386–95.
32. Sarganas G, Garbe E, Klümpe A, Hering RC, Bronder E, Haverkamp W. Epidemiology of symptomatic drug-induced long QT syndrome and Torsade de pointes in Germany. *Europace*. 2014;16:101–8.
33. Ninan B, Wertheimer A. Withdrawing drugs in the US versus other countries. *Innov Pharm*. 2012;3:1–12.
34. Shah RR. Drugs, QTc interval prolongation and final ICH E14 guideline: an important milestone with challenges ahead. *Drug Saf*. 2005;28:1009–28.

35. Woosley RL, Romero K. Assessing cardiovascular drug safety for clinical decision-making. *Nat Rev Cardiol.* 2013;13:330–7.
36. Barra S, Agarwal S, Begley D, Providência R. Post-acute management of the acquired long QT syndrome. *Postgrad Med J.* 2014;90:348–58.
37. Florian JA, Tornøe CW, Brundage R, Parekh A, Garnett CE. Population pharmacokinetics and concentration - QTc models for moxifloxacin: pooled analysis of 20 thorough QT studies. *J Clin Pharmacol.* 2011;51:1152–62.
38. Ackerman MJ, Splawski I, Makielski JC, Tester DJ, Will ML, Timothy KW, et al. Spectrum and prevalence of cardiac sodium channel variants among Black, White, Asian, and Hispanic individuals: implications for arrhythmogenic susceptibility and Brugada/long QT syndrome genetic testing. *Heart Rhythm.* 2004;1:600–7.
39. Manini AF, Stimmel B, Vlahov D. Racial susceptibility for QT prolongation in acute drug overdoses. *J Electrocardiol.* 2014;47:244–50.
40. Sauer AJ, Moss AJ, McNitt S, et al. Long QT syndrome in adults. *J Am Coll Cardiol.* 2007;49:329–37.
41. Conrath CE, Wilde AA, Jongbloed RJ, Alders M, Van Langen IM, Van Tiltelen JP, et al. Gender difference in the long QT syndrome: effects of beta-adrenoreceptor blockade. *Cardiovasc Res.* 2002;53:770–6.
42. Buber J, Mathew J, Moss AJ, et al. Risk of recurrent cardiac events after onset of menopause in women with congenital Long QT syndrome type 1 and 2. *Circulation.* 2011;123:2784–91.
43. Drici MD, Clement N. Is gender a risk factor for adverse drug reactions? The example of drug induced long QT syndrome. *Drug Saf.* 2001;24:575–85.
44. Coker SJ. Drugs for men and women-how important is gender as risk factor for TdP? *Pharmacol Ther.* 2009;119:186–94.
45. Roden DM. Drug-induced prolongation of the QT interval. *N Engl J Med.* 2004;350:1013–22.
46. Slama G, Bett GCL. Sex differences in the mechanism underlying long QT syndrome. *Am J Physiol Heart Circ Physiol.* 2014;307:H640–8.
47. Odening KE, Koren G. How do sex hormones modify arrhythmogenesis in long QT syndrome? Sex hormones effects on arrhythmogenic substrate and trigger activity. *Heart Rhythm.* 2014;11:2107–15.
48. El-Sherif N, Himel HG, Yue Y, Boutjdir M, Restivo M. Electrophysiological substrates for gender difference in the incidence of Torsade de Pointes Arrhythmias. In: Shenasa M, Hindricks G, Borggreffe M, Breithardt G, editors. *Cardiac mapping.* 5th ed: Elsevier; 2018.. In press.
49. Zipes DP, Camm AJ, Borggreffe M, Buxton AE, Chaitman B, Fromer M, et al. ACC/AHA/ESC guidelines for management of patients with ventricular arrhythmias and the prevention of sudden cardiac death: a report of the American College of Cardiology/American Heart Association Task Force and the European Society of Cardiology Committee for practice guidelines (writing committee to develop guidelines for Management of Patients with ventricular arrhythmias and the prevention of sudden cardiac death) developed in collaboration with the European Heart Rhythm Association and the Heart Rhythm Society. *Circulation.* 2006;114:e385–484.
50. Drew BJ, Ackerman MJ, Funk M, Gibler WB, Kligfield P, Menon V, et al. Prevention of torsade de pointes in hospital setting: a scientific statement from the American Heart Association and the American College of Cardiology Foundation. *Circulation.* 2010;121:1047–60.
51. Kaye P, O'Sullivan I. Role of magnesium in the emergency department. *Emerg Med J.* 2002;19:288–91.
52. Diness T, Yeh YH, Qi XY, Chartier D, Tsuji Y, Hansen RS, et al. Antiarrhythmic properties of rapid delayed-rectifier current activator in rabbit models of acquired long QT syndrome. *Cardiovasc Res.* 2008;79:61–9.
53. Testai L, Cecchetti V, Sabatini S, Martelli A, Breschi MC, Calderone V. Effects of K openers on the QT prolongation induced by HERG-blocking drugs in Guinea-pigs. *J Pharmacol.* 2010;62:924–30.
54. Priori SG, Wilde AA, Horie M, Cho Y, Behr ER, Berul C, et al. Executive summary: HRS/ EHRA/ APhRS expert consensus statement on the diagnosis and management of patients with inherited primary arrhythmia syndromes. *Europace.* 2013;15:1389–406.
55. Lang CN, Koren G, Odening KE. Transgenic rabbit models to investigate the cardiac ion channel disease long QT syndrome. *Prog Biophys Mol Biol.* 2016;21:142–56.
56. Vos MA, de Groot SH, Verduyn SC, van der Zande J, Leunissen HD, Cleutjens JP, et al. Enhanced susceptibility for acquired torsade de pointes arrhythmias in the dog with chronic complete av block is related to cardiac hypertrophy and electrical remodeling. *Circulation.* 1998;98:1125–35.
57. Kozhevnikov DO, Yamamoto K, Robotis D, Restive M, El-Sherif N. Electrophysiological mechanisms of enhanced susceptibility of hypertrophied heart to acquired torsade de pointes arrhythmias: tri-dimensional mapping of activation and recovery. *Circulation.* 2002;105:1128–34.
58. El-Sherif N, Zeiler RH, Craelius W, Gough WB, Henkin R. QTc prolongation and polymorphic ventricular tachyarrhythmias due to bradycardia-dependent early after depolarizations. *Circ Res.* 1988;63:286–305.
59. El-Sherif N, Fozzard HA, Hanck DA. Dose-dependent modulation of the cardiac sodium channel by the sea anemone toxin ATXII. *Circ Res.* 1992;70:285–301.
60. Bennett PB, Yazawa K, Makita N, George AL Jr. Molecular mechanism for an inherited cardiac arrhythmia. *Nature.* 1995;37:683–5.
61. Wang O, Shen J, Splawski I, Atkinson D, Li Z, Robinson JL, et al. SCN5A mutations associated with an inherited cardiac arrhythmia, long QT syndrome. *Cell.* 1995;80:805–11.
62. El-Sherif N, Boutjdir M. Role of pharmacotherapy in cardiac ion channelopathy. *Pharmacol Ther.* 2015;155:132–42.

63. El-Sherif N, Caref EB, Yin H, Restivo M. The electrophysiological mechanism of ventricular tachyarrhythmias in the long QT syndrome. Tridimensional mapping of activation and recovery patterns. *Circ Res.* 1996;79:474–92.
64. El-Sherif N, Chinushi M, Caref EB, Restivo M. Electrophysiological mechanism of the characteristic electrocardiographic morphology of torsade de pointes tachyarrhythmias in the long-QT syndrome. Detailed analysis of ventricular tridimensional activation patterns. *Circulation.* 1997;96:4392–9.
65. Schreiner KD, Voss F, Senges JC, Becker R, Kraft P, Bauer A, et al. Tridimensional activation patterns of acquired torsade de pointes tachycardia on dogs with chronic AV block. *Basic Res Cardiol.* 2004;99:1128–34.
66. Caref EB, Boutjdir M, Himel HD, El-Sherif N. Role of subendocardial Purkinje network in triggering torsade de pointes arrhythmias in experimental long QT syndrome. *Europace.* 2008;10:1218–23.
67. Spido KR, Varro A, Eisner D. Sodium calcium exchange as a target for antiarrhythmic therapy. *Handb Exp Pharmacol.* 2006;171:159–99.
68. Pogwizd SM, Bers DM. Cellular basis of triggered arrhythmias in heart failure. *Trends Cardiovasc Med.* 2004;14:61–6.
69. Milberg P, Pott C, Fink M, Frommeyer G, Matsuda T, Baba A, et al. Inhibition of the Na⁺/Ca²⁺ exchanger suppresses torsade de pointes in an intact heart model of long QT syndrome-2 and long QT syndrome-3. *Heart Rhythm.* 2008;5:1444–52.
70. Vandersickel N, de Boer TP, Vos MA, Panfilov AV. Perpetuation of torsade de pointes in heterogeneous hearts: competing foci or re-entry. *J Physiol.* 2016;594:6865–78.
71. Vandersickel N, Bossu A, De Neve J, Dunnik A, Meijborg VMF, Van der Heyden MAG, et al. Short-lasting episodes of torsade de pointes in the chronic atrioventricular block dog model have focal mechanism, while longer-lasting episodes are maintained by re-entry. *JACC Clin Electrophysiol.* 2017;3:1565–76.
72. Gray RA, Jalife J, Panfilov A. Non stationary vortex-like reentrant activity as a mechanism of polymorphic ventricular tachycardia in the isolated rabbit heart. *Circulation.* 1995;91:2454–69.
73. Winfree AT. Mechanism of cardiac fibrillation,---reply. *Science.* 1995;270:1225.
74. Nayyar S, Porta-Sanchez A, Nanthakumar K. Twisting and turning to find an explanation for torsade de pointes. *JACC Clin Electrophysiol.* 2017;3:1577–9.
75. Walton RD, Martinez ME, Bishop MJ, Hocini M, Haissaguerre M, Plank G, et al. Influence of the Purkinje-muscle junction on transmural repolarization heterogeneity. *Cardiovasc Res.* 2014;103:629–40.
76. Sicouri S, Antzelevitch C. Electrophysiologic characteristics of M cells in the canine left ventricular free wall. *J Cardiovasc Electrophysiol.* 1995;6:591–603.
77. Sato D, Xie L-H, Sovari AA, Tran DX, Morita N, Xie F, et al. Synchronization of chaotic early afterdepolarizations in the genesis of cardiac arrhythmias. *Proc Natl Acad Sci.* 2009;106:2983–8.
78. Hoffman BF, Rosen MR. Cellular mechanisms for cardiac arrhythmias. *Circ Res.* 1981;49:1–15.
79. El-Sherif N. Mechanism of ventricular arrhythmias in the long QT syndrome: on hermeneutics. *J Cardiovasc Electrophysiol.* 2001;12:973–6.
80. Payne TH, Hines LE, Chan RC, Hartman S, Kapusnik-Uner J, Russ AL, et al. Recommendations to improve the usability of drug-drug interaction clinical decision support alerts. *J Am Med Inform Assoc.* 2015;22:1243–50.
81. Woosley RL, Whyte J, Mohamadi A, Romero K. Medical decision support systems and therapeutics: the role of autopilots. *Clin Pharmacol Ther.* 2016;99:161–4.



Pathogenesis of Autoimmune-Associated Long QT Syndrome

Mohamed Boutjdir, Pietro Enea Lazzarini,
Pier Leopoldo Capecchi, Franco Laghi-Pasini,
and Nabil El-Sherif

Long QT Syndrome

Long QT syndrome (LQTS) manifests as prolongation of the QT interval on the surface electrocardiogram (ECG), predisposing to life-threatening ventricular arrhythmias particularly torsades de pointes (TdP) [1–4]. The QT interval in the ECG is a surrogate measure of the average duration of the ventricular action potential. Whenever a channel dysfunction induces an increase in the inward Na^+ or Ca^{++} currents and/or a decrease in an outward K^+ current resulting in an inward shift in the balance of net current, the action potential duration prolongs and hence the QT interval. LQTS can be congenital and caused by mutations in ion channel or associated protein-coding genes, or acquired often drug-induced [1, 2]. In most cases of drug-induced QT prolon-

gation, the target ion channel, is the hERG (human Ether-à-go-Related Gene) encoding the pore-forming subunits ($\text{Kv}11.1$) of the rapidly activating delayed K^+ channel conducting I_{Kr} [5]. I_{Kr} plays a major role during repolarization of the cardiac action potential and its reduction by drugs or genetic defects causes delayed repolarization and prolongation of the QT interval [1, 2, 6]. Regardless of the specific ion channel dysfunction involved, the prolongation of action potential duration leads to an increased susceptibility to develop oscillations at the plateau level (early afterdepolarizations). When they reach the threshold for activation of the inward Ca^{++} current in the presence of a vulnerable window created by differences in action potential duration lengthening across the ventricular wall (transmural dispersion of depolarization), a triggered ectopic activity is generated that can induce reentrant arrhythmias, particularly TdP. Although frequently terminating spontaneously, TdP can degenerate into ventricular fibrillation and sudden cardiac death [1, 2].

M. Boutjdir (✉)

Department of Medicine and Physiology, SUNY Downstate Medical Center, Brooklyn, NY, USA

State University of New York Downstate Medical Center, New York, NY, USA

NYU School of Medicine, New York, NY, USA

P. E. Lazzarini · P. L. Capecchi · F. Laghi-Pasini
Department of Medical Sciences, Surgery and Neurosciences, University of Siena, Siena, Italy

N. El-Sherif

Department of Medicine and Physiology, State University of New York Downstate Medical Center, VA New York Harbor Healthcare Center, Brooklyn, NY, USA

Anti-Ro/SS Autoantibody System and Autoimmunity

Ro/SSA antigens are intracellular proteins that associate with small cytoplasmic RNAs and form Ro-ribonucleoprotein (Ro-RNP) complex [7, 8]. Ro/SSA antigens consist of two different proteins, Ro52kD/SSA and Ro60kD/SSA. While the Ro60 kD/SSA autoantigen is a ring-shaped RNA-binding

Table 12.1 Prevalence of anti-Ro SSA antibodies in different autoimmune diseases and general population [26–28]

Status	Anti-Ro/SSA antibodies (%)
Sjögren's syndrome (SS)	70
Systemic lupus erythematosus (SLE)	24–60
Scleroderma	35.6
Rheumatoid arthritis (RA)	3–5
Systemic sclerosis (SSc)	3–11
Myositis	5–15
General asymptomatic population	2–3

protein [9], Ro52kD/SSA functions as an E3 ubiquitin ligase [10] and is involved in the ubiquitination of interferon regulatory factor 3 and IRF7 post toll-like receptor stimulation, suggesting an avenue for the immune system to protect the host from prolonged immune system activation [11, 12]. It is not clear why the self-body generates autoantibodies against these endogenous antigens in the first place but nevertheless, the corresponding autoantibodies are important clinical markers for several autoimmune diseases (Table 12.1). Specifically, anti-Ro52kD/SSA antibody is emerging as a unique antibody with direct pathogenic disease involvement and distinct clinical properties [13]. As such, anti-Ro52kD/SSA antibodies are being associated with clinical and laboratory markers of disease [13].

Long-QT Syndrome and Autoimmunity

In the recent years, accumulating evidence indicates that autoimmune mechanisms are involved in the pathogenesis of cardiac arrhythmias [14, 15]. Indeed, a number of autoantibodies are able to interfere with the electrical properties of the heart by directly targeting specific molecules expressed on the cardiomyocyte surface, including β -adrenergic and muscarinic receptors, Na/K-ATPase, and ion channels [14–19]. The term “autoimmune cardiac channelopathies” was recently proposed to define a novel pathogenic mechanism for cardiac arrhythmias in patients with autoimmune disease as well as in apparently healthy subjects with idiopathic rhythm disturbances to account for a number of unexplained, molecular autopsy-negative sud-

den cardiac deaths (SCDs) [15]. In this regard, an acquired autoimmune-associated LQTS has been reported in patients with autoimmune diseases carrying pathogenic autoantibodies, namely, anti-Ro/SSA antibodies [20–25]. These anti-Ro/SSA antibodies are prevalent in several autoimmune diseases such as Sjögren's syndrome, systemic lupus erythematosus, scleroderma, rheumatoid arthritis, systemic sclerosis, and myositis and also in the general otherwise healthy population (Table 12.1) [26–28]. As such, autoimmunity is emerging as a novel mechanism of cardiac arrhythmias, not only in patients with autoimmune diseases but also in healthy subjects [14, 15, 29]. Different types of arrhythmogenic autoantibodies have been identified and affect cardiac ion channels by directly targeting the corresponding proteins at the myocyte surface [14, 29]. In particular, some of these autoantibodies can significantly interfere with the function of specific ion channels critically involved in determining ventricular action potential duration (*autoimmune cardiac channelopathies*), thus leading to a new acquired forms of LQTS of autoimmune origin [15]. Autoimmune cardiac channelopathies are mediated by circulating autoantibodies directly interacting with different cardiac ion channels: based on the specific channel type involved, three main groups of autoimmune cardiac channelopathies are currently recognized, i.e., Ca^{++} , K^{+-} , and Na^{++} -channelopathies [15]. To date, the most investigated autoimmune cardiac channelopathy associated with LQTS is related to the presence of anti-Ro/SSA antibodies cross-reacting with the hERG- K^+ channel [30, 31], hence to focus in this book chapter. Other autoantibodies recognizing Ca^{++} channels, other K^+ channels, and receptors have been recently reviewed elsewhere [15].

Autoimmune Potassium Channelopathies Associated with LQTS

Several pro-arrhythmic anti- K^+ channel autoantibodies have been identified in patients with manifest autoimmune diseases or in otherwise healthy subjects [15]. By targeting specific K , α -subunits

such as $K_v11.1/hERG$ [23, 31, 32] and $K_v1.4$ [33–35], these autoantibodies exert different electrophysiological effects resulting in LQTS.

Autoantibodies Against $K_v1.4$ Channel

Although less investigated, LQTS-inducing autoimmune channelopathy is related to anti- $K_v1.4$ - K^+ channel antibodies, detected in ~10–20% of myasthenia gravis patients [33–35]. Anti- $K_v1.4$ -positive subjects frequently showed QTc prolongation and significant mortality for lethal QT-associated arrhythmias [33–35]. Even though pathogenesis studies are currently not available, LQTS may likely result from an autoantibody inhibition of the $K_v1.4$ -related current, the slow transient outward current, I_{os} , leading to prolongation of the ventricular repolarization.

Anti-Ro/SSA Autoantibodies Against $K_v11.1-hERG$ Channel

Unlike anti- $K_v1.4$ autoantibodies, the functional and molecular mechanisms of autoantibodies (anti-Ro/SSA antibodies) targeting the $hERG-K^+$ channel have been well characterized [23, 31, 32, 36] and proposed as a novel form of acquired LQTS [15]. The arrhythmogenicity of anti-Ro/SSA antibodies, including the anti-Ro52kD/SSA and anti-Ro60kD/SS subtypes, is well established from many years, specifically in the pathogenesis of autoimmune-associated congenital heart block [37–40]. More recently, patients with autoimmune connective tissue diseases tested positive for anti-Ro/SSA antibodies, commonly show QTc prolongation correlating with autoantibody levels (particularly anti-Ro52kD/SSA) and with complex ventricular arrhythmia [21, 22, 25]. In addition to patients with connective tissue

diseases, anti-Ro/SSA antibodies have been also associated with QTc prolongation and TdP occurrence in the general population, in most cases independent of the presence of a concomitant autoimmune diseases [23]. Below, we present and discuss the functional and molecular basis of anti-Ro/SSA-associated LQTS.

Functional and Molecular Basis of Autoimmune-Associated LQTS

An increasing body of experimental data points to $hERG-K^+$ channel as the molecular target responsible for anti-Ro/SSA-associated LQTS [23, 31, 32, 36].

In Vivo Experiments Addressing Reproducibility of the Clinical LQTS Phenotype

To demonstrate the pathogenic role of anti-Ro/SSA antibodies in the development of QTc prolongation in the absence of other confounding risk factors usually present in patients with autoimmune diseases, healthy guinea pigs were actively immunized with Ro/SSA antigen [31]. ECGs were measured and anti-Ro/SSA antibody titers were quantified by enzyme-linked immunosorbent assay (ELISA) at regular intervals to insure proper immune response (Table 12.2). Indeed, QT interval and corrected QT (QTc) were significantly prolonged in immunized guinea pigs compared to nonimmunized guinea pigs (Fig. 12.1a, b) without any measurable changes in heart rate, PR interval, and QRS duration (Table 12.2). The observed QTc prolongation was explained by anti-Ro/SSA antibodies' lengthening of guinea pig ventricular action potential (Fig. 12.2c) resulting from the inhibition of the native I_{Kr} (Fig. 12.2d) as well as I_{Kr}

Table 12.2 Anti-Ro/SSA antibodies Levels and ECG parameters before and after immunization

	Anti-Ro/SSA antibodies range (OD)	QTc (ms)	Heart rate	PR interval (ms)	QRS duration (ms)	Anti-Ro Antibody Range (OD)
Baseline	0.02–0.04	248.3 ± 30	294.4 ± 12	50.5 ± 2.9	19.1 ± 1.0	0.02–0.04
Immunized	1.14–2.16*	272.5 ± 23*	280.2 ± 42	56.5 ± 1.4	19.2 ± 2.0	1.4–2.16*

OD indicates optical density and * $P < 0.05$

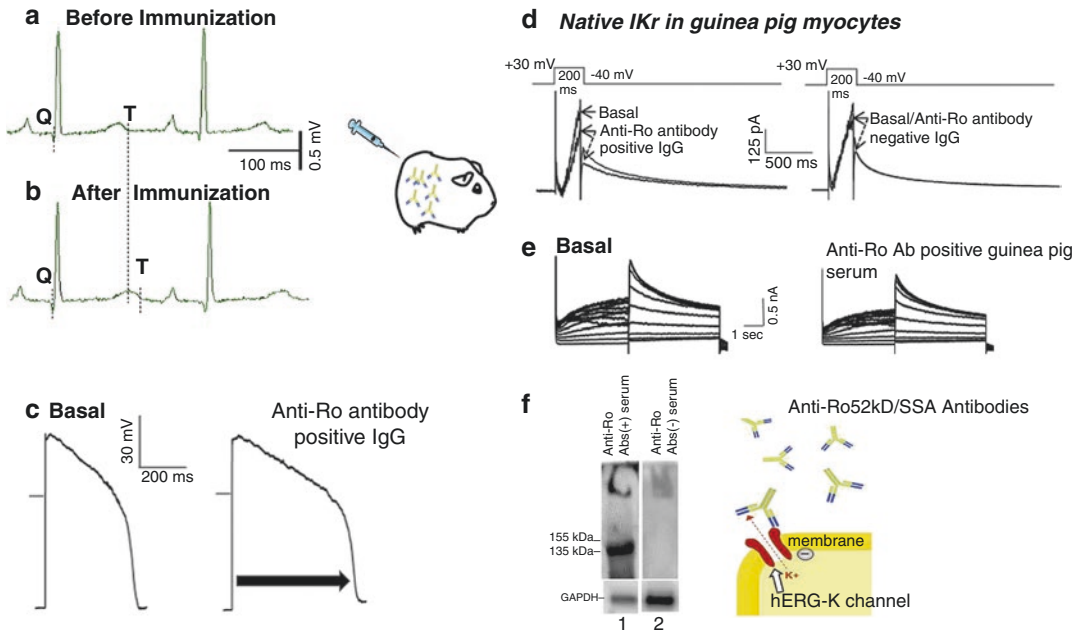


Fig. 12.1 Immunization of guinea pigs with Ro52kD/SSA antigen causes delay in repolarization, prolongation of action potential, and inhibition of hERG-K⁺ channel. Representative ECGs from a guinea pig (a) before immunization and (b) after immunization with Ro52kD/SSA antigen. Vertical dashed lines indicate QT interval. (c) Effects of anti-Ro/SSA antibody-positive IgG from serum of a patient with connective tissue disease and QTc prolongation on action potential duration and (d) on I_{Kr} current recorded from guinea pig ventricular myocytes. (e)

Representative I_{Kr} tracings from HEK293 cells stably expressing the hERG channel, at basal (left) and after the application of anti-Ro/SSA antibody-positive serum from an immunized guinea pig (right). (f) Western blot of guinea pig ventricles probed with anti-Ro/SSA antibody-positive (lane 1) and anti-Ro/SSA antibody-negative (lane 2) guinea pig sera. A schematic representation of direct anti-Ro/SSA antibody block of hERG-K⁺ channel is shown on the right of panel F. (Based on data from Yue et al. [31])

recorded from HEK293 cells stably expressing the hERG channel (Fig. 12.2e). This inhibition occurred likely by direct binding of anti-Ro/SSA antibodies from immunized guinea pig sera with guinea pig ERG channel proteins (Fig. 12.2f, left panel) as proposed in the schematic of Fig. 12.2f, right panel. Collectively, these findings are consistent and support the clinical observation that the sole presence of anti-Ro/SSA antibodies is associated with QTc prolongation and constitute a nonconventional risk factor for the development of ventricular arrhythmias such as TdP [23, 32].

In Vitro Experiments Demonstrating the Pathogenesis of anti-Ro/SSA Antibodies

To directly address whether the actual anti-Ro/SSA antibodies from patients with autoim-

mune diseases are pathogenic, sera, purified IgG, and affinity purified, anti-Ro/SSA antibodies from patients with connective tissue disease with a documented long QTc, were tested on I_{Kr} recorded from HEK293 cells stably expressing hERG channel. Indeed, not only sera and purified IgG but also affinity purified IgG containing anti-Ro/SSA antibodies from these patients inhibited I_{Kr} in a time- and dose-dependent manner without affecting the I_{Kr} kinetics suggesting a direct channel block (Fig. 12.2a–h). This premise is further supported by the Western blot data, demonstrating the direct interaction of these anti-Ro/SSA antibodies from connective tissue disease patients with the hERG channel proteins by Western blots (Fig. 12.2i). Similar findings were first reported by Nakamura et al. [32], demonstrating that anti-Ro/SSA antibodies from serum and purified IgG of a female patient

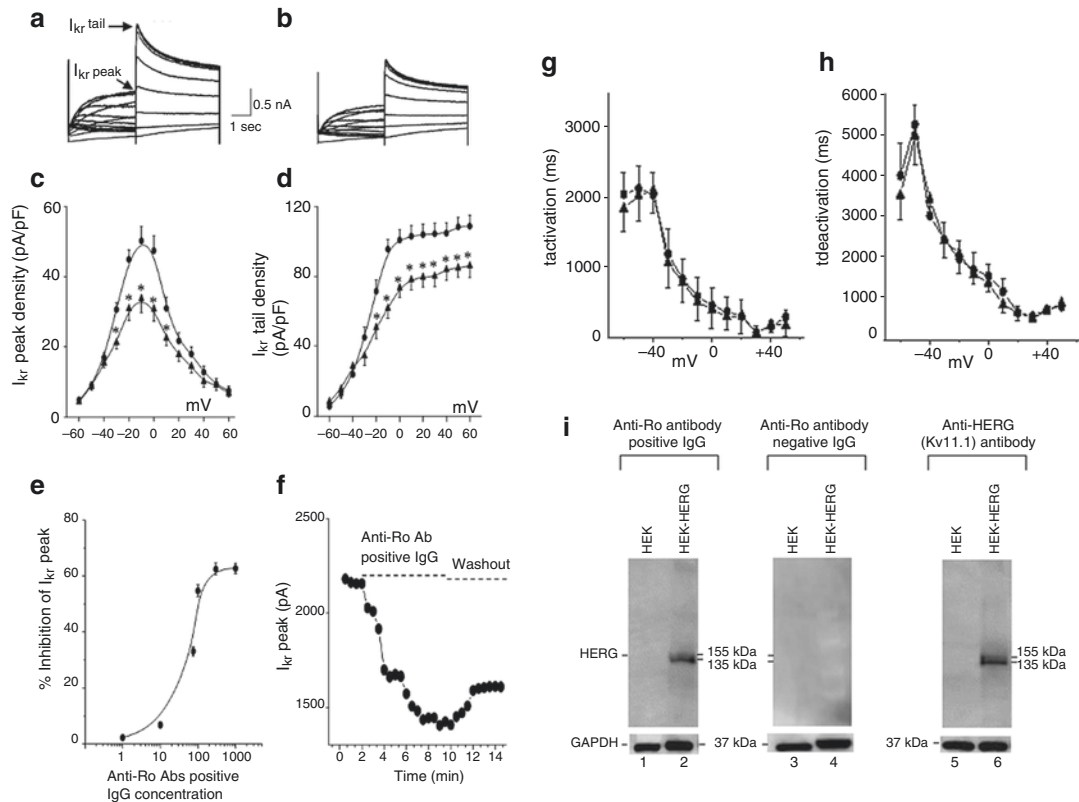


Fig. 12.2 Electrophysiologic and biochemical effects of anti-Ro/SSA antibodies on hERG- K^+ channel. Representative currents (I_{Kr}) were recorded from HEK293 cells stably expressing hERG channels under basal (a) conditions and (b) in the presence of 75 $\mu\text{g/ml}$ anti-Ro/SSA antibody-positive IgG from a patient with connective tissue disease and QTc prolongation. I-V relationships of I_{Kr} peak (c) and tail (d) current densities during basal (circles) and anti-Ro/SSA antibody-positive IgG application (triangles). (e) Dose-response curve of anti-Ro/SSA antibody-positive IgG resulted in an $\text{EC}_{50} = 87.3 \mu\text{g/ml}$. (f) Time course of anti-Ro/SSA antibody-positive IgG (75 $\mu\text{g/ml}$) on I_{Kr} peak. The dashed lines indicate the time of IgG application and washout, as indicated. The Boltzmann fit of I_{Kr} activation (g) and deactivation (h) before (circle) and after anti-Ro/SSA antibody-positive IgG application (triangle). (i) Proteins from un-transfected

(lane 1) and transfected HEK293 cells with hERG channels (lane 2) were probed with anti-Ro/SSA antibody-positive IgG from a patient with connective tissue disease and QTc prolongation and QTC prolongation. Bands at 155 kD and 135 kD correspond to glycosylated and endoplasmic reticulum-retained hERG channels in lane 2. Proteins from un-transfected (lane 3) and transfected HEK293 cells with hERG channels (lane 4) where probed with anti-Ro/SSA antibody-negative IgG from a control patient with connective tissue disease but normal QTc. Proteins from un-transfected (lane 5) and transfected HEK293 cells with hERG channels (lane 6) were probed with a commercial anti-hERG channel antibodies. Bands at 155 kD and 135 kD were seen in lane 6 only as in lane 2 with anti-Ro/SSA antibody-positive IgG. The 37 kD band represents GAPDH. (*) indicates statistical significance at $p < 0.05$. (Based on data from Yue et al. [31])

whose QTc was excessively prolonged (700 ms) with episodes of TdP, functionally inhibited and biochemically interacted with the hERG channel proteins in a dose-dependent manner. However, these effects were observed only when HEK293 cells in culture were incubated with anti-Ro/SSA antibodies for 1–5 days but no acute effects (5 min) were observed. It is possible that longer period of time than the 5 min exposure, is necessary to

see an acute effect as reported above. Nevertheless, both studies agree that anti-Ro/SSA antibodies are pathogenic.

In Silico Experiments Demonstrating Epitope Mimics on hERG Channel

As mentioned earlier, the native target of anti-Ro/SSA antibodies is SSA/Ro antigen, which is

intracellularly located and as thus not accessible to the circulating antibodies in the normal myocyte (Fig. 12.3a). As such it seems reasonable to hypothesize that anti-Ro/SSA antibodies must then recognize an epitope mimic on the extracellular side of the hERG channel which shares homology with Ro52kD/SSA antigen. To test this hypothesis linear homology analysis revealed 44% homology between Ro52kD/SSA antigen (aa302-aa321) and the hERG $\alpha 1$ subunit

(aa574-aa598) at the pore region of which 25% are identical (Fig. 12.3b) [31]. The presence of this homology at the pore region may be sufficient for anti-Ro52kD/SSA antibodies' binding to the hERG channel at this epitope mimic, especially in the tetrameric conformation of the channel where the four pore extracellular loops come together and are accessible to the antibodies (Fig. 12.3c). To test this, a 31 aa peptide (hERG E-pore peptide) corresponding to a pore

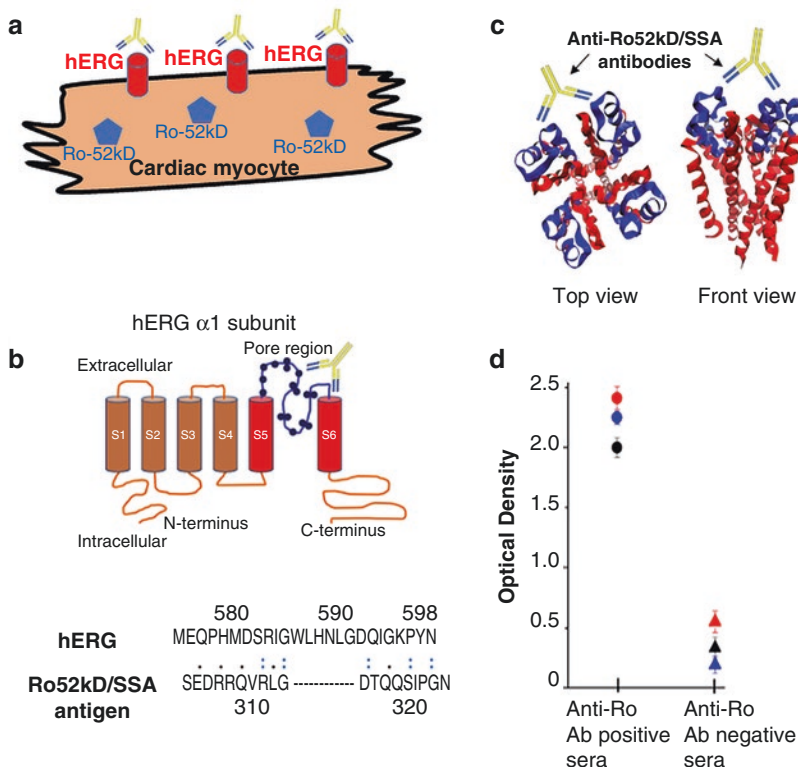


Fig. 12.3 Secondary and tetrameric structure of hERG- K^+ channel pore region and reactivity of the corresponding peptide to sera from patients with connective tissue diseases. (a) Cartoon depiction of a cardiac myocyte showing the inaccessible intracellularly located Ro/SSA antigen and the accessible hERG- K^+ channels to anti-Ro/SSA antibodies. (b) The upper panel is a schematic representation of the secondary structure of a single hERG channel $\alpha 1$ subunit. The six segments (S1–S6) are shown, along with the intracellularly located N and C termini. The pore-forming extracellular loop is located between S5 and S6, where single and double circles illustrate similar and identical amino acids (aa) between

the 52-kDa Ro (52Ro) protein and hERG channel, respectively. The lower panel shows the linear homology analysis between the Ro52kD/SSA protein and hERG channel at the pore region. (c) Tetrameric structure of the hERG channel model at the pore region based on KcsA crystal structure. Left, top view, and (right) front view of the pore region. Red represents segment S5/S6 helices, and blue indicates the predicted anti-Ro/SSA antibody binding sites in the extracellular loop between S5/S6 sites based on the homology shown in (b). (d) Reactivity of connective tissue disease patient's sera to the peptide corresponding to the pore-forming region of hERG. (Based on data from Yue et al. [31])

tion of the hERG extracellular loop at the pore region between S5 and S6 was designed, synthesized, and tested against sera from anti-Ro/SSA antibody-positive and anti-Ro/SSA antibody-negative connective tissue disease patients. Significant reactivity to the peptide was observed in only anti-Ro/SSA antibody-positive patient's sera [31], thus implicating this pore region as a potential binding epitope for the autoantibodies. Further support of this view are data from guinea pig immunization with this hERG E-pore peptide (but not with a scrambled peptide) demonstrating significant QTc prolongation correlating with the antibody titers [36]. Sera from hERG E-pore peptide-immunized animals inhibited I_{Kr} and prolonged action potential, without any evidence of structural heart modifications [36].

Anti-Ro/SSA-Positive Sera from Patients with Connective Tissue Diseases or TdP Shows High Reactivity to the hERG E-pore Peptide

If the hERG E-pore region is the target of anti-Ro/SSA antibodies, then reactivity with patients' sera containing these autoantibodies is expected. In this regard, serum samples from patients with connective tissue diseases, anti-Ro/SSA positive, and with documented QTc prolongation [20, 22] demonstrate high reactivity to the hERG E-pore peptide [36]. No reactivity was observed with sera from patients with connective tissue diseases that were anti-Ro/SSA negative and had a normal QTc (control group) [36].

As mentioned above, anti-Ro/SSA antibodies are present in up to ~3% of the general population (Table 12.1) [26], where they could significantly contribute to SCD risk [23]. Indeed, anti-Ro52kD/SSA antibodies exerting hERG-blocking properties were frequently found (60%) in unselected TdP patients, mainly without manifest autoimmune diseases [23]. The reactivity of these patients' sera with the hERG E-pore peptide and its scrambled form were tested by

ELISA. Interestingly, anti-Ro/SSA-positive sera showed significant reactivity to the hERG E-pore peptide compared with the scrambled peptide and with anti-Ro/SSA-negative sera suggesting the hERG E-pore peptide bound to the anti-Ro/SSA antibodies [23]. Altogether, the sera reactivity findings open new avenues in peptide-based diagnostic and/or therapeutic approaches to pathogenic anti-Ro/SSA antibodies and associated arrhythmogenesis (Fig. 12.4).

Clinical Significance and Conclusions

Emerging and recent evidence indicates that autoimmunity is involved in the pathogenesis of cardiac arrhythmias, not only those occurring in patients with overt autoimmune diseases but also in a number of rhythm disorders currently classified as "idiopathic." Because arrhythmogenic anti-Ro/SSA antibodies are prevalent in several autoimmune diseases and also in healthy individuals, they should be considered as a risk factor for the development of QTc prolongation, TdP, and SCD. Thus, it is warranted that such individuals be screened for these antibodies, considering performing routine ECGs and counselling for those who may have congenital or medication-related QTc prolongation. In fact, although anti-Ro/SSA antibodies are in most cases probably not per se able to induce a QTc prolongation as critical as to induce TdP (but actually this is true for all recognized causes of LQTS, when present alone), nevertheless they can reduce the ventricular repolarization reserve, thereby significantly increasing the risk of life-threatening arrhythmias in the presence of other classical QT-prolonging factors (drugs, electrolyte imbalances, genetic polymorphisms, etc.). While it is well conceivable that these events may take place in patients with autoimmune chronic inflammatory diseases, thus putatively contributing to explain the increased risk of sudden death observed in the course of connective tissue diseases [41], nevertheless asymptomatic circulating

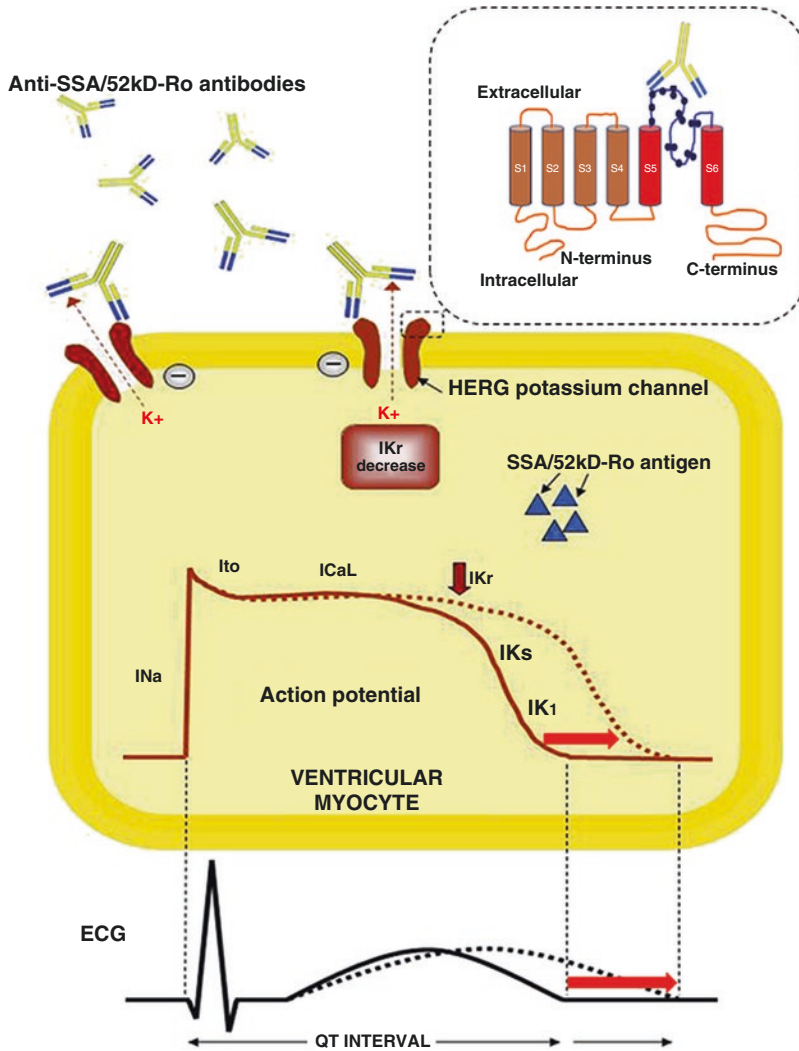


Fig. 12.4 The molecular and electrophysiologic basis of anti-Ro/SSA-associated QTc prolongation, from the cell to the surface ECG. Circulating anti-Ro52/SSA antibodies cross-react with the extracellular loop of the pore-forming region of the hERG K^+ channel (inset) as a result of a molecular mimicry mechanism with Ro52kD/SSA antigen (blue triangles) that are located inside the cardiac myocyte but are not accessible to autoantibodies. The

autoantibody-hERG channel interaction results in the inhibition of the related I_{Kr} current, thus leading to an increase in the cardiomyocyte action potential duration (dotted lines). The clinical correlate of these electrophysiologic changes is a prolongation of the QT interval on the surface ECG (dotted lines). (Reprinted from Boutjdir et al. [30], with permission from Elsevier)

anti-Ro/SSA may be also silently involved, as a predisposing factor, in a number of unexpected life-threatening arrhythmias, including drug-induced TdP, and sudden deaths occurring in the general population.

From a therapeutic point of view, the evidence that pathogenic activities of anti-Ro/SSA autoantibodies are functional, thus potentially revers-

ible, suggests that treatments targeting the immune-inflammatory system might effectively reduce arrhythmic risk in these subjects. In addition, since these autoantibodies induce channelopathies by directly cross-reacting with specific amino acid sequences on ion channels, an innovative therapeutic approach could be proposed based on the use of short decoy peptides

distracting the pathogenic antibodies from channel binding sites.

Acknowledgement Supported in part by Cardiovascular Research program, a MERIT Award Number I01BX007080 from Biomedical Laboratory Research & Development Service of Veterans Affairs Office of Research and Development (MB), and the Narrows Institute for Biomedical Research and Education (NES).

References

- El-Sherif N, Turitto G, Boutjdir M. Congenital long QT syndrome and torsade de pointes. *Ann Noninvasive Electrocardiol.* 2017;22(6):e12481.
- El-Sherif N, Turitto G, Boutjdir M. Acquired long QT syndrome and torsade de pointes. *Pacing Clin Electrophysiol.* 2018;41:414.
- El-Sherif N, Turitto G. Torsade de pointes. *Curr Opin Cardiol.* 2003;18(1):6–13.
- Schwartz PJ, Periti M, Malliani A. The long Q-T syndrome. *Am Heart J.* 1975;89(3):378–90.
- Roden DM. Cellular basis of drug-induced torsades de pointes. *Br J Pharmacol.* 2008;154(7):1502–7.
- Farkas AS, Nattel S. Minimizing repolarization-related proarrhythmic risk in drug development and clinical practice. *Drugs.* 2010;70(5):573–603.
- Lerner MR, Boyle JA, Hardin JA, Steitz JA. Two novel classes of small ribonucleoproteins detected by antibodies associated with lupus erythematosus. *Science.* 1981;211(4480):400–2.
- Yoshimi R, Ueda A, Ozato K, Ishigatsubo Y. Clinical and pathological roles of Ro/SSA autoantibody system. *Clin Dev Immunol.* 2012;2012:606195.
- Sim S, Wolin SL. Emerging roles for the Ro 60-kDa autoantigen in noncoding RNA metabolism. *Wiley Interdiscip Rev RNA.* 2011;2(5):686–99.
- Kong HJ, Anderson DE, Lee CH, Jang MK, Tamura T, Tailor P, et al. Cutting edge: autoantigen Ro52 is an interferon inducible E3 ligase that ubiquitinates IRF-8 and enhances cytokine expression in macrophages. *J Immunol.* 2007;179(1):26–30.
- Higgs R, Lazzari E, Wynne C, Ni Gabhann J, Espinosa A, Wahren-Herlenius M, et al. Self protection from anti-viral responses--Ro52 promotes degradation of the transcription factor IRF7 downstream of the viral Toll-Like receptors. *PLoS One.* 2010;5(7):e11776.
- Higgs R, Ni Gabhann J, Ben Larbi N, Breen EP, Fitzgerald KA, Jefferies CA. The E3 ubiquitin ligase Ro52 negatively regulates IFN-beta production post-pathogen recognition by polyubiquitin-mediated degradation of IRF3. *J Immunol.* 2008;181(3):1780–6.
- Lee AYS. A review of the role and clinical utility of anti-Ro52/TRIM21 in systemic autoimmunity. *Rheumatol Int.* 2017;37(8):1323–33.
- Lee HC, Huang KT, Wang XL, Shen WK. Autoantibodies and cardiac arrhythmias. *Heart Rhythm.* 2011;8(11):1788–95.
- Lazzerini PE, Capecci PL, Laghi-Pasini F, Boutjdir M. Autoimmune channelopathies as a novel mechanism in cardiac arrhythmias. *Nat Rev Cardiol.* 2017;14(9):521–35.
- Bornholz B, Roggenbuck D, Jahns R, Boege F. Diagnostic and therapeutic aspects of beta1-adrenergic receptor autoantibodies in human heart disease. *Autoimmun Rev.* 2014;13(9):954–62.
- Patel PA, Hernandez AF. Targeting anti-beta-1-adrenergic receptor antibodies for dilated cardiomyopathy. *Eur J Heart Fail.* 2013;15(7):724–9.
- Matsui S, Fu M. Pathological importance of anti-G-protein coupled receptor autoantibodies. *Int J Cardiol.* 2006;112(1):27–9.
- Li J, Seyler C, Wiedmann F, Schmidt C, Schweizer PA, Becker R, et al. Anti-KCNQ1 K(+) channel autoantibodies increase IKs current and are associated with QT interval shortening in dilated cardiomyopathy. *Cardiovasc Res.* 2013;98(3):496–503.
- Lazzerini PE, Acampa M, Guideri F, Capecci PL, Campanella V, Morozzi G, et al. Prolongation of the corrected QT interval in adult patients with anti-Ro/SSA-positive connective tissue diseases. *Arthritis Rheum.* 2004;50(4):1248–52.
- Lazzerini PE, Capecci PL, Acampa M, Morozzi G, Bellisai F, Bacarelli MR, et al. Anti-Ro/SSA-associated corrected QT interval prolongation in adults: the role of antibody level and specificity. *Arthritis Care Res (Hoboken).* 2011;63(10):1463–70.
- Lazzerini PE, Capecci PL, Guideri F, Bellisai F, Selvi E, Acampa M, et al. Comparison of frequency of complex ventricular arrhythmias in patients with positive versus negative anti-Ro/SSA and connective tissue disease. *Am J Cardiol.* 2007;100(6):1029–34.
- Lazzerini PE, Yue Y, Srivastava U, Fabris F, Capecci PL, Bertolozzi I, et al. Arrhythmogenicity of anti-Ro/SSA antibodies in patients with torsades de pointes. *Circ Arrhythm Electrophysiol.* 2016;9(4):e003419.
- Cimaz R, Stramba-Badiale M, Brucato A, Catelli L, Panzeri P, Meroni PL. QT interval prolongation in asymptomatic anti-SSA/Ro-positive infants without congenital heart block. *Arthritis Rheum.* 2000;43(5):1049–53.
- Bourré-Tessier J, Clarke AE, Huynh T, Bernatsky S, Joseph L, Belisle P, et al. Prolonged corrected QT interval in anti-Ro/SSA-positive adults with systemic lupus erythematosus. *Arthritis Care Res (Hoboken).* 2011;63(7):1031–7.
- Hayashi N, Koshiba M, Nishimura K, Sugiyama D, Nakamura T, Morinobu S, et al. Prevalence of disease-specific antinuclear antibodies in general population: estimates from annual physical examinations of residents of a small town over a 5-year period. *Mod Rheumatol.* 2008;18(2):153–60.

27. Satoh M, Chan EK, Ho LA, Rose KM, Parks CG, Cohn RD, et al. Prevalence and sociodemographic correlates of antinuclear antibodies in the United States. *Arthritis Rheum.* 2012;64(7):2319–27.
28. Guo YP, Wang CG, Liu X, Huang YQ, Guo DL, Jing XZ, et al. The prevalence of antinuclear antibodies in the general population of China: a cross-sectional study. *Curr Ther Res Clin Exp.* 2014;76:116–9.
29. Lazzerini PE, Capecchi PL, Guideri F, Acampa M, Selvi E, Bisogno S, et al. Autoantibody-mediated cardiac arrhythmias: mechanisms and clinical implications. *Basic Res Cardiol.* 2008;103(1):1–11.
30. Boutjdir M, Lazzerini PE, Capecchi PL, Laghi-Pasini F, El-Sherif N. Potassium channel block and novel autoimmune-associated long QT syndrome. *Card Electrophysiol Clin.* 2016;8(2):373–84.
31. Yue Y, Castrichini M, Srivastava U, Fabris F, Shah K, Li Z, et al. Pathogenesis of the novel autoimmune-associated long-QT syndrome. *Circulation.* 2015;132(4):230–40.
32. Nakamura K, Katayama Y, Kusano KF, Haraoka K, Tani Y, Nagase S, et al. Anti-KCNH2 antibody-induced long QT syndrome: novel acquired form of long QT syndrome. *J Am Coll Cardiol.* 2007;50(18):1808–9.
33. Suzuki S, Satoh T, Yasuoka H, Hamaguchi Y, Tanaka K, Kawakami Y, et al. Novel autoantibodies to a voltage-gated potassium channel Kv1.4 in a severe form of myasthenia gravis. *J Neuroimmunol.* 2005;170(1–2):141–9.
34. Suzuki S, Baba A, Kaida K, Utsugisawa K, Kita Y, Tsugawa J, et al. Cardiac involvements in myasthenia gravis associated with anti-Kv1.4 antibodies. *Eur J Neurol.* 2014;21(2):223–30.
35. Romi F, Suzuki S, Suzuki N, Petzold A, Plant GT, Gilhus NE. Anti-voltage-gated potassium channel Kv1.4 antibodies in myasthenia gravis. *J Neurol.* 2012;259(7):1312–6.
36. Fabris F, Yue Y, Qu Y, Chahine M, Sobie E, Lee P, et al. Induction of autoimmune response to the extracellular loop of the HERG channel pore induces QTc prolongation in guinea pigs. *J Physiol.* 2016;594(21):6175–87.
37. Karnabi E, Boutjdir M. Role of calcium channels in congenital heart block. *Scand J Immunol.* 2010;72(3):226–34.
38. Strandberg LS, Cui X, Rath A, Liu J, Silverman ED, Liu X, et al. Congenital heart block maternal sera autoantibodies target an extracellular epitope on the alpha1G T-type calcium channel in human fetal hearts. *PLoS One.* 2013;8(9):e72668.
39. Ambrosi A, Sonesson SE, Wahren-Herlenius M. Molecular mechanisms of congenital heart block. *Exp Cell Res.* 2014;325(1):2–9.
40. Qu Y, Baroudi G, Yue Y, Boutjdir M. Novel molecular mechanism involving alpha1D (Cav1.3) L-type calcium channel in autoimmune-associated sinus bradycardia. *Circulation.* 2005;111(23):3034–41.
41. Maradit-Kremers H, Crowson CS, Nicola PJ, Ballman KV, Roger VL, Jacobsen SJ, et al. Increased unrecognized coronary heart disease and sudden deaths in rheumatoid arthritis: a population-based cohort study. *Arthritis Rheum.* 2005;52(2):402–11.



The Role of Inflammation and Autoimmunity in Long QT Syndrome

Pietro Enea Lazzerini, Franco Laghi-Pasini,
Nabil El-Sherif, Mohamed Boutjdir,
and Pier Leopoldo Capecchi

The long QT syndrome (LQTS) is a cardiac electric disorder characterized by the presence of a prolonged heart rate-corrected QT interval (QTc) on the electrocardiogram (ECG) and an increased susceptibility to life-threatening ventricular arrhythmias, particularly torsades de pointes (TdP) [1, 2]. LQTS can be the result of a wide number of etiologic factors, both congenital and acquired, often variously associated in a single patient and synergistically operating to promote TdP [2–5]. Indeed, different QT-prolonging factors interfere with the function of one or more cardiac ion channels determining the duration of

ventricular repolarization, leading to an inward shift in the balance of current as a result of an increase in the inward sodium (Na^+) or calcium (Ca^{++}) currents and/or a decrease in an outward potassium (K^+) current [2, 3].

While congenital LQTS is a rare disease with an estimated prevalence of ~1:2000 apparently healthy live births [6], acquired forms are quite common occurring in up to 1 every 4 hospitalized patients [7–9]. Drugs, electrolyte imbalances, and structural heart diseases are the most common acquired QT-prolonging factors involved, although also bradyarrhythmias, endocrine diseases, liver disorders, nervous system injuries, HIV infection, starvation, hypothermia, and toxins are recognized causes of acquired LQTS in the general population [1–3, 5, 10–12].

However, “classical” risk factors cannot fully explain LQTS/TdP occurrence in a fraction of subjects, thereby pointing to the existence of a number of “nonclassical” risk factors, currently unrecognized and largely overlooked. In this view, accumulating evidence identified inflammation and autoimmunity as novel pathogenic mechanisms of acquired LQTS, actively cooperating with classical risk factors to increase the risk of TdP, and sudden cardiac death (SCD) [13]. By integrating basic and clinical research, in this chapter we provide an updated overview of this subject, also discussing practical implications and future therapeutic perspectives.

Franco Laghi-Pasini, Nabil El-Sherif, Mohamed Boutjdir, and Pier Leopoldo Capecchi contributed equally to this work.

P. E. Lazzerini (✉) · F. Laghi-Pasini · P. L. Capecchi
Department of Medical Sciences, Surgery and
Neurosciences, University of Siena, Siena, Italy
e-mail: lazzerini7@unisi.it

N. El-Sherif
Department of Medicine and Physiology, State
University of New York Downstate Medical Center,
VA New York Harbor Healthcare Center,
Brooklyn, NY, USA

M. Boutjdir
Department of Medicine and Physiology, SUNY
Downstate Medical Center, Brooklyn, NY, USA

State University of New York Downstate Medical
Center, New York, NY, USA

NYU School of Medicine, New York, NY, USA

The Role of Inflammation in Long QT Syndrome

Clinical Evidence

The risk of developing acquired LQTS and TdP is significantly increased in several pathologic conditions characterized by cardiac and/or systemic inflammatory activation.

Inflammatory Heart Diseases

In inflammatory heart disease, particularly myocarditis, QTc prolongation is a rather common finding, sometimes complicated by TdP. QTc lengthening was found to be the most frequent ECG abnormality in biopsy-proven myocarditis [14], and a significant association between QTc prolongation and the occurrence of complex ventricular arrhythmias during 24-hour electrocardiographic recordings was demonstrated in patients with myocarditis [15]. These findings were confirmed in a large cohort of almost 200 myocarditis patients, where a QTc \geq 440 occurred in ~25% of the cases, also representing

a predictor of poor clinical outcome, including cardiac death [16]. Increasing evidence indicates that TdP risk is particularly high when the QT interval is prolonged as a result of an increase in the terminal portion of the T wave, from the peak of the T wave to its end (Tpeak-Tend interval, Tp-Te) [2, 17]. Recently, Gunes et al. reported that also Tp-Te duration and Tp-Te/QTc ratio were significantly increased in myocarditis patients when compared to healthy controls (Table 13.1) [18]. In addition, 14 cases of TdP in patients with acute myo-/endocarditis have been reported in the literature, regardless of the specific etiologic agent implicated [19–32]. Moreover, in a prospective cohort of 40 consecutive, unselected TdP patients from the general population, 2 subjects (5% incidence) were found to be affected with acute infective endocarditis [33].

Further evidence supporting a significant prolonging effect of cardiac inflammation on ventricular repolarization derives from patients with specific forms of inflammatory heart diseases, such as Chagas disease (ChD) and acute rheu-

Table 13.1 Clinical studies showing an association between QTc prolongation and inflammatory heart diseases

Authors	Study population	Subjects <i>n</i>	Controls <i>n</i>	Main results
Ramamurthy et al. [14]	Myocarditis	20	–	QTc prolongation occurred in 70% of the patients
Karjalainen et al. [15]	Myocarditis	26	–	QTc prolongation was associated with complex ventricular arrhythmias
Ukena et al. [16]	Myocarditis	186	–	QTc prolongation occurred in 25% of the patients and predicted cardiac death
Gunes et al. [18]	Myocarditis	30	25	Tp-e and Tp-e/QT were higher in myocarditis patients than in controls
Williams-Blangero et al. [37]	Chagas disease	722	667	<i>T. Cruzi</i> -seropositive subjects showed a longer QTc when compared to controls
Sabino et al. [38]	Chagas disease	546	483	Chagas disease/ <i>T. Cruzi</i> PCR-positive subjects showed a longer QTc when compared to controls
Salles et al. [36]	Chagas disease	738	–	QTc max independently predicted SCD
Bradfield et al. [39]	Chagas disease	31	31	Tp-e was longer in Chagas disease patients than controls and associated with increased mortality
Alp et al. [45]	Acute rheumatic carditis	64	41	QTc was significantly longer in patients with acute rheumatic fever than in controls and predicted the presence of carditis
Balli et al. [48]	Acute rheumatic carditis	73	–	QTc prolongation occurred in 2/3 of patients with carditis and strongly correlated with levels of acute phase reactants

QTc corrected QT interval, Tp-e interval from the peak to the end of the T wave, Tp-e/QT interval from the peak to the end of the T wave/QT interval ratio, PCR polymerase chain reaction

matic carditis. ChD is a diffuse myocarditis triggered by the protozoan parasite *Trypanosoma cruzi* and then maintained by immune-mediated mechanisms [34]. The disease is endemic in Latin America and is burdened by a high risk of life-threatening arrhythmias and SCD [35]. In ChD, QTc prolongation is common, and maximal QTc independently predicts SCD [36–38]. Also Tp-Te duration was found to be increased in these patients and associated with the risk of death (Table 13.1) [39]. QT prolongation has been reproduced in murine models of the disease [40–42], where an increased propensity to drug-induced TdP and ventricular fibrillation (VF) was demonstrated [43]. Moreover, in these animals QT length and the extent of cardiac inflammation at the histological examination significantly correlated [41]. Acute rheumatic carditis is an immune-mediated inflammatory heart disease frequently presenting with QTc prolongation [44, 45], occasionally complicated with TdP [46, 47]. Notably, the presence of carditis and high levels of inflammatory markers (C-reactive protein (CRP) and erythrocyte sedimentation rate (ESR)) were found to be significant predictors of a prolonged QTc in patients with acute rheumatic fever (Table 13.1) [48].

Systemic Inflammatory Diseases

A growing body of evidence, mostly derived from patients with chronic autoimmune diseases such as rheumatoid arthritis (RA) and connective tissue diseases (CTD), demonstrated that systemic inflammatory activation is associated with an increased incidence of acquired LQTS (Table 13.2).

RA is a chronic joint disease characterized by persistent high-grade systemic inflammation [49], which is burdened by a ~2-fold higher risk of SCD [50] and cardiac arrest [51] when compared to the general population. RA patients frequently show QTc prolongation, correlating with disease activity and inflammatory markers, also predicting mortality [52]. Indeed, after we demonstrated for the first time that in RA patients QTc was longer than in spondyloarthritis and control subjects, also correlating with CRP levels [53], several other authors confirmed this finding.

In a larger retrospective study, Chauhan et al. [54] found that the cumulative incidence of QTc prolongation at 20 years after RA incidence was significantly higher among RA than non-RA subjects and ESR values associated with risk of idiopathic QTc prolongation. Moreover, any QTc prolongation independently predicted all-cause mortality [54]. Accordingly, in a prospective cohort of 357 RA patients, Panoulas et al. [55] found that a prolonged QTc was a strong predictor of death, with a doubling of the all-cause mortality risk for each 50 ms increase in QTc. In these patients, QTc prolongation independently correlated with CRP levels, and the value of QTc in predicting mortality was lost after the adjustment for CRP [55]. More recently, Geraldino-Pardilla et al. [56] reported that in RA, CRP levels and disease activity score in 28 joints (DAS-28) were associated with an increased QTc length, while Acar et al. [57] demonstrated that also Tp-Te and Tp-Te/QT ratio were increased in these patients and significantly correlated with CRP, ESR, and DAS-28 score. These data are further supported by the evidence that in RA patients circulating levels of inflammatory cytokines (TNF α , IL-1 β , IL-6, IL-10) associated with QTc duration [58] and that anti-IL6 therapy with tocilizumab (TCZ) led to a rapid and significant QTc shortening, which correlated with both the decrease in CRP and TNF α levels [59]. In addition, although no data are currently available on TdP prevalence in the RA population, cases of marked QTc prolongation and TdP have been reported in RA patients with elevated CRP and IL-6 levels [60]. Notably, these subjects accounted for 5% of the cases in a cohort of 40 consecutive TdP patients [33], an incidence 5–10 times higher than expected in the general population (0.5–1%) [49].

QTc prolongation is common also in CTD. Several studies in patients with different CTD reported a high prevalence of QTc prolongation [61–65], also being independently predicted by IL-1 β serum level [65]. Consistently, systemic lupus erythematosus (SLE) patients show a longer QTc than controls [66–69], with QTc prolongation occurring in 7–17% of the patients [70–72]. QTc duration correlated with

Table 13.2 Clinical studies showing an association between QTc prolongation and systemic inflammatory diseases

Authors	Study population	Subjects <i>n</i>	Controls <i>n</i>	Main results
Lazznerini et al. [53]	RA	25	20	Mean QTc longer in RA patients than healthy controls and significantly correlated with CRP levels
Chauhan et al. [54]	RA	518	499	Cumulative incidence of QTc prolongation higher in RA than non-RA patients; any QTc prolongation independently associated with all-cause mortality; risk of idiopathic QTc prolongation correlated with ESR (HR 1.14 per 10 mm/h increase; 95% CI, 1.03–1.27)
Panoulas et al. [55]	RA	357	–	QTc prolongation was independently associated with CRP levels and predicted all-cause mortality
Geraldino-Pardilla et al. [56]	RA	139	–	QTc length correlated with CRP levels and disease activity (each unit higher DAS28-CRP score associated with a 1.5- and 1.6-fold higher odds of having a QTc \geq 460 ms and \geq 480 ms, respectively)
Acar et al. [57]	RA	96	50	Tp-e was higher in RA patients than controls and correlated with CRP, ESR, and DAS-28
Adlan et al. [58]	RA	112	–	QTc prolongation correlated with circulating levels of inflammatory cytokines
Lazznerini et al. [59]	RA	17	–	Anti-IL-6 therapy (TCZ) was associated with a rapid (within 12 weeks) QTc shortening, which correlated with the decrease in both CRP and TNF α levels
Acar et al. [92]	AS	62	50	Tp-e and Tp-e/QT were higher in AS patients than controls and correlated with CRP levels
Senel et al. [99]	AS	21	–	Anti-TNF therapy (IFX) significantly reduced QTc duration, along with disease activity scores, ESR, and CRP
Lazznerini et al. [61]	CTD	57	–	QTc prolongation in 31% of patients
Costedoat-Ch et al. [62]	CTD	89	–	QTc prolongation in 12% of patients
Lazznerini et al. [63]	CTD	46	–	QTc prolongation (28% of patients) correlated with complex ventricular arrhythmias
Lazznerini et al. [64]	CTD	49	–	QTc prolongation in 32% of patients
Pisoni et al. [65]	CTD	73	–	QTc prolongation (15% of patients) was independently predicted by circulating IL-1 β levels
Cardoso et al. [66]	SLE	140	37	Mean QTc longer in patients than healthy controls
Milovanović et al. [67]	SLE	52	41	Mean QTc longer in patients than healthy controls
Rivera-Lopez et al. [68]	SLE	93	109	Mean QTc longer in patients than healthy controls
Bourrè-Tessier et al. [70]	SLE (two studies)	150 278	– –	QTc prolongation (7% of SLE patients) was independently associated with SDI
Bourrè-Tessier et al. [71]	SLE	779	–	QTc prolongation (15% of SLE patients) was independently associated with SDI
Myung et al. [72]	SLE	235	–	QTc prolongation in 17% of patients
Teixera et al. [74]	SLE	317	–	Marked QTc prolongation (>500 ms) in 3% of SLE patients
Sham et al. [69]	SLE	100	100	Mean QTc was longer in SLE patients than healthy controls and correlated with disease activity
Avci et al. [73]	SLE	69	57	Tp-e and Tp-e/QT were higher in SLE patients than controls and correlated with disease duration
Sgreccia et al. [85]	SSc	38	17	Mean QTc longer in SSc patients than healthy controls

Table 13.2 (continued)

Authors	Study population	Subjects <i>n</i>	Controls <i>n</i>	Main results
Rosato et al. [86]	SSc	20	NA	Mean QTc longer in SSc patients than healthy controls; QTc associated with disease severity
Massie et al. [88]	SSc	689	–	QTc prolongation (25% of SSc patients) independently associated with disease duration and severity
De Luca et al. [90]	SSc	100	–	QTc prolongation in 11% of patients
Foocharoen et al. [89]	SSc	103	–	QTc prolongation (14.6% of SSc patients) associated with disease severity
Okutucu et al. [87]	SSc	107	100	Tp-e and Tp-e/QT were higher in SSc patients than controls and correlated with ESR and CRP levels
Diederichsen et al. [91]	PM/DM	76	48	Mean QTc longer in PM/DM patients than healthy controls; QTc prolongation occurred in 5% of patients
Pattanshetty et al. [94]	IBD	142	–	QTc prolongation in 46% of patients
Simsek et al. [95]	Psoriasis	94	51	QTc max was longer in psoriasis patients than healthy controls
Poorzand et al. [97]	Psoriasis	30	30	QTc was longer in psoriasis patients than healthy controls
Arisoy et al. [98]	Psoriasis	74	74	QTc, Tp-e, and Tp-e/QT were higher in psoriasis patients than controls; Tp-e/QT correlated with CRP
Soylu et al. [96]	Psoriasis	71	70	Tp-e and Tp-e/QT were higher in psoriasis patients than controls and correlated with disease severity
Tisdale et al. [101]	ICU patients	900	–	Sepsis was a strong and independent predictor of QTc prolongation (OR, 2.7; 95% CI, 1.5–4.8)
Wasserstrum et al. [101]	Sepsis	257	–	QTc duration independently predicts mortality
Ozdemir et al. [102]	Sepsis	93	103	Tp-e and Tp-e/QT were higher in patients with sepsis than controls; Tp-e/QT independently predicted mortality
Lazzerini et al. [33]	Inflammatory diseases ^a	46	–	QTc prolongation in 26% of patients; CRP reduction was associated with significant QTc shortening, which correlated with IL-6 level decrease

RA rheumatoid arthritis, AS ankylosing spondylitis, CRP C-reactive protein, ESR erythrocyte sedimentation rate, TCZ tocilizumab, CTD connective tissue disease, SLE systemic lupus erythematosus, SSc systemic sclerosis, PM/DM polymyositis/dermatomyositis, IBD inflammatory bowel disease, ICU intensive care unit, QTc corrected QT interval, Tp-e interval from the peak to the end of the T wave, Tp-e/QT ratio interval from the peak to the end of the T wave/QT interval ratio, ESR erythrocyte sedimentation rate, TNF α tumor necrosis factor alpha, IL-1 β interleukin-1 beta, IL-6 interleukin-6, DAS28 disease activity score in 28 joints, OR odds ratio, HR hazard ratio, NA not available

^aInflammatory diseases of different origin (infective, immuno-inflammatory, others)

disease activity, increasing during severe flares [69], and with overall inflammatory burden [70, 71]. Moreover, also Tp-Te and Tp-Te/QT ratio significantly increase in SLE, positively associating with disease duration [73]. A marked QTc prolongation (>500 ms) is demonstrated in ~3% of patients [74], and 10 reports of TdP in SLE have been described in the literature [75–84]. In systemic sclerosis (SSc) patients, where values of QTc, Tp-e, and Tp-e/QT are significantly higher in comparison to controls [85–87], QTc prolongation has a prev-

alence ranging from 11% to 25%, also correlating with disease duration and severity [88–90]. Notably, Tp-Te and Tp-Te/QT showed also a specific association with ESR and CRP levels [87]. In addition, recent studies provided evidence that QTc and Tp-Te are also increased in polymyositis/dermatomyositis [91], as well as other autoimmune inflammatory diseases, such as ankylosing spondylitis [92], inflammatory bowel disease [93, 94], and psoriasis [95–98], also correlating with disease severity and CRP [92, 96, 98]. Finally, in ankylosing spondylitis

patients a 6-month anti-TNF treatment with infliximab significantly reduced both inflammatory markers and QTc duration [99], and occurrence of TdP or premonitory ECG signs of TdP (marked QTc prolongation with macroscopic T-wave alternans) have been recently reported in both polymyalgia rheumatica and psoriatic arthritis patients with elevated CRP and IL-6 levels [60, 100].

Besides immune-mediated inflammatory activation, increasing evidence suggests that also infections, particularly severe forms such as sepsis, can be associated with QTc prolongation and increased TdP risk. Indeed, in patients with sepsis QTc is frequently prolonged, and Tp-Te and Tp-Te/QT values are significantly higher than in controls, all independently predicting short-term mortality [101, 102]. Moreover, by studying 900 consecutive patients admitted to cardiac care units, Tisdale et al. [103] identified sepsis as one of strongest independent predictors of QTc prolongation. Several cases of TdP in patients with sepsis have been reported [104–110], and in a recent study performed in our Institution we found that an acute infection (more commonly a sepsis) was demonstrable in 30% of cases in a cohort of 40 consecutive TdP patients [33].

Altogether, these data strongly suggest that systemic inflammation per se represents a risk factor for QTc prolongation and TdP, regardless of its origin and pathogenesis. Accordingly, in the above cited study on unselected TdP patients, elevated CRP and IL-6 levels were present in most cases (80%), including several patients in whom a specific inflammatory disease was not detected [33]. In support of this view, we demonstrated that in subjects with elevated CRP levels from different inflammatory conditions (infective, immune-mediated, others), QTc prolongation was common, but rapidly and significantly shortened as soon as CRP and IL-6 decreased following specific treatments (Fig. 13.1) [33].

Noninflammatory Heart Diseases and Congenital Long QT Syndrome

Recent evidence suggests that systemic inflammation may also play a role in modulating QTc duration/arrhythmia development in patients

with noninflammatory heart diseases (Table 13.3) and congenital LQTS.

By studying 466 hypertensive patients, Chang et al. [111] found that low-grade chronic systemic inflammation as assessed by high-sensitivity CRP (hsCRP) levels was strictly correlated with QTc length, also independently predicting the presence of a prolonged QTc. Consistent findings were reported in patients with coronary artery disease (CAD), where a significant association between QTc duration and circulating hsCRP was demonstrated [112]. Moreover, in CAD patients short-term exposure to ambient particulate air pollution leading to hsCRP increase is associated with a significant prolongation of QTc duration [113]. In Takotsubo cardiomyopathy, QTc prolongation is frequently observed, also predicting occurrence of ventricular arrhythmias, TdP, and death [114, 115]. Among these patients, those developing a prolonged QTc showed ~3 times higher hsCRP levels when compared to subjects with a normal QTc [116]. In addition, we demonstrated that in patients with cardiovascular diseases who developed marked QTc prolongation and TdP, CRP and IL-6 levels were markedly higher than in those who did not (~5–15 times, respectively), in about a half of cases in the presence of a definite, concomitant inflammatory disease [33].

Finally, recent data point to a role for inflammatory activation also in increasing electrical instability in patients with congenital LQTS. In fact, Rizzo et al. [117] provided evidence that in subjects who underwent left cardiac sympathetic denervation for malignant intractable arrhythmias, inflammatory infiltrates including activated T lymphocytes and macrophages, suggestive of a chronic T-cell-mediated stellate ganglionitis, were demonstrable. Consistent findings, already described in early reports in single cases/case series of LQTS patients who died suddenly [118–120], were also recently found in stellate ganglia from patients with cardiomyopathy and refractory ventricular arrhythmias [121]. These data suggest that locally released inflammatory mediators may be arrhythmogenic by enhancing efferent sympathetic tone on the heart, in turn representing a

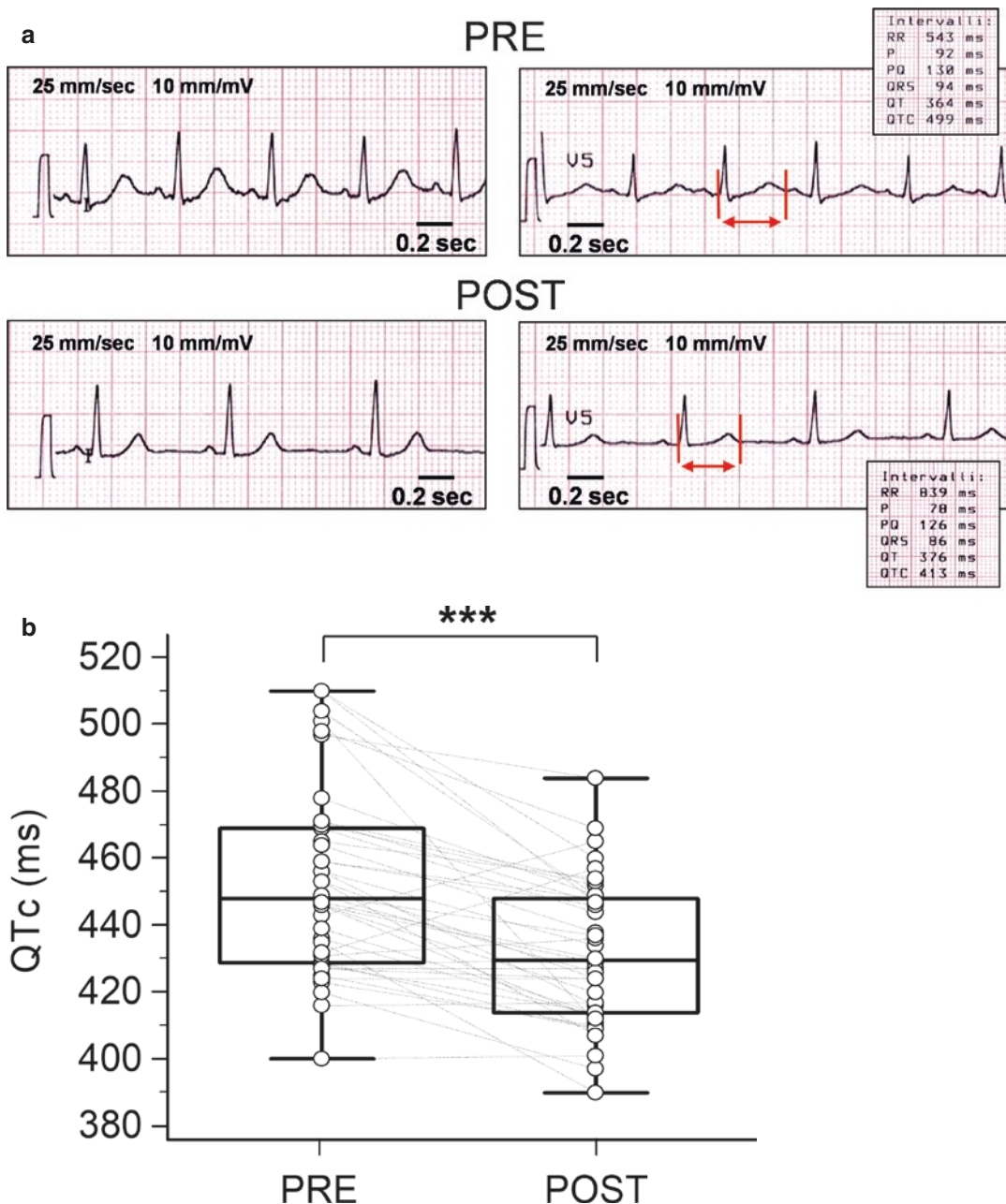


Fig. 13.1 Changes in the corrected QT (QTc) interval duration in patients with active inflammatory diseases during active disease (PRE) and after therapeutic interventions resulting in a CRP decrease >75% when compared to the baseline (POST). (a) Representative ECG strips of a patient with acute pancreatitis, during active disease (PRE; CRP 27.0 mg/dl) and after a 13-day treat-

ment with gabesate mesilate (POST; CRP 1.64 mg/dl). Red vertical lines in lead V5 show QT interval. (b) QTc changes observed before (PRE) and after (POST) treatment in the entire study population. Patients, $n = 46$. Two-tail Student's paired "t" test, $***p < 0.0001$. (Reproduced from Lazzarini et al. [33], with permission from BMJ Publishing Group)

Table 13.3 Clinical studies showing an association between QTc duration/TdP occurrence and inflammatory activation in patients with noninflammatory heart diseases or apparently healthy subjects of the general population

Authors	Study population	Subjects <i>n</i>	Controls <i>n</i>	Main results
Chang et al. [111]	Arterial hypertension	466	–	CRP levels correlated with QTc duration and independently predicted QTc prolongation
Yue et al. [112]	Coronary artery disease	52	–	CRP levels correlated with QTc duration
Song et al. [116]	Takotsubo cardiomyopathy	105	–	Patients with QTc prolongation had higher CRP levels than those with normal QTc
Lazznerini et al. [33]	Torsades de pointes	40	30	Increased CRP levels in most subjects (80%); IL-6 levels were elevated and comparable with those observed in patients with severe active RA and markedly higher than controls
Kazumi et al. [128]	Healthy subjects	179	–	QTc length independently correlated with CRP
Kim et al. [129]	Healthy subjects	4758	–	QTc prolongation independently associated with elevated CRP
Medenwald et al. [130]	Healthy subjects	1716	–	Soluble TNF-receptor 1 levels independently correlated with QTc duration in women

TdP torsades de pointes, *QTc* corrected QT interval, *Tp-e* interval from the peak to the end of the T wave, *Tp-e/QT* ratio interval from the peak to the end of the T wave/*QT* interval ratio, *CRP* C-reactive protein

well-recognized trigger for malignant arrhythmias in LQTS [122]. Accordingly, Wang et al. [123] demonstrated that IL-1 β injection into the left stellate ganglion increased ganglion activity, sympathetic indices of heart rate variability, and VA occurrence in canine hearts. Indeed, acute inflammatory processes are increasingly recognized as possible precipitant factors of malignant arrhythmias/electrical storms in congenital LQTS subjects [124, 125]. Although fever can be per se arrhythmogenic by altering temperature-sensitive biophysical properties of mutant channels [126, 127], it is conceivable that in these patients high levels of cytokines may further contribute to arrhythmia susceptibility by directly affecting cardiomyocyte APD (see below, *Molecular basis and pathophysiology*), as well as by indirectly increasing sympathetic output in the heart.

General Population

Subclinical low-grade chronic inflammation may be associated with an increased risk of QTc prolongation also in apparently healthy subjects (Table 13.3). Based on preliminary evidence by Kazumi et al. [128] who demonstrated that in male college students QTc duration independently correlated with hsCRP, two large community-based studies supported the existence of a strict link between inflammatory

markers and QTc in both middle-aged and elderly individuals of the general population. The Korean Health and Genome Study found that hsCRP levels independently predicted the presence of QTc prolongation among 4758 subjects aged 40–69 years [129]. Consistently, in the Cardiovascular Diseases, Living and Ageing in Halle (CARLA) Study analyzing 1716 subjects aged 45–83 years, Medenwald et al. [130] demonstrated that circulating markers of inflammation correlated with QTc length, particularly the TNF α system, as reflected by soluble TNF-receptor 1 levels (sTNF-R1), in women.

These findings, together with the evidence from large prospective population studies that hsCRP and IL-6 are strong independent predictors of SCD in apparently healthy persons [131–133], intriguingly suggest that low-grade chronic systemic inflammation may increase the susceptibility of long QT-associated malignant arrhythmias also in the general population, specifically TdP rapidly degenerating to ventricular fibrillation.

Molecular Basis and Pathophysiology

Accumulating evidence points to inflammatory cytokines, particularly TNF α , IL-1, and IL-6, as the key mediators linking inflammatory activation

Table 13.4 Effects of inflammatory cytokines on cardiac ion channels, ventricular APD, and QT interval: evidence from in vitro and animal studies

Cytokine	Ion currents	Molecular mechanisms	APD	QT/QTc interval
TNF α	I _{to} decrease [137–140]	Reduced expression of K _v 4.2/K _v 4.3 potassium channels [137, 139, 140], mediated by iNOS induction [140], ROS generation [140], and KChIP-2 inhibition [139]	Prolongation [136, 140, 141]	Prolongation [134, 135, 144]
	I _{Kr} decrease [141]	Functional impairment of hERG potassium channel, mediated by TNF-receptor 1 engagement and ROS production [141]		
	I _{Ks} decrease [142]	Mediated by sphingosine-1-phosphate generation and cyclic AMP decrease [142]		
	I _{Kur} decrease [137, 138]	Reduced expression of K _v 1.5 potassium channel [137]		
IL-1	I _{to} decrease [145]	NA	Prolongation [145, 146]	Prolongation [145]
	I _{CaL} increase [146]	Mediated by activation of cyclooxygenase and lipoxygenase pathways [146]		
IL-6	I _{CaL} increase [152]	Enhancement of Ca _v 1.2 calcium channel function [150, 152], dependent on a SHP2/ERK-mediated phosphorylation of the serine residue at the position 1829 [151]	Prolongation [152]	NA

Modified from: Lazzarini et al. [13]

TNF α tumor necrosis factor alpha, IL-1 interleukin-1, IL-6 interleukin-6, ROS reactive oxygen species, hERG human Ether-a-go-go-Related Gene K⁺ channel, I_{to} transient K⁺ outward current, I_{Kur} ultrarapidly activating component of the delayed outward rectifying current, I_{Kr} rapidly activating component of the delayed outward rectifying current, I_{Ks} slowly activating component of the delayed outward rectifying current, iNOS inducible nitric oxide synthase, KChIP-2 K(+) channel-interacting protein, SHP/ERK Src homology 2 domain-containing phosphatase/extracellular signal-regulated kinase, APD action potential duration, QTc corrected QT interval, NA data not available

to QTc prolongation, via direct electrophysiological effects on the myocardium (Table 13.4) [13]. In fact, several experimental studies provided evidence that such molecules can prolong ventricular APD by modulating the expression and/or function of several ion channels of the cardiomyocyte (*inflammatory channelopathies*), resulting in an inward shift in the balance of currents [13, 52]. The best documented are the inhibitory effects exerted by TNF α on outward potassium currents. In mouse models, cardiac-specific overexpression of TNF α is associated with QT/QTc interval prolongation [134, 135]. Ex vivo experiments demonstrated that perfused hearts from transgenic mice overexpressing TNF α showed APD prolongation and increased propensity to reentrant ventricular arrhythmias, in the presence of a significant reduction of the transient outward potassium current (I_{to}) and the rapidly activating, slowly inactivating delayed rectifier currents (I_{Kslow1}, I_{Kslow2}) in left ventricular myocytes [136, 137]. Consistent inhibitory effects on these currents were also found by Grandy et al. [138] in cardiomyocytes from ventricles of mice chronically

injected with TNF α , resulting in elevated circulating levels of this cytokine. Notably, such changes were associated with a parallel expression decrease of related channel proteins (K_v4.2, K_v4.3, and K_v1.5) in the TNF α -overexpressing model only [137, 138], possibly depending on the higher cardiac tissue TNF α concentrations reached in these animals [138]. Moreover, two further studies reported significant I_{to} and K_v4.2 downregulation in rat ventricular myocytes cultured in vitro with TNF α , also demonstrating the involvement of an intracellular pathway including overexpression of nitric oxide synthase, generation of reactive oxygen species (ROS), and inhibition of potassium channel-interacting protein 2 [139, 140]. Evidence indicates that also the rapid and the slow components of the delayed rectifier potassium current (I_{Kr} and I_{Ks}, respectively) are significantly reduced by TNF α . By using both HEK293 cells and canine cardiomyocytes, Wang et al. [141] found that TNF α prolonged APD and decreased I_{Kr} by impairing human Ether-a-go-go-Related Gene (hERG) potassium channel function, via TNF-receptor 1 engagement and ROS

production [141]. Moreover, in guinea pig ventriculocytes Hatada et al. [142] proved the inhibitory effect of TNF α on isoproterenol-activated I $_{Ks}$, possibly mediated by sphingosine-1-phosphate generation and cyclic AMP decrease. The in vivo relevance of all these electrophysiological effects has been recently confirmed by the group of Kollias in two TNF α -overexpressing mouse models developing polyarthritis, where QTc prolongation (*Tg197* model) [143] and premature mortality associated with increased incidence of fatal arrhythmic events (*Tnf^{ARE}* model) [144] have been demonstrated.

Although less extensively investigated, emerging experimental data support a significant QT-prolonging potential also for IL-1 and IL-6, able to increase ventricular APD by inhibiting outward K $^+$ and/or enhancing inward Ca $^{++}$ currents. A recent study by Monnerat et al. [145] showed that IL-1 β incubation increases APD in ventricular rat cardiomyocytes as well as field potential duration (FPD) in human induced pluripotent stem cell-derived cardiomyocytes, along with a ~35% reduction of I $_{to}$. Moreover, the same authors demonstrated that in diabetic rats showing QTc prolongation and increased susceptibility to arrhythmias, the genetic deletion of the IL-1-receptor or the treatment with the IL-1-receptor antagonist anakinra was sufficient to prevent both electric abnormalities in these animals [145]. A further possible mechanism by which IL-1 β could increase QTc length is the enhancement of L-type Ca $^{++}$ current (I $_{CaL}$), although available data are conflicting. In fact, while Li et al. [146] found that IL-1 β significantly augmented I $_{CaL}$ density and prolonged APD via cyclooxygenase and lipoxygenase pathways in guinea pig papillary myocytes, other authors reported opposite effects on such current (despite no concomitant data on APD were provided) [147–149]. Regarding IL-6, several studies provided evidence that it can increase I $_{CaL}$ in cardiomyocytes [150–152], a mechanism probably accounting for the ventricular APD prolongation induced by such cytokine [152]. In particular, IL-6 activates a SHP2/ERK (Src homology 2 domain-containing phosphatase/extracellular signal-regulated kinase)-mediated signaling cas-

cade leading to I $_{CaL}$ enhancement as a result of the phosphorylation of the serine residue at the position 1829 of the Cav1.2 calcium channel subunit [151]. In addition, IL-6 also inhibits I $_{Kr}$, by activating Janus kinase signaling cascade [unpublished data].

Altogether, these data provide robust mechanistic support to the hypothesis that TNF α , IL-1 β , and IL-6 represent key mediators of inflammation-induced QTc prolongation. The previously reported evidence that circulating levels of these cytokines correlated with QTc length in patients with inflammatory diseases [33, 58, 59, 65] as well as apparently healthy subjects [130], strongly indicates that these pathophysiological mechanisms are also crucially involved in vivo, a conclusion also supported by several animal models of cardiac or systemic inflammation. In mice with experimental autoimmune myocarditis (EAM), APD is significantly prolonged along with increased tissue expression of IL-6 and TNF α , reduced I $_{to}$ current density, and enhanced susceptibility to triggered ventricular arrhythmias [153, 154]. Moreover, in a murine model of myocardial infarction (MI), lipopolysaccharide (LPS)-induced systemic inflammation markedly increases APD and ventricular arrhythmia propensity, when compared to non-LPS-injected MI animals [155]. Such electric changes, showing an association with the degree of macrophage activity and IL-1 β expression in the myocardium [155], were significantly attenuated by anti-IL1 treatment with anakinra [156]. Other authors demonstrated the key role of IL-1 β in increasing APD and QTc interval, as well as ventricular arrhythmia vulnerability in diabetic mice [145]. Moreover, in cardiac-specific liver kinase B1 knockout mice, a model of spontaneous cardiac and systemic inflammation, QTc prolongs as much as circulating levels of CRP, TNF α , and IL-6 increase [157]. Notably, in these animals SCD was a common finding, frequently resulting from ventricular arrhythmias, including TdP degenerating to ventricular fibrillation [157].

Finally, increasing evidence suggests that inflammation could promote QTc prolongation also in an indirect manner, by inducing cytokine-mediated cardiac autonomic dysfunction via

central (*inflammatory reflex*) and peripheral mechanisms (left stellate ganglia activation) [13]. These changes could intriguingly have an important role in precipitating life-threatening arrhythmias during inflammatory activation, given that cardiac sympathetic overactivity is a well-recognized trigger for arrhythmic events in patients with LQTS [122].

The Role of Autoimmunity in Long QT Syndrome

Autoimmunity is recently emerging as a novel mechanism of cardiac arrhythmias, not only in patients with autoimmune diseases (AD) but also in otherwise healthy subjects with “idiopathic” rhythm disorders [158]. Different types of arrhythmogenic autoantibodies affecting cardiac electrophysiology by directly targeting proteins expressed on the myocyte surface have been identified [158, 159]. In particular, some of these autoantibodies can significantly interfere with the function of specific ion channels critically involved in determining ventricular APD (*autoimmune channelopathies*), thus leading to acquired forms of LQTS of autoimmune origin [160]. To date, the most investigated autoimmune channelopathy associated with LQTS is related to the presence of anti-Ro/SSA antibodies (anti-Ro/SSA) cross-reacting with the hERG-K⁺ channel [161, 162]. Recent data suggest that other autoantibodies recognizing K⁺ or Ca⁺⁺ channels, i.e., anti-voltage-gated potassium channel K_v1.4 antibodies and agonist-like anti-L-type Ca⁺⁺ antibodies, might also promote life-threatening arrhythmias by prolonging APD/QTc interval [160].

Clinical Evidence

Anti-Ro/SSA, including the two main subtypes anti-Ro/SSA-52kD and anti-Ro/SSA-60kD, primarily recognize the Ro/SSA antigen, an intracellular ribonucleoprotein constituted by two subunits of different molecular weight, named Ro52/E3 ubiquitin-protein ligase and Ro60,

respectively [163]. Maternal anti-Ro/SSA, particularly anti-Ro/SSA-52kD, play a key pathogenic role in autoimmune congenital heart block (ACHB) [164], at least in part mediated by an inhibitory cross-reaction with L-type Ca⁺⁺ channels in the cardiac conduction system of the fetus [165, 166]. Anti-Ro/SSA are frequently detected in patients with AD, particularly Sjögren’s syndrome and SLE [163], but also in a non-negligible percentage of apparently healthy subjects (0.5–2.7%) [166–169]. Notably, although techniques such as immunoenzymatic tests (ELISA, FEIA) and line blot immunoassay (LIA) are routinely used, evidence points to immuno-Western blot (IWB), as the most sensitive method to detect arrhythmogenic autoantibodies [170].

Besides conduction system, accumulating clinical data indicate that ventricular repolarization represents another potential target of anti-Ro/SSA pathogenic activity, both in fetal and in adult hearts. In fact, several studies in the last two decades provided evidence that circulating anti-Ro/SSA are associated with a higher risk of developing acquired LQTS [161], as well as the occurrence of ventricular arrhythmias [63, 171], including TdP (Tables 13.5 and 13.6) [172, 173].

The first data were obtained in newborns in early 2000s, when Cimaz et al. [174] reported how infants from anti-Ro/SSA-positive mothers presented a QTc interval significantly prolonged when compared to those born from negative mothers, despite no development of ACHB. Notably, in a prospective follow-up study the same authors demonstrated that such abnormality was transient, as it spontaneously recovered during the first year of life in parallel with the disappearance of acquired maternal anti-Ro/SSA in the blood [175]. Both such findings were later confirmed by two independent groups, one from England showing that QTc was significantly longer in children born from anti-Ro/SSA-positive vs. anti-Ro/SSA-negative mothers [176] and the other one from Canada reporting that among 116 newborns without ACHB, 17 (15%) had transient QTc prolongation [177]. Although none of these studies reported concomitant occurrence of life-threatening arrhythmias/SCD, a case of QTc prolongation complicated with pre-

Table 13.5 Clinical studies on anti-Ro/SSA antibodies and QTc in newborns

Authors	Study population	Anti-Ro/ SSA+ patients (n)	Anti-Ro/ SSA- patients (n)	Main results
Cimaz et al. [174]	Children of CTD mothers	21	7	Mean QTc significantly longer in anti-Ro/SSA-positive subjects
Gordon et al. [176]	Children of CTD mothers	38	7	Mean QTc significantly longer in children of anti-Ro/SSA-positive mothers
Cimaz et al. [175]	Children of anti-Ro/SSA-positive mothers	21	–	Concomitant disappearance of QTc prolongation and acquired maternal antibodies at 1-year follow-up
Costedoat-Chalumeau et al. [182]	Children of CTD mothers	58	85	No differences in mean QTc duration or in QTc prolongation prevalence between groups
Duke et al. [171]	Child of an anti-Ro/SSA-positive mother	1	–	QTc prolongation and ventricular tachycardia
Motta et al. [179]	Children of CTD mothers	51	50	Mean QTc slightly longer in children of anti-Ro/SSA-positive mothers ($p = 0.06$)
Gerosa et al. [183]	Children of AD mothers	60	30	No difference in the prevalence of QTc prolongation between the groups
Jaeggi et al. [177]	Children of anti-Ro/SSA-positive mothers	116	–	Transient QTc prolongation in 14.6% of cases

CTD connective tissue disease, AD autoimmune disease, QTc corrected QT interval

natal ventricular tachycardia was described in a ACHB fetus born from an anti-Ro/SSA-positive mother [171].

The existence of a link between anti-Ro/SSA, QTc prolongation, and ventricular arrhythmias was confirmed and further characterized by several other studies performed in adults. In our Institution, we first provide evidence that anti-Ro/SSA-positive CTD patients showed a high prevalence of QTc prolongation, with a mean QTc length significantly increased when compared to negative patients [61]. In a following 24-hour ECG monitoring study, we also demonstrated that such abnormality persisted throughout the day-night time and correlated with an increased incidence of complex ventricular arrhythmias [63]. Consistent data were later reported by Bourre-Tessier et al. [70] in two large consecutive studies involving SLE patients, where the presence of anti-Ro/SSA positivity was associated with a 5–12 times higher risk of presenting QTc prolongation. Moreover, the authors found that such a risk increased as much as autoantibody levels were high and that the association between anti-Ro/SSA and QTc prolongation strongly persisted over a 17-month follow-up [70]. The key pathogenic role of circu-

lating anti-Ro/SSA concentrations was also confirmed in our own CTD cohort, where the existence of a direct correlation between antibody levels and QTc length was demonstrated. In addition, we provided evidence that anti-Ro/SSA specificity is crucial, as when considered separately only anti-Ro/SSA-52kD subtype levels remained significantly associated with QTc duration [64]. More recently, other supportive studies have been published. Pisoni et al. [65] showed that QTc prolongation was more common in anti-Ro/SSA-positive (20%) vs. anti-Ro/SSA-negative CTD patients (0%), and Sham et al. [69] found that anti-Ro/SSA positivity was associated with a significantly prolonged QTc in a SLE cohort. Besides reporting that anti-Ro/SSA-52kD-positive CTD patients had higher QTc maximum values when compared to both negative subjects and healthy controls, Tufan et al. [178] demonstrated that also Tp-Te and Tp-Te/QT were significantly increased in these patients, with a strong direct correlation between Tp-Te duration and anti-Ro/SSA-52kD titer. In addition, evidence exists that, in adult patients, anti-Ro/SSA positivity is associated with TdP, regardless of the presence of a manifest AD, thus possibly representing a silent risk factor for life-

Table 13.6 Clinical studies on anti-Ro/SSA antibodies and QTc/TdP in adults

Author, year	Study population	Anti-Ro/SSA+ patients (<i>n</i>)	Anti-Ro/SSA- patients (<i>n</i>)	Main results
Gordon et al. [180]	AD patients	49	62	Mean QTc slightly longer in anti-Ro/SSA-positive patients ($p = 0.06$)
Lazzerini et al. [61]	CTD patients	31	26	Mean QTc significantly longer and prevalence of QTc prolongation significantly higher in anti-Ro/SSA-positive subjects
Costedoat-Chalumeau et al. [62]	CTD patients	32	57	No differences in mean QTc duration or in QTc prolongation prevalence between groups
Lazzerini et al. [63]	CTD patients	26	20	Mean QTc significantly longer and prevalence of QTc prolongation significantly higher in anti-Ro/SSA-positive subjects; QTc prolongation significantly associated with the presence of complex ventricular arrhythmias
Bourrè-Tessier et al. [70]	SLE patients (two studies)	57 113	93 165	5.1–12.6 times higher risk of QTc prolongation in anti-Ro/SSA-positive vs. anti-Ro/SSA-negative group
Lazzerini et al. [64]	CTD patients	25	24	Mean QTc significantly longer and prevalence of QTc prolongation significantly higher in anti-Ro/SSA-positive subjects; significant correlation between anti-Ro/SSA-52kD concentration and QTc duration
Nomura et al. [181]	SLE patients	43	47	Anti-Ro/SSA positivity slightly more frequent among SLE patients with QTc prolongation ($p = 0.08$)
Teixeira et al. [74]	SLE patients	111	206	No difference in the prevalence of marked QTc prolongation (>500 msec) between groups
Massie et al. [88]	SSc patients	148	541	No difference in the prevalence of QTc prolongation between groups
Bourrè-Tessier et al. [71]	SLE patients	283	314	Prevalence of QTc prolongation slightly higher in anti-Ro/SSA-positive subjects, but not significantly for wide confidence intervals
Pisoni et al. [65]	AD patients	55	18	Anti-Ro/SSA positivity significantly more frequent among CTD patients with QTc prolongation (all patients with QTc prolongation were anti-Ro/SSA positive)
Sham et al. [69]	SLE patients	47	53	Mean QTc significantly longer in anti-Ro/SSA-positive subjects
Nakamura et al. [172]	TdP patient	1	–	Marked QTc prolongation and TdP in an anti-Ro/SSA-positive woman without AD
Lazzerini et al. [173]	TdP patients	25	–	High prevalence of anti-Ro/SSA-52kD in unselected TdP patients (60%)
Geraldino-Pardilla et al. [56]	SLE patients	28	22	No association between anti-Ro/SSA positivity and QTc length
Tufan et al. [178]	CTD patients	15	39	QTc maximum, Tp-e, and Tp-e/QT ratio higher in anti-Ro/SSA-52kD-positive vs. anti-Ro/SSA-52kD-negative CTD patients (and healthy controls, $n = 22$); Tp-Te duration strongly correlated with anti-Ro/SSA-52kD titer

CTD connective tissue disease, AD autoimmune disease, SLE systemic lupus erythematosus, SSc systemic sclerosis, QTc corrected QT interval, TdP torsades de pointes, Tp-e interval from the peak to the end of the T wave, Tp-e/QT ratio interval from the peak to the end of the T wave/QT interval ratio

threatening arrhythmias/SCD in the apparently healthy population. Nakamura et al. [172] reported for the first time the case of an otherwise healthy woman developing TdP, despite

intensive search excluded genetic or acquired known causes of QT prolongation. In this patient, asymptomatic for AD, only specific testing revealed high circulating levels of anti-Ro/

SSA. These data were confirmed and expanded in a cohort of 25 consecutive TdP patients, where anti-Ro/SSA-52kD positivity was detected in 60% of cases, almost always in the absence of a concomitant AD (Fig. 13.2) [173]. Notably, likewise in ACHB [170] and CTD patients [64], also in these subjects IWB was the most sensitive technique in detecting arrhythmogenic autoantibodies. Finally, it must be mentioned that a num-

ber of other studies found near statistically significant differences in QTc duration and/or QTc prevalence between anti-Ro/SSA-positive and anti-Ro/SSA-negative patients, possibly due to relatively small sample sizes. Motta et al. [179] showed that mean QTc of infants born from anti-Ro/SSA-positive mothers was slightly longer than controls ($p = 0.06$), and consistent findings were reported by Gordon et al. [180] by

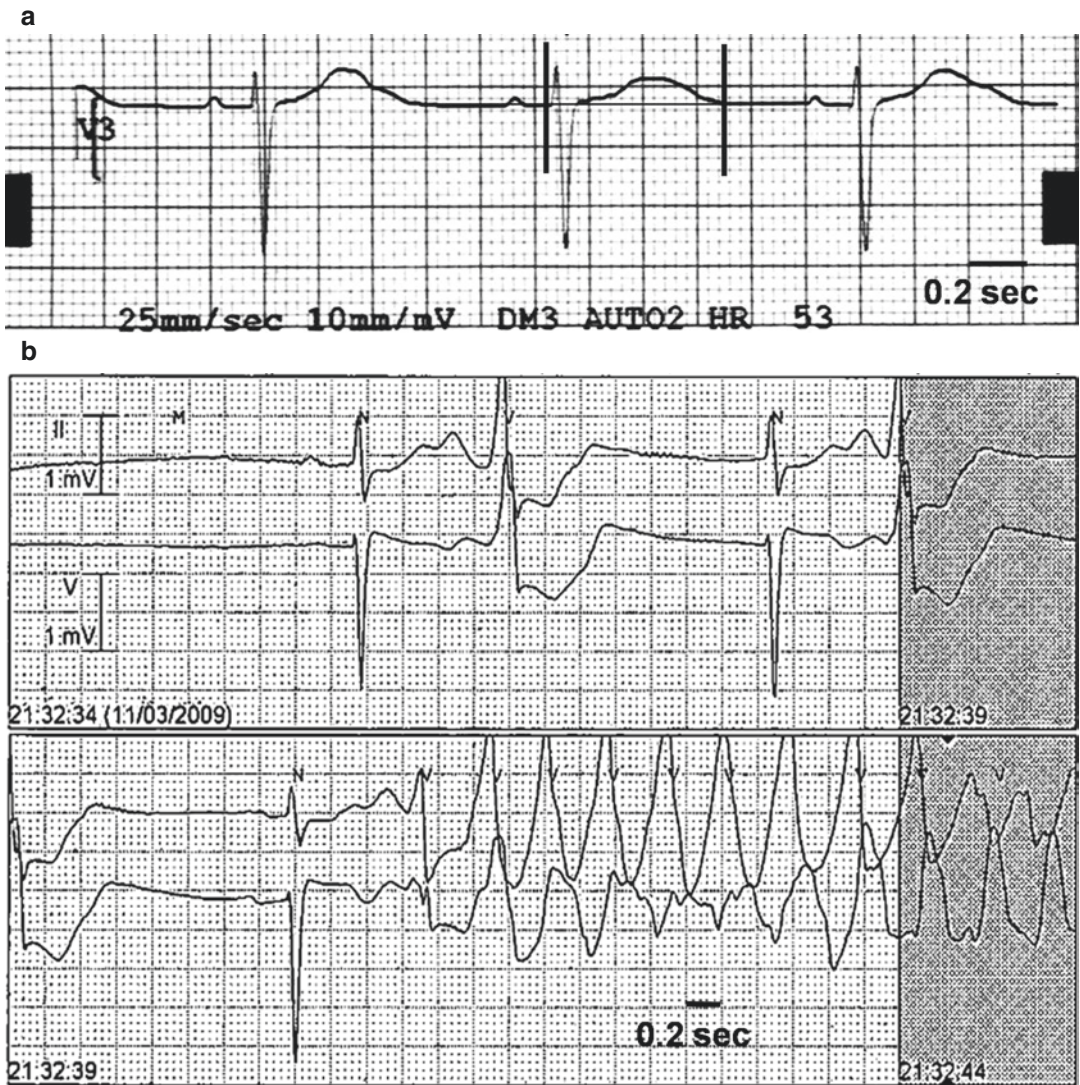


Fig. 13.2 QTc prolongation and torsades de pointes in a patient with circulating anti-Ro/SSA antibodies. ECG strip in sinus rhythm (a) and during torsades de pointes (b) from a patient who is anti-Ro/SSA positive and has a

QTc of 620 ms. Vertical lines in lead V3 show QT interval. (Reproduced/adapted from Lazznerini et al. [173], with permission from Wolters Kluwer Health)

comparing anti-Ro/SSA-positive vs. anti-Ro/SSA-negative adults with CTD ($p = 0.06$). Moreover, two studies performed in adult SLE patients [71, 181] found that anti-Ro/SSA positivity was slightly more frequent among subjects with QTc prolongation ($p = 0.08$) [181] and vice versa the percentage of patients presenting with a prolonged QTc was slightly higher in the anti-Ro/SSA-52kD-positive group, but not significantly for wide confidence intervals (Tables 13.5 and 13.6) [71].

Altogether, these data strongly support the existence of a clinical association between anti-Ro/SSA and LQTS. Nevertheless, it should be remarked that some authors found conflicting results, both in newborns [182, 183] and in adults [56, 62, 74, 88] (Tables 13.5 and 13.6), and, even in positive studies, prevalence of QTc prolongation varied significantly, from 10% to 60% [64, 161]. Several factors may account for such discrepancies throughout the studies, including disease-specific differences in autoantibody titers (specifically the anti-Ro/SSA-52kD subtype [184], by most authors not separately evaluated), as well as QTc measurement methods and QTc prolongation cutoffs used. Moreover, electrophysiological considerations related to the aptitude of anti-Ro/SSA to concomitantly interact with multiple ion channels

on the cardiomyocyte could also contribute to explain discrepancies [160, 185] (see below *Pathogenesis and pathophysiology* and chapter titled “Pathogenesis of Autoimmune-Associated LQTS”).

Recent clinical evidence preliminary suggests that anti-ion channel autoantibodies other than anti-Ro/SSA might be also responsible for acquired LQTS and life-threatening arrhythmias [160] (Table 13.7). Anti-K_v1.4 antibodies, recognizing the cardiac channel that by conducting I_{to} critically determines the early repolarization phase of the AP [186], are found in up to 20% of patients with myasthenia gravis (MG) [187–189]. The group of Suzuki demonstrated that anti-K_v1.4-positive MG subjects frequently showed QTc prolongation (15–35%) [188, 189], also providing evidence of an association between such electrocardiographic abnormality and TdP/SCD [189]. Agonist-like anti-L-type Ca⁺⁺ antibodies exerting APD-prolonging effects were detected in a significant percentage of patients with idiopathic and ischemic cardiomyopathies, where represented independent predictors of ventricular tachycardia and SCD [190, 191]. However, although electrophysiological considerations predict that circulating anti-L-type Ca⁺⁺ antibodies may be associated with a LQTS electrocardiographic phenotype [190,

Table 13.7 Clinical studies demonstrating an association between anti-Kv1.4 or agonist-like anti-L-type Ca⁺⁺ channel antibodies and QTc prolongation/ventricular arrhythmias/SCD

Authors	Study population	Antibody+ patients (n)	Antibody- patients (n)	Main results
Suzuki et al. [188]	MG patients	11	45	QTc prolongation prevalence significantly higher in anti-Kv1.4-positive patients (36% vs. 0%)
Suzuki et al. [189]	MG patients	70	–	QTc prolongation in 14% of anti-Kv1.4-positive patients, who presented high prevalence (20%) of fatal QT-associated arrhythmias
Xiao et al. [190]	DCM patients	39	41	Increased incidence of ventricular tachycardia and SCD in anti-L-type Ca ⁺⁺ channel-positive patients; anti-L-type Ca ⁺⁺ channel positivity was the strongest independent predictor of SCD
Yu et al. [191]	DCM patients	43	689	Increased incidence of SCD in anti-L-type Ca ⁺⁺ channel-positive patients; anti-L-type Ca ⁺⁺ channel positivity was an independent predictor of SCD
	ICM patients	51	1048	

MG myasthenia gravis, QTc corrected QT interval, DCM dilated cardiomyopathy, ICM ischemic cardiomyopathy, SCD sudden cardiac death

[192], studies specifically focused at determining occurrence and prevalence of QTc prolongation in these patients are currently lacking.

Molecular Basis and Pathophysiology

An increasing body of experimental data point to hERG-K⁺ channel as the molecular target responsible for anti-Ro/SSA-associated LQTS (Table 13.8) [160–162, 172, 173, 193]. The chapter titled “Pathogenesis of Autoimmune-Associated LQTS” covers the basic aspects of the pathogenesis. Notably, it is well demonstrated that anti-Ro/SSA can also block cardiac Ca⁺⁺ channels [165, 194–197], and this multi-channel electrophysiological interference could contribute to explain the above-reported discrepancies in clinical studies on QTc prolongation. In fact, simulation studies support the hypothesis that a concomitant inhibitory effect of anti-Ro/SSA on I_{CaL} during the plateau phase can partially counteract the I_{Kr} inhibition-dependent prolongation of APD and as a result determines the net duration of QTc in vivo [193]. Nevertheless, since I_{Kr} is activated after the peak of T wave [186, 198], specific measurement of T_p-T_{end} interval on the electrocardiogram should in any case reveal if anti-Ro/SSA are interfering on the ventricular repolarization of a patient. Accordingly, the recent demonstra-

tion by Tufan et al. [178] that Tp-Te is significantly prolonged in anti-Ro/SSA-52kD-positive CTD subjects, also when the QTc was found normal, confirms this view and points to this parameter as a better reflection of the anti-Ro/SSA-mediated I_{Kr} inhibition in vivo.

Regarding the other anti-ion channel autoantibodies possibly associated with LQTS, much less information on the potential underlying mechanisms is currently available (Table 13.8). Although it is proposed that anti-Kv1.4 antibodies can prolong QTc by inhibiting I_{to} via direct binding with the channel [187], at the moment no mechanistic studies specifically tested such a hypothesis. The evidence that some anti-Kv1.4-positive MG patients developed signs of myocarditis suggests that besides functional interference, also inflammatory heart changes may contribute to LQTS and TdP occurrence [188, 189]. More investigated are the molecular arrhythmogenic mechanisms of agonist-like anti-L-type Ca⁺⁺ channel antibodies, probably triggered by an increased Ca⁺⁺ influx during the AP plateau phase. Indeed, experimental evidence indicates that such autoantibodies can directly activate the channel by recognizing an intracellular epitope at the N-terminus of the Ca_v1.2 subunit [190, 192]. Xiao et al. demonstrated that affinity-purified autoantibodies from dilated cardiomyopathy patients enhance I_{CaL} in oocytes, prolong APD, and promote early after-

Table 13.8 Effects of anti-ion channel autoantibodies on cardiac ion currents, ventricular APD, and QT interval: evidence from in vitro and animal studies

Autoantibody	Functional effect	Ion current	Binding site	APD	QTc interval
Anti-hERG-K ⁺ channel (anti-Ro/SSA)	Inhibiting [162, 172, 173, 193]	I _{Kr} decrease [162, 172, 173, 193]	Pore region (extracellular loop between S5-S6 of D1) [162, 173, 193]	Prolongation [162, 193]	Prolongation [162, 193]
Anti-L-type -Ca ⁺⁺ channel	Agonist-like [190, 192]	I _{CaL} decrease [190, 192]	Intracellular N-terminus of D1 [190, 192]	Prolongation (with EAD occurrence and VT induction) [190]	NA
Anti-K _v 1.4 channel	Inhibiting ^a	I _{to} decrease ^a	NA	NA	NA

hERG human Ether-a-go-go-Related Gene K⁺ channel, I_{Kr} rapidly activating component of the delayed outward rectifying current, I_{CaL} L-type calcium current, I_{to} transient K⁺ outward current, S5–S6 5th–6th transmembrane segments, D1 domain 1 of the channel α₁ subunit, AP action potential, APD action potential duration, EADs early afterdepolarizations, VT ventricular tachycardia, QTc corrected QT interval, NA data not available

^aProposed, as no direct evidence is currently available

depolarizations in rat ventricular myocytes, also inducing ventricular tachycardia in perfused hearts [190, 192].

Conclusions and Clinical Perspectives

Inflammation and autoimmunity are increasingly recognized as causative factors of LQTS and TdP in patients with immuno-inflammatory diseases, but also in apparently healthy subjects, where asymptomatic low-grade chronic inflammation and/or circulating anti-ion channel autoantibodies (particularly anti-Ro/SSA) might represent occult predisposing factors for unexpected life-threatening arrhythmias/SCD [13, 160]. In fact, likewise other better recognized determinants of LQTS, both genetic [199] and acquired [200], inflammatory and autoimmune mechanisms alone are not able in most cases to prolong QTc as critically as to precipitate TdP development. Nevertheless, by reducing the ventricular repolarization reserve [201], they could significantly enhance the risk of malignant arrhythmias when other classical QT-prolonging factors (drugs, electrolyte imbalances, genetic mutations/polymorphisms, etc.) are concomitantly present [33, 173, 202–205]. However, the potential impact of inflammatory and autoimmune channelopathies on ventricular repolarization is to date largely overlooked in the clinical practice and therefore poorly considered in terms of diagnostic and therapeutic implications in LQTS, even when an immuno-inflammatory disease is clinically evident. In this view, increasing awareness to the existence of these forms is essential to identify and adequately manage those patients. Indeed, systemic inflammatory activation, also subclinical, may be easily revealed by routine markers, particularly CRP. Anti-Ro/SSA testing is largely available in the clinical practice worldwide, although IWB technique is recommended for detecting arrhythmogenic subtypes [64, 173].

Given that arrhythmogenic effects of cytokines and autoantibodies are due to a functional and thereby potentially reversible electrophysio-

logical interference with the channel function [13, 52, 160], anti-inflammatory and immunomodulating interventions might represent an innovative anti-arrhythmic approach in a number of subjects. Accordingly, preliminary data suggest a rapid effectiveness of immunosuppressive therapies in reducing QTc duration in patients with inflammatory or anti-Ro/SSA-associated LQTS [33, 59, 99, 206]. Moreover, based on ex vivo studies with sera from anti-Ro/SSA-positive TdP subjects [173] or affinity-purified anti-L-type Ca^{++} channel autoantibodies from DCM patients [190, 192], showing how competing peptides can prevent autoantibody recognition of the channel binding site, as well as electrophysiological changes and VA occurrence, short decoy peptide-based therapy distracting the pathogenic antibodies could be also intriguingly proposed in autoimmune channelopathies.

Finally, induction of functional anti-ion channel antibodies by peptide vaccination might represent an original anti-arrhythmic approach in inherited channelopathies, specifically in congenital LQTS patients refractory to conventional treatments, as recently hypothesized by Li et al. [207]. Indeed, these authors demonstrated that immunization against $K_v1.7$ channel peptide accelerates cardiac repolarization and ameliorates drug-induced QTc prolongation in a rabbit model via induction of agonist-like anti- $K_v1.7$ antibodies increasing I_{Ks} . Based on such theoretical premises, the evidence that guinea pig vaccination with a hERG channel pore-derived peptide generates I_{Kr} -inhibiting antibodies which slow ventricular repolarization [193] might also lead to speculate on a therapeutic potential for hERG channel immunization in selected patients with congenital short QT syndrome.

References

1. Moss AJ, Long QT. Syndrome. JAMA. 2003;289(16):2041–4.
2. Drew BJ, Ackerman MJ, Funk M, Gibler WB, Kligfield P, Menon V, et al. Prevention of torsade de pointes in hospital settings: a scientific statement from the American Heart Association and the

- American College of Cardiology Foundation. *J Am Coll Cardiol*. 2010;55(9):934–47.
3. El-Sherif N, Turitto G. Torsade de pointes. *Curr Opin Cardiol*. 2003;18(1):6–13.
 4. El-Sherif N, Turitto G, Boutjdir M. Congenital long QT syndrome and torsade de pointes. *Ann Noninvasive Electrocardiol*. 2017;22(6):e12481.
 5. El-Sherif N, Turitto G, Boutjdir M. Acquired long QT syndrome and torsade de pointes. *Pacing Clin Electrophysiol*. 2018;41:414–21.
 6. Schwartz PJ, Stramba-Badiale M, Crotti L, Pedrazzini M, Besana A, Bosi G, et al. Prevalence of the congenital long-QT syndrome. *Circulation*. 2009;120(18):1761–7.
 7. Tisdale JE, Wroblewski HA, Overholser BR, Kingery JR, Trujillo TN, Kovacs RJ. Prevalence of QT interval prolongation in patients admitted to cardiac care units and frequency of subsequent administration of QT interval-prolonging drugs: a prospective, observational study in a large urban academic medical center in the US. *Drug Saf*. 2012;35(6):459–70.
 8. Pickham D, Helfenbein E, Shinn JA, Chan G, Funk M, Weinacker A, et al. High prevalence of corrected QT interval prolongation in acutely ill patients is associated with mortality: results of the QT in Practice (QTIP) Study. *Crit Care Med*. 2012;40(2):394–9.
 9. Pasquier M, Pantet O, Hugli O, Pruvot E, Buclin T, Waeber G, et al. Prevalence and determinants of QT interval prolongation in medical inpatients. *Intern Med J*. 2012;42(8):933–40.
 10. Viskin S. Long QT syndromes and torsade de pointes. *Lancet*. 1999;354(9190):1625–33.
 11. Møller S, Bernardi M. Interactions of the heart and the liver. *Eur Heart J*. 2013;34(36):2804–11.
 12. Gonzalez CD, de Serey M, Sinay I, Santoro S. Endocrine therapies and QTc prolongation. *Curr Drug Saf*. 2010;5(1):79–84.
 13. Lazznerini PE, Capecchi PL, Laghi-Pasini F. Long QT syndrome: an emerging role for inflammation and immunity. *Front Cardiovasc Med*. 2015;2:26.
 14. Ramamurthy S, Talwar KK, Goswami KC, Shrivastava S, Chopra P, Broor S, et al. Clinical profile of biopsy proven idiopathic myocarditis. *Int J Cardiol*. 1993;41(3):225–32.
 15. Karjalainen J, Viitasalo M, Kala R, Heikkilä J. 24-hour electrocardiographic recordings in mild acute infectious myocarditis. *Ann Clin Res*. 1984;16(1):34–9.
 16. Ukena C, Mahfoud F, Kindermann I, Kandolf R, Kindermann M, Böhm M. Prognostic electrocardiographic parameters in patients with suspected myocarditis. *Eur J Heart Fail*. 2011;13(4):398–405.
 17. Panikkath R, Reinier K, Uy-Evanado A, Teodorescu C, Hattenhauer J, Mariani R, et al. Prolonged Tpeak-to-tend interval on the resting ECG is associated with increased risk of sudden cardiac death. *Circ Arrhythm Electrophysiol*. 2011;4(4):441–7.
 18. Güneş HM, Babur Güler G, Güler E, Demir GG, Teber MK, Kızıllırmak F, et al. Assessment of repolarization abnormalities in baseline electrocardiograms of patients with myocarditis. *Turk J Med Sci*. 2017;47(5):1333–9.
 19. Finley JP, Radford DJ, Freedom RM. Torsade de pointes ventricular tachycardia in a newborn infant. *Br Heart J*. 1978;40(4):421–4.
 20. Mitamura E, Mifune J, Kanamori K, Hifumi N, Shimizu O, Yamamura I, et al. A case of torsade de pointes tachycardia complicating diphtheria. *Kokyo To Junkan*. 1985;33(2):223–8.
 21. Sareli P, Schamroth CL, Passias J, Schamroth L. Torsade de pointes due to coxsackie B3 myocarditis. *Clin Cardiol*. 1987;10(5):361–2.
 22. Devriendt J, Staroukine M, Schils E, Sivaciyan B, Van Beers D. Legionellosis and “torsades de pointes”. *Acta Cardiol*. 1990;45(4):329–33.
 23. Badorff C, Zeiher AM, Hohnloser SH. Torsade de pointes tachycardia as a rare manifestation of acute enteroviral myocarditis. *Heart*. 2001;86(5):489–90.
 24. Izawa A, Yazaki Y, Hayashi S, Imamura H, Kusama Y, Isobe M. Transient left ventricular aneurysm and hypertrophy accompanied by polymorphic ventricular tachycardia in a patient suspected of acute myocarditis. *Jpn Heart J*. 2000;41(1):97–102.
 25. Gowani SA, Kumar A, Arora S, Lahiri B. Legionella pneumonia complicated by myocarditis and torsades de pointes: a case report and review of literature. *Conn Med*. 2013;77(6):331–4.
 26. Jensen TB, Dalsgaard D, Johansen JB. Cardiac arrest due to torsades de pointes ventricular tachycardia in a patient with Lyme carditis. *Ugeskr Laeger*. 2014;176(35):pii: V03140168.
 27. Khazan M, Mathis AS. Probable case of torsades de pointes induced by fluconazole. *Pharmacotherapy*. 2002;22(12):1632–7.
 28. Sayar N, Terzi S, Yilmaz HY, Atmaca H, Kocak F, Dayi SU, et al. A case of prosthetic mitral valve Brucella endocarditis complicated with torsades de pointes. *Heart Vessel*. 2006;21(5):331–3.
 29. Irie T, Kaneko Y, Nakajima T, Saito A, Kurabayashi M. QT interval prolongation and torsade de pointes induced by propofol and hypoalbuminemia. *Int Heart J*. 2010;51(5):365–6.
 30. Aypar E, Kendirli T, Tutar E, Çiftçi E, Ince E, Ileri T, et al. Voriconazole-induced QT interval prolongation and torsades de pointes. *Pediatr Int*. 2011;53(5):761–3.
 31. Tounsi A, Abid L, Akrouf M, Hentati M, Kammoun S. QT prolongation complicated with torsades de pointes in prosthetic mitral valve endocarditis: a case report. *Case Rep Med*. 2012;2012:574923.
 32. Aleksova N, Juneau D, Dick A, Green M, Birmie D, Beanlands RS, et al. Role of 18F-fluorodeoxyglucose/positron emission tomography imaging to demonstrate resolution of acute myocarditis. *Can J Cardiol*. 2017;33(2):293.e3–5.
 33. Lazznerini PE, Laghi-Pasini F, Bertolozzi I, Morozzi G, Lorenzini S, Simpatico A, et al. Systemic inflammation as a novel QT-prolonging risk fac-

- tor in patients with torsades de pointes. *Heart*. 2017;103(22):1821–9.
34. Cunha-Neto E, Chevillard C. Chagas disease cardiomyopathy: immunopathology and genetics. *Mediat Inflamm*. 2014;2014:683230.
 35. Rassi A, Rassi SG. Predictors of mortality in chronic Chagas disease: a systematic review of observational studies. *Circulation*. 2007;115(9):1101–8.
 36. Salles G, Xavier S, Sousa A, Hasslocher-Moreno A, Cardoso C. Prognostic value of QT interval parameters for mortality risk stratification in Chagas' disease: results of a long-term follow-up study. *Circulation*. 2003;108(3):305–12.
 37. Williams-Blangero S, Magalhaes T, Rainwater E, Blangero J, Corrêa-Oliveira R, Vandenberg JL. Electrocardiographic characteristics in a population with high rates of seropositivity for *Trypanosoma cruzi* infection. *Am J Trop Med Hyg*. 2007;77(3):495–9.
 38. Sabino EC, Ribeiro AL, Lee TH, Oliveira CL, Carneiro-Proietti AB, Antunes AP, et al. Detection of *Trypanosoma cruzi* DNA in blood by PCR is associated with Chagas cardiomyopathy and disease severity. *Eur J Heart Fail*. 2015;17(4):416–23.
 39. Bradfield J, Woodbury B, Traina M, Hernandez S, Sanchez D, Wachsnier R, et al. Repolarization parameters are associated with mortality in chagas disease patients in the United States. *Indian Pacing Electrophysiol J*. 2014;14(4):171–80.
 40. Garcia S, Ramos CO, Senra JF, Vilas-Boas F, Rodrigues MM, Campos-de-Carvalho AC, et al. Treatment with benznidazole during the chronic phase of experimental Chagas' disease decreases cardiac alterations. *Antimicrob Agents Chemother*. 2005;49(4):1521–8.
 41. Eickhoff CS, Lawrence CT, Sagartz JE, Bryant LA, Labovitz AJ, Gala SS, et al. ECG detection of murine chagasic cardiomyopathy. *J Parasitol*. 2010;96(4):758–64.
 42. Navarro IC, Ferreira FM, Nakaya HI, Baron MA, Vilar-Pereira G, Pereira IR, et al. MicroRNA transcriptome profiling in heart of trypanosoma cruzi-infected mice: parasitological and cardiological outcomes. *PLoS Negl Trop Dis*. 2015;9(6):e0003828.
 43. Alvarado-Tapias E, Rivas-Coppola M, Alvarado A, Bello M, Briceño M, Rodríguez-Bonfante C, et al. Adenosine induces ventricular arrhythmias in hearts with chronic chagas cardiomyopathy. *Rev Esp Cardiol*. 2010;63(4):478–82.
 44. Saraiva LR, Santos CL, de Aguiar IR. The prolongation of the QT interval in the acute rheumatic carditis: an enigma. *Arq Bras Cardiol*. 2006;87(6):e254–6.
 45. Alp H, Baysal T, Altın H, Karataş Z, Karaarslan S. QT and P-wave dispersions in rheumatic heart disease: prospective long-term follow up. *Pediatr Int*. 2014;56(5):681–8.
 46. Kaul UA, Gambhir DS, Khalilullah M. Torsade de pointes: manifestation of acute rheumatic carditis. *Indian Heart J*. 1983;35(2):117–9.
 47. Liberman L, Hordof AJ, Alfayyadh M, Salafia CM, Pass RH. Torsade de pointes in a child with acute rheumatic fever. *J Pediatr*. 2001;138(2):280–2.
 48. Balli S, Oflaz MB, Kibar AE, Ece I. Rhythm and conduction analysis of patients with acute rheumatic fever. *Pediatr Cardiol*. 2013;34(2):383–9.
 49. Scott DL, Wolfe F, Huizinga TW. Rheumatoid arthritis. *Lancet*. 2010;376(9746):1094–108.
 50. Maradit-Kremers H, Crowson CS, Nicola PJ, Ballman KV, Roger VL, Jacobsen SJ, et al. Increased unrecognized coronary heart disease and sudden deaths in rheumatoid arthritis: a population-based cohort study. *Arthritis Rheum*. 2005;52(2):402–11.
 51. Pujades-Rodriguez M, Duyx B, Thomas SL, Stogiannis D, Rahman A, Smeeth L, et al. Rheumatoid arthritis and incidence of twelve initial presentations of cardiovascular disease: a population record-linkage cohort study in England. *PLoS One*. 2016;11(3):e0151245.
 52. Lazzarini PE, Capecchi PL, Laghi-Pasini F. Systemic inflammation and arrhythmic risk: lessons from rheumatoid arthritis. *Eur Heart J*. 2017;38(22):1717–27.
 53. Lazzarini PE, Acampa M, Capecchi PL, Hammoud M, Maffei S, Bisogno S, et al. Association between high sensitivity C-reactive protein, heart rate variability and corrected QT interval in patients with chronic inflammatory arthritis. *Eur J Intern Med*. 2013;24(4):368–74.
 54. Chauhan K, Ackerman MJ, Crowson CS, Matteson EL, Gabriel SE. Population-based study of QT interval prolongation in patients with rheumatoid arthritis. *Clin Exp Rheumatol*. 2015;33(1):84–9.
 55. Panoulas VF, Toms TE, Douglas KM, Sandoo A, Metsios GS, Stavropoulos-Kalinoglou A, et al. Prolonged QTc interval predicts all-cause mortality in patients with rheumatoid arthritis: an association driven by high inflammatory burden. *Rheumatology (Oxford)*. 2014;53(1):131–7.
 56. Geraldino-Pardilla L, Gartshsteyn Y, Piña P, Cerrone M, Giles JT, Zartoshti A, et al. ECG non-specific ST-T and QTc abnormalities in patients with systemic lupus erythematosus compared with rheumatoid arthritis. *Lupus Sci Med*. 2016;3(1):e000168.
 57. Acar GR, Akkoyun M, Nacar AB, Dirnak I, Yıldırım Çetin G, Nur Yıldırım M, et al. Evaluation of Tp-e interval and Tp-e/QT ratio in patients with rheumatoid arthritis. *Turk Kardiyol Dern Ars*. 2014;42(1):29–34.
 58. Adlan AM, Panoulas VF, Smith JP, Fisher JP, Kitas GD. Association between corrected QT interval and inflammatory cytokines in rheumatoid arthritis. *J Rheumatol*. 2015;42(3):421–8.
 59. Lazzarini PE, Acampa M, Capecchi PL, Fineschi I, Selvi E, Moscadelli V, et al. Antiarrhythmic potential of anticytokine therapy in rheumatoid arthritis: tocilizumab reduces corrected QT interval by controlling systemic inflammation. *Arthritis Care Res (Hoboken)*. 2015;67(3):332–9.

60. Lazzarini PE, Capecchi PL, Bertolozzi I, Morozzi G, Lorenzini S, Simpatico A, et al. Marked QTc prolongation and torsades de pointes in patients with chronic inflammatory arthritis. *Front Cardiovasc Med.* 2016;3:31.
61. Lazzarini PE, Acampa M, Guideri F, Capecchi PL, Campanella V, Morozzi G, et al. Prolongation of the corrected QT interval in adult patients with anti-Ro/SSA-positive connective tissue diseases. *Arthritis Rheum.* 2004;50(4):1248–52.
62. Costedoat-Chalumeau N, Amoura Z, Hulot JS, Ghillani P, Lechat P, Funck-Brentano C, et al. Corrected QT interval in anti-SSA-positive adults with connective tissue disease: comment on the article by Lazzarini et al. *Arthritis Rheum.* 2005;52(2):676–7; author reply 7–8.
63. Lazzarini PE, Capecchi PL, Guideri F, Bellisai F, Selvi E, Acampa M, et al. Comparison of frequency of complex ventricular arrhythmias in patients with positive versus negative anti-Ro/SSA and connective tissue disease. *Am J Cardiol.* 2007;100(6):1029–34.
64. Lazzarini PE, Capecchi PL, Acampa M, Morozzi G, Bellisai F, Bacarelli MR, et al. Anti-Ro/SSA-associated corrected QT interval prolongation in adults: the role of antibody level and specificity. *Arthritis Care Res (Hoboken).* 2011;63(10):1463–70.
65. Pisoni CN, Reina S, Arakaki D, Eimon A, Carrizo C, Borda E. Elevated IL-1 β levels in anti-Ro/SSA connective tissue diseases patients with prolonged corrected QTc interval. *Clin Exp Rheumatol.* 2015;33(5):715–20.
66. Cardoso CR, Sales MA, Papi JA, Salles GF. QT-interval parameters are increased in systemic lupus erythematosus patients. *Lupus.* 2005;14(10):846–52.
67. Milovanović B, Stojanović L, Milićević N, Vasić K, Bjelaković B, Krotin M. Cardiac autonomic dysfunction in patients with systemic lupus, rheumatoid arthritis and sudden death risk. *Srp Arh Celok Lek.* 2010;138(1–2):26–32.
68. Rivera-López R, Jiménez-Jáimez J, Sabio JM, Zamora-Pasadas M, Vargas-Hitos JA, Martínez-Bordonado J, et al. Relationship between QT interval length and arterial stiffness in systemic lupus erythematosus (SLE): a cross-sectional case-control study. *PLoS One.* 2016;11(4):e0152291.
69. Sham S, Madheshwaran M, Tamilselvam T, Rajeswari S. Correlation of QT interval with disease activity in newly detected SLE patients at baseline and during flare. *Indian J Rheumatol.* 2015;10(3):121–4.
70. Bourré-Tessier J, Clarke AE, Huynh T, Bernatsky S, Joseph L, Belisle P, et al. Prolonged corrected QT interval in anti-Ro/SSA-positive adults with systemic lupus erythematosus. *Arthritis Care Res (Hoboken).* 2011;63(7):1031–7.
71. Bourré-Tessier J, Urowitz MB, Clarke AE, Bernatsky S, Krantz MJ, Huynh T, et al. Electrocardiographic findings in systemic lupus erythematosus: data from an international inception cohort. *Arthritis Care Res (Hoboken).* 2015;67(1):128–35.
72. Myung G, Forbess LJ, Ishimori ML, Chugh S, Wallace D, Weisman MH. Prevalence of resting-ECG abnormalities in systemic lupus erythematosus: a single-center experience. *Clin Rheumatol.* 2017;36(6):1311–6.
73. Avci A, Demir K, Altunkeser BB, Yilmaz S, Yilmaz A, Ersecgin A, et al. Assessment of inhomogeneities of repolarization in patients with systemic lupus erythematosus. *Ann Noninvasive Electrocardiol.* 2014;19(4):374–82.
74. Teixeira RA, Borba EF, Pedrosa A, Nishioka S, Viana VS, Ramires JA, et al. Evidence for cardiac safety and antiarrhythmic potential of chloroquine in systemic lupus erythematosus. *Europace.* 2014;16(6):887–92.
75. Hodak SP, Moubarak JB, Rodriguez I, Gelfand MC, Alijani MR, Tracy CM. QT prolongation and near fatal cardiac arrhythmia after intravenous tacrolimus administration: a case report. *Transplantation.* 1998;66(4):535–7.
76. Amankwa K, Krishnan SC, Tisdale JE. Torsades de pointes associated with fluoroquinolones: importance of concomitant risk factors. *Clin Pharmacol Ther.* 2004;75(3):242–7.
77. Letsas KP, Alexanian IP, Pappas LK, Kounas SP, Efremidis M, Sideris A, et al. QT interval prolongation and torsade de pointes associated with indapamide. *Int J Cardiol.* 2006;112(3):373–4.
78. Chen CY, Wang FL, Lin CC. Chronic hydroxychloroquine use associated with QT prolongation and refractory ventricular arrhythmia. *Clin Toxicol (Phila).* 2006;44(2):173–5.
79. Pham CP, de Feiter PW, van der Kuy PH, van Mook WN. Long QTc interval and torsade de pointes caused by fluconazole. *Ann Pharmacother.* 2006;40(7–8):1456–61.
80. Heinrich TW, Biblo LA, Schneider J. Torsades de pointes associated with ziprasidone. *Psychosomatics.* 2006;47(3):264–8.
81. Ahmed N, Rai R, Riaz K, Khalid MA, Wase A. Levofloxacin-induced torsades de pointes. *Resid Staff Physician.* 2007;53(1):51–4.
82. Stas P, Faes D, Noyens P. Conduction disorder and QT prolongation secondary to long-term treatment with chloroquine. *Int J Cardiol.* 2008;127(2):e80–2.
83. Newton-Cheh C, Lin AE, Baggish AL, Wang H. Case records of the Massachusetts General Hospital. Case 11-2011. A 47-year-old man with systemic lupus erythematosus and heart failure. *N Engl J Med.* 2011;364(15):1450–60.
84. Kandan SR, Saha M. Severe primary hypothyroidism presenting with torsades de pointes. *BMJ Case Rep.* 2012;2012:bcr1220115306.
85. Sgreccia A, Morelli S, Ferrante L, Perrone C, De Marzio P, De Vincentis G, et al. QT interval and QT dispersion in systemic sclerosis (scleroderma). *J Intern Med.* 1998;243(2):127–32.

86. Rosato E, Gigante A, Liberatori M, Gasperini ML, Sardo L, Amoroso A, et al. QTc interval prolongation in systemic sclerosis: correlations with clinical variables. *Int J Cardiol.* 2015;182:20–2.
87. Okutucu S, Karakulak UN, Aksoy H, Sabanoglu C, Hekimsoy V, Sahiner L, et al. Prolonged Tp-e interval and Tp-e/QT correlates well with modified Rodnan skin severity score in patients with systemic sclerosis. *Cardiol J.* 2016;23(3):242–9.
88. Massie C, Hudson M, Tatibouet S, Steele R, Huynh T, Fritzler MJ, et al. Absence of an association between anti-Ro antibodies and prolonged QTc interval in systemic sclerosis: a multicenter study of 689 patients. *Semin Arthritis Rheum.* 2014;44(3):338–44.
89. Foocharoen C, Pussadhamma B, Mahakkanukrauh A, Suwannaroj S, Nanagara R. Asymptomatic cardiac involvement in Thai systemic sclerosis: prevalence and clinical correlations with non-cardiac manifestations (preliminary report). *Rheumatology (Oxford).* 2015;54(9):1616–21.
90. De Luca G, Bosello SL, Canestrari G, Cavalli G, Dagna L, Ferraccioli G. QTc interval prolongation in systemic sclerosis: correlations with clinical variables and arrhythmic risk. *Int J Cardiol.* 2017;239:33.
91. Diederichsen LP, Simonsen JA, Diederichsen AC, Hvidsten S, Hougaard M, Junker P, et al. Cardiac abnormalities in adult patients with polymyositis or dermatomyositis as assessed by non-invasive modalities. *Arthritis Care Res (Hoboken).* 2016;68(7):1012–20.
92. Acar G, Yorgun H, Inci MF, Akkoyun M, Bakan B, Nacar AB, et al. Evaluation of Tp-e interval and Tp-e/QT ratio in patients with ankylosing spondylitis. *Mod Rheumatol.* 2014;24(2):327–30.
93. Curione M, Aratari A, Amato S, Colotto M, Barbato M, Leone S, et al. A study on QT interval in patients affected with inflammatory bowel disease without cardiac involvement. *Intern Emerg Med.* 2010;5(4):307–10.
94. Pattanshetty DJ, Gajulapalli RD, Anna K, Sappati Biyyani RS. Prevalence of QT interval prolongation in inflammatory bowel disease. *Turk J Gastroenterol.* 2016;27(2):136–42.
95. Simsek H, Sahin M, Akyol A, Akdag S, Ozkol HU, Gumrukcuoglu HA, et al. Increased risk of atrial and ventricular arrhythmia in long-lasting psoriasis patients. *ScientificWorldJournal.* 2013;2013:901215.
96. Soyul K, İnci S, Aksan G, Nar G, Yüksel EP, Ocal HS, et al. Evaluation of inhomogeneities of repolarization in patients with psoriasis vulgaris. *Arch Med Sci.* 2016;12(6):1225–31.
97. Poorzand H, Kiafar B, Asadzadeh Heravi F, Vejdanparast M, Saki A, Tayebi M, et al. Cardiogoniometry in psoriatic patients and its comparison with a control group. *Indian Heart J.* 2017;69(1):75–80.
98. Arısoy A, Karaman K, Karayakalı M, Demirelli S, Seçkin HY, Çelik A, et al. Evaluation of ventricular repolarization features with novel electrocardiographic parameters (Tp-e, Tp-e/QT) in patients with psoriasis. *Anatol J Cardiol.* 2017;18(6):397–401.
99. Senel S, Cobankara V, Taskoylu O, Guclu A, Evrengul H, Kaya MG. Effect of infliximab treatment on QT intervals in patients with ankylosing spondylitis. *J Investig Med.* 2011;59(8):1273–5.
100. Lazzarini PE, Bertolozzi I, Acampa M, Fulceri R, Laghi-Pasini F, Capecci PL. Torsades de pointes in patients with polymyalgia rheumatica. *Curr Pharm Des.* 2018;24(3):323–40.
101. Wasserstrum Y, Lotan D, Itelman E, Barbarova I, Kogan M, Klempfner R, et al. Corrected QT interval anomalies are associated with worse prognosis among patients suffering from sepsis. *Intern Med J.* 2016;46(10):1204–11.
102. Ozdemir R, Isguder R, Kucuk M, Karadeniz C, Ceylan G, Katipoglu N, et al. A valuable tool in predicting poor outcome due to sepsis in pediatric intensive care unit: Tp-e/QT ratio. *J Trop Pediatr.* 2016;62(5):377–84.
103. Tisdale JE, Jaynes HA, Kingery JR, Mourad NA, Trujillo TN, Overholser BR, et al. Development and validation of a risk score to predict QT interval prolongation in hospitalized patients. *Circ Cardiovasc Qual Outcomes.* 2013;6(4):479–87.
104. Varriale P, Ramaprasad S. Septic cardiomyopathy as a cause of long QT syndrome. *J Electrocardiol.* 1995;28(4):327–9.
105. Esch JJ, Kantoch MJ. Torsades de pointes ventricular tachycardia in a pediatric patient treated with fluconazole. *Pediatr Cardiol.* 2008;29(1):210–3.
106. Soutodeh R, Götz J, Tebbe U, Cuneo A. Acquired long QT interval in a recurrent septic female patient with polymorphic ventricular tachycardia due to primary acute adrenal insufficiency. *Clin Res Cardiol.* 2011;100(4):373–7.
107. Yelve K, Phatak S, Patil MA, Pazare AR. Syncope in a patient being treated for hepatic and intestinal amoebiasis. *BMJ Case Rep.* 2012;2012:bcr2012006687.
108. Kang DG, Kim SE, Park MS, Kim EJ, Lee JH, Park DG, et al. Acquired long QT syndrome manifesting with torsades de pointes in a patient with panhypopituitarism due to radiotherapy. *Korean Circ J.* 2013;43(5):340–2.
109. Panos G, Velissaris D, Karamouzou V, Matzaroglou C, Tylianakis M. Long QT syndrome leading to multiple cardiac arrests after posaconazole administration in an immune-compromised patient with sepsis: an unusual case report. *Am J Case Rep.* 2016;17:295–300.
110. Patel N, Shenoy A, Dous G, Kamran H, El-Sherif N. Sepsis-induced takotsubo cardiomyopathy leading to torsades de pointes. *Case Rep Cardiol.* 2016;2016:2384752.
111. Chang KT, Shu HS, Chu CY, Lee WH, Hsu PC, Su HM, et al. Association between C-reactive protein, corrected QT interval and presence of QT prolongation in hypertensive patients. *Kaohsiung J Med Sci.* 2014;30(6):310–5.

112. Yue W, Schneider A, Rückerl R, Koenig W, Marder V, Wang S, et al. Relationship between electrocardiographic and biochemical variables in coronary artery disease. *Int J Cardiol.* 2007;119(2):185–91.
113. Yue W, Schneider A, Stölzel M, Rückerl R, Cyrus J, Pan X, et al. Ambient source-specific particles are associated with prolonged repolarization and increased levels of inflammation in male coronary artery disease patients. *Mutat Res.* 2007;621(1–2):50–60.
114. Madias C, Fitzgibbons TP, Alsheikh-Ali AA, Bouchard JL, Kalsmith B, Garlitski AC, et al. Acquired long QT syndrome from stress cardiomyopathy is associated with ventricular arrhythmias and torsades de pointes. *Heart Rhythm.* 2011;8(4):555–61.
115. Imran TF, Rahman I, Dikdan S, Shah R, Niazi OT, Thirunahari N, et al. QT prolongation and clinical outcomes in patients with takotsubo cardiomyopathy. *Pacing Clin Electrophysiol.* 2016;39(6):607–11.
116. Song BG, Chung SM, Kim SH, Kim HJ, Kang GH, Park YH, et al. The QT prolongation and clinical features in patients with takotsubo cardiomyopathy: experiences of two tertiary cardiovascular centers. *Anadolu Kardiyol Derg.* 2014;14(2):162–9.
117. Rizzo S, Basso C, Troost D, Aronica E, Frigo AC, Driessen AH, et al. T-cell-mediated inflammatory activity in the stellate ganglia of patients with ion-channel disease and severe ventricular arrhythmias. *Circ Arrhythm Electrophysiol.* 2014;7(2):224–9.
118. James TN, Zipes DP, Finegan RE, Eisele JW, Carter JE. Cardiac ganglionitis associated with sudden unexpected death. *Ann Intern Med.* 1979;91(5):727–30.
119. James TN, Froggatt P, Atkinson WJ, Lurie PR, McNamara DG, Miller WW, et al. De subitaneis mortibus. XXX. Observations on the pathophysiology of the long QT syndromes with special reference to the neuropathology of the heart. *Circulation.* 1978;57(6):1221–31.
120. Pfeiffer D, Fiehring H, Henkel HG, Rostock KJ, Rathgen K. Long QT syndrome associated with inflammatory degeneration of the stellate ganglia. *Clin Cardiol.* 1989;12(4):222–4.
121. Ajijola OA, Hoover DB, Simerly TM, Brown TC, Yanagawa J, Biniwale RM, et al. Inflammation, oxidative stress, and glial cell activation characterize stellate ganglia from humans with electrical storm. *JCI Insight.* 2017;2(18):pii: 94715.
122. Schwartz PJ. Cardiac sympathetic denervation to prevent life-threatening arrhythmias. *Nat Rev Cardiol.* 2014;11(6):346–53.
123. Wang M, Li S, Zhou X, Huang B, Zhou L, Li X, et al. Increased inflammation promotes ventricular arrhythmia through aggravating left stellate ganglion remodeling in a canine ischemia model. *Int J Cardiol.* 2017;248:286–93.
124. Silva Marques J, Veiga A, Nóbrega J, Correia MJ, de Sousa J. Electrical storm induced by H1N1 A influenza infection. *Europace.* 2010;12(2):294–5.
125. Lim SM, Pak HN, Lee MH, Kim SS, Joung B. Fever-induced QTc prolongation and ventricular fibrillation in a healthy young man. *Yonsei Med J.* 2011;52(6):1025–7.
126. Amin AS, Herfst LJ, Delisle BP, Klemens CA, Rook MB, Bezzina CR, et al. Fever-induced QTc prolongation and ventricular arrhythmias in individuals with type 2 congenital long QT syndrome. *J Clin Invest.* 2008;118(7):2552–61.
127. Amin AS, Klemens CA, Verkerk AO, Meregalli PG, Asghari-Roodsari A, de Bakker JM, et al. Fever-triggered ventricular arrhythmias in Brugada syndrome and type 2 long-QT syndrome. *Neth Heart J.* 2010;18(3):165–9.
128. Kazumi T, Kawaguchi A, Hirano T, Yoshino G. C-reactive protein in young, apparently healthy men: associations with serum leptin, QTc interval, and high-density lipoprotein-cholesterol. *Metabolism.* 2003;52(9):1113–6.
129. Kim E, Joo S, Kim J, Ahn J, Kimm K, Shin C. Association between C-reactive protein and QTc interval in middle-aged men and women. *Eur J Epidemiol.* 2006;21(9):653–9.
130. Medenwald D, Kors JA, Loppnow H, Thiery J, Kluttig A, Nuding S, et al. Inflammation and prolonged QT time: results from the Cardiovascular Disease, Living and Ageing in Halle (CARLA) study. *PLoS One.* 2014;9(4):e95994.
131. Albert CM, Ma J, Rifai N, Stampfer MJ, Ridker PM. Prospective study of C-reactive protein, homocysteine, and plasma lipid levels as predictors of sudden cardiac death. *Circulation.* 2002;105(22):2595–9.
132. Empana JP, Jouven X, Canoui-Poitrine F, Luc G, Tafflet M, Haas B, et al. C-reactive protein, interleukin 6, fibrinogen and risk of sudden death in European middle-aged men: the PRIME study. *Arterioscler Thromb Vasc Biol.* 2010;30(10):2047–52.
133. Hussein AA, Gottdiener JS, Bartz TM, Sotoodehnia N, DeFilippi C, See V, et al. Inflammation and sudden cardiac death in a community-based population of older adults: the Cardiovascular Health Study. *Heart Rhythm.* 2013;10(10):1425–32.
134. Saba S, Janczewski AM, Baker LC, Shusterman V, Gursoy EC, Feldman AM, et al. Atrial contractile dysfunction, fibrosis, and arrhythmias in a mouse model of cardiomyopathy secondary to cardiac-specific overexpression of tumor necrosis factor- α . *Am J Physiol Heart Circ Physiol.* 2005;289(4):H1456–67.
135. Sawaya SE, Rajawat YS, Rami TG, Szalai G, Price RL, Sivasubramanian N, et al. Downregulation of connexin40 and increased prevalence of atrial arrhythmias in transgenic mice with cardiac-restricted overexpression of tumor necrosis factor. *Am J Physiol Heart Circ Physiol.* 2007;292(3):H1561–7.
136. London B, Baker LC, Lee JS, Shusterman V, Choi BR, Kubota T, et al. Calcium-dependent arrhythmias in transgenic mice with heart failure. *Am J Physiol Heart Circ Physiol.* 2003;284(2):H431–41.

137. Petkova-Kirova PS, Gursoy E, Mehdi H, McTiernan CF, London B, Salama G. Electrical remodeling of cardiac myocytes from mice with heart failure due to the overexpression of tumor necrosis factor- α . *Am J Physiol Heart Circ Physiol*. 2006;290(5):H2098–107.
138. Grandy SA, Fiset C. Ventricular K⁺ currents are reduced in mice with elevated levels of serum TNF α . *J Mol Cell Cardiol*. 2009;47(2):238–46.
139. Kawada H, Niwano S, Niwano H, Yumoto Y, Wakisaka Y, Yuge M, et al. Tumor necrosis factor- α downregulates the voltage gated outward K⁺ current in cultured neonatal rat cardiomyocytes: a possible cause of electrical remodeling in diseased hearts. *Circ J*. 2006;70(5):605–9.
140. Fernández-Velasco M, Ruiz-Hurtado G, Hurtado O, Moro MA, Delgado C. TNF- α downregulates transient outward potassium current in rat ventricular myocytes through iNOS overexpression and oxidant species generation. *Am J Physiol Heart Circ Physiol*. 2007;293(1):H238–45.
141. Wang J, Wang H, Zhang Y, Gao H, Nattel S, Wang Z. Impairment of HERG K⁽⁺⁾ channel function by tumor necrosis factor- α : role of reactive oxygen species as a mediator. *J Biol Chem*. 2004;279(14):13289–92.
142. Hatada K, Washizuka T, Horie M, Watanabe H, Yamashita F, Chinushi M, et al. Tumor necrosis factor- α inhibits the cardiac delayed rectifier K current via the sphingomyelin pathway. *Biochem Biophys Res Commun*. 2006;344(1):189–93.
143. Ntari L, Sakkou M, Chouvardas P, Mourouzis I, Prados A, Denis MC, et al. Comorbid TNF-mediated heart valve disease and chronic polyarthritis share common mesenchymal cell-mediated aetiopathogenesis. *Ann Rheum Dis*. 2018;77(6):926–34.
144. Sakkou M, Chouvardas P, Ntari L, Prados A, Moreth K, Fuchs H, et al. Mesenchymal TNFR2 promotes the development of polyarthritis and comorbid heart valve stenosis. *JCI Insight*. 2018;3(7):pii: 98864.
145. Monnerat G, Alarcón ML, Vasconcellos LR, Hochman-Mendez C, Brasil G, Bassani RA, et al. Macrophage-dependent IL-1 β production induces cardiac arrhythmias in diabetic mice. *Nat Commun*. 2016;7:13344.
146. Li YH, Rozanski GJ. Effects of human recombinant interleukin-1 on electrical properties of guinea pig ventricular cells. *Cardiovasc Res*. 1993;27(3):525–30.
147. Liu S, Schreuer KD. G protein-mediated suppression of L-type Ca²⁺ current by interleukin-1 beta in cultured rat ventricular myocytes. *Am J Phys*. 1995;268(2 Pt 1):C339–49.
148. Schreuer KD, Liu S. Involvement of ceramide in inhibitory effect of IL-1 beta on L-type Ca²⁺ current in adult rat ventricular myocytes. *Am J Phys*. 1997;272(6 Pt 2):H2591–8.
149. El Khoury N, Mathieu S, Fiset C. Interleukin-1 β reduces L-type Ca²⁺ current through protein kinase C α activation in mouse heart. *J Biol Chem*. 2014;289(32):21896–908.
150. Murata M, Fukuda K, Ishida H, Miyoshi S, Koura T, Kodama H, et al. Leukemia inhibitory factor, a potent cardiac hypertrophic cytokine, enhances L-type Ca²⁺ current and [Ca²⁺]_i transient in cardiomyocytes. *J Mol Cell Cardiol*. 1999;31(1):237–45.
151. Takahashi E, Fukuda K, Miyoshi S, Murata M, Kato T, Ita M, et al. Leukemia inhibitory factor activates cardiac L-type Ca²⁺ channels via phosphorylation of serine 1829 in the rabbit Cav1.2 subunit. *Circ Res*. 2004;94(9):1242–8.
152. Hagiwara Y, Miyoshi S, Fukuda K, Nishiyama N, Ikegami Y, Tanimoto K, et al. SHP2-mediated signaling cascade through gp130 is essential for LIF-dependent I CaL, [Ca²⁺]_i transient, and APD increase in cardiomyocytes. *J Mol Cell Cardiol*. 2007;43(6):710–6.
153. Less H, Shilkut M, Rubinstein I, Berke G, Binah O. Cardiac dysfunction in murine autoimmune myocarditis. *J Autoimmun*. 1999;12(3):209–20.
154. Park H, Lee D, Oh S, Lim J, Hwang HJ, Park S, et al. Increased phosphorylation of Ca⁽²⁺⁾ handling proteins as a proarrhythmic mechanism in myocarditis. *Circ J*. 2014;78(9):2292–301.
155. De Jesus NM, Wang L, Herren AW, Wang J, Shenasa F, Bers DM, et al. Atherosclerosis exacerbates arrhythmia following myocardial infarction: role of myocardial inflammation. *Heart Rhythm*. 2015;12(1):169–78.
156. De Jesus NM, Wang L, Lai J, Rigor RR, Francis Stuart SD, Bers DM, et al. Antiarrhythmic effects of interleukin 1 inhibition after myocardial infarction. *Heart Rhythm*. 2017;14(5):727–36.
157. Ozcan C, Battaglia E, Young R, Suzuki G. LKB1 knockout mouse develops spontaneous atrial fibrillation and provides mechanistic insights into human disease process. *J Am Heart Assoc*. 2015;4(3):e001733.
158. Lazzarini PE, Capecchi PL, Guideri F, Acampa M, Selvi E, Bisogno S, et al. Autoantibody-mediated cardiac arrhythmias: mechanisms and clinical implications. *Basic Res Cardiol*. 2008;103(1):1–11.
159. Lee HC, Huang KT, Wang XL, Shen WK. Autoantibodies and cardiac arrhythmias. *Heart Rhythm*. 2011;8(11):1788–95.
160. Lazzarini PE, Capecchi PL, Laghi-Pasini F, Boutjdir M. Autoimmune channelopathies as a novel mechanism in cardiac arrhythmias. *Nat Rev Cardiol*. 2017;14(9):521–35.
161. Boutjdir M, Lazzarini PE, Capecchi PL, Laghi-Pasini F, El-Sherif N. Potassium channel block and novel autoimmune-associated long QT syndrome. *Card Electrophysiol Clin*. 2016;8(2):373–84.
162. Yue Y, Castrichini M, Srivastava U, Fabris F, Shah K, Li Z, et al. Pathogenesis of the novel

- autoimmune-associated long-QT syndrome. *Circulation*. 2015;132(4):230–40.
163. Franceschini F, Cavazzana I. Anti-Ro/SSA and La/SSB antibodies. *Autoimmunity*. 2005;38(1):55–63.
 164. Brito-Zerón P, Izmirly PM, Ramos-Casals M, Buyon JP, Khamashta MA. The clinical spectrum of autoimmune congenital heart block. *Nat Rev Rheumatol*. 2015;11(5):301–12.
 165. Karnabi E, Boutjdir M. Role of calcium channels in congenital heart block. *Scand J Immunol*. 2010;72(3):226–34.
 166. Lazzerini PE, Capecchi PL, Laghi-Pasini F. Anti-Ro/SSA antibodies and cardiac arrhythmias in the adult: facts and hypotheses. *Scand J Immunol*. 2010;72(3):213–22.
 167. Hayashi N, Koshiha M, Nishimura K, Sugiyama D, Nakamura T, Morinobu S, et al. Prevalence of disease-specific antinuclear antibodies in general population: estimates from annual physical examinations of residents of a small town over a 5-year period. *Mod Rheumatol*. 2008;18(2):153–60.
 168. Satoh M, Chan EK, Ho LA, Rose KM, Parks CG, Cohn RD, et al. Prevalence and sociodemographic correlates of antinuclear antibodies in the United States. *Arthritis Rheum*. 2012;64(7):2319–27.
 169. Guo YP, Wang CG, Liu X, Huang YQ, Guo DL, Jing XZ, et al. The prevalence of antinuclear antibodies in the general population of China: a cross-sectional study. *Curr Ther Res Clin Exp*. 2014;76:116–9.
 170. Buyon JP, Winchester RJ, Slade SG, Arnett F, Copel J, Friedman D, et al. Identification of mothers at risk for congenital heart block and other neonatal lupus syndromes in their children. Comparison of enzyme-linked immunosorbent assay and immunoblot for measurement of anti-SS-A/Ro and anti-SS-B/La antibodies. *Arthritis Rheum*. 1993;36(9):1263–73.
 171. Duke C, Stuart G, Simpson JM. Ventricular tachycardia secondary to prolongation of the QT interval in a fetus with autoimmune mediated congenital complete heart block. *Cardiol Young*. 2005;15(3):319–21.
 172. Nakamura K, Katayama Y, Kusano KF, Haraoka K, Tani Y, Nagase S, et al. Anti-KCNH2 antibody-induced long QT syndrome: novel acquired form of long QT syndrome. *J Am Coll Cardiol*. 2007;50(18):1808–9.
 173. Lazzerini PE, Yue Y, Srivastava U, Fabris F, Capecchi PL, Bertolozzi I, et al. Arrhythmogenicity of anti-Ro/SSA antibodies in patients with torsades de pointes. *Circ Arrhythm Electrophysiol*. 2016;9(4):e003419.
 174. Cimaz R, Stramba-Badiale M, Brucato A, Catelli L, Panzeri P, Meroni PL. QT interval prolongation in asymptomatic anti-SSA/Ro-positive infants without congenital heart block. *Arthritis Rheum*. 2000;43(5):1049–53.
 175. Cimaz R, Meroni PL, Brucato A, Fesstová V, Panzeri P, Goulene K, et al. Concomitant disappearance of electrocardiographic abnormalities and of acquired maternal autoantibodies during the first year of life in infants who had QT interval prolongation and anti-SSA/Ro positivity without congenital heart block at birth. *Arthritis Rheum*. 2003;48(1):266–8.
 176. Gordon PA, Khamashta MA, Hughes GR, Rosenthal E. Increase in the heart rate-corrected QT interval in children of anti-Ro-positive mothers, with a further increase in those with siblings with congenital heart block: comment on the article by Cimaz et al. *Arthritis Rheum*. 2001;44(1):242–3.
 177. Jaeggi E, Laskin C, Hamilton R, Kingdom J, Silverman E. The importance of the level of maternal anti-Ro/SSA antibodies as a prognostic marker of the development of cardiac neonatal lupus erythematosus a prospective study of 186 antibody-exposed fetuses and infants. *J Am Coll Cardiol*. 2010;55(24):2778–84.
 178. Tufan AN, Sag S, Oksuz MF, Ermurat S, Coskun BN, Gullulu M, et al. Prolonged Tpeak-Tend interval in anti-Ro52 antibody-positive connective tissue diseases. *Rheumatol Int*. 2017;37(1):67–73.
 179. Motta M, Rodriguez-Perez C, Tincani A, Lojaco A, Chirico G. Outcome of infants from mothers with anti-SSA/Ro antibodies. *J Perinatol*. 2007;27(5):278–83.
 180. Gordon PA, Rosenthal E, Khamashta MA, Hughes GR. Absence of conduction defects in the electrocardiograms [correction of echocardiograms] of mothers with children with congenital complete heart block. *J Rheumatol*. 2001;28(2):366–9.
 181. Nomura A, Kishimoto M, Takahashi O, Deshpande GA, Yamaguchi K, Okada M. Prolongation of heart rate-corrected QT interval is a predictor of cardiac autonomic dysfunction in patients with systemic lupus erythematosus. *Rheumatol Int*. 2014;34(5):643–7.
 182. Costedoat-Chalumeau N, Amoura Z, Lupoglazoff JM, Huong DL, Denjoy I, Vauthier D, et al. Outcome of pregnancies in patients with anti-SSA/Ro antibodies: a study of 165 pregnancies, with special focus on electrocardiographic variations in the children and comparison with a control group. *Arthritis Rheum*. 2004;50(10):3187–94.
 183. Gerosa M, Cimaz R, Stramba-Badiale M, Goulene K, Meregalli E, Trespidi L, et al. Electrocardiographic abnormalities in infants born from mothers with autoimmune diseases—a multicentre prospective study. *Rheumatology (Oxford)*. 2007;46(8):1285–9.
 184. Dugar M, Cox S, Limaye V, Gordon TP, Roberts-Thomson PJ. Diagnostic utility of anti-Ro52 detection in systemic autoimmunity. *Postgrad Med J*. 2010;86(1012):79–82.
 185. Lazzerini PE, Capecchi PL, Laghi-Pasini F. Assessing QT interval in patients with autoimmune chronic inflammatory diseases: perils and pitfalls. *Lupus Sci Med*. 2016;3(1):e000189.
 186. Grant AO. Cardiac ion channels. *Circ Arrhythm Electrophysiol*. 2009;2(2):185–94.
 187. Romi F, Suzuki S, Suzuki N, Petzold A, Plant GT, Gilhus NE. Anti-voltage-gated potassium channel Kv1.4 antibodies in myasthenia gravis. *J Neurol*. 2012;259(7):1312–6.

188. Suzuki S, Satoh T, Yasuoka H, Hamaguchi Y, Tanaka K, Kawakami Y, et al. Novel autoantibodies to a voltage-gated potassium channel Kv1.4 in a severe form of myasthenia gravis. *J Neuroimmunol.* 2005;170(1-2):141-9.
189. Suzuki S, Baba A, Kaida K, Utsugisawa K, Kita Y, Tsugawa J, et al. Cardiac involvements in myasthenia gravis associated with anti-Kv1.4 antibodies. *Eur J Neurol.* 2014;21(2):223-30.
190. Xiao H, Wang M, Du Y, Yuan J, Cheng X, Chen Z, et al. Arrhythmogenic autoantibodies against calcium channel lead to sudden death in idiopathic dilated cardiomyopathy. *Eur J Heart Fail.* 2011;13(3):264-70.
191. Yu H, Pei J, Liu X, Chen J, Li X, Zhang Y, et al. Calcium channel autoantibodies predicted sudden cardiac death and all-cause mortality in patients with ischemic and nonischemic chronic heart failure. *Dis Markers.* 2014;2014:796075.
192. Xiao H, Wang M, Du Y, Yuan J, Zhao G, Tu D, et al. Agonist-like autoantibodies against calcium channel in patients with dilated cardiomyopathy. *Heart Vessel.* 2012;27(5):486-92.
193. Fabris F, Yue Y, Qu Y, Chahine M, Sobie E, Lee P, et al. Induction of autoimmune response to the extracellular loop of the HERG channel pore induces QTc prolongation in guinea-pigs. *J Physiol.* 2016;594(21):6175-87.
194. Xiao GQ, Hu K, Boutjdir M. Direct inhibition of expressed cardiac l- and t-type calcium channels by igg from mothers whose children have congenital heart block. *Circulation.* 2001;103(11):1599-604.
195. Xiao GQ, Qu Y, Hu K, Boutjdir M. Down-regulation of L-type calcium channel in pups born to 52 kDa SSA/Ro immunized rabbits. *FASEB J.* 2001;15(9):1539-45.
196. Karnabi E, Qu Y, Wadgaonkar R, Mancarella S, Yue Y, Chahine M, et al. Congenital heart block: identification of autoantibody binding site on the extracellular loop (domain I, S5-S6) of alpha(1D) L-type calcium channel. *J Autoimmun.* 2010;34(2):80-6.
197. Salomonsson S, Sonesson SE, Ottosson L, Muhallab S, Olsson T, Sunnerhagen M, et al. Ro/SSA autoantibodies directly bind cardiomyocytes, disturb calcium homeostasis, and mediate congenital heart block. *J Exp Med.* 2005;201(1):11-7.
198. Artyeva NV, Goshka SL, Sedova KA, Bernikova OG, Azarov JE. What does the T(peak)-T(end) interval reflect? An experimental and model study. *J Electrocardiol.* 2013;46(4):296.e1-8.
199. Priori SG, Wilde AA, Horie M, Cho Y, Behr ER, Berul C, et al. HRS/EHRA/APHRS expert consensus statement on the diagnosis and management of patients with inherited primary arrhythmia syndromes: document endorsed by HRS, EHRA, and APHRS in May 2013 and by ACCF, AHA, PACES, and AEPC in June 2013. *Heart Rhythm.* 2013;10(12):1932-63.
200. Turker I, Ai T, Itoh H, Horie M. Drug-induced fatal arrhythmias: acquired long QT and Brugada syndromes. *Pharmacol Ther.* 2017;176:48-59.
201. Roden DM. Repolarization reserve: a moving target. *Circulation.* 2008;118(10):981-2.
202. Yang P, Kanki H, Drolet B, Yang T, Wei J, Viswanathan PC, et al. Allelic variants in long-QT disease genes in patients with drug-associated torsades de pointes. *Circulation.* 2002;105(16):1943-8.
203. Kääh S, Crawford DC, Sinner MF, Behr ER, Kannankeril PJ, Wilde AA, et al. A large candidate gene survey identifies the KCNE1 D85N polymorphism as a possible modulator of drug-induced torsades de pointes. *Circ Cardiovasc Genet.* 2012;5(1):91-9.
204. Itoh H, Crotti L, Aiba T, Spazzolini C, Denjoy I, Fressart V, et al. The genetics underlying acquired long QT syndrome: impact for genetic screening. *Eur Heart J.* 2016;37(18):1456-64.
205. Lazzarini PE, Bertolozzi I, Finizola F, Acampa M, Natale M, Vanni F, et al. Proton pump inhibitors and serum magnesium levels in patients with torsades de pointes. *Front Pharmacol.* 2018;9:363.
206. Saribayev M, Tufan F, Oz F, Erer B, Ozpolat T, Ozturk GB, et al. Corticosteroid treatment normalizes QTc prolongation and improves heart block in an elderly patient with anti-Ro-positive systemic lupus erythematosus. *Aging Clin Exp Res.* 2014;26(3):337-9.
207. Li J, Maguy A, Duverger JE, Vigneault P, Comtois P, Shi Y, et al. Induced KCNQ1 autoimmunity accelerates cardiac repolarization in rabbits: potential significance in arrhythmogenesis and antiarrhythmic therapy. *Heart Rhythm.* 2014;11(11):2092-100.

Part III

Pathophysiology, Molecular Biology, and Clinical Aspects of Early Repolarization Syndromes



Genetics, Molecular Biology, and Emerging Concepts of Early Repolarization Syndrome

14

Charles Antzelevitch and Gregory Dendramis

Abbreviations and Acronyms

AP	action potential
ECG	electrocardiogram
EG	electrogram
ERS	early repolarization syndrome
BrS	Brugada syndrome
JWS	J wave syndromes
LV	left ventricle
P2R	phase-2-reentry
RFA	radiofrequency ablation
RVOT	right ventricular outflow tract
VF	ventricular fibrillation
VT	ventricular tachycardia

Introduction

An early repolarization pattern (ERP) in the electrocardiogram (ECG), characterized by a distinct J wave or J point elevation (when part

of the J wave is “buried” inside the QRS), a notch or slur of the terminal part of the QRS (with or without ST segment elevation), has traditionally been viewed as benign [1, 2]. When accompanied by arrhythmic symptoms, ERP is referred to as early repolarization syndrome (ERS) and is considered to be one of the J wave syndromes.

The appearance of prominent J waves in the ECG and their association with sudden cardiac death (SCD) due to life-threatening cardiac arrhythmias has long been recognized and reported in clinical cases of hypothermia [3–5], hypercalcemia [6, 7], and ischemia [8]. Accentuated J waves have recently been associated more with inherited life-threatening cardiac arrhythmia disorders including Brugada syndrome (BrS) and ERS, the so-called J wave syndromes (JWS).

The risk for SCD in patients afflicted with ERS was not fully appreciated until recently. Its benign nature was challenged in 2000 [9] on the basis of experimental data obtained using canine ventricular wedge preparations [9–12] showing that an ERP was associated with imminent development of polymorphic ventricular tachycardia and fibrillation (VT/VF). Clinical evidence in support of this hypothesis was provided 8 years later by Haïssaguerre et al. [13], Nam et al. [14], and Rosso et al. [15].

C. Antzelevitch (✉)

Department of Cardiovascular Research, Lankenau
Institute for Medical Research,
Wynnewood, PA, USA

Lankenau Heart Institute, Wynnewood, PA, USA

Sidney Kimmel Medical School, Thomas Jefferson
University, Philadelphia, PA, USA

G. Dendramis

Cardiovascular Division, Pietro Cosma Hospital,
Padova, Italy

Diagnosis of ERS

ERP is most often encountered in apparently healthy individuals, particularly in young males, black individuals, and athletes. Early repolarization is recognized with the appearance of: (1) an *end QRS notch (J wave)* or *slur* on the downslope of a prominent R wave (with or without ST segment elevation). The onset of the J wave is referred to as J_0 , (2) a distinct J wave with a peak (designated as J_p) ≥ 0.1 mV in two or more contiguous ECG leads, excluding leads V1–V3; and (3) a QRS duration (measured in leads in which a notch or slur is absent) must be <120 ms. The end of the *J wave* or that of the *QRS slur* or *notch* is designated as J_T (Fig. 14.1) [16].

Electrocardiographically, three distinct forms of ERP are recognized. ER is characterized by distinct J waves, J_0 elevation, notch or slur of the terminal part of the QRS and ST segment, or J_T elevation in the lateral (*Type I*), in infero-lateral (*Type II*), or in infero-lateral + (anterior) right precordial leads (*Type III*) [10].

Unlike in BrS, sodium channel blockers generally do not unmask or accentuate the J wave manifestation on the surface ECG of patients with ERS. These agents may indeed reduce the amplitude of the J wave in individuals with ERS [17]. This has been suggested to mean that the pathophysiological basis for ERS and BrS is fundamentally different, but this is not necessarily the case. A recent study by Nakagawa et al. reported that J waves recorded using unipolar LV epicardial leads in ERS patients are augmented following provocative drug testing with a sodium channel blocker, while the J waves concurrently recorded in the lateral precordial leads are diminished, demonstrating that the J waves in the surface leads are reduced because they are engulfed by the widening QRS [17, 18]. Support for the hypothesis that the pathophysiological basis for ERS and BrS is closely related also comes from reports of cases in which ERS transitions into ERS plus BrS phenotypes [19, 20].

Table 14.1 shows the Shanghai Score System recently proposed for the diagnosis of ERS [21].

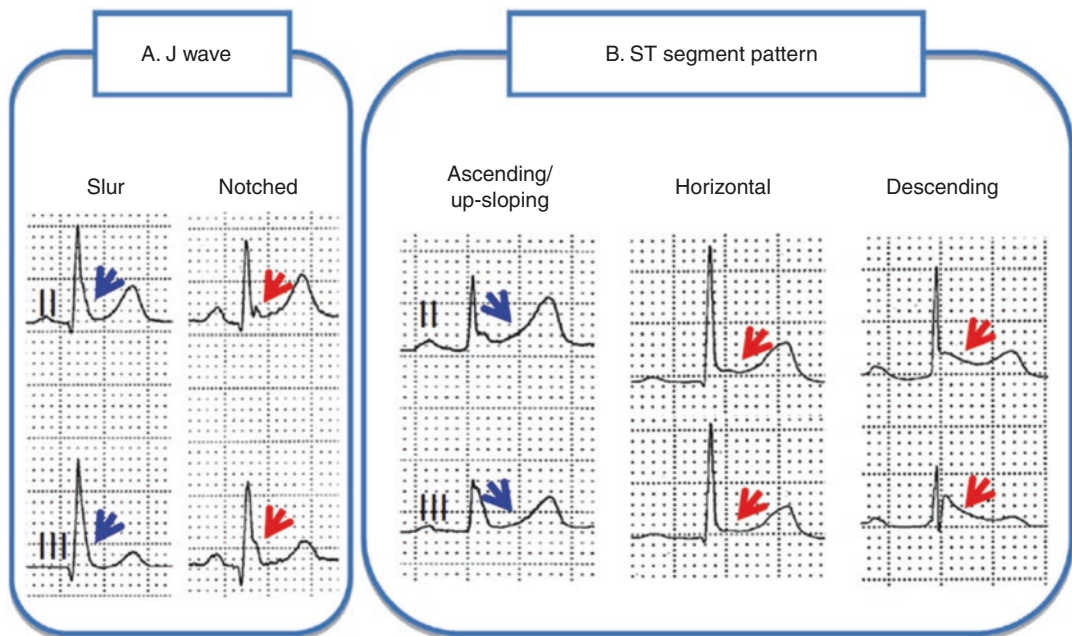


Fig. 14.1 Different manifestations of early repolarization. (a) The J wave may be distinct or appear as a slur. In the latter case, part of the J wave is buried inside the QRS, resulting in an elevation of J_0 . Patients with a **very prominent J waves have a worse prognosis**. (b) The ST seg-

ment may be upsloping, horizontal, or descending. **Horizontal and descending ST segments are associated with a worse prognosis**. (Reproduced from Antzelevitch et al., Copyright 2016 [21], with permission from Elsevier)

Table 14.1 Shanghai Score System for diagnosis of early repolarization syndrome

	Points
I. Clinical history	
A. Unexplained cardiac arrest, documented VF, or polymorphic VT	3
B. Suspected arrhythmic syncope	2
C. Syncope of unclear mechanism/unclear etiology <i>*Only award points once for highest score within this category</i>	1
II. Twelve-lead ECG	
A. ER ≥ 0.2 mV in ≥ 2 inferior and/or lateral ECG leads with horizontal/descending ST segment	2
B. Dynamic changes in J point elevation (≥ 0.1 mV) in \geq inferior and/or lateral ECG leads	1.5
C. ≥ 0.1 mV J point elevation in at least 2 inferior and/or lateral ECG leads <i>*Only award points once for highest score within this category</i>	1
III. Ambulatory ECG monitoring	
A. Short-coupled PVCs with R on ascending limb or peak of T wave	2
IV. Family history	
A. Relative with definite ERS	2
B. ≥ 2 first-degree relatives with a II.A. ECG pattern	2
C. First-degree relative with a II.A. ECG pattern	1
D. Unexplained sudden cardiac death <45 years in a first- or second-degree relative <i>*Only award points once for highest score within this category</i>	0.5
V. Genetic test result	
A. Probably pathogenic ERS susceptibility mutation	0.5
Score (requires at least 1 ECG finding)	
≥ 5 points: Probable/definite ERS	
3–4.5 points: Possible ERS	
< 3 points: Nondiagnostic	

Reproduced from Antzelevitch et al., Copyright 2016 [21], with permission from Elsevier
ER early repolarization, *ERS* early repolarization syndrome, *PVC* premature ventricular contraction, *VF* ventricular fibrillation, *VT* ventricular tachycardia

A similar scoring system was proposed for BrS and recently validated by Kawada and co-workers [22]. Clinical validation of the ERS scoring system has not as yet been reported.

Prevalence of ERP and Arrhythmic Risk

It is important to recognize that the discovery of a J wave on a routine ECG should not be routinely interpreted to be a marker of risk for SCD. Rosso et al. reported that the presence of a J wave on the ECG increases the probability of VF from 3.4:100,000 to 11:100,000 [15, 23]. However, careful attention needs to be paid to subjects with “high-risk” ER or J waves.

J waves in the lateral ECG leads have a high prevalence but are generally associated with a very low arrhythmic risk. Patients displaying a rapidly ascending ST segment elevation also have a high prevalence and low risk. In contrast, J waves appearing in the inferior leads or inferolateral leads are associated with a much higher risk, particularly when displaying a flat or descending ST segment [24]. J waves appearing globally in the ECG have a very low prevalence, but are thought to be associated with a relatively high level of arrhythmic risk as are subjects resuscitated from cardiac arrest [21].

The prevalence of an ER pattern in the inferior and/or lateral leads with a J point (J_0) elevation of ≥ 0.1 mV ranges between 1% and 24% and for J_0 elevation of ≥ 0.2 mV ranges between 0.6% and 6.4% [25–27]. Unlike BrS, where prevalence is high in individuals of Asian or Southeast Asian origin, no significant regional differences are reported in the prevalence of an ER pattern [28].

Similarities and Difference Between BrS and ERS

ERS and BrS have several clinical similarities, which once again suggest a closely related pathophysiology [11, 19, 29–31]. Males predominate in both syndromes [32, 33]. In general, the occurrence of accentuated J waves and ST segment elevation is concurrent with bradycardia or pauses [34, 35], and thus VF often occurs during sleep or at a low level of physical activities [17, 36]. They may be totally asymptomatic

until presenting with cardiac arrest. The highest incidence of VF or SCD occurs in the third decade of life in both syndromes [37].

ERS and BrS also share similarities with respect to the response to pharmacological therapy. Electrical storms (and the associated accentuated J waves) can be suppressed with β -adrenergic agonists [38–41]. Chronic oral administration of quinidine [42, 43], bepridil [40], denopamine [38, 44], and cilostazol [38, 40, 44–48] is reported to prevent VT/VF in both syndromes, probably secondary to inhibition of I_{to} and/or augmentation of I_{Ca} [14, 45, 49].

There are a number of differences between the two syndromes. These include: (1) the region of the heart most affected (RVOT in BrS vs. inferior LV in ERS); (2) the incidence of late potentials in signal-averaged ECGs (SAECG), 60% in BrS/7% in ERS [17]; (3) greater elevation of J_O , J_B , or J_T (ST segment elevation) in response to sodium channel blockers in BrS vs. ERS; (4) higher prevalence of atrial fibrillation in BrS vs. ERS [50]; and (5) the presence of subtle structural abnormalities in BrS, which as yet have not been reported in ERS [51].

Steep and localized repolarization gradients in the inferior and lateral regions of the LV have been reported in ERS patients in conjunction with normal ventricular activation [52]. In contrast, fractionated electrogram activity was recorded in the RVOT of BrS patients in addition to a steep dispersion of repolarization gradients [53].

Several studies indicate that ERS patients are at greater risk of VF during hypothermia [54–58] as well as in the event of an acute myocardial infarction [59]. BrS patients are known to be at greater risk of VF in febrile states [60, 61] as well as when accompanied by an ER pattern in the infero-lateral leads [62].

Genetics

ERS has been associated with variants in seven different genes (Table 14.2).

An ER pattern in the ECG is known to be familial [63–65]. Consistent with experimental

Table 14.2 Gene defects associated with the early repolarization and Brugada syndromes

	Locus	Gene/protein	Ion channel
ERS1	12p11.23	<i>KCNJ8, Kir6.1</i>	$\uparrow I_{K-ATP}$
ERS2	12p13.3	<i>CACNA1C, Ca_v1.2</i>	$\downarrow I_{Ca}$
ERS3	10p12.33	<i>CACNB2b, Ca_vβ2b</i>	$\downarrow I_{Ca}$
ERS4	7q21.11	<i>CACNA2D1, Ca_vα2δ1</i>	$\downarrow I_{Ca}$
ERS5	12p12.1	<i>ABCC9, SUR2A</i>	$\uparrow I_{K-ATP}$
ERS6	3p21	<i>SCN5A, Na_v1.5</i>	$\downarrow I_{Na}$
ERS7	3p22.2	<i>SCN10A, Na_v1.8</i>	$\downarrow I_{Na}$

Listed in chronological order of discovery

findings that I_{K-ATP} activation can generate an ER pattern in canine ventricular wedge preparations, variants in *KCNJ8* and *ABCC9*, responsible for the pore-forming and ATP-sensing subunits of the I_{K-ATP} channel, have been reported in patients with ERS [66–68]. Loss-of-function variations in the $\alpha 1$, $\beta 2$, and $\alpha 2\delta$ subunits of the cardiac L-type calcium channel (*CACNA1C*, *CACNB2*, and *CACNA2D1*) and the α subunit of Nav1.5 and Nav1.8 (*SCN5A* and *SCN10A*) have also been reported in patients with ERS [69–71].

It is important to point out that only a small fraction of identified genetic variants in the genes associated with BrS and ERS have been examined using functional expression studies to ascertain causality and establish a plausible contribution to pathogenesis. The lack of functional or biological validation of mutation effects remains the most severe limitation of genetic test interpretation, as highlighted by Schwartz et al. [72].

To date a large number of variants remain in “genetic purgatory” and this number will only increase as the use of exome/genome sequencing becomes more utilized. This then demands the development and utilization of a uniform variant repository that would include clinical assertions and evidence for variant classification. Even with these issues, the emergence of exome/genome sequencing holds promise for the opportunity to study genetic variation like never before, holding the promise of improvements in diagnostic, prognostic, and therapeutics for the JWSs and the other heritable cardiac channelopathies.

Recent efforts have led to exhaustive studies using American College of Medical Genetics

and Genomics and Association for Molecular Pathology guidelines of genes and variants currently catalogued as deleterious and causative of inherited syndromes. This has been performed for BrS and the result is that 20 of the 21 genes identified as being causative of the disease have been reclassified as *disputed* with regard to any assertions of disease causality. Such a rigorous study has yet to be performed for ERS. Accordingly, we recommend that great care be taken with these previously reported genes and variants for ERS until their clinical validity can be further tested.

Ionic and Cellular Mechanisms of ERS

The first studies to explore the basis of J point elevation in the ECG appeared in the early 1950s. Osborn reported the appearance of J point elevation secondary to severe hypothermia and acidosis in a canine model. Although it was unclear which of the two factors caused the ECG change, he speculated that the appearance of J waves in lead II of the surface ECG represented a “current of injury” J point elevation was consistently associated with VF in the hypothermic dogs [73].

The J wave in the ECG is due to the presence of a prominent I_{to} -mediated action potential (AP) notch in ventricular epicardium but not endocardium [31, 74, 75]. The transmural gradient and associated J wave are much greater in the right vs. left ventricle, especially in the region of the RVOT [76]. This is the basis for why BrS is a right ventricular disease. An end of QRS notch, resembling a J wave, may also be due to an intramural conduction delay and these two possibilities could be discerned on the basis of the response to increase in heart rate, with the latter showing accentuation at faster rates [16, 77].

Koncz et al. [78] provided evidence that in ERS, as in BrS, accentuation of transmural gradient of the I_{to} -mediated action potential notch in the LV wall is responsible for the repolarization abnormalities underlying the ECG phenotype. This and subsequent studies provided evidence for the hypothesis that an outward shift in the bal-

ance of current contributing to the early phase of the left ventricular (LV) epicardial action potential (AP) either via an increase in ATP-sensitive potassium current (I_{K-ATP}) or transient outward current (I_{to}) or via a decrease in calcium inward current (I_{Ca}) in LV wedge preparations can recapitulate the ECG and arrhythmic manifestations of ERS (Fig. 14.2). Pharmacologic modeling of the genetic defects responsible for ERS, using pinacidil and NS5806 to increase I_{K-ATP} and I_{to} , respectively, and verapamil and acetylcholine (ACh) to reduce I_{Ca} , was shown to give rise to a substrate capable of inducing phase 2 reentry and polymorphic VT/VF [78].

Vagal activity has long been implicated in the development of an ER pattern in the ECG [79, 80] and recent clinical observations suggest that parasympathetic tone contributes to the electrocardiographic and arrhythmic manifestations of ERS [81, 82]. Sleep is commonly associated with spontaneous VF in patients with ERS [17].

Koncz et al. also provided evidence in support of the hypothesis that higher levels of I_{to} in the inferior wall can explain why an ER pattern in the inferior ECG leads is associated with a higher risk for sudden cardiac arrest [78].

Rudy and colleagues provided additional evidence for repolarization abnormalities in patients with ERS using noninvasive ECGI techniques. They demonstrated short activation-recovery intervals and marked dispersion of repolarization in the inferior and lateral regions of the LV in ERS patients [52].

Approaches to Therapy of ERS

Implantable Cardioverter Defibrillator

The approach to therapy of ERS as recommended in the 2016 HRS/APHRS/EHRA/SOLAECE Consensus Statement is presented in Fig. 14.3. The most effective therapy for the prevention of SCD in high-risk ERS patients is an implantable cardioverter defibrillator (ICD) [83, 84]. However, ICDs are associated with complications, especially in young active individuals [85,

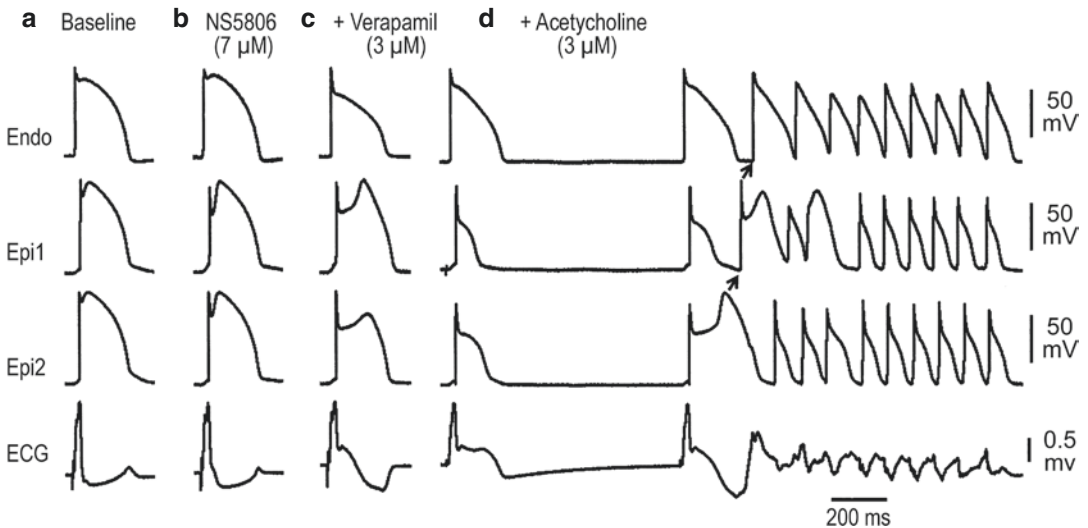


Fig. 14.2 Cellular mechanism underlying the development of polymorphic VT in ERS. Each panel shows simultaneous recordings from one endocardial (Endo) and two epicardial (Epi) sites together with a pseudo-ECG recorded from a canine left ventricular coronary wedge preparation. (a) Control. (b and c) The combination of calcium channel block using verapamil (3 μ M) and accentuation of the transient outward current (I_{to}) using

(NS5806, 7 μ M) caused an ER pattern to develop in the left ventricular wedge preparation, but no arrhythmogenic substrate. (d) The addition of ACh, used to mimic increased vagal tone (ACh, 3 μ M), led to the development of phase 2 reentry and polymorphic VT/ventricular fibrillation. Basic cycle length = 1000 ms. (Reprinted from Koncz et al., Copyright 2014 [78], with permission from Elsevier)

86], and, over time, inappropriate shocks and lead failure are not uncommon. Remote monitoring can identify lead failure and prevent inappropriate shocks [87]. The advent of subcutaneous ICDs is a welcome innovation associated with fewer complications over a lifetime [88].

Pacemaker Therapy

Although life-threatening arrhythmias and SCD in JWS are generally associated with slow heart rates, the potential therapeutic benefit for cardiac pacing at relatively fast rates remains largely unexplored [89–91].

Radiofrequency Ablation (RFA) Therapy

Few clinical data are available with respect to the effectiveness of RFA in patients with ERS. RFA has been shown to suppress arrhythmogenesis by eliminating the extrasystoles precipitating VT/

VF in patients with ERS [92–95]. Low-voltage fractionated electrogram activity and high-frequency LP are observed in the LV epicardium of patients with ERS [18]. Nademanee et al. [96] in their seminal studies targeted such activity in the RVOT for RFA in patients with BrS, demonstrating a significantly reduced arrhythmia risk [97]. Additional evidence in support of the effectiveness of epicardial RVOT ablation in BrS patients was provided by Sacher et al., Shah et al., and Brugada and co-workers [98–100]. RF ablation is also an option in BrS patients with frequent appropriate ICD shocks due to repeated electrical storms [101].

Although no clinical data are available with respect to epicardial RFA in cases of ERS, recent experimental evidence of its effectiveness has been reported [102]. Yoon and co-workers [102] showed that in experimental models of ERS, low-voltage fractionated electrical activity and high-frequency late potentials recorded from the epicardial surface of the left ventricle can identify regions of abnormal repolarization responsible for ventricular tachycardia/ventricular fibrillation

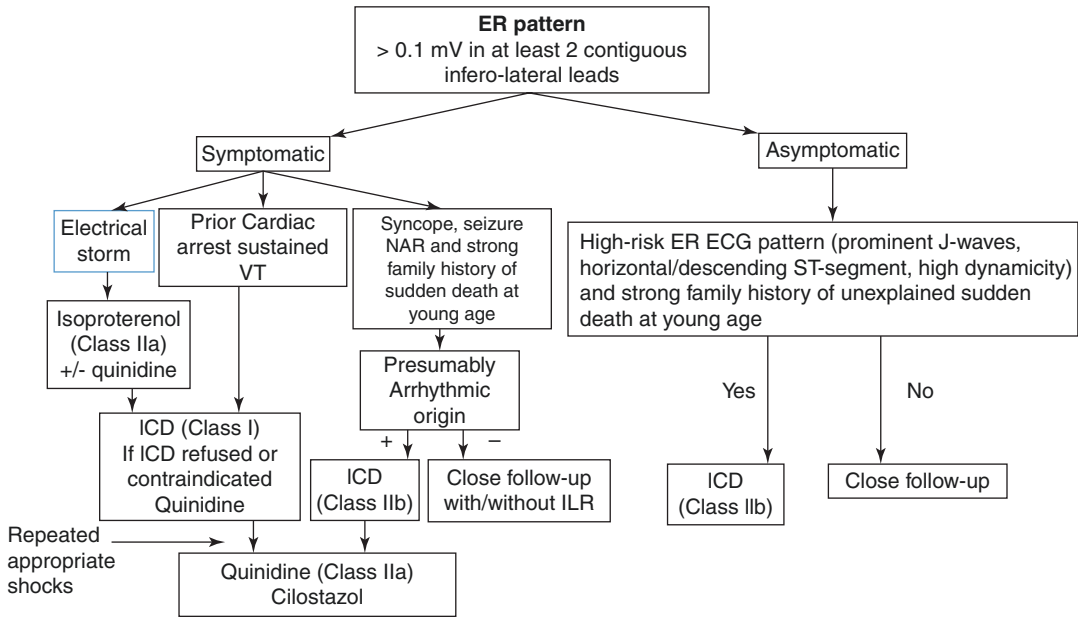


Fig. 14.3 Indications for therapy of patients with early repolarization syndrome. Recommendations with class designations are taken from the 2013 HRS/EHRA/APHS expert consensus statement on the diagnosis and management of patients with inherited primary arrhythmia syndromes. Heart Rhythm [147] and the 2015 ESC Guidelines for the management of patients with ventricular arrhythmias and the prevention of sudden cardiac death [148]. Recommendations without class designa-

tions are derived from unanimous consensus of the authors of the 2016 HRS/APHS/EHRA/SOLAECE J wave syndrome expert consensus report [21]. (Reproduced from Antzelevitch et al., Copyright 2016 [21], with permission from Elsevier. ER early repolarization, ICD implantable cardioverter defibrillator, ILR implantable loop recorder, NAR nocturnal agonal respiration, VT ventricular tachycardia)

and that radiofrequency ablation of these regions in left ventricular epicardium can suppress VT/VF by destroying regions of ER.

Pharmacologic Therapy

ICD implantation often leads to complications, particularly in children and active young adults, and is unaffordable in many regions of the world. A pharmacologic approach to therapy is therefore desirable. Because the presence of a prominent I_{to} is believed to be a prerequisite for the development of both ERS and BrS, partial inhibition of this current is thought to be effective regardless of the underlying ionic or genetic basis for these syndromes. Unfortunately, ion channel-specific and cardio-selective I_{to} blockers are not available at present. The best drug currently available in the clinic capable of blocking I_{to} is

quinidine. Quinidine was first recommended as therapy for BrS by our group in 1999 based on experimental evidence obtained using coronary-perfused RV wedge models of BrS [11, 103–107]. A large volume of clinical data point to the effectiveness of quinidine in BrS [40, 43, 47, 108–120]. Belhassen, Viskin, and colleagues, who pioneered the use of quinidine in VF [121], reported a 90% efficacy in prevention of VF induction following treatment with quinidine, despite the use of very aggressive protocols of extrastimulation [121]. Much less information is available relative to the effectiveness of quinidine in ERS. The effectiveness of quinidine to suppress arrhythmogenesis in a case of ERS was reported by Sacher and co-workers in 2014 [122].

Agents that increase the L-type calcium channel current, such as isoproterenol or orciprenaline, are useful as well in treating patients with JWS [11, 40, 44, 117, 123, 124]. Augmentation of I_{Ca}

prevents arrhythmogenesis associated with *JWS* by opposing early repolarization forces during phase 1 of the action potential, thus restoring the epicardial AP dome in both ERS [125] and BrS [126]. Isoproterenol, sometimes in combination with quinidine, has been used to successfully control VF storms and normalizing ST elevation [38–41, 101, 109, 110, 115, 127–137].

Another promising pharmacologic approach for *JWS* is *cilostazol*, a phosphodiesterase (PDE) III inhibitor [40, 44, 46] which normalizes the ST segment by augmenting I_{Ca} as well as by reducing I_{to} secondary to an increase in cAMP and heart rate [138]. Iguchi and co-workers [45] reported a case in which *cilostazol* was effective in suppressing recurrent VT in a patient with ERS.

Milrinone, another PDE III inhibitor, has been identified as a more potent alternative to *cilostazol* in suppressing ST segment elevation and arrhythmogenesis in an experimental models of ERS [125, 139] and BrS [106, 126]. No clinical data are available as yet.

Wenxin Keli, a traditional Chinese medicine, has recently been shown to inhibit I_{to} and suppress arrhythmogenesis in experimental models of *BrS* when combined with low concentrations of quinidine (5 μ M) [105]. No experimental or clinical data are available concerning its efficacy in ERS.

Agents that increase peak and late I_{Na} , including *bepidil* and *dimethyl lithospermate B* (dmLSB), have been suggested to be of value in both ERS and BrS. *Bepidil* has been reported to suppress VT/VF in several studies of patients with ERS or BrS [40, 48, 137, 140–143]. The drug's action is thought to be mediated by: (1) inhibition of I_{to} , (2) augmentation of I_{Na} via upregulation of the sodium channels [144], and (3) prolongation of QT interval at slow rates, thus increasing the QT/RR slope [140, 142].

Dimethyl lithospermate B, an extract of *Danshen*, a traditional Chinese herbal remedy, has been reported to slow inactivation of I_{Na} , thus increasing I_{Na} during the early phases of the AP, thereby reducing the AP notch and restoring the epicardial AP dome and, in the process, suppress-

ing arrhythmogenesis in experimental models of BrS [145]. No clinical data are available as yet.

Acacetin, a natural flavone produced by several plants including snow lotus, damiana, and black locust, has proved useful for multiple purposes, including treatment of rheumatoid arthritis, impotence, irregular menses, asthma, bronchitis, cough, and altitude sickness [146]. *Acacetin* has been shown to inhibit I_{to} in human atrial myocytes in a frequency-dependent manner [146]. The potential ameliorative effect of this agent in experimental models of BrS and ERS is currently under study by our group and holds promise as a safe and effective therapy for *JWS*.

Funding We acknowledge support from NIH-NHLBI Grant #HL47678, the W.W. Smith Charitable Trust Grant #1820 and from the Martha and Wistar Morris Fund.

References

1. Wasserburger RH, Alt WJ. The normal RS-T segment elevation variant. *Am J Cardiol*. 1961;8:184–92.
2. Mehta MC, Jain AC. Early repolarization on scalar electrocardiogram. *Am J Med Sci*. 1995;309(6):305–11.
3. Clements SD, Hurst JW. Diagnostic value of ECG abnormalities observed in subjects accidentally exposed to cold. *Am J Cardiol*. 1972;29:729–34.
4. Thompson R, Rich J, Chmelik F, Nelson WL. Evolutionary changes in the electrocardiogram of severe progressive hypothermia. *J Electrocardiol*. 1977;10:67–70.
5. Eagle K. Images in clinical medicine. Osborn waves of hypothermia. *N Engl J Med*. 1994;10:680.
6. Kraus F. Ueber die wirkung des kalziums auf den kreislauf I. *Dtsch Med Wochenschr*. 1920;46(8):201–3.
7. Sridharan MR, Horan LG. Electrocardiographic J wave of hypercalcemia. *Am J Cardiol*. 1984;54:672–3.
8. Sato A, Tanabe Y, Chinushi M, Hayashi Y, Yoshida T, Ito E, et al. Analysis of J waves during myocardial ischaemia. *Europace*. 2012;14(5):715–23.
9. Gussak I, Antzelevitch C. Early repolarization syndrome: clinical characteristics and possible cellular and ionic mechanisms. *J Electrocardiol*. 2000;33(4):299–309.
10. Antzelevitch C, Yan GX. J wave syndromes. *Heart Rhythm*. 2010;7(4):549–58.
11. Yan GX, Antzelevitch C. Cellular basis for the Brugada syndrome and other mechanisms of arrhythmogenesis associated with ST segment elevation. *Circulation*. 1999;100(15):1660–6.

12. Shu J, Zhu T, Yang L, Cui C, Yan GX. ST-segment elevation in the early repolarization syndrome, idiopathic ventricular fibrillation, and the Brugada syndrome: cellular and clinical linkage. *J Electrocardiol.* 2005;38(4 Suppl):26–32.
13. Haissaguerre M, Derval N, Sacher F, Jesel L, Deisenhofer I, De Roy L, et al. Sudden cardiac arrest associated with early repolarization. *N Engl J Med.* 2008;358(19):2016–23.
14. Nam GB, Kim YH, Antzelevitch C. Augmentation of J waves and electrical storms in patients with early repolarization. *N Engl J Med.* 2008;358(19):2078–9.
15. Rosso R, Kogan E, Belhassen B, Rozovski U, Scheinman MM, Zeltser D, et al. J-point elevation in survivors of primary ventricular fibrillation and matched control subjects: incidence and clinical significance. *J Am Coll Cardiol.* 2008;52(15):1231–8.
16. Macfarlane P, Antzelevitch C, Haissaguerre M, Huikuri HPMRR, Sacher F, Tikkanen J, Wellens H, Yan G-X. Consensus paper- early repolarization pattern. *J Am Coll Cardiol.* 2015; In Press.
17. Kawata H, Noda T, Yamada Y, Okamura H, Satomi K, Aiba T, et al. Effect of sodium-channel blockade on early repolarization in inferior/lateral leads in patients with idiopathic ventricular fibrillation and Brugada syndrome. *Heart Rhythm.* 2012;9(1):77–83.
18. Nakagawa K, Nagase S, Morita H, Ito H. Left ventricular epicardial electrogram recordings in idiopathic ventricular fibrillation with inferior and lateral early repolarization. *Heart Rhythm.* 2013;11(2):314–7.
19. McIntyre WF, Perez-Riera AR, Femenia F, Baranchuk A. Coexisting early repolarization pattern and Brugada syndrome: recognition of potentially overlapping entities. *J Electrocardiol.* 2012;45(3):195–8.
20. Nam GB, Ko KH, Kim J, Park KM, Rhee KS, Choi KJ, et al. Mode of onset of ventricular fibrillation in patients with early repolarization pattern vs. Brugada syndrome. *Eur Heart J.* 2010;31(3):330–9.
21. Antzelevitch C, Yan GX, Ackerman MJ, Borggreffe M, Corrado D, Guo J, et al. J-Wave syndromes expert consensus conference report: emerging concepts and gaps in knowledge. *Heart Rhythm.* 2016;32(5):315–39.
22. Kawada SMH, Antzelevitch C, Morimoto Y, Nakagawa K, Atsuyuki W, Nishii N, Nakamura K, Ito H. The Shanghai score system for diagnosis of Brugada syndrome. *JACC Clin Electrophysiol.* In press, 2018.
23. Rosso R, Adler A, Halkin A, Viskin S. Risk of sudden death among young individuals with J waves and early repolarization: putting the evidence into perspective. *Heart Rhythm.* 2011;8(6):923–9.
24. Tikkanen JT, Junttila MJ, Anttonen O, Aro AL, Luttinen S, Kerola T, et al. Early repolarization: electrocardiographic phenotypes associated with favorable long-term outcome. *Circulation.* 2011;123(23):2666–73.
25. Tikkanen JT, Anttonen O, Junttila MJ, Aro AL, Kerola T, Rissanen HA, et al. Long-term outcome associated with early repolarization on electrocardiography. *N Engl J Med.* 2009;361(26):2529–37.
26. Sinner MF, Reinhard W, Muller M, Beckmann BM, Martens E, Perz S, et al. Association of early repolarization pattern on ecg with risk of cardiac and all-cause mortality: a population-based prospective cohort study (MONICA/KORA). *PLoS Med.* 2010;7(7):e1000314.
27. Haruta D, Matsuo K, Tsuneto A, Ichimaru S, Hida A, Sera N, et al. Incidence and prognostic value of early repolarization pattern in the 12-lead electrocardiogram. *Circulation.* 2011;123:2931–7.
28. Hayashi M, Shimizu W, Albert CM. The spectrum of epidemiology underlying sudden cardiac death. *Circ Res.* 2015;116(12):1887–906.
29. Nam GB. Idiopathic ventricular fibrillation, early repolarization and other J wave-related ventricular fibrillation syndromes. *Circ J.* 2012;76(12):2723–31.
30. Antzelevitch C. J wave syndromes: molecular and cellular mechanisms. *J Electrocardiol.* 2013;46(6):510–8.
31. Yan GX, Antzelevitch C. Cellular basis for the electrocardiographic J wave. *Circulation.* 1996;93(2):372–9.
32. Benito B, Sarkozy A, Mont L, Henkens S, Berruezo A, Tamborero D, et al. Gender differences in clinical manifestations of Brugada syndrome. *J Am Coll Cardiol.* 2008;52(19):1567–73.
33. Kamakura T, Kawata H, Nakajima I, Yamada Y, Miyamoto K, Okamura H, et al. Significance of non-type 1 anterior early repolarization in patients with inferolateral early repolarization syndrome. *J Am Coll Cardiol.* 2013;62(17):1610–8.
34. Kalla H, Yan GX, Marinchak R. Ventricular fibrillation in a patient with prominent J (Osborn) waves and ST segment elevation in the inferior electrocardiographic leads: a Brugada syndrome variant? *J Cardiovasc Electrophysiol.* 2000;11(1):95–8.
35. Aizawa Y, Sato A, Watanabe H, Chinushi M, Furushima H, Horie M, et al. Dynamicity of the J-wave in idiopathic ventricular fibrillation with a special reference to pause-dependent augmentation of the J-wave. *J Am Coll Cardiol.* 2012;59(22):1948–53.
36. Nademane K. Sudden unexplained death syndrome in Southeast Asia. *Am J Cardiol.* 1997;79(6A):10–1.
37. Matsumoto AM. Fundamental aspects of hypogonadism in the aging male. *Rev Urol.* 2003;5(Suppl 1):S3–s10.
38. Shimizu W, Kamakura S. Catecholamines in children with congenital long QT syndrome and Brugada syndrome. *J Electrocardiol.* 2001;34(Suppl):173–5.
39. Suzuki H, Torigoe K, Numata O, Yazaki S. Infant case with a malignant form of Brugada syndrome. *J Cardiovasc Electrophysiol.* 2000;11:1277–80.
40. Ohgo T, Okamura H, Noda T, Satomi K, Suyama K, Kurita T, et al. Acute and chronic management in patients with Brugada syndrome associated with electrical storm of ventricular fibrillation. *Heart Rhythm.* 2007;4(6):695–700.

41. Watanabe A, Fukushima KK, Morita H, Miura D, Sumida W, Hiramatsu S, et al. Low-dose isoproterenol for repetitive ventricular arrhythmia in patients with Brugada syndrome. *Eur Heart J*. 2006;27(13):1579–83.
42. Hermida JS, Denjoy I, Clerc J, Extramiana F, Jarry G, Milliez P, et al. Hydroquinidine therapy in Brugada syndrome. *J Am Coll Cardiol*. 2004;43(10):1853–60.
43. Belhassen B, Glick A, Viskin S. Efficacy of quinidine in high-risk patients with Brugada syndrome. *Circulation*. 2004;110:1731–7.
44. Tsuchiya T, Ashikaga K, Honda T, Arita M. Prevention of ventricular fibrillation by cilostazol, an oral phosphodiesterase inhibitor, in a patient with Brugada syndrome. *J Cardiovasc Electrophysiol*. 2002;13(7):698–701.
45. Iguchi K, Noda T, Kamakura S, Shimizu W. Beneficial effects of cilostazol in a patient with recurrent ventricular fibrillation associated with early repolarization syndrome. *Heart Rhythm*. 2013;10(4):604–6.
46. Agac MT, Erkan H, Korkmaz L. Conversion of Brugada type I to type III and successful control of recurrent ventricular arrhythmia with cilostazol. *Arch Cardiovasc Dis*. 2013.
47. Hasegawa K, Ashihara T, Kimura H, Jo H, Itoh H, Yamamoto T, et al. Long-term pharmacological therapy of Brugada syndrome: is J-wave attenuation a marker of drug efficacy? *Intern Med*. 2014;53(14):1523–6.
48. Shinohara T, Ebata Y, Ayabe R, Fukui A, Okada N, Yufu K, et al. Combination therapy of cilostazol and bepridil suppresses recurrent ventricular fibrillation related to J-wave syndromes. *Heart Rhythm*. 2014;11(8):1441–5.
49. Haissaguerre M, Sacher F, Nogami A, Komiya N, Bernard A, Probst V, et al. Characteristics of recurrent ventricular fibrillation associated with inferolateral early repolarization role of drug therapy. *J Am Coll Cardiol*. 2009;53(7):612–9.
50. Junttila MJ, Tikkanen JT, Kentta T, Anttonen O, Aro AL, Porthan K, et al. Early repolarization as a predictor of arrhythmic and nonarrhythmic cardiac events in middle-aged subjects. *Heart Rhythm*. 2014;11(10):1701–6.
51. Nademanee K, Raju H, de Noronha SV, Papadakis M, Robinson L, Rothery S, et al. Fibrosis, Connexin-43, and conduction abnormalities in the Brugada syndrome. *J Am Coll Cardiol*. 2015;66(18):1976–86.
52. Ghosh S, Cooper DH, Vijayakumar R, Zhang J, Pollak S, Haissaguerre M, et al. Early repolarization associated with sudden death: insights from noninvasive electrocardiographic imaging. *Heart Rhythm*. 2010;7(4):534–7.
53. Zhang J, Sacher F, Hoffmayer K, O'Hara T, Strom M, Cuculich P, et al. Cardiac electrophysiological substrate underlying the ECG phenotypic and electrogram abnormalities in Brugada syndrome patients. *Circulation*. 2015;131(22):1950–9.
54. Noda T, Shimizu W, Tanaka K, Chayama K. Prominent J wave and ST segment elevation: serial electrocardiographic changes in accidental hypothermia. *J Cardiovasc Electrophysiol*. 2003;14(2):223.
55. Bastiaenen R, Hedley PL, Christiansen M, Behr ER. Therapeutic hypothermia and ventricular fibrillation storm in early repolarization syndrome. *Heart Rhythm*. 2010;7(6):832–4.
56. Federman NJ, Mechulan A, Klein GJ, Krahn AD. Ventricular fibrillation induced by spontaneous hypothermia in a patient with early repolarization syndrome. *J Cardiovasc Electrophysiol*. 2013;24:586–8.
57. Kowalczyk E, Kasprzak JD, Lipiec P. Giant J-wave and Brugada-like pattern in a patient with severe hypothermia. *Acta Cardiol*. 2014;69(1):66–7.
58. RuDusky BM. The electrocardiogram in hypothermia—the J wave and the Brugada syndrome. *Am J Cardiol*. 2004;93(5):671–2.
59. Patel RB, Ng J, Reddy V, Chokshi M, Parikh K, Subacius H, et al. Early repolarization associated with ventricular arrhythmias in patients with chronic coronary artery disease. *Circ Arrhythm Electrophysiol*. 2010;3(5):489–95.
60. Amin AS, Meregalli PG, Bardai A, Wilde AA, Tan HL. Fever increases the risk for cardiac arrest in the Brugada syndrome. *Ann Intern Med*. 2008;149(3):216–8.
61. Rattanawong P, Vutthikraivit W, Charoensri A, Jongraksak T, Prombandankul A, Kanjanahattakij N, et al. Fever-induced Brugada syndrome is more common than previously suspected: a cross-sectional study from an endemic area. *Ann Noninvasive Electrocardiol*. 2015.
62. Kawata H, Morita H, Yamada Y, Noda T, Satomi K, Aiba T, et al. Prognostic significance of early repolarization in inferolateral leads in Brugada patients with documented ventricular fibrillation: a novel risk factor for Brugada syndrome with ventricular fibrillation. *Heart Rhythm*. 2013;10(8):1161–8.
63. Noseworthy PA, Tikkanen JT, Porthan K, Oikarinen L, Pietila A, Harald K, et al. The early repolarization pattern in the general population clinical correlates and heritability. *J Am Coll Cardiol*. 2011;57(22):2284–9.
64. Reinhard W, Kaess BM, Debiec R, Nelson CP, Stark K, Tobin MD, et al. Heritability of early repolarization: a population-based study. *Circ Cardiovasc Genet*. 2011;4(2):134–8.
65. Nunn LM, Bhar-Amato J, Lowe MD, Macfarlane PW, Rogers P, McKenna WJ, et al. Prevalence of J-point elevation in sudden arrhythmic death syndrome families. *J Am Coll Cardiol*. 2011;58(3):286–90.
66. Haissaguerre M, Chatel S, Sacher F, Weerasooriya R, Probst V, Loussouarn G, et al. Ventricular fibrillation with prominent early repolarization associated with a rare variant of KCNJ8/K_{ATP} channel. *J Cardiovasc Electrophysiol*. 2009;20(1):93–8.

67. Medeiros-Domingo A, Tan BH, Crotti L, Tester DJ, Eckhardt L, Cuoretti A, et al. Gain-of-function mutation S422L in the KCNJ8-encoded cardiac K(ATP) channel Kir6.1 as a pathogenic substrate for J-wave syndromes. *Heart Rhythm*. 2010;7(10):1466–71.
68. Barajas-Martinez H, Hu D, Ferrer T, Onetti CG, Wu Y, Burashnikov E, et al. Molecular genetic and functional association of Bugada and early repolarization syndromes with S422L missense mutation in *KCNJ8*. *Heart Rhythm*. 2012;9(4):548–55.
69. Burashnikov E, Pfeiffer R, Barajas-Martinez H, Delpon E, Hu D, Desai M, et al. Mutations in the cardiac L-type calcium channel associated J wave syndrome and sudden cardiac death. *Heart Rhythm*. 2010;7(12):1872–82.
70. Watanabe H, Nogami A, Ohkubo K, Kawata H, Hayashi Y, Ishikawa T, et al. Electrocardiographic characteristics and *SCN5A* mutations in idiopathic ventricular fibrillation associated with early repolarization. *Circ Arrhythm Electrophysiol*. 2011;4(6):874–81.
71. Hu D, Barajas-Martinez H, Pfeiffer R, Dezi F, Pfeiffer J, Buch T, et al. Mutations in *SCN10A* are responsible for a large fraction of cases of Brugada syndrome. *J Am Coll Cardiol*. 2014;64(1):66–79.
72. Schwartz PJ, Ackerman MJ, George AL Jr, Wilde AA. Impact of genetics on the clinical management of channelopathies. *J Am Coll Cardiol*. 2013;62(3):169–80.
73. Osborn JJ. Experimental hypothermia: respiratory and blood pH changes in relation to cardiac function. *Am J Phys*. 1953;175:389–98.
74. Litovsky SH, Antzelevitch C. Transient outward current prominent in canine ventricular epicardium but not endocardium. *Circ Res*. 1988;62(1):116–26.
75. Litovsky SH, Antzelevitch C. Differences in the electrophysiology of ventricular epicardium and endocardium as the basis for the Osborne wave. *Circulation*. 1989;80:II-129.
76. Di Diego JM, Sun ZQ, Antzelevitch C. I_{to} and action potential notch are smaller in left vs. right canine ventricular epicardium. *Am J Phys*. 1996;271:H548–H61.
77. Antzelevitch C, Yan GX. J-wave syndromes: Brugada and early repolarization syndromes. *Heart Rhythm*. 2015;12(8):1852–66.
78. Koncez I, Gurabi Z, Patocskai B, Panama BK, Szel T, Hu D, et al. Mechanisms underlying the development of the electrocardiographic and arrhythmic manifestations of early repolarization syndrome. *J Mol Cell Cardiol*. 2014;68C:20–8.
79. Wilhelm M, Brem MH, Rost C, Klinghammer L, Hennig FF, Daniel WG, et al. Early repolarization, left ventricular diastolic function, and left atrial size in professional soccer players. *Am J Cardiol*. 2010;106(4):569–74.
80. Marcus RR, Kalisetti D, Raxwal V, Kiratli BJ, Myers J, Perkash I, et al. Early repolarization in patients with spinal cord injury: prevalence and clinical significance. *J Spinal Cord Med*. 2002;25(1):33–8.
81. Mizumaki K, Nishida K, Iwamoto J, Nakatani Y, Yamaguchi Y, Sakamoto T, et al. Vagal activity modulates spontaneous augmentation of J-wave elevation in patients with idiopathic ventricular fibrillation. *Heart Rhythm*. 2012;9(2):249–55.
82. Koutbi L, Roussel M, Haissaguerre M, Deharo JC. Hyperpnea test triggering malignant ventricular arrhythmia in a child with early repolarization. *Heart Rhythm*. 2012;9(7):1153–6.
83. Brugada J, Brugada R, Brugada P. Pharmacological and device approach to therapy of inherited cardiac diseases associated with cardiac arrhythmias and sudden death. *J Electrocardiol*. 2000;33(Suppl):41–7.
84. Nademanee K, Veerakul G, Mower M, Likittanasombat K, Krittayapong R, Bhuripanyo K, et al. Defibrillator versus beta-blockers for unexplained death in Thailand (DEBUT): a randomized clinical trial. *Circulation*. 2003;107(17):2221–6.
85. Sacher F, Probst V, Maury P, Babuty D, Mansourati J, Komatsu Y, et al. Outcome after implantation of cardioverter-defibrillator in patients with Brugada syndrome: a Multicenter Study - Part 2. *Circulation*. 2013;128(16):1739–47.
86. Conte G, Sieira J, Ciconte G, de Asmundis C, Chierchia GB, Baltogiannis G, et al. Implantable cardioverter-defibrillator therapy in brugada syndrome: a 20-year single-center experience. *J Am Coll Cardiol*. 2015;65(9):879–88.
87. Sacher F, Probst V, Bessouet M, Wright M, Maluski A, Abbey S, et al. Remote implantable cardioverter defibrillator monitoring in a Brugada syndrome population. *Europace*. 2009;11(4):489–94.
88. De Maria E, Oлару A, Cappelli S. The entirely subcutaneous defibrillator (s-icd): state of the art and selection of the ideal candidate. *Curr Cardiol Rev*. 2015;11(2):180–6.
89. van Den Berg MP, Wilde AA, Viersma TJW, Brouwer J, Haaksma J, van der Hout AH, et al. Possible bradycardic mode of death and successful pacemaker treatment in a large family with features of long QT syndrome type 3 and Brugada syndrome. *J Cardiovasc Electrophysiol*. 2001;12(6):630–6.
90. Bertomeu-Gonzalez V, Ruiz-Granell R, Garcia-Civera R, Morell-Cabedo S, Ferrero A. Syncopal monomorphic ventricular tachycardia with pleomorphism, sensitive to antitachycardia pacing in a patient with Brugada syndrome. *Europace*. 2006;8(12):1048–50.
91. Lee KL, Lau C, Tse H, Wan S, Fan K. Prevention of ventricular fibrillation by pacing in a man with Brugada syndrome. *J Cardiovasc Electrophysiol*. 2000;11(8):935–7.
92. Haissaguerre M, SFDNJLDidRPLJLNABDY-MSAFA. Early repolarization in the inferolateral leads: a new syndrome associated with sudden cardiac death. *J Interv Card Electrophysiol*. 2007;18:281.
93. Chatzidou S, Repasos E, Plastiras S, Kontogiannis C, Kosmopoulos M, Tsilimigras DI, et al. Repetitive-incessant electrical storm triggered by

- early repolarization. *Ann Noninvasive Electrocardiol.* 2017.
94. Latcu DG, Bun SS, Zargane N, Saoudi N. Ablation of left ventricular substrate in early repolarization syndrome. *J Cardiovasc Electrophysiol.* 2016;27(4):490–1.
 95. Kakiyama J, Takagi M, Hayashi Y, Tatsumi H, Doi A, Yoshiyama M. Radiofrequency catheter ablation for treatment of premature ventricular contractions triggering ventricular fibrillation from the right ventricular outflow tract in a patient with early repolarization syndrome. *HeartRhythm Case Rep.* 2016;2(4):342–6.
 96. Nademane K, Veerakul G, Chandanamatta P, Chaothawe L, Ariyachaiapanich A, Jirasirojanakorn K, et al. Prevention of ventricular fibrillation episodes in Brugada syndrome by catheter ablation over the anterior right ventricular outflow tract epicardium. *Circulation.* 2011;123(12):1270–9.
 97. Cortez-Dias N, Placido R, Marta L, Bernardes A, Sobral S, Carpinteiro L, et al. Epicardial ablation for prevention of ventricular fibrillation in a patient with Brugada syndrome. *Rev Port Cardiol.* 2014;33(5):305.
 98. Shah AJ, Hocini M, Lamaison D, Sacher F, Derval N, Haissaguerre M. Regional substrate ablation abolishes Brugada syndrome. *J Cardiovasc Electrophysiol.* 2011;22(11):1290–1.
 99. Sacher F, Jesel L, Jais P, Haissaguerre M. Insight into the mechanism of Brugada syndrome: epicardial substrate and modification during ajmaline testing. *Heart Rhythm.* 2014;11(4):732–4.
 100. Brugada J, Pappone C, Berruzo A, Vicedomini G, Manguso F, Ciconte G, et al. Brugada syndrome phenotype elimination by epicardial substrate ablation. *Circ Arrhythm Electrophysiol.* 2015;8:1373.
 101. Priori SG, Wilde AA, Horie M, Cho Y, Behr ER, Berul C, et al. Executive summary: HRS/EHRA/APHRS expert consensus statement on the diagnosis and management of patients with inherited primary arrhythmia syndromes. *Heart Rhythm.* 2013;15(10):1389–406.
 102. Yoon N, Patocskai B, Antzelevitch C. Epicardial substrate as a target for radiofrequency ablation in an experimental model of early repolarization syndrome. *Circ Arrhythm Electrophysiol.* 2018; In press.
 103. Antzelevitch C, Brugada P, Brugada J, Brugada R, Nademane K, Towbin JA. Clinical approaches to tachyarrhythmias. *The Brugada syndrome*, vol. 1999. Armonk: Futura Publishing Company, Inc.; 1999.
 104. Minoura Y, Di Diego JM, Barajas-Martinez H, Zygmunt AC, Hu D, Sicouri S, et al. Ionic and cellular mechanisms underlying the development of acquired Brugada syndrome in patients treated with antidepressants. *J Cardiovasc Electrophysiol.* 2012;23(4):423–32.
 105. Minoura Y, Panama BK, Nesterenko VV, Betzenhauser M, Barajas-Martinez H, Hu D, et al. Effect of Wenxin Keli and quinidine to suppress arrhythmogenesis in an experimental model of Brugada syndrome. *Heart Rhythm.* 2013;10(7):1054–62.
 106. Szel T, Antzelevitch C. Abnormal repolarization as the basis for late potentials and fractionated electrograms recorded from epicardium in experimental models of brugada syndrome. *J Am Coll Cardiol.* 2014;63(19):2037–45.
 107. Johson P, Lesage A, Floyd WL, Young WG Jr, Sealy WC. Prevention of ventricular fibrillation during profound hypothermia by quinidine. *Ann Surg.* 1960;151:490–5.
 108. Belhassen B, Shapira I, Shoshani D, Paredes A, Miller H, Laniado S. Idiopathic ventricular fibrillation: inducibility and beneficial effects of class I antiarrhythmic agents. *Circulation.* 1987;75(4):809–16.
 109. Belhassen B, Viskin S, Antzelevitch C. The Brugada syndrome: is an implantable cardioverter defibrillator the only therapeutic option? *Pacing Clin Electrophysiol.* 2002;25(11):1634–40.
 110. Alings M, Dekker L, Sadee A, Wilde A. Quinidine induced electrocardiographic normalization in two patients with Brugada syndrome. *Pacing Clin Electrophysiol.* 2001;24(9 Pt 1):1420–2.
 111. Belhassen B, Viskin S. Pharmacologic approach to therapy of Brugada syndrome: quinidine as an alternative to ICD therapy? In: Antzelevitch C, Brugada P, Brugada J, Brugada R, editors. *The Brugada syndrome: from bench to bedside.* Oxford: Blackwell Futura; 2004. p. 202–11.
 112. Viskin S, Wilde AA, Tan HL, Antzelevitch C, Shimizu W, Belhassen B. Empiric quinidine therapy for asymptomatic Brugada syndrome: time for a prospective registry. *Heart Rhythm.* 2009;6(3):401–4.
 113. Belhassen B, Glick A, Viskin S. Excellent long-term reproducibility of the electrophysiologic efficacy of quinidine in patients with idiopathic ventricular fibrillation and Brugada syndrome. *Pacing Clin Electrophysiol.* 2009;32(3):294–301.
 114. Marquez MF, Bonny A, Hernandez-Castillo E, De SA, Gomez-Flores J, Nava S, et al. Long-term efficacy of low doses of quinidine on malignant arrhythmias in Brugada syndrome with an implantable cardioverter-defibrillator: a case series and literature review. *Heart Rhythm.* 2013;9(12):1995–2000.
 115. Pellegrino PL, Di BM, Brunetti ND. Quinidine for the management of electrical storm in an old patient with Brugada syndrome and syncope. *Acta Cardiol.* 2013;68(2):201–3.
 116. Probst V, Evain S, Gournay V, Marie A, Schott JJ, Boisseau P, et al. Monomorphic ventricular tachycardia due to brugada syndrome successfully treated by hydroquinidine therapy in a 3-year-old child. *J Cardiovasc Electrophysiol.* 2006;17(1):97–100.
 117. Schweizer PA, Becker R, Katus HA, Thomas D. Successful acute and long-term management of electrical storm in Brugada syndrome using oriprenaline and quinine/quinidine. *Clin Res Cardiol.* 2010;99(7):467–70.

118. Marquez MF, Rivera J, Hermosillo AG, Iturralde P, Colin L, Moragrega JL, et al. Arrhythmic storm responsive to quinidine in a patient with Brugada syndrome and vasovagal syncope. *Pacing Clin Electrophysiol.* 2005;28(8):870–3.
119. Viskin S, Antzelevitch C, Marquez MF, Belhassen B. Quinidine: a valuable medication joins the list of 'endangered species'. *Europace.* 2007;12(12):1105–6.
120. Rosso R, Glick A, Glikson M, Wagshal A, Swissa M, Rosenhek S, et al. Outcome after implantation of cardioverter defibrillator in patients with Brugada syndrome: a multicenter Israeli study (ISRABRU). *Isr Med Assoc J.* 2008;10(6):435–9.
121. Belhassen B, Rahkovich M, Michowitz Y, Glick A, Viskin S. Management of Brugada Syndrome: a 33-year experience using electrophysiologically-guided therapy with class IA antiarrhythmic drugs. *Circ Arrhythm Electrophysiol.* 2015;8:1393.
122. Sacher F, Derval N, Horlitz M, Haissaguerre M. J wave elevation to monitor quinidine efficacy in early repolarization syndrome. *J Electrocardiol.* 2014;47(2):223–5.
123. Antzelevitch C. The Brugada syndrome: ionic basis and arrhythmia mechanisms. *J Cardiovasc Electrophysiol.* 2001;12(2):268–72.
124. Kyriazis K, Bahlmann E, van der SH, Kuck KH. Electrical storm in Brugada syndrome successfully treated with orciprenaline; effect of low-dose quinidine on the electrocardiogram. *Europace.* 2009;11(5):665–6.
125. Gurabi Z, Koncz I, Patocskaï B, Nesterenko VV, Antzelevitch C. Cellular mechanism underlying hypothermia-induced VT/VF in the setting of early repolarization and the protective effect of quinidine, cilostazol and milrinone. *Circ Arrhythm Electrophysiol.* 2014;7(1):134–42.
126. Szel T, Koncz I, Antzelevitch C. Cellular mechanisms underlying the effects of milrinone and cilostazol to suppress arrhythmogenesis associated with Brugada syndrome. *Heart Rhythm.* 2013;10(11):1720–7.
127. Shimizu W, Matsuo K, Takagi M, Tanabe Y, Aiba T, Taguchi A, et al. Body surface distribution and response to drugs of ST segment elevation in Brugada syndrome: clinical implication of eighty-seven-lead body surface potential mapping and its application to twelve-lead electrocardiograms. *J Cardiovasc Electrophysiol.* 2000;11(4):396–404.
128. Tanaka H, Kinoshita O, Uchikawa S, Kasai H, Nakamura M, Izawa A, et al. Successful prevention of recurrent ventricular fibrillation by intravenous isoproterenol in a patient with Brugada syndrome. *Pacing Clin Electrophysiol.* 2001;24(8 Pt 1):1293–4.
129. Mok NS, Chan NY, Chi-Suen CA. Successful use of quinidine in treatment of electrical storm in Brugada syndrome. *Pacing Clin Electrophysiol.* 2004;27(6P1):821–3.
130. Miyazaki T, Mitamura H, Miyoshi S, Soejima K, Aizawa Y, Ogawa S. Autonomic and antiarrhythmic drug modulation of ST segment elevation in patients with Brugada syndrome. *J Am Coll Cardiol.* 1996;27:1061–70.
131. Maury P, Couderc P, Delay M, Boveda S, Brugada J. Electrical storm in Brugada syndrome successfully treated using isoprenaline. *Europace.* 2004;6(2):130–3.
132. Maury P, Hocini M, Haissaguerre M. Electrical storms in Brugada syndrome: review of pharmacologic and ablative therapeutic options. *Indian Pacing Electrophysiol J.* 2005;5(1):25–34.
133. Jongman JK, Jepkes-Bruin N, Ramdat Misier AR, Beukema WP, Delnoy PP, Oude LH, et al. Electrical storms in Brugada syndrome successfully treated with isoproterenol infusion and quinidine orally. *Neth Heart J.* 2007;15(4):151–5.
134. Sharif-Kazemi MB, Emkanjoo Z, Tavoosi A, Kafi M, Kheirkhah J, Alizadeh A, et al. Electrical storm in Brugada syndrome during pregnancy. *Pacing Clin Electrophysiol.* 2011;34(2):e18–21.
135. Furniss G. Isoprenaline and quinidine to calm Brugada VF storm. *BMJ Case Rep.* 2012.
136. Roten L, Derval N, Sacher F, Pascale P, Scherr D, Komatsu Y, et al. Heterogeneous response of J wave syndromes to beta-adrenergic stimulation. *Heart Rhythm.* 2012;9(12):1970–6.
137. Kaneko Y, Horie M, Niwano S, Kusano K, Takatsuki S, Kurita T, et al. Electrical storm in patients with Brugada syndrome is associated with early repolarization. *Circ Arrhythm Electrophysiol.* 2014;7:1122.
138. Kanlop N, Chattipakorn S, Chattipakorn N. Effects of cilostazol in the heart. *J Cardiovasc Med (Hagerstown).* 2011;12(2):88–95.
139. Patocskaï B, Barajas-Martinez H, Hu D, Gurabi Z, Koncz I, Antzelevitch C. Cellular and ionic mechanisms underlying the effects of cilostazol, milrinone, and isoproterenol to suppress arrhythmogenesis in an experimental model of early repolarization syndrome. *Heart Rhythm.* 2016;13(6):1326–34.
140. Sugao M, Fujiki A, Nishida K, Sakabe M, Tsuneda T, Iwamoto J, et al. Repolarization dynamics in patients with idiopathic ventricular fibrillation: pharmacological therapy with bepridil and disopyramide. *J Cardiovasc Pharmacol.* 2005;45(6):545–9.
141. Murakami M, Nakamura K, Kusano KF, Morita H, Nakagawa K, Tanaka M, et al. Efficacy of low-dose bepridil for prevention of ventricular fibrillation in patients with Brugada syndrome with and without SCN5A mutation. *J Cardiovasc Pharmacol.* 2010;56(4):389–95.
142. Aizawa Y, Yamakawa H, Takatsuki S, Katsumata Y, Nishiyama T, Kimura T, et al. Efficacy and safety of bepridil for prevention of ICD shocks in patients with Brugada syndrome and idiopathic ventricular fibrillation. *Int J Cardiol.* 2013;168(5):5083–5.
143. Aizawa Y, Chinushi M, Hasegawa K, Naiki N, Horie M, Kaneko Y, et al. Electrical storm in idiopathic ventricular fibrillation is associated with early repolarization. *J Am Coll Cardiol.* 2013;62(11):1015–9.
144. Kang L, Zheng MQ, Morishima M, Wang Y, Kaku T, Ono K. Bepridil up-regulates cardiac Na⁺ channels

- as a long-term effect by blunting proteasome signals through inhibition of calmodulin activity. *Br J Pharmacol.* 2009;157(3):404–14.
145. Fish JM, Welchons DR, Kim YS, Lee SH, Ho WK, Antzelevitch C. Dimethyl lithospermate B, an extract of danshen, suppresses arrhythmogenesis associated with the Brugada syndrome. *Circulation.* 2006;113(11):1393–400.
146. Li GR, Wang HB, Qin GW, Jin MW, Tang Q, Sun HY, et al. Acacetin, a natural flavone, selectively inhibits human atrial repolarization potassium currents and prevents atrial fibrillation in dogs. *Circulation.* 2008;117(19):2449–57.
147. Priori SG, Wilde AA, Horie M, Cho Y, Behr ER, Berul C, et al. HRS/EHRA/APHRS expert consensus statement on the diagnosis and management of patients with inherited primary arrhythmia syndromes: document endorsed by HRS, EHRA, and APHRS in May 2013 and by ACCF, AHA, PACES, and AEPC in June 2013. *Heart Rhythm.* 2013;10(12):1932–63.
148. Priori SG, Blomstrom-Lundqvist C, Mazzanti A, Blom N, Borggrefe M, Camm J, et al. 2015 ESC Guidelines for the management of patients with ventricular arrhythmias and the prevention of sudden cardiac death: The Task Force for the Management of Patients with Ventricular Arrhythmias and the Prevention of Sudden Cardiac Death of the European Society of Cardiology (ESC) Endorsed by: Association for European Paediatric and Congenital Cardiology (AEPC). *Eur Heart J.* 2015;36:2793.



Electrocardiographic J Wave and Cardiovascular Risk in the General Population

15

Heikki V. Huikuri

Preface

The electrocardiographic (ECG) pattern of early repolarization (ER) has historically been regarded as a benign ECG variant, but during the past few years, this concept has been challenged based on multiple reports linking the ER pattern in the inferior and/or lateral leads of the standard 12-lead ECG with an increased risk of sudden cardiac death. Case-control studies have unambiguously shown that patients resuscitated from cardiac arrest without a known etiology have higher prevalence of ECG pattern of ER in the inferior and/or lateral leads (=ER syndrome) than matched controls. Epidemiological follow-up studies have also shown that ER pattern carries an increased risk of future arrhythmic death. Although the prevalence of ER pattern is relatively high especially in young asymptomatic males, there is increasing information about the ECG and phenotype characteristics, which can help in separating ER syndrome from benign patterns of ER. This chapter presents the current knowledge of the prevalence and significance of ECG pattern of ER in general population.

History of Early Repolarization ECG Pattern

Early repolarization (ER) is a common electrocardiographic (ECG) pattern characterized by J point and ST segment elevation in 2 or more contiguous leads. The presence of ER pattern in the precordial leads (V1–V3) is still considered a benign phenomenon and it has been generally viewed as a marker of good health. Most recommendations for standardization and interpretation of the ECG include a statement that the term ER is used to describe a normal QRS-T variant with ST segment elevation especially in the left precordial leads [1], and most clinicians have considered ER as nonspecific ST elevation.

Shipley and Hallaran referred to QRS notching and slurring in the electrocardiogram (ECG) of 200 apparently healthy subjects in 1936 using four unconventional ECG leads [2]. Myers et al. reported in 1947 that an elevation of the RS-T of 0.05–0.2 mV may be considered a normal variant, provided that the ST segment begins to rise above the RS-T junction in an arc with upward concavity to end in a tall upright T wave [3]. Later, Goldman noted in 25 subjects that there was elevation of 0.2–0.4 mV of the RS-T segment in leads V4–V6, which was regarded as a normal variant and occurred more commonly in young black males [4]. In 1961, Wasserburger et al. also described the normal RS-T segment elevation variant, which was termed “early repolarization” [5].

H. V. Huikuri (✉)
Research Unit of Internal Medicine, University
Hospital of Oulu, Oulu, Finland
e-mail: heikki.huikuri@oulu.fi

Osborn described the classic *J* wave in experimental hypothermia in 1953 [1]. Dogs subjected to hypothermia developed spontaneous ventricular fibrillation (VF) that was preceded by the development of *J* waves [6]. The *J* wave, which was attributed to a current of injury (hence the term “*J*”), was later coined the Osborn wave. Later experiments have demonstrated that *J* waves are the ECG reflection of increased dispersion of repolarization [7–9]. After some case reports pointing to an arrhythmogenic potential of ER, a series of case-control studies have described an apparent over-presentation of *J* waves, i.e., terminal QRS notching and/or slurring in infero-lateral leads with and without ST segment elevation, in patients with idiopathic VF [10–15]. Thereafter infero-lateral QRS notching and slurring, referred to as ER ECG pattern, have also been demonstrated to carry an increased risk of sudden cardiac death (SCD) and mortality in general population [16–18].

There are conflicting data regarding the prognosis of subjects with ECG pattern of ER, but as discussed later, there has been a major lack of consistence between these studies in the pattern definition as well the duration of the follow-up [16–23]. There seems to be variability in the magnitude of risk between different ECG patterns. Especially *J* wave distribution, *J* wave amplitude, and dynamicity and morphology of the ST segment modify the risk. This article summarizes the current knowledge of the prevalence of ER and of arrhythmic risk associated with various *J* wave patterns and intentionally elides any debate on the underlying pathophysiology as this has been discussed in several articles [7–9].

Terminology and Definitions

A recent consensus paper was aimed at harmonizing the terminology and definitions of *J* waves and ER patterns from standard 12-lead ECG [24]. Notched *J* was defined as notching in the final 50% of the downslope of the R wave occurring in the final segment of the QRS complex (Fig. 15.1a). It should be distinguished from a notch in the middle part of the downslope of R

wave, which should be classified as the fragmentation of the QRS complex. Slurred *J* wave is the apparent slowing of the waveform at the end of the QRS complex and it merges with the ST segment (Fig. 15.1b). A slur should also occur in the final 50% of the downslope of the R wave. The consensus paper recommends the following terminology: (i) *J* onset (Jo) should represent the onset of a notch, (ii) *J* peak (Jp) should represent the peak of a notch or onset of a slur, and (iii) *J* termination (Jt) should represent the end of a notch or slur (Fig. 15.1a, b). In the case of a slur, Jo and Jp are the same points. The amplitude of early repolarization or *J* point elevation equates with the Jp amplitude. The ST segment slope should be measured from Jt. It should be regarded as horizontal or downsloping if the amplitude of the ST segment 100 ms after Jt is the same or smaller than the amplitude of Jt (Fig. 15.2). The ST segment should be regarded as upward sloping if the amplitude of the ST segment 100 ms after Jt is higher than the amplitude of Jt (Fig. 15.1a, b).

The consensus report proposed new definitions of early repolarization as follows: (i) there is an end QRS notch or slur on the downslope of a prominent R wave. If there is a notch, it should lie entirely above the baseline. The onset of a slur must also be above the baseline, and (ii) $J_p \geq 0.1$ mV in two or more contiguous leads of the 12-lead ECG, excluding leads V1–V3. If the ST segment is upward sloping and followed by a tall symmetrical upright T wave, the pattern should be described as early repolarization with ascending ST segment. If the segment is horizontal or downward sloping, the pattern should be described as early repolarization with horizontal or descending ST segment.

Prevalence of Early Repolarization in the Inferior and/or Lateral ECG Leads

ER ECG pattern in the inferior/lateral leads occurs in 1–24% of the middle-aged general population [16–26] (see Table 15.1) and in 15–70% of idiopathic VF cases [3–11]. Male sex is

Fig. 15.1 Example *J* wave patterns in two young and healthy athletes illustrating terminal QRS notching (a) and slurring (b) with rapidly ascending ST segments. (Reprinted with permission from Wolters Kluwer from: Tikkanen et al. [29])



Fig. 15.2 Example *J* wave patterns in two middle-aged individuals with QRS changes and horizontal ST segments. (Reprinted with permission from Wolters Kluwer from: Tikkanen et al. [29])



strongly associated with ER ECG pattern, since over 70% of subjects with ER are males. The prevalence of ER ECG pattern declines from early adulthood until middle age in males, and gender difference diminishes with age, suggesting a hormonal influence, probably testosterone, on the presence of ER [27]. The ER pattern is more common in young physically active indi-

viduals, athletes (up to 40%), and African Americans [28]. There is an increased prevalence of ER reported in Southeast Asians (27%) [18]. ER is associated with high vagal tone, as well as hypothermia. ECG features of bradycardia, prolonged QRS duration, short QT interval, and left ventricular hypertrophy assessed by the Sokolow-Lyon index are also associated with ER [25].

Table 15.1 Prevalence of early repolarization in inferior and/or lateral leads in different ethnic and age groups

Study	Number of subjects	Prevalence if ER (%)	ER with horizontal/descending ST segment (%)	Origin	Age (years)
Tikkanen et al. [29]	10,288	5,6	4,0	Whites/Finland	44 ± 8
Noseworthy et al. [25]	3955	6,1	–	Blacks and Whites/USA	40 ± 8
Noseworthy et al. [25]	5489	3,3	–	Whites/Finland	49 ± 11
Sinner et al. [17]	6213	13,1	–	Whites/Germany	
Haruta et al. [18]	5976	23,9	–	Whites/Japan	43
Olson et al. [19]	15,141	12,3	–	Blacks and Whites/USA	54 ± 6
Tikkanen et al. [29]	503	31,0	3,1	Athletes/USA	17–24
Sager et al. [26]	719	17,0	3,0	Blacks and Whites/USA	8–12
Sager et al. [26]	755	16,0	3,0	Blacks and Whites/USA	21–25
Aagaard et al. [20]	211,920	2,2	–	African Americans/USA	18–75
Aagaard et al. [20]		1,5	–	Hispanics/USA	18–75
Aagaard et al. [20]		0,9	–	Non-Hispanics, Whites/USA	18–75

The ER pattern with rapidly ascending ST segment and tall peaked T waves is commonly observed in healthy, young athletes and is considered as a benign normal variant [29]. Its prevalence declines rapidly with aging. The pattern with horizontal/downsloping ST segment following the *J* wave is not age dependent and its prevalence is relatively consistent (3–4%) in different populations and in different age groups.

Prognostic Significance of Early Repolarization in General Population

Table 15.2 summarizes the results of studies assessing the prognostic significance of ER pattern in the inferior and/or lateral ECG leads in various populations. It should be emphasized that the ER pattern is more predictive of sudden arrhythmic death than overall cardiovascular mortality or all-cause mortality. Majority of the studies using the criteria by Haissaguerre et al. for diagnosing the ER pattern have shown that the ER, especially in the inferior ECG leads, pre-

Table 15.2 Prognosis of patients with early repolarization in inferior and/or lateral ECG leads

Study	Number of subjects	All-cause mortality (adjusted relative risk)	Arrhythmic death/sudden cardiac death ^a (adjusted relative risk)
Tikkanen et al. [16]	10,288	1.14 (1.03–1.26)	1.30 (1.00–1.70)
Olson et al. [19]	15,141	1.35 (1.24–1.48)	2.20 (1.63–2.97)
Haruta et al. [18]	5976	0.88 (0.80–0.96)	1.75 (1.10–2.80)
Sinner et al. [17]	6213	1.08 (0.95–1.24)	1.40 (1.13–1.74) ^a
Rollin A et al. [23]	1161	2.45 (1.44–1.45)	5.60 (2.27–11.8) ^a
Wu et al. (meta-analysis) [22]	126,583	1.06 (0.85–1.31)	1.70 (1.19–2.42)
Aagaard et al. [20]	211,920	0.98 (0.89–1.07)	–

dicts cardiac and arrhythmic death. The negative studies in this field have usually used different diagnostic criteria for ER pattern, such as ST segment elevation or no ST segment elevation, or

included ER in the precordial leads in their analysis. Furthermore, negative studies have usually had a relatively short follow-up and/or have not included sudden cardiac death or arrhythmic death as a major endpoint [21].

The lack of consistency in the diagnostic criteria of ECG pattern of ER may partly explain the large heterogeneity in the prevalence and prognostic significance of this ECG pattern between the different studies. A consensus group has now created criteria for diagnostics, which will hopefully result in more homogeneous interpretations of the ER patterns [23]. Importantly, fragmented QRS complex of the downward sloping R wave should clearly be separated from the ER pattern, which should be linked to the ST segment and occur clearly in the terminal portion of the QRS complex.

The seminal study by Tikkanen et al. showed that ER pattern with a rapidly ascending ST segment is not associated with an increased risk of arrhythmic death, but the pattern with horizontal/downsloping ST segment with a high amplitude of *J* wave (>0.2 mV) is a strong predictor of arrhythmic death [29]. An interesting discovery of this study was that the survival curves for cardiac mortality started to diverge 15 years after the baseline recordings (in the early 1980s) and continued to diverge at a constant rate throughout the follow-up period, even though the treatment and prognosis for patients with cardiac disease overall have improved during recent years [16, 29]. The arrhythmic deaths seemed to occur at a relatively high age (>55 years), in which age group the SCD has been most commonly caused by an acute ischemic coronary event in the Finnish population. This led to the hypothesis that ER pattern may be a trigger of fatal events during myocardial ischemia. Later, in a case-control layout, it was found that there was a significant and independent association in the general population sample between ER, documented in a random ECG recording prior and remote to the event and the risk of sudden cardiac death at the time of an ischemic event [30]. The risk for sudden death was doubled even after multivariate adjustments, with the highest risk being observed for ER with hori-

zontal or descending ST segments, which supported the hypothesis of reduced ischemia tolerance. Although there were demographic and clinical differences between the victims and controls, the association between ER and sudden cardiac death was independent of those factors suggesting, although not confirming, the vulnerability of individuals with ER to suffer malignant arrhythmias during ischemia. Furthermore, the victims of sudden cardiac death had a lower prevalence of previously diagnosed cardiac disease in support to the concept that ER increases the risk of SCD in those subjects who suffer sudden death as their first manifestation of cardiac disease. Furthermore, the risk for ventricular fibrillation during the first 48 hours after myocardial infarction has been shown to be higher in patients who exhibited ER with horizontal/descending ST segments in the premonitory ECG [31, 32]. These studies provide one plausible mechanistic link between ER and risk of SCD: the presence of ER might act as a factor facilitating the occurrence of fatal arrhythmia during an acute ischemic event. In patients with ST elevation myocardial infarction (STEMI), previous ER was more common in patients with subsequent ventricular tachyarrhythmias (26% vs 4%), especially when present in the inferior leads [33]. A recent study has suggested that ER ECG pattern increases the risk of mortality also in chronic heart failure [34]. When these observations are combined, it can be speculated that subjects with ER ECG pattern suffer an increased risk for ventricular fibrillation during events such as those present in myocardial ischemia or heart failure that further shorten the action potential and increase the repolarization dispersion.

The amplitude and dynamicity of *J* waves are major modifiers of risk. In the general population, the risk of arrhythmic death increases significantly if *J* wave amplitude exceeds 0.2 mV, and this observation seems to hold true in a larger scale [16]. Although higher amplitude has been associated with a higher risk, the dynamic nature of *J* waves should also be acknowledged. In some patients both major high amplitude *J* waves and completely normal ECGs can be observed.

Especially in those with the ER syndrome, *J* waves are dynamic and increase in amplitude prior to VF episodes [35–37], and thus the *J* wave amplitude at random ECG does not always accurately define the possible underlying risk. However, when dynamicity of *J* waves is observed, it might be a significant marker of risk as pause-dependent augmentation of *J* waves has been reported to have a 100% specificity and high positive predictive value for idiopathic VF in ER syndrome patients [38–41]. These observations together suggest that higher amplitude and transient augmentation of *J* wave patterns should be recognized as signs of a high risk of fatal arrhythmias. However, it should also be noted that the benign forms of ER followed by rapidly ascending ST segment observed often in young athletes are also rate dependent, i.e., their amplitude increases at slow heart rates [42].

Third major mediator of risk in those with *J* waves seems to be the following ST segment morphology. First observed in unselected general population individuals [29], ER pattern with horizontal or descending ST segment has been shown to possess the highest risk of arrhythmic events in IVF patient samples [43], patients with myocardial ischemia, as well as in other general population samples [30, 31]. The definition of calling an ST segment non-ascending has been that it has to “stay flat” (under 0.1 mV) at least 100 ms after the preceding *J* wave. However, this concept lacks both the sensitivity and specificity as in several IVF patients the *J* waves are followed by ascending ST segments, and horizontal ST segments are observed quite commonly also in healthy individuals without any events on follow-up. However, for example, in patients with IVF and early repolarization those with ascending ST segments usually have other pathological co-findings, such as short QT interval or Brugada-type ECG pattern. Overall, evidence is accumulating in support of the finding that terminal QRS changes in the absence of ST elevation confer the highest risk of fatal arrhythmias.

There is also some evidence of the prognostic significance of *J* wave morphology, as the presence of QRS notching over terminal QRS slurring has been proposed to confer an increased

risk of sudden death. Terminal QRS notching has been commonly observed in some IVF patients, and in meta-analysis it has been associated with significant risk of sudden death [22]. This concept however has not uniformly distinguished the risk in all studies and its sensitivity and specificity to predict fatal arrhythmias is weak.

Characteristics of a Benign ECG Pattern of ER

Overall, not all manifestations of *J* wave patterns across the ECG leads seem to be equally proarrhythmic. In asymptomatic healthy individuals, *J* point elevation with high takeoff ST elevation is most prominently seen in mid-precordial leads, and terminal QRS notching accompanied by ST elevation in left precordial leads is likewise a common finding among young healthy individuals. These classical types of ER have for long been demonstrated to possess a benign prognosis, also in the current era. ER is commonly observed in the young, especially in fit and highly trained athletes, and therefore it is not surprising that our information of the ECG characteristics found in healthy individuals comes mainly from athlete populations, in which the prognosis of ER has also been found to be benign. Prevalence of *J* waves also in the inferior and lateral leads in athletes ranges up to 40%, but in >80% of cases the following ST segments are rapidly ascending [29]. *J* waves with rapidly ascending ST elevations have not predicted a high risk of arrhythmic death in the general population [29] or in IVF patients [43]. Therefore, this ER pattern can generally be considered as a benign phenomenon similar to ER patterns in the precordial leads in asymptomatic subjects. In conclusion, the ECG characteristics of benign ER patterns include *J* wave distribution mainly in the anterior, lateral, or inferior leads, tall peaked R waves, and the hallmark of athlete ER: rapidly ascending ST elevations. These patterns found especially in young and bradycardic athletic males, presumably with high testosterone levels and high Sokolow score, are with the current knowledge most likely normal variants.

Conclusions

The terminology and the criteria of *J* point elevations, *J* waves, and ER have been under debate in recent years. In addition, it is not completely resolved, whether the ER ECG pattern reflects depolarization or repolarization abnormality. Regardless of terminology and electrophysiological background, the ER pattern has the potential for arrhythmia prediction that can be seen in ECG tracing several years or decades before the actual risk for sudden death.

With the present knowledge, any screening for ER in completely asymptomatic individuals is not legitimate. The identification of individuals with ER patterns at high risk of ventricular arrhythmias and sudden death continues to be a challenge as the various ECG phenotypes are fairly common in the general population, but only a small subset experiences an arrhythmic event. It should be acknowledged that part of the data for risk stratification has been collected from heterogeneous populations, and observations from general population might not be straightforward applicable to those patients with ER syndrome, as the mechanisms of the onset of VF might vary. Given these limitations, on the ECG interpretation, emphasis should be put to the distribution and magnitude of *J* waves, most likely also to the following ST segments, but probably also to the dynamicity of *J* waves in order to unveil those with the highest risk for fatal arrhythmias. Finally, young athletes with a benign ECG pattern of ER should not be alerted to be at any risk for life-threatening arrhythmias.

References

1. Rautaharju PM, Surawicz B, Gettes LS. AHA/ACCF/HRS recommendations for the standardization and interpretation of the electrocardiogram: part IV: the ST segment, T and U waves, and the QT interval: a scientific statement from the American Heart Association electrocardiography and arrhythmias committee, council on clinical cardiology; the American college of cardiology foundation; and the heart rhythm society: endorsed by the international society for computerized electrocardiology. *Circulation*. 2009;119:e241–50.
2. Shipley RA, Hallaran WR. The four-lead electrocardiogram in two hundred normal men and women. *Am Heart J*. 1936;11:325–45.
3. Myers GB, Klein HA, Stofer BE, Hiraztka T. Normal variation in multiple precordial leads. *Am Heart J*. 1947;34:785–807.
4. Goldman MJ. RS-T segment elevation in mid and left precordial leads as a normal variant. *Am Heart J*. 1953;46:817–20.
5. Wasserburger RH, Alt WJ. The normal RS-T segment elevation variant. *Am J Cardiol*. 1961;8:184–92.
6. Osborn JJ. Experimental hypothermia: respiratory and blood pH changes in relation to cardiac function. *Am J Phys*. 1953;175:389–98.
7. Gussak I, Antzelevitch C. Early repolarization syndrome: clinical characteristics and possible cellular and ionic mechanisms. *J Electrocardiol*. 2000;33(4):299–309.
8. Antzelevitch C, Yan GX. J wave syndromes. *Heart Rhythm*. 2010;7:549–58.
9. Koncz I, Gubari Z, Patocskaï B, Panama BK, Szel T, Hu D, et al. Mechanisms underlying the development of the electrocardiographic and arrhythmic manifestations of early repolarization syndrome. *J Mol Cell Cardiol*. 2014;68:20–8.
10. Haïssaguerre M, Derval N, Sacher F, Jesel L, Deisenhofer I, de Roy L, et al. Sudden cardiac arrest associated with early repolarization. *N Engl J Med*. 2008;358:2016–23.
11. Rosso R, Kogan E, Belhassen B, Rozovski U, Scheinman MM, Zeltser D, et al. J-point elevation in survivors of primary ventricular fibrillation and matched control subjects: incidence and clinical significance. *J Am Coll Cardiol*. 2008;52:1231–8.
12. Abe A, Ikeda T, Tsukada T, Ishiguro H, Miwa Y, Miyakoshi M, et al. Circadian variation of late potentials in idiopathic ventricular fibrillation associated with J-waves: insight into alternative pathophysiology and risk stratification. *Heart Rhythm*. 2010;7:675–82.
13. Nam GB, Ko KH, Kim J, Park KM, Rhee KS, Choi KJ, et al. Mode of onset of ventricular fibrillation in patients with early repolarization pattern vs. Brugada syndrome. *Eur Heart J*. 2010;31:330–9.
14. Derval N, Simpson CS, Birnie DH, Healey J, Chauhan V, Champagne J, et al. Prevalence and characteristics of early repolarization in the CASPER registry. *J Am Coll Cardiol*. 2011;58:722–8.
15. Rosso R, Adler A, Halkin A, Viskin S. Risk of sudden death among young individuals with J waves and early repolarization: putting the evidence into perspective. *Heart Rhythm*. 2011;8:923–9.
16. Tikkanen JT, Anttonen O, Junttila MJ, Aro AL, Kerola T, Rissanen HA, et al. Long-term outcome associated with early repolarization on electrocardiography. *N Engl J Med*. 2009;361:2529–37.
17. Sinner MF, Reinhard W, Müller M, Beckmann BM, Martens E, Perz S, et al. Association of early repolarization pattern on ecg with risk of cardiac and all-cause mortality: a population-based prospective cohort study (MONICA/KORA). *PLoS Med*. 2010;7:e1000314.

18. Haruta D, Matsuo K, Tsuneto A, Ichimaru S, Hida A, Sera N, et al. Incidence and prognostic value of early repolarization pattern in the 12-lead electrocardiogram. *Circulation*. 2011;123:2931–7.
19. Olson KA, Viera AJ, Soliman EZ, Crow RS, Rosamond WD. Long-term prognosis associated with J-point elevation in a large middle-aged biracial cohort: the ARIC study. *Eur Heart J*. 2011;32:3098–106.
20. Aagaard P, Shulman E, Di Biase L, Fisher JD, Gross JN, Kargoli F, et al. Prognostic value of automatically detected early repolarization. *Am J Cardiol*. 2014;114:1431–6.
21. Uberoi A, Jain NA, Perez M, Weinkopff A, Ashley E, Hadley D, et al. Early repolarization in an ambulatory clinical population. *Circulation*. 2011;124:2208–14.
22. Wu S-H, Lin X-X, Cheng Y-J, Qiang C-C, Zhang J. Early repolarization and risk for arrhythmic death. *J Am Coll Cardiol*. 2013;61:645–50.
23. Rollin A, Maury P, Bongard V, Sacher F, Delay M, Duparc A, et al. Prevalence, prognosis, and identification of the malignant form of early repolarization pattern in a population-based study. *Am J Cardiol*. 2012;110:1302–8.
24. Macfarlane PW, Antzelevitch C, Haissaguerre M, Huikuri HV, Potse M, Rosso R, et al. The early repolarization pattern. A consensus paper. *J Am Coll Cardiol*. 2015;66(4):470–7. Erratum in *J Am Coll Cardiol*. 2015;66(10):1206.
25. Noseworthy PA, Tikkanen JT, Porthan K, Oikarinen L, Pietilä A, Harald K, et al. The early repolarization pattern in the general population: clinical correlates and heritability. *J Am Coll Cardiol*. 2011;57:2284–9.
26. Sager SJ, Hoosien M, Junttila MJ, Tanawuttiwat T, Perry AC, Myerburg RJ. Comparison of inferolateral early repolarization and its electrocardiographic phenotypes in pre- and postadolescent populations. *Am J Cardiol*. 2013;112:444–8.
27. Junttila MJ, Tikkanen JT, Porthan K, Oikarinen L, Jula A, Kenttä T, et al. Relationship between testosterone levels and early repolarization in 12-lead electrocardiogram in males. *J Am Coll Cardiol*. 2013;62:1633–4.
28. Junttila MJ, Sager SJ, Freiser M, McGonagle S, Castellanos A, Myerburg RJ. Inferolateral early repolarization in athletes. *J Interv Card Electrophysiol*. 2011;31:33–8.
29. Tikkanen JT, Junttila MJ, Anttonen O, Aro AL, Luttinen S, Kerola T, et al. Early repolarization: electrocardiographic phenotypes associated with favorable long-term outcome. *Circulation*. 2011;123:2666–73.
30. Tikkanen JT, Wichmann V, Junttila MJ, Rainio M, Hookana E, Lappi OP, et al. Association of early repolarization and sudden cardiac death during an acute coronary event. *Circ Arrhythm Electrophysiol*. 2012;5:714–8.
31. Rudic B, Veltmann C, Kuntz E, Behnes M, Elmas E, Konrad T, et al. Early repolarization pattern is associated with ventricular fibrillation in patients with acute myocardial infarction. *Heart Rhythm*. 2012;9:1295–300.
32. Naruse Y, Tada H, Harimura Y, Hayashi M, Noguchi Y, Sato A, et al. Early repolarization is an independent predictor of occurrences of ventricular fibrillation in the very early phase of acute myocardial infarction. *Circ Arrhythm Electrophysiol*. 2012;5:506–13.
33. Patel RB, Ng J, Reddy V, Chokshi M, Parikh K, Subacius H, et al. Early repolarization associated with ventricular arrhythmias in patients with chronic coronary artery disease. *Circ Arrhythm Electrophysiol*. 2010;3:489–95.
34. Furukawa Y, Yamada T, Morita T, Iwasaki Y, Kawasaki M, Kikuchi A, et al. Early repolarization pattern associated with sudden cardiac death: long-term follow-up in patients with chronic heart failure. *J Cardiovasc Electrophysiol*. 2013;24:632–9.
35. Kitazawa H, Wakasugi T, Sugimoto T, Yamamoto K, Yoshii S, Aizawa Y. Evolving J waves prior to ventricular fibrillation postoperative coronary bypass. *Intern Med*. 2011;50:2337–40.
36. Nam GB, Kim YH, Antzelevitch C. Augmentation of J waves and electrical storms in patients with early repolarization. *N Engl J Med*. 2008;358:2078–9.
37. Tereshchenko L, McCabe A, Han L, Sur S, Huang T, Marine JE, et al. Intracardiac J-point elevation before the onset of polymorphic ventricular tachycardia and ventricular fibrillation in patients with an implantable cardioverter-defibrillator. *Heart Rhythm*. 2012;9:1594–602.
38. Shinohara T, Takahashi N, Saikawa T, Yoshimatsu H. Characterization of J wave in a patient with idiopathic ventricular fibrillation. *Heart Rhythm*. 2006;3:1082–4.
39. Aizawa Y, Sato A, Watanabe H, Chinushi M, Furushima H, Horie M, et al. Dynamicity of the J-wave in idiopathic ventricular fibrillation with a special reference to pause-dependent augmentation of the J-wave. *J Am Coll Cardiol*. 2012;59:1948–53.
40. Aizawa Y, Chinushi M, Hasegawa K, Naiki N, Horie M, Kaneko Y, et al. Electrical storm in idiopathic ventricular fibrillation is associated with early repolarization. *J Am Coll Cardiol*. 2013;62:1015–9.
41. Mizumaki K, Nishida K, Iwamoto J, Nakatani Y, Yamaguchi Y, Sakamoto T, et al. Vagal activity modulates spontaneous augmentation of J-wave elevation in patients with idiopathic ventricular fibrillation. *Heart Rhythm*. 2012;9:249–55.
42. Huikuri HV. Separation of benign from malignant J waves. *Heart Rhythm*. 2015;12:384–5.
43. Rosso R, Glikson E, Belhassen B, Katz A, Halkin A, Steinvil A, et al. Distinguishing “benign” from “malignant early repolarization”: the value of the ST-segment morphology. *Heart Rhythm*. 2012;9:225–9.



Benign Versus Malignant Early Repolarization Patterns

16

Raphael Rosso and Sami Viskin

Distinguishing the “benign” from the “malignant” patterns of early repolarization is of utmost importance [1–3]. While the former electrocardiogram (ECG) pattern is frequently observed in healthy individuals (particularly young, male [4–6], athletic [7, 8], and of African American origin [5, 9]), the latter is clearly associated with idiopathic ventricular fibrillation (VF) in case-control studies [10–13]. In simple terms, the goal is to identify the isolated individual at increased risk from the “silent majority” who has an excellent prognosis [14].

There have been serious attempts to precisely define and even quantitate each component of the early repolarization pattern in the ECG [15, 16]. However, we believe it is important to keep the approach to the patients with early repolarization as simple as possible [1], and we have called for a separate analysis of the two components of the “early repolarization pattern,” namely, the J-wave (or J-point elevation) and the ST-segment [2]. More recently, the importance of a third ECG component, which is the amplitude of the T-wave, has been emphasized [17, 18]. All three components will be first analyzed for the early repolarization related to hypothermia, accepting that hypothermia represents a prototype of highly arrhythmogenic early repolarization [19].

The Arrhythmogenic Early Repolarization of Hypothermia

The ECG pattern recorded during hypothermia can be regarded as a classic example of highly arrhythmogenic early repolarization because of the following: (1) As originally described by Osborn in animal studies [20], dogs exposed to hypothermia consistently develop prominent J-waves in their ECG. Moreover, with deeper degrees of hypothermia, the J-waves increase in amplitude (Fig. 16.1a) and virtually all the hypothermic animals develop spontaneous VF [21]. (2) Experiments involving differential cooling of cardiac-wedge preparations [22] or cooling of preparations mimicking early repolarization [23] demonstrate that hypothermia-related J-waves are the ECG reflection of increased dispersion of repolarization caused by disproportionate abbreviation of the epicardial action potential, eventually leading to phase 2 reentry and VF (Fig. 16.1b) [19]. (3) Therapeutic and accidental hypothermia are well-described causes of spontaneous VF in humans [24–26]. Importantly, although the prominent J-wave (also known as “Osborn wave”) has been traditionally viewed as the hallmark ECG marker of hypothermia, careful analysis of the ECG recorded during hypothermia reveals that the “arrhythmogenic early repolarization” actually has three characteristics: tall J-waves, a flat ST-segment *without* ST-segment elevation and low-amplitude T-waves (Fig. 16.1). The value of each of these features for telling

R. Rosso · S. Viskin (✉)
Department of Cardiology, Tel Aviv Medical Center
and Sackler School of Medicine, Tel Aviv University,
Tel Aviv-Yafo, Israel

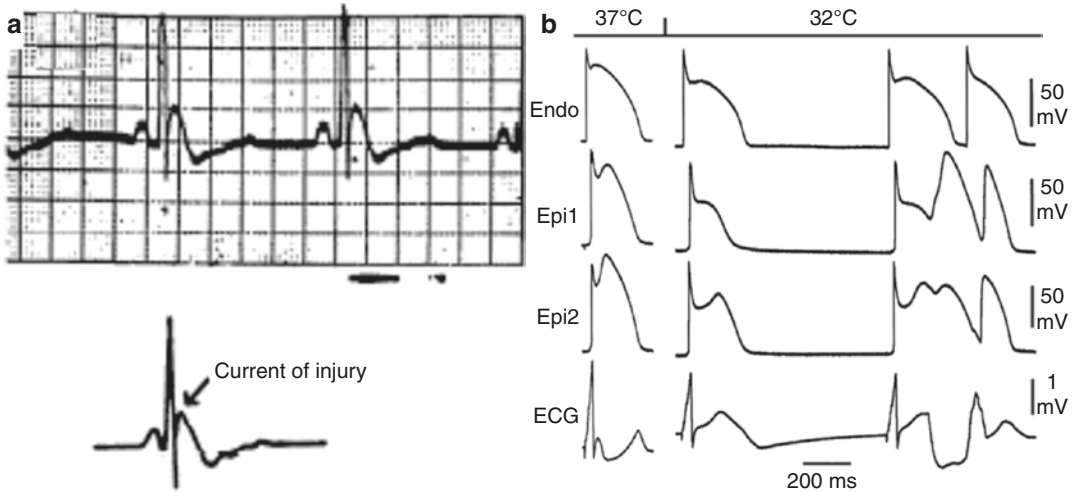


Fig. 16.1 Prominent J-waves in response to hypothermia in the classic study by Osborn (panel **a**). The prominent J-wave observed during deep hypothermia was labelled by Osborn as “current of injury” because it preceded the onset of spontaneous ventricular fibrillation in studied dogs. Note also the absence of ST-segment elevation and the low-amplitude T-wave. (Reprinted with permission from Osborn [10]). Arrhythmogenic effect of hypothermia in the setting of early repolarization (panel **b**). Traces recorded at 2 epicardial (Epi) and 1 endocardial (Endo)

sites, together with a pseudo-electrocardiogram in a model of “early repolarization” created with infusion of NS5806, verapamil, and acetylcholine to the coronary perfusate at 37 °C. The second grouping was recorded 10 minutes after lowering of the perfusate to 32 °C. *Hypothermia in the setting of early repolarization leads to the development of phase 2 reentry and polymorphic ventricular tachycardia.* (Reproduced with permission from Gurabi et al. [23])

apart the benign from the malignant patterns of early repolarization will now be reviewed.

The Amplitude of the J-Wave

In a case-controlled study comparing 206 patients with idiopathic VF to 412 healthy subjects matched for age, sex, race, and level of physical activity, Haissaguerre et al. demonstrated, for the first time, that early repolarization is more frequently observed in the ECG of idiopathic VF survivors than in control subjects (31% vs. 5%, $P < 0.001$) [10]. In the same study, the amplitude of the J-waves (i.e., the height of the J-point elevation) was greater in idiopathic VF patients with early repolarization than in controls (2.0 ± 0.9 mm vs. 1.2 ± 0.4 mm; $P < 0.001$) [10]. In our own case-controlled study, published the same year [11], we also found that idiopathic VF survivors had taller J-waves than matched controls (0.14 vs. 0.09 mV), but the difference did not reach statistical significance because of the smaller patient

population in our study [11]. Thus, the amplitude of the J-wave does matter. However, there is significant overlap between the amplitude of “malignant” vs. “benign” J-waves. Moreover, in a carefully conducted large population study where 20% of ostensibly healthy adults displayed early repolarization in their ECG [14], 8.2% of adults had J-waves taller than and 1.5 mV and 5% had J-waves taller than 2 mV (representing a J-point elevation of 2 mm or more at standard gain) without adverse prognostic events. In a more recent publication, 7% of athletes had J-waves taller than 2 mV [27]. This suggests that except for rare cases with “monstrous J-waves” (as in the examples shown in Fig. 16.2), the amplitude of the observed J-waves will not have sufficient deterministic value for clinical decision making in patients with asymptomatic early repolarization. One small study suggests that for J-waves of comparable height, those of idiopathic VF patients are wider and therefore have a wider angle from the QRS [27]. Finally, data from Japan suggest that the J-waves of patients with

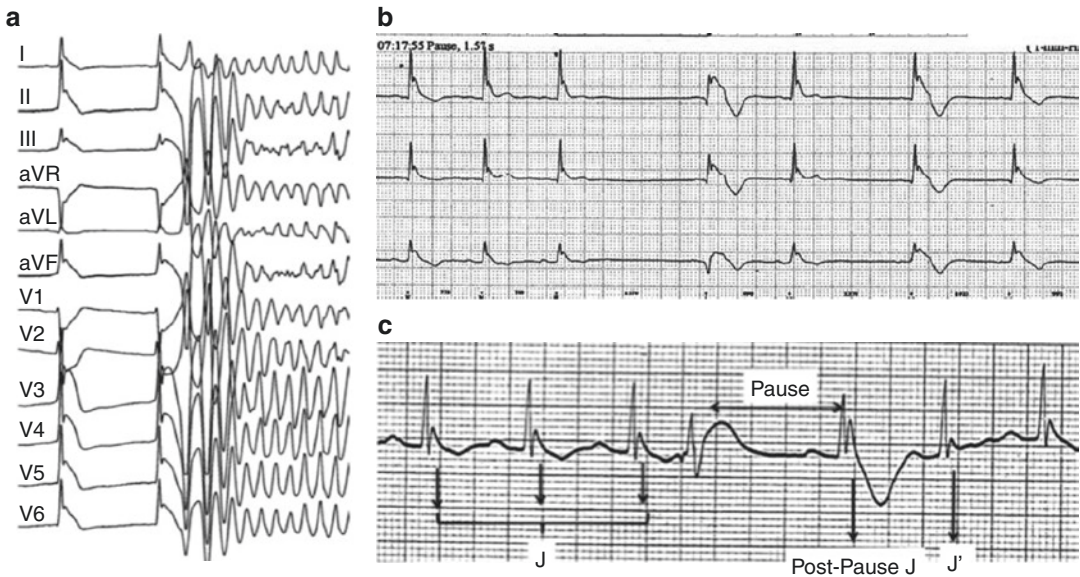


Fig. 16.2 Examples of monstrous J-waves. The examples here are from two unrelated cases with idiopathic ventricular fibrillation. *Panels (a, b)* are electrocardiograms from a 14-year-old female with arrhythmic storm. Coronary spasm was excluded by coronary angiography performed when this bizarre electrocardiogram was recorded. (Reproduced with permission from Haissaguerre et al. [32]). *Panel (c)* demonstrates the dynamicity of the

J-waves as a function of the heart rate. (Reprinted from Aizawa et al. [33], with permission from Elsevier). Note that the very tall J-waves are followed by flat (horizontal and not elevated) S-segments and by flat or even inverted T-waves. Also, note that in both cases, the sudden decrease in heart rate leads to further augmentation of the J-wave amplitude and deeper negative T-waves (panels **b, c**)

idiopathic VF *increase* when the heart rate suddenly *decreases* (Fig. 16.2), while the opposite is true for healthy individuals with J-waves [28].

The Contour of the ST-Segment

Tikkanen et al. were the first to notice in a large population study (including over 10,000 subjects) that healthy athletes who have early repolarization almost invariably have their J-waves followed by a “rapidly ascending ST-segment” (defined as a 0.1 mV elevation [1 mm elevation at standard gain recordings]) of the ST-segment within 100 ms after the J point as it approaches the T-wave, or as a persistently elevated ST-segment of 0.1 mV (1 mm) throughout the ST-segment [7]. They then speculated that this “rapidly ascending ST-segment pattern” would prove to be benign, whereas the other pattern observed in their population study, namely, the “horizontal or descending ST-segment” pattern,

is the one associated with increased risk during long-term follow-up [7]. Indeed, among individuals with early repolarization at their baseline ECG, only the horizontal/descending ST-segment variant was associated with an increased risk of arrhythmic death (relative risk 1.43; 95% confidence interval 1.05–1.94). Furthermore, when limited to high-amplitude J-waves (J-waves of 0.2 mV [2 mm] or more) in the inferior leads, the presence of the horizontal/descending ST-segment variant was associated with a threefold increased risk of arrhythmic death (95% confidence interval 1.56–6.30). In contrast, in subjects with early repolarization who had the “benign” rapidly ascending ST variant, the relative risk for arrhythmic death was not increased (0.89; 95% confidence interval 0.52–1.55) [7].

Following this important observation by Tikkanen [7], we revisited our original case-controlled study of idiopathic VF [11] and noted that the presence of J-waves was associated with a history of idiopathic VF with an odds ratio of

4.0 (95% confidence intervals 2.0–7.9), but having *both* J-waves *and* horizontal ST-segment yielded an odds ratio of 14 (95% confidence intervals 5.1–37.2) for having idiopathic VF [29]. Recognizing the importance of this observation, numerous studies focused on the contour of the ST-segment in early repolarization in further attempts to define its diagnostic/prognostic value. In 2013 we summarized all studies on early repolarization reporting on the type of ST-segment pattern by that date [3]. As clearly seen in Fig. 16.3, reproduced from our 2013 publication [3], as one moves from cohorts with the best prognosis (asymptomatic athletes on the far left of the figure followed by asymptomatic adults) to patient groups at higher risk (patients with acute myocardial infarction complicated by VF on the right) and highest risk (idiopathic VF survivors on the extreme right), the partition of individuals who have early repolarization into individuals with J-waves and rapidly ascending pattern (blue columns) and patients with J-waves followed by horizontal or descending ST-segment (red columns) changes accordingly. Thus, among athletes [except for the study by Cappato et al. [30], which was a case-controlled study of athletes with and without cardiac arrest], virtually all individuals with early repolarization have J-waves followed by rapidly ascending ST-segment, whereas the opposite pattern (horizontal/descending) is far more prevalent among idiopathic VF survivors [3]. Clearly then, the pattern of the ST-segment in early repolarization matters. However, as discussed earlier for the value of the J-wave amplitude, the diagnostic and prognostic value of the ST-segment contour are too limited for clinical decision making for the asymptomatic individual. This is because (as also seen in Fig. 16.3), among healthy adults with early repolarization, the horizontal/descending ST-segment pattern is observed as commonly as the rapidly ascending pattern [3]. Furthermore, in a more recent population study including more than 20,000 individuals who had their baseline ECG carefully evaluated by experts in electrocardiography [14], the presence of J-waves followed by a horizontal/descending ST-segment did not correlate with cardiovascular death during

17 years of follow-up [14]. Regrettably, information on arrhythmic death was not available for this cohort [14]. Note, however, that the very rare cases of monstrous J-waves also demonstrate flat ST-segments (Fig. 16.2).

The Amplitude of the T-Waves

Pursuing the idea that the other ECG components of early repolarization (and not only the J-wave) are important for risk stratification, Roten et al. (Haissaguerre's group) looked at the value of T-wave amplitude in a case-controlled study of 92 idiopathic VF survivors and 247 matched controls [17]. Importantly, both groups had early repolarization on their electrocardiogram (defined as J-waves of ≥ 0.1 mV in the inferior or inferolateral leads). "Low-amplitude T-waves" were defined as any T-wave in leads I, II, or V4–V6 that were either inverted, biphasic, or had an amplitude that was both ≤ 0.1 mV and $\leq 10\%$ of its respective R-wave [17]. Using this definition, "low-amplitude T-waves" were observed in 29% of idiopathic VF survivors but in only 3% of controls ($p < 0.001$) [17]. Moreover, although both the presence of large-amplitude J-waves and flat ST-segment correlated with a history of VF, the best correlation between a history of idiopathic VF and an ECG parameter of early repolarization was with low T/R-wave ratio [17]. This study has not been reproduced but it agrees with our (unpublished) impression. Since this is a relatively new finding, there is no data from large population-based studies on the frequency of "low-amplitude T-waves" in other unselected populations. Consequently, caution should be exercised when analyzing the ECG of an asymptomatic patient.

Unmet Needs and Future Directions

Although important advances in our understanding of the phenomenon of early repolarization have been made during the last decade, our ability for risk stratification of patients with early repolarization in the absence of warning

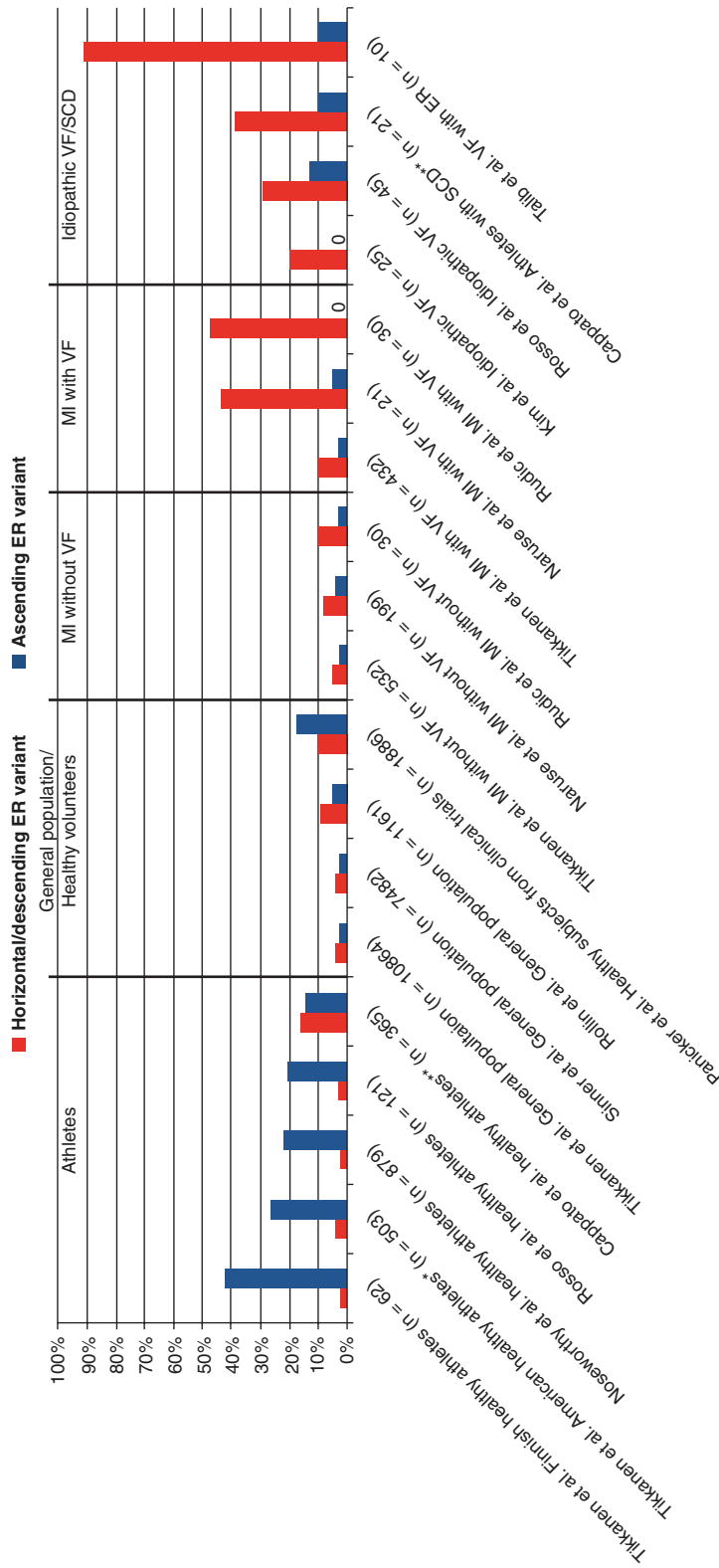


Fig. 16.3 Incidence of early repolarization with rapidly ascending ST-segment (blue bars) and with horizontal ST-segment (red bars) in different populations. The numbers in parentheses represent the number of patients included in each study. (Reprinted from Adler et al. [3], with permission from Elsevier)

symptoms is still very limited. J-waves of large amplitude followed by a flat ST-segment and flat or inverted T-waves are signs of relatively increased risk. However, except for very rare cases with monstrous J-waves (as those shown in Fig. 16.2), the majority of asymptomatic patients with these features ought to be treated conservatively. Recently, noninvasive mapping of the epicardial substrate of patients with early repolarization with ECGI (electrocardiographic imaging techniques) has demonstrated that the epicardial depolarization of patients with idiopathic VF with J-waves is normal, while their epicardial surface has an area with steep repolarization gradients caused by areas with very short action potentials in the areas correlating with the presence of J-waves in their surface ECG [31]. Unfortunately, the healthy controls used in this study did not have early repolarization on their ECG. More studies are needed to define if ECGI techniques can reliably be used to tell apart individuals with benign vs. malignant early repolarization.

References

1. Viskin S, Rosso R, Halkin A. Making sense of early repolarization. *Heart Rhythm*. 2012;9(4):566–8.
2. Rosso R, Adler A, Halkin A, Viskin S. Risk of sudden death among young individuals with J waves and early repolarization: putting the evidence into perspective. *Heart Rhythm*. 2011;8(6):923–9.
3. Adler A, Rosso R, Viskin D, Halkin A, Viskin S. What do we know about the “malignant form” of early repolarization? *J Am Coll Cardiol*. 2013;62(10):863–8.
4. Ezaki K, Nakagawa M, Taniguchi Y, Nagano Y, Teshima Y, Yufu K, et al. Gender differences in the ST segment: effect of androgen-deprivation therapy and possible role of testosterone. *Circ J*. 2010;74(11):2448–54.
5. Walsh JA 3rd, Ilkhanoff L, Soliman EZ, Prineas R, Liu K, Ning H, et al. Natural history of the early repolarization pattern in a biracial cohort: CARDIA (Coronary Artery Risk Development in Young Adults) Study. *J Am Coll Cardiol*. 2013;61(8):863–9.
6. Panicker GK, Manohar D, Karnad DR, Salvi V, Kothari S, Lokhandwala Y. Early repolarization and short QT interval in healthy subjects. *Heart Rhythm*. 2012;9(8):1265–71.
7. Tikkanen JT, Junttila MJ, Anttonen O, Aro AL, Luttinen S, Kerola T, et al. Early repolarization: electrocardiographic phenotypes associated with favorable long-term outcome. *Circulation*. 2011;123(23):2666–73.
8. Noseworthy PA, Weiner R, Kim J, Keelara V, Wang F, Berkstresser B, et al. Early repolarization pattern in competitive athletes: clinical correlates and the effects of exercise training. *Circ Arrhythm Electrophysiol*. 2011;4(4):432–40.
9. Perez MV, Uberoi A, Jain NA, Ashley E, Turakhia MP, Froelicher V. The prognostic value of early repolarization with ST-segment elevation in African Americans. *Heart Rhythm*. 2012;9(4):558–65.
10. Haissaguerre M, Derval N, Sacher F, Jesel L, Deisenhofer I, de Roy L, et al. Sudden cardiac arrest associated with early repolarization. *N Engl J Med*. 2008;358(19):2016–23.
11. Rosso R, Kogan E, Belhassen B, Rozovski U, Scheinman MM, Zeltser D, et al. J-point elevation in survivors of primary ventricular fibrillation and matched control subjects incidence and clinical significance. *J Am Coll Cardiol*. 2008;52(15):1231–8.
12. Kim SH, Kim do Y, Kim HJ, Jung SM, Han SW, Suh SY, et al. Early repolarization with horizontal ST segment may be associated with aborted sudden cardiac arrest: a retrospective case control study. *BMC Cardiovasc Disord*. 2012;12:122.
13. Talib AK, Sato N, Asanome A, Myojo T, Nishiura T, Yamaki M, et al. Impaired ventricular repolarization dynamics in patients with early repolarization syndrome. *J Cardiovasc Electrophysiol*. 2013;24(5):556–61.
14. Pargaonkar VS, Perez MV, Jindal A, Mathur MB, Myers J, Froelicher VF. Long-term prognosis of early repolarization with J-wave and QRS slur patterns on the resting electrocardiogram: a Cohort Study. *Ann Intern Med*. 2015;163(10):747–55.
15. Macfarlane PW, Antzelevitch C, Haissaguerre M, Huikuri HV, Potse M, Rosso R, et al. The early repolarization pattern: a consensus paper. *J Am Coll Cardiol*. 2015;66(4):470–7.
16. Surawicz B, Macfarlane PW. Inappropriate and confusing electrocardiographic terms: J-wave syndromes and early repolarization. *J Am Coll Cardiol*. 2011;57(15):1584–6.
17. Roten L, Derval N, Maury P, Mahida S, Pascale P, Leenhardt A, et al. Benign vs. malignant inferolateral early repolarization: focus on the T wave. *Heart Rhythm*. 2016;13(4):894–902.
18. Viskin S, Havakuk O, Antzelevitch C, Rosso R. Malignant early repolarization: It’s the T-wave, stupid. *Heart Rhythm*. 2016;13(4):903–4.
19. Viskin S, Rosso R. J-wave syndromes. In: Zipes DP, Jalife J, Stevenson WG, editors. *Cardiac electrophysiology: from cell to bedside*. 7th ed: Philadelphia: Elsevier; 2017.
20. Osborn JJ. Experimental hypothermia; respiratory and blood pH changes in relation to cardiac function. *Am J Phys*. 1953;175(3):389–98.
21. Johnson P, Lesage A, Floyd WL, Young WG Jr, Sealy WC. Prevention of ventricular fibrillation dur-

- ing profound hypothermia by quinidine. *Ann Surg.* 1960;151:490–5.
22. Fish JM, Antzelevitch C. Link between hypothermia and the Brugada syndrome. *J Cardiovasc Electrophysiol.* 2004;15(8):942–4.
 23. Gurabi Z, Koncz I, Patocsikai B, Nesterenko VV, Antzelevitch C. Cellular mechanism underlying hypothermia-induced ventricular tachycardia/ventricular fibrillation in the setting of early repolarization and the protective effect of quinidine, cilostazol, and milrinone. *Circ Arrhythm Electrophysiol.* 2014;7(1):134–42.
 24. Bastiaenen R, Hedley PL, Christiansen M, Behr ER. Therapeutic hypothermia and ventricular fibrillation storm in early repolarization syndrome. *Heart Rhythm.* 2010;7(6):832–4.
 25. Federman NJ, Mechulan A, Klein GJ, Krahn AD. Ventricular fibrillation induced by spontaneous hypothermia in a patient with early repolarization syndrome. *J Cardiovasc Electrophysiol.* 2013;24(5):586–8.
 26. Kanna B, Wani S. Giant J wave on 12-lead electrocardiogram in hypothermia. *Ann Noninvasive Electrocardiol.* 2003;8(3):262–5.
 27. Cristoforetti Y, Biasco L, Giustetto C, De Backer O, Castagno D, Astegiano P, et al. J-wave duration and slope as potential tools to discriminate between benign and malignant early repolarization. *Heart Rhythm.* 2016;13(3):806–11.
 28. Aizawa Y, Takatsuki S, Nishiyama T, Kimura T, Kohsaka S, Kaneko Y, et al. Tachycardia-induced J-wave changes in patients with and without idiopathic ventricular fibrillation. *Circ Arrhythm Electrophysiol.* 2017;10(7):pii:e005214.
 29. Rosso R, Glikson E, Belhassen B, Katz A, Halkin A, Steinvil A, et al. Distinguishing “benign” from “malignant early repolarization”: the value of the ST-segment morphology. *Heart Rhythm.* 2012;9(2):225–9.
 30. Cappato R, Furlanello F, Giovinazzo V, Infusino T, Lupo P, Pittalis M, et al. J wave, QRS slurring, and ST elevation in athletes with cardiac arrest in the absence of heart disease: marker of risk or innocent bystander? *Circ Arrhythm Electrophysiol.* 2010;3(4):305–11.
 31. Zhang J, Hocini M, Strom M, Cuculich PS, Cooper DH, Sacher F, et al. The electrophysiological substrate of early repolarization syndrome: noninvasive mapping in patients. *JACC Clin Electrophysiol.* 2017;3(8):894–904.
 32. Haissaguerre M, et al. Ventricular fibrillation with prominent early repolarization associated with a rare variant of KCNJ8/K_{ATP} channel. *J Cardiovasc Electrophysiol.* 2009;20:93.
 33. Aizawa Y, et al. Dynamicity of the J-wave in idiopathic ventricular fibrillation with a special reference to pause-dependent augmentation of the J-wave. *JACC.* 2012;59:1948.



Genetic Architecture, Pathophysiology, and Clinical Management of Brugada Syndrome

John R. Giudicessi and Michael J. Ackerman

Abbreviations

ACC	American College of Cardiology
AHA	American Heart Association
BrS	Brugada syndrome
ClinGen	Clinical Genome Resource
EHRA	European Heart Rhythm Association
EPS	Electrophysiology study
ESC	European Society of Cardiology
ExAC	Exome Aggregation Consortium
gnomAD	Genome Aggregation Database
GUS	Gene of uncertain significance
GWAS	Genome-Wide Association Study
HRS	Heart Rhythm Society
ICD	Implantable cardioverter-defibrillator
PVC	Premature ventricular contraction
RVOT	Right ventricular outflow tract
SCD	Sudden cardiac death
VF	Ventricular fibrillation
VT	Ventricular tachycardia
VUS	Variant of uncertain significance

J. R. Giudicessi
Department of Cardiovascular Medicine,
Mayo Clinic, Rochester, MN, USA

M. J. Ackerman (✉)
Departments of Cardiovascular Medicine,
Pediatric and Adolescent Medicine, and Molecular
Pharmacology and Experimental Therapeutics,
Mayo Clinic Genetic Heart Rhythm Clinic and the
Windland Smith Rice Sudden Death Genomics
Laboratory, Rochester, MN, USA
e-mail: ackerman.michael@mayo.edu

Introduction

Brugada syndrome (BrS) is considered classically to be a primary electrical disorder characterized clinically by spontaneous or class I antiarrhythmic-provoked coved ST-segment elevation ≥ 2 mm in ≥ 1 right precordial leads (V_1 or V_2 ; Fig. 17.1a) and an increased risk of sudden cardiac death (SCD), often during rest, sleep, or febrile episodes, in the absence of overt structural heart disease [1–3]. However, a growing body of evidence suggests BrS may represent a subtle cardiomyopathy that arises from both electroanatomic and structural abnormalities located within and around the right ventricular outflow tract (RVOT) [4–6]. Additional clinical manifestations observed commonly in BrS include conduction delay (i.e., slight PR prolongation and QRS widening) and supraventricular tachyarrhythmias (i.e., atrial fibrillation) [7], which suggest the pathogenic substrate(s) that underlie BrS may extend beyond the RVOT in some cases. However, whether the supraventricular and ventricular arrhythmias observed in BrS arise secondary to impaired conduction, abnormal repolarization, both, or neither remains the subject of lively debate and ongoing investigation.

Classically, BrS is considered a monogenic (i.e., single gene/variant) disorder that follows an autosomal-dominant pattern of inheritance. Whereas ~20–30% of BrS cases are attributed to pathogenic loss-of-function variants in the *SCN5A*-encoded $Na_v1.5$ cardiac sodium channel

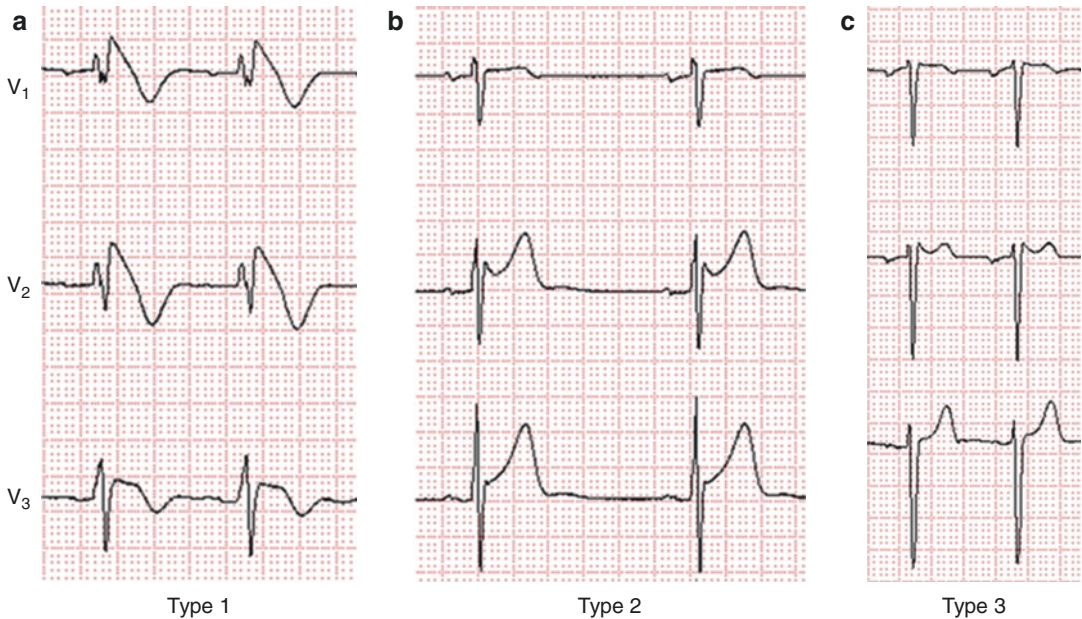


Fig. 17.1 The three types of ST-segment elevation associated with Brugada syndrome. (a) Type 1 BrS ECG pattern. The only pattern that is considered diagnostic for the disease. (b) Type 2 BrS ECG pattern. (c) Type 3 BrS ECG

pattern. Abbreviations: BrS, Brugada syndrome, and ECG, electrocardiogram. (Adapted from Anztelevitch et al. [17] with permission from Elsevier)

[8], at least 20 additional minor BrS-susceptibility genes have been reported to date. However, the majority of these genes were discovered using hypothesis-driven, mutational analysis of biologically plausible candidate genes in an era before the true burden of background amino acid-altering genetic variation was known [9]. As a result, the gene-disease association strength of most minor (i.e., non-*SCN5A*) BrS-susceptibility genes is rightfully in question [10].

Furthermore, even among families with a BrS-causative pathogenic *SCN5A* variant, disease penetrance is relatively low (~16%). Although this phenomenon may be explained, in part, by i) a strong male predominance, ii) late disease onset (third and fourth decades of life), and iii) genetic background (BrS is more common among individuals of Asian descent), mounting evidence suggests that a larger number of BrS cases may have an oligogenic/polygenic (i.e., ≥ 2 genes/variants) basis than anticipated previously.

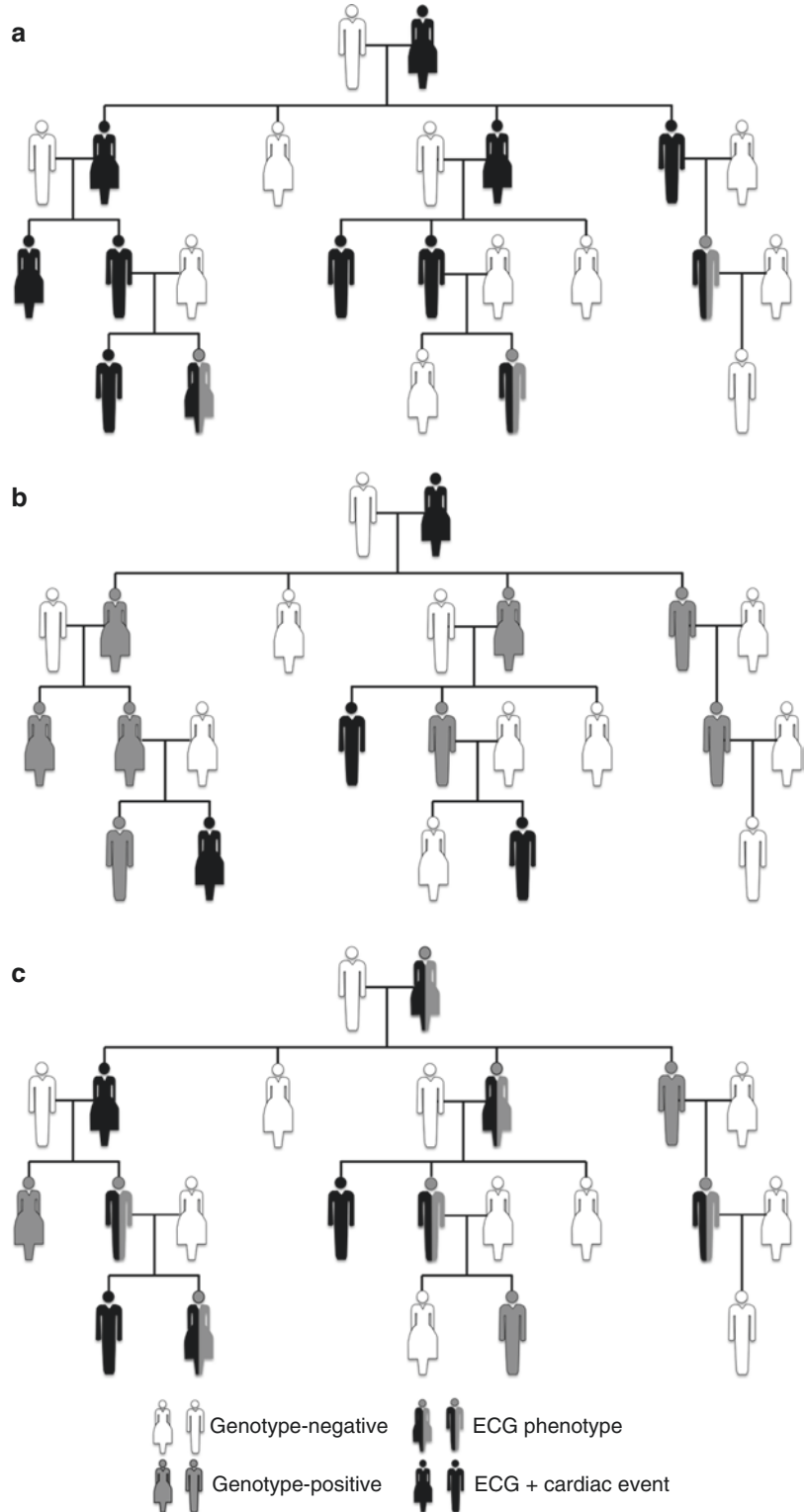
In this chapter, we review succinctly the current paradigms surrounding the genetic basis and electrophysiological mechanism(s) underlying

BrS, ongoing efforts to redefine BrS genetic architecture, and recent advances in the diagnosis, risk stratification, and clinical management of BrS.

Genetics and Pathophysiology of BrS

Classically, BrS is considered a Mendelian disorder that follows an autosomal-dominant pattern of inheritance, albeit with low/incomplete penetrance and variable expressivity (Fig. 17.2) [11, 12]. As a result, family members with the same putative BrS-causative variant frequently assume vastly different clinical courses ranging from manifest electrocardiographic abnormalities (i.e., spontaneous coved-type ST elevation in V_1 – V_2) with a history of ventricular arrhythmia-triggered cardiac events (i.e., syncope, seizures, or SCD) to the complete absence of spontaneous or provoked electrocardiographic features and a lifelong asymptomatic state (Fig. 17.2) [11]. Furthermore, many cases of BrS arise sporadically and efforts

Fig. 17.2 Penetrance and expressivity in Brugada syndrome. (a) Representative multigenerational pedigree displaying complete penetrance (100%) for electrocardiographic hallmarks (i.e., coved-type ST-segment elevation in leads V₁ and V₂ for BrS) and disease-related symptomatology (i.e., arrhythmic syncope, SCA, or SCD). (b) Representative multigenerational pedigree displaying incomplete penetrance (33%) for the electrocardiographic hallmarks and disease-related symptomatology. (c) Representative multigenerational pedigree displaying incomplete penetrance (66%) and variable expressivity as some individuals display the electrocardiographic hallmarks of the disease without symptomatology. Abbreviations: BrS, Brugada syndrome; SCA, sudden cardiac arrest; and SCD, sudden cardiac death. (Adapted from Giudicessi and Ackerman [11] with permission from Elsevier)



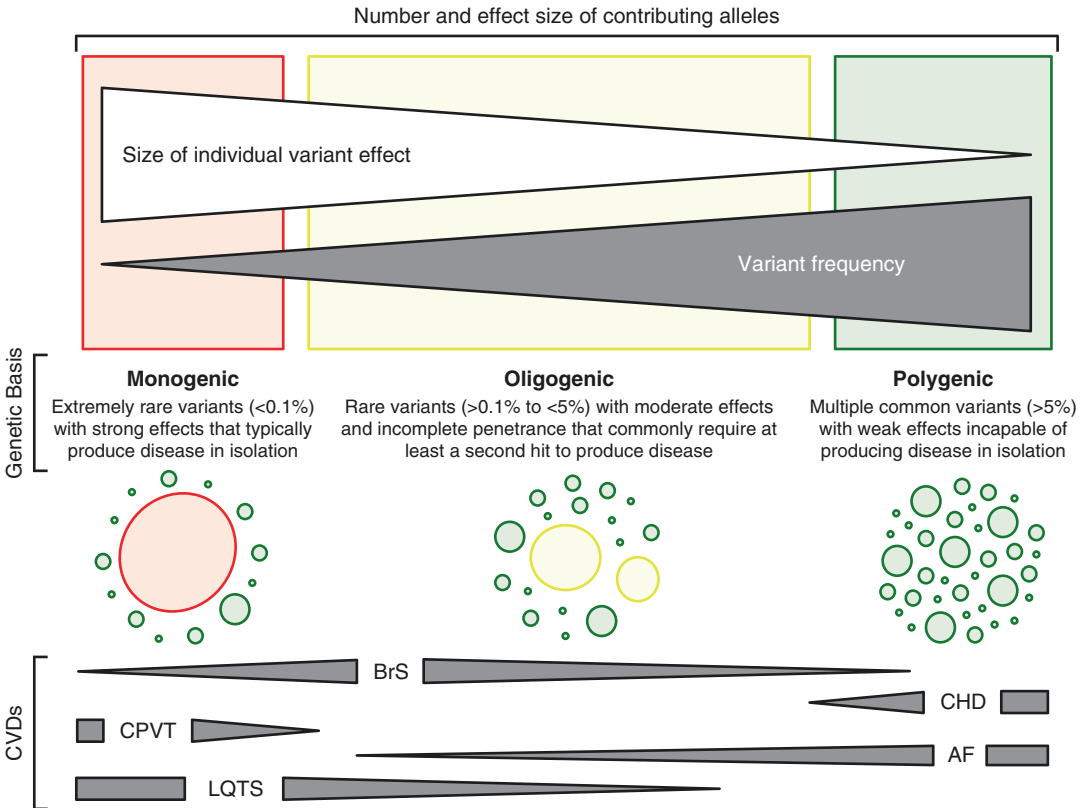


Fig. 17.3 The spectrum of genetic variation underlying the heritable component of commonly encountered cardiovascular disorders (CVDs). At the severe (red) end of the spectrum are extremely rare disease-causative mutations with strong effects on gene function that typically result in monogenic disorders such as catecholaminergic polymorphic ventricular tachycardia (CPVT), long QT syndrome (LQTS), and some cases of Brugada syndrome (BrS). In the middle of the spectrum (yellow) are rare variants with moderate effects on gene function that rarely produce disease in isolation, but in the presence of one or more second hits result in disease as seen in some instances of BrS with a high burden of relatively common

HEY2 and *SCN10A* variants. Lastly, at the benign (green) end of the spectrum are common variants with weak effects on gene function that are incapable of producing disease in isolation, but may confer disease risk when multiple risk-associated common variants are present within the genome of an individual with environmental risk factors for disorders such as coronary heart disease (CHD) and atrial fibrillation (AF). In recognition that the genetic basis of most heritable CVDs is variable, dark gray triangles denote the spectrum of genetic variation underlying each CVD or class of CVDs. (Adapted from Giudicessi [14] with permission from Elsevier)

to utilize linkage analysis to identify novel monogenic (i.e., single gene; Fig. 17.3) causes of BrS have largely proven unsuccessful [13–15]. As such, a growing body of evidence, discussed later in this chapter, suggests that many cases of BrS may follow a complex inheritance model (i.e., oligogenic/polygenic disease) akin to that observed for most atrial fibrillation and atherosclerotic coronary heart disease cases (Fig. 17.3) [13, 14]. Nevertheless, in the ensuing sections, we review briefly the classic Mendelian genetic

basis of *SCN5A*- and non-*SCN5A*-mediated BrS as well as their suspected underlying electrophysiological mechanism(s).

SCN5A-Mediated BrS

As discussed previously, 20–30% of BrS arises secondary to loss-of-function genetic variants in the *SCN5A*-encoded $\text{Na}_v1.5$ cardiac sodium channel that either i) decrease *SCN5A* expression (i.e.,

haploinsufficiency secondary to nonsense variants) or ii) encode defective $\text{Na}_v1.5$ channels that reach the sarcolemma, but fail to conduct I_{Na} current or have abnormal gating properties (i.e., delayed activation or faster inactivation). Each of these mechanisms in turn decrease peak I_{Na} current during phase 0 of the cardiac action potential and slow cardiac conduction. However, the precise electrophysiological mechanism(s) that link decreased I_{Na} current to right precordial ST-segment elevation and ventricular arrhythmia susceptibility remains the subject of great debate.

At present, two distinct hypotheses have been advanced. The “repolarization” hypothesis, advanced largely on the basis that the heterogeneous distribution of the transient outward potassium current ($\text{Kv}4.3/I_{\text{to}}$) results in an epicardial > endocardial transmural voltage gradient in canine RV wedge preparations [16], postulates that decreased I_{Na} outwardly shifts the balance of currents in the RV epicardium predisposing to phase 2 reentry and the generation of closely coupled premature ventricular contractions (PVCs) capable of ventricular arrhythmias [17]. In contrast, the “depolarization” hypothesis, advanced largely on data obtained from diagnostic electrophysiology studies (EPS) and more recently concomitant RVOT endomyocardial biopsies, suggests that decreased I_{Na} current [6, 18–20], perhaps mediated or exacerbated by myocardial inflammation [6], predisposes to pathological remodeling in the epicardial RVOT and anterior RV wall (i.e., focal myocardial fibrosis/connexin 43 downregulation) that leads to conduction slowing and ultimately electrical instability [17].

Although the “repolarization” and “depolarization” hypotheses are not necessarily mutually exclusive, evidence from recent imaging [21, 22], postmortem necropsy [23], and concomitant electroanatomic mapping/targeted endomyocardial biopsy [6] studies all suggest structural alterations in the RVOT/anterior RV free wall play a prominent role in the pathogenesis of BrS. Interestingly, endomyocardial biopsies obtained from living patients with in vitro loss-of-function BrS-causative *SCN5A* pathogenic variants display increased rates of myocyte apoptosis and cardiomyopathy-like changes such as

myocyte hypertrophy, vacuolization, and cytoplasmic degeneration [24]. This has led to speculation that perturbations in cellular sodium homeostasis (i.e., decreased I_{Na}), which influences cellular pH, calcium homeostasis, and excitation-contraction coupling, may lead to increased rates of myocyte apoptosis/necrosis and trigger a reactive immune-mediated process that ultimately leads to focal myocardial inflammation and fibrosis within the RVOT/anterior RV [6, 24]. As such, the pathophysiological mechanisms underlying BrS appear to be more in line with arrhythmogenic cardiomyopathy than primary electrical disorders such as long QT syndrome.

Non-*SCN5A*-Mediated BrS

Following the sentinel discovery that pathogenic variants in *SCN5A* underlie a subset of BrS cases [25], more than 20 additional BrS-susceptibility genes have been reported in the literature (Table 17.1). Not surprisingly, many of the “minor” BrS-susceptibility genes encode components of the $\text{Na}_v1.5$ macromolecular complex and have been shown, in vitro, to confer a similar I_{Na} loss of function to that observed in *SCN5A*-mediated BrS (Table 17.1). In addition, variants in genes known to encode pore-forming α - and accessory β -subunits that impart either a loss of function to the depolarizing L-type calcium current ($I_{\text{Ca,L}}$) or a gain of function to repolarizing $\text{Kv}4.3/I_{\text{to}}$ and ATP-sensitive potassium (I_{KATP}) currents have been implicated in BrS (Table 17.1).

However, with advances in sequencing technology, it has become increasingly clear that *SCN5A* is the only BrS-causative gene identified to date where a greater burden of rare variants is observed in BrS cases versus controls [26]. As such, great caution must be taken when interpreting rare variants identified in any of the alleged minor BrS-susceptibility genes. Lastly, even if the 20+ BrS-susceptibility genes are included, after over 20 years of genetic investigations, nearly two-thirds of BrS cases still remain genetically elusive. When coupled with

Table 17.1 Reported Brugada syndrome-susceptibility genes

Gene	Historical convention	OMIM	Protein	Functional effect	Reported frequency	Key reference
ClinGen definitive evidence						
<i>SCN5A</i>	BrS1	601,144	Cardiac sodium channel alpha subunit (Na _v 1.5)	↓ I _{Na}	20%–30%	[25]
ClinGen disputed evidence						
<i>ABCC9</i>	BrS13	N/A	ATP-binding cassette, subfamily C member 9	↑ I _{KATP}	2%	[50]
<i>CACNA1C</i>	BrS3	611,875	Voltage-gated L-type calcium channel (Ca _v 1.2)	↓ I _{Ca,L}	6.6%	[51]
<i>CACNA2D1</i>	BrS9	N/A	Voltage-gated L-type calcium channel 2 delta 1 subunit	↓ I _{Ca,L}	1.8%	[52]
<i>CACNB2</i>	BrS4	611,876	Voltage-gated L-type calcium channel beta 2 subunit	↓ I _{Ca,L}	4.8%	[51]
<i>FGF12</i>	BrS16	N/A	Fibroblast growth factor 12	↓ I _{Na}	Rare	[53]
<i>GPD1L</i>	BrS2	611,777	Glycerol-3-phosphate dehydrogenase 1-like	↓ I _{Na}	Rare	[30]
<i>HCN4</i>	N/A	N/A	Hyperpolarization-activated cyclic nucleotide-gated channel 4	↓ I _f	Rare	[54]
<i>KCND3</i>	BrS10	616,399	Voltage-gated potassium channel alpha subunit (K _v 4.3)	↑ I _{to}	Rare	[31]
<i>KCNE3</i>	BrS6	613,119	Potassium channel beta subunit 3 (MiRP2)	↑ I _{to}	Rare	[55]
<i>KCNE5</i>	N/A	N/A	Potassium channel beta subunit 5	↑ I _{to}	Rare	[56]
<i>KCNH2</i>	N/A	N/A	Voltage-gated potassium channel alpha subunit (hERG; K _v 11.1)	↑ I _{Kr}	Rare	[57]
<i>KCNJ8</i>	BrS8	613,601	Inwardly rectifying potassium channel alpha subunit (K _r 6.1)	↑ I _{KATP}	2%	[58]
<i>RANGRF</i>	BrS11	N/A	RAN guanine nucleotide release factor 1	↓ I _{Na}	Rare	[59]
<i>PKP2</i>	BrS15	N/A	Plakophilin-2	↓ I _{Na}	Rare	[60]
<i>SCN10A</i>	BrS17	N/A	Voltage-gated sodium channel alpha subunit (Na _v 1.8)	↓ I _{Na}	5%–16.7%	[35]
<i>SCN1B</i>	BrS5	612,838	Sodium channel beta 1	↓ I _{Na}	1.1%	[61]
<i>SCN2B</i>	BrS14	N/A	Sodium channel beta 2	↓ I _{Na}	Rare	[62]
<i>SCN3B</i>	BrS7	613,120	Sodium channel beta 3	↓ I _{Na}	Rare	[63]
<i>SEMA3A</i>	N/A	N/A	Semaphorin 3A	↑ I _{to}	Rare	[64]
<i>SLMAP</i>	BrS12	N/A	Sarcolemma associated protein	↓ I _{Na}	Rare	[65]
<i>TRPM4</i>	N/A	N/A	Transient receptor potential cation channel, subfamily M, member 4	↓ I _{Na}	Rare	[66]

Abbreviations: BrS, Brugada syndrome; ClinGen, Clinical Genome Resource; and OMIM, Online Mendelian Inheritance in Man

the large number of sporadic/nonfamilial BrS cases, substantial genetic heterogeneity, and low penetrance/variable expressivity observed even in familial *SCN5A*-mediated BrS, the number of

BrS cases that remain genetically elusive suggests strongly that the genetic architecture of BrS may be substantially more complex than anticipated initially.

Reappraising the Nature of Non-*SCN5A*/Minor BrS Gene-Disease Associations

Following the completion of the human genome, rapid advances in sequencing technology have allowed for the discovery of novel disease-susceptibility genes in situations (i.e., unrelated singletons, small kindreds, etc.) not amenable to classic linkage analysis. As a result, nearly half of all gene-disease associations in existence today [27], including the majority of the 20+ BrS-susceptibility genes (Table 17.1), were discovered over the last ~10 years using largely hypothesis-driven, mutational analysis of biologically plausible genes and their gene-encoded proteins. Unfortunately, many of these genes were discovered before large-scale next-generation sequencing projects such as the Exome Aggregation Consortium (ExAC)/Genome Aggregation Database (gnomAD) illuminated the true burden of amino acid-altering genetic variation in the human genome. Furthermore, the level of clinical, genetic, and experimental evidence to support existing gene-disease associations, including those in BrS, is widely variable. In the ensuing sections, we examine efforts to systematically reclassify the minor BrS-susceptibility genes and the impact of these efforts on clinical BrS genetic testing.

Systematic Efforts to Reappraise Minor BrS-Susceptibility Gene-Disease Associations

The clinical utility of genetic testing, for any disease, is predicated on the assembly of a sufficiently evidence-based gene panel. Unfortunately, from the onset of clinical genetic testing for BrS and other SCD-predisposing genetic disorders, the prevailing mindset has been that “bigger is better” in terms of the number of genes included on a given gene panel. As a result, current clinical genetic tests for a myriad of Mendelian/monogenic disorders, including BrS, are littered with so-called genes of uncertain significance (GUS) with a paucity of genetic and experimental evidence to definitively confirm or deny their role in disease pathogenesis.

In an effort to improve the validity of genes included on clinical genetic tests, the National Institutes of Health-funded Clinical Genome Resource (ClinGen) consortium developed a semiquantitative, evidence-based framework designed to standardize how the strength of genetic and functional evidence supporting a given gene-disease association is assessed and reported [28]. With the assistance of three independent gene curation teams and a panel of genetic heart disease experts, the ClinGen framework was used recently to reappraise the gene-disease association strength of 21 genes associated previously with BrS. The results were sobering as 20/21 (95%) or BrS-susceptibility genes assessed received a “disputed” evidence classification (Table 17.1) [10].

Not surprisingly, the primary justification for these reclassifications were (i) insufficient co-segregation data, (ii) excess prevalence of putative disease-causative variants in public exome/genome databases such as ExAC/gnomAD, and (iii) an overreliance on experimental evidence obtained exclusively from *in vitro* heterologous expression systems [10]. Interestingly, even *GPD1L*, a minor BrS-susceptibility gene discovered initially using classical linkage analysis and characterized functionally *in vitro* [29, 30], was demoted to “disputed” status due to the excess frequency of the sentinel p.Ala280Val-*GPD1L* variant in public exomes/genomes and concern that alternative causes in the large genomic region containing *GPD1L* discovered by genetic linkage were not fully explored [10].

Impact of ClinGen Reclassifications on Clinical BrS Genetic Testing

One might expect that the recent demotion of ~95% of BrS-susceptibility genes included currently on commercial gene panels to “disputed” status would impact negatively the clinical utility of genetic testing in BrS [10]. However, genetic testing in BrS, unlike long QT syndrome and catecholaminergic polymorphic ventricular tachycardia, has never been shown to play a substantive role in the diagnosis, prognostication, or

clinical management of patients with BrS [31]. As such, current American Heart Association (AHA)/American College of Cardiology (ACC) [3], European Society of Cardiology (ESC) [2], and Heart Rhythm Society (HRS)/European Heart Rhythm Association (EHRA) [1, 31]

expert consensus guidelines, which largely suggest that *SCN5A*-specific genetic testing of BrS index cases may be helpful in facilitating the screening of first-degree relatives, are not affected by the recent ClinGen BrS gene reclassification efforts (Fig. 17.4).

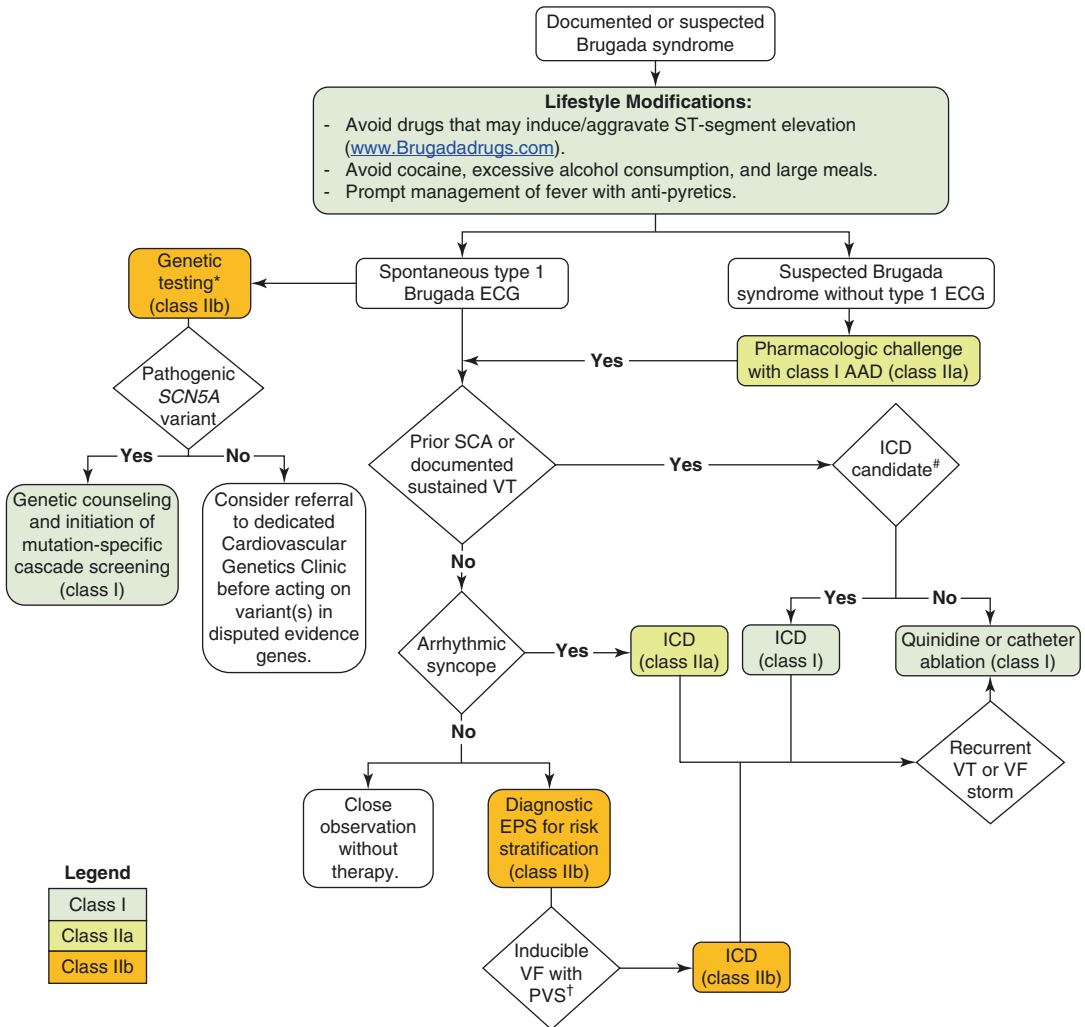


Fig. 17.4 Prevention of ventricular arrhythmias and SCD in Brugada syndrome. Colored boxes indicate strength of recommendation [class I (green/strong), recommended; class IIa (yellow/moderate), reasonable; and class IIb (orange/weak), may be reasonable]. *At present, the majority of commercially available genetic tests contain a large number of weak/disputed evidence genes. In the absence of an ACMG pathogenic/likely pathogenic variant in *SCN5A*, the decision to pursue cascade screening of first-degree relatives based on a variant of uncertain significance (VUS) in a weak/limited evidence gene is best accomplished in the setting of a dedicated Cardiovascular Genetics Clinic. #ICD candidacy determined by functional

status, life expectancy, feasibility, and patient preference. †ICD implantation may be considered in patients with a diagnosis of Brugada syndrome with inducible VF during diagnostic EPS with PVS (one or two extrastimuli at ≥ 2 sites). This recommendation was endorsed by the current ESC and HRS/EHRA guidelines, but not the AHA/ACC guidelines. Abbreviations: AAD antiarrhythmic drug, ECG electrocardiogram, EPS electrophysiological study, ICD implantable cardioverter-defibrillator, SCA sudden cardiac arrest, VF ventricular fibrillation, VT ventricular tachycardia. (Adapted from Al-Khatib et al. [3, 67] with permission from Wolters Kluwer Health, Inc.)

However, from a practical perspective, most commercially available BrS genetic tests are likely to include a number of “disputed” evidence genes on their respective panels for the foreseeable future. Given the interpretative nightmare the discovery of a novel variant of uncertain significance (VUS) in a weak/disputed evidence gene (i.e., GUS) poses and the elevated potential that misinterpretation of such variants could lead to potentially harmful diagnostic miscues, referral of patients with ambiguous BrS genetic testing findings to dedicated Cardiovascular Genetics Clinics represents a reasonable and prudent approach (Fig. 17.4).

Genetic Architecture of BrS: Monogenic, Polygenic, or Both?

In light of the large number of BrS cases that remain genetically elusive [32], low penetrance and variable expressivity of BrS-causative *SCN5A* pathogenic variants [12], and questionable validity of many putative BrS-susceptibility minor genes [10], it is becoming increasingly evident that BrS is not a predominantly Mendelian/monogenic disorder. Instead, if the rest of BrS is genetically driven, then an oligenic/polygenic basis must be considered.

To this end, a genome-wide association study (GWAS) identified and validated the association of three genetic loci located within or near the *SCN5A* (rs11708996), *SCN10A* (rs10428132), and *HEY2* (rs9388451) genes with BrS [13]. Interestingly, the risk of developing BrS rose substantially as individuals accumulated risk alleles within these genetic loci (i.e., 2 risk alleles, odds ratio of 1.9 vs >4 risk alleles, odds ratio of 21.5) [13]. However, as ~1.5% of individuals of European descent are expected to possess >4 risk alleles in the identified *SCN5A*, *SCN10A*, and *HEY2* BrS-associated genetic loci, it is unlikely that common genetic variation in these three genetic loci alone is sufficient to cause BrS, a disorder with an estimated prevalence of no more than 1:2000 (0.05%) [13, 17].

Unlike most novel genetic loci discovered through GWAS, potential mechanisms underlying the BrS-associated GWAS genetic loci in

SCN10A (rs10428132) and *HEY2* (rs9388451) have both been elucidated [33]. Although the *SCN10A* rs10428132 BrS risk allele has not been studied directly, it is known to be in tight linkage disequilibrium with a functional variant (rs6801957) that affects T-box transcription factor (TBX3 and TBX5) binding and thereby the activity of an intronic cardiac enhancer region in *SCN10A* [34]. Through a complicated series of in vivo murine and ex vivo human studies, van den Boogaard demonstrated subsequently that *SCN10A* rs6801957 likely weakens the affinity of the *SCN10A* intronic cardiac enhancer for the *SCN5A* promoter [33]. This results in a modest overall reduction in *SCN5A* expression and may alter the pattern/gradient of *SCN5A* expression [33]. As such, *SCN10A* rs6801957 and by virtue of linkage disequilibrium *SCN10A* rs10428132 appear to confer BrS risk through genomic dysregulation of *SCN5A* expression rather than through the controversial role of *SCN10A*-encoded Na_v1.8 sodium channel in cardiac electrophysiology [33, 35, 36].

Similarly, data derived from human and murine left ventricular transcriptome studies suggests that the *HEY2* rs9388451 BrS risk allele results in increased expression of a *HEY2*-encoded basic helix-loop-helix transcriptional repressor, predominantly expressed in the ventricular subepicardium, which regulates transmural ion channel patterning in the heart [37]. Interestingly, *HEY2* haploinsufficiency in mice (i.e., *HEY2*^{+/-}) flattens the epicardial-to-endocardial transmural electrophysiological gradient in the RV via effects on both depolarizing I_{Na} and repolarizing I_{to} currents and results in less prominent J-waves [37]. Although the direct effect of increased *HEY2* expression has yet to be assessed directly in vivo, accentuation of the I_{Na}- and I_{to}-mediated epicardial-to-endocardial transmural electrophysiological gradient in the RVOT is consistent with existing models of BrS pathogenesis.

Collectively, the aforementioned BrS GWAS and subsequent elucidation of potential mechanisms underlying the BrS risk associated with *SCN10A* rs10428132 and *HEY2* rs9388451 risk alleles provide compelling evidence that common genetic variation that influences the

transmural expression/patterning of cardiac ion channels may contribute to the pathogenesis of BrS. However, it remains to be seen if (i) these GWAS-identified BrS risk alleles underlie the marked incomplete penetrance and variable expressivity observed in *SCN5A*-mediated BrS and (ii) larger/better powered multicenter GWAS will unearth additional novel BrS-associated genetic loci. Furthermore, how common and rare genetic risk factors interact with environmental risk factors such as gender (i.e., sex hormones), age (fibrosis/biophysical changes in I_{Na}), and comorbid conditions (i.e., hypertension) in BrS pathogenesis requires further investigation. Hopefully, ongoing studies in these areas will help refine/redefine our current understanding of the genetic architecture(s) underlying BrS.

Advances in the Diagnosis, Risk Stratification, and Clinical Management of BrS

As discussed previously, according to current AHA/ACC (2017) [3], ESC (2015) [2], and HRS/EHRA (2013) [1] consensus guidelines for the management of patients with ventricular arrhythmias/SCD, BrS is diagnosed in a patient with either spontaneous or class I antiarrhythmic-induced coved-type ST-segment elevations ≥ 2 mm in ≥ 1 right precordial leads (V1 or V2; Fig. 17.1a) positioned in either the 2nd, 3rd, or fourth intercostal position. This specific ECG morphology is often referred to as a type 1 Brugada ECG pattern. However, due to concerns that the inclusion of a class I antiarrhythmic-provoked type I Brugada ECG pattern could result in overdiagnosis, the recent HRS/EHRA J-wave syndrome task force recommended that a diagnosis of BrS in this circumstance also require at least one of the following: documented ventricular fibrillation (VF)/polymorphic ventricular tachycardia (VT), arrhythmic syncope, family history of autopsy-negative SCD, type I Brugada ECG pattern in relatives, or nocturnal agonal respirations [17].

As a result of the complexities surrounding the diagnosis of BrS, particularly the role of a drug-induced type 1 Brugada ECG pattern and nonspecific type 2 (saddle-back)/type 3 ST-segment elevations (Fig. 17.1b, c), the J-wave syndrome task force proposed a weighted diagnostic BrS diagnostic scorecard termed the “Shanghai Score System” (Table 17.2) [17]. Although the Shanghai Score is based entirely on expert opinion and not directly derived from large-scale BrS outcome/risk stratification data, its recent independent validation [38] supports its ongoing use, especially by non-experts, when considering a potential BrS diagnosis.

In the following sections, we detail current expert consensus approaches to the risk stratification and clinical management of patients with a clinical diagnosis of BrS.

Risk Stratification Approaches in BrS

Numerous prior studies have indicated that the single strongest predictor of subsequent cardiac events in patients diagnosed ultimately with BrS is initial clinical presentation (i.e., asymptomatic < arrhythmic syncope < aborted sudden cardiac arrest) [39, 40]. Furthermore, the presence of a *spontaneous* type 1 Brugada ECG pattern is a widely accepted, independent predictor of risk [40, 41].

A number of additional electrocardiographic markers (i.e., QRS fragmentation, concomitant inferolateral early repolarization pattern) [42, 43] appear to signify increased risk as does VF inducibility with programmed electrical stimulation during diagnostic EPS using a nonaggressive protocol (i.e., ≤ 2 extrastimuli from the RV apex) [44]. However, it remains to be seen whether these additional ECG parameters and/or the results of a diagnostic EPS with programmed electrical stimulation are robust enough to alter clinical decision-making, particularly in asymptomatic patients, and remain the subject of ongoing study and expert debate.

Fortunately, the majority of patients with a newly rendered diagnosis of BrS are asymptomatic

Table 17.2 Proposed “Shanghai Score” Brugada syndrome diagnostic scorecard

Clinical criteria	Points
<i>Electrocardiographic criteria (requires ≥ 1 finding on 12-lead ECG or ambulatory Holter monitoring)</i>	
Spontaneous type 1 Brugada ECG pattern at nominal or high leads	3.5
Fever-induced type 1 Brugada ECG pattern at nominal or high leads	3
Type 2 or 3 Brugada ECG pattern that converts with provocative drug challenge	2
<i>*Only award points for highest score in this category</i>	
<i>Clinical history</i>	
Unexplained cardiac arrest or documented VF/ polymorphic VT	3
Nocturnal agonal respirations	2
Suspected arrhythmic syncope	2
Syncope of unclear mechanism/unclear etiology	1
Atrial flutter/fibrillation in patients <30 years without alternative etiology	0.5
<i>*Only award points for highest score in this category</i>	
<i>Family history</i>	
First- or second-degree relative with definite BrS	2
Suspicious SCD (fever, nocturnal, Brugada aggravating drugs) in a first- or second-degree relative	1
Unexplained SCD <45 years in first- or second- degree relative with negative autopsy	0.5
<i>*Only award points for highest score in this category</i>	
<i>Genetic test result^a</i>	
ACMG pathogenic or likely pathogenic variant in BrS-susceptibility gene	0.5
<i>Shanghai BrS score (requires at least 1 electrocardiographic criteria)</i>	
≥3.5 points: High pretest probability of BrS (probable/definite BrS; ≥ 90% likelihood)	
2–3 points: Intermediate pretest probability of BrS (possible BrS; ~50% likelihood)	
<2 points: Low pretest probability of BrS (nondiagnostic)	

Adapted from Anztelevitch et al. [17] with permission from Elsevier

Abbreviations: ACMG American College of Medical Genetics and Genomics, BrS Brugada syndrome, ECG electrocardiogram, SCD sudden cardiac death, VF ventricular fibrillation, VT ventricular tachycardia

^aOnly *SCN5A* is definitively associated with BrS. Extreme caution should be exercised when adjudicating/interpreting variants identified in the 20+ weak/disputed evidence minor BrS-susceptibility genes

(~63%) and are therefore associated with relatively low annual risk (~0.5%) [39, 40]. In these patients, it is important to remember that neither a family history of SCD nor the detection of a pathogenic *SCN5A* variant influences prognosis [39, 40]. As such, family history and genetic testing results have no bearing on clinical decision-making, including the decision to pursue implantable cardioverter-defibrillator (ICD) implantation.

Invasive Management of Previously Symptomatic BrS

At present, the only proven SCD prevention strategy in high-risk BrS patients (i.e., those with a history of SCA, documented VF/sustained VT, or arrhythmic syncope) is an ICD. As outlined in Fig. 17.4, current AHA/ACC, ESC, and HRS/EHRA guidelines all recommend an ICD as first-line therapy for all BrS patients with a life expectancy >1 year that either i) presented with aborted SCD or ii) have documented evidence of sustained VT/VF (class I recommendation) [1–3].

In addition, current ESC and HRS/EHRA, but not AHA/ACC, guidelines recommend consideration of an ICD in i) symptomatic BrS patients with a clinical history strongly suggestive of arrhythmic syncope (class IIa recommendation) and ii) asymptomatic BrS patients with a spontaneous type I Brugada ECG and inducible VT/VF during a diagnostic EPS with programmed ventricular stimulation (PVS) limited to ≤2 extra-stimuli (Fig. 17.4) [1–3].

Lastly, although the use of diagnostic EPS with PVS is reemerging as a risk stratification strategy (currently a class IIb recommendation in the AHA/ACC, ESC, and HRS/EHRA guidelines), the role of therapeutic radiofrequency ablation in BrS is currently limited to previously symptomatic patients who (i) are not candidates for or refuse an ICD, (ii) have experienced frequent appropriate ICD therapies, and (iii) have a history of electrical storm (Fig. 17.4) [1–3]. As our understanding of the pathophysiology of BrS continues to evolve, particularly as it relates to the role of structural alterations in the RVOT/

anterior RV free wall, and better powered outcome studies with longer follow-up duration emerge, radiofrequency ablation may assume a larger role in the treatment of BrS in the future [18, 19, 45]. However, until such data emerge, a prophylactic epicardial RVOT ablation in asymptomatic patients with BrS should be discouraged [20].

Pharmacologic Management of Previously Symptomatic BrS

Unfortunately, in some patients (i.e., infants/young children, individuals from developing nations), an ICD may be refused or not physically/financially feasible. In these cases, quinidine, a class Ia antiarrhythmic that blocks I_{to} nonspecifically, suppresses spontaneous ventricular arrhythmias in BrS [46–49]. As such, the AHA/ACC, ESC, and HRS/EHRA guidelines on the management of patients with ventricular arrhythmias/SCD all support the use of quinidine in BrS patients with i) symptomatic ventricular arrhythmias who either are not candidates for or decline an ICD, ii) a history of recurrent polymorphic VT shocks or VF storm, and iii) supra-ventricular arrhythmias requiring pharmacologic management (Fig. 17.4) [1–3].

Future Directions

As illustrated in this chapter, our understanding of the genetic architecture and pathophysiological mechanisms underlying BrS is currently in a state of active flux. Although BrS was once considered a primary electrical disorder, emerging electro-anatomic and pathologic evidence suggest BrS may, mechanistically, have more in common with the arrhythmogenic cardiomyopathies than its long presumed cousin long QT syndrome. Furthermore, in light of the substantial rate of amino acid-altering genetic variation within most genes in the human genome and techniques employed in the discovery of most BrS-susceptibility genes, it comes as little surprise that many of the genes/variants associated previously

with BrS may represent background genetic noise and deserve rightfully their current ClinGen “disputed” evidence label.

However, as illustrated by the discovery of BrS-associated common variants in *HEY2* and *SCN10A* by GWAS, the genetic architecture of BrS is likely more complicated than envisioned previously. As such, some of the genes/variants in “disputed” evidence minor BrS-susceptibility genes may, in reality, represent strong contributors to an oligogenic/polygenic disease. In this light, developing a better understanding of the mechanistic link between decreased I_{Na} current and/or disruptions in transmural ion channel gradients conferred by rare and common genetic variants in *SCN5A*, *HEY2*, *SCN10A*, and perhaps some “disputed” evidence genes and subtle structural alterations in the RVOT/anterior RV is of utmost important.

Furthermore, developing a better mechanistic understanding of the complex interplay between established genetic and environmental risk factors such as gender, age, inflammation, and other comorbid conditions is sorely needed. With an enhanced understanding of how potentially modifiable environmental risk factors interact with genetic predisposition, development of approaches to slow or prevent the formation of a high-risk BrS substrate in the RVOT/anterior RV may one day be feasible.

Lastly, the ICD, with its inherent risk of inappropriate therapies and other nontrivial complications, remains the only widely accepted SCD prevention strategy in high-risk BrS patients. As such, ongoing assessment of the role of diagnostic EPS with programmed ventricular stimulation in risk stratification, durability of epicardial ablation, and the development of additional therapeutic approaches promises to provide physicians with better therapeutic options that will hopefully improve substantially the lives of patients with this potentially lethal condition.

Funding Sources This work was supported by the Mayo Clinic Windland Smith Rice Sudden Comprehensive Sudden Cardiac Death Program (to Dr. Ackerman). Dr. Giudicessi thanks the Mayo

Clinic Cardiovascular Diseases Fellowship and Clinician Investigator Training Programs for fostering an outstanding environment for physician-scientist training.

Conflict of Interest Disclosures Dr. Ackerman is a consultant for Audentes Therapeutics, Boston Scientific, Gilead Sciences, Invitae, Medtronic, MyoKardia, and St. Jude Medical. From 2004 to 2016, M.J.A. and Mayo Clinic received sales-based royalties from Transgenomic for their FAMILION-LQTS and FAMILION-CPVT genetic tests. M.J.A. and Mayo Clinic have an equity/royalty relationship (without remuneration so far) with AliveCor, Blue Ox Health, and StemoniX. However, none of these entities participated in this study. Dr. Giudicessi declares no conflicts.

References

- Priori SG, Wilde AA, Horie M, Cho Y, Behr ER, Berul C, et al. HRS/EHRA/APHRs expert consensus statement on the diagnosis and management of patients with inherited primary arrhythmia syndromes: document endorsed by HRS, EHRA, and APhRS in May 2013 and by ACCF, AHA, PACES, and AEPC in June 2013. *Heart Rhythm*. 2013;10(12):1932–63.
- Priori SG, Blomstrom-Lundqvist C, Mazzanti A, Blom N, Borggrefe M, Camm J, et al. 2015 ESC guidelines for the management of patients with ventricular arrhythmias and the prevention of sudden cardiac death: the task force for the management of patients with ventricular arrhythmias and the prevention of sudden cardiac death of the European Society of Cardiology (ESC). Endorsed by: Association for European Paediatric and Congenital Cardiology (AEPC). *Eur Heart J*. 2015;36(41):2793–867.
- Al-Khatib SM, Stevenson WG, Ackerman MJ, Bryant WJ, Callans DJ, Curtis AB, et al. 2017 AHA/ACC/HRS guideline for management of patients with ventricular arrhythmias and the prevention of sudden cardiac death: executive summary: A report of the American College of Cardiology/American Heart Association task force on clinical practice guidelines and the Heart Rhythm Society. *J Am Coll Cardiol*. 2018;72(14):1677–749.
- Morita H, Fukushima-Kusano K, Nagase S, Takenaka-Morita S, Nishii N, Kakishita M, et al. Site-specific arrhythmogenesis in patients with Brugada syndrome. *J Cardiovasc Electrophysiol*. 2003;14(4):373–9.
- Pappone C, Ciccone G, Manguso F, Vicedomini G, Mecarocci V, Conti M, et al. Assessing the malignant ventricular arrhythmic substrate in patients with Brugada syndrome. *J Am Coll Cardiol*. 2018;71(15):1631–46.
- Pieroni M, Notarstefano P, Oliva A, Campuzano O, Santangeli P, Coll M, et al. Electroanatomic and pathologic right ventricular outflow tract abnormalities in patients with Brugada syndrome. *J Am Coll Cardiol*. 2018;72(22):2747–57.
- Morita H, Kusano-Fukushima K, Nagase S, Fujimoto Y, Hisamatsu K, Fujio H, et al. Atrial fibrillation and atrial vulnerability in patients with Brugada syndrome. *J Am Coll Cardiol*. 2002;40(8):1437–44.
- Kapflinger JD, Tester DJ, Alders M, Benito B, Berthet M, Brugada J, et al. An international compendium of mutations in the SCN5A-encoded cardiac sodium channel in patients referred for Brugada syndrome genetic testing. *Heart Rhythm*. 2010;7(1):33–46.
- Ackerman MJ, Splawski I, Makielski JC, Tester DJ, Will ML, Timothy KW, et al. Spectrum and prevalence of cardiac sodium channel variants among black, white, Asian, and Hispanic individuals: implications for arrhythmogenic susceptibility and Brugada/long QT syndrome genetic testing. *Heart Rhythm*. 2004;1(5):600–7.
- Hosseini SM, Kim R, Udupa S, Costain G, Jobling R, Liston E, et al. Reappraisal of reported genes for sudden arrhythmic death. *Circulation*. 2018;138(12):1195–205.
- Giudicessi JR, Ackerman MJ. Determinants of incomplete penetrance and variable expressivity in heritable cardiac arrhythmia syndromes. *Transl Res*. 2013;161(1):1–14.
- Priori SG, Napolitano C, Gasparini M, Pappone C, Della Bella P, Brignole M, et al. Clinical and genetic heterogeneity of right bundle branch block and ST-segment elevation syndrome: a prospective evaluation of 52 families. *Circulation*. 2000;102(20):2509–15.
- Bezzina CR, Barc J, Mizusawa Y, Remme CA, Gourraud JB, Simonet F, et al. Common variants at SCN5A-SCN10A and HEY2 are associated with Brugada syndrome, a rare disease with high risk of sudden cardiac death. *Nat Genet*. 2013;45(9):1044–9.
- Giudicessi JR, Kullo IJ, Ackerman MJ. Precision cardiovascular medicine: state of genetic testing. *Mayo Clin Proc*. 2017;92(4):642–62.
- Hermida JS, Dassonville E, Six I, Amant C, Coviaux F, Clerc J, et al. Prospective evaluation of the familial prevalence of the brugada syndrome. *Am J Cardiol*. 2010;106(12):1758–62.
- Yan GX, Antzelevitch C. Cellular basis for the electrocardiographic J wave. *Circulation*. 1996;93(2):372–9.
- Antzelevitch C, Yan GX, Ackerman MJ, Borggrefe M, Corrado D, Guo J, et al. J-wave syndromes expert consensus conference report: emerging concepts and gaps in knowledge. *Heart Rhythm*. 2016;13(10):e295–324.
- Nademanee K, Veerakul G, Chandanamattha P, Chaothawee L, Ariyachaiapanich A, Jirasirojanakorn

- K, et al. Prevention of ventricular fibrillation episodes in Brugada syndrome by catheter ablation over the anterior right ventricular outflow tract epicardium. *Circulation*. 2011;123(12):1270–9.
19. Sacher F, Jesel L, Jais P, Haissaguerre M. Insight into the mechanism of Brugada syndrome: epicardial substrate and modification during ajmaline testing. *Heart Rhythm*. 2014;11(4):732–4.
 20. Brugada J, Pappone C, Berruezo A, Vicedomini G, Manguso F, Ciconte G, et al. Brugada syndrome phenotype elimination by epicardial substrate ablation. *Circ Arrhythm Electrophysiol*. 2015;8(6):1373–81.
 21. Bastiaenen R, Cox AT, Castelletti S, Wijeyeratne YD, Colbeck N, Pakroo N, et al. Late gadolinium enhancement in Brugada syndrome: a marker for subtle underlying cardiomyopathy? *Heart Rhythm*. 2017;14(4):583–9.
 22. Gray B, Gnanappa GK, Bagnall RD, Femia G, Yeates L, Ingles J, et al. Relations between right ventricular morphology and clinical, electrical and genetic parameters in Brugada syndrome. *PLoS One*. 2018;13(4):e0195594.
 23. Papadakis M, Raju H, Behr ER, De Noronha SV, Spath N, Kouloubinis A, et al. Sudden cardiac death with autopsy findings of uncertain significance: potential for erroneous interpretation. *Circ Arrhythm Electrophysiol*. 2013;6(3):588–96.
 24. Frustaci A, Priori SG, Pieroni M, Chimenti C, Napolitano C, Rivolta I, et al. Cardiac histological substrate in patients with clinical phenotype of Brugada syndrome. *Circulation*. 2005;112(24):3680–7.
 25. Chen Q, Kirsch GE, Zhang D, Brugada R, Brugada J, Brugada P, et al. Genetic basis and molecular mechanism for idiopathic ventricular fibrillation. *Nature*. 1998;392(6673):293–6.
 26. Le Scouarnec S, Karakachoff M, Gourraud JB, Lindenbaum P, Bonnaud S, Portero V, et al. Testing the burden of rare variation in arrhythmia-susceptibility genes provides new insights into molecular diagnosis for Brugada syndrome. *Hum Mol Genet*. 2015;24(10):2757–63.
 27. Chong JX, Buckingham KJ, Jhangiani SN, Boehm C, Sobreira N, Smith JD, et al. The genetic basis of Mendelian phenotypes: discoveries, challenges, and opportunities. *Am J Hum Genet*. 2015;97(2):199–215.
 28. Strande NT, Riggs ER, Buchanan AH, Ceyhan-Birsoy O, DiStefano M, Dwight SS, et al. Evaluating the clinical validity of gene-disease associations: an evidence-based framework developed by the Clinical Genome Resource. *Am J Hum Genet*. 2017;100(6):895–906.
 29. Weiss R, Barmada MM, Nguyen T, Seibel JS, Cavlovich D, Kornblit CA, et al. Clinical and molecular heterogeneity in the Brugada syndrome: a novel gene locus on chromosome 3. *Circulation*. 2002;105(6):707–13.
 30. London B, Michalec M, Mehdi H, Zhu X, Kerchner L, Sanyal S, et al. Mutation in glycerol-3-phosphate dehydrogenase 1 like gene (GPD1-L) decreases cardiac Na⁺ current and causes inherited arrhythmias. *Circulation*. 2007;116(20):2260–8.
 31. Giudicessi JR, Ye D, Tester DJ, Crotti L, Mugione A, Nesterenko VV, et al. Transient outward current (I_{to}) gain-of-function mutations in the KCND3-encoded Kv4.3 potassium channel and Brugada syndrome. *Heart Rhythm*. 2011;8(7):1024–32.
 32. Crotti L, Marcou CA, Tester DJ, Castelletti S, Giudicessi JR, Torchio M, et al. Spectrum and prevalence of mutations involving BrS1- through BrS12-susceptibility genes in a cohort of unrelated patients referred for Brugada syndrome genetic testing: implications for genetic testing. *J Am Coll Cardiol*. 2012;60(15):1410–8.
 33. van den Boogaard M, Smemo S, Burnicka-Turek O, Arnolds DE, van de Werken HJ, Klous P, et al. A common genetic variant within SCN10A modulates cardiac SCN5A expression. *J Clin Invest*. 2014;124(4):1844–52.
 34. van den Boogaard M, Wong LY, Tessadori F, Bakker ML, Dreizehnter LK, Wakker V, et al. Genetic variation in T-box binding element functionally affects SCN5A/SCN10A enhancer. *J Clin Invest*. 2012;122(7):2519–30.
 35. Hu D, Barajas-Martinez H, Pfeiffer R, Dezi F, Pfeiffer J, Buch T, et al. Mutations in SCN10A are responsible for a large fraction of cases of Brugada syndrome. *J Am Coll Cardiol*. 2014;64(1):66–79.
 36. Behr ER, Savio-Galimberti E, Barc J, Holst AG, Petropoulou E, Prins BP, et al. Role of common and rare variants in SCN10A: results from the Brugada syndrome QRS locus gene discovery collaborative study. *Cardiovasc Res*. 2015;106(3):520–9.
 37. Veerman CC, Podliesna S, Tadros R, Lodder EM, Mengarelli I, de Jonge B, et al. The Brugada syndrome susceptibility gene HEY2 modulates cardiac transmural ion channel patterning and electrical heterogeneity. *Circ Res*. 2017;121(5):537–48.
 38. Kawada S, Morita H, Antzelevitch C, Morimoto Y, Nakagawa K, Watanabe A, et al. Shanghai score system for diagnosis of Brugada syndrome: validation of the score system and reclassification of the patients. *JACC Clin Electrophysiol*. 2018;4(6):724–30.
 39. Kamakura S, Ohe T, Nakazawa K, Aizawa Y, Shimizu A, Horie M, et al. Long-term prognosis of probands with Brugada-pattern ST-elevation in leads V1–V3. *Circ Arrhythm Electrophysiol*. 2009;2(5):495–503.
 40. Probst V, Veltmann C, Eckardt L, Merregalli PG, Gaita F, Tan HL, et al. Long-term prognosis of patients diagnosed with Brugada syndrome: results from the FINGER Brugada syndrome registry. *Circulation*. 2010;121(5):635–43.
 41. Priori SG, Gasparini M, Napolitano C, Della Bella P, Ottonelli AG, Sassone B, et al. Risk stratification in Brugada syndrome: results of the PRELUDE (PRogrammed ELectrical stimulation preDICTive valuE) registry. *J Am Coll Cardiol*. 2012;59(1):37–45.
 42. Morita H, Kusano KF, Miura D, Nagase S, Nakamura K, Morita ST, et al. Fragmented QRS as a marker of conduction abnormality and a predictor of prognosis of Brugada syndrome. *Circulation*. 2008;118(17):1697–704.

43. Kawata H, Morita H, Yamada Y, Noda T, Satomi K, Aiba T, et al. Prognostic significance of early repolarization in inferolateral leads in Brugada patients with documented ventricular fibrillation: a novel risk factor for Brugada syndrome with ventricular fibrillation. *Heart Rhythm*. 2013;10(8):1161–8.
44. Sroubek J, Probst V, Mazzanti A, Delise P, Hevia JC, Ohkubo K, et al. Programmed ventricular stimulation for risk stratification in the Brugada syndrome: a pooled analysis. *Circulation*. 2016;133(7):622–30.
45. Shah AJ, Hocini M, Lamaison D, Sacher F, Derval N, Haissaguerre M. Regional substrate ablation abolishes Brugada syndrome. *J Cardiovasc Electrophysiol*. 2011;22(11):1290–1.
46. Hermida JS, Denjoy I, Clerc J, Extramiana F, Jarry G, Milliez P, et al. Hydroquinidine therapy in Brugada syndrome. *J Am Coll Cardiol*. 2004;43(10):1853–60.
47. Belhassen B, Glick A, Viskin S. Efficacy of quinidine in high-risk patients with Brugada syndrome. *Circulation*. 2004;110(13):1731–7.
48. Belhassen B, Rahkovich M, Michowitz Y, Glick A, Viskin S. Management of Brugada syndrome: thirty-three-year experience using electrophysiologically guided therapy with class IA antiarrhythmic drugs. *Circ Arrhythm Electrophysiol*. 2015;8(6):1393–402.
49. Viskin S, Wilde AA, Tan HL, Antzelevitch C, Shimizu W, Belhassen B. Empiric quinidine therapy for asymptomatic Brugada syndrome: time for a prospective registry. *Heart Rhythm*. 2009;6(3):401–4.
50. Hu D, Barajas-Martinez H, Terzic A, Park S, Pfeiffer R, Burashnikov E, et al. ABCC9 is a novel Brugada and early repolarization syndrome susceptibility gene. *Int J Cardiol*. 2014;171(3):431–42.
51. Antzelevitch C, Pollevick GD, Cordeiro JM, Casis O, Sanguinetti MC, Aizawa Y, et al. Loss-of-function mutations in the cardiac calcium channel underlie a new clinical entity characterized by ST-segment elevation, short QT intervals, and sudden cardiac death. *Circulation*. 2007;115(4):442–9.
52. Burashnikov E, Pfeiffer R, Barajas-Martinez H, Delpon E, Hu D, Desai M, et al. Mutations in the cardiac L-type calcium channel associated with inherited J-wave syndromes and sudden cardiac death. *Heart Rhythm*. 2010;7(12):1872–82.
53. Hennessey JA, Marcou CA, Wang C, Wei EQ, Wang C, Tester DJ, et al. FGF12 is a candidate Brugada syndrome locus. *Heart Rhythm*. 2013;10(12):1886–94.
54. Biel S, Aquila M, Hertel B, Berthold A, Neumann T, DiFrancesco D, et al. Mutation in S6 domain of HCN4 channel in patient with suspected Brugada syndrome modifies channel function. *Pflugers Arch*. 2016;468(10):1663–71.
55. Delpon E, Cordeiro JM, Nunez L, Thomsen PE, Guerschicoff A, Pollevick GD, et al. Functional effects of KCNE3 mutation and its role in the development of Brugada syndrome. *Circ Arrhythm Electrophysiol*. 2008;1(3):209–18.
56. Ohno S, Zankov DP, Ding WG, Itoh H, Makiyama T, Doi T, et al. KCNE5 (KCNE1L) variants are novel modulators of Brugada syndrome and idiopathic ventricular fibrillation. *Circ Arrhythm Electrophysiol*. 2011;4(3):352–61.
57. Verkerk AO, Wilders R, Schulze-Bahr E, Beekman L, Bhuiyan ZA, Bertrand J, et al. Role of sequence variations in the human ether-a-go-go-related gene (HERG, KCNH2) in the Brugada syndrome. *Cardiovasc Res*. 2005;68(3):441–53.
58. Medeiros-Domingo A, Tan BH, Crotti L, Tester DJ, Eckhardt L, Cuoretti A, et al. Gain-of-function mutation S422L in the KCNJ8-encoded cardiac K(ATP) channel Kir6.1 as a pathogenic substrate for J-wave syndromes. *Heart Rhythm*. 2010;7(10):1466–71.
59. Kattygnarath D, Maugenre S, Neyroud N, Balse E, Ichai C, Denjoy I, et al. MOG1: a new susceptibility gene for Brugada syndrome. *Circ Cardiovasc Genet*. 2011;4(3):261–8.
60. Cerrone M, Lin X, Zhang M, Agullo-Pascual E, Pfenniger A, Chkourko Gusky H, et al. Missense mutations in plakophilin-2 cause sodium current deficit and associate with a Brugada syndrome phenotype. *Circulation*. 2014;129(10):1092–103.
61. Watanabe H, Koopmann TT, Le Scouarnec S, Yang T, Ingram CR, Schott JJ, et al. Sodium channel beta1 subunit mutations associated with Brugada syndrome and cardiac conduction disease in humans. *J Clin Invest*. 2008;118(6):2260–8.
62. Riuro H, Beltran-Alvarez P, Tarradas A, Selga E, Campuzano O, Verges M, et al. A missense mutation in the sodium channel beta2 subunit reveals SCN2B as a new candidate gene for Brugada syndrome. *Hum Mutat*. 2013;34(7):961–6.
63. Hu D, Barajas-Martinez H, Burashnikov E, Springer M, Wu Y, Varro A, et al. A mutation in the beta 3 subunit of the cardiac sodium channel associated with Brugada ECG phenotype. *Circ Cardiovasc Genet*. 2009;2(3):270–8.
64. Boczek NJ, Ye D, Johnson EK, Wang W, Crotti L, Tester DJ, et al. Characterization of SEMA3A-encoded semaphorin as a naturally occurring Kv4.3 protein inhibitor and its contribution to Brugada syndrome. *Circ Res*. 2014;115(4):460–9.
65. Ishikawa T, Sato A, Marcou CA, Tester DJ, Ackerman MJ, Crotti L, et al. A novel disease gene for Brugada syndrome: sarcolemmal membrane-associated protein gene mutations impair intracellular trafficking of hNav1.5. *Circ Arrhythm Electrophysiol*. 2012;5(6):1098–107.
66. Liu H, Chatel S, Simard C, Syam N, Salle L, Probst V, et al. Molecular genetics and functional anomalies in a series of 248 Brugada cases with 11 mutations in the TRPM4 channel. *PLoS One*. 2013;8(1):e54131.
67. Al-Khatib SM, et al. 2017 AHA/ACC/HRS guideline for management of patients with ventricular arrhythmias and the prevention of sudden cardiac death. *Circulation*. 2018;138(13):e272–391.

Part IV

Pathophysiology and Clinical Aspects of Special Cardiac Repolarization Syndromes



The Short QT Syndrome

18

Chiara Scrocco, Fiorenzo Gaita,
and Carla Giustetto

Introduction

The short QT syndrome (SQTS) is a rare familial ion channel disease characterized by shortened cardiac repolarization and increased susceptibility to life-threatening arrhythmias, in the absence of structural heart disease.

The first speculation about the potential malignant effects of a short QT interval dates back to 1993, when a retrospective analysis of 24-hour Holter recordings in 6693 subjects highlighted that both prolonged (>440 ms) and shortened (<400 ms) mean QTc interval were associated with a doubled risk of sudden death (SD) as compared with QTc values comprised between 400 and 440 ms [1]. The first report of a short QT interval at ECG associated with cardiac symptoms is from Gussak et al. [2], who reported a family of three (one of whom aged 17 suffered from paroxysmal atrial fibrillation (AF)) and an unrelated subject who had died suddenly. All of

them showed QT and QTc intervals <300 ms. In 2003 the inherited nature of the condition and its role in familial SD was highlighted by Gaita et al. [3] with the description of two unrelated families in which QT intervals between 210 and 280 ms (with QTc always <300 ms) were associated with palpitations (in some case with evidence of AF), syncope, and SD across several generations.

Diagnosis

QT and QTc Interval

The hallmark of SQTS is a constantly short QT interval on ECG (Fig. 18.1). As the QT interval reflects the duration of the repolarization, it is influenced by fluctuations in heart rate and vagal tone, as well as by hormonal factors linked to age, race, and sex and also by electrolyte abnormalities and certain drugs [4, 5]. To overcome the rate dependence of the QT interval, different correction formulas have been introduced. The most commonly used is the one proposed by Bazett ($QTc = QT/\sqrt{RR}$) [6], despite its tendency to underestimate the QT interval at low frequencies and to overestimate it at high heart rates. In 1992 a formula by which the expected QT interval (predicted QT, QTp) can be calculated for a specific heart rate was developed [7], but this is seldom used in the clinical practice. Although alternative formulas have been developed (Fridericia's formula, Framingham's formula), it has become apparent that a universal correction model may not

C. Scrocco
Clinical Cardiology Academic Group, Molecular and
Clinical Sciences Research Centre, St George's
University of London, London, UK

F. Gaita
Department of Medical Sciences, University of Turin,
and Clinica Pinna Pintor, Turin, Italy

C. Giustetto (✉)
Division of Cardiology, Department of Medical
Sciences, University of Turin, "Città della Salute e
della Scienza" Hospital, Turin, Italy
e-mail: carla.giustetto@unito.it

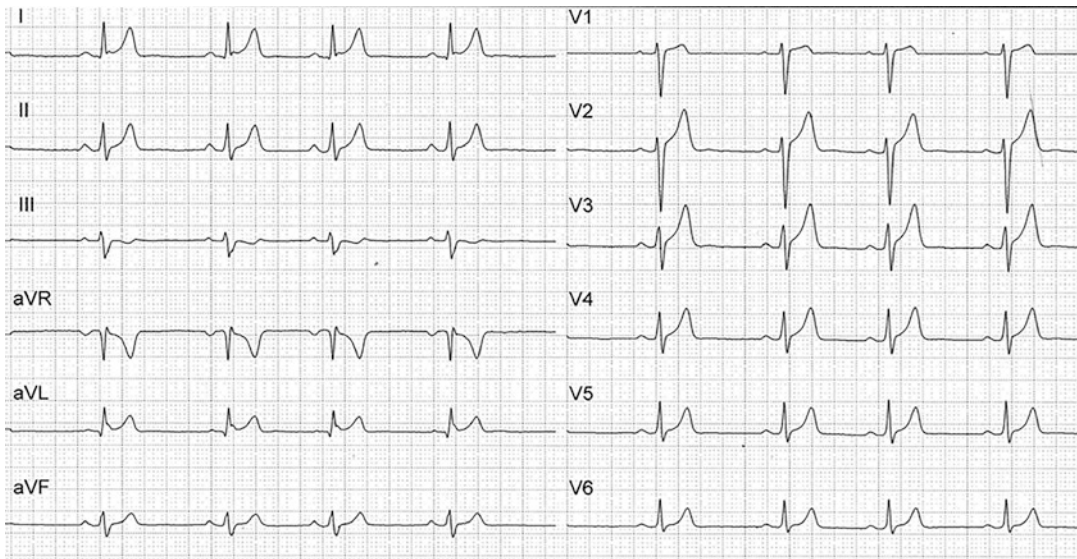


Fig. 18.1 A 18-year-old male with unknown mutation. HR 57 bpm, QT 340 ms, QTc 330 ms

be feasible, and therefore it is advisable that QT interval should be measured as close as possible to 60 beats/min.

Based on the observation that the QT values follow a Gaussian distribution in the general population [8–12], the lower limit of normality for the QT interval can be set at 2 standard deviations from the mean, that is, 360 ms in men and 370 ms in women [2, 13]. On the contrary, the precise cut-off value for the diagnosis of SQTS is controversial. In the 2013 *HRS/EHRA/APHRs Expert Consensus Statement on the Diagnosis and Management of Patients with Inherited Primary Arrhythmia Syndromes*, a cut-off value ≤ 330 ms was recommended for the diagnosis, while in the 2015 *ESC Guidelines for the management of patients with ventricular arrhythmias and the prevention of sudden cardiac death*, the threshold is set to 340 ms [14, 15]. Both documents agree that borderline values (up to 360 ms) may be considered for the diagnosis only in the presence of a confirmed pathogenic mutation, a family history of SQTS or of SD at age <40 years, and personal history of VT/VF episode in the absence of heart disease.

In the aforementioned epidemiological studies, the presence of shorter than normal QT-QTc intervals was not associated with an increased risk of SD. Due to this overlap between SQTS patients and general population, it appears that a

single QTc value cannot distinguish all affected from healthy individuals.

J-Tpeak Interval

In the first described SQTS patients, very impressive ECGs with tall, peaked, and symmetrical T waves together with a “virtual” ST segment had been observed [3]. In 2009, Anttonen et al. analyzed the differences in ECG between SQTS patients, subjects with short QT intervals from the general population, and subjects with normal QTc values. The main finding of this study was that SQTS subjects exhibited shorter QT and QTc values, together with shorter J-Tpeak intervals (between 80 and 120 ms) [16]. This observation was confirmed in a larger population of SQTS patients in 2011 [17].

PQ Segment Depression

PQ segment depression (PQD) is a well-defined ECG marker of acute pericarditis. It is also associated with extensive myocardial damage and atrial fibrillation. In a paper by Tulumen et al., it emerged that 52/74 (81%) of SQTS patients displayed PQD at ECG, defined as >0.05 mV

(0.5 mm) depression from the isoelectric line. This finding, though present also in 24% of healthy control subjects, has been interpreted as a consequence of the heterogeneous abbreviation of atrial repolarization [18].

QT/HR Relationship

A relevant feature in patients with SQTS is the lack of adaptation of the QT interval to the vari-

ations in the HR, with relatively little shortening in response to an increasing HR [19]. In 2015, the usefulness of exercise test in the diagnosis of SQTS was evaluated comparing the QT/HR relationship during exercise in 21 SQTS patients and 20 control subjects with short QT intervals [20]. SQTS patients showed a steeper β slope of the HR/QT linear relationship (≤ -0.90 ms/beat/min), together with a significantly lower mean QT variation from rest to peak exercise (48 ± 14 ms vs. 120 ± 20 ms) (Fig. 18.2).

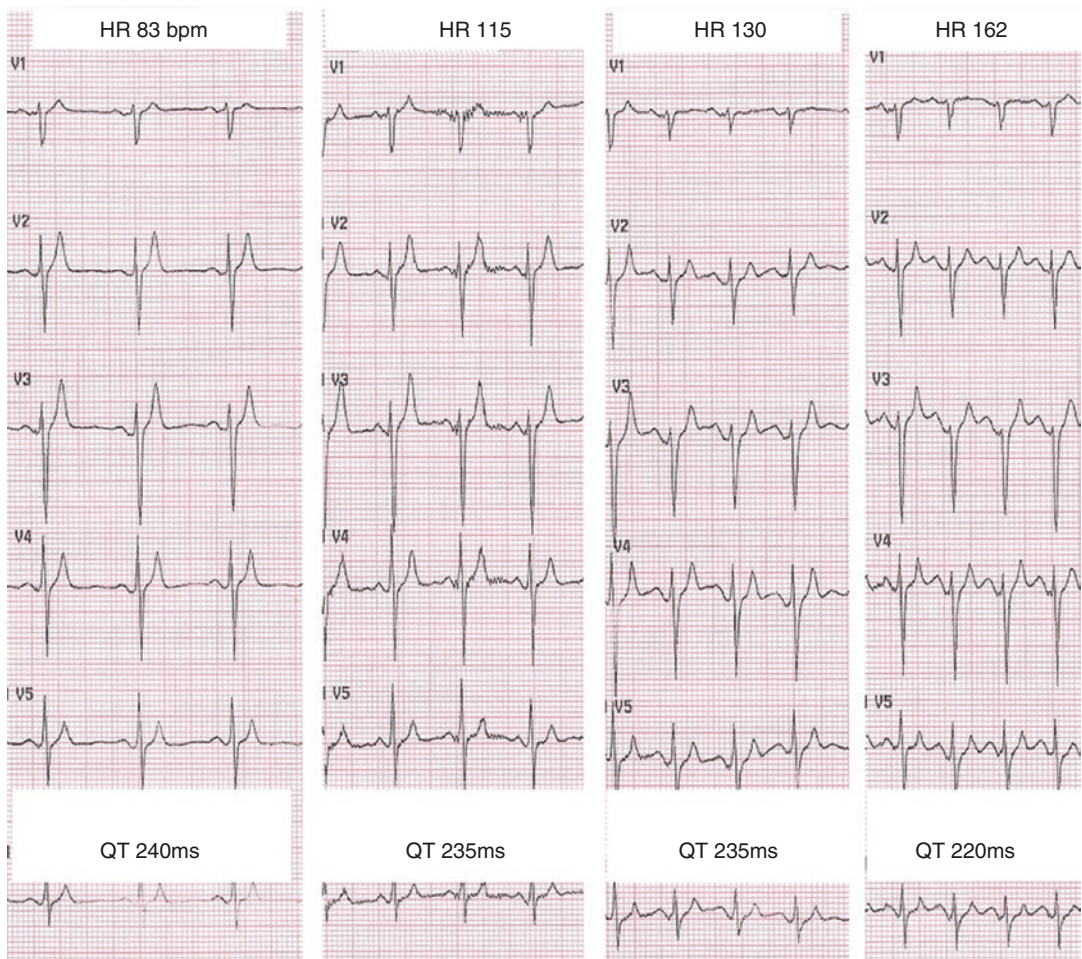


Fig. 18.2 A 31-year-old female patient with *KCNH2* (N588K) mutation. During the stress test a normal increase in heart rate was observed with only a slight further decrease of the QT interval duration. HR, heart rate

Ventricular Effective Refractory Periods (VERPs)

Electrophysiological study (EPS) has a role in confirming the diagnosis of SQTS. In fact, both atrial and ventricular effective refractory periods (VERPs) have been shown to be shorter in SQTS subjects as compared to controls (140–200 ms at a cycle length between 500 and 600 ms), both at baseline and after premature extrastimuli [3, 17, 21].

In 2011 a diagnostic score system in the style of that used for long QT syndrome, defining the probability of having SQTS as “high,” “intermediate,” and “low,” has been proposed [22]. The analyzed variables comprised clinical manifestations, family history, ECG parameters, and genetic analysis. The data were not drawn from a population of SQTS patients, but from several reports in worldwide literature, which included mainly symptomatic subjects. This score has not been validated in an independent population of SQTS patients and is not currently recommended for the diagnosis of SQTS.

Genetics and Molecular Basis

SQTS is considered to have an autosomal dominant inheritance, with high penetrance in families and variable expressivity. To date, the molecular basis of the disease has been associated with mutations in six genes, which encode the potassium (SQTS1–3) and the L-type calcium (SQTS4–6) channel [23–27]:

- *KCNH2* (rapidly activating delayed rectifier potassium channel [IKr], SQTS1)
- *KCNQ1* (slowly activating delayed rectifier potassium channel [IKs], SQTS2)
- *KCNJ2* (inward rectifier potassium channel [IK1], SQTS3)
- *CACNA1C* [ICa] (SQTS4)
- *CACNB2b* [ICa] (SQTS5)
- *CACNA2D1* [ICa] (SQTS6)

These mutations determine either an increase in the outward potassium currents or a decrease

in the inward calcium current, which eventually results in acceleration of the repolarization process and an abnormal abbreviation of the QT interval at surface ECG.

Several genetic variants in *KCNH2* gene have been reported in the literature [28, 29], even though not in all cases a clear role in pathogenesis has been proved [30, 31]. It has also been speculated that some modifier gene variants may affect the QT interval duration and the potassium currents and possibly the response to therapy in some affected patients [32]. Mutations in the L-type calcium channel have been detected in a high percentage of probands with J-wave syndromes, Brugada syndrome, and early repolarization syndrome.

Clinical Manifestations

Since its first description, less than 200 subjects with SQTS have been described in the literature worldwide. Few case series have been published so far: results from the Euroshort Registry, including 29 and 53 subjects, respectively, were published in 2006 and 2011 [17, 19]. Other registries included a cohort of 73 adults [33] and 25 pediatric patients [34].

SQTS affects predominantly males (above 75% of cases), with a mean age at observation below 25 years. More than a half (53–62%) of patients had experienced symptoms at the time of first clinical observation, of which cardiac arrest is the first in up to one-third of cases (26–32%). SD can be observed in individuals of all ages and its distribution shows two peaks: one in the first year of life and another between 20 and 40 years. It has been estimated that the probability of experiencing CA between birth and 40 years of age is between 40% and 50% [33]. With regard to the circumstances in which cardiac arrest or SD occurs, there are no clear triggers for arrhythmias, although a higher number of events have occurred during sleep or at rest. Syncope of presumed arrhythmic origin is the first clinical presentation in less than 20% of cases (13–16%), and short episodes of fast nsVT can be detected in both previously symptomatic and asymptomatic subjects

(Fig. 18.3). The presence of AF or atrial flutter at a young age has been documented in 11% of subjects in the Euroshort series [17] (Fig. 18.4), while in other series its prevalence has not been reported.

The incidence of events at follow-up in the available series ranges from 3.2% to 4.9% per year, with an estimated annual CA rate of 10.6% in SD survivors [33].

Due to the limited number of patients reported so far, and to the low yield of genetic testing, precise data on genotype-phenotype correlation in the setting of SQTs are not available.

Data from the EuroShort Registry showed that SQTs1 patients exhibit shorter QT, QTc, and J-Tpeak intervals at ECG (Fig. 18.5), shorter VERPs at electrophysiological study, and steeper slope of the QT/HR relationship during exercise [17, 20]. A recent review on 64 mutation-posi-

tive SQTs patients from the literature reported that 34 SQTs1 patients showed a later onset of symptoms as compared with other SQTs types, with a mean age at clinical manifestation of 35 ± 19 years [35]. However, several reports highlighted the high incidence of SD in children and newborns in SQTs1 families [3, 17, 19, 28], and although a definitive diagnosis could not be made due to the absence of available ECGs or molecular analysis on autoptotic tissue, it is likely that these events represent a manifestation of the disease. Another observation from the study by Harrell and colleagues is that SSS or bradycardia were significantly more prevalent in SQT2 patients (6/8, 75%) than non-SQT2 patients (5/57, 9%; $p < 0.001$). In their study no significant differences in the QTc values between different genotypes emerged.

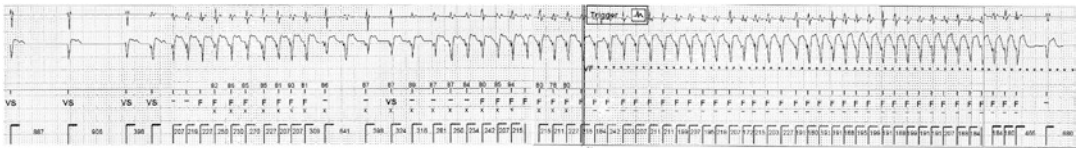


Fig. 18.3 Episode of nsVT recorded by the ICD in a 43-year-old asymptomatic female with KCNH2 (N588K) mutation and family history of SD. The ICD had been implanted in primary prevention 11 years before

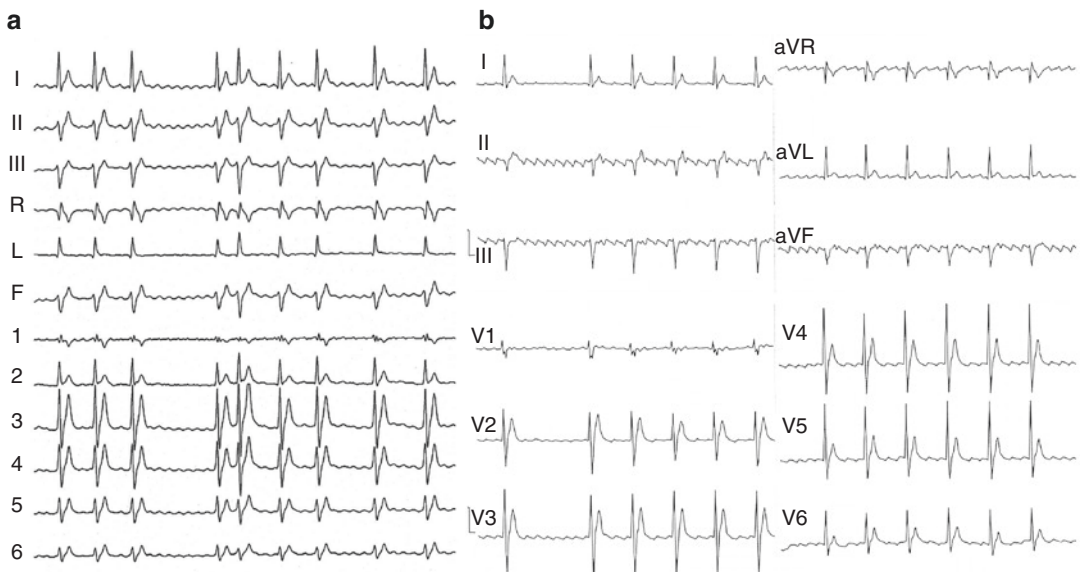
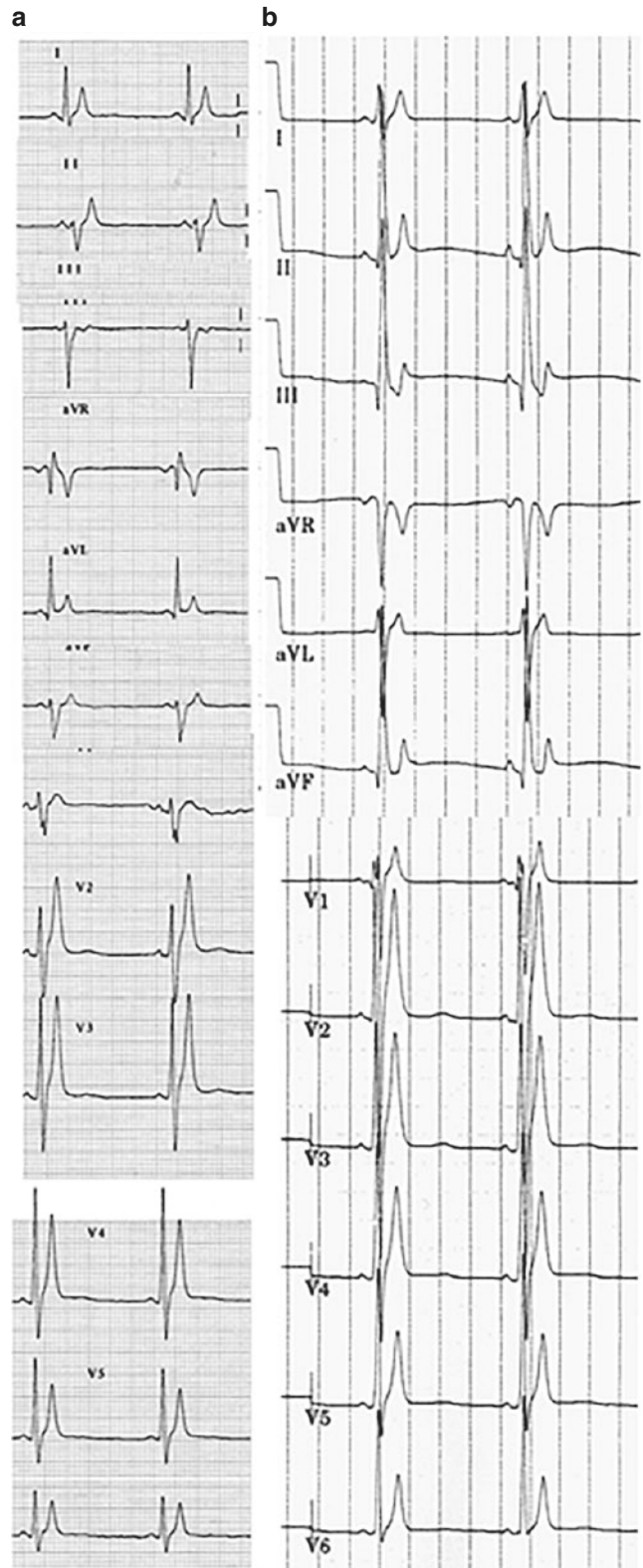


Fig. 18.4 33-year-old male with N588K mutation in KCNH2. (a) Atrial fibrillation with coarse and regular *f* waves. (b), common atrial flutter with very short FF intervals, suggesting very short atrial refractory periods

Fig. 18.5 ECG from two male patients with KCNH2 (N588K) mutation. Panel **a**: HR 52 bpm, QT 260 ms, QTc 280 ms. Panel **b**: HR 62 bpm, QT 248 ms, QTc 252 ms. (Courtesy of Prof. M. Borggreffe, Department of Medicine–Cardiology, University Hospital Mannheim, first Department of Medicine–Cardiology, Mannheim, Germany)



Risk Stratification and Management

Precise data on the risk stratification in SQTs are limited by the small number of subjects reported. In the three largest available series, neither sex nor age were significantly different in subjects with or without major arrhythmic events. Similarly, several ECG parameters, including QTc and JTp values, failed to demonstrate a clear correlation with the occurrence of symptoms [17, 33, 34]. Also the induction of sustained ventricular arrhythmias at EPS is not helpful in predicting CA, having a sensitivity below 40% [17, 33]. In a univariate analysis including the abovementioned parameters and others such as familial versus sporadic disease, family history of CA, mutation-positive status, and prior symptoms, only a personal history of aCA resulted to be associated with an increased risk of events at follow-up. A modified Gollob's diagnostic score had been proposed as a valuable tool to predict events in a pediatric cohort of SQTs patients [34] but failed to reproduce similar results in a cohort of adult patients [33].

Given the lack of precise risk stratification tools and the high incidence of SD, an implantable cardioverter-defibrillator (ICD) represents the treatment of choice for high-risk individuals, those with aborted CA or syncope [14]. Particular considerations with regard to the programming of the device must be made to reduce the risk of inappropriate shocks due to T wave oversensing in SQTs subjects; in fact, the high-amplitude T waves occurring shortly after the R wave may lead to double counting and inappropriate therapies [36, 37]. The intravenous ICD experience in the SQTs is burdened by a high incidence of complications (inappropriate shocks, lead fractures, infections requiring extraction of the device, and psychological distress) with rates up to 51% in adults [17] and 80% in children [34], not to mention the technical challenges of the implant in pediatric patients related to the small body and heart size, the difficult vascular access, and the need for modifications of the implant system during growth. Conversely, data on the use of subcutaneous ICD are still limited [38].

Concerning the pharmacological approach to the electrophysiological abnormalities underlying the SQTs, the first study with several antiarrhythmic drugs has been carried out in 2004 [39]. Selective IKr blocking agents were tested (sotalol and ibutilide) but failed to produce an increase in the QT interval in patients with SQT1, and subsequent genetic studies showed that the N588K mutation in *KCNH2* reduced the sensitivity of the channel to sotalol [40]. More recently, in vitro studies demonstrated that the T618I-*KCNH2* mutation is associated with a smaller loss of the inhibitory effect of sotalol on IKr channel, due to a less profound effect on inactivation of HERG current [27]. However, these findings were not confirmed in a SQTs1 family with the T618I mutation and the K897 T polymorphism in *KCNH2* gene [32].

A robust evidence on the efficacy of hydroquinidine (HQ) in SQTs exists. After the first report highlighting the prolongation of QT intervals and VERPs, and the non-inducibility of arrhythmias at EPS in treated subjects [39], its long-term efficacy in reducing life-threatening arrhythmias has been confirmed by the results of the EuroShort Registry cohort follow-up in 2011 [17]. Twelve patients had been receiving HQ for a mean period of 76 ± 30 months. HQ induced normalization of the QT interval and of the VERPs in patients with *KCNH2* mutations, both those with the N588K and T618I mutations. A lower and less homogeneous QTc increment was observed in patients with different or unknown genotype; however, HQ prevented both induction of VF at EPS and arrhythmic events at follow-up regardless of genotype. Similar results have been reported in 2017 in a cohort of 15 subjects, with a reduction in the annual rate of late arrhythmic events from 12% while off-HQ to 0 while on-HQ [41].

Among the other drugs, flecainide caused only a slight QT prolongation (mainly due to an increase in the QRS duration) in 4 patients [39]. Isolated reports on the efficacy of dofetilide (QT prolongation and AF suppression), amiodarone (polymorphic VT recurrences prevention), and isoproterenol (management of electrical storm) have been published [17, 34, 42].

References

- Algra A, Tijssen JG, Roelandt JR, Pool J, Lubsen J. QT interval variables from 24 hour electrocardiography and the two year risk of sudden death. *Br Heart*. 1993;70(5):421–7.
- Gussak I, Brugada P, Brugada J, Wright RS, Kopecky SL, Chaitman BR. Idiopathic short QT interval: a new clinical syndrome? *Cardiology*. 2000;94(2):99–102.
- Gaita F, Giustetto C, Bianchi F, Wolpert C, Schimpf R, Riccardi R, et al. Short QT syndrome: a familial cause of sudden death. *Circulation*. 2003;108(8):965–70.
- Surawicz B, Parikh SR. Differences between ventricular repolarization in men and women: description, mechanism and implications. *Ann Noninvasive Electrocardiol*. 2003;8(4):333–40.
- Garberoglio L, Giustetto C, Wolpert C, Gaita F. Is acquired short QT due to digitalis intoxication responsible for malignant ventricular arrhythmias? *J Electrocardiol*. 2007;40(1):43–6.
- Bazett HC. An analysis of the time relations of the electrocardiograms. *Heart*. 1920;7:353–70.
- Rautaharju PM, Zhou SH, Wong S, Calhoun HP, Berenson GS, Prineas R, et al. Sex differences in the evolution of the electrocardiographic QT interval with age. *Can J Cardiol*. 1992;8(7):690–5.
- Gallagher MM, Magliano G, Yap YG, Padula M, Morgia V, Postorino C, et al. Distribution and prognostic significance of QT intervals in the lowest half centile in 12,012 apparently healthy persons. *Am J Cardiol*. 2006;98(7):933–5.
- Funada A, Hayashi K, Ino H, Fujino N, Uchiyama K, Sakata K, et al. Assessment of QT intervals and prevalence of short QT syndrome in Japan. *Clin Cardiol*. 2008;31(6):270–4.
- Kobza R, Roos M, Niggli B, Abächerli R, Lupi GA, Frey F, et al. Prevalence of long and short QT in a young population of 41,767 predominantly male Swiss conscripts. *Heart Rhythm*. 2009;6(5):652–7.
- Anttonen O, Junttila MJ, Rissanen H, Reunanen A, Viitasalo M, Huikuri HV. Prevalence and prognostic significance of short QT interval in a middle-aged Finnish population. *Circulation*. 2007;116(7):714–20.
- Dhutia H, Malhotra A, Parpia S, Gabus V, Finocchiaro G, Mellor G, et al. The prevalence and significance of a short QT interval in 18,825 low-risk individuals including athletes. *Br J Sports Med*. 2016;50(2):124–9.
- Viskin S. The QT interval: too long, too short or just right. *Heart Rhythm*. 2009;6(5):711–5.
- Priori SG, Wilde AA, Horie M, Cho Y, Behr ER, Berul C. HRS/EHRA/APHR expert consensus statement on the diagnosis and management of patients with inherited primary arrhythmia syndromes. *Europace*. 2013;15(10):1389–406.
- Priori SG, Blomström-Lundqvist C, Mazzanti A, Blom N, Borggrefe M, Camm J, et al. 2015 ESC guidelines for the management of patients with ventricular arrhythmias and the prevention of sudden cardiac death: the task force for the management of patients with ventricular arrhythmias and the prevention of sudden cardiac death of the European Society of Cardiology (ESC). Endorsed by: Association for European Paediatric and Congenital Cardiology (AEPC). *Eur Heart J*. 2015;36(41):2793–867.
- Anttonen O, Junttila MJ, Maury P, Schimpf R, Wolpert C, Borggrefe M, et al. Differences in twelve-lead electrocardiogram between symptomatic and asymptomatic subjects with short QT interval. *Heart Rhythm*. 2009;6(2):267–71.
- Giustetto C, Schimpf R, Mazzanti A, Scrocco C, Maury P, Anttonen O, et al. Long-term follow-up of patients with short QT syndrome. *J Am Coll Cardiol*. 2011;58(6):587–95.
- Türlümen E, Giustetto C, Wolpert C, Maury P, Anttonen O, Probst V, et al. PQ segment depression in patients with short QT syndrome: a novel marker for diagnosing short QT syndrome? *Heart Rhythm*. 2014;11:1024–30.
- Giustetto C, Di Monte F, Wolpert C, Borggrefe M, Schimpf R, Sbragia P, et al. Short QT syndrome: clinical findings and diagnostic–therapeutic implications. *Short QT syndrome: clinical findings and diagnostic–therapeutic implications*. *Eur Heart J*. 2006;27(20):2440–7.
- Giustetto C, Scrocco C, Schimpf R, Maury P, Mazzanti A, Levetto M, et al. Usefulness of exercise test in the diagnosis of short QT syndrome. *Europace*. 2015;17(4):628–34.
- Rollin A, Gandjbakch E, Giustetto C, Scrocco C, Fourcade C, Monteil B, et al. Shortening of the short refractory periods in short QT syndrome. *J Am Heart Assoc*. 2017;6:e005684.
- Gollob MH, Redpath CJ, Roberts JD. The short QT syndrome: proposed diagnostic criteria. *J Am Coll Cardiol*. 2011;57(7):802–12.
- Brugada R, Hong K, Dumaine R, Cordeiro J, Gaita F, Borggrefe M, et al. Sudden death associated with short-QT syndrome linked to mutations in HERG. *Circulation*. 2004;109(1):30–5.
- Belloq C, Van Ginneken ACG, Bezzina CR, Alders M, Escande D, Mannens MM, et al. Mutation in the KCNQ1 gene leading to the short QT-interval syndrome. *Circulation*. 2004;109(20):2394–7.
- Priori S, Pandit SV, Rivolta I, Berenfeld O, Ronchetti E, Dhamoon A, et al. A novel form of short QT syndrome (SQT3) is caused by a mutation in the KCNJ2 gene. *Circ Res*. 2005;96(7):800–7.
- Antzelevitch C, Pollevick GD, Cordeiro JM, Casis O, Sanguinetti MC, Aizawa Y, et al. Loss-of function mutations in the cardiac calcium channel underlie a new clinical entity characterized by ST-segment elevation, short QT intervals and sudden cardiac death. *Circulation*. 2007;115(4):442–9.
- Templin C, Ghadri JR, Rougier JS, Baumer A, Kaplan V, Albesa M, et al. Identification of a novel loss-of-function calcium channel gene mutation in short QT syndrome (SQTS6). *Eur Heart J*. 2011;32(9):1077–88.

28. Sun Y, Quan XQ, Fromme S, Cox RH, Zhang P, Zhang L, et al. A novel mutation in the KCNH2 gene associated with short QT syndrome. *J Mol Cell Cardiol.* 2011;50(3):433–41.
29. Hu D, Li Y, Zhang Y, Pfeiffer R, Gollob MH, Healey J, et al. The phenotypic spectrum of a mutation hotspot responsible for the short QT syndrome. *JACC Clin Electrophysiol.* 2017;3(7):727–43.
30. Itoh H, Sakaguchi T, Ashihara T, Ding WG, Nagaoka I, Oka Y, et al. A novel KCNH2 mutation as a modifier for short QT interval. *Int J Cardiol.* 2009;137(1):83–5.
31. Redpath CJ, Green MS, Birnie DH, Gollob MH. Rapid genetic testing facilitating the diagnosis of short QT syndrome. *Can J Cardiol.* 2009;25(4):e133–5.
32. Giustetto C, Scrocco C, Giachino D, Rapezzi C, Mognetti B, Gaita F. The lack of effect of sotalol in SQTS patients carrying the T618I mutation in the KCNH2 gene. *HeartRhythm Case Rep.* 2015;1(5):373–8.
33. Mazzanti A, Kanthan A, Monteforte N, Memmi M, Bloise R, Novelli V, et al. Novel insight into the natural history of short QT syndrome. *J Am Coll Cardiol.* 2014;63(13):1300–8.
34. Villafañe J, Atallah J, Gollob MH, Maury P, Wolpert C, Gebauer R, et al. Long-term follow-up of a pediatric cohort with short QT syndrome. *J Am Coll Cardiol.* 2013;61(11):1183–91.
35. Harrell DT, Ashihara T, Ishikawa T, Tominaga I, Mazzanti A, Takahashi K, et al. Genotype-dependent differences in age of manifestation and arrhythmia complications in short QT syndrome. *Int J Cardiol.* 2015;190:393–402.
36. Schimpf R, Wolpert C, Bianchi F, Giustetto C, Gaita F, Bauersfeld U, et al. Congenital short QT syndrome and implantable cardioverter defibrillator treatment: inherent risk for inappropriate shock delivery. *J Cardiovasc Electrophysiol.* 2003;14(12):1273–7.
37. Sun Y, Zhang P, Li X, Guo J. Inappropriate ICD discharge due to T-wave oversensing in a patient with short QT syndrome. *PACE.* 2010;33(1):113–6.
38. Mondoly P, Cardin C, Rollin A, Duparc A, Maury P. Use of a subcutaneous ICD in a patient with short QT syndrome. *Clin Case Rep.* 2015;4(1):35–8.
39. Gaita F, Giustetto C, Bianchi F, Schimpf R, Haissaguerre M, Calò L, et al. Short QT syndrome: pharmacological treatment. *J Am Coll Cardiol.* 2004;43(8):1494–9.
40. Wolpert C, Schimpf R, Giustetto C, Antzelevitch C, Cordeiro J, Dumaine R, et al. Further insights into the effect of quinidine in short QT syndrome caused by a mutation in HERG. *J Cardiovasc Electrophysiol.* 2005;16(1):54–8.
41. Mazzanti A, Maragna R, Vacanti G, Kostopoulou A, Marino M, Monteforte N, et al. Hydroquinidine prevents life-threatening arrhythmic events in patients with short QT syndrome. *J Am Coll Cardiol.* 2017;70(24):3010–5.
42. Bun S, Maury P, Giustetto C, Deharo JC. Electrical storm in short-QT syndrome successfully treated with isoproterenol. *J Cardiovasc Electrophysiol.* 2012;23(9):1028–30.



Microvolt T-Wave Alternans: Pathophysiology and Clinical Aspects

19

Richard L. Verrier

Abbreviations

ABCD	Alternans Before Cardioverter Defibrillator (NCT00187291)
AECG	Ambulatory electrocardiogram
CAD	Coronary artery disease
ECG	Electrocardiogram
EU-CERT-ICD	Comparative Effectiveness Research to Assess the Use of Primary Prophylactic Implantable Cardioverter Defibrillators in Europe (NCT02064192)
FINCAVAS	Finnish Cardiovascular Study
HRT	Heart rate turbulence
ICD	Implantable cardioverter-defibrillator
LQTS	Long QT syndrome
LVEF	Left ventricular ejection fraction
MADIT II	Multicenter Automatic Defibrillator Implantation Trial II

MASTER	Microvolt T Wave Alternans Testing for Risk Stratification of Post-Myocardial Infarction Patients (NCT00305240)
MERLIN TIMI 36	Metabolic Efficiency with Ranolazine for Less Ischemia in Non-ST-Elevation Acute Coronary Syndrome-Thrombolysis in Myocardial Infarction – TIMI 36 (NCT00099788)
MMA	Modified Moving Average
NPV	Negative predictive value
PPV	Positive predictive value
REFINE-ICD	Risk Estimation Following Infarction Noninvasive Evaluation – ICD (NCT00673842)
SCD	Sudden cardiac death
SCD-HeFT	Sudden Cardiac Death in Heart Failure Trial (NCT00000609)
SWORD	Survival With Oral <i>d</i> -Sotalol
TdP	Torsade de pointes
TWA	T-wave alternans
VF	Ventricular fibrillation
VT	Ventricular tachycardia

R. L. Verrier (✉)
 Department of Medicine, Harvard Medical School,
 Beth Israel Deaconess Medical Center,
 Boston, MA, USA
 e-mail: rverrier@bidmc.harvard.edu



Fig. 19.1 Precordial (V₄) electrocardiogram rhythm strip (left panel) and high-resolution template of QRS-aligned complexes (right panel) during routine exercise tolerance testing from a patient with coronary artery disease who experienced cardiovascular death at 12 months following

the recording. The template illustrates T-wave alternans (TWA) as a separation between ST-T segments in A and B beats. mV, millivolt. Sec, second. (Reproduced with permission from Elsevier from Verrier et al. [1])

Introduction

Fascination with T-wave alternans (TWA), a beat-to-beat fluctuation in ST-segment or T-wave morphology (Fig. 19.1) [1], can be traced to the dawn of electrocardiology. In 1910, less than a decade after Einthoven's invention of the electrocardiograph, Sir Thomas Lewis noted, when TWA was visible in the electrocardiogram (ECG) of his patients with angina pectoris, that there was elevated risk for premature death [2]. For decades, macroscopic, visible TWA, observed episodically in cases of long QT syndrome (LQTS), acute coronary syndrome, and adverse drug responses, was regarded as a relatively rare but ominous sign. It was not until the late 1980s, when systematic attempts were made to apply advanced signal processing techniques including frequency-domain spectral analysis and time-domain recursive averaging to quantifying TWA, that it was realized that this phenomenon is prevalent in diverse pathologic conditions.

This review addresses the following questions:

1. What are the main pathologic conditions responsible for sudden cardiac death? And what is the evidence that TWA might be useful in risk assessment in these main arrhythmogenic states?
2. What are the electrophysiologic mechanisms underlying TWA's predictive capacity?

3. What analysis methods are approved for clinical use by the United States Food and Drug Administration? And what clinical studies support their utility?
4. What is the rationale for quantitative analysis of TWA?

Pathophysiology of Sudden Cardiac Death and Rationale for T-Wave Alternans Testing

Identification of people at risk for sudden cardiac death (SCD) continues to present a major challenge in contemporary cardiology. SCD is responsible for 1.5 million deaths annually worldwide, including 512,000 in the United States [3]. In 45–50% of cases, death is the first expression of heart disease [4, 5]. Epidemiological findings reveal that coronary artery disease (CAD) is the main culprit in 80% of life-threatening arrhythmias [6] (Fig. 19.2). Dilated and hypertrophic cardiomyopathies are the second most frequent cause of SCDs, in the range of 10–15%. Other disorders, such as valvular or congenital heart diseases, acquired infiltrative disorders, primary electrophysiological disorders, and genetically determined ion channel abnormalities, are responsible for a small proportion, ~1%, of SCDs that occur in the general population. Two main processes leading to malignant arrhythmias have been observed in patients with ischemic heart dis-

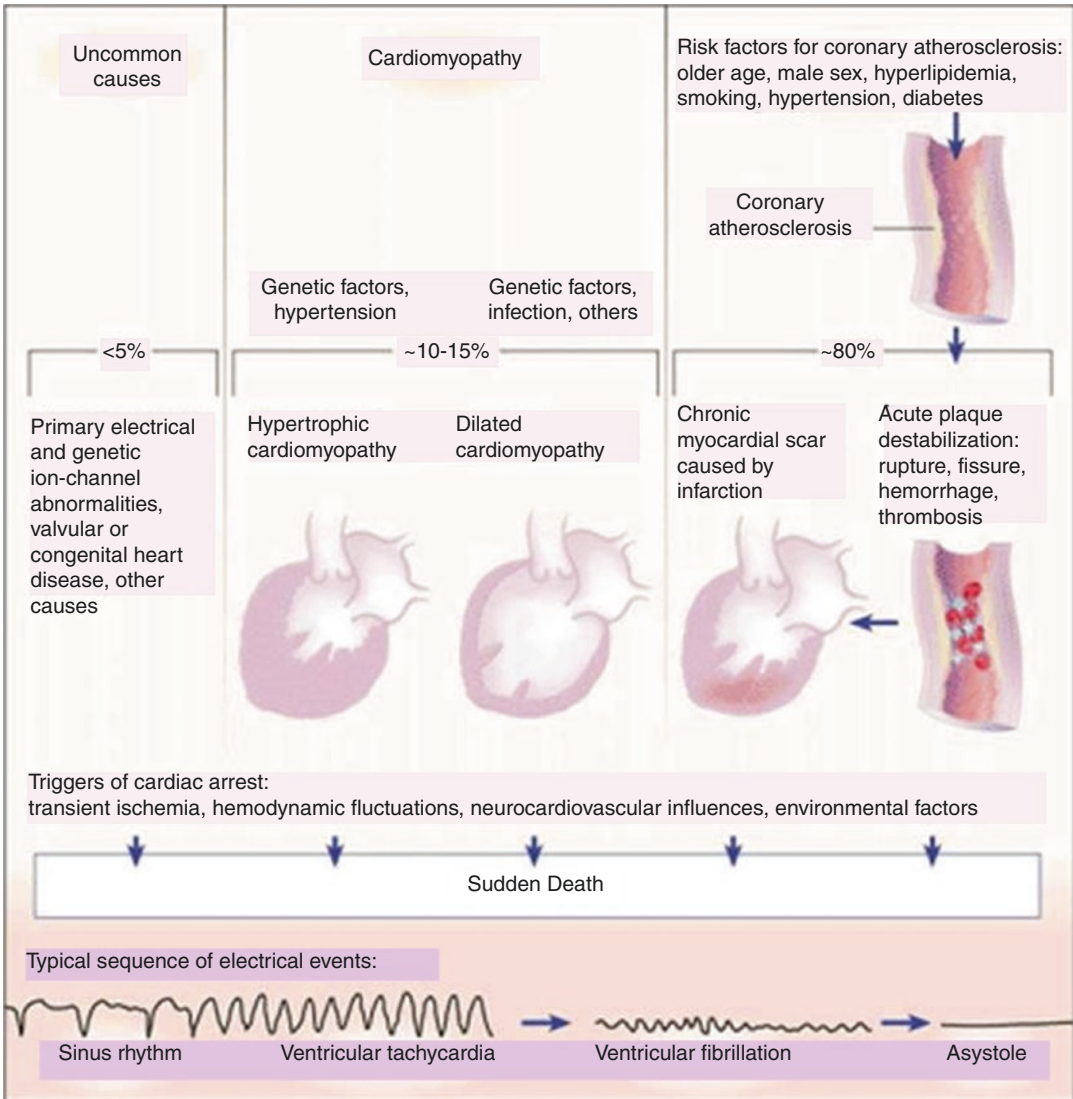


Fig. 19.2 Pathophysiology and epidemiology of sudden death from cardiac causes. (Published with permission from Massachusetts Medical Society from Huikuri et al. [6])

ease. These include ventricular tachyarrhythmia triggered by acute myocardial ischemia in individuals with or without preexisting myocardial scar and ventricular tachyarrhythmia attributable to an anatomical substrate, usually scarring from a previous infarction, without active or identifiable myocardial ischemia. Acute myocardial ischemia is considered to be the primary factor that triggers lethal arrhythmias. Additional factors have been implicated, specifically, systemic metabolic and hemodynamic alterations, neuro-

chemical and neurophysiological influences, and exogenous toxic or proarrhythmic drugs. These precipitating factors can interact with ischemia or cardiac structural abnormalities culminating in SCD due to ventricular arrhythmia [6].

While conventional cardiovascular risk factors including smoking, hypertension, and hyperlipidemia correlate with cardiovascular disease, they are not adequate markers of risk for SCD. The primary contemporary risk factor is depressed left ventricular ejection fraction (LVEF). Its value in

identifying patients who would benefit from placement of implantable cardioverter defibrillators (ICDs) is based on the randomized, controlled Multicenter Automatic Defibrillator Implantation Trial (MADIT) II trial, which demonstrated that ICDs confer improved survival over conventional pharmacologic therapy in patients with LVEF $\leq 30\%$ [7]. However, in the general population, LVEF does not have adequate sensitivity and specificity to guide ICD implantation, as the majority of individuals who succumb to SCD have relatively preserved LVEF, and only 1 of 8 patients who receive ICDs based on MADIT II criteria experience appropriate device discharge to terminate ventricular tachycardia/fibrillation (VT/VF) across the lifetime of the ICD [8]. The findings from the large Israeli National ICD Registry suggest that the number of patients needed to treat in a “real-world setting” may be even less favorable, specifically 1 of 20 [9].

Extensive data showing that TWA is useful in risk assessment in most of these pathophysiologic conditions has been reported in >13,000 individuals. An overview of the clinical studies supporting this assertion is provided in Table 19.1 [10–32].

Synopsis of Electrophysiologic Mechanisms and Physiologic Influences

TWA’s utility for evaluating risk for cardiovascular mortality and SCD is based on the extent of heterogeneity of repolarization [33] and of derangements in intracellular calcium cycling (Fig. 19.3) [34–36]. In turn, these abnormalities result in a beat-to-beat alternation of action potential duration culminating in alternating changes in the size and shape of the T wave. TWA can be either spatially concordant, when action potentials in adjoining cell regions alternate in phase, or discordant, when they are out of phase [34, 37]. The transition from concordant to discordant TWA is an established indicator of increased risk for serious arrhythmias [33].

Investigations of TWA in integrative physiology studies with regard to clinical correlates and pharmacologic influences are summarized in Table 19.2 [32, 38–65]. Surges in heart rate, adrenergic activity, and myocardial ischemia and reperfusion increase TWA level while also enhancing arrhythmia risk. Conversely, vagus nerve stimulation, beta-adrenergic receptor

Table 19.1 Clinical studies of prediction of sudden cardiac death or life-threatening arrhythmias by quantitative T-wave alternans with the time-domain modified moving average method

First author, year (trial)	Patient population (enrollment, disease, mean age)	Mean LVEF	TWA hazard ratios (95% CI), AUC, NVP, PPV for SCD, or life-threatening arrhythmias
Verrier et al. 2003 (ATRAMI) [10]	Acute post-MI; case-control analysis (15 cases, 29 controls) from 1284 ATRAMI patients; 60–62 years	Moderately depressed (42 ± 3%)	4.2 (1.1–16.3, $p < 0.04$) to 7.9 (1.9–33.1, $p < 0.005$) for cardiac arrest or arrhythmic death at 21 ± 8 months for a priori 75th percentile cut point (47 μV); patients were monitored at 15 ± 10 days post-MI
Slawnych et al. 2009 (REFINE and FINCAVAS) [11]	322 post-MI patients; 62 (interquartile range 53–70) years	Moderately depressed (38%–48%)	3.7 (1.4–9.7, $p = 0.008$) monitored during postexercise recovery at 10–14 weeks after event for CV death at 47 months for TWA $\geq 60 \mu\text{V}$; NPV = 95%; PPV = 14%; sensitivity = 20%; specificity = 92%; 2.6 (1.0–6.6, $p = 0.05$) for SCD. AUC = 0.69
Stein et al. 2008 (EPHESUS) [12]	Acute post-MI, LVEF $\leq 40\%$, and heart failure; Case-control analysis (46 cases, 92 controls) from 493 EPHESUS patients in AECG substudy; 68 ± 11 years	Depressed (34 ± 5%)	5.5 (2.2–13.8, $p < 0.001$) for SCD at 16.4 months for 47 μV ; patients were monitored at 2–10 days post-MI. For SCD, AUC = 0.73 for lead V ₁ and 0.70 for lead V ₃ ($p < 0.001$)
Sakaki et al. 2009 [13]	295 consecutive patients with ischemic or nonischemic cardiomyopathy and left ventricular dysfunction; 66 ± 16 years	Depressed (34 ± 6%)	17.1 (6.3–46.6, $p < 0.001$) for CV death, 22.6 (2.6–193.7, $p < 0.005$) for witnessed SCD at 1.1 year for TWA $\geq 65 \mu\text{V}$; NPV for CV death = 97%; PPV = 37%; sensitivity = 74%; specificity = 87%

(continued)

Table 19.1 (continued)

First author, year (trial)	Patient population (enrollment, disease, mean age)	Mean LVEF	TWA hazard ratios (95% CI), AUC, NVP, PPV for SCD, or life-threatening arrhythmias
Maeda et al. 2009 [14]	63 consecutive patients including 21 controls, 21 post-MI patients without VT, and 21 post-MI patients with VT; 65 ± 11 years	Depressed (36–43%) for post-MI group	6.1 (1.1–34.0, $p < 0.041$) for sustained VT or VF at 6 years for TWA ≥65 μV; patients were monitored at 1–3 months after event
Stein et al. 2010 (CHS) [15]	General population patients ≥65 years old; case-control analysis (49 cases, 97 controls) from 1649 CHS patients; 73 ± 5 years	Not tested, assumed preserved	4.84 (1.48–15.81, $p < 0.009$) for SCD across 4.7 ± 3.0 (range 0.2–10.4) years for TWA ≥37 μV
Leino et al. 2011 [16–19]	3598 consecutive patients referred for exercise tolerance testing, 56 ± 13 years	Mostly preserved	1.55 (1.150–2.108, $p < 0.004$) for CV death; 1.58 (1.041–2.412, $p < 0.033$) for SCD per 20 μV TWA in lead V ₅
Hoshida et al. 2012 [20]	313 consecutive post-MI patients, 70 ± 12 years	48%	3.6 (1.3–10.4, $p < 0.0174$) for cardiac mortality; 5.8 (1.6–20.8, $p < 0.0072$) for SCD for TWA ≥65 μV at 3.3 years; patients were monitored >2 weeks after event
Ren et al. 2012 [21]	173 consecutive post-MI patients with and without diabetes mellitus; 66 years	46%	AUC = 0.708 for cardiac mortality at 1.6 years; patients were monitored at 1–3 weeks after event
Shimada et al. 2012 [22]	40 consecutive patients with vasospastic angina, 59 years	66%	15.5 (1.7–142.0, $p = 0.009$) for VT at 2.9 years for TWA ≥65 μV during asymptomatic periods
Sulimov et al. 2012 [23]	111 post-MI patients, 64.1 years	46.6%	5.01 (1.5–17.0, $p < 0.005$) for SCD at 1 year for TWA >53.5 μV at heart rate of 100 bpm, NPV = 93.9%; PPV = 24.4%; sensitivity = 73.3%, specificity = 64.6%; patients were monitored at 2 months to 36 years after event
Hou et al. 2013 [24]	219 consecutive acute post-MI patients, 56 years	>35% in 201; ≤35% in 18	15.07 (2.88–78.68, $p < 0.0031$) for SCD within 16 ± 7 months for TWA ≥47 μV; patients were monitored at 7 ± 4 days after event
Verrier et al. 2013 [25]	48 acute STEMI patients; 61 years	51%	AUC = 0.87; NPV = 79%; PPV = 71% for NSVT during or after PCI
Arisha et al. 2013 [26]	199 consecutive post-MI patients, 61.7 years	45%	ROC = 0.64 for SCD or life-threatening ventricular arrhythmias within 6 months; ROC = 0.80 for TWA combined with HRT onset; ROC = 0.86 for TWA combined with HRT onset in patients with LVEF <40%
Nieminen et al. 2014 (MERLIN) [27]	210 ACS patients, 68 years	<40%	2.35 (1.03–5.37, $p = 0.04$) for 1 year mortality for TWA ≥47 μV; patients were monitored in-hospital at onset of ACS
Uchimura et al. 2014 [28]	45 Brugada syndrome patients, 45 ± 15 years	[not stated]	7.217 (2.503–35.504, $p = 0.002$) for VT history
Takasugi et al. 2016 [29]	32 consecutive LQTS patients, 13 (range: 11–17.5) years	[not stated]	100% sensitivity for VT history at ≥42 μV cut point
Chung et al. 2016 [30]	63 ARVD/C patients, 44.7 ± 14.8 years	Preserved	1.06 (1.03–1.10, $p < 0.001$)
Yamada et al. 2018 [31]	215 hospitalized decompensated heart failure patients, 62 ± 14.5 years	Both depressed and preserved	1.015 (1.003–1.027, $p = 0.016$)
Summary	5884 patients in full-cohort prospective studies 391 patients in case-control studies	Both depressed and preserved	

Expanded from Verrier and Ikeda [32]

Key: ACS acute coronary syndrome, AUC area under the curve, CAD coronary artery disease, EPS electrophysiologic study, ICD implantable cardioverter-defibrillator, LQTS long QT syndrome, MI myocardial infarction, NSVT nonsustained ventricular tachycardia, PCI percutaneous coronary intervention, SCD sudden cardiac death, STEMI ST-segment elevation myocardial infarction, SUDEP sudden unexplained death in epilepsy patients, TdP torsade de pointes, TWA T-wave alternans, VF ventricular fibrillation, VNS vagus nerve stimulation, VT ventricular tachycardia

Table 19.2 Physiologic and pharmacologic influences on T-wave alternans: experimental and clinical correlates

Experimental intervention	Clinical correlates
<i>Increase TWA</i>	
Elevated heart rate and rapid atrial pacing [38]	Right atrial pacing or exercise increases TWA [39]
Adrenergic stimuli and behavioral stress [40]	Anger recall and mental arithmetic increase TWA in ICD patients [41] Anger-induced TWA predicts ICD discharge [42]
Myocardial ischemia [38, 43–45]	TWA predicts intraprocedural VT during PCI in STEMI patients (AUC = 0.87) [25] TWA stratifies risk for 1-year mortality in ACS patients [27]
Reperfusion (initial minutes) [38, 44, 45]	Surge in TWA prior to VT/VF during PCI [46]
I _{Kr} blockade [47]	d-Sotalol increased arrhythmia in CAD patients [48]; penicillin provoked TWA and TdP [49]
Flecainide [50]	Flecainide provoked proarrhythmia in patients with CAD [51]; clinical effects on TWA have not been reported
<i>Decrease TWA</i>	
Stellectomy [44]	Reduced SCD in LQTS [52] and post-MI patients [53]
VNS [54]	VNS reduced SUDEP [55] and TWA [56, 57] in patients with epilepsy
Beta-blockade [40]	Metoprolol reduced SCD in post-MI patients [58] Beta-blockade during fixed-rate EPS [59–61] or graded exercise [62] decreased TWA
Calcium channel blockade [63]	Decreased NSVT and TWA in patients with vasospastic angina [22]
Late I _{Na} blockade [47, 50]	Decreased VT [64, 65] and TWA [27, 65]

Key: *ACS* acute coronary syndrome, *AUC* area under the curve, *CAD* coronary artery disease, *EPS* electrophysiologic study, *ICD* implantable cardioverter-defibrillator, *LQTS* long QT syndrome, *MI* myocardial infarction, *NSVT* nonsustained ventricular tachycardia, *PCI* percutaneous coronary intervention, *SCD* sudden cardiac death, *STEMI* ST-segment elevation myocardial infarction, *SUDEP* sudden unexplained death in epilepsy patients, *TdP* torsade de pointes, *TWA* T-wave alternans, *VF* ventricular fibrillation, *VNS* vagus nerve stimulation, *VT* ventricular tachycardia

blockade, calcium channel antagonism, inhibition of late I_{Na}, and sympathetic denervation, which reduce susceptibility to ventricular tachyarrhythmias, also diminish TWA level. Experimentally induced myocardial ischemia increases TWA magnitude in parallel with vulnerability to ischemia-induced VF [38, 43, 44]. Abnormalities in both calcium cycling and conduction are linked to the development of TWA during myocardial ischemia. Studies with luminescent dye have demonstrated both concordant and discordant alternation in calcium transients during myocardial ischemia [35]. Heart failure augments TWA level in parallel with vulnerability to arrhythmias and reduction in the heart rate threshold for TWA as a consequence of impaired intracellular calcium cycling [66]. Abnormal calcium handling and action potential alternans have been documented in patients with systolic dysfunction and VT and/or VF but not in normal individuals [67]. TWA level has been found to be correlated to extent of scar tissue [68, 69].

Clinical Methodologies

Two methods have been cleared by the United States Food and Drug Administration to determine microvolt levels of TWA for risk stratification for arrhythmic death, namely, the Spectral and Modified Moving Average (MMA) Methods. Other implementations have been used in a variety of clinical and preclinical studies.

The spectral method employs an exercise-based system that was formerly commercialized by Cambridge Heart, Inc. (Tewksbury MA, USA). This method is based on a fast Fourier transform to measure the amplitude of the spectrum at 0.5 cycle/beat (Fig. 19.4) [70, 71]. The average alternans level across the ST-T wave is determined. The spectral method requires increasing and maintaining the subject's heart rate at 105–110 beats per minute and use of specialized electrodes. Tests with TWA levels $\geq 1.9 \mu\text{V}$ with signal-to-noise ratio $K = 3$ sustained for 2 minutes are classified as positive

tests; tests with TWA values below this level are considered negative. Due to the relatively high incidence (20–40%) of tests with excessive ectopy, inability to raise heart rate to 105–110 bpm, or transient TWA (Fig. 19.4, lower left panel), the classification “abnormal due to patient factors” is used [72] and these tests are considered “nonnegative” and combined with positive tests in clinical studies of risk assessment. Recordings with muscle, respiration, or other movement artifacts or electrode noise are regarded as “technically indeterminate.”

The MMA method, commercialized by GE Healthcare, Inc. (Milwaukee WI, USA), operates on two platforms: ambulatory ECGs (AECGs) employing a MARS or Getemed (Berlin, Germany) reader and the CASE 8000 treadmill system for routine, symptom-limited exercise tolerance testing. MMA is a time-domain analytical approach that involves the noise-rejection principle of recursive averaging (Fig. 19.4, right panel) [73]. The algorithm continuously transfers odd and even beats into separate bins and generates median complexes for each bin. The maximum separation between the A and B beats within the ST-T wave is demarcated with a vertical line in the template of superimposed beats; this separation indicates the patient’s TWA level and is used for risk assessment. This method does not require elevation or stabilization of heart rate or use of specialized electrodes. A TWA level of $\geq 47 \mu\text{V}$ is classified as abnormal and $\geq 60 \mu\text{V}$ as severely abnormal in terms of elevated risk for SCD and/or cardiovascular mortality [1]. Indeterminate results are few (3–5%) with the MMA method because reaching a target heart rate is not required.

MMA-based TWA can be analyzed during routine exercise tolerance testing, permitting patients to be monitored in the flow of clinical evaluation. AECG-based TWA reflects the influences of daily activity, behavioral stress, and sleep, trigger factors that cannot be duplicated by exercise tolerance tests. The peak TWA value during the entire 24-hour period has proved to be more informative than brief recordings. Nocturnal TWA monitoring is important with regard to the fact that 20–30% of SCDs in individuals with

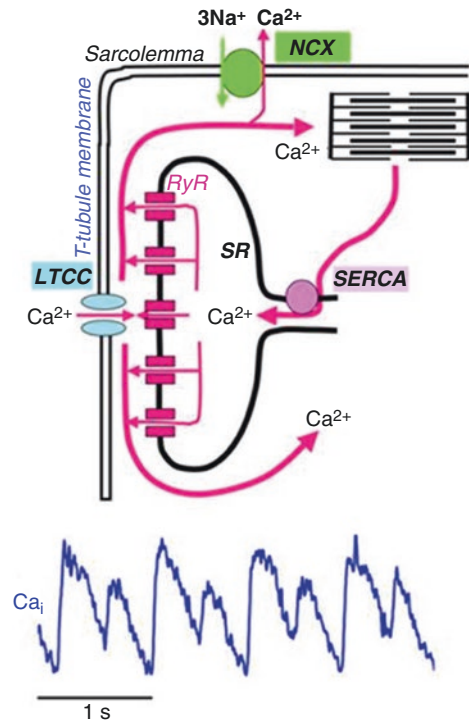


Fig. 19.3 Intracellular calcium cycling dynamics in cardiac myocytes. Upper panel: Schematic of calcium (Ca^{2+}) cycling, illustrating that a small amount of Ca^{2+} entering the cell through L-type Ca^{2+} channels (LTCC) triggers release of a large amount of Ca^{2+} from internal stores (sarcoplasmic reticulum, SR) by activating SR Ca^{2+} release channels (ryanodine receptors, RyR). Ca^{2+} is then pumped back into the SR by sarcoplasmic reticulum calcium ATPase (SERCA) pumps or removed from the cell by sodium (Na^+)-calcium exchange (NCX). Lower panel: Calcium transient (Ca_i) alternans is under the dual influences of membrane voltage and the dynamics of intracellular Ca^{2+} handling by the SR. Action potential duration (APD) alternans occurs when perturbations in membrane voltage arise and/or when elevated heart rate or other physiologic or pathophysiologic factors disrupt the myocytes’ capacity to cycle calcium. (Adapted with permission from Wolters Kluwer from Weiss et al. [34])

CAD and/or heart failure occur during nighttime [74]. Nocturnal precipitating factors include REM sleep-associated bursts in sympathetic nerve activity and disturbed nighttime breathing due to apneas, which occur in 50% of heart failure patients. In specific disease states such as the Brugada syndrome, TWA is rate-suppressed, and thus TWA should not be measured during exercise tolerance testing [75]. Monitoring these patients at rest or during nighttime, when their

peak TWA levels occur [28], is preferable. Moreover, AECG-based monitoring offers the distinct advantage of permitting TWA measurement in patients who cannot exercise.

The four- to ten-fold difference in TWA values reported by the two methods is largely a consequence of differences in the extent of signal averaging and filtering [1]. Another basis for the lower values reported by the spectral method as compared to the MMA method is that with the former, the average TWA value across the ST-T wave is calculated, while with the latter, the peak TWA level is provided.

Clinical Evidence of Prediction

An AHA/ACC/ESC guideline committee [76] assigned Class I Level of Evidence A to TWA monitoring on AECG to assess risk or to evaluate therapy and Class IIa Level of Evidence A for TWA monitoring on AECG or exercise tolerance test recordings to improve diagnosis and risk assessment in individuals with ventricular arrhythmias. A subsequent consensus guideline statement sponsored by the International Society for Holter and Noninvasive Electrocardiology recommended that TWA analysis be considered “whenever there is suspicion of vulnerability to lethal cardiac arrhythmias” [1]. However, the document also recognized the unmet need to provide evidence of the potential of TWA to guide device and medical therapy.

TWA testing with the spectral method has demonstrated its predictive capacity in prospective studies enrolling 7200 patients with diverse cardiovascular diseases, including myocardial infarction, congestive heart failure, ischemic cardiomyopathy, and nonischemic dilated cardiomyopathy [1]. No further studies with the spectral method have been announced.

Using routine exercise tolerance testing protocols, the MMA method has stratified risk for cardiovascular death and SCD in ~3600 patients with generally preserved LVEF enrolled in the Finnish Cardiovascular Study [16–19]. This investigation is the largest TWA study conducted with any method. TWA analysis on AECG using

the MMA method has proven to predict cardiovascular mortality and SCD in nearly 2300 patients with CAD, acute myocardial infarction, acute coronary syndrome, heart failure, LQTS, Brugada syndrome, vasospastic angina, ischemic and nonischemic cardiomyopathy with differing degrees of left ventricular dysfunction, and arrhythmogenic right ventricular dysplasia/cardiomyopathy (ARVD/C) as well as in the general population (Table 19.1). In all MMA studies, TWA was measured while patients continued chronic medications, including beta-adrenergic blocking agents. All studies in which the commercialized MMA method was accurately performed have been predictive.

An important recent discovery is that microvolt TWA is far more prevalent in LQTS patients than previously reported, 69%, and above the cut point of 42 μ V is strongly associated with TdP history [29]. The authors recommended that TWA should be monitored from precordial leads in LQTS patients, as they surmised that use of a limited set of ECG leads in conventional monitoring led to underestimation of the prevalence of TWA and its association with TdP. The reader is referred to several chapters in this book for discussion of the cellular, genetic, and molecular bases for arrhythmogenesis in LQTS.

Odds ratios generated by the spectral and MMA methods for all studies are comparable based on multivariate analyses adjusted for standard clinical variables for cardiovascular disease, namely, demographic factors (e.g., age, sex, and race) and traditional cardiovascular risk markers (e.g., smoking, blood pressure, history, medications, and depressed LVEF) [1]. Specifically, for predictive studies using the Spectral Method, the odds ratios ranged from 2.1 to ∞ for SCD/arrhythmic death in patients with depressed LVEF and from 5.9 to 23.5 for SCD/arrhythmic death in patients with better preserved LVEF. For the MMA method, odds ratios ranged from 2.94 to 17.1 for cardiovascular death and from 4.8 to 22.6 for SCD in patients with both depressed and preserved LVEF. A head-to-head comparison of the spectral and MMA methods in 322 post-myocardial infarction patients reported that the odds ratios for estimating cardiovascular mortal-

ity and SCD were equivalent, at 2.75 for the spectral method and at 2.94 for the MMA method [11, 77]. Across all studies, the negative predictive value (NPV) averages 97.2% for the spectral method and ranges from 94 to 99% for the MMA method. For both techniques, the positive predictive value (PPV) is variable, consistent with the fact that PPV is based on the prevalence of disease in the study population.

Importance of Quantitative Analysis of TWA to Enhance Clinical Prediction

In light of the fact that TWA reflects a spectrum of cardiac electrical instability, its quantification can enhance the potential for diagnosing degrees of risk and for improving prognostic capacity, because treating a continuous variable as binary reduces its predictive power by 33–50% [78]. Analysis of the FINCAVAS database demonstrated that risk for cardiovascular death and SCD increased by 55% and 58%, respectively, for each 20- μ V increase in MMA-based TWA [19] (Fig. 19.4, right panel). Quantitative TWA analysis may permit dynamic tracking of changes in risk across time. This consideration is relevant to post-MI remodeling, changing status of cardiac disease or heart failure, or response to medical therapy or cardiac exercise rehabilitation.

Moreover, TWA quantification permits comparison of risk levels among different populations and disease conditions, whose range of TWA levels correlates with established degrees of risk (Fig. 19.5) [32]. For example, TWA is markedly elevated (≥ 60 μ V) in patients who receive dialysis, even in the absence of a prior cardiovascular event, a finding consistent with their well-known heightened risk for SCD [79]. Also, patients with drug-resistant epilepsy exhibit markedly elevated TWA levels during the interictal period, in the range of 70 microvolts [56, 57, 80], consistent with the >threefold increased risk for SCD over the general population [81, 82] and with emerging evidence of cardiovascular comorbidities [83].

TWA Assessment to Guide Device-Based Therapy

The primary contemporary application foreseen for microvolt TWA was to identify patients with reduced LVEF who would not benefit from ICD placement. This application was spearheaded by investigators using the spectral method and was based on the presence or absence of criterion levels of TWA. Unfortunately, the overall experience did not prove satisfactory as the MASTER trial (NCT 00305240, NCT00305214) [84] and the TWA substudy of the Sudden Cardiac Death in Heart Failure Trial (SCD-HeFT, NCT00000609) [85] did not demonstrate prediction. One potential explanation for this failure is washout of beta-adrenergic blocking agents prior to the test to allow patients to achieve the target heart rate requirement of 105 to 110 beats/min and resumption of these agents following the test. In studies using the spectral method in which beta-blockers were washed out, the hazard ratios were four-fold lower than those in which beta-blockade was maintained (Fig. 19.6) [86]. The present recommendation is that TWA testing should be performed while patients maintain chronic medications including beta-blockers [1]. Employing ICD discharge as a surrogate endpoint for SCD has also been suggested as the explanation for the absence of prediction [87] in the MASTER trial [84] and SCD-HeFT TWA substudy [85]. It is worth noting that the Alternans Before Cardiac Defibrillator (ABCD) trial (NCT00187291) indicated similar 1-year success as electrophysiologic study in identifying patients who would not benefit from ICD placement [88].

The Risk Estimation Following Infarction Noninvasive Evaluation-ICD (REFINE-ICD) randomized controlled trial (NCT00673842), which is testing whether ICD placement guided by both MMA-based TWA and the autonomic indicator heart rate turbulence (HRT) can alter SCD risk, is ongoing in Canada. The available data indicate that the presence of both abnormal TWA and impaired HRT in patients with relatively preserved left ventricular function identifies patients with a nearly tenfold increased risk

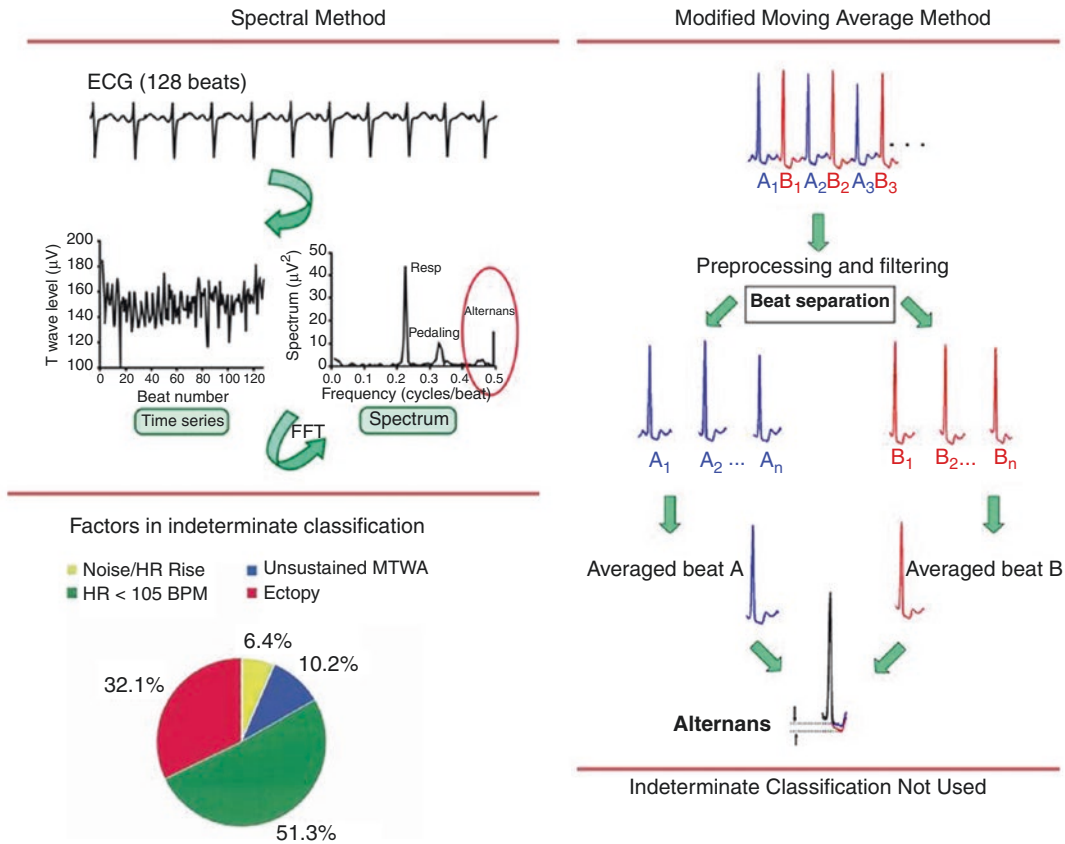


Fig. 19.4 Left panel, upper figure: Schematic representation of T-wave alternans (TWA) assessment of the electrocardiogram (ECG) with the Spectral Method. FFT, fast Fourier transform. (Reproduced with permission from Elsevier from Verrier et al. [1])
 Left panel, lower figure: Causes of indeterminate microvolt TWA (MTWA) tests. Only 6.4% of the indeterminate

MTWA results were due to technical factors; the remainder was due to patient factors. BPM, beats/min; HR, heart rate. (Reproduced with permission from Elsevier from Kaufman et al. [72]). Right panel: Flow chart of the major components of the Modified Moving Average Method of TWA analysis. (Reproduced with permission from Elsevier from Verrier et al. [1])

TWA Magnitude in AECGs and “Ladder” of SCD Risk

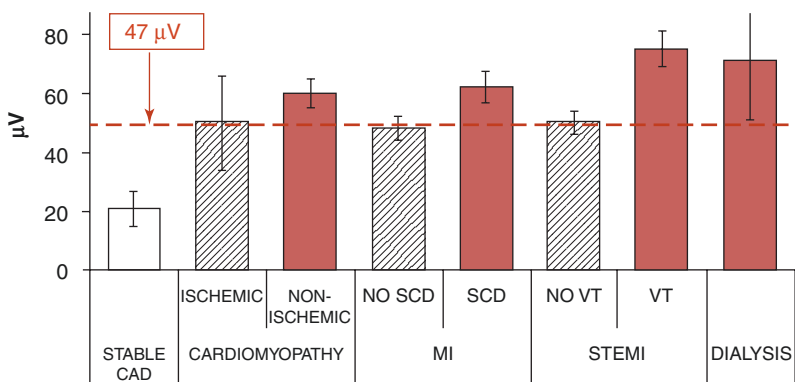


Fig. 19.5 TWA magnitude determined by the MMA method in ambulatory ECGs showing “ladder” of risk. Mean values of peak TWA are from patients with stable coronary artery disease (CAD), cardiomyopathy, acute post-myocardial

(MI) patients with and without sudden cardiac death (SCD), ST-elevation MI (STEMI) patients with and without ventricular tachycardia (VT), and dialysis patients. (Reproduced with permission from Elsevier from Verrier and Ikeda [32])

of cardiac death compared to those who do not meet both of these criteria [89]. The sizeable Comparative Effectiveness Research to Assess the Use of Primary Prophylactic Implantable Cardioverter Defibrillators in Europe (EU-CERT-ICD, NCT02064192) study, which employs MMA-based TWA together with HRT, has completed enrollment and the results are pending.

TWA Assessment to Guide Antiarrhythmic Drug Therapy

Sakabe and colleagues [90] demonstrated that administration of antiarrhythmic agents does not interfere with the capacity of TWA to predict outcomes. Using the Spectral Method, the investigators prospectively evaluated patients with ischemic or nonischemic dilated cardiomyopathy and a history of sustained VT or VF during empirically guided therapy with amiodarone, beta-blockade, and/or angiotensin-converting enzyme inhibitors. TWA but not LVEF predicted the recurrence of VT during the ensuing 13 ± 11 months. Effects of different classes of antiarrhythmic drugs on TWA have been reviewed in detail [91] and are summarized below, providing evidence of TWA's suitability to serve as a therapeutic target for antiarrhythmic medications.

Sodium Channel Blockade

Traditional sodium channel blocking agents have not been shown to be effective in reducing malignant ventricular arrhythmias [47], and accordingly, there is little or no evidence in the literature of an effect of this class of agents on TWA. By contrast, inhibition of the late I_{Na} current has yielded promising results. Increases in late I_{Na} , which are known to be arrhythmogenic because they result in excess intracellular calcium, have been shown to occur under diverse pathologic conditions, specifically myocardial ischemia, heart failure, reperfusion, and the long QT3 syndrome [92]. The prototypical late I_{Na} inhibitor, ranolazine, was shown using the MMA method to reduce ischemia-induced TWA in parallel with a protective effect on VF threshold in a large animal model of coronary artery stenosis [48]. Conversely,

in the same model, flecainide increased ischemia-induced TWA concurrently with an increase in the incidence of spontaneous VF [50], a finding consistent with the drug's known proarrhythmic effects and its contraindication in patients with CAD [51]. Clinically, ranolazine suppressed ventricular tachyarrhythmias in the Metabolic Efficiency with Ranolazine for Less Ischemia in Non-ST-Elevation Acute Coronary Syndrome-Thrombolysis in Myocardial Infarction 36 (MERLIN TIMI 36, NCT00099788) trial [64]. A reduction in 1-year mortality in patients with TWA $\geq 47 \mu V$ in the MERLIN TIMI 36 TWA sub-study was found using the MMA method [27].

Beta-Adrenergic Blockade

Using the Spectral Method, a decrease in TWA by beta-adrenergic blockade was demonstrated during electrophysiologic study with atrial pacing, indicating a heart rate-independent antiarrhythmic effect as one mechanism underlying its well-known capacity to reduce susceptibility to SCD [58, 59]. Specifically, metoprolol, a relatively cardioselective beta-blocker, and d,l-sotalol, a beta-blocker with Class III antiarrhythmic actions, similarly reduced TWA in patients with malignant VT and diminished the incidence of positive TWA tests by 67% (from 12 to 4) in 54 patients [59]. Esmolol reduced positive TWA tests by 50% (from 42 to 21) in 60 patients with ischemic cardiomyopathy and inducible sustained VT [60]. Propranolol decreased the number of positive TWA tests by 36% (from 11 to 7) in 15 patients with ventricular tachyarrhythmia [61]. In response to graded exercise, metoprolol, carvedilol, or other beta-blockers reduced the incidence of positive TWA tests by 31% (from 26 to 18) in 26 patients with nonischemic heart disease [62].

Calcium Channel Blockade

Although calcium channel blocking agents decrease TWA in experimental models in parallel with reducing ischemia-induced ventricular tachyarrhythmia [63], their antiarrhythmic actions may be offset by their negative inotropic

effects in clinical studies, particularly in individuals with myocardial infarction complicated by pulmonary congestion [93]. Clinical investigations relevant to effects of this class of compounds on TWA have been limited to patients with vasospastic angina. Shimada and colleagues [21] using the MMA method reported high levels of TWA during asymptomatic phases, especially in patients with tachyarrhythmias during vasospasm, but not in matched control patients; calcium channel blockade decreased arrhythmias and TWA level. The hazard ratio for TWA in predicting ventricular tachyarrhythmias was 15.5 (95% confidence interval, 1.7 to 142.0, $p < 0.01$). The authors proposed that repolarization abnormalities monitored even during the asymptomatic period could indicate increased risk for life-threatening ventricular arrhythmias during ischemic attacks.

T-Wave Alternans in Detecting Proarrhythmia

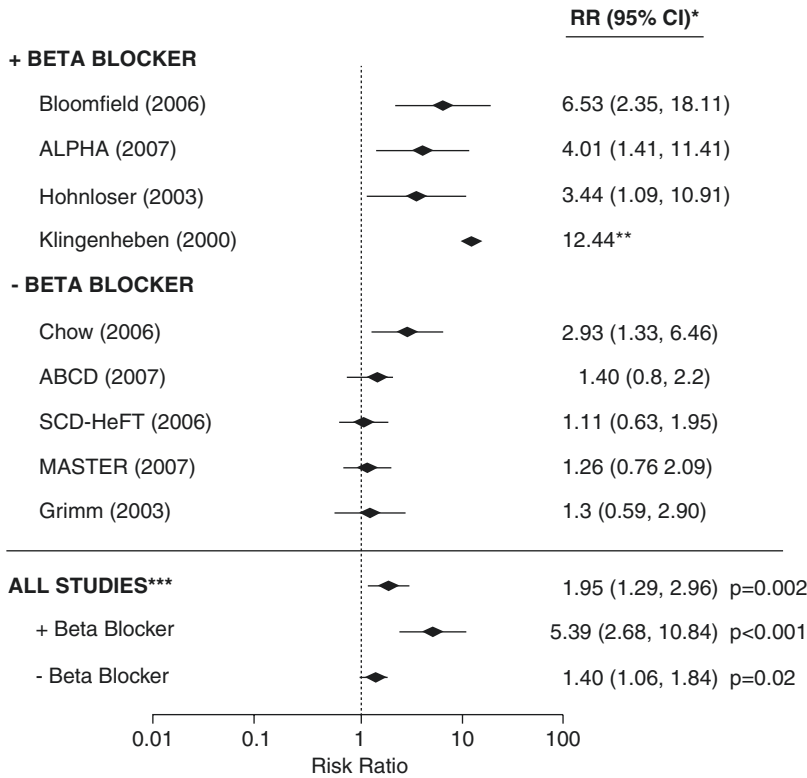
Case reports of TWA in association with proarrhythmia have recurred [49, 91, 94]. Notably, Hohnloser [94] reported visible TWA in association with torsade de pointes (TdP) in patients who received high doses of amiodarone to manage atrial fibrillation. Subsequent administration of magnesium sulfate suppressed both ventricular arrhythmia and TWA. It is well-known that d-sotalol, which inhibits I_{Kr} , proved to be proarrhythmic in the Survival With Oral d-Sotalol (SWORD) trial [48]; inhibition of I_{Kr} has also been shown experimentally to increase MMA-based TWA during myocardial ischemia [47]. Penicillin, an antibiotic that can inhibit I_{Kr} , was reported to induce macroscopic TWA followed by TdP during hospitalization for pneumonia (Fig. 19.7) [49]. Such observations may represent the tip of the iceberg. The potential use of TWA in identifying proarrhythmia deserves systematic study, particularly using quantitative measures of microvolt levels of TWA rather than relying solely on the appearance of visible, macroscopic TWA or a positive TWA test by a binary analysis approach.

Perspective and Future Directions

Based on a 30-year experience in studying the phenomenon of TWA, both in the experimental laboratory and in analyses of clinical data, the following perspective is provided. The most effective use of TWA should involve quantitative analysis and be performed in the context of provocative testing with either exercise or AECG monitoring to incorporate stimuli of daily activities including mental and physical stressors.

When elevated TWA is detected, the primary objective should be to determine the root cause. A number of prevalent clinical conditions associated with elevated TWA can be readily addressed prior to the decision to place an ICD. Primary, manageable causes of elevated TWA are the persistence of myocardial ischemia [95–97], which can be addressed by revascularization. Compliance with anti-SCD medications such as beta-blockers [98], which is standard of care following myocardial infarction and in LQTS patients, is reported to decrease by 43% during the high-risk period at 30–90 days post-MI [99], by >50% at 4 years following MI [100], and by 51% in LQTS patients [101]. As beta-blockade significantly reduces TWA, this parameter could fill an unmet need to determine whether SCD risk is present due to noncompliance to prescription medications. Another practical area of future application of TWA is to serve as a therapeutic target for antiarrhythmic drug efficacy and drug-induced proarrhythmia, which has been implicated in the context of antibiotics, particularly agents with I_{Kr} inhibition (Fig. 19.7) [49] and amiodarone [94]. An important implication of TWA's sensitivity to antiarrhythmic therapy is that retesting must be performed after a new drug regimen is instituted (Fig. 19.8) [71].

The potential value of TWA in tracking effectiveness of cardiac rehabilitation therapy should be duly considered, as this intervention has been shown to reduce TWA significantly [102]. Other new applications include TWA's capacity to sense risk for rehospitalization during discharge in patients with heart failure [31, 103], as an aid to diagnose ARVD/C [104], and



*study estimates for meta-analysis were hazard or risk ratios
 **No events in MTWA negative group ($p = 0.04$). RR of 12.44 reflects 0.5 correction factor; therefore, no 95% CI depicted
 ***test for heterogeneity; $p = .0025$

Fig. 19.6 Relative risks of TWA for ventricular arrhythmic events, stratified by continuation or discontinuation of beta-blocker therapy. Significant heterogeneity was observed among studies ($p = 0.025$). Subgroup analyses found a strong, consistent, fivefold increased risk for ventricular arrhythmic events in studies where beta-blocker

therapy was not discontinued prior to TWA assessment. In contrast, a weak association between an abnormal TWA test and risk for arrhythmic events was observed in studies that withheld beta-blocker therapy prior to TWA assessment and then resumed therapy. (Reproduced with permission from Wiley from Chan et al. [86])

to detect coronary artery stenosis [95–97] as well as scar tissue [57, 69].

Neural triggers acting on a vulnerable myocardial substrate are a critical factor in SCD. Combined monitoring of TWA and autonomic parameters, particularly HRT, could prove particularly valuable. Recent evidence that combined assessment of HRT and TWA can prove useful in assessing risk for hospital readmission and cardiovascular mortality in patients with heart failure carries important implications and deserves further exploration [31, 103].

Finally, there is considerable merit in moving from a “snapshot” approach for TWA monitoring to more frequent and sustained assessment of the

phenomenon by taking advantage of ECG patch monitors [105]. These devices, with or without capacity for mobile cardiac telemetry, can extend monitoring to 2 weeks to include initiation of therapy and recovery of cardiac electrical stability in patients after myocardial infarction as well as in epilepsy patients with sporadic VT [106].

Collectively, the body of knowledge that has been accrued in the recent three decades using state-of-the-art signal processing techniques points to promising expanding horizons for TWA testing, including the broad spectrum of pathologic conditions predisposing to SCD, supported by evidence of TWA’s predictive capacity in Table 19.1.

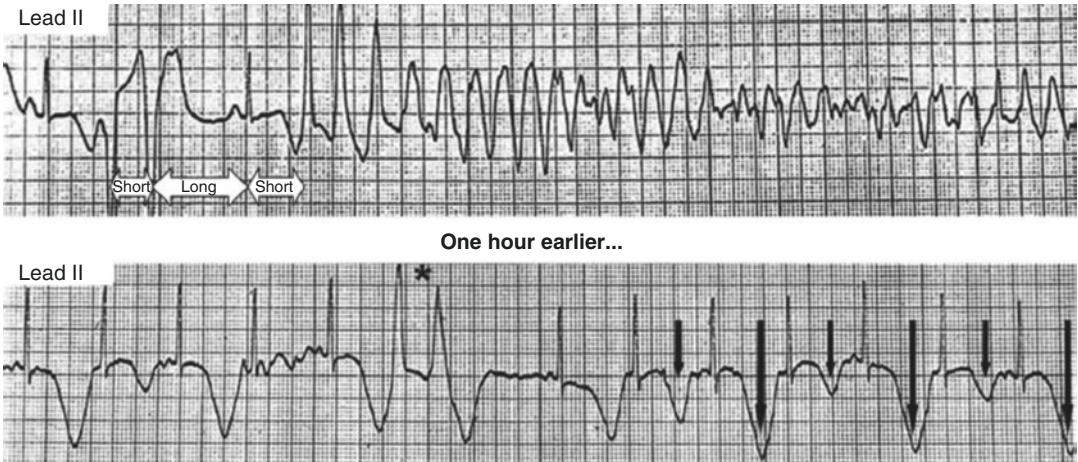


Fig. 19.7 Top rhythm strip: TdP culminating in ventricular fibrillation in an 83-year-old female in the intensive care unit with pneumonia. Intravenous erythromycin was commenced several hours prior to cardiac arrest. Lower rhythm strip, ECG at 1 hour before the development of TdP reveals pronounced prolongation of the QT interval (QTc in cycles with larger T waves = 730 ms), a ventricu-

lar couplet (*), and macroscopic T-wave alternans (TWA, vertical arrows). If these indicators of risk for TdP had been recognized, termination of the culprit agent and administration of magnesium might have prevented the subsequent cardiac arrest. (Reprinted with permission from Wolters Kluwer from Drew et al. [49])

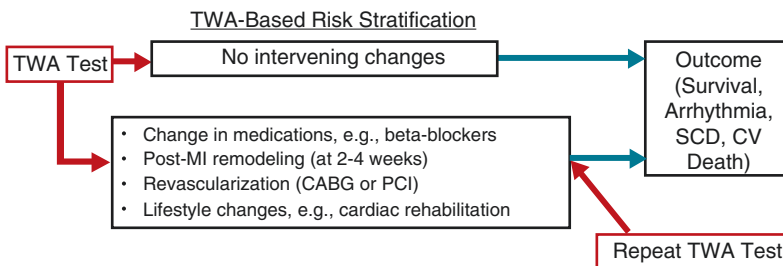


Fig. 19.8 A number of established clinical factors that affect TWA and thereby impact on prediction. These include changes in medications [83], post-MI remodeling [77], revascularization [25], and exercise rehabilitation [98]. Thus, TWA testing should be repeated following any of these significant changes. The availability of routine

exercise testing and ambulatory ECG monitoring using standard electrodes facilitates retesting TWA. Key: CABG coronary artery bypass graft surgery, CV cardiovascular, MI myocardial infarction, PCI percutaneous coronary intervention, SCD sudden cardiac death, TWA T-wave alternans. (Reprinted with permission from Elsevier from Verrier and Sroubek [71])

References

- Verrier RL, Klinghenben T, Malik M, El-Sherif N, Exner D, Hohnloser S, Ikeda T, Martinez JP, Narayan S, Nieminen T, Rosenbaum DS. Microvolt T-wave alternans: physiologic basis, methods of measurement, and clinical utility. Consensus guideline by the International Society for Holter and Noninvasive Electrocardiology. *J Am Coll Cardiol*. 2011;44:1309–24.
- Lewis T. Notes on alternation of the heart. *Quarterly Med J*. 1910;4:141–4.
- Mozaffarian D, Benjamin EJ, Go AS, et al. Heart disease and stroke statistics—2016 update: a report from the American Heart Association. *Circulation*. 2016;133:e38–e360.
- Stecker EC, Vickers C, Waltz J, Sosatearu C, John BT, Mariani R, McAnulty JH, Gunson K, Jui J, Chugh SS. Population-based analysis of sudden cardiac death with and without left ventricular systolic dysfunction: two-year findings from the Oregon Sudden Unexpected Death Study. *J Am Coll Cardiol*. 2006;47:1161–6.
- Wellens HJJ, Schwartz PJ, Lindemans FW, et al. Risk stratification for sudden cardiac death: current

- status and challenges for the future. *Eur Heart J*. 2014;35:1642–51.
6. Huikuri HV, Castellanos A, Myerburg RJ. Sudden death due to cardiac arrhythmias. *N Engl J Med*. 2001;345:1473–82.
 7. Moss AJ, Zareba W, Hall WJ, Klein H, Wilber DJ, Cannom DS, Daubert JP, Higgins SL, Brown MW, Andrews ML. Prophylactic implantation of a defibrillator in patients with myocardial infarction and reduced ejection fraction. *N Engl J Med*. 2002;346:877–83.
 8. Buxton AE. Risk stratification for sudden death in patients with coronary artery disease. *Heart Rhythm*. 2009;6:836–47.
 9. Sabbag A, Suleiman M, Laish-Farkash A, Samania N, Kazatsker M, Goldenberg I, Glikson M, Beinart R, Israeli Working Group of Pacing and Electrophysiology. Contemporary rates of appropriate shock therapy in patients who receive implantable device therapy in a real-world setting: from the Israeli ICD Registry. *Heart Rhythm*. 2015;12:2426–33.
 10. Verrier RL, Nearing BD, LaRovere MT, Pinna GD, Mittleman MA, Bigger JT, Schwartz PJ, ATRAMI Investigators. Ambulatory ECG-based tracking of T-wave alternans in post-myocardial infarction patients to assess risk of cardiac arrest or arrhythmic death. *J Cardiovasc Electrophysiol*. 2003;14:705–11.
 11. Slawnych MP, Nieminen T, Kahonen M, Kavanagh KM, Lehtimäki T, Ramadan D, et al. Postexercise assessment of cardiac repolarization alternans in patients with coronary artery disease using the modified moving average method. *J Am Coll Cardiol*. 2009;53:1130–7.
 12. Stein PK, Sanghavi D, Domitrovich PP, Mackey RA, Deedwania P. Ambulatory ECG-based T-wave alternans predicts sudden cardiac death in high-risk post-MI patients with left ventricular dysfunction in the EPHEBUS study. *J Cardiovasc Electrophysiol*. 2008;19:1037–42.
 13. Sakaki K, Ikeda T, Miwa Y, Miyakoshi M, Abe A, Tsukada T, et al. Time-domain T-wave alternans measured from Holter electrocardiograms predicts cardiac mortality in patients with left ventricular dysfunction: a prospective study. *Heart Rhythm*. 2009;6:332–7.
 14. Maeda S, Nishizaki M, Yamawake N, et al. Ambulatory ECG-based T-wave alternans and heart rate turbulence predict high risk of arrhythmic events in patients with old myocardial infarction. *Circ J*. 2009;73:2223–8.
 15. Stein PK, Sanghavi D, Sotoodehnia N, Siscovick DS, Gottdiener J. Association of Holter-based measures including T-wave alternans with risk of sudden cardiac death in the community-dwelling elderly: the cardiovascular health study. *J Electrocardiol*. 2010;43:251–9.
 16. Nieminen T, Lehtimäki T, Viik J, Lehtinen R, Nikus K, Kööbi T, et al. T-wave alternans predicts mortality in a population undergoing a clinically indicated exercise test. *Eur Heart J*. 2007;28:2332–7.
 17. Minkkinen M, Kähönen M, Viik J, Nikus K, Lehtimäki T, Lehtinen R, et al. Enhanced predictive power of quantitative TWA during routine exercise testing in the Finnish Cardiovascular Study. *J Cardiovasc Electrophysiol*. 2009;20:408–15.
 18. Leino J, Minkkinen M, Nieminen T, Lehtimäki T, Viik J, Lehtinen R, et al. Combined assessment of heart rate recovery and T-wave alternans during routine exercise testing improves prediction of total and cardiovascular mortality: The Finnish Cardiovascular Study. *Heart Rhythm*. 2009;6:1765–71.
 19. Leino J, Verrier RL, Minkkinen M, Lehtimäki T, Viik J, Lehtinen R, et al. Importance of regional specificity of T-wave alternans in assessing risk for cardiovascular mortality and sudden cardiac death during routine exercise testing. *Heart Rhythm*. 2011;8:385–90.
 20. Hoshida K, Miwa Y, Miyakoshi M, et al. Simultaneous assessment of T-wave alternans and heart rate turbulence on Holter electrocardiograms as predictors for serious cardiac events in patients after myocardial infarction. *Circ J*. 2013;77:432–8.
 21. Ren L-N, Fang X-H, Ren L-D, et al. Ambulatory ECG-based T-wave alternans and heart rate turbulence can predict cardiac mortality in patients with myocardial infarction with or without diabetes mellitus. *Cardiovasc Diabetol*. 2012;11:104–11.
 22. Shimada H, Nishizaki M, Fujii H, Yamawake N, Fukamizu S, Sakurada H, et al. Ambulatory electrocardiogram-based T-wave alternans in patients with vasospastic angina during asymptomatic periods. *Am J Cardiol*. 2012;110:1446–51.
 23. Sulimov V, Okisheva E, Tsaregorodtsev D. Non-invasive risk stratification for sudden cardiac death by heart rate turbulence and microvolt T wave alternans in patients after myocardial infarction. *Europace*. 2012;14:1786–92.
 24. Hou Y, Fang PH, Wu Y, et al. Prediction of sudden cardiac death in patients after acute myocardial infarction using T-wave alternans: a prospective study. *J Electrocardiol*. 2012;45:60–5.
 25. Verrier RL, Nearing BD, Ghanem RN, Olson RE, Garberich RF, Katsiyiannis WT, et al. Elevated T-wave alternans predicts nonsustained ventricular tachycardia in association with percutaneous coronary intervention in ST-segment elevation myocardial infarction (STEMI) patients. *J Cardiovasc Electrophysiol*. 2013;24:658–63.
 26. Arisha MM, Girerd N, Chauveau S, Bresson D, Scridon A, Bonnefoy E, et al. In-hospital heart rate turbulence and microvolt T-wave alternans abnormalities for prediction of early life-threatening ventricular arrhythmia after acute myocardial infarction. *Ann Noninvasive Electrocardiol*. 2013;18:530–7.
 27. Nieminen T, Scirica BM, Pegler JRM, Tavares C, Pagotto VPF, Kanas AF, et al. Relation of T-wave alternans to mortality and nonsustained ventricular tachycardia in patients with non-ST segment eleva-

- tion acute coronary syndrome from the MERLIN-TIMI 36 trial of ranolazine versus placebo. *Am J Cardiol.* 2014;114:17–23.
28. Uchimura-Makita Y, Nakano Y, Tokuyama T, Fujiwara M, Watanabe Y, Sairaku A, et al. Time-domain T-wave alternans is strongly associated with a history of ventricular fibrillation in patients with Brugada Syndrome. *J Cardiovasc Electrophysiol.* 2014;25:1021–7.
 29. Takasugi N, Goto H, Takasugi M, Verrier RL, Kuwahara T, Kubota T, et al. Prevalence of microvolt T-wave alternans in patients with long QT syndrome and its association with torsade de pointes. *Circ Arrhythm Electrophysiol.* 2016;9:e003206.
 30. Chung FP, Lin YJ, Chong E, Chang SL, Lo LW, Hu YF, et al. The application of ambulatory electrocardiographically-based T-wave alternans in patients with arrhythmogenic right ventricular dysplasia/cardiomyopathy. *Can J Cardiol.* 2016;32:1355.e15–22.
 31. Yamada S, Yoshihisa A, Sato Y, Sato T, Kamioka M, Kaneshiro T, et al. Utility of heart rate turbulence and T-wave alternans to assess risk for readmission and cardiac death in hospitalized heart failure patients. *J Cardiovasc Electrophysiol.* 2018; <https://doi.org/10.1111/jce.13639>.
 32. Verrier RL, Ikeda T. Ambulatory ECG-based T-wave alternans monitoring for risk assessment and guiding medical therapy: Mechanisms and clinical applications. *Prog Cardiovasc Dis.* 2013;56:172–85. <https://doi.org/10.1016/j.pcad.2013.07.002>.
 33. Nearing BD, Verrier RL. Tracking heightened cardiac electrical instability by computing interlead heterogeneity of T-wave morphology. *J Appl Physiol.* 2003;95:2265–72.
 34. Weiss JN, Karma A, Shiferaw Y, Chen P-S, Garfinkel A, Qu Z. From pulsus to pulseless: the saga of cardiac alternans. *Circ Res.* 2006;98:1244–53.
 35. Clusin WT. Mechanisms of calcium transient and action potential alternans in cardiac cells and tissues. *Am J Physiol Heart Circ Physiol.* 2008;294:H1–10.
 36. Cutler MJ, Rosenbaum DS. Explaining the clinical manifestations of T wave alternans in patients at risk for sudden cardiac death. *Heart Rhythm.* 2009;6:S22–8.
 37. Chinushi M, Kozhevnikov D, Caref EB, Restivo M, El-Sherif N. Mechanism of discordant T wave alternans in the in vivo heart. *J Cardiovasc Electrophysiol.* 2003;14:632–8.
 38. Nearing BD, Oesterle SN, Verrier RL. Quantification of ischaemia-induced vulnerability by precordial T-wave alternans analysis in dog and human. *Cardiovasc Res.* 1994;28:1440–9.
 39. Rashba EJ, Osman AF, MacMurdy K, Kirk MM, Sarang S, Peters RW, et al. Exercise is superior to pacing for T wave alternans measurement in subjects with chronic coronary artery disease and left ventricular dysfunction. *J Cardiovasc Electrophysiol.* 2002;13:845–50.
 40. Kovach JA, Nearing BD, Verrier RL. An angerlike behavioral state potentiates myocardial ischemia-induced T-wave alternans in canines. *J Am Coll Cardiol.* 2001;37:1719–25.
 41. Kop WJ, Krantz DS, Nearing BD, Gottdiener JS, Quigley JF, O'Callahan M, et al. Effects of acute mental and exercise stress on T-wave alternans in patients with implantable cardioverter defibrillators and controls. *Circulation.* 2004;109:1864–9.
 42. Lampert R, Shusterman V, Burg M, McPherson C, Batsford W, Goldberg A, et al. Anger-induced T-wave alternans predicts future ventricular arrhythmias in patients with implantable cardioverter-defibrillators. *J Am Coll Cardiol.* 2009;53:774–8.
 43. Konta T, Ikeda K, Yamaki M, Nakamura K, Honma K, Kubota I, et al. Significance of discordant ST alternans in ventricular fibrillation. *Circulation.* 1990;82:2185–9.
 44. Nearing BD, Huang AH, Verrier RL. Dynamic tracking of cardiac vulnerability by complex demodulation of the T-wave. *Science.* 1991;252:437–40.
 45. Smith JM, Clancy EA, Valeri CR, Ruskin JN, Cohen RJ. Electrical alternans and cardiac electrical instability. *Circulation.* 1988;77:110–21.
 46. Nearing BD, Wellenius GA, Mittleman MA, Josephson ME, Burger AJ, Verrier RL. Crescendo in depolarization and repolarization heterogeneity heralds development of ventricular tachycardia in hospitalized patients with decompensated heart failure. *CIRCEP.* 2012;5:84–90.
 47. Waldo AL, Camm AJ, deRuyter H, Friedman PL, MacNeil DJ, Pauls JF, SWORD investigators, et al. Effect of d-sotalol on mortality in patients with left ventricular dysfunction after recent and remote myocardial infarction. *Survival With Oral d-Sotalol.* *Lancet.* 1996;348:7–12.
 48. Nieminen T, Nanbu DY, Datti IP, Vaz GR, Tavares CAM, Pegler JRM, et al. Antifibrillatory effect of ranolazine during severe coronary stenosis in the intact porcine model. *Heart Rhythm.* 2011;8:608–14.
 49. Drew BJ, Ackerman MJ, Funk M, Gibler WB, Kligfield P, Menon V, et al. Prevention of torsade de pointes in hospital settings: a scientific statement from the American Heart Association and the American College of Cardiology Foundation. *J Am Coll Cardiol.* 2010;55:934–47.
 50. Bonatti R, Garcia Silva AF, Pereira Batatinha JA, Sobrado LF, Machado AD, Varone BB, et al. Selective late sodium current blockade with GS-458967 markedly reduces ischemia-induced atrial and ventricular repolarization alternans and ECG heterogeneity. *Heart Rhythm.* 2014;11:1827–35.
 51. Echt DS, Liebson PR, Mitchell LB, Peters RW, Obias-Manno D, Barker AH, CAST Investigators, et al. Mortality and morbidity in patients receiving encainide, flecainide, or placebo. The Cardiac Arrhythmia Suppression Trial. *N Engl J Med.* 1991;324:781–8.
 52. Schwartz PJ, Malliani A. Electrical alternation of the T-wave: clinical and experimental evidence of its relationship with the sympathetic nervous sys-

- tem and with the long Q-T syndrome. *Am Heart J*. 1975;89:45–50.
53. Schwartz PJ, Motolese M, Pollavini G, Lotto A, Ruberti U, Trazzi R, Italian Sudden Death Prevention Group, et al. Prevention of sudden cardiac death after a first myocardial infarction by pharmacologic or surgical antiadrenergic interventions. *J Cardiovasc Electrophysiol*. 1992;3:2–16.
 54. Verrier RL, Nearing BD. Electrophysiologic basis for T-wave alternans as an index of vulnerability to ventricular fibrillation. *J Cardiovasc Electrophysiol*. 1994;5:445–61.
 55. Ryvlin P, So EL, Gordon CM, Hesdorffer DC, Sperling MR, Devinsky O, et al. Long-term surveillance of SUDEP in drug-resistant epilepsy patients treated with VNS therapy. *Epilepsia*. 2018;59(3):562–72.
 56. Schomer AC, Nearing BD, Schachter SC, Verrier RL. Vagus nerve stimulation reduces cardiac electrical instability assessed by quantitative T-wave alternans analysis in patients with drug-resistant focal epilepsy. *Epilepsia*. 2014;55:1996–2002.
 57. Verrier RL, Nearing BD, Olin B, Boon P, Schachter SC. Baseline elevation and reduction in cardiac electrical instability assessed by quantitative T-wave alternans in patients with drug-resistant epilepsy treated with vagus nerve stimulation in the AspireSR E-36 trial. *Epilepsy Behav*. 2016;62:85–9.
 58. Olsson G, Wikstrand J, Warnold I, Manger Cats V, McBoyle D, Herlitz J, et al. Metoprolol-induced reduction in postinfarction mortality: pooled results from five doubleblind randomized trials. *Eur Heart J*. 1992;13:28–32.
 59. Klungenheben T, Gronefeld G, Li YG, Hohnloser SH. Effect of metoprolol and d,l-sotalol on microvolt-level T-wave alternans. Results of a prospective, double-blind, randomized study. *J Am Coll Cardiol*. 2001;38:2013–9.
 60. Rashba EJ, Cooklin M, Macmurdy K, Kavesh N, Kirk M, Sarang S, et al. Effects of selective autonomic blockade on T-wave alternans in humans. *Circulation*. 2002;105:837–42.
 61. Komiya N, Seto S, Nakao K, Yano K. The influence of beta-adrenergic agonists and antagonists on T-wave alternans in patients with and without ventricular tachyarrhythmia. *Pacing Clin Electrophysiol*. 2005;28:680–4.
 62. Murata M, Harada M, Shimizu A, Kubo M, Mitani R, Dairaku Y, et al. Effect of long-term beta-blocker therapy on microvolt-level T-wave alternans in association with the improvement of the cardiac sympathetic nervous system and systolic function in patients with nonischemic heart disease. *Circ J*. 2003;67:821–5.
 63. Nearing BD, Hutter JJ, Verrier RL. Potent anti-fibrillatory effect of combined blockade of calcium channels and 5-HT₂ receptors with nexopamil during myocardial ischemia and reperfusion in canines: comparison to diltiazem. *J Cardiovasc Pharmacol*. 1996;27:777–87.
 64. Scirica BM, Braunwald E, Belardinelli L, Hedgepeth CM, Spinar J, Wang W, et al. Relationship between nonsustained ventricular tachycardia after non-ST elevation acute coronary syndrome and sudden cardiac death: observations from the Metabolic Efficiency with Ranolazine for Less Ischemia in Non-ST-Elevation Acute Coronary Syndrome-Thrombolysis in Myocardial Infarction 36 (MERLIN-TIMI 36) randomized controlled trial. *Circulation*. 2010;122:455e462.
 65. Murdock D, Kaliebe J, Overton N. Ranolazine-induced suppression of ventricular tachycardia in a patient with nonischemic cardiomyopathy: a case report. *PACE*. 2008;31:765–8.
 66. Wilson LD, Jeyaraj D, Wan X, Hoeker GS, Said TH, Gittinger M, et al. Heart failure enhances susceptibility to arrhythmogenic cardiac alternans. *Heart Rhythm*. 2009;6:251–9.
 67. Narayan SM, Bayer JD, Lalani G, Trayanova NA. Action potential dynamics explain arrhythmic vulnerability in human heart failure: a clinical and modeling study implicating abnormal calcium handling. *J Am Coll Cardiol*. 2008;52:1782–92.
 68. Sakamoto N, Sato N, Oikawa K, Karim Talib A, Sugiyama E, Minoshima A, et al. Late gadolinium enhancement of cardiac magnetic resonance imaging indicates abnormalities of time-domain T-wave alternans in hypertrophic cardiomyopathy with ventricular tachycardia. *Heart Rhythm*. 2015;12(8):1747–55.
 69. Mewton N, Strauss DG, Rizzi P, Verrier RL, Liu CY, Tereshchenko LG, et al. Screening for cardiac magnetic resonance scar features by 12-lead ECG in patients with preserved ejection fraction. *Ann Noninvasiv Electrocardiol*. 2016;21:49–59.
 70. Rosenbaum DS, Jackson LE, Smith JM, Garan H, Ruskin JN, Cohen RJ. Electrical alternans and vulnerability to ventricular arrhythmias. *N Engl J Med*. 1994;330:235–41.
 71. Verrier RL, Sroubek J. Quantitative T-wave alternans analysis for sudden cardiac death risk assessment and guiding therapy: answered and unanswered questions. *J Electrocardiol*. 2016;49:429–38.
 72. Kaufman ES, Bloomfield DM, Steinman RC, Namerow PB, Costantini O, Cohen RJ, et al. “Indeterminate” microvolt T-wave alternans tests predict high risk of death or sustained ventricular arrhythmias in patients with left ventricular dysfunction. *J Am Coll Cardiol*. 2006;48:1399–404.
 73. Nearing BD, Verrier RL. Modified moving average method for T-wave alternans analysis with high accuracy to predict ventricular fibrillation. *J Appl Physiol*. 2002;92:541–9.
 74. Verrier RL, Josephson ME. Cardiac arrhythmogenesis during sleep: mechanisms, diagnosis, and therapy. In: Kryger MH, Roth T, Dement WC, editors. *Principles and practice of sleep medicine*. 5th ed. Philadelphia: WB Saunders; 2010. p. 1363–9.
 75. Nishizaki M, Fujii H, Sakurada H, Kimura A, Hiraoka M. Spontaneous T wave alternans in a

- patient with Brugada syndrome—responses to intravenous administration of class I antiarrhythmic drug, glucose tolerance test, and atrial pacing. *J Cardiovasc Electrophysiol.* 2005;16:217–20.
76. Zipes DP, Camm AJ, Borggrefe M, Buxton AE, Chaitman B, Fromer M, et al. ACC/AHA/ESC 2006 guidelines for management of patients with ventricular arrhythmias and the prevention of sudden cardiac death: a Report of the American College of Cardiology/American Heart Association Task Force and the European Society of Cardiology Committee for Practice Guidelines. *J Am Coll Cardiol.* 2006;48:e247–346.
 77. Exner DV, Kavanagh KM, Slawnych MP, Mitchell LB, Ramadan D, Aggarwal SG, et al. Noninvasive risk assessment early after a myocardial infarction the REFINe study. *J Am Coll Cardiol.* 2007;50:2275–84.
 78. Royston P, Altman DG, Sauerbrei W. Dichotomizing continuous predictors in multiple regression: a bad idea. *Stat Med.* 2006;25:127–41.
 79. Secemsky EA, Verrier RL, Cooke G, Ghossein C, Subacius H, Manuchehry A, et al. High prevalence of cardiac autonomic dysfunction and T-wave alternans in dialysis patients. *Heart Rhythm.* 2011;8:592–8.
 80. Strzelczyk A, Adjei P, Scott CA, Bauer S, Rosenow F, Walker MC, Surges R. Postictal increase in T-wave alternans after generalized tonic-clonic seizures. *Epilepsia.* 2011;52:2112–7.
 81. Bardai A, Lamberts RJ, Blom MT, Spanjaart AM, Berdowski J, van der Staal SR, et al. Epilepsy is a risk factor for sudden cardiac arrest in the general population. *PLoS One.* 2012;7:e42749. 10.1371/annotation/847ccb3-45b2-4338-9ff3-ee5f35c58551.
 82. Stecker EC, Reinier K, Uy-Evanado A, Teodorescu C, Chugh H, Gunson K, et al. Relationship between seizure episode and sudden cardiac arrest in patients with epilepsy. *Circ Arrhythm Electrophysiol.* 2013;6:912–6.
 83. Verrier RL, Schachter SC. Is heart disease in chronic epilepsy a consequence of seizures or a fellow traveler? *Epilepsy Behav.* 2018;86:211–3.
 84. Chow T, Kereiakes DJ, Onufer J, Woelfel A, Gursoy S, Peterson BJ, et al. Does microvolt T-wave alternans testing predict ventricular tachyarrhythmias in patients with ischemic cardiomyopathy and prophylactic defibrillators? The MASTER (Microvolt T-wave Alternans Testing for Risk Stratification of Post-Myocardial Infarction Patients) trial. *J Am Coll Cardiol.* 2008;52:1607–15.
 85. Gold MR, Ip JH, Costantini O, Poole JE, McNulty S, Mark DB, et al. Role of microvolt T-wave alternans in assessment of arrhythmia vulnerability among patients with heart failure and systolic dysfunction: Primary results from the T-wave Alternans Sudden Cardiac Death in Heart Failure Trial substudy. *Circulation.* 2008;118:2022–8.
 86. Chan PS, Gold MR, Nallamothu BK. Do beta-blockers impact microvolt T-wave alternans testing in patients at risk for ventricular arrhythmias? A meta-analysis. *J Cardiovasc Electrophysiol.* 2010;21:1009–14.
 87. Hohnloser SH, Ikeda T, Cohen RJ. Evidence regarding clinical use of microvolt T-wave alternans. *Heart Rhythm.* 2009;6:S36–44.
 88. Costantini O, Hohnloser SH, Kirk MM, Lerman BB, Baker JH, Sethuraman B, et al. The ABCD (Alternans Before Cardioverter Defibrillator) trial: strategies using T-wave alternans to improve efficiency of sudden cardiac death prevention. *J Am Coll Cardiol.* 2009;53:471–9.
 89. Exner CV, Kavanagh KM, Hruczkowski TW, Hersi AS, Thibault B, Philippon F, et al. Combined assessment of autonomic tone and cardiac repolarization identifies patients with better-preserved left ventricular systolic function at high risk of death following a myocardial infarction [abstract]. *Circulation.* 2016;134:A20441.
 90. Sakabe K, Ikeda T, Sakata T, Kawase A, Kumagai K, Tezuka N, et al. Predicting the recurrence of ventricular tachyarrhythmias from T-wave alternans assessed on antiarrhythmic pharmacotherapy: a prospective study in patients with dilated cardiomyopathy. *Ann Noninvasive Electrocardiol.* 2001;6:203–8.
 91. Verrier RL, Nieminen T. T-wave alternans as a therapeutic marker for antiarrhythmic agents. *J Cardiovasc Pharmacol.* 2010;55:544–54.
 92. Belardinelli L, Liu G, Smith-Maxwell C, Wang W-Q, El-Bizri N, Hirakawa R, et al. A novel, potent, and selective inhibitor of cardiac late sodium current suppresses experimental arrhythmias. *J Pharmacol Exp Ther.* 2013;344:23–32.
 93. Multicenter Diltiazem Postinfarction Trial Research Group. The effect of diltiazem on mortality and reinfarction after myocardial infarction. *N Engl J Med.* 1988;319:385–92.
 94. Hohnloser SH. Macroscopic T wave alternans as a harbinger of sudden death. *J Cardiovasc Electrophysiol.* 1999;10:625.
 95. Floré V, Claus P, Vos MA, Vandenberg B, Van Soest S, Sipido KR, et al. T-wave alternans is linked to microvascular obstruction and to recurrent coronary ischemia after myocardial infarction. *J Cardiovasc Transl Res.* 2015;8:484–92.
 96. Figliozzi S, Stazi A, Pinnacchio G, Laurito M, Parrinello R, Villano A, et al. Use of T-wave alternans in identifying patients with coronary artery disease. *J Cardiovasc Med.* 2016;17:20–5.
 97. Somuncu MU, Erturk M, Karakurt H, Demir AR, Bulut U, Kurtar A, et al. Microvolt T-wave alternans in young myocardial infarction patients with preserved cardiac function treated with single-vessel primary percutaneous coronary intervention. *Arch Med Sci Atheroscler Dis.* 2016;1:e68–74.
 98. Rasmussen JN, Chong A, Alter DA. Relationship between adherence to evidence-based pharmacotherapy and long-term mortality after acute myocardial infarction. *JAMA.* 2007;297:177–86.

99. Kramer JM, Hammill B, Anstrom KJ, Fetterolf D, Snyder R, Charde JP, et al. National evaluation of adherence to beta-blocker therapy for 1 year after acute myocardial infarction in patients with commercial health insurance. *Am Heart J.* 2006;152:454.e1–8.
100. Shah ND, Dunlay SM, Ting HH, Montori VM, Thomas RJ, Wagie AE, et al. Long-term medication adherence after myocardial infarction: experience of a community. *Am J Med.* 2009;122:961.e7–13.
101. Waddell-Smith KE, Li J, Smith W, Crawford J, Skinner JR, on behalf of the Cardiac Inherited Disease Group New Zealand. β -Blocker adherence in familial long QT syndrome. *Circ Arrhythm Electrophysiol.* 2016;9:e003591.
102. Kentta T, Tulppo MP, Nearing BD, Karjalainen JJ, Hautala AJ, Kiviniemi AM, et al. Effects of exercise rehabilitation on cardiac electrical instability assessed by T-wave alternans during ambulatory electrocardiogram monitoring in coronary artery disease patients without versus with diabetes mellitus. *Am J Cardiol.* 2014;114:832–7.
103. Verrier RL. Assessing risk for rehospitalization and cardiac death in patients with heart failure: can the dynamic duo of heart rate turbulence and T-wave alternans help? [Editorial]. *J Cardiovasc Electrophysiol.* 2018;29:1–3. <https://doi.org/10.1111/jce.13660>.
104. Yalin K, Golcuk E, Aksu T, Tiryakioglu SK, Bilge AK, Adalet K. Distinguishing right ventricular cardiomyopathy from idiopathic right ventricular outflow tract tachycardia with T-wave alternans. *Am J Med Sci.* 2015;350:463–6.
105. Verrier RL. The power of the patch: a smart way to track risk for torsades de pointes in congenital and drug-induced long QT syndromes? *Int J Cardiol.* 2018;266:145–6.
106. Pang TD, Nearing BD, Krishnamurthy KB, Olin B, Schachter SC, Verrier RL. Cardiac electrical instability in newly diagnosed/chronic epilepsy tracked by Holter and EKG patch. *Neurology*, in press.



Action Potential Dynamics in Human Atrial Fibrillation

20

Junaid Ahmed Bakhtiyar Zaman,
Sanjiv M. Narayan, and Michael R. Franz

Introduction

While there is intense debate over the mechanisms for atrial fibrillation (AF), a clear consensus exists on an apparent interplay between triggers and substrate [1]. While triggers (focal beats) for AF often lay at or near the pulmonary veins [2], the mechanisms responsible for maintenance (substrate) of AF appear to be remote to these areas based on the limited success of pulmonary vein isolation in such patients and the results of newer specific mapping techniques (Fig. 20.1) [3]. Electrical remodeling of the atria and structural changes are recognized as key substrates for persistence of atrial fibrillation. While studies increasingly demonstrate the structural substrate for AF using imaging techniques [4], its electrical characterization has for years focused on clinical electrograms. Intracardiac electro-

grams, however, are not direct markers of atrial action potentials, can be challenging to interpret for their precise activation time (especially during AF), and do not provide insight into atrial *repolarization* and thus the determinants of block, reentry or after depolarizations.

This chapter will discuss key experimental data from monophasic action potentials (MAPs) during rapid pacing, the mechanistic sequelae of this with respect to initiation of atrial fibrillation in humans, and implications for the atrial substrate.

Action Potential Duration

Atrial action potentials can be measured in vivo in patients using the monophasic action potential (MAP) catheter. Early work by Franz et al. validated this recording to correspond to transmural action potential [6].

Precise measurement of total atrial action potential duration is difficult because of its asymptotic terminus. Clinically, human atrial AP duration is usually determined at a repolarization level of 90% (or another fraction) with respect to the AP amplitude, i.e., recovery from plateau voltage to 90% of fully repolarized “resting membrane potential.” The monophasic AP (MAP) amplitude is defined as the distance from the baseline to the crest of the MAP plateau voltage, not its upstroke peak (Fig. 20.2) [6]. The intersection between the diastolic baseline and a

J. A. B. Zaman
Royal Brompton Heart and Vascular Institute,
London, UK

Department of Medicine, Stanford University,
Stanford, CA, USA

S. M. Narayan (✉)
Department of Medicine, Stanford University,
Stanford, CA, USA
e-mail: Sanjiv1@stanford.edu

M. R. Franz
Division of Cardiology, Veterans Affairs Medical
Center, Washington, DC, USA

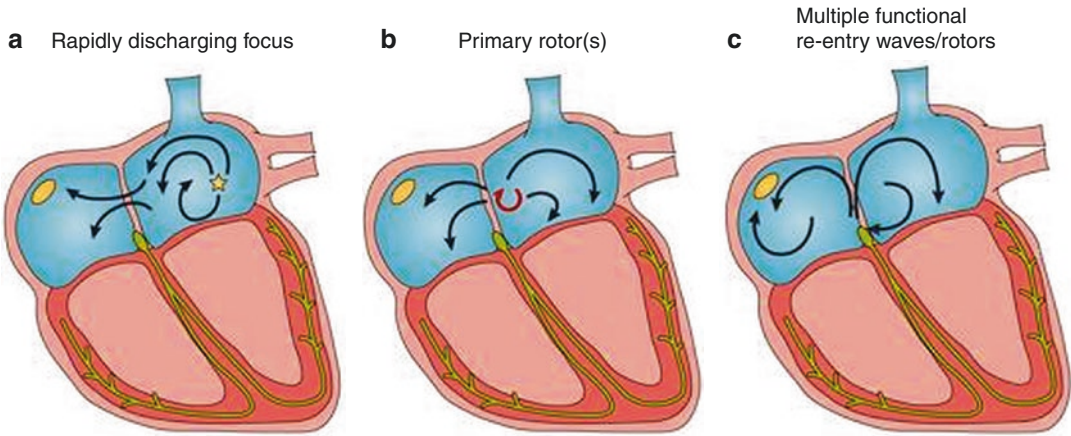
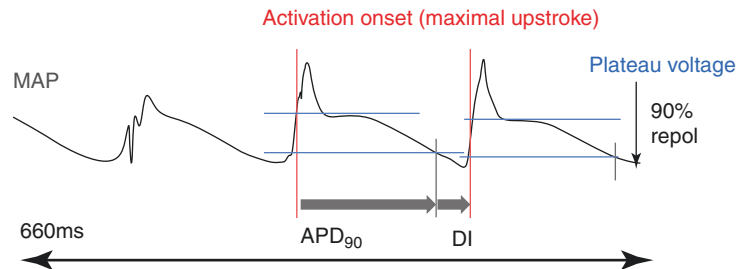


Fig. 20.1 Summary of AF mechanisms. (a) Rapidly discharging focal beats, often near pulmonary veins, act as triggers. (b) Primary reentrant driver (rotor) driving downstream fibrillatory conduction, often remote to pul-

monary veins, still represents a localized substrate. (c) Multiple functional reentries, a global distributed substrate. (Reprinted with permission from Springer Nature: Lip et al. [5])

Fig. 20.2 Graphical representation of monophasic action potential (MAP) recorded from a patient with atrial fibrillation. Note notation of action potential duration 90% (APD₉₀). DI = diastolic interval



tangent placed on phase three of the action potential may also determine MAP duration, but typically yields more arbitrary results. In human atrium, MAPD₉₀ (the duration of time for the MAP to return to 90% of its repolarized voltage) has been correlated to effective refractory period during pacing [7].

and 20.5) [8, 9]. A modified technique for describing the APD-CL relationship, referred to as the “dynamic” restitution curve (DRC), exhibits the relationship between APD and different steady cycle lengths determined during the early phases of rate adaptation.

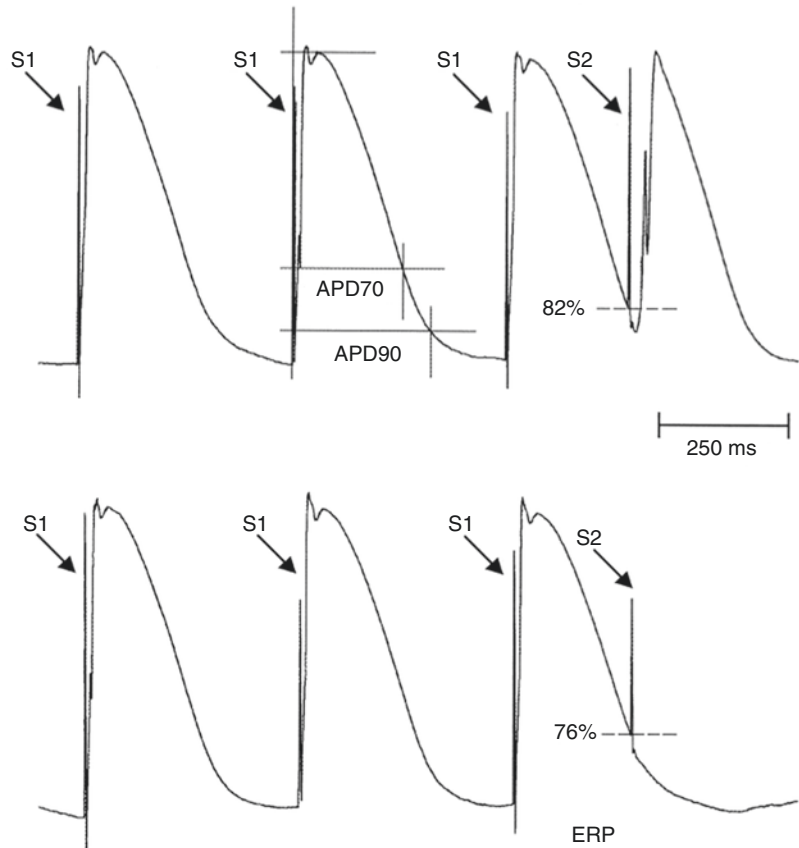
Action Potential Restitution

An electrical restitution curve (ERC) is obtained by pacing at a constant S1–S1 interval, followed by an S2, a single premature stimulus. S1–S2 coupling interval is progressively shortened until block of the premature pulse or the effective refractory period. The graphical relationship between APD 90% (or another fraction) to its preceding DI or CL is the ERC (Figs. 20.3, 20.4

Initiation of Human AF May Be Preceded by Atrial APD Alternans

CL-dependent changes in APD are proposed mechanisms for arrhythmogenesis and, in particular, fibrillation [12, 13]. As ERCs are described, progressive shortening of CL and DI accentuate changes in APD. Increasing APD “alternans” leads to larger wavelength oscillations and points of wavebreak resulting in temporal heterogeneity

Fig. 20.3 Simultaneous measurement of atrial ERP and APD₇₀ and APD₉₀ with the combination catheter. S1 and S2 denote the basic and extrastimulus artifacts. Repolarization levels (n%) at which extrastimuli are superimposed onto the preceding repolarization phase are visualized. (From Bode et al. [10]. Used with permission from Elsevier)



and reentry. The mechanisms by which APD alternans may contribute to electrical instability have been described utilizing computer and numeric simulations [14, 15]. The demonstration of APD alternans at high stimulus rates provides mechanistic support for this concept [16–18]. APD alternans has also been linked to ventricular fibrillation vulnerability [19, 20]. Evidence now exists that APD alternans may contribute to the onset and potentially maintenance of atrial fibrillation and its transition from atrial flutter in animal models [21, 22], in numerical simulations [23], and directly in humans [24], discussed later in this chapter.

Quantifying Atrial APD Alternans

APD alternans was historically assessed by visual inspection [25], but this does not allow for rapid

assessment or quantification. More recently, APD alternans has been detected and quantified spectrally. APs for a contiguous number of beats are each denoted by beat number and time sample. APs are time-aligned such that APs for successive beats (as voltage-time series) can be visualized in a third dimension for the number N of beats (Fig. 20.6).

A fast Fourier transform is used to compute power spectra *across beats* at each time sample to produce a spectrum for that time sample, which are then summated across all time samples to produce a spectral estimate of oscillations for the entire AP [26]. The magnitude of APD alternans is represented by the dimensionless k -score (Fig. 20.6).

It has been suggested that the slope of the ERC (see Fig. 20.5) may produce APD alternans and hence wavebreak and serve as an electrical substrate for reentry. A steeper ERC slope means

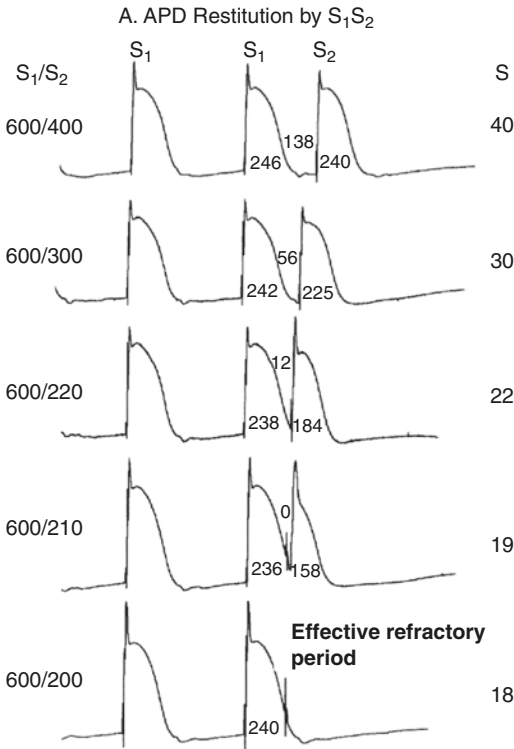


Fig. 20.4 Examples of MAP recorded at the high lateral wall of the right atrium by S_1S_2 in patients with persistent AF. A single extrastimulus (S_2) was given at progressively shorter S_1S_2 intervals. As diastolic interval decreased from 138 to 0 ms, the APD_{90} decreased from 240 to 158 ms and then reached effective refractory period (ERP) with a coupling interval of 200 ms. (From Kim et al. [11]. Used with permission from Elsevier)

that a relatively small change in DI may render large changes in APD and refractoriness which in turn cause reciprocal changes in DI for the next cycle, causing an opposite APD change and thus producing oscillations. The “restitution hypothesis” suggests that when the ERC slope >1 , augmented APD “alternans” results in larger wavelength oscillations and points of wavebreak. Alternatively, when ERC slope <1 , oscillations progressively decrease and ultimately achieve a new steady state [12, 28–30].

However, several findings question this otherwise attractive hypothesis for ventricular [26] and atrial [29, 31] arrhythmias. A major issue is that patients with advanced persistent AF

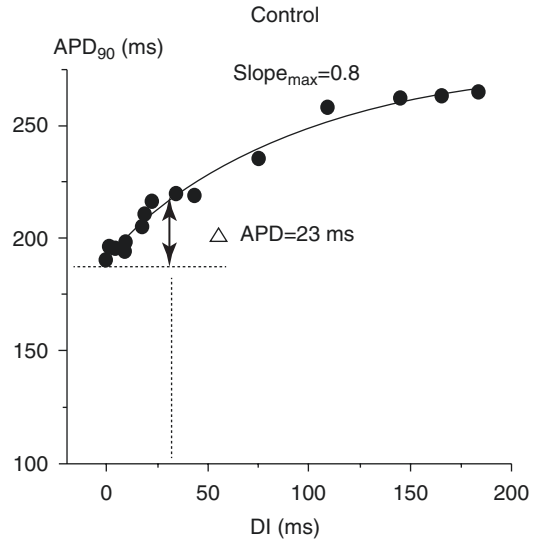


Fig. 20.5 An ERC by S_1S_2 . The decrease in APD_{90} with increasing prematurity resulted in an ERC slope of 0.8. (From Kim et al. [11]. Used with permission from Elsevier)

appear to have less steep atrial APD restitution curves than patients with less advanced paroxysmal AF [29]. Accordingly, work from our laboratory and others have moved to examine the shape of the human atrial action potential as a potentially more revealing pathophysiological marker than the single point of MAPD alone. In Fig. 20.6 we applied spectral analysis to quantify alternans across the entire atrial MAP duration, which we have related more recently to atrial electrical remodeling and potential cellular mechanisms [32].

Atrial Action Potentials to Mark Electrophysiologic Remodeling in Atrial Fibrillation

Atrial electrophysiologic remodeling as a consequence of AF was significantly advanced by work conducted in animal models [33, 34]. Further studies also suggested that AF induced atrial APD shortening and action potential plateau phase depression in animals [35, 36] as well as

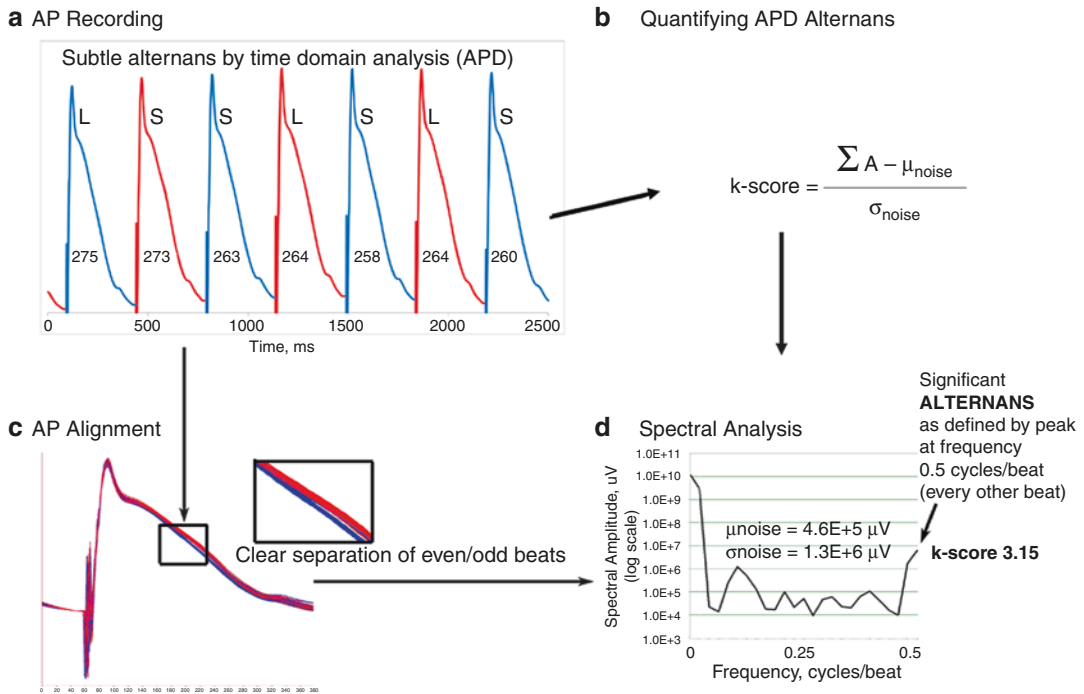


Fig. 20.6 Measurement of atrial alternans. **(a)** Left atrial monophasic action potentials during atrial fibrillation, with APD values listed beneath. **(b)** APD alternans quantification. ΣA is spectral magnitude at 0.5 cycles/beat, and μ_{noise} and σ_{noise} are the mean and standard deviation of

noise. A $k > 0$ indicates that alternans exceeds noise. **(c)** AP amplitude shows marked alternans, shown by the separation of even (blue line) and odd (red line) beats. **(d)** Significant AP alternans with k -score 3.15. (From: Lalani et al. [27]. Used with permission from Wolters Kluwer)

humans [37], due to quantifiable remodeling in ion channels [32, 38]. AF induces abnormal cellular calcium handling that may promote compensatory downregulation of inward L-type Ca^{2+} current (I_{CaL}) [39–41]. It is theorized that this reduction in I_{CaL} activity mitigates the plateau phase and largely explains the accentuated shortening of atrial APD [42, 43]. Transient outward K^+ current (I_{TO}) is also reduced in chronic AF [44], which seems puzzling but may help explain additional effects of AF on APD [32]. Chronic AF also exhibits an increase in inward rectifying K^+ current I_{K1} [45] which primarily controls the resting potential of the atrial myocyte. In sum, a complex interplay of currents in atrial AF myocytes renders a shorter APD and mitigation of the plateau phase.

An interesting phenomenon noted by Wijffels et al. [33] was an alteration to physiologic rate adaptation. As expected, normal goats in sinus rhythm exhibited atrial APD shortening at shorter pacing intervals. Goats artificially maintained in AF over 24–48 hours, however, lost physiological adaptation and exhibited either constant or shorter APD at slower heart rates. Further, normal heart rate adaptation was restored within a few days after cardioversion to sinus rhythm. A later study by Van Der Velden et al. added that increasing pacing rates rendered longer APD in a post-cardioversion chronic AF goat model [46]. This constitutes an AF-induced, paradoxical physiological adaptation of the atrial APD to changes in heart rate. This maladaptation of the atrial APD had been observed in prior human studies [24, 47].

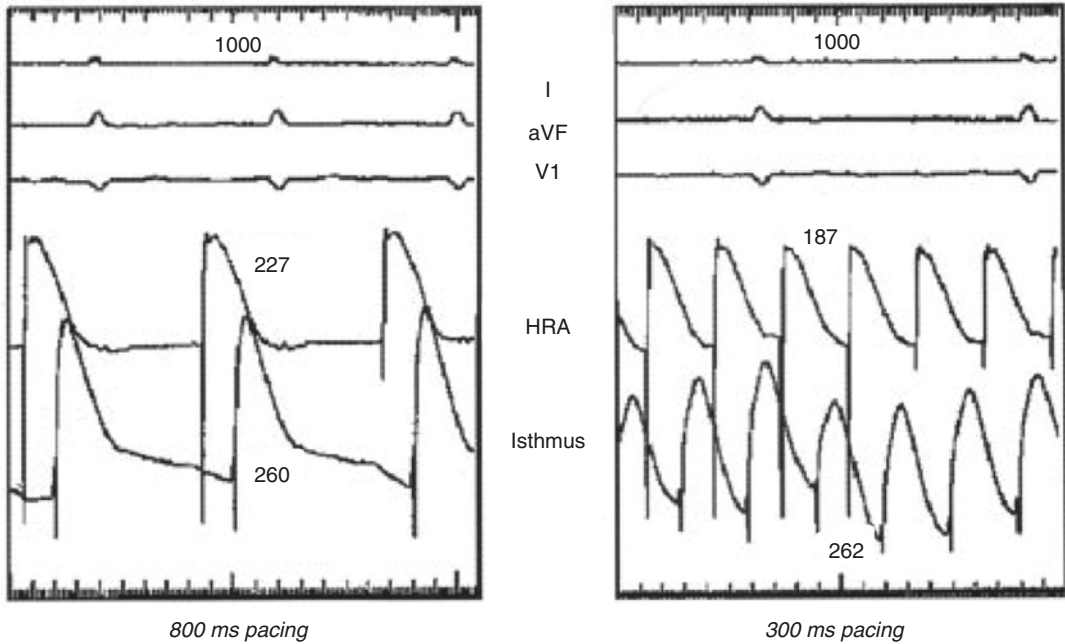


Fig. 20.7 APD-CL nonuniformity between the isthmus and high right atria (HRA) in a patient who developed AF. APD is longer at the isthmus than the HRA at pacing CL of 800 ms (left) and CL of 300 ms (right). Notably, APD at the isthmus failed to shorten with CL (right), although shortening was appropriate at the HRA. APD

rate maladaptation at the isthmus versus HRA eliminated the diastolic interval, caused the MAP to encroach on subsequent beats, and became more pronounced at faster pacing. (From Narayan et al. [24]. Used with permission from Wolters Kluwer)

We documented atrial APD alternans in humans during transitions of atrial flutter (Afl) to AF and noted that rate maladaptation leads to APD alternans preceding all such transitions [24]. Conversely, much less APD alternans was seen in patients in whom AF did not initiate. A critical observation was of spatial heterogeneity within the atria [48], with such APD alternans observed in certain regions (in this case, in the cavotricuspid isthmus, which may explain breakdown of otherwise stable typical AFL; Fig. 20.7) and heterogeneous rate maladaptation in Afl and AF known to contribute to AF [49].

We also demonstrated that continued incremental pacing enhanced APD alternans until beat-to-beat conduction was unable to be maintained physiologically, leading to 2:1 conduction block, which was also noted in prior investigation [11]. We posited that, as a result of a maladaptive APD rate response, spatially heterogeneous APD alternans at



Fig. 20.8 APD alternans with 2:1 capture block at the isthmus during pacing CL of 230 ms, while 1:1 capture is maintained at the His and distal coronary sinus (DCS) sites; this preceded AF initiation. APD₉₀ alternans in the isthmus first appeared in this patient at CL of 250 ms. (From Narayan et al. [34]. Used with permission from Wolters Kluwer)

increasing heart rates leads to wavefront fractionation and wavebreak, conduction block, and the eventual transition to AF [24]. See Figs. 20.8 and 20.9.

Heterogeneity of APD Maladaptation

We evaluated the concept of heterogeneity of APD maladaptation and AP oscillations during AF initiation in the electrophysiology laboratory in patients with and without clinical AF [31]. We hypothesized that AF-induced atrial remodeling may cause APD alternans at slower heart rates. Using an incremental pacing technique, we studied left and right atrial APD₉₀, APD restitution curve, APD alternans, and non-alternating complex APD oscillations on transitions to AF in patients with persistent AF, paroxysmal AF, and control subjects without clinical AF.

The development of APD alternans was elicited at near resting rates in patients with persistent AF, at intermediate rates in those with paroxysmal AF, and only at very rapid rates just prior to AF in controls. Moreover, the amplitude of APD alternans also varied by group and was greatest in those with persistent AF, intermediate in those with paroxysmal AF, and smallest just before AF induction in controls. A representative patient with persistent AF is shown in Fig. 20.9, in whom marked left atrial APD alternans was seen at CL 600 ms (100 beats/min) and CL 500 ms (120 beats/min, illustrated). At faster rates (shorter CLs), APD alternans disorganized to complex APD oscillation immediately preceding AF transition. In stark contrast, Fig. 20.10 shows a representative control subject in whom APD alternans did not arise until very fast rates (CL 200–250 ms), just prior to AF onset. No control subject had APD alternans at CL greater than or equal to 250 ms and, when exhibited, alternans had very small magnitude.

The APD rate-response relationship and APD alternans directly indicated AF “substrates,” presumably caused by electrical remodeling. The CL onset of APD alternans and CL range varied among the three groups. As delineated in the figure below, persistent and paroxysmal AF subjects exhibited APD alternans at all rates while controls only exhibited APD alternans around CL 250 ms (Fig. 20.11).

Refining Electrical APD Restitution in AF

We explored the potential role of APD restitution in patients with different forms of AF and in control subjects without AF. Notably, initiation of APD alternans was observed in some control subjects as well as a few paroxysmal AF subjects in whom ERC slope was >1 . This is consistent with, and may explain, spontaneous AF initiation by triggering premature atrial complexes such as those from the PVs (Fig. 20.12).

However, this did not explain AF onset in all patients. The ERC slope in all paroxysmal and persistent AF subjects was <1 at the onset of APD alternans, even if maximum slope was >1 at faster rates. Persistent AF enabled onset of APD alternans at relatively slower heart rates (see Fig. 20.9), suggesting that some other facet of electrical remodeling than ERC slope was operative. As noted earlier, AF is thought to affect several aspects of atrial myocyte character and function, including abnormal intracellular Ca²⁺ handling [42], membrane ion current remodeling changes [50], and atrial conduction slowing [51].

Nevertheless, atrial APD alternans was noted to precede every AF transition, supporting prior studies [29] and suggesting a critical role for APD alternans in AF onset. Accordingly, we suggest that, in addition to spontaneous premature atrial complexes, APD alternans amplification or complex oscillation preceding AF transition at fast rates represent period multiplying in nonlinear systems, another suspected trigger for AF. Proposed mechanisms to elucidate this phenomenon remain under intense scrutiny.

Future Directions

There is renewed interest in recording action potential-like signals in human cardiac chambers as the ability to view repolarization is a pre-requisite for interpreting complex electrograms and detecting reentry. The interaction of head meets tail at rotational cores requires accu-

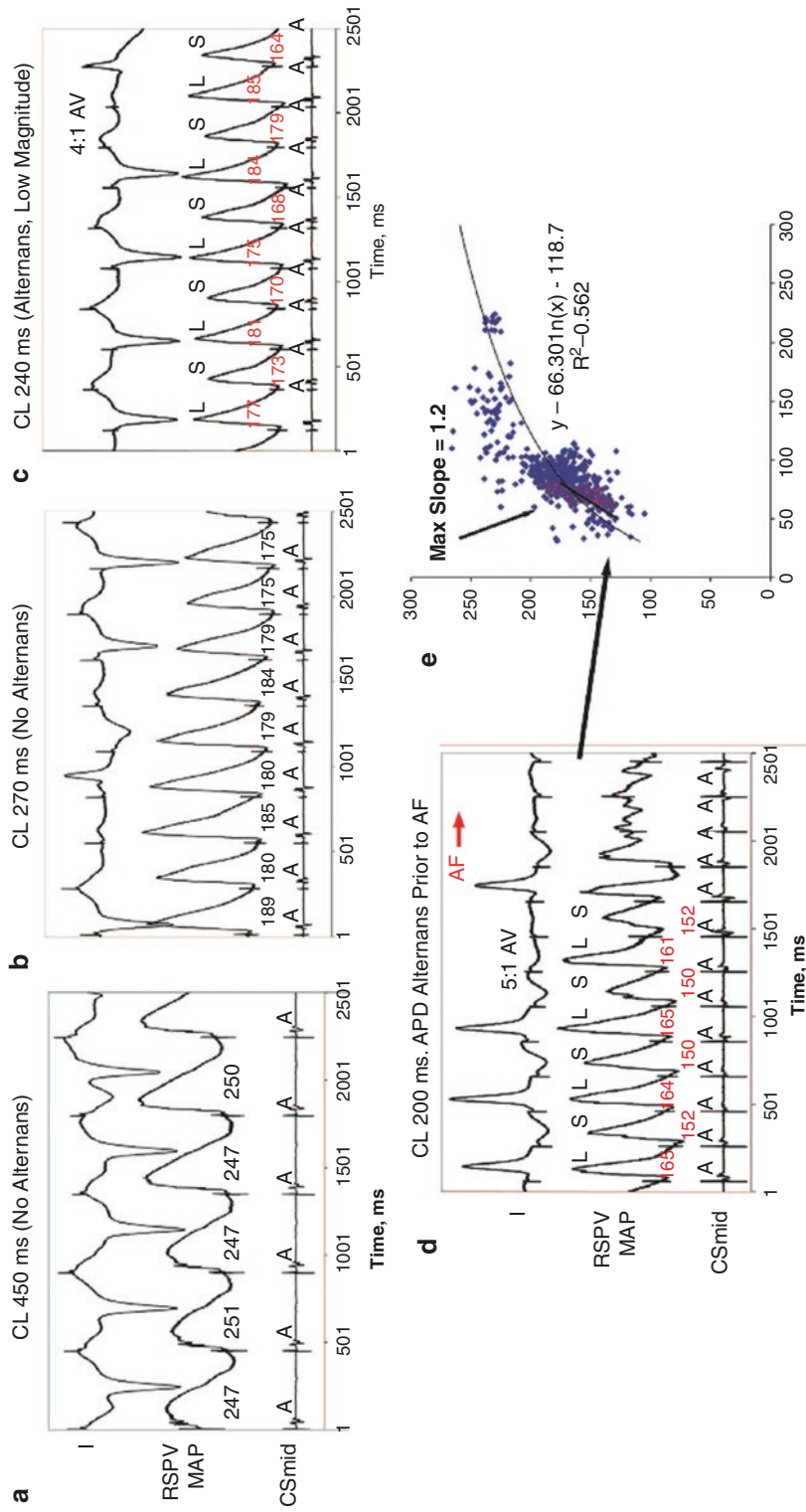


Fig. 20.10 Control subject with APD alternans only at very fast rates preceding AF. This patient showed no APD alternans at (a) CL 500 ms to (b) CL 240 ms. (c) APD alternans appeared at CL 210 ms during 1:1 and 2:1 AV conduction. (d) At CL 180ms, APD alternans amplified to 6.5% of APD immediately preceding AF initiation. ERC slope 1 at the fast rates of APD alternans onset. (From Narayan et al. [31]. Used with permission from Wolters Kluwer)

rate spatial awareness of wavefront curvature and can only be visualized directly by action potential data, such as human heart ex vivo optical mapping [52]. In clinical practice, limited tools exist to quantify repolarization from electrograms, but novel methods are under investigation

[53] and may shed further light onto AF mechanisms [54].

Viewing repolarization also is instrumental in assessing conduction velocity (CV) as it relates to the proximity of the preceding depolarization. CV is minimal closest to the refractoriness of the preceding AP and then recovers quickly as the DI increases (CV restitution). CV is the major determinant of the AP wavelength and thus may be important to assess the number of reentry wavelets in play during closely spaced depolarizations (as in AF). There is considerable research interest in measurement of conduction velocity in the human atria [51, 55–57], but measurements during fibrillation itself require knowledge of wavelet direction a priori, which can limit extrapolation from paced data preinitiation.

Because the MAP reflects repolarization at the cellular level, MAP recordings could also be used to define clinical phenotypes anchored on cellular mechanisms, and current modeling and translational studies are exploring this possibility for patients with atrial fibrillation as well as those at risk for sudden death. Finally, assessments of repolarization can also thus be used to suggest individuals who may or may not benefit from anti-arrhythmic drug therapy, for instance, using novel tools such as induced pluripotent

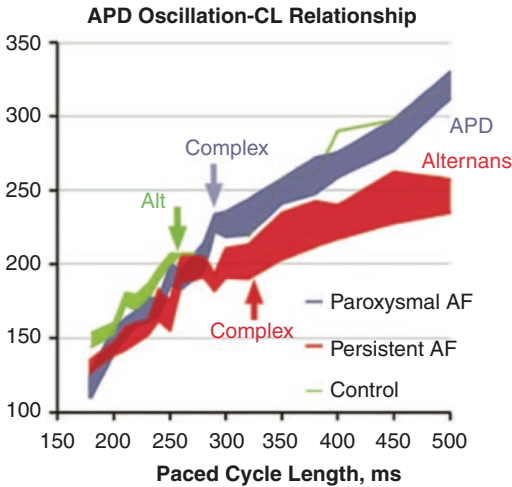
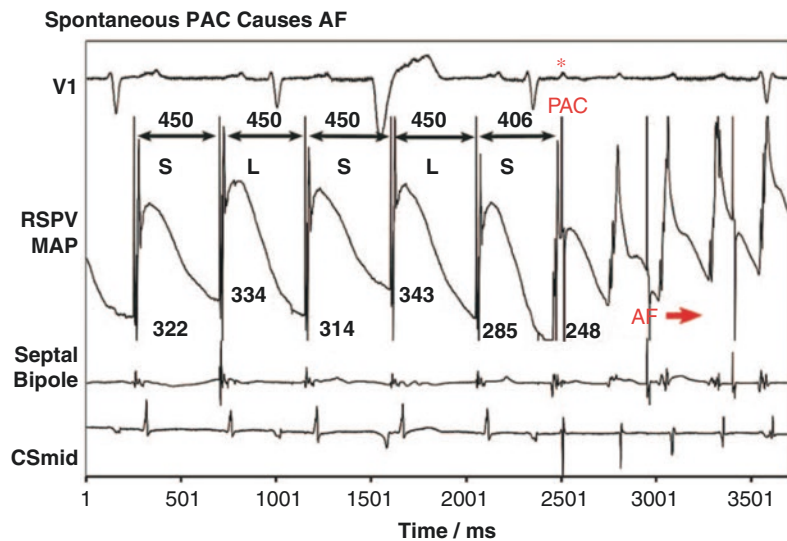


Fig. 20.11 APD oscillation and CL. AF patients show marked APD oscillations (alternans at slow rates transitioning to complex oscillations at faster rate), whereas controls show APD alternans only at very short CL. (From Narayan et al. [31]. Used with permission from Wolters Kluwer)

Fig. 20.12 Spontaneous premature atrial complex (PAC, marked by *) initiates AF in the milieu of APD alternans at relatively slow rates. This happened multiple times in this patient at various rates. (From Narayan et al. [31]. Used with permission from Wolters Kluwer)



stem cell-derived cardiomyocytes in individual patients [58].

Conclusions

Cardiac arrhythmias are dependent upon a complex interplay of impulse formation, spatially heterogeneous conduction slowing, and abnormal repolarization. Monophasic action potential data is uniquely suited to reveal abnormalities in these human tissue properties in vivo that escape traditional unipolar or bipolar electrogram measurements. A number of studies using this technique have demonstrated the role of abnormal electrical restitution, alternans and complex oscillations in action potential shape and duration, and spatial heterogeneities which may directly enable the initiation and maintenance of complex arrhythmias. The MAP can thus be used to delineate novel clinical phenotypes based on cellular remodeling, can be used to assist in mapping for complex arrhythmias, and thus may have an important role in guiding therapy.

Disclosures Junaid Zaman was funded by a Fulbright Foundation-British Heart Foundation award. Sanjiv M. Narayan is the author of intellectual property owned by the University of California Regents and Stanford University and discloses consulting income from Abbott, Medtronic, Uptodate, and the American College of Cardiology and funding from the National Institutes of Health (HL83559, HL103800). Michael R Franz reports no disclosures relevant to this work.

References

- Nattel S. New ideas about atrial fibrillation 50 years on. *Nature*. 2002;415:219–26.
- Haïssaguerre M, Jaïs P, Shah DC, Takahashi A, Hocini M, Quiniou G, et al. Spontaneous initiation of atrial fibrillation by ectopic beats originating in the pulmonary veins. *N Engl J Med*. 1998;339:659–66.
- Zaman JAB, Rogers AJ, Narayan SM. Rotational drivers in atrial fibrillation. *Circ Arrhythmia Electrophysiol*. 2017;10:e006022.
- Oakes RS, Badger TJ, Kholmovski EG, Akoum N, Burgon NS, Fish EN, Blauer JJE, et al. Detection and quantification of left atrial structural remodeling with delayed-enhancement magnetic resonance imaging in patients with atrial fibrillation. *Circulation*. 2009;119:1758–67.
- Lip GYH, Fauchier L, Freedman SB, Van Gelder I, Natale A, Gianni C, et al. Atrial fibrillation. *Nat Rev Dis Prim*. 2016;2:16016.
- Franz MR. Long-term recording of monophasic action potentials from human endocardium. *Am J Cardiol*. 1983;51:1629–34.
- Franz MR, Karasik PL, Li C, Moubarak J, Chavez M. Electrical remodeling of the human atrium: similar effects in patients with chronic atrial fibrillation and atrial flutter. *J Am Coll Cardiol*. 1997;30:1785–92.
- Koller M, Riccio M, Gilmour RF. Dynamic restitution of action potential duration during electrical alternans and ventricular fibrillation. *Am J Phys*. 1998;275:H1635–42.
- Taggart P, Lab M. Cardiac mechano-electric feedback and electrical restitution in humans. *Prog Biophys Mol Biol*. 2008;97:452–60.
- Bode F, Kilborn M, Karasik P, Franz MR. The repolarization-excitability relationship in the human right atrium is unaffected by cycle length, recording site and prior arrhythmias. *J Am Coll Cardiol*. 2001;37:920–5.
- Kim B-S, Kim Y-H, Hwang G-S, Pak H-N, Lee SC, Shim WJ, et al. Action potential duration restitution kinetics in human atrial fibrillation. *J Am Coll Cardiol*. 2002;39:1329–36.
- Franz MR. The electrical restitution curve revisited: steep or flat slope-which is better? *J Cardiovasc Electrophysiol*. 2003;14:S140–7.
- Knollmann BC, Tranquillo J, Sirenko SG, Henriquez C, Franz MR. Microelectrode study of the genesis of the monophasic action potential by contact electrode technique. *J Cardiovasc Electrophysiol*. 2002;13:1246–52.
- Liu J, Gong Y, Xia L, Zhao X. In silico investigation into cellular mechanisms of cardiac Alternans in myocardial ischemia. *Comput Math Methods Med*. 2016;2016:1–9.
- Qu Z, Garfinkel A, Chen PS, Weiss JN. Mechanisms of discordant alternans and induction of reentry in simulated cardiac tissue. *Circulation*. 2000;102:1664–70.
- Cao JM, Qu Z, Kim YH, Wu TJ, Garfinkel A, Weiss JN, et al. Spatiotemporal heterogeneity in the induction of ventricular fibrillation by rapid pacing: importance of cardiac restitution properties. *Circ Res*. 1999;84:1318–31.
- Pastore JM, Girouard SD, Laurita KR, Akar FG, Rosenbaum DS. Mechanism linking T-wave Alternans to the genesis of cardiac fibrillation. *Circulation*. 1999;99:1385–94.
- Walker ML, Rosenbaum DS. Cellular alternans as mechanism of cardiac arrhythmogenesis. *Heart Rhythm*. 2005;2:1383–6.
- Keldermann RH, ten Tusscher KHWJ, Nash MP, Hren R, Taggart P, Panfilov AV. Effect of heterogeneous APD restitution on VF organization in a model of the human ventricles. *Am J Physiol Circ Physiol*. 2008;294:H764–74.

20. ten Tusscher KHWJ, Panfilov AV. Alternans and spiral breakup in a human ventricular tissue model. *Am J Physiol Circ Physiol*. 2006;291:H1088–100.
21. Lu Z, Cui B, He B, Hu X, Wu W, Wu L, et al. Distinct restitution properties in vagally mediated atrial fibrillation and six-hour rapid pacing-induced atrial fibrillation. *Cardiovasc Res*. 2011;89:834–42.
22. Pruvot E, Jousset F, Ruchat P, Vesin J-M, Prudat Y, Zerm T, et al. Propagation velocity kinetics and repolarization alternans in a free-behaving sheep model of pacing-induced atrial fibrillation. *Europace*. 2007;9(Suppl 6):vi83–8.
23. Gong Y, Xie F, Stein KM, Garfinkel A, Cuianu C, Lerman BB, et al. Mechanism underlying initiation of paroxysmal atrial flutter/atrial fibrillation by ectopic foci: a simulation study. *Circulation*. 2007;115:2094–102.
24. Narayan SM, Bode F, Karasik P, Franz MR. Alternans of atrial action potentials during atrial flutter as a precursor to atrial fibrillation. *Circulation*. 2002;106:1968–73.
25. Narayan SM, Krummen DE, Kahn AM, Karasik PL, Franz MR. Evaluating fluctuations in human atrial fibrillatory cycle length using monophasic action potentials. *Pacing Clin Electrophysiol*. 2006;29:1209–18.
26. Narayan SM, Bayer JD, Lalani G, Trayanova N. Action potential dynamics explain arrhythmic vulnerability in human heart failure: a clinical and modeling study implicating abnormal calcium handling. *J Am Coll Cardiol*. 2008;52:1782–92.
27. Lalani GG, Schricker AA, Clopton P, Krummen DE, Narayan SM. Frequency analysis of atrial action potential alternans: a sensitive clinical index of individual propensity to atrial fibrillation. *Circ Arrhythm Electrophysiol*. 2013;6:859–67.
28. Weiss JN, Qu Z, Chen P-S, Lin S-F, Karagueuzian HS, Hayashi H, et al. The dynamics of cardiac fibrillation. *Circulation*. 2005;112:1232–40.
29. Narayan SM, Kazi D, Krummen DE, Rappel W-J. Repolarization and activation restitution near human pulmonary veins and atrial fibrillation initiation: a mechanism for the initiation of atrial fibrillation by premature beats. *J Am Coll Cardiol*. 2008;52:1222–30.
30. Gilmour RF, Chialvo DR. Electrical restitution, critical mass, and the riddle of fibrillation. *J Cardiovasc Electrophysiol*. 1999;10:1087–9.
31. Narayan SM, Franz MR, Clopton P, Pruvot EJ, Krummen DE. Repolarization Alternans reveals vulnerability to human atrial fibrillation. *Circulation*. 2011;123:2922–30.
32. Ni H, Zhang H, Grandi E, Narayan SM, Giles W. Transient outward K⁺ current can strongly modulate action potential duration and initiate Alternans in human atrium. *Am J Physiol Heart Circ Physiol*. 2018;316(3):H527–42; ajpheart.00251.2018
33. Wijffels MCEF, Kirchhof CJHJ, Dorland R, Allessie MA. Atrial fibrillation begets atrial fibrillation: a study in awake chronically instrumented goats. *Circulation*. 1995;92:1954–68.
34. Morillo CA, Klein GJ, Jones DL, Guiraudon CM. Chronic rapid atrial pacing. Structural, functional, and electrophysiological characteristics of a new model of sustained atrial fibrillation. *Circulation*. 1995;91:1588–95.
35. Gaspo R, Bosch RF, Talajic M, Nattel S. Functional mechanisms underlying tachycardia-induced sustained atrial fibrillation in a chronic dog model. *Circulation*. 1997;96:4027–35.
36. Hara M, Shvilkin A, Rosen MR, Danilo P, Boyden PA. Steady-state and nonsteady-state action potentials in fibrillating canine atrium: abnormal rate adaptation and its possible mechanisms. *Cardiovasc Res*. 1999;42:455–69.
37. Daoud EG, Zeidan Z, Hummel JD, Weiss R, Houmsse M, Augostini R, et al. Identification of repetitive activation patterns using novel computational analysis of multielectrode recordings during atrial fibrillation and flutter in humans. *JACC Clin Electrophysiol*. 2017;3:207–16.
38. Schoonderwoerd BA, Van Gelder IC, Van Veldhuisen DJ, Van den Berg MP, Crijns HJGM. Electrical and structural remodeling: role in the genesis and maintenance of atrial fibrillation. *Prog Cardiovasc Dis*. 2005;48:153–68.
39. Van Wagoner DR, Pond AL, Lamorgese M, Rossie SS, McCarthy PM, Nerbonne JM. Atrial L-type Ca²⁺ currents and human atrial fibrillation. *Circ Res*. 1999;85:428–36.
40. Hatem SN, Coulombe A, Balse E. Specificities of atrial electrophysiology: clues to a better understanding of cardiac function and the mechanisms of arrhythmias. *J Mol Cell Cardiol*. 2010;48:90–5.
41. Yue L, Feng J, Gaspo R, Li GR, Wang Z, Nattel S. Ionic remodeling underlying action potential changes in a canine model of atrial fibrillation. *Circ Res*. 1997;81:512–25.
42. Van Wagoner DR. Electrophysiological remodeling in human atrial fibrillation. *Pacing Clin Electrophysiol*. 2003;26:1572–5.
43. Escande D, Coulombe A, Faivre JF, Coraboeuf E. Characteristics of the time-dependent slow inward current in adult human atrial single myocytes. *J Mol Cell Cardiol*. 1986;18:547–51.
44. Schotten U, Verheule S, Kirchhof P, Goette A. Pathophysiological mechanisms of atrial fibrillation: a translational appraisal. *Physiol Rev*. 2011;91:265–325.
45. Bosch RF, Zeng X, Grammer JB, Popovic K, Mewis C, Kühlkamp V. Ionic mechanisms of electrical remodeling in human atrial fibrillation. *Cardiovasc Res*. 1999;44:121–31.
46. van der Velden HMW, van der Zee L, Wijffels MC, van Leuven C, Dorland R, Vos M, et al. Atrial fibrillation in the goat induces changes in monophasic action potential and mRNA expression of ion channels involved in repolarization. *J Cardiovasc Electrophysiol*. 2000;11:1262–9.
47. Boutjdir M, Le Heuzey JY, Lavergne T, Chauvaud S, Guize L, Carpentier A, et al. Inhomogeneity of cellular refractoriness in human atrium: factor of

- arrhythmia? *Pacing Clin Electrophysiol.* 1986;9:1095–100.
48. Roberts-Thomson KC, Stevenson IH, Kistler PM, Haqqani HM, Goldblatt JC, Sanders P, et al. Anatomically determined functional conduction delay in the posterior left atrium. Relationship to structural heart disease. *J Am Coll Cardiol.* 2008;51:856–62.
 49. Tse HF, Lau CP, Ayers GM. Heterogeneous changes in electrophysiologic properties in the paroxysmal and chronically fibrillating human atrium. *J Cardiovasc Electrophysiol.* 1999;10:125–35.
 50. Caballero R, de la Fuente MG, Gómez R, Barana A, Amorós I, Dolz-Gaitón P, et al. In humans, chronic atrial fibrillation decreases the transient outward current and ultrarapid component of the delayed rectifier current differentially on each atria and increases the slow component of the delayed rectifier current in both. *J Am Coll Cardiol.* 2010;55:2346–54.
 51. Lalani GG, Schrickler A, Gibson M, Rostamian A, Krummen DE, Narayan SM. Atrial conduction slows immediately before the onset of human atrial fibrillation: a bi-atrial contact mapping study of transitions to atrial fibrillation. *J Am Coll Cardiol.* 2012;59:595–606.
 52. Hansen BJ, Zhao J, Csepe T, Moore BT, Li N, Jayne L, et al. Atrial fibrillation driven by micro-anatomic intramural re-entry revealed by simultaneous sub-epicardial and sub-endocardial optical mapping in explanted human hearts. *Eur Heart J.* 2015;36:2390–401.
 53. Verrier RL, Fuller H, Justo F, Nearing BD, Rajamani S, Belardinelli L. Unmasking atrial repolarization to assess alternans, spatiotemporal heterogeneity, and susceptibility to atrial fibrillation. *Hear Rhythm.* 2016;13:953–61.
 54. Narayan SM, Zaman JAB, Baykaner T, Franz MR. Atrial fibrillation: can electrograms be interpreted without repolarization information? *Hear Rhythm.* 2016;13:962–3.
 55. Roney CH, Cantwell CD, Qureshi NA, Ali RL, Chang ETY, Lim PB, et al. An automated algorithm for determining conduction velocity, Wavefront direction and origin of focal cardiac arrhythmias using a multipolar catheter. *IEEE.* 2014;2014:1583–6.
 56. Honarbakhsh S, Schilling RJ, Orini M, Providencia R, Keating E, Finlay M, et al. Structural remodeling and conduction velocity dynamics in the human left atrium: relationship with reentrant mechanisms sustaining atrial fibrillation. *Heart Rhythm.* 2018;16(1):18–25.
 57. Zaman JAB, Peters NS. The rotor revolution: conduction at the eye of the storm in atrial fibrillation. *Circ Arrhythmia Electrophysiol.* 2014;7:1230–6.
 58. Sharma A, McKeithan WL, Serrano R, Kitani T, Burridge PW, del Álamo JC, et al. Use of human induced pluripotent stem cell-derived cardiomyocytes to assess drug cardiotoxicity. *Nat Protoc.* 2018;13:3018–41.

Index

A

- Abnormal repolarization, 132, 133
- Abu-Zeitone's analysis, 169
- Acquired long QT syndrome
 - acute and long term management, 208, 209
 - drug-induced LQTS, 207
 - ECG characteristics, 202, 204
 - ethnicity and gender differences, 207, 208
 - etiology, 204, 205
 - pharmacogenetics, 205–207
 - QT/T wave alternans, 202, 203, 205
- Action potential (AP)
 - cardiac, 109, 110
 - different phases, 109, 110
 - profile, 77
 - of small animals, 88
- Action potential duration (APD), 77
 - AF mechanisms, 333, 334
 - atrial electrophysiologic remodeling, 336–339
 - conduction velocity, 342
 - decrease in outward potassium currents
 - delayed rectifier K⁺ currents I_{Kr} and I_{Ks}, 79, 80
 - inward I_{K1} density, 80
 - transient outward potassium current (I_{to}), 79
 - dynamic restitution curve, 334
 - electrical remodeling, 333
 - electrical restitution curve, 334, 336
 - heterogeneity, 340–342
 - human AF, 334, 335
 - increase in inward currents
 - altered Ca²⁺ current, 81
 - calcium transient, 81
 - late inward sodium current, 80–81
 - magnitude, 335
 - MAP amplitude, 333
 - MAP catheter, 333
 - rapid assessment or quantification, 335, 337
 - refining electrical restitution, 339, 340, 342
 - restitution hypothesis, 336
 - spectral analysis, 336
- Acute rheumatic carditis, 228–229
- Adrenergic stimulation, 50, 51
- Affinity-purified autoantibodies, 242
- Age-related QTc-interval changes, 120–121
- Andersen's syndrome mutations, 27
- Andersen-Tawil syndrome, 143
- Antiadrenergic therapy, 165, 166
- Antiarrhythmic drug therapy, 113
 - beta-adrenergic blockade, 323
 - calcium channel blocking agents, 323
 - in detecting proarrhythmia, 324
 - sodium channel blocking agents, 323
- Antiarrhythmic neuromodulations
 - cardiac sympathetic blockade, 65
 - cardiac sympathetic denervation, 65
 - isoproterenol as antiarrhythmic drug, 67
 - sympathetic nervous system, 65
 - vagus nerve stimulation, 66
- Anti-Kv1.4 antibodies, 241
- Anti-Ro/SSA antibodies, 218
 - arrhythmogenic, 223
 - hERG E-pore region, 223
 - in silico experiments, 221, 223
 - in vitro experiments, 220, 221
 - Kv11.1-hERG channel, 219
 - pathogenic activities, 224
 - pathogenic role, 219
- APD-CL nonuniformity, 338
- Arizona's Center for Education and Research on Therapeutics (AZCERT), 188–190
- Arrhythmia mechanisms, 67
- Arrhythmias in J-wave syndromes, 67
- Arrhythmogenic autoantibodies, 218
- Arrhythmogenic early repolarization, 277
- Artificial neural networks, 97
- Atrial alternans, 337
- Atrial electrophysiologic remodeling, 336–339
- Atrial flutter (Afl), 338
- Autoimmune cardiac channelopathies, 218
- Autoimmune channelopathy, 218, 237
- Autoimmune-congenital heart block (ACHB), 237
- Autoimmunity
 - anti-Ro SSA antibodies, 218, 237–241
 - autoimmune cardiac channelopathies, 218
 - autoimmune potassium channelopathies, 219
 - cardiac arrhythmias, 218
 - clinical significance, 223, 224
 - clinical studies, 241
 - hERG E-pore region, 223
 - in silico experiments, 222, 223

- Autoimmunity (*cont.*)
 in vitro experiments, 220, 221
 in vivo experiments, 219–220
 molecular basis and pathophysiology, 242
 QTc/TdP, 238, 239
- Autonomic nervous system (ANS)
 adrenergic stimulation, 50, 51
 beta-1 adrenergic receptor stimulation, 50
 complex anatomy, 49
 proarrhythmic effects, 50, 51
 sympathetic stimulation, 50
 temporal VR heterogeneities, 51
 three-component system, 49
 type 2 muscarinic receptor stimulation, 50
- Autosomal-dominant pattern of inheritance, 285
- B**
- Bazett's formula, 131
 Beat-to-beat evaluation, 59–60
 Beta-1 adrenergic receptor stimulation, 50
 Beta-adrenergic blockade, 323
 Beta-adrenergic stimulation, 67
 Beta-blocker therapy
 2017 AHA/ACC/HRS Guideline, 171
 aborted cardiac arrest, 167, 168
 Abu-Zeitone's analysis, 169
 cardiac events, risk of, 167
 Cox regression analysis, 170
 dose dependency of response, 166
 evaluated effects, 166
 hERG channel, 169
 left cervicothoracic sympathetic ganglionectomy, 166
 life-threatening arrhythmic events, 167, 168
 QTc before *vs.* after, 166
 significant effect, 166
 therapy of choice, 166
 time-dependent Cox regression analyses, 168
 time-dependent variable, 168
- Bradycardia-induced QT prolongation, 67
- Brugada syndrome (BrS), 63, 64, 92, 136
 conduction delay, 285
 diagnosis, 294
 genetic architecture, 293–294
 genetics and pathophysiology
 non-SCN5A-Mediated BrS, 289, 290
 penetrance and variable expressivity, 286, 287
 SCN5A-mediated BrS, 288, 289
 ST-segment elevation, 286
 variation, 288
 invasive management, 295–296
 monogenic disorder, 285
 non-SCN5A/minor BrS gene-disease associations
 ClinGen reclassifications, 291, 293
 susceptibility genes, 290, 291
 systematic efforts, 291
 pharmacologic management, 292, 296
 risk-stratification approaches, 294
 ST-segment elevation, 285
 subtle cardiomyopathy, 285
 supraventricular tachyarrhythmias, 285
 type 1 Brugada ECG pattern, 294
- C**
- Ca²⁺-activated and Na⁺-activated K⁺ channels, 31, 32
 Ca_v channel accessory subunits, 18, 19
 Calcium channel blocking agents, 323
 Calcium transient (CaT), 81
 Cardiac action potential, 110
 Cardiac arrhythmias, 87, 89
 Cardiac channelopathies, 119
 Cardiac electrical stability, 325
 Cardiac ion channels, 119
 Cardiac pacing, 174
 Cardiac rehabilitation therapy, 324
 Cardiac repolarization disorders model
 Brugada syndrome, 92
 catecholaminergic polymorphic ventricular tachycardia, 92
 long QT syndrome, 90, 91
 short QT syndrome, 91, 92
 Cardiac repolarization reserve, 194
 Cardiac resynchronization therapy (CRT), 78
 Cardiac sympathetic denervation (CSD), 65
 Catecholaminergic polymorphic ventricular tachycardia (CPVT), 64, 92
 Caveolin-3, 143
 Cell-attached macropatch technique, 113
 Cell maturity, 98
 Chagas's disease (ChD), 228
 Channelopathic-related disorders, 143
 Channelopathies, 112, 113
 Class I antiarrhythmic drugs, 113
 Class I antiarrhythmic-provoked type I Brugada ECG pattern, 294
 Classic Coumel's triangle, 49
 Classic J-wave, 270
 ClinGen framework, 291
 ClinGen reclassifications, 291, 293
 Clinical decision support system (CDSS), 192, 193, 195
 Comprehensive In vitro Proarrhythmia Assay (CiPA) Initiative, 97
 Computer model simulations, 113
 Conduction velocity (CV), 342
 Congenital long QT syndrome (cLQTS), 185, 232, 234
 Connective tissue diseases (CTD), 229
 Cox regression analysis, 170
 C-type inactivation, 111
- D**
- Delayed afterdepolarization (DAD)-triggered activity, 211
 Delayed rectifier K⁺ currents I_{Kr} and I_{Ks}, 8, 9, 79, 80
 Depolarization hypothesis, 136
 Drug-induced long QT syndrome (diLQTS)
 cellular mechanism, 187, 188
 clinical scenario specific risk, 194
 clinical sequelae, 188

CredibleMeds risk categorization, 188–190
 death, 191, 192
 diagnosis, 185
 drug specific risk factors, 193
 genetic factors, 194, 195
 history, 186, 187
 incidence, 190, 191
 international impact, 185
 pathophysiology, 185, 186
 patient specific risk factors, 192, 193
 prevention, 192
 QTdrugs lists, 190
 Drug-induced type 1 Brugada ECG pattern, 294
 Dynamic clamp, 96
 Dynamic restitution curve (DRC), 334
 Dyssynchronous heart failure (DHF), 78

E

Early after depolarizations (EADs), 50, 78
 Early repolarization syndrome (ERS), 63, 64
 amplitude, 273, 274
 arrhythmic death, 273, 274
 ascending ST segments, 274
 benign ECG pattern, 274
 benign vs. malignant
 ECGI techniques, 282
 horizontal/descending ST-segment
 variant, 279, 280
 hypothermia, 277, 278
 J-wave, amplitude of, 277–279
 low amplitude T-waves, 280
 non-invasive mapping, 282
 rapidly ascending ST-segment, 279–281
 risk stratification of patients, 280
 ST-segment, 277
 definitions, 270
 diagnostic criteria, 272, 273
 downward sloping R-wave, 273
 dynamicity, J waves, 273, 274
 history, 269, 270
 non-ascending ST segments, 274
 normal QRS-T variant with ST segment
 elevation, 269
 prevalence, 270–272
 prognosis, 272
 ST segment morphology, 274
 terminology, 270
 ECG-derived evaluation
 arrhythmic events, 131
 J wave syndromes, 136
 microvolt T-wave alternans, 134, 135
 periodic repolarization dynamics, 134
 QT and corrected QT (QTc) interval, 131, 132
 QT dispersion, 132, 133
 QT dynamicity, 134
 static parameters, 131
 sudden cardiac death, 131, 132, 134
 Tpeak -Tend, 133
 Tpeak-Tend/QT ratio, 133

variables, 133
 Electrical properties, 78
 Electrical remodeling, 333
 Electrical restitution curve (ERC), 334, 336
 Electrocardiographic imaging techniques (ECGI), 282
 Electrophysiologic studies, 143
 Electrophysiological mechanisms
 delayed after depolarization-triggered activity, 211
 experimental models, 206, 209
 reentrant and focal activity, 210
 self-terminating vs. non self-terminating, 212, 213
 Epinephrine testing, 148, 149
 Excitation-contraction (EC) coupling, 79
 Exercise-induced T-wave alternans, 148
 Exome Aggregation Consortium (ExAC), 291
 Experimental autoimmune myocarditis (EAM), 236

F

Fast inactivation process, 111
 Field potentials (FP), 93
 Fluorescent dyes, 94
 Fridericia's formula, 132
 Functional phenotype
 fluorescent dyes, 94, 95
 multi electrode array technology, 93, 94
 patch clamp technique, 93, 94
 video-based analyses, 94–96

G

Gain of sodium function, 113
 Genes of uncertain significance (GUS), 291
 Genetic architecture, 293–294
 Genome Aggregation Database (gnomAD), 291
 Genome editing, 97, 98
 Genome-wide association study (GWAS), 293
 Global QT duration, 52, 53
 Guinea-pig ventricular action potential, 219

H

Heart failure (HF)
 electrical stability, 77
 late sodium current, 113
 prevalence, 77
 Hereditary arrhythmogenic disorder, 141
 Heterogeneity, 340–342
 Heterologous systems, 87
 Holter recordings, 148
 Horizontal or descending ST-segment pattern, 279, 280
 HR/QT linear relationship, 305
 HRS/EHRA J-wave syndrome, 294
 Human and murine left ventricular transcriptome
 studies, 293
 Human embryonic stem cells (hESC), 88
 Human embryonic stem cells-cardiomyocytes
 (hESC-CMs), 88
 Human induced pluripotent stem cells-cardiomyocytes
 (hiPSC-CMs), 88, 89

Hydroquinidine (HQ), 309
Hypothermia, 277, 278

I

Ibutilide infusion, 122
I_{Na}- and I_{to}-mediated epicardial-to-endocardial transmural electrophysiological gradient, 293
I_{K(ACh)} channels, 11
ICa-T, 110
I_{K1} channels, 11
I_{KATP} channels, 11
Impaired intracellular calcium cycling, 318
Implanted cardioverter-defibrillators (ICDs), 316
 2017 AHA/ACC/HRS Guideline, 175
 appropriate ICD rendered shocks, 179
 appropriate therapy, 177–179
 class I indication, 175
 mutations, 178
 risk score, 178
 sudden cardiac death, 176
In silico mathematical model, 96
In vitro heterologous expression systems, 291
Incremental pacing technique, 340
Induced pluripotent stem cells (iPSCs), 88, 89
Inflammation
 congenital long-QT syndrome, 232, 234
 cytokines, 235
 electrophysiological effects, 236
 ex-vivo experiments, 235
 general population, 234
 inflammation-induced QTc prolongation, 236
 inflammatory cytokines, 234
 inflammatory heart disease, 228, 229
 inhibitory effects, 235
 intracellular pathway, 235
 molecular basis, 235
 non-inflammatory heart diseases, 232, 234
 pathophysiological mechanisms, 236
 QTc prolongation, 228, 229, 236
 systemic inflammatory diseases, 229–232
Inflammatory channelopathies, 235
Inflammatory cytokines, 235
Inflammatory heart diseases, 228, 229
Inherited arrhythmia syndromes, 54–55
Intracellular calcium cycling dynamics, 319
Inward I_{K1} density, 80
Inwardly rectifying cardiac K⁺ (Kir) channel pore-forming α subunits, 26–28
Inwardly rectifying K⁺ channel currents, 10
Ion-channel structure and function, 143–145
Ionic mechanism(s), 210
Isogenic controls, 97
Isoproterenol as antiarrhythmic drug, 67

J

J wave syndromes, 136
Jervell and Lange-Nielsen syndrome, 142

J-Tpeak interval, 304
J-wave (J-point elevation), 277
 amplitude of, 278–279
 ECG characteristics, 136
 syndromes, 63, 64

K

K⁺ current expression, 10

L

Labile process, 78
Late (delayed) after depolarizations, 113
Late sodium current
 channelopathies, 112, 113
 heart failure, 113
 molecular mechanisms and pathophysiology, 111, 112
 pharmacology
 class 1 antiarrhythmic drugs, 113
 ranolazine, 114, 115
Left cardiac sympathetic denervation (LCSD), 174
Left cervicothoracic sympathetic ganglionectomy, 166
Life-threatening arrhythmias, 314
Long QT syndrome (LQTS), 54, 90, 91, 112, 132
 acquired QT-prolonging factors, 227
 autoimmunity
 anti-Ro/SSA, 218, 237–241
 autoimmune cardiac channelopathies, 218
 autoimmune potassium channelopathies, 219
 cardiac arrhythmias, 218
 clinical significance, 223, 224
 clinical studies, 241
 hERG E-pore region, 223
 in silico experiments, 222, 223
 in vitro experiments, 220, 221
 in vivo experiments, 219–220
 molecular basis and pathophysiology, 242
 QTc/TdP, 238, 239
 beta-blocker therapy
 2017 AHA/ACC/HRS Guideline, 171
 aborted cardiac arrest, 167, 168
 Abu-Zeitone's analysis, 169
 cardiac events, risk of, 167
 Cox regression analysis, 170
 evaluated effects, 166
 hERG channel, 169
 left cervicothoracic sympathetic ganglionectomy, 166
 life-threatening arrhythmic events, 167, 168
 QTc before *vs.* after, 166
 significant effect, 166
 therapy of choice, 166
 time-dependent Cox regression analyses, 168
 time-dependent variable, 168
 cardiac pacing, 174
 classical and non-classical risk factors, 227
 clinical course

adolescence through age 40 years, 152, 153
 after fourth decade of life, 153, 154
 pre-adolescent LQTS patients, 151–153
 sex hormones, 154, 155
 clinical management, 181
 arrhythmic events, 165
 QTc shortening, 165
 sudden cardiac death, 165
 diagnosis
 epinephrine testing, 148, 149
 exercise induced repolarization changes, 147
 exercise-induced T-wave alternans, 148
 genetic testing, 149
 Holter recordings, 148
 score, 146–147
 in Standard 12-lead ECG, 145
 T-amplitude/RR slope, 148
 TpTe dynamics, 148
 T wave morphology, 146
 etiologic factors, 227
 gain of function, 142
 genetics, 143
 genotype-phenotype correlations, 150
 implanted cardioverter-defibrillator
 2017 AHA/ACC/HRS Guideline, 175
 appropriate ICD rendered shocks, 179
 appropriate therapy, 177–179
 class I indication, 175
 mutations, 178
 risk score, 178
 sudden cardiac death, 176
 inflammation
 congenital long-QT syndrome, 232, 234
 cytokines, 235
 electrophysiological effects, 236
 ex-vivo experiments, 235
 general population, 234
 inflammation-induced QTc prolongation, 236
 inflammatory cytokines, 234
 inflammatory heart disease, 228, 229
 inhibitory effects, 235
 intracellular pathway, 235
 molecular basis, 235
 non-inflammatory heart diseases, 232, 234
 pathophysiological mechanisms, 236
 QTc prolongation, 228, 229, 236
 systemic inflammatory diseases, 229–232
 ion-channel structure and function, 143–145
 left cardiac sympathetic denervation, 174
 loss of function/prolonged depolarization, 142
 manifestation, 217
 mutation, 142, 143
 pattern of inheritance, 142
 pharmacotherapy targeting ion channel dysfunction
 potassium channel mutations, 173
 sodium channel mutations, 171–173
 phenotype-genotype relationship, 141
 prevalence, 141, 227
 preventive measures, 165, 166

risk stratification
 type 1, 155–158
 type 2, 158–160
 type 3, 160, 161
 Low amplitude T-waves, 280
 LQTS type 1 (LQT1), 142
 LQTS type 2 (LQT2), 143
 LQTS type 3 (LQT3), 143
 LQTS type 4-17 (LQT 4-17), 143
 L-type calcium channels, 17

M

Mammalian heart

action potentials, 3
 delayed rectifier K⁺ currents, I_K, 8, 9
 electrophysiological studies, 4
 I_{K(ACh)} channels, 11
 I_{K1} channels, 11
 I_{K(ATP)} channels, 11
 I_{KCa1}, 11
 inwardly rectifying K⁺ channel currents, 10
 K⁺ current expression, 10
 transient outward K⁺ current channels, I_{to}, 7–8
 ventricular K⁺ currents
 Ca²⁺-activated and Na⁺-activated K⁺ channels, 31, 32
 inwardly rectifying cardiac K⁺ (Kir) channel pore-forming α subunits, 26–28
 two pore domain K⁺ channels, 29, 30
 voltage-gated Ca²⁺ channels, (CaV) pore-forming α subunits, 15, 16, 18
 voltage-gated calcium (Ca²⁺) currents/channels, 6
 voltage-gated K channel expression, 9, 10
 voltage-gated K⁺ current diversity
 K_v subunits and ventricular delayed rectifier K⁺ channels, 25
 K_v subunits and ventricular transient outward K⁺ channels, 24–25
 voltage-gated K⁺ (K_v) channel accessory subunits, 22
 voltage-gated K⁺ channel (K_v) pore-forming (α) subunits, 19
 voltage-gated Na⁺ (Na_v) channel pore-forming (α) subunits, 12, 14
 voltage-gated Na⁺ channel (Na) accessory β subunits, 15
 voltage-gated Na⁺ channels, 5, 6
 Membrane depolarization, 110
 Mendelian randomization, 196
 Menopause, 124, 125
 Menstrual cycle, 122, 123
 Menstrual phase, 122
 Microvolt T-wave alternans (TWA)
 antiarrhythmic drug therapy
 beta-adrenergic blockade, 323
 calcium channel blocking agents, 323
 in detecting proarrhythmia, 324
 sodium channel blocking agents, 323

- Microvolt T-wave alternans (TWA) (*cont.*)
 application, 324
 cardiac electrical stability, 325
 cardiac rehabilitation therapy, 324
 Clinical Evidence of Prediction, 320–321
 compliance, 324
 device-based therapy, 321, 323
 experimental and clinical correlates, 318
 high-resolution template, 314
 implication, 325
 life-threatening arrhythmias, 314–316
 MMA method, 318–322
 neural triggers, 325
 precordial (V_4) electrocardiogram
 rhythm strip, 314
 quantitative analysis, 321, 324
 relative risks, 325
 spectral method, 319–323
 sudden cardiac death, 314–316
- Modal gating, 109, 111
- Modified moving average (MMA)
 method, 135, 318–322
- Monophasic action potentials (MAPs), 333, 334
- Monstrous J-waves, 278, 279
- Multi electrode array (MEA) technology, 93, 94
- Multiple cell culture formats, 88, 90
- N**
- $Na_v1.5$, 111
- Neuromodulation
 ventricular arrhythmias
 catecholaminergic polymorphic ventricular
 tachycardia, 64
 clinical data, 61
 congenital long QT syndrome, 62, 63
 congenital short QT syndrome, 63
 ischemic and non-ischemic
 cardiomyopathy, 62
 J-wave syndromes, 63, 64
 life-threatening ventricular arrhythmias, 62
 ventricular repolarization
 beat to beat evaluation, 59–60
 global QT duration, 52, 53
 inherited arrhythmia syndromes, 54–55
 long QT syndrome, 54
 QT interval and risk stratification, 54
 QT/RR dependency, 55, 56
 QT-RR hysteresis, 56, 58
 short QT syndrome, 55
 Tpeak to Tend interval, 58, 59
- Non-inflammatory heart diseases, 232, 234
- Non-invasive mapping, 282
- Non-SCN5A/minor BrS gene-disease associations
 ClinGen reclassifications, 291, 293
 susceptibility genes, 290, 291
 systematic efforts, 291
- Non-SCN5A-Mediated BrS, 289, 290
- Non-specific type 2 (saddle-back)/type 3 ST-segment
 elevations, 294
- Normal RS-T segment elevation variant, 269
- O**
- Optogenetics, 96, 97
- Osborn wave, 277
- P**
- Paroxysmal supraventricular tachycardia
 (SVT), 122
- Patch clamp technique, 93, 94
- Periodic repolarization dynamics, 134
- Pharmacotherapy targeting ion channel dysfunction
 potassium channel mutations, 173
 sodium channel mutations, 171–173
- Pluripotent stem cells
 derived cardiomyocytes, 88, 89
 in cardiac arrhythmias, 89
- Post-cardioversion chronic AF goat model, 337
- Postmenopausal arrhythmogenesis, 124
- PQ segment depression (PQD), 304
- Precordial (V_4) electrocardiogram rhythm strip, 314
- Proarrhythmic effect, 50, 51
- Q**
- QT and QTc interval, 303, 304
- QT apex (QTa), 134
- QT dispersion (QTD), 132, 133
- QT dynamicity, 134
- QT end (QTe), 134
- QT factors, 166
- QTc-interval
 age-related QTc-interval changes, 120–121
 cardiac ion channels, 119
 electrophysiological basis, 120
 HPG-axis, 121
 hypothetical changes, 125
 phases, 120
 prolongation, 112
 racial differences, 121
 sex differences, 121
 sex hormones, 121
 menopausal period, 124, 125
 menstrual cycle, 122, 123
 pregnancy, 123, 124
- QT/RR dependency, 55, 56
- QT-RR hysteresis, 56, 58
- R**
- Ranolazine, 114, 115
- Rapidly ascending ST-segment, 279–281
- Repolarization hypothesis, 136
- Repolarization remodeling
 action potential duration (*see* Action potential
 duration (APD))
 failure, 81
 labile process, 78
 left myocardial hypertrophy, 81
 metabolic transcripts, 81, 82
- Resolution X-ray crystallographic analysis, 145
- Restitution hypothesis, 336

Rheumatoid arthritis (RA), 229
Romano-Ward syndrome, 142

S

SCN5A mutations, 112
SCN5A-mediated BrS, 288, 289
Sex hormones, 121
 menopausal period, 124, 125
 menstrual cycle, 122, 123
 pregnancy, 123, 124
Short QT syndrome (SQTS), 55, 63, 91, 92, 132
 clinical manifestations, 306–308
 diagnosis
 HR/QT linear relationship, 305
 J-Tpeak interval, 304
 PQ segment depression, 304
 QT and QTc interval, 303, 304
 genetics and molecular basis, 306
 risk stratification and management, 309
Sodium channel blocking agents, 323
Sodium-calcium exchange mechanism, 113
Spectral method, 135, 318–323
SQTS type 1 (SQT1), 91
Standard deviation of RR intervals (SDNN), 62
ST-elevation myocardial infarction (STEMI), 273
Stem cells
 cardiac repolarization disorders model
 Brugada syndrome, 92
 catecholaminergic polymorphic ventricular tachycardia, 92
 long QT syndrome, 90, 91
 short QT syndrome, 91, 92
 functional phenotype
 fluorescent dyes, 94, 95
 multi electrode array technology, 93, 94
 patch clamp technique, 93, 94
 video-based analyses, 94–96
 limitations
 cell maturity, 98
 translational capabilities, 98
 pluripotent stem cells
 in cardiac arrhythmias, 89
 derived cardiomyocytes, 88, 89
 technological advancements
 computational capabilities, 97
 dynamic clamp, 96
 genome editing, 97, 98
 optogenetics, 96, 97
Subtle cardiomyopathy, 285
Sudden cardiac death (SCD), 49, 77, 314
Sudden Cardiac Death-Heart Failure Trial (SCD-HeFT), 62
Sympathetic neural ablation procedures, 62
Sympathetic stimulation, 50
Systemic inflammatory diseases, 229–232
Systemic lupus erythematosus (SLE), 229

T

Takotsubo cardiomyopathy, 51
Temporal VR heterogeneities, 51

Therapeutic and accidental hypothermia, 277
Three-component system, 49
III-IV linker, 111
Time-dependent Cox regression analyses, 168
Timothy's syndrome, 143
Torsade de Pointes (TdP)
 acquired long QT syndrome
 acute and long term management, 208, 209
 drug-induced LQTS, 207
 ECG characteristics, 202, 204
 ethnicity and gender differences, 207, 208
 etiology, 204, 205
 pharmacogenetics, 205–207
 QT/T wave alternans, 202, 203, 205
 comprehensive electrophysiological mechanisms
 delayed afterdepolarization (DAD)-triggered activity, 211
 experimental models, 206, 209
 reentrant and focal activity, 210
 self-terminating vs. non self-terminating, 212, 213
 congenital long QT syndrome, 201
Torsades-de-pointes (TdP), 67, 185
 AZCERT, 189
 CDSS, 195
 cellular mechanisms, 187
 clinical decision support system, 192, 193, 195
 death, 191
 drug induced, 186, 187
 drug specific risk factors, 193
 genomics, 195
 hERG channels, 193
 history, 186
 incidence, 191
 medical autopilots, 195
 risks, 188
 symptomatic QT prolongation, 191
 types, 185
Tpeak to Tend (TpTe) interval, 58, 59, 133
Trafficking, 143
Transient outward K⁺ current channels, I_{to}, 7–8, 79
T-wave alternans (TWA), 134, 135
T wave morphology, 146
Two pore domain K⁺ channels, 29, 30
Type 1 Brugada ECG pattern, 294
Type 2 muscarinic receptors stimulation, 50
Type 3 long QT syndrome (LQTS3), 112–114

V

Vagus nerve stimulation (VNS), 66
Ventricular action potential, 3, 217
Ventricular arrhythmias
 catecholaminergic polymorphic ventricular tachycardia, 64
 clinical data, 61
 congenital long QT Syndrome, 62, 63
 congenital short QT syndrome, 63
 ischemic and non-ischemic cardiomyopathy, 62
 J-wave syndromes, 63, 64
 life-threatening ventricular arrhythmias, 62
Ventricular effective refractory periods (VERPs), 306

Ventricular fibrillation (VF), 49, 273

Ventricular repolarization (VR)

ANS

- adrenergic stimulation, 50, 51
- beta-1 adrenergic receptor stimulation, 50
- complex anatomy, 49
- proarrhythmic effects, 50, 51
- sympathetic stimulation, 50
- temporal VR heterogeneities, 51
- three-component system, 49
- type 2 muscarinic receptor stimulation, 50

antiarrhythmic neuromodulations

- cardiac sympathetic blockade, 65
- cardiac sympathetic denervation, 65
- isoproterenol as antiarrhythmic drug, 67
- sympathetic nervous system, 65
- vagus nerve stimulation, 66

neuromodulation

- beat to beat evaluation, 59–60
- global QT duration, 52, 53
- inherited arrhythmia syndromes, 54–55

long QT syndrome, 54

QT interval and risk stratification, 54

QT/RR dependency, 55, 56

QT-RR hysteresis, 56, 58

short QT syndrome, 55

T_{peak} to T_{end} interval, 58, 59

Video-based analyses, 94–96

Voltage-gated Ca²⁺ channels, (Ca_v) pore-forming α subunits, 15, 16, 18

Voltage-gated calcium (Ca²⁺) currents/channels, 6

Voltage-gated K channel expression, 9, 10

Voltage-gated K⁺ (K_v) channel accessory subunits, 22

Voltage-gated K⁺ channel (K_v) pore-forming (α) subunits, 19

Voltage-gated Na⁺ (Na_v) channel pore-forming (α) subunits, 12, 14

Voltage-gated Na⁺ channel (Na) accessory β subunits, 15

Voltage-gated outward potassium (K⁺) currents, 3

Voltage-gated sodium channels, 109

function, 111

structure, 111